MOUSE MODELS OF B CELL MALIGNANCIES

EDITED BY: Gema Perez-Chacon, Christelle Vincent-Fabert and Juan M. Zapata

PUBLISHED IN: Frontiers in Immunology

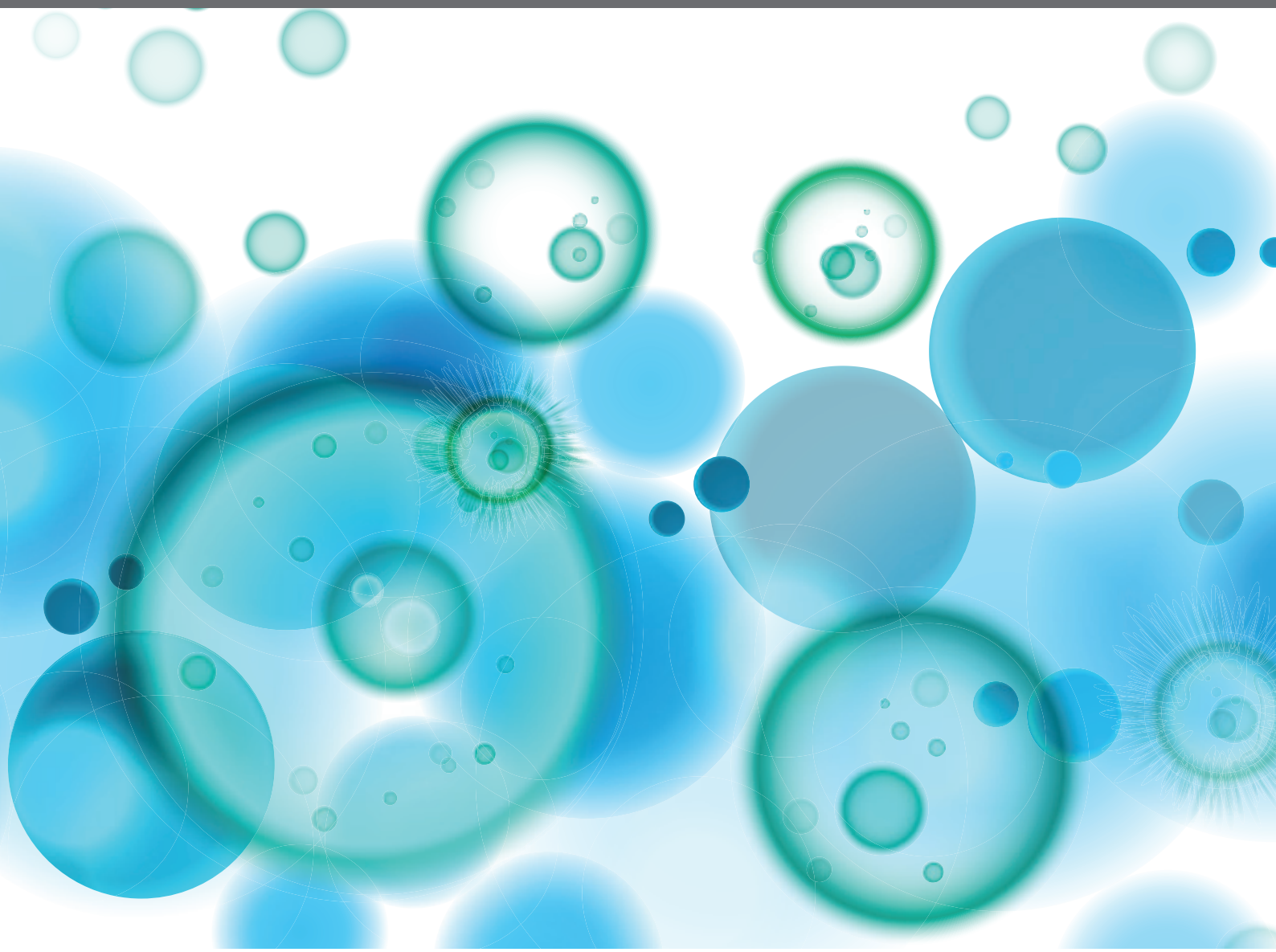

frontiers Research Topics

ISSN 1664-8714
ISBN 978-2-88971-896-2
DOI 10.3389/978-2-88971-896-2

About Frontiers

Frontiers is more than just an open-access publisher of scholarly articles: it is a pioneering approach to the world of academia, radically improving the way scholarly research is managed. The grand vision of Frontiers is a world where all people have an equal opportunity to seek, share and generate knowledge. Frontiers provides immediate and permanent online open access to all its publications, but this alone is not enough to realize our grand goals.

Frontiers Journal Series

The Frontiers Journal Series is a multi-tier and interdisciplinary set of open-access, online journals, promising a paradigm shift from the current review, selection and dissemination processes in academic publishing. All Frontiers journals are driven by researchers for researchers; therefore, they constitute a service to the scholarly community. At the same time, the Frontiers Journal Series operates on a revolutionary invention, the tiered publishing system, initially addressing specific communities of scholars, and gradually climbing up to broader public understanding, thus serving the interests of the lay society, too.

Dedication to Quality

Each Frontiers article is a landmark of the highest quality, thanks to genuinely collaborative interactions between authors and review editors, who include some of the world's best academicians. Research must be certified by peers before entering a stream of knowledge that may eventually reach the public - and shape society; therefore, Frontiers only applies the most rigorous and unbiased reviews.
Frontiers revolutionizes research publishing by freely delivering the most outstanding research, evaluated with no bias from both the academic and social point of view. By applying the most advanced information technologies, Frontiers is catapulting scholarly publishing into a new generation.

What are Frontiers Research Topics?

Frontiers Research Topics are very popular trademarks of the Frontiers Journals Series: they are collections of at least ten articles, all centered on a particular subject. With their unique mix of varied contributions from Original Research to Review Articles, Frontiers Research Topics unify the most influential researchers, the latest key findings and historical advances in a hot research area! Find out more on how to host your own Frontiers Research Topic or contribute to one as an author by contacting the Frontiers Editorial Office: frontiersin.org/about/contact

MOUSE MODELS OF B CELL MALIGNANCIES

Topic Editors:
Gema Perez-Chacon, Spanish National Cancer Research Center (CNIO), Spain
Christelle Vincent-Fabert, UMR7276 Contrôle des réponses immunes B et des lymphoprolifération (CRIBL), France
Juan M. Zapata, Consejo Superior de Investigaciones Científicas (CSIC), Spain

Citation: Perez-Chacon, G., Vincent-Fabert, C., Zapata, J. M., eds. (2021). Mouse Models of B Cell Malignancies. Lausanne: Frontiers Media SA.
doi: 10.3389/978-2-88971-896-2

Table of Contents

frontiers in Immunology

EDITORIAL
published: 28 October 2021
doi: 10.3389/fimmu.2021.789901

Editorial: Mouse Models of B Cell Malignancies

Gema Perez-Chacon[1]*, *Christelle Vincent-Fabert*[2,3]* *and Juan M. Zapata*[4,5]*

[1] Centro Nacional de Investigaciones Oncológicas (CNIO), Madrid, Spain, [2] UMR CNRS 7276/INSERM U1262 CRIBL, University of Limoges, Limoges, France, [3] Hematology Laboratory of Dupuytren, Hospital University Center (CHU) of Limoges, Limoges, France, [4] Instituto de Investigaciones Biomédicas "Alberto Sols", CSIC-UAM, Madrid, Spain, [5] Instituto de Investigación Sanitaria La Paz (IdIPAZ), Madrid, Spain

Keywords: genetically engineered mouse models, GEMM, mouse lymphoma, mouse leukemia, B cell neoplasms, immunosurveillance

Editorial on the Research Topic

Mouse Models of B Cell Malignancies

B cell malignancies represent a vast group of different entities arising from the multiple differentiation stages of B cells. In humans, there is a large variety of B cell malignancies, most of which have counterparts in mice. Prognosis and treatment for these malignancies would be largely dependent on their type, stage and grade.

Malignant B cells, like their normal counterparts, can disseminate around the body and have the remarkable ability to generate clonal diversity by mutation, often resulting in the development of treatment resistances. The microenvironment is crucial to drive tumor evolution, and we cannot yet adequately recapitulate *ex vivo* the complexity of the crosstalk between malignant B cells, normal lymphoid cells and stroma. Mouse models of B cell malignancies offer the possibility to study these complex relations *in vivo*. They also provide insights into the cellular and molecular mechanisms driving tumor evolution and may provide a preclinical platform for testing new therapies against leukemia and lymphoma.

Genetically engineered mouse models (GEMMs) mimicking the alterations in the expression and/or bearing cancer-driving mutations of candidate genes (oncogenes and tumor suppressors) implicated in B cell tumorigenesis are essential tools to assess the role of these genes in cancer. In addition, the unexpected development of B cell malignancies by genetically modified mice helped to uncover neoplastic functions of a variety of genes, unveiling new targets for therapy. Furthermore, the next generation sequencing has opened new possibilities for forward and reverse genetic screenings to identify gene mutations involved in tumor development, progression, evasion and relapse, both in human and mice, shaping the field for an exciting future.

This Research Topic is a collection of 13 articles that provides an overview on the recent developments in the field, including comprehensive reviews on the existing mouse models of B cell leukemia and lymphoma and on the new techniques available to characterize these models. In addition, original research articles describing new mouse models of monoclonal gammopathy of undetermined significance (MGUS), Waldenström macroglobulinemia (WM) and chronic lymphocytic leukemia (CLL) provide new insights into the role of a variety of oncogenes on the development of these B cell neoplasms.

OPEN ACCESS

Edited and reviewed by:
Harry W. Schroeder, University of Alabama at Birmingham, United States

***Correspondence:**
Gema Perez-Chacon
gperez@cnio.es
Christelle Vincent-Fabert
christelle.vincent-fabert@unilim.fr
Juan M. Zapata
jmzapata@iib.uam.es

Specialty section:
This article was submitted to B Cell Biology, a section of the journal Frontiers in Immunology

Received: *05 October 2021*
Accepted: *13 October 2021*
Published: *28 October 2021*

Citation:
Perez-Chacon G, Vincent-Fabert C and Zapata JM (2021) Editorial: Mouse Models of B Cell Malignancies. Front. Immunol. 12:789901. doi: 10.3389/fimmu.2021.789901

The new methodologies involving forward and reverse genetics and their applications in mouse research to identify new pro-oncogenic gene mutations as drivers of B cell malignancies is reviewed by Uren and Dawes. This timely and comprehensive review focuses on the experimental high throughput genetic approaches as tools to identify and validate large numbers of candidate genes. The authors overview how forward genetic screening in mice using insertional mutagenesis, chemical mutagenesis and exome sequencing can help to identify cooperating mutations at rates not possible using human tumor genomes. Uren and Dawes also address the usefulness of reverse genetic models and screenings that use CRISPR-Cas9, ORFs and shRNAs to provide high throughput *in vivo* proof of oncogenic function.

NEW MOUSE MODELS OF PLASMA CELL NEOPLASMS

Plasma cell neoplasms are tumor entities composed of post-germinal center (GC), terminally differentiated Ig producing B cells. There are distinct subclasses, including MGUS), WM, plasmacytoma and multiple myeloma (MM). Among those, MM is the most aggressive and the second most frequent leukemia (1), still causing the death of many patients due to the development of treatment resistances. Pisano et al. provide an insightful review of the available mouse models of plasma cell neoplasms, including transplantation-based and transgenic mouse models. The authors discuss the strengths and weaknesses of these mouse models for the study of MM and other plasma cell neoplasms, highlighting past achievement, current developments and future directions in the field aimed to develop new therapies that improve the outcome of patients with MM.

Schmidt et al. and Ouk et al. present original research providing conclusive evidence on the role of constitutive MyD88 activation on the development of plasma cell neoplasm. A mutation in the *MyD88* gene introducing a leucine in position 265 instead of a proline causing constitutive MyD88 dimerization and NFKB and JAK activation is found in a variety of human B cell neoplasms (2), including in most patients with WM (3). Schmidt et al. developed three genetically engineered conditional mouse models harboring floxed-*Myd88*^{L252P} (the mouse homolog of the human L265P mutation), one with *Cre* under the control of CD19 (CD19-Cre mice), where Myd88^{L252P} expression is enforced in all B cells, a second mouse strain with *Cre* under the control of Cγ1 promoter (Cγ1-Cre mice), thus limiting *Myd88*^{L252P} expression to GC cell, and a third mouse line with restricted *MyD88*^{L252P} expression to a few random B cells (CD19-CreERT2 mice). All these models developed distinct manifestations of IgM plasma cell hyperplasia, with the *Myd88*^{L252P}*;CD19-Cre*^{ERT2} mice developing monoclonal IgM paraproteins and IgM-expressing plasma cell expansions consistent with MGUS, the premalignant condition preceding WM. In addition, Ouk et al. independently generated a transgenic mice constitutively expressing Myd88^{L252P} in CD19 B cells (*Myd88*^{L252P}-IRES-*Yfp*;*CD19-Cre*). They show that these mice accumulate plasma cells in bone marrow and develop serum hyper-gammaglobulinemia, similar to the *Myd88*^{L252P}; *CD19-Cre* model described by Schmidt et al. Interestingly, although Schmidt et al. did not observe a path to plasma cell transformation in their model, Ouk et al. performed a longitudinal analysis that show that most of their mice develop with aging a monoclonal IgM peak and spleen lymphoplasmacytic-like B cell lymphoma with a transcriptomic signature consistent with WM. These two excellent works highlight the key role of the *Myd88*^{L252P} mutation and constitutive Myd88 activation in plasma cell transformation. Interestingly, the results with the two *Myd88*^{L252P}*;CD19-Cre mice* also raise questions on whether a different microbial and mouse housing environments, and even mouse genetic backgrounds, might influence the transformation outcome.

TNF-Receptor Associated Factor (TRAF)-3 controls Toll-like Receptors (TLR) signaling by recruiting and regulating MyD88 function (4). Remarkably, transgenic mice with enforced expression of TRAF3 in B lymphocytes also cause plasma cell expansions, hypergammaglobulinemia and exacerbated TLR responses (5) In addition, a role of TRAF3 in B cell lymphomagenesis is highlighted by the fact that mouse models with B cell-restricted upregulated TRAF3 expression (6) or TRAF3 deficiency (7) develop post-GC and mostly pre-GC B cell lymphomas, respectively. Looking for the mechanisms involved in TRAF3-deficiency-mediated B cell transformation, Liu et al. have uncovered a new role for TRAF3 in regulating B cell viability. The results provided by Liu et al. indicate that, in response to survival and/or growth factors deprivation, TRAF3 is mobilized to mitochondria, where, through its interaction with MFF, triggers mitochondria-dependent apoptosis. This new role of TRAF3 in controlling mitochondria homeostasis might have key implications in the role of TRAF3 in B cell transformation, providing new insights into why TRAF3-deficient mice (7) and TRAF3xBCL2 tg mice (6) (the later with protected mitochondria by means of BCL2 overexpression) develop distinct types of B cell neoplasia.

MOUSE MODELS OF C-MYC-DRIVEN LYMPHOMAS

c-MYC is a major transcriptional regulator controlling proliferation, cell growth, and apoptosis. Dysregulation of *c-MYC* is a trademark of a variety of B-cell lymphomas, where translocations of this gene lead to overexpression of intact c-MYC protein (8). *c-MYC* translocation is a primary transformation event in Burkitt´s lymphoma but its occurrence as a secondary event in diffuse large B-cell lymphoma, plasmablastic lymphoma, mantle cell lymphoma, or double-hit lymphoma fuels the aggressiveness of these lymphomas. Ferrad et al. overview the various *c-Myc*-driven mouse models of lymphoma focusing on those mouse models of c-myc overexpression regulated by the two main enhancers in the Igh locus, namely, Eμ and 3´RR enhancer. The authors comment on

the strengths and limitations of these mouse models with deregulated *c-Myc* expression for the study of lymphoma etiology.

In addition, Malaney et al. also overview the various transgenic mouse models of B cell lymphoma based on c-MYC upregulation, with particular emphasis on the heterogeneous nuclear ribonucleoprotein K (hnRNP K) as a driver of B cell lymphoma through its role on c-Myc regulation. hnRNP K is a ssDNA and RNA binding protein that regulates a plethora of processes controlling transcription and translation (9) and its over- and under-expression is causative of cancer (10). hnRNP K has been shown to be upregulated in DLBCL and Burkitt´s lymphoma patients and the oncogenic role of *hnRNP K* was previously confirmed by the authors by means of a B cell specific Eμ-*hnRNP K* transgenic mice that develop B cell lymphomas with high latency and high incidence (11). hnRNP K's oncogenic potential stems from its ability to regulate c-MYC expression at post-transcriptional and translational level, without requiring *c-MYC* translocations. In this review, Melaney et al. discuss the usefulness of the Eμ-*hnRNP K* mouse models in the study of B cell malignancies and as a preclinical platform for the assessment of novel therapeutics.

MOUSE MODELS OF FL AND GCB-DLBCL

Mossadegh-Keller et al. and Meyer et al. provide two comprehensive reviews on the available mouse models of GC-derived B cell lymphomas, which are the most frequent lymphoma types in humans. Mossadegh-Keller et al. pay particular attention to follicular lymphoma (FL) and the GC B cell-like subtype of DLBCL, providing a review of the various mouse models of FL and GCB-DLBCL and their respective key genetic and epigenetic characteristics. The authors overview the role of 1) apoptosis dysregulation, as indicated by the fundamental role of *Bcl2* dysregulation in FL and GCB-DLBCL lymphomagenesis, 2) epigenetic dysregulation (i.e. *Ezh2, Crebbp, Kmt2D*), 3) the tumor microenvironment as a driver of tumor progression and evasion from the immune system, and 4) the metabolism adaptations fueling tumor progression. Meyer et al. provide a thorough overview on the mouse models of Burkitt´s lymphoma, FL and DLBCL based on the key oncogenic events found in the human counterparts of these tumor subtypes, highlighting the pros and cons of each of these mouse models in the context of human disease and their potential therapeutic utility. Meyer et al. also review the different techniques currently available for creating a GEMM and comment on the development of patient-derived xenografts (PDXs) and their usefulness in lymphoma research.

MOUSE MODELS OF CHRONIC LYMPHOCYTIC LEUKEMIA

CLL remains as the most common leukemia in Western countries. CLL is an incurable disease with a variable clinical course consisting of at least two distinct subtypes based on the mutational status of the immunoglobulin heavy chain variable IGHV genes, which could be mutated (M) (good prognosis) or unmutated (UM) (bad prognosis) (12). The establishment of CLL PDXs have been challenging, in part because CLL cells, unlike many other B cell neoplasms, are low-proliferating cells, mostly quiescent and with dysregulated apoptosis. Only a small percentage are proliferating cells, which makes difficult their expansion in immunodeficient mice. Patten et al. provide a thorough analysis of the critical parameters supporting engraftment and growth of patient´s CLL cells in NGS immunodeficient mice. The authors find that *in vitro* pre-activation of CLL-derived T cells is key to support reliable implantation of CLL cells in a fully autologous system. The authors also show that patient´s CLL and T cells implantation follow distinct dynamics that could be differentiated in 4 temporal phases. The usefulness of this PDX approach is illustrated by assessing the effects of a bispecific antibody reactive with B and T cells.

Due to the difficulties in stablishing reliable CLL PDXs as described above, an intense effort has been invested in developing CLL mouse models (13). The most profusely studied CLL mouse model, the *Eμ-TCL-1* transgenic (14), as well as other reported mouse CLL models, only develop UM CLL, thus leaving unrepresented the M-CLL subtype. Another mouse model of CLL is the *Traf2*DN/*BCL2*-double-tg mice, that develop CLL/Small Lymphocytic Lymphoma (SLL) with high penetrance with aging. This mouse model has unbridled BAFF signaling and constitutive NFKB2 activation, causing the expansion of marginal zone (MZ) B cells (15) and, together with BCL2 overexpression, which is a CLL trademark, predispose MZ B cells to transformation into CLL/SLL. Perez-Chacon and Zapata provide original research showing that the CLL/SLL arising in the *Traf2*DN/*BCL2*-tg double-tg mice consists of both expanded M- and UM-CLL/SLL clones. Expanded clones show a biased IGHV gene usage, stereotypy and express HCDR3 that are similar to those recognizing autoantigens and pathogen antigens, thus closely resembling human CLL.

PATHOGENS AND IMMUNE EVASION IN LYMPHOMAGENESIS

The role of pathogens in promoting B cell transformation is reviewed by Huang and Yasuda, who focus on the role of Epstein-Barr virus (EBV) infection in lymphomagenesis. EBV is endemic in humans, with approximately 95% of the world's population sustaining an asymptomatic life-long infection. EBV may cause a variety of immune diseases in immunosuppressed individuals, including tumorigenesis when infected cells evade immunosurveillance (16). Huang and Yasuda summarize the role of EBV proteins and RNAs in promoting lymphomagenesis, the types of EBV-associated lymphomas and the available mouse models to study EBV-driven lymphoma.

The key role of immunosurveillance in preventing tumorigenesis is addressed by Lemasson et al., who evaluates how GEMMs could help in assessing the specific role of the distinct immune checkpoints in immunosurveillance and how B

cell lymphomas scape from their control. The authors review the mouse models of B cell lymphoma that have been used to study the involvement of the PD-1/PD-L1 axis, CTLA-4, MHC-II and NKG2 in lymphoma immune evasion. The authors also overview the relevance for the human disease of these mouse models and the usefulness of these models to pharmacologically target these checkpoint molecules to improve current treatments.

Overall, the original articles and reviews contained in this Research Topic provide a broad and updated view on the current GEMMs of B cell malignancies, highlighting the essential role of genetically modified mice in understanding all aspects of B cell lymphoma and leukemia, including development, progression, immune evasion and evolution to refractory disease.

AUTHOR CONTRIBUTIONS

All authors listed have made substantial, direct and intellectual contribution to the article and approved it for publication.

FUNDING

GP-C and JMZ were supported by a grant from the Agencia Estatal de Investigacion (PID2019-110405RB-I00/AEI/ 10.13039/ 501100011033). CV-F was supported by the France Lymphome Espoir association of patients and the Ligue contre le cancer.

REFERENCES

1. van de Donk N, Pawlyn C, Yong KL. Multiple Myeloma. *Lancet* (2021) 397 (10272):410–27. doi: 10.1016/S0140-6736(21)00135-5
2. Ngo VN, Young RM, Schmitz R, Jhavar S, Xiao W, Lim KH, et al. Oncogenically Active MYD88 Mutations in Human Lymphoma. *Nature* (2011) 470(7332):115–9. doi: 10.1038/nature09671
3. Xu L, Hunter ZR, Yang G, Zhou Y, Cao Y, Liu X, et al. MYD88 L265P in Waldenstrom Macroglobulinemia, Immunoglobulin M Monoclonal Gammopathy, and Other B-Cell Lymphoproliferative Disorders Using Conventional and Quantitative Allele-Specific Polymerase Chain Reaction. *Blood* (2013) 121(11):2051–8. doi: 10.1182/blood-2012-09-454355
4. Yu X, Du Y, Cai C, Cai B, Zhu M, Xing C, et al. Inflammasome Activation Negatively Regulates MyD88-IRF7 Type I IFN Signaling and Anti-Malaria Immunity. *Nat Commun* (2018) 9(1):4964. doi: 10.1038/s41467-018-07384-7
5. Zapata JM, Llobet D, Krajewska M, Lefebvre S, Kress CL, Reed JC. Lymphocyte-Specific TRAF3 Transgenic Mice Have Enhanced Humoral Responses and Develop Plasmacytosis, Autoimmunity, Inflammation, and Cancer. *Blood* (2009) 113(19):4595–603. doi: 10.1182/blood-2008-07-165456
6. Perez-Chacon G, Adrados M, Vallejo-Cremades MT, Lefebvre S, Reed JC, Zapata JM. Dysregulated TRAF3 and BCL2 Expression Promotes Multiple Classes of Mature Non-Hodgkin B Cell Lymphoma in Mice. *Front Immunol* (2018) 9:3114. doi: 10.3389/fimmu.2018.03114
7. Moore CR, Liu Y, Shao C, Covey LR, Morse HC3rd, Xie P. Specific Deletion of TRAF3 in B Lymphocytes Leads to B-Lymphoma Development in Mice. *Leukemia* (2012) 26(5):1122–7. doi: 10.1038/leu.2011.309
8. Ahmadi SE, Rahimi S, Zarandi B, Chegeni R, Safa M. MYC: A Multipurpose Oncogene With Prognostic and Therapeutic Implications in Blood Malignancies. *J Hematol Oncol* (2021) 14(1):121. doi: 10.1186/s13045-021-01111-4
9. Zhu S, Wang Z, Xu J. Connecting Versatile lncRNAs With Heterogeneous Nuclear Ribonucleoprotein K and Pathogenic Disorders. *Trends Biochem Sci* (2019) 44(9):733–6. doi: 10.1016/j.tibs.2019.06.001
10. Gallardo M, Hornbaker MJ, Zhang X, Hu P, Bueso-Ramos C, Post SM. Aberrant hnRNP K Expression: All Roads Lead to Cancer. *Cell Cycle* (2016) 15 (12):1552–7. doi: 10.1080/15384101.2016.1164372
11. Gallardo M, Malaney P, Aitken MJL, Zhang X, Link TM, Shah V, et al. Uncovering the Role of RNA-Binding Protein hnRNP K in B-Cell Lymphomas. *J Natl Cancer Inst* (2020) 112(1):95–106. doi: 10.1093/jnci/djz078
12. Kipps TJ, Stevenson FK, Wu CJ, Croce CM, Packham G, Wierda WG, et al. Chronic Lymphocytic Leukaemia. *Nat Rev Dis Primers* (2017) 3:16096. doi: 10.1038/nrdp.2016.96
13. Perez-Chacon G, Zapata JM. Mouse Models of Chronic Lymphocytic Leukemia. In: P Oppezzo, editor. *Chronic Lymphocytic Leukemia*. Rijeka, Croatia: InTech (2012). p. 203–28.
14. Bresin A, D'Abundo L, Narducci MG, Fiorenza MT, Croce CM, Negrini M, et al. TCL1 Transgenic Mouse Model as a Tool for the Study of Therapeutic Targets and Microenvironment in Human B-Cell Chronic Lymphocytic Leukemia. *Cell Death Dis* (2016) 7:e2071. doi: 10.1038/cddis.2015.419
15. Perez-Chacon G, Llobet D, Pardo C, Pindado J, Choi Y, Reed JC, et al. TNFR-Associated Factor 2 Deficiency in B Lymphocytes Predisposes to Chronic Lymphocytic Leukemia/Small Lymphocytic Lymphoma in Mice. *J Immunol* (2012) 189(2):1053–61. doi: 10.4049/jimmunol.1200814
16. Young LS, Yap LF, Murray PG. Epstein-Barr Virus: More Than 50 Years Old and Still Providing Surprises. *Nat Rev Cancer* (2016) 16(12):789–802. doi: 10.1038/nrc.2016.92

Conflict of Interest: The authors declare that the research was conducted in the absence of any commercial or financial relationships that could be construed as a potential conflict of interest.

frontiers in Immunology

MINI REVIEW
published: 23 July 2020
doi: 10.3389/fimmu.2020.01564

Mouse Models of *c-myc* Deregulation Driven by IgH Locus Enhancers as Models of B-Cell Lymphomagenesis

*Melissa Ferrad, Nour Ghazzaui, Hussein Issaoui, Jeanne Cook-Moreau and Yves Denizot**

Inserm U1262, UMR CNRS 7276, Equipe Labellisée LIGUE 2018, Université de Limoges, Limoges, France

Chromosomal translocations linking various oncogenes to transcriptional enhancers of the immunoglobulin heavy chain (IgH) locus are often implicated as the cause of B-cell malignancies. Two major IgH transcriptional enhancers have been reported so far. The E_μ enhancer located upstream of the C_μ gene controls early events in B-cell maturation such as VDJ recombination. The 3' regulatory region (3'RR) located downstream from the C_α gene controls late events in B-cell maturation such as IgH transcription, somatic hypermutation, and class switch recombination. Convincing demonstrations of the essential contributions of both E_μ and 3'RR in B-cell lymphomagenesis have been provided by transgenic and knock-in animal models which bring the oncogene *c-myc* under E_μ/3'RR transcriptional control. This short review summarizes the different mouse models so far available and their interests/limitations for progress in our understanding of human *c-myc*-induced B-cell lymphomagenesis.

Keywords: MYC, B-cell lymphoma, transgenic mouse models, IgH locus, IgH transcriptional enhancers

OPEN ACCESS

Edited by:
Gema Perez-Chacon, Spanish National Cancer Research Center (CNIO), Spain

Reviewed by:
Ignacio Moreno De Alborán, Consejo Superior de Investigaciones Científicas (CSIC), Spain
Anne Corcoran, Babraham Institute (BBSRC), United Kingdom

****Correspondence:***
Yves Denizot
yves.denizot@unilim.fr

Specialty section:
This article was submitted to B Cell Biology, a section of the journal Frontiers in Immunology

Received: *29 April 2020*
Accepted: *15 June 2020*
Published: *23 July 2020*

Citation:
Ferrad M, Ghazzaui N, Issaoui H, Cook-Moreau J and Denizot Y (2020) Mouse Models of c-myc Deregulation Driven by IgH Locus Enhancers as Models of B-Cell Lymphomagenesis. Front. Immunol. 11:1564. doi: 10.3389/fimmu.2020.01564

INTRODUCTION

RAG-induced recombination, AID-induced DNA breaks and mutations throughout B-cell development make the IgH locus a hotspot for translocations (1) (**Figures 1A,B**). Bcl-2 translocation, the typical hallmark of follicular lymphomas (FL), occurs during RAG-induced VDJ recombination. Cyclin D1 translocation, associated with mantle cell lymphomas (MCL), occurs either during AID-induced somatic hypermutation (SHM) or AID-induced class switch recombination (CSR). *C-myc* translocation, the typical hallmark of Burkitt lymphoma (BL), takes place during AID-induced SHM and CSR. Finally, several translocations (such as *c-myc*, *c-maf*, *cyclin D1/D3*) found in myelomas are also related to AID-induced CSR. During CSR, AID-induced DNA double strand breaks (DSB) appear in the switch (*S*) donor region (usually S_μ) and in the *S* acceptor region (for example $S_{\gamma 1}$ and S_α for CSR toward IgG1 and IgA, respectively). *S* regions are of various lengths (for example 3.5 and 10 kb long for S_μ and $S_{\gamma 1}$, respectively) and are unusually G-rich. AID deaminates C into U at preferential AID hotspot motifs located throughout *S* regions. The AID-introduced U in *S* region DNA is removed by UNG to generate an abasic site that is recognized by the endonuclease APE1 generating a nick. A closely spaced, similarly created nick on the opposite strand induces a staggered DSB. Translocation of the DNA fragment encompassing *c-myc* is due to an off target AID effect on the chromosome bearing *c-myc*. Since AID transforms C to U all along *S* donor/acceptor regions, there is no common breakpoint identified in *S* regions for mature B-cell lymphomas. It is the same AID effect for SHM where AID targets the VDJ rearranged segments (and up to several kB in 3') and can induce DNA DSB for *c-myc* translocation. Similarly to CSR, there is no common breakpoint established in VDJ regions for mature B-cell lymphomas.

During VDJ recombination RAG binds to recombination signal sequences adjacent to V, D, and J coding segments and induces DNA DSB. *C-myc* translocation could take place during this process. Similarly to CSR/SHM, there is no common breakpoint singled out in VDJ regions for B-cell lymphomas. The common point for all these c-myc translocations is the occurrence of DSB in the IgH locus during its remodeling required for B-cell repertoire formation and B-cell maturation. All remodeling events of the IgH locus (VDJ recombination, SHM, and CSR) require transcription to occur (2). Transcriptional control and remodeling of the IgH locus are under the control of several *cis*-regulatory elements located throughout the IgH locus. In the murine IgH locus seven regions of interest can be defined including *cis*-regulatory elements, matrix attachment regions (MARs), and hypersensitivity (hs) sites with potential transcriptional enhancer or insulator activity: 4 hs sites located 5' of the first V segments, 6 hs sites in the V–D intergenic region, the DQ52 promoter–enhancer, the E_μ enhancer (between J_H and C_μ) and its flanking MARs, the γ1 enhancer element, the 3' regulatory region (3'RR) downstream from C_α with its four enhancers (hs3a, hs1,2, hs3b, and 4) and the 3'CBE insulator region (hs5, 6, 7, 8) as the 3' boundary of the locus (**Figure 1A**). Two potent transcriptional enhancers act during B-cell maturation: E_μ (during early B-cell maturation stages) and 3'RR (during late B-cell maturation stages) (**Figure 1A**). These elements obviously intervene in oncogene-induced B-cell lymphomagenesis as reported by several transgenic mouse models (using both transgene and knock-in (KI) strategies) developed in order to mimic human mature B-cell lymphomagenesis. Since c-myc is a key regulator of cell growth through its action on cell cycle progression, metabolism, differentiation, death receptor signaling, and DNA damage recovery, the vast majority of available models use *c-myc* as a deregulated oncogene (3). This short review describes how E_μ and 3'RR enhancers might play a critical role in *c-myc* deregulation during c-myc-induced mature B-cell lymphomas, why these models are not silver bullets to totally mimic human B-cell lymphomagenesis and why it is possible that targeting the 3'RR would be an interesting strategy in human B-cell lymphomagenesis.

THE E_μ *cis*-TRANSCRIPTIONAL IGH ENHANCER AND *c-myc* DEREGULATION

Forty years ago, E_μ was the first discovered IgH *cis*-transcriptional enhancer (4–6). It is located upstream of the C_μ gene (**Figure 1A**). E_μ-deficient mice revealed its role in controlling IgH locus access at immature B-cell stages and thus its key role for efficient VDJ recombination (7, 8). In contrast, E_μ is dispensable for late B-cell maturation events such as IgH locus transcription for Ig synthesis and CSR (9, 10). In 1985, transgenic mice bearing *c-myc* coupled to the E_μ enhancer were reported to consistently develop immature (pre-B) and sometimes mature B-cell lymphomas (11). Our entire knowledge of E_μ involvement in *c-myc* oncogenic deregulation for B-cell lymphoma development was built from this model. Since 1985, 183 papers with "E_μ-*Myc* mice" in their abstract have been referenced. Of note, 153 have been published in the last 15 years showing the great interest of the scientific community for this transgenic mouse model of B-cell lymphoma. It is thus impossible in this short review to reference them all. Therefore, the authors apologize in advance for the numerous interesting manuscripts which have not been cited in the present review. Lymphomas from Eμ-Myc mice range from the pre-B to the mature B-cell stages (**Figure 1C**). They are usually all positive for the CD45R (B220), CD19 and CD93 (AA4.1) B-cell specific markers and negative for the CD3 T-cell marker. Tumors of pre-B-cell type are characterized by the lack of membrane IgM and no Ig light chain (IgL) rearrangements. Tumors of immature B-cell types are more mature and express membrane IgM after efficient IgL rearrangements. Tumors of mature B-cell types are even more mature and express both membrane IgM and IgD. The majority of lymphomas in Eμ-Myc mice are at the pre-B and immature B-cell stages. In their original study, Adams et al. (11) stated that "these *myc* mice should aid study of lymphoma development, B-cell ontogeny and Ig regulation." Clearly 35 years later this is the case. Creation of these mice resulted in the dissection of many mechanisms implicated in B-cell lymphomagenesis (**Figure 1D**). They have highlighted the importance of several signaling pathways (such as Ras/Mapk, mTOR, and Akt) (12–14), several cell cycle check-points (such as Mdm2/p53/p73) (15, 16) and processes that affect c-myc stability and action (17, 18). Using these mice clearly demonstrated the importance of numerous (new and well-known) tumor suppressor genes (such as FoxO3, CDK4, Mtap, and Smchd1) (19–22). This model reinforced our knowledge concerning the signaling/regulation of the B-cell apoptotic program (members of the Bcl-2 family of apoptosis regulator) and deficiencies in apoptotic pathways leading to B-cell lymphomagenesis (23–28). To our knowledge the influence of genetic background in the development of B-cell lymphomas in Eμ-*Myc* mice has not been documented. The E_μ-*Myc* model has also opened a new area of research concerning the role of tumor microenvironment via release of angiocrine/chemokine factors (29–31) and the importance of cells from the vascular niche for NK cell surveillance, senescence, and homing of B-cell lymphomas (32–34). Perhaps most importantly, this model is at the origin of a wide number of publications investigating new therapeutic treatments or combinations of drugs in order to affect (among various targets) DNA synthesis (cytarabine, doxyrubicin, cyclophosphamide), mTOR signaling (rapamycin analogs), microtubule formation (vincristine), c-myc (decursin), apoptosis (venetoclax and BET inhibitors), protein synthesis (silvestrol), or B-cell receptor (BCR)-induced, or chemokine-mediated signaling (ibrutinib) (35–42). The rapid occurrence of lymphoma in E_μ-*Myc* mice and its high penetrance make this mouse model an accurate, reliable, easy, and fast experimental model not only to test new therapeutic approaches but also combinatory associations. This model is also unique by providing the possibility to monitor the assay of new NK therapeutic vaccination strategies (43, 44), to stimulate immune defenses for tumor rejection (45) and to test protocols for monoclonal antibody therapies (46). E_μ-*Myc* mice have thus proven their great potential as a model to study human B-cell lymphomagenesis during the

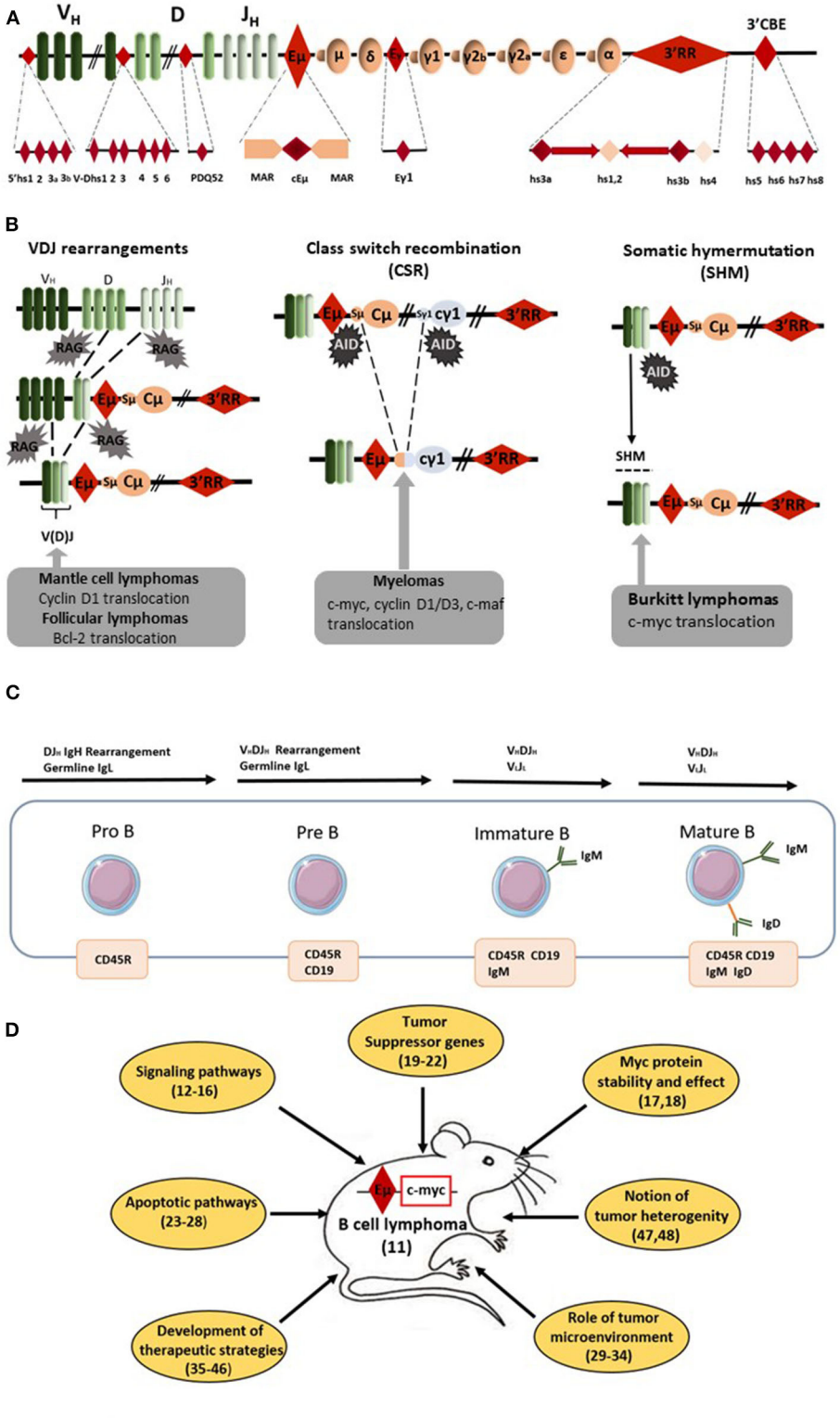

FIGURE 1 | E_{μ}-*Myc* mice as a model of B-cell lymphomagenesis. **(A)** Schematic diagrams of the mouse IgH locus. Locations of the various IgH *cis*-regulatory elements with enhancer or insulator activity are reported: four hs sites located 5' of the first V segments, six hs sites in the V–D intergenic region, the DQ52

(Continued)

FIGURE 1 | promoter-enhancer, the E_μ enhancer (the core region (cEμ) and its flanking MARs), the γ1 enhancer, the 3' regulatory region (3'RR) [four enhancers (namely hs3a, hs1,2, hs3b, and 4) with flanking inverted repeats] and the 3'CBE insulator region (hs5, 6, 7, and 8) as the 3' boundary of the locus. **(B)** Schematic representation of oncogene translocation affecting the IgH locus during VDJ recombination, CSR and SHM. Arrows indicate the site of oncogene translocation found during follicular lymphomas, mantle cell lymphomas, myelomas, and Burkitt lymphomas. **(C)** Schematic representation of B-cell development from pro-B to mature B-cells. Lymphomas from E_μ-*Myc* mice are from the pre-B to the mature B-cell stages. The immature B-cell stage is characterized by the expression of membrane IgM whereas membrane IgD occurs at the mature B-cell stage. **(D)** Schematic representation of the various field of research developed with E_μ-*Myc* mice. Bibliographic references are reported (number in parenthesis).

past decade. Moreover, arising lymphomas are heterogeneous (47, 48) mirroring genomic differences observed between human BL, germinal center B-cell lymphomas (GCBCL), activated B-cell lymphomas (ABCL), and diffuse large B-cell lymphomas (DLBCL). The different genomic signatures (toward specific proliferative and/or apoptotic pathways) of B-cell lymphomas in E_μ-*Myc* mice might be used as biomarkers of response against specific therapeutic strategies. Thus, and especially with the development of transcriptomic tools, E_μ-*Myc* mice can serve as relevant model for human B-cell lymphoma subtype experimental or associated treatments. The only but nevertheless major drawback of E_μ-*Myc* mice relates to the window of activity for E_μ which has been clearly demonstrated to occur at the immature pro-B/pre-B B-cell stages (49, 50). E_μ is not implicated in IgH hypertranscription occurring at the mature/plasma cell stages. E_μ is also not implicated in DNA breaks occurring during SHM/CSR and thus clearly not implicated in oncogenic translocation induced by off target AID action occurring during CSR or SHM in the majority of human mature B-cell lymphoma subtypes. As confirmation of this fact, the great majority of lymphomas from E_μ-Myc mice have a pre-B/immature B-cell stage.

THE 3'RR *cis*-TRANSCRIPTIONAL IgH ENHANCER AND *c-myc* DEREGULATION

The second transcriptional enhancer located in the IgH locus is the 3'RR (**Figure 1**). The 3'RR is a complex element with four transcriptional enhancers (namely hs3a, hs1,2, hs3b, and hs4) encompassed in a unique and functional 3D palindromic architecture (51). The 3'RR controls μ transcription (7), CSR (52, 53), and SHM (54) in mature B-cells. The transcriptional activity of the 3'RR occurs from pre-B to mature B-cell stages (55) and thus has a much larger window of activity than the E_μ enhancer. In 1994, Madisen and Groudine reported (in stable transfection assays in plasmacytomas and BL cells) that the 3'RR was efficient and sufficient to deregulate c-*myc* transcription (56). Convincing demonstration of 3'RR involvement in lymphomagenesis has been produced by a transgenic 3'RR-deficient model of B-cell lymphomas with IgH-*c-myc* translocations (57). The integrity of the 3'RR (deletion of hs3b to hs4) has been shown to be dispensable for development of pro-B-cell lymphomas with V(D)J recombination-initiated translocations suggesting the key role of E_μ. In contrast, 3'RR integrity (for its optimal transcriptional activity) is required for B-cell lymphomas with CSR-associated translocations (57). In another study modeling murine plasmacytomas with T (12, 15) translocations, the same hs3b-hs4 deletion of the 3'RR in Bcl-xL transgenic mice was without effect for *Myc* deregulation and mouse plasmacytoma generation (58). However, total 3'RR deletion in these plasmacytomas lowered Myc expression and cell growth confirming 3'RR involvement for myc deregulation by T (12, 15). Nevertheless, these models are not sufficient to monitor in detail and to modulate signaling pathways for B-cell lymphoma development. The same comments can be made for the transgenic mouse model of Wang and Boxer (59) which develops mature B-cell lymphomas ($CD19^+B220^+IgM^+IgD^{low}$) after the KI of a 3'RR cassette upstream of the endogenous *c-myc* gene (this model is the reverse of natural *c-myc* translocation into the human IgH locus) (**Figure 2**). More than 15 years after the development of transgenic E_μ-*Myc* mice, transgenic *Myc*-3'RR mice were generated and were shown to develop BL-like proliferations and diffuse anaplastic B-cell lymphomas (60). All these lymphomas exhibited a mature B-cell phenotype ($CD19^+B220^+IgM^+IgD^+$) but differed by their Ki67 status (low and high for diffuse anaplastic B-cell lymphomas and BL lymphomas, respectively). This model was used to study the role of second hits such as p53 deficiency, Cdk4 mutation, and change of class-specific B cell receptor (BCR) tonic signals. Results clearly demonstrated that a second hit affects the phenotype of B-cell lymphomas, their aggressiveness and transcriptomic signatures differently (61–64). This model was, however, progressively abandoned due to its medium B-cell lymphoma penetrance (compared to E_μ-*Myc* mice), long delay for B-cell lymphoma development (compared to E_μ-*Myc* mice), key differences with human B-cell lymphomas (such as mutations lacking for the p53-ARF-Mdm2 apoptotic pathways in numerous cases) and the description that the occurrence of B-cell lymphomas was much too sensitive to genetic background [C57Bl/6 mice developed BL-like lymphomas while none occurred in a Balb/c background (65)]. All these points argued against the use of *Myc*-3'RR mice as an accurate experimental model to test new pharmacologic or vaccination strategies.

THE COMBINATION OF E_μ AND 3'RR *cis*-TRANSCRIPTIONAL ENHANCERS AND *c-myc* DEREGULATION

As reported above, a transgenic model with IgH-*c-myc* translocations in response to pristine demonstrated the involvement of IgH *cis*-transcriptional enhancers in B-cell lymphomagenesis (57). In another manner, this study confirmed results obtained with three transgenic mouse models with a *c-myc* KI in various locations in the IgH locus (i.e., under the

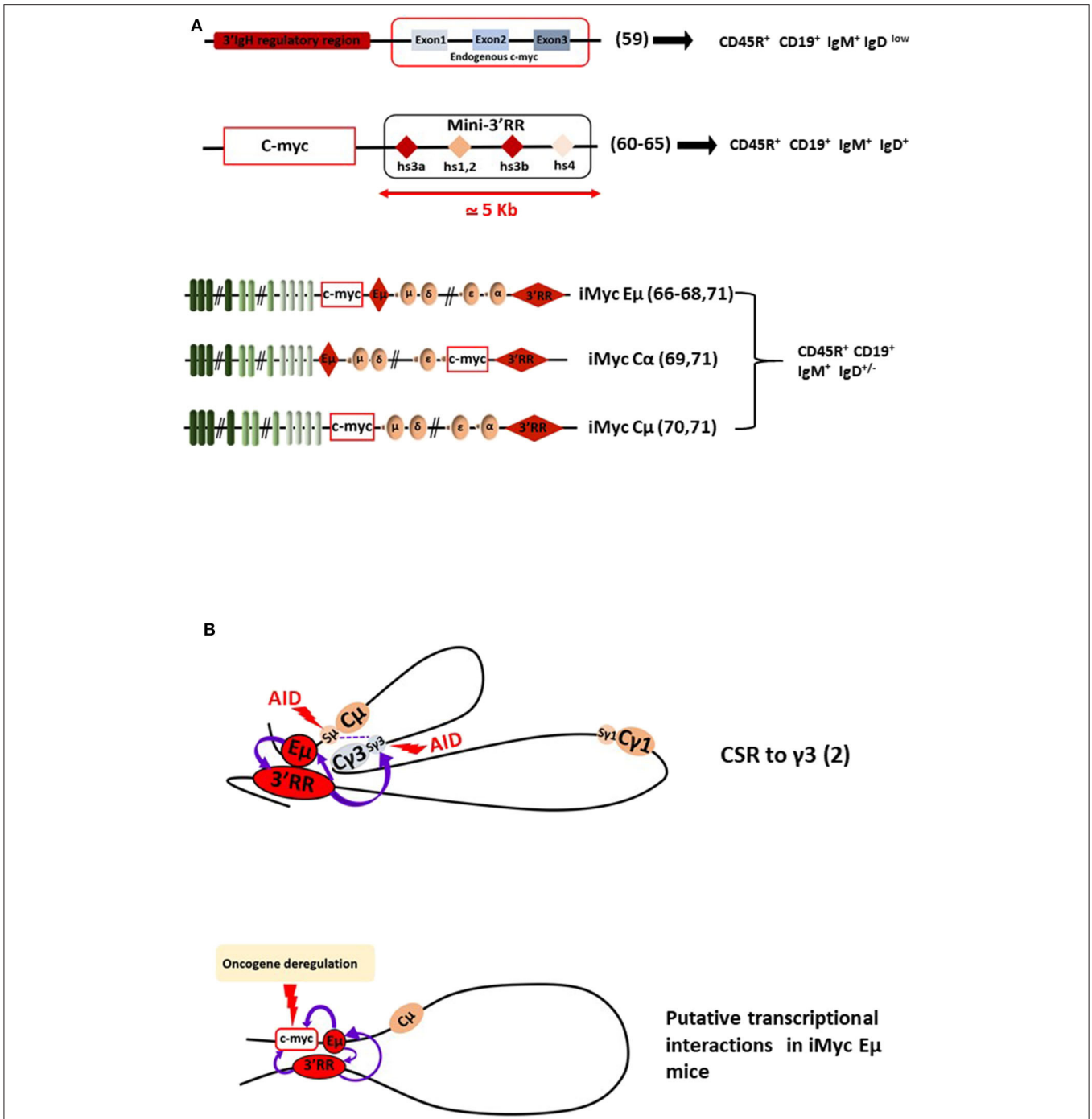

FIGURE 2 | The 3'RR and B-cell lymphomagenesis. **(A)** Schematic representation of several transgenic mouse models reporting *c-myc* 3'RR-driven deregulation leading to B-cell lymphomagenesis. B-cell lymphoma phenotypes are reported. Bibliographic references are reported (number in parenthesis). The "Mini-3'RR" contains the four transcriptional enhancers hs3a, hs1,2, hs3b, and hs4 but not the 3'RR palindromic sequences flanking hs1,2 and the DNA sequence between hs3a and hs4. **(B)** Long-range loop interactions between chromatin segments of the IgH locus comprise the mechanism of normal gene transcription regulation by the E_μ and 3'RR transcriptional enhancers. The example of the IgG_3 CSR process is schematized. Putative long-range interactions leading to c-myc oncogene deregulation in $iMycE_\mu$ mice are schematized.

dependence of both E_μ and 3'RR elements) (**Figure 2**). These models provided the most convincing data for the essential roles of both E_μ and 3'RR in c-*myc* B-cell lymphomagenesis. The KI of *c-myc* in the mouse IgH locus just 5′ to E_μ (namely i*Myc*E_μ mice), thus modeling human endemic BL, induced, as expected, B-cell lymphoma development with alterations

in the $p19^{Arf}$-Mdm2-p53 tumor suppressor axis (66) and NF?B/STAT3/PI3K signaling (67). In this model, *c-myc* is under the control of both E_μ and 3'RR at immature and mature B-cell stages, respectively. i*Myc*Eμ mice also mimic T (12, 15) mouse plasmacytoma translocation and thus also lead to plasmacytomas (68). KI of *c-myc* directly into C_α just 5' to the 3'RR (i*Myc*C_α mice) produced B-cell lymphomas with low kinetics which were increased after overexpression of the anti-apoptotic Bcl-X_L gene (69). In this model, *c-myc* is located in a site where E_μ has no transcriptional influence, *c-myc* transcription being only under the dependence of 3'RR at mature B-cell stages. *c-myc* KI in the mouse IgH locus just 5′ to C_μ with E_μ deletion (namely i*Myc*C_μ mice), thus modeling human sporadic BL, confirmed that 3'RR alone is sufficient to deregulate *c-myc* in the B-cell lineage and to induce B-cell lymphoma development (70). Taken altogether, these KI models carrying *c-myc* at the IgH locus are prone to B-cell lymphomas of various penetrance, kinetics, and fate as recently reported in a study comparing the three mouse models (71). The lymphoma signatures are also heterogeneous even comparing lymphomas from a specific KI, mirroring the genomic differences observed between the various subtypes of human mature B-cell lymphomas and those previously reported with the model of transgenic E_μ-*Myc* mice. In our opinion, these transgenic mouse models represent the "most physiological" experimental mouse models by mimicking the direct effect of c-*myc* in the context of the endogenous IgH locus. However, the main drawbacks of these various KI mice (and similarly to *Myc*-3'RR mice) remain their low lymphoma penetrance and their low kinetics of B-cell lymphoma development arguing against their use as efficient and easy experimental models to test new experimental therapeutic approaches. The low kinetics of B-cell lymphoma development compared with 3'RR-*Myc* mice would be related to the 3'CBE insulator region at the 3' boundary of the endogenous IgH locus (72, 73). This region is not present in the transgenic mouse model of 3'RR-induced *c-myc* deregulation. The 3'CBE insulator region contains a high density of binding sites for CCCTC-binding factor (CTCF), a protein associated with mammalian insulator activity. Deletion of the 3'CBE insulator region resulted in significant effects on VDJ rearrangement, IgH locus compaction, and IgH locus insulation. Furthermore, physical interactions occur in B-cells between 3'CBE and 3'RR enhancers suggesting that the entire 3' region (3'RR enhancers + 3'CBE insulators) works as a physical unit. The lack of 3'CBE in 3'RR-*Myc* mice could induced stronger and longer ***c****-myc* deregulation (and thus faster lymphoma emergence) than that obtained when *c-myc* is inserted into the IgH locus under the control of the entire (enhancer + insulator) region.

CONCLUSION

Knock-out mice models have clarified the functions of E_μ and 3'RR enhancers as essential for DNA remodeling and IgH locus transcription at specific stages of B-cell development and maturation. Thus, these enhancers have a major potential to be oncogene deregulators for IgH-translocated oncogenes, even when the breakpoints lie several 100 kb away from them. All these models contribute different but interesting data to our understanding of human B-cell lymphoma development and treatments especially with regards to the great functional and structural similarities found between human and mouse IgH loci (74). However, we must keep in mind that these mice are experimental models that do not reflect 100% of what happens in humans. For example, if the vast majority of human mature B-cell lymphomas are mutated in their VDJ region (highlighting their post-germinal center status) it is not the case in mice where mature B-cell lymphomas are unmutated (highlighting their pre-germinal center status) (75). Long-range loop interactions between chromatin segments of the IgH locus comprise the mechanism of normal and abnormal gene transcription regulation by the 3'RR (2, 76) (**Figure 2B**). Therefore, it is possible to suggest that targeted inhibition of the 3'RR would be a therapeutic approach for the treatment of some mature B-cell lymphomas. Finally, it is also of importance to mention that the *c-myc* oncogene driven by Ig light chain enhancers also induces B-cell lymphoid malignancy in transgenic mice (11, 77). These models highlight not only the importance of all Ig enhancers for B-cell lymphoma development but also that a 3'RR targeting strategy (if any) would not be a silver bullet to treat all B-cell lymphomas but at best some mature B-cell subtypes.

AUTHOR CONTRIBUTIONS

All authors listed have made a substantial, direct and intellectual contribution to the work, and approved it for publication.

FUNDING

This work was supported by grants from Equipe Labellisée LIGUE 2018 and ANR Episwitch 2016. MF was supported by a grant from Université de Limoges and Région Nouvelle Aquitaine. NG and HI were supported by ANR Episwitch 2016.

REFERENCES

1. Lieber MR. Mechanisms of human lymphoid chromosomal translocations. *Nat Rev Cancer.* (2016) 16:387–98. doi: 10.1038/nrc.2016.40
2. Pinaud E, Marquet M, Fiancette R, Peron S, Vincent-Fabert C, Denizot Y, et al. The IgH locus 3' regulatory region: pulling the strings from behind. *Adv Immunol.* (2011) 110:27–70. doi: 10.1016/B978-0-12-387663-8.00002-8
3. Kuzyk A, Mai S. C-MYC induced genomic instability. *Cold Spring Harb Perspect Med.* (2014) 4:a014373. doi: 10.1101/cshperspect.a014373
4. Alt FW, Rosenberg N, Casanova RJ, Thomas E, Baltimore D. Immunoglobulin heavy-chain expression and class switching in a murine leukaemia cell line. *Nature.* (1982) 296:325–331. doi: 10.1038/296325a0
5. Gillies SD, Morrison SL, Oi VT, Tonegawa S. A tissue-specific transcription. enhancer element is located in the major

intron of a rearranged immunoglobulin heavy chain gene. *Cell.* (1983) 33:717–28. doi: 10.1016/0092-8674(83)90014-4
6. Banerji J, Olson L, Schaffner W. A lymphocyte-specific cellular enhancer is located downstream of the joining region in immunoglobulin heavy chain genes. *Cell.* (1983) 33:729–40. doi: 10.1016/0092-8674(83)90015-6
7. Perlot T, Alt FW, Bassing CH, Heikyung S, Pinaud E. Elucidation of IgH intronic enhancer functions via germ-line deletion. *Proc Natl Acad Sci USA.* (2005) 102:14362–7. doi: 10.1073/pnas.0507090102
8. Marquet M, Garot A, Bender S, Carrion C, Rouaud P, Lecardeur S, et al. The Eμ enhancer region influences H chain expression and B cell fate without impacting IgVH repertoire and immune response *in vivo*. *J Immunol.* (2014) 193:1171–83. doi: 10.4049/jimmunol.1302868
9. Saintamand A, Rouaud P, Garot A, Carrion C, Oblet C, Cogné M, et al. The IgH 3' regulatory region governs μ chain transcription in mature B lymphocytes and the B cell fate. *Oncotarget.* (2015) 6:4845–52. doi: 10.18632/oncotarget.3010
10. Issaoui H, Ghazzaui N, Ferrad M, Boyer F, Denizo Y. Class switch recombination junctions are not affected by the absence of the immunoglobulin heavy chain E_{μ} enhancer. *Cell Mol Immunol.* (2019) 16:671–3. doi: 10.1038/s41423-019-0229-x
11. Adams JM, Harris AW, Pinkert CA, Corcoran LM, Alexander W, Cory S, et al. The c-myc oncogene driven by immunoglobulin enhancers induces lymphoid malignancy in transgenic mice. *Nature.* (1985) 318:533–8. doi: 10.1038/318533a0
12. Hussain S, Bedekovics T, Liu Q, Hu W, Jeon H, Johnson H, et al. UCH-L1 bypasses mTOR to promote protein biosynthesis and is required for MYC-driven lymphomagenesis in mice. *Blood.* (2018) 132:2564–74. doi: 10.1182/blood-2018-05-848515
13. Hussain S, Foreman O, Perkins SL, Witzig TE, Miles RR, van Deursen J, et al. The de-ubiquitinase UCH-L1 is an oncogene that drives the development of lymphoma *in vivo* by deregulating PHLPP1 and Akt signaling. *Leukemia.* (2010) 24:1641–55. doi: 10.1038/leu.2010.138
14. Gramling MW, Eischen CM. Suppression of Ras/Mapk pathway signaling inhibits Myc-induced lymphomagenesis. *Cell Death Differ.* (2012) 19:1220–7. doi: 10.1038/cdd.2012.1
15. Nemajerova A, Petrenko O, Trümper L, Palacios G, Moll UM. Loss of p73 promotes dissemination of Myc-induced B cell lymphomas in mice. *J Clin Invest.* (2010) 120:2070–80. doi: 10.1172/JCI40331
16. Odvody J, Vincent T, Arrate M, Pgrieb B, Wang S, Garriga J, et al. A deficiency in Mdm2 binding protein inhibits Myc-induced B-cell proliferation and lymphomagenesis. *Oncogene.* (2010) 29:3287–96. doi: 10.1038/onc.2010.82
17. Chen J, Shin JH, Zhao R, Phan L, Wang H, Xue Y, et al. CSN6 drives carcinogenesis by positively regulating Myc stability. *Nat Commun.* (2014) 5:5384. doi: 10.1038/ncomms6384
18. Wong DM, Li L, Jurado S, King A, Bamford R, Wall M, et al. The transcription factor ASCIZ and its target DYNLL1 are essential for the development and expansion of MYC-driven B cell lymphoma. *Cell Rep.* (2016) 14:1488–99. doi: 10.1016/j.celrep.2016.01.012
19. Kadariya Y, Tang B, Wang L, Al-Saleem T, Hayakawa K, Slifker MJ, et al. Germline mutations in *Mtap* cooperate with *Myc* to accelerate tumorigenesis in mice. *PLoS ONE.* (2013) 8:e67635. doi: 10.1371/journal.pone.0067635
20. Leong HS, Kelan C, Hilton DJ, Blewitt ME, Yifang HU, Lee S, et al. Epigenetic regulator Smchd1 functions as a tumor suppressor. *Cancer Res.* (2012) 73:1591–9. doi: 10.1158/0008-5472.CAN-12-3019
21. Lu Y, Wu Y, Feng X, Shen R, Wang JH, Fallahi M, et al. CDK4 deficiency promotes genomic instability and enhances Myc-driven lymphomagenesis. *J Clin Invest.* (2014) 124:1672–84. doi: 10.1172/JCI63139
22. Vandenberg CJ, Motoyama N, Cory S. FoxO3 suppresses Myc driven lymphomagenesis. *Cell Death Dis.* (2016) 7:e2046. doi: 10.1038/cddis.2015.396
23. Olive V, Sabio E, Bennett MJ, De Jong CS, Biton A, McGann JC, et al. A component of the mir-17-92 polycistronic oncomir promotes oncogene-dependent apoptosis. *Elife.* (2013) 2:e00822. doi: 10.7554/eLife.00822
24. Chu B, Kon N, Chen D, Li T, Liu T, Jiang L, et al. ALOX12 is required for p53-mediated tumour suppression through a distinct ferroptosis pathway. *Nat Cell Biol.* (2019) 21:579–91. doi: 10.1038/s41556-019-0305-6
25. Takahashi Y, Young MM, Serfass JM, Hori T, Wang HG. Sh3glb1/Bif-1 and mitophagy. *Autophagy.* (2013) 9:1107–9. doi: 10.4161/auto.24817
26. Tuzlak S, Haschka MD, Mokina AM, Rülicke T, Cory S, Labi V, et al. Differential effects of Vav-promoter-driven overexpression of BCLX and BFL1 on lymphocyte survival and B cell lymphomagenesis. *FEBS J.* (2018) 285:1403–18. doi: 10.1111/febs.14426
27. Sochalska M, Schuler F, Weiss JG, Prchal-Murphy M, Sexl V, Villunger A. MYC selects against reduced BCL2A1/A1 protein expression during B-cell lymphomagenesis. *Oncogene.* (2017) 36:2066–73. doi: 10.1038/onc.2016.362
28. Nguyen HV, Vandenberg CJ, Ng AP, Robati MR, Anstee NS, Rimes J, et al. Development and survival of MYC-driven lymphomas require the Myc antagonist MNT to curb MYC-induced apoptosis. *Blood.* (2020) 135:1019–31. doi: 10.1182/blood.2019003014
29. Vecchio E, Fiume G, Mignogna C, Iaccino E, Mimmi S, Maisano D, et al. IBTK haploinsufficiency affects the tumor microenvironment of Myc-driven lymphoma in E-myc mice. *Int J Mol Sci.* (2020) 21:885. doi: 10.3390/ijms21030885
30. Rehm A, Mensen A, Schradi K, Gerlach K, Wittstock S, Winter S, et al. Cooperative function of CCR7 and lymphotoxin in the formation of a lymphoma-permissive niche within murine secondary lymphoid organs. *Blood.* (2011) 118:1020–33. doi: 10.1182/blood-2010-11-321265
31. Cao Z, Ding BS, Guo P, Lee SB, Butler JM, Casey C, et al. Angiocrine factors deployed by tumor vascular niche induce B cell lymphoma invasiveness and chemotresistance. *Cancer Cell.* (2014) 25:350–65. doi: 10.1016/j.ccr.2014.02.005
32. Reimann M, Lee S, Loddenkemper C, Dorr JR, Tabor V, Aichele P, et al. Tumor stroma-derived TGF-b limits myc-driven lymphomagenesis via Suv39h1-dependent senescence. *Cancer Cell.* (2010) 17:262–72. doi: 10.1016/j.ccr.2009.12.043
33. Sauer M, Schuldner M, Hoffmann N, Cetintas A, Reiners KS, Shatnyeva O, et al. CBP/p300 acetyltransferases regulate the expression of NKG2D ligands on tumor cells. *Oncogene.* (2017) 36:933–41. doi: 10.1038/onc.2016.259
34. Rehm A, Gätjen M, Gerlach K, Scholz F, Mensen A, Gloger M, et al. Dendritic cell-mediated survival signals in Eμ-Myc B-cell lymphoma depend on the transcription factor C/EBPμ. *Nat Comm.* (2014) 5:5057. doi: 10.1038/ncomms6057
35. Lasorsa E, Smonksey M, Kirk JS, Rosario S, Hernandez-Ilizaliturri FJ, Ellis L, et al. Mitochondrial protection impairs BET bromodomain inhibitor-mediated cell death and provides rationale for combination therapeutic strategies. *Cell Death Dis.* (2015) 6:e2014. doi: 10.1038/cddis.2015.352
36. Hogg SJ, Newbold A, Vervoort SJ, Cluse LA, Martin BP, Gregory P, et al. BET inhibition induces apoptosis in aggressive B-cell lymphoma via epigenetic regulation of BCL-2 family members. *Mol Cancer Ther.* (2016) 15:2030–41. doi: 10.1158/1535-7163.MCT-15-0924
37. Lin CJ, Robert F, Sukarieh R, Michnick S, Pelletier J. The antidepressant sertraline inhibits translation initiation by curtailing mammalian target of rapamycin signaling. *Cancer Res.* (2010) 70:3199–208. doi: 10.1158/0008-5472.CAN-09-4072
38. Rava M, D'Andrea A, Nicoli P, Gritti I, Donati G, Doni M, et al. Therapeutic synergy between tigecycline and venetoclax in a preclinical model of Myc/BCL2 double-hit B cell lymphoma. *Sci Transl Med.* (2018) 10:eaan8723. doi: 10.1126/scitranslmed.aan8723
39. Ross J, Rashkovan M, Fraszczak J, Beauparlant CJ, Vadnais C, Winkler R, et al. C and B-ALL/lymphoma mouse models. *Cancer Res*. 79:4184–95. doi: 10.1158/0008-5472.CAN-18-3038
40. Reiff SD, Mantel R, Smith LL, Greene JT, Muhowski EM, Fabian A, et al. The BTK inhibitor ARQ531 targets ibrutinib-resistant CLL and richter transformation. *Cancer Discov.* (2018) 8:1300–15. doi: 10.1158/2159-8290.CD-17-1409
41. Wall M, Poortinga G, Stanley KL, Lindemann RK, Bots M, Chan J, et al. The mTORC1 inhibitor everolimus prevents and treats em-Myc lymphoma by restoring oncogene-induced senescence. *Cancer Discov.* (2013) 3:82–95. doi: 10.1158/2159-8290.CD-12-0404
42. Rodrigo M, Cencic R, Roche SP, Pelletier J, Porco JA Jr. Synthesis of rocaglamide hydroxamates and related compounds as eukaryotic translation inhibitors: synthetic and biological studies. *J Med Chem*. (2012) 55:558–62. doi: 10.1021/jm201263k
43. Mattarollo SR, West AC, Steegh K, Duret H, Paget C, Martin B, et al. NKT cell adjuvant-based tumor vaccine for treatment

of myc oncogene-driven mouse B-cell lymphoma. *Blood.* (2012) 120:3019–29. doi: 10.1182/blood-2012-04-426643
44. Kobayashi T, Doff BL, Rearden RC, Leggatt GR, Mattarollo SR. NKT cell-targeted vaccination plus anti-4-1BB antibody generates persistent CD8 T cell immunity against B cell lymphoma. *OncoImmunology.* (2015) 4:e990793. doi: 10.4161/2162402X.2014.990793
45. Croxford JL, Tang ML, Pan MF, Huang CW, Kamran N, Phua M, et al. ATM-dependent spontaneous regression of early Eμ-myc-induced murine B-cell leukemia depends on natural killer and T cells. *Blood.* (2013) 121:2512–21. doi: 10.1182/blood-2012-08-449025
46. Westwood JA, Matthews GM, Shortt J, Faulkner D, Pegram HJ, Duong P, et al. Combination anti-CD137 and anti-CD40 antibody therapy in murine myc-driven hematological cancers. *Leukemia Res.* (2014) 38:948–54. doi: 10.1016/j.leukres.2014.05.010
47. Johnston HE, Carter MJ, Cox KL, Dunscombe M, Manousopoulou A, Townsend A, et al. Integrated cellular and plasma proteomics of contrasting B-cell cancers reveals common unique and systemic signatures. *Mol Cell Proteomics.* (2017) 16:386–406. doi: 10.1074/mcp.M116.063511
48. Rempel RE, Jiang X, Fullerton P, Tan TZ, Ye J, Lau A, et al. Utilization of the Eμ-Myc mouse to model heterogeneity of therapeutic response. *Mol Cancer Ther.* (2014) 13:3219–29. doi: 10.1158/1535-7163.MCT-13-0044
49. Guglielmi L, Truffinet V, Carrion C, Le Bert M, Cogné N, Cogné M, et al. The 5'HS4 insulator element is an efficient tool to analyse the transient expression of an Eμ-GFP vector in a transgenic mouse model. *Trans Res.* (2005) 14:361–4. doi: 10.1007/s11248-005-3239-7
50. Ghazzaui N, Issaoui H, Boyer F, Martin OA, Saintamand A, Denizot Y. 3'RR and 5'Eμ immunoglobulin heavy chain enhancers are independent engines of locus remodeling. *Cell Mol Immunol.* (2019) 16:198–200. doi: 10.1038/s41423-018-0171-3
51. Saintamand A, Vincent-Fabert C, Garot A, Rouaud P, Oruc Z, Magnone V, et al. Deciphering the importance of the palindromic architecture of the immunoglobulin heavy chain 3' regulatory region. *Nat Commun.* (2016) 7:10730. doi: 10.1038/ncomms10730
52. Vincent-Fabert C, Fiancette R, Pinaud E, Truffinet V, Cogné N, Cogné M, et al. Genomic deletion of the whole IgH 3' regulatory region (hs3a, hs1,2, hs3b, hs4) dramatically affects class switch recombination and Ig secretion to all isotypes. *Blood.* (2010) 116:1895–98. doi: 10.1182/blood-2010-01-264689
53. Saintamand A, Rouaud P, Saad F, Rios G, Cogné M, Denizot Y. Elucidation of IgH 3' region regulatory role during class switch recombination via germline deletion. *Nat Commun.* (2015) 6:7084. doi: 10.1038/ncomms8084
54. Rouaud P, Vincent-Fabert C, Saintamand A, Fiancette R, Marquet M, Robert I, et al. The IgH 3' regulatory region controls AID-induced somatic hypermutation in germinal centre B-cells in mice. *J Exp Med.* (2013) 210:1501–7. doi: 10.1084/jem.20130072
55. Guglielmi L, Le Bert M, Truffinet V, Cogné M, Denizot Y. Insulators to improve expression of a 3'IgH LCR-driven reporter gene in transgenic mouse models. *Biochem Biophys Res Commun.* (2003) 307:466–71. doi: 10.1016/S0006-291X(03)01185-9
56. Madisen L, Groudine M. Identification of a locus control region in the immunoglobulin heavy-chain locus that deregulates C-Myc expression in plasmacytoma and Burkitt's lymphoma cells. *Genes Dev.* (1994) 8:2212–26. doi: 10.1101/gad.8.18.2212
57. Gostissa M, Yan CT, Bianco JM, Cogné M, Pinaud E, Alt FW. Long-range oncogenic activation of Igh-c-myc translocations by the Igh 3' regulatory region. *Nature.* (2009) 462:803–8. doi: 10.1038/nature08633
58. Kovalchuk AL, Sakai T, Qi CF, Du Bois W, Dunnick WA, Congé M, et al. (2018) 3'Igh enhancers hs3b/hs4 are dispensable for Myc deregulation in mouse plasmacytomas with T(12;15) translocations. *Oncotarget.* 9:34528–42. doi: 10.18632/oncotarget.26160
59. Wang J, Boxer LM. Regulatory elements in the immunoglobulin heavy chain gene 3'-enhancers induce c-myc deregulation and lymphomagenesis in murine B cells. *J Biol Chem.* (2006) 280:12766–73. doi: 10.1074/jbc.M412446200
60. Truffinet V, Pinaud E, Cogné N, Petit B, Guglielmi L, Cogné M, et al. The 3' IgH locus control region is sufficient to deregulate a c-myc transgene and promote mature B cell malignancies with a predominant Burkitt-like phenotype. *J Immunol.* (2007) 179:6033–42. doi: 10.4049/jimmunol.179.9.6033
61. Fiancette R, Rouaud P, Vincent-Fabert C, Laffleur B, Magnone V, Cogné M, et al. A p53 defect sensitizes various stages of B cell development to lymphomagenesis in mice carrying an IgH 3' regulatory region-driven c-myc transgene. *J Immunol.* (2011) 187:5772–82. doi: 10.4049/jimmunol.1102059
62. Vincent-Fabert C, Fiancette R, Rouaud P, Baudet C, Truffinet V, Magnone V, et al. A defect of the INK4-Cdk4 checkpoint and c-myc collaborate in blastoid mantle cell lymphoma (MCL)-like lymphoma formation in mice. *Am J Pathol.* (2012) 180:1688–701. doi: 10.1016/j.ajpath.2012.01.004
63. Rouaud P, Fiancette R, Vincent-Fabert C, Magnone V, Cogné M, Dubus P, et al. Mantle cell lymphoma-like lymphomas in c-myc-3'RR/p53+/- mice and c-myc-3'RR/Cdk4R24C mice: differential oncogenic mechanisms but similar cellular origin. *Oncotarget.* (2012) 3:586–93. doi: 10.18632/oncotarget.474
64. Amin R, Marfak A, Pangault C, Oblet C, Chanut A, Tarte K, et al. The class-specific BCR tonic signal modulates lymphomagenesis in a c-myc deregulation transgenic model. *Oncotarget.* (2014) 15:8995–9006. doi: 10.18632/oncotarget.2297
65. Vincent-Fabert C, Fiancette R, Truffinet V, Cogné N, Cogné M, Denizot Y. Genetic background modulates susceptibility to oncogen-driven proliferation and lymphoma occurrence in mice carrying a deregulated c-myc transgene. *Leuk Res.* (2009) 33:e203–6. doi: 10.1016/j.leukres.2009.05.018
66. Park SS, Kim JS, Tessarollo L, Owens JD, Peng L, Su Han S, et al. Insertion of c-Myc into Igh induces B-cell and plasma-cell neoplasms in mice. *Cancer Res.* (2005) 65:1306–15. doi: 10.1158/0008-5472.CAN-04-0268
67. Han SS, Yun H, Son DJ, Tompkins VS, Peng L, Chung T, et al. NF-kappaB/STAT3/PI3K signaling crosstalk in iMyc E mu B lymphoma. *Mol Cancer.* (2010) 9:97. doi: 10.1186/1476-4598-9-97
68. Park SS, Shaffer AL, Kim JS, Dubois W, Potter M, Staudt M, et al. Insertion of Myc into Igh accelerates peritoneal plasmacytomas in mice. *Cancer Res.* (2005) 65:7644–52. doi: 10.1158/0008-5472.CAN-05-1222
69. Cheung WC, Kim JS, Linden M, Peng L, Van Ness B. Novel targeted deregulation of c-myc cooperates with Bcl-XL to cause plasma cell neoplasms in mice. *J Clin Invest.* (2004) 113:1763–73. doi: 10.1172/JCI200420369
70. Rosean TR, Holman CJ, Tompkins VS, Jing X, Krasowski MD, Rose-John S, et al. KSHV-encoded vIL6 collaborates with deregulated c-MYC to drive plasmablastic neoplasm in mice. *Blood Cancer J.* (2016) 6:e398. doi: 10.1038/bcj.2016.6
71. Ghazzaui N, Issaoui H, Ferrad M, Carrion C, Cook-Moreau J, Denizot Y, et al. Eμ and 3'RR transcriptional enhancers of the IgH locus cooperate to promote c-myc-induced mature B-cell lymphomas. *Blood Adv.* (2020) 4:28–39. doi: 10.1182/bloodadvances.2019000845
72. Volpi SA, Verma-Gaur J, Hassan R, Ju Z, Roa S, Chatterjee S, et al. Germline deletion of Igh 3′ regulatory region elements hs 5, 6, 7 (hs5–7) affects B cell-specific regulation, rearrangement, and insulation of the Igh locus. *J Immunol.* (2012) 188: 2556–66. doi: 10.4049/jimmunol.1102763
73. Birshtein BK. Epigenetic regulation of individual modules of the immunoglobulin heavy chain locus 3' regulatory region. *Front Immunol.* (2014) 5:163. doi: 10.3389/fimmu.2014.00163
74. D'addabbo P, Scascitelli M, Giambra V, Rocchi M, Frezza D. Position and sequence conservation in amniota of polymorphic enhancer HS1,2 within the palindrome of IgH 3' regulatory region. *BMC Evol Biol.* (2011) 11:71. doi: 10.1186/1471-2148-11-71
75. Saintamand A, Garot A, Saad F, Moulinas R, Denizot Y. Pre-germinal center origin for mature mouse B cell lymphomas: a major discrepancy with human mature lymphomas. *Cell Cycle.* (2015) 14:3656–8. doi: 10.1080/15384101.2015.1093708
76. Duan H, Xiang H, Ma L, Boxer LM. Functionals long-range interactions of the IgH 3' enhancers with the bcl-2 promoter region in t(14;18) lymphoma cells. *Oncogene.* (2008) 27:6720–8. doi: 10.1038/onc.2008.286

77. Kovalchuk AL, Qi CF, Torrey TA, Taddesse-Heath L, Feigenbaum L, Park SS, et al. Burkitt lymphoma in the mouse. *J Exp Med.* (2000) 192:1183–90. doi: 10.1084/jem.192.8.1183

Conflict of Interest: The authors declare that the research was conducted in the absence of any commercial or financial relationships that could be construed as a potential conflict of interest.

frontiers in Immunology

ORIGINAL RESEARCH
published: 01 December 2020
doi: 10.3389/fimmu.2020.602868

B-Cell-Specific Myd88 L252P Expression Causes a Premalignant Gammopathy Resembling IgM MGUS

Kristin Schmidt[1], Ulrike Sack[1†], Robin Graf[1], Wiebke Winkler[2], Oliver Popp[3], Philipp Mertins[3], Thomas Sommermann[1], Christine Kocks[1,4] and Klaus Rajewsky[1]*

[1] Immune Regulation and Cancer, Max Delbrück Center for Molecular Medicine in the Helmholtz Association, Berlin, Germany, [2] Biology of Malignant Lymphomas, Max Delbrück Center for Molecular Medicine in the Helmholtz Association, Berlin, Germany, [3] Proteomics, Max Delbrück Center for Molecular Medicine in the Helmholtz Association, Berlin, Germany, [4] Transgenics, Max Delbrück Center for Molecular Medicine in the Helmholtz Association, Berlin, Germany

A highly recurrent somatic L265P mutation in the TIR domain of the signaling adapter MYD88 constitutively activates NF-κB. It occurs in nearly all human patients with Waldenström's macroglobulinemia (WM), a B cell malignancy caused by IgM-expressing cells. Here, we introduced an inducible leucine to proline point mutation into the mouse Myd88 locus, at the orthologous position L252P. When the mutation was introduced early during B cell development, B cells developed normally. However, IgM-expressing plasma cells accumulated with age in spleen and bone, leading to more than 20-fold elevated serum IgM titers. When introduced into germinal center B cells in the context of an immunization, the Myd88^{L252P} mutation caused prolonged persistence of antigen-specific serum IgM and elevated numbers of antigen-specific IgM plasma cells. Myd88^{L252P}-expressing B cells switched normally, but plasma cells expressing other immunoglobulin isotypes did not increase in numbers, implying that IgM expression may be required for the observed cellular expansion. In order to test whether the Myd88^{L252P} mutation can cause clonal expansions, we introduced it into a small fraction of CD19-positive B cells. In this scenario, five out of five mice developed monoclonal IgM serum paraproteins accompanied by an expansion of clonally related plasma cells that expressed mostly hypermutated VDJ regions. Taken together, our data suggest that the Myd88^{L252P} mutation is sufficient to promote aberrant survival and expansion of IgM-expressing plasma cells which in turn can cause IgM monoclonal gammopathy of undetermined significance (MGUS), the premalignant condition that precedes WM.

Keywords: monoclonal gammopathy of unknown significance, IgM MGUS, MYD88 L265P mutation, Waldenström's macroglobulinemia, B cell abnormalities, B cell lymphoma, lymphomagenesis, IgM paraprotein

OPEN ACCESS

Edited by:
Juan M. Zapata, Instituto de Investigaciones Biomédicas Alberto Sols (CSIC), Spain

Reviewed by:
Siegfried Janz, Medical College of Wisconsin, United States
Gina Doody, University of Leeds, United Kingdom

****Correspondence:***
Klaus Rajewsky
klaus.rajewsky@mdc-berlin.de

†Present address:
Ulrike Sack, Bayer Pharma AG, Berlin, Germany

Specialty section:
This article was submitted to B Cell Biology, a section of the journal Frontiers in Immunology

Received: *04 September 2020*
Accepted: *19 October 2020*
Published: *01 December 2020*

Citation:
Schmidt K, Sack U, Graf R, Winkler W, Popp O, Mertins P, Sommermann T, Kocks C and Rajewsky K (2020) B-Cell-Specific Myd88 L252P Expression Causes a Premalignant Gammopathy Resembling IgM MGUS. Front. Immunol. 11:602868. doi: 10.3389/fimmu.2020.602868

INTRODUCTION

Waldenström's macroglobulinemia (WM) is an incurable low-grade lymphoplasmacytic lymphoma, characterized by bone marrow (BM) infiltration of small, IgM-positive lymphocytes with varying degrees of plasmacytoid or plasma cell differentiation and the presence of monoclonal immunoglobulin M (IgM) paraproteins (M-spikes) in the serum (1–5). The great majority of

malignant WM cells are monoclonal and carry somatically mutated antibody V region rearrangements, suggesting that transformation occurs at a mature, antigen-experienced B cell stage (6–11).

More than 90% of WM patients harbor a T794C gain-of-function mutation in the myeloid differentiation primary response gene 88 (MYD88), which results in an L265P amino acid substitution in the MYD88 TIR domain (12), promoting an increased propensity for Myd88 oligomerization (13). MYD88 is the canonical adaptor protein for inflammatory signaling pathways downstream of various toll-like receptor (TLR) and interleukin (IL)-1 receptor family members (14). First described in activated B-cell (ABC)-like subtype of diffuse large B-cell lymphoma (DLBCL) [where it occurs in 21% of patients (15)], the $MYD88^{L265P}$ mutation constitutively activates NF-κB and JAK kinase signaling through TLR9, IRAK1 and IRAK4 (16, 17), and independently through BTK (18), conferring a pro-survival advantage to mutated B cells. In line with these findings, an earlier attempt to model the $Myd88^{L265P}$ mutation in mice *in vivo* produced fulminant B lymphoproliferative disease and occasional ABC-DLBCL-type lymphoma (19), while a more recent study reported low-grade lymphoproliferative disease with certain pathological features of WM (20). However, in both mouse models the observed lymphoproliferation was polyclonal.

WM is diagnosed late in life at a median age of 73 years in Caucasians (21). Symptomatic WM is preceded by prolonged asymptomatic phases classified as smoldering (or asymptomatic) WM and IgM monoclonal gammopathy of unknown significance (MGUS) (22–26). With increasingly sensitive methods $Myd88^{L265P}$ mutation could be detected in up to 87% of IgM MGUS patients, suggesting that it is an early event in WM pathogenesis (27–33). A second somatic, highly recurrent genetic event in WM consists of activating C-terminal mutations in the CXCR4 gene, which appear to enhance tumor cell dissemination and survival (34–37) and mostly occur in the context of a mutated Myd88 allele (36, 38, 39). CXCR4 mutations are less frequent (25–40% of WM patients) and probably acquired later during disease progression (36, 38–41).

Consistent with such a scenario, we here present evidence that targeting endogenous expression of the dominant $Myd88^{L265P}$ mutation to a small number of cells in the mouse B cell compartment (at the orthologous position L252P in mouse Myd88) is—by itself—sufficient to cause IgM MGUS, the premalignant condition which precedes WM.

MATERIAL AND METHODS

Gene Targeting

The gene targeting strategy was based on the NCBI mouse transcript *NM_010851.2*, where wildtype exons 5 and 6 were flanked with *loxP* sites (4.3kb region). Exons 5 and 6 were duplicated and inserted downstream of the distal *loxP* site followed by an IRES-GFP reporter. The L252P mutation was introduced into the duplicated Exon 5 and a Neo^R marker (flanked by *frt* sites) inserted between wildtype Exon 6 and mutated Exon 5. The targeting vector was generated by amplifying the genomic region of Myd88 using BAC clones from the *C57BL/6J* RPCIB-731 BAC library and subsequent introduction of the point mutation. The linearized targeting vector was co-transfected with sgRNA and a Cas-9-expression vector into the Artemis B6/3 C57BL/6 ES cell line. Targeted clones were isolated using positive (Neo^R) selection and correct integration was verified by Southern blotting. The conditional $Myd88^{L252P}$ allele was obtained in a germline-transmitting transgenic animal after *in vivo* Flp-mediated removal of the selection markers.

Cell Culture of B Cells *Ex Vivo*

Splenic B cells were enriched by depletion of $CD43^+$ cells with magnetic anti-mouse-CD43 microbeads (Miltenyi Biotech Cat# 130-049-801, RRID: AB_2861373), transduced with in-house generated TAT-Cre recombinase (42, 43), cultured in the absence or presence of LPS (20 μg/ml, *Escherichia coli* 055:B5; Sigma Cat# L2880) or $F(ab')_2$ fragment anti-IgM (1.2 μg/ml; Jackson ImmunoResearch Labs Cat# 115-006-020; RRID: AB_2338469) and 1 μM BrdU or cultured with LPS plus recombinant mouse IL-4 (10–20 units/ml; Peprotech Cat# 214-14).

Flow Cytometry, Cell Sorting, and Detection of *In Vivo* Proliferation

Red blood cells were lysed with Gey's solution and single-cell suspensions (in PBS pH7.2 supplemented with 1% FCS and 1 mM EDTA) from spleen or femur-derived bone marrow were stained with antibody conjugates (**Supplementary Table 1**) and analyzed using FlowJo software (BD FlowJo, RRID : SCR_008520) on an LSRFortessa (BD Biosciences) or sorted on a FACSAria (BD Biosciences). NIP-BSA-APC: 4-Hydroxy-3-iodo-5-nitrophenylacetyl hapten (NIP) conjugated to Bovine Serum Albumin (BSA) was generated in-house from BSA fraction V (Roth Cat# 8076.3) and NIP-OSu (Biosearch Technologies Cat# N-1080-100) and then labeled with Allophycocyanin (APC) using the Allophycocyanin labeling kit-SH (Dojindo Cat# LK24). For 5-Bromo-2'-deoxyuridine (BrdU) labeling, we used BrdU Kits (BD Biosciences Cat# 552598, RRID: AB_2861367). Mice were injected intraperitoneally with 2 mg BrdU and analyzed by flow cytometry.

Laboratory Mice and Immunizations

Cγ1-Cre (44), *R26StopFLeYFP* (45), CD19-Cre (46), and CD19-Cre^{ERT2} alleles (47) have been described. Mice were bred and maintained under specific pathogen-free conditions. Unless specifically indicated (**Supplementary Figures 1B, C**), mice used in this study were heterozygous for the Cre and $Myd88^{L252P}$ alleles (designated Cre;$Myd88^{L252P}$). To activate Cre^{ERT2}, four mg of tamoxifen (Sigma Cat# T5648), dissolved in sunflower oil (Sigma Cat# S5007), was fed by oral gavage (47). Eight to 12 weeks old mice were immunized intraperitoneally with 100 μg alum-precipitated 4-Hydroxy-3-nitrophenylacetyl

hapten conjugated to Chicken Gamma Globulin (NP-CGG, Ratio 10-19) (LGC Biosearch Technologies Cat# N-5055B-5) followed by secondary immunization intravenously with 100 µg soluble NP-CGG.

Immunohistochemistry

Tissues were embedded in Tissue-Tek O.C.T. Compound (Sakura Cat# 4583), stored at -80°C and cryosectioned (7 µm thickness). Sections were fixed in 100% acetone and stained with DAPI (eBioScience Cat# D1306), and the antibody conjugates and reagents listed in **Supplementary Table 1**.

Enzyme-Linked Immuno Assays, Serum Protein Electrophoresis, and Immunofixation

Enzyme-linked immunosorbent assays (ELISAs) were done as described (48) with addition of 0.05% Tween 20 in block and wash buffers. 4-Hydroxy-3-nitrophenylacetyl hapten (NP) conjugated to BSA (NP-BSA, Ratio 28) was generated in-house with BSA fraction V (Roth Cat# 8076.3) and NP-OSu (Biosearch Technologies Cat# N1010-100). Plates were coated with 2 µg/ml NP-BSA or 1 µg/ml anti-light chain antibodies and developed with 1 µg/ml anti-isotype antibodies and the standards listed in **Supplementary Table 1**. For enzyme-linked immuno spot (ELISPOT) assays MultiScreen$_{HTS}$ IP Filter Plates (Merck Cat# MSIPS4510) were coated and developed as described above for the ELISA plates, incubated with cells overnight, washed with 0.1% Tween 20 and processed according to the manufacturer's instructions. For serum protein electrophoresis or immunofixation 10 µl serum was run on buffered agarose gels, pH8.6 Hydragel PROTEIN(E) (Sebia Cat# PN4100) or pH9.2 DOUBLE IF K20 (Sebia Cat# PN3036), and processed according to the manufacturer's instructions. For proteomics, serum samples were run on multiple lanes of pH8.6 agarose gels and stained with InstantBlue Ultrafast Protein Stain (Sigma Cat# ISB1L). Excised bands were processed and analyzed by tandem mass spectrometry as described below.

Sequence Analysis of IgH V Gene Rearrangements

IgH V gene rearrangements were PCR-amplified (40 cycles) from genomic DNA (isolated from sorted, GFP-reporter-positive TACI^{+}CD138^{+} plasma cells) using the Expand High Fidelity PCR System (Roche Cat# 03310256103) with a forward primer for J558/VH1 family genes [pos. 37–57 (IMTG) ARG CCT GGG RCT TCA GTG AAG] and a reverse primer for the IgH intronic enhancer (CTCCACCAGACCTCTCTAGACAGC). A 0.9 kb fragment corresponding to JH4 rearrangements was gel-purified, cloned (Zero Blunt TOPO PCR Cloning Kit, Invitrogen Cat# 450031) and subclones sequenced on one strand. VDJ sequences were aligned with IgBLAST (49) software (IgBLAST, RRID : SCR_002873) against V, D, J genes in the IMGT (50) database (IMGT—the international ImMunoGeneTics information system, RRID : SCR_012780) and analysed for clonality (identical or related CDR3) and somatic mutations. The mixed *C57BL/6* and *129* background of the Cγ1-Cre allele (44) was taken into account.

Ig Isotype Quantification by Tandem Mass Spectrometry

Excised gel pieces were subjected to tryptic in-gel digest (51) followed by purification on C18 stage-tips (52). Samples were measured on a Q Exactive HF-x orbitrap mass spectrometer (ThermoFisher Scientific) connected to an EASY-nLC system (ThermoFisher Scientific). HPLC-separation occurred on an in-house prepared nano-LC column (0.074 × 250 mm, 3 µm Reprosil C18, Dr. Maisch GmbH) using a flow rate of 250 nl/min on a 45 min gradient with an acetonitrile concentration ramp from 4.7 to 46.5% (v/v) in 0.1% (v/v) formic acid. MS acquisition was performed at a resolution of 60,000 in the scan range from 350 to 1,800 m/z. MS2 scans were carried out at a resolution of 15,000 with the isolation window of 1.3 m/z and a maximum injection time of 100 ms. Dynamic exclusion was set to 20 s and the normalized collision energy was specified to 26.

For analysis, the MaxQuant software package (RRID : SCR_014485) version 1.6.3.4 was used (53, 54). An FDR of 0.01 was applied for peptides and proteins, and the andromeda search was performed using Uniprot (Universal Protein Resource, RRID : SCR_002380) (mouse database release July 2018, including isoforms). For protein identification a minimum of one unique peptide was required. Further analysis was done using R (R Project for Statistical Computing, RRID : SCR_001905). Proteins of non-mouse origin were considered contaminants and filtered out. All protein groups belonging to one immunoglobulin isotype were collapsed into one group by summing their individual intensities and were compared against the total intensity per sample.

Statistical Analysis

Prism software (GraphPad Prism, RRID : SCR_002798) version 7 was used for pair-wise comparisons between mutant and control samples using non-parametric, unpaired, two-tailed Mann-Whitney U tests. Asterisks indicate statistical significance for p-values ≤0.05 (single), ≤0.01 (double), ≤0.001 (triple), ≤0.0001 (quadruple). Data are represented as individual points or means (bar graphs or horizontal lines) and error bars represent SD.

RESULTS

Myd88^{L252P} Leads to NF-κB Activation and Short-Term Proliferation of Primary B Cells *Ex Vivo*

In order to investigate and track the consequences of the human MYD88^{L265P} mutation in mouse B cells, we generated a conditional Myd88 allele which expresses the mutation at the orthologous position L252P (as well as GFP) upon Cre-mediated recombination from the endogenous mouse Myd88 locus (**Figure 1A** and **Supplementary Figures 1A–D**). Endogenous Myd88^{L252P} expression induced a transient expansion of transgenic B cells in the absence or presence of added mitogens (**Supplementary Figure 1E**) consistent with the effect of retroviral overexpression of Myd88^{L252P} in mouse B cells *ex vivo* as previously reported (55). Myd88^{L252P} caused this effect at least partially by enhancing proliferation (**Supplementary**

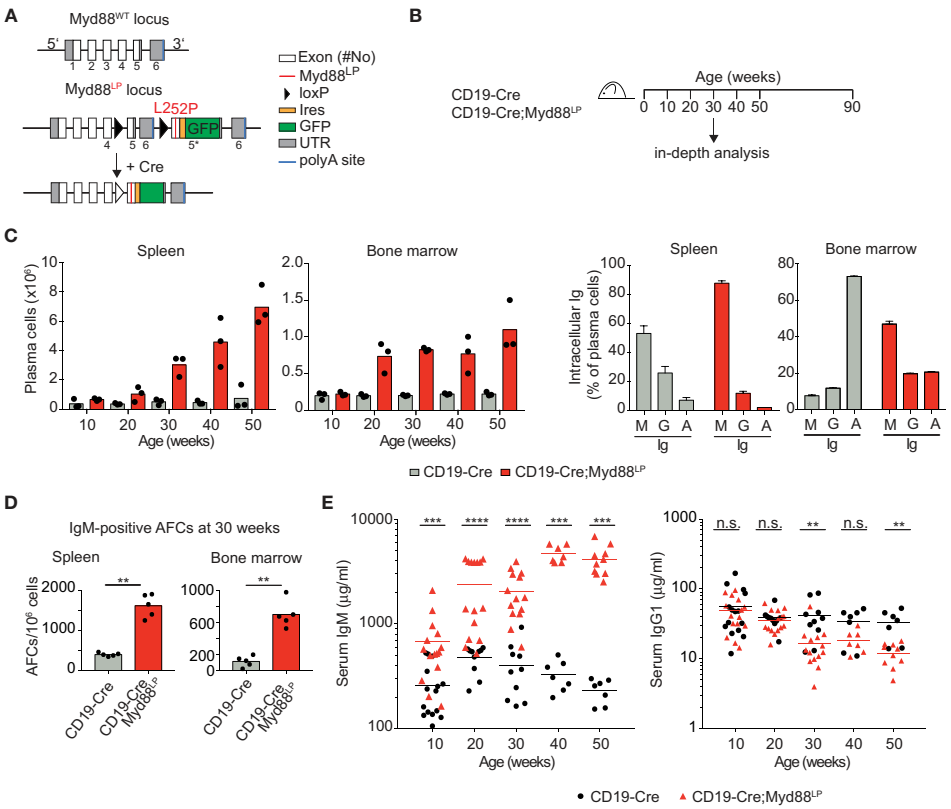

FIGURE 1 | B-cell-specific Myd88^{L252P} expression causes increased IgM plasma cell and serum IgM levels. **(A)** Gene targeting strategy: Myd88^{L252P}-IRES-GFP was targeted into the endogenous *Myd88* locus by homologous recombination. The wildtype exons 5 and 6 were flanked by loxP sites that can be recombined by Cre recombinase, leading to expression of the mutant version. **(B)** Outline of the experiments shown in C–E and **Table 1**. Mice of the indicated genotypes were observed for 90 weeks. **(C)** FACS analysis of spleen and bone marrow. Left: TACI^{+}CD138^{+} plasma cell numbers increase over time. Right panels: Plasma cells expressed mostly IgM (30 weeks of age). **(D)** ELISPOT analysis in spleen and bone marrow at 30 weeks of age. IgM secreting antibody forming cells (AFCs) were elevated. **(E)** Serum immunoglobulin levels measured by ELISA. IgM titers increased over time while IgG1 titers decreased slightly. Results are representative of three independent experiments. **(C–E)** Each symbol represents one mouse. **p ≤ 0.01, ***p ≤ 0.001, ****p ≤ 0.0001, n.s. = not significant. (See also **Supplementary Figures 1–4**).

Figure 1F). As shown previously, these effects are likely due to Myd88^{L252P} activated NF-κB signaling (16–19, 55), concomitant with increased NF-κB negative regulatory feedback — through A20 (TNFAIP3) (55) and NF-κB p65 phosphorylation (56).

B-Cell-Specific Myd88^{L252P} Expression *In Vivo* Leads to an Increase in IgM^{+} Plasma Cells and Serum IgM

In order to address whether B cell-specific expression of Myd88^{L252P} influences B cell development or homeostasis, we used the CD19-Cre allele (46) which is expressed from an early B cell stage on, and monitored mice until 90 weeks of age (**Figure 1B**). In this and all following experiments, mice heterozygous for the Cre and mutant Myd88 alleles were used, designated Cre; Myd88^{L252P}. B cell development in the bone marrow appeared unchanged (**Supplementary Figure 2**), as indicated by the fractions of precursor, immature and mature B cells over time, absence of selection of AA4.1-positive Myd88^{L252P}-expressing B lineage cells over YFP reporter expressing control cells and normal bone marrow histology. Two of thirteen mice

TABLE 1 | Myd88^{L252P} does not promote B lymphomagenesis.

Genotype	Number of animals	Age (weeks)	Phenotype at endpoint (90 weeks)
CD19-Cre	1	74	T cell tumor (TCRβ^{+})
	10	90	Healthy, end of experiment
CD19-Cre; Myd88^{L252P}	1	70	T cell tumor (TCRβ^{+}GFP^{-})
	1	74	GC B cell tumor (reporter-positive) (B220^{+}CD19^{+}CD38^{low}FAS^{high}GFP^{+})
	1	78	GC B cell tumor (reporter-negative) (B220^{+}CD19^{+}CD38^{low}FAS^{high}GFP^{-})
	1	90	T cell tumor (TCRβ^{+}GFP^{-})
	9	90	Healthy, end of experiment

CD19-Cre and CD19-Cre;Myd88^{L252P} mice were observed for 90 weeks and monitored for the appearance of tumors. Tumors were analyzed and characterized by flow cytometry. Tumor incidence appeared comparable to control animals and likely was due to the genetic C57BL/6 background (57).

developed a B cell lymphoma (at 70 and 74 weeks of age; **Table 1** and **Supplementary Figure 3A**). However, only one of these tumors expressed the Myd88^{L252P} reporter, indicating that these tumors arose spontaneously due to the *C57BL/6* genetic background (57).

Starting at 30 weeks of age CD19-Cre;Myd88^{L252P} animals developed a mildly enlarged spleen with more than 95% of splenic B cells expressing the GFP reporter (**Supplementary Figures 3B, C**). While the percentage of follicular and marginal zone B cells appeared unchanged, germinal center (CG) B cells increased in frequency and number over time (**Supplementary Figures 3D–F**).

The most prominent phenotype in CD19-Cre;Myd88^{L252P} mice was an enlarged plasma cell compartment in the spleen, and to a lesser extent, in the bone marrow: Both the frequency and the absolute numbers of the TACI^{+}CD138^{+} plasma cells from 50 weeks old CD19-Cre;Myd88^{L252P} mice were increased compared to CD19-Cre control mice (**Figure 1C** and **Supplementary Figure 4A**). The majority of these expanded plasma cells expressed the Myd88^{L252P} reporter GFP, indicating that the plasma cell expansion was driven by the Myd88^{L252P} mutation (**Supplementary Figure 3C**). Strikingly, the majority of the expanded plasma cells also expressed and secreted IgM (**Figures 1C, D**; **Supplementary Figure 4B**). Correspondingly, serum IgM titers increased as early as ten weeks after birth and continued to increase over time up to twenty-fold, while other Ig isotypes were unchanged or slightly decreased (**Figure 1E**).

Taken together, our results suggest that the Myd88^{L252P} mutation causes elevated serum IgM levels and confers a subtle survival or growth advantage on IgM-expressing B cells that encompass a spectrum of differentiation states, including GC B cells and plasma cells.

Ig Class Switching Is Unchanged in Myd88^{L252P}-Expressing B Cells

It has remained unclear whether the malignant B cells in WM are unable to switch Ig isotype from IgM to another class or whether switched WM cells might disappear over time *in vivo* (7, 8, 58–61). In order to gain insight into whether the Myd88^{L252P} mutation inhibits class switching, we crossed the Myd88^{L252P} mice with Cγ1-Cre mice which express Cre in early GCs at a mature, activated B cell stage just prior to class switching (44). Cγ1-Cre;Myd88^{L252P} animals were immunized with hapten-carrier conjugate as shown in **Figure 2A**. Antigen-specific GFP-reporter-positive and negative B cells did not differ in their ability to switch to IgG1 *in vivo*, neither after primary nor secondary immunization (**Figures 2B, C**). Supporting this result, *ex vivo* B cells transduced with TAT-Cre recombinase showed comparable Ig class switching efficiency in cell culture, irrespective of Myd88^{L252P} expression (**Supplementary Figure 5A**). We also assessed class switch in CD19-Cre mice (in which >95% of B cells are GFP-reporter-positive), and could not detect any change in the frequency of switched cells in either the spleen (IgG1), mesenteric lymph nodes (IgG1) or Peyer's Patches (IgA) (**Supplementary Figure 5B**).

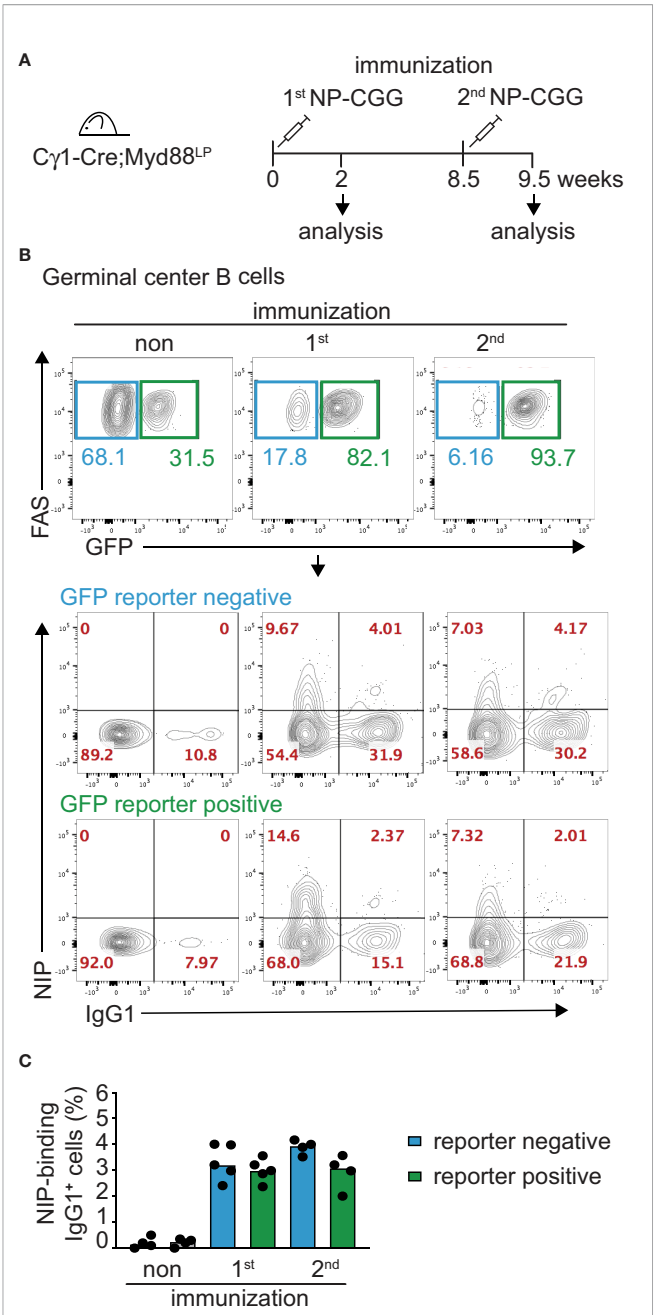

FIGURE 2 | Myd88^{L252P}-expressing B cells switch isotype normally. The Myd88^{L252P} allele was crossed into the B-cell-specific Cγ1-Cre strain which activates Cre-expression in mature B cells upon germline transcription of the IgH Cγ1 switch region. **(A)** Cγ1-Cre;Myd88^{L252P} and littermate control animals were immunized with hapten carrier conjugate (NP-CGG) and analyzed at the indicated time points. **(B)** Representative flow cytometry plots of germinal center (GC) B cells (B220^{+}CD19^{+}CD38^{low}FAS^{high}). Upper panels: Myd88^{L252P} GFP-reporter-positive cells increased upon primary and secondary immunization. Lower panels: Antigen-specific, reporter-negative and -positive GC cells switch to IgG1 to similar extents during primary and secondary immune responses. **(C)** Percentage of IgG1-positive, antigen-positive GC cells. Each dot represents one mouse (n ≥ 4). (See also **Supplementary Figure 5**).

Collectively, these results indicate that the Myd88^{L252P} mutation does not interfere with Ig class switching. They rather suggest that the mutation specifically impacts the fitness of B cells expressing an IgM B cell receptor (BCR).

Myd88^{L252P} Causes Prolonged Persistence of IgM^{+} Antigen-Specific Plasma Cells and Serum IgM

In order to test directly whether IgM-expressing Myd88^{L252P}-mutated B cells can persist for prolonged times *in vivo*, we followed reporter-positive antigen-specific B cells in Cγ1-Cre;Myd88^{L252P} animals until 50 weeks after primary immunization with hapten-carrier conjugate NP-CGG (**Figure 3A**). As shown in **Figure 3B**, hapten-specific IgM-producing cells in spleen and bone marrow remained elevated up to 50 weeks after immunization. Consistent with this finding, NP-specific serum IgM titers remained elevated, while the NP-specific IgG1 titers decreased as in the controls (**Figure 3C**).

The same mice also showed an overall increase in the number of plasma cells (>80% reporter-positive) and elevated total serum IgM, similar to the CD19-Cre;Myd88^{L252P} mice described above, albeit to a lesser extent (**Supplementary Figures 6A, B**). BrdU-labeling over 16 h revealed an increased number of labeled splenic GC B cells and plasma cells compared to controls (**Supplementary Figure 6C**). Histology of the spleen suggested that this proliferation occurred mostly in plasma cell precursors, since CD138-positive plasma cells showed little active proliferation and were mostly Ki67-negative (**Supplementary Figure 6D**). Reminiscent of malignant Waldenström B cells, Myd88^{L252P} reporter-positive, IgM^{+} plasma cells carried increased numbers of somatic mutations compared to IgM^{+} plasma cells from controls (**Supplementary Figures 4C, 6E**).

Our results thus suggest that the Myd88^{L252P} mutation confers a survival and proliferation advantage to IgM-expressing B cells and plasma cell progenitors. Taking into account the capacity of these cells to switch isotype normally, these findings imply that surface IgM expression is required for the observed cellular expansion.

Myd88^{L252P} Expression in a Small Number of B Cells Leads to Serum IgM Paraproteins (M-Spikes)

In WM patients, the MYD88^{L265P} mutation presumably arises as a rare event in a tumor progenitor cell. Therefore, to mimic the disease etiology more closely, we restricted mouse Myd88^{L252P} expression to a small fraction of B cells by a tamoxifen-inducible Cre allele (CD19-Cre^{ERT2}) (47) which induces Cre-mediated recombination in only a few percent of B cells (**Figure 4**, **Supplementary Figure 7**). Ten days after a single dose of tamoxifen expression of Myd88^{L252P} led to a 15-fold increase in the reporter-positive plasma cell population in the spleen, an effect not observed in tamoxifen-treated YFP reporter control mice (**Supplementary Figure 7**). Importantly, 70 weeks after a single tamoxifen injection IgM-secreting plasma cells still persisted in spleen and bone marrow (**Figures 4A, B**). Correspondingly, serum IgM levels were also increased in the mutant animals (**Figure 4C**), all of which displayed discrete paraprotein bands in the γ-globulin zone upon serum protein electrophoresis. Such paraproteins are indicative of clonally restricted plasma cell expansions and occur in IgM MGUS, the precursor condition of WM (**Figure 4D** and **Supplementary Figure 8A**). Immunofixation confirmed that five out of five mice had developed a paraprotein of IgM isotype (**Figure 4D**).

IgM paraprotein bands occasionally also appeared in Cγ1-Cre;Myd88^{L252P} mice, whereas we never observed paraprotein bands in sera of CD19-Cre;Myd88^{L252P} mice (**Supplementary Figure 8B**). Both in aged Cγ1-Cre;Myd88^{L252P} and CD19-Cre^{ERT2};Myd88^{L252P} mice 70 weeks after tamoxifen injection, Myd88^{L252P}-reporter-positive cells—while detectable only in low in numbers—consisted of B220^{+} B cells and varying proportions of differentiated, mostly IgM-positive plasma cells (B220^{low}TACI^{+}CD138^{+}) (**Supplementary Figures 8C, D**).

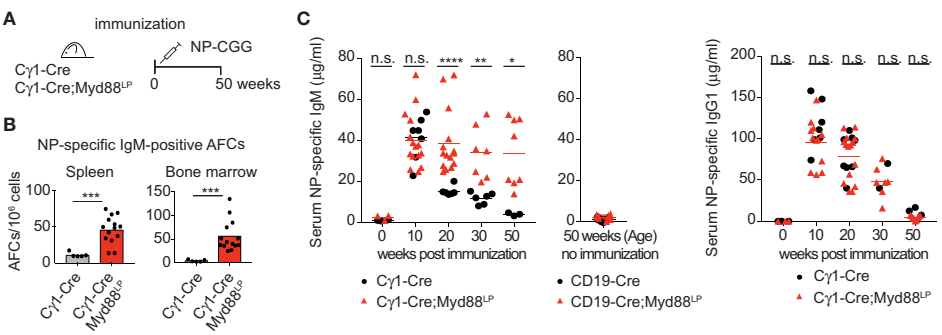

FIGURE 3 | Myd88^{L252P} causes persistence of antigen-specific IgM plasma cells and serum IgM. **(A)** Cγ1-Cre;Myd88^{L252P} and littermate control animals were immunized with hapten carrier conjugate (NP-CGG) and analyzed at the indicated time points. **(B)** ELISPOT analysis in spleen and bone marrow at 50 weeks of age. Antigen-specific IgM secreting antibody forming cells (AFCs) were elevated. **(C)** Serum immunoglobulin levels measured by ELISA. Antigen-specific IgM titers remained elevated while IgG1 titers declined normally. Results are representative of three (NP-specific IgM) or two (NP-specific IgG1) independent experiments. **(B, C)** Each symbol represents one mouse (n ≥ 3). *p ≤ 0.05, **p ≤ 0.01, ***p ≤ 0.001, ****p ≤ 0.0001, n.s. = not significant. (See also **Supplementary Figure 6**).

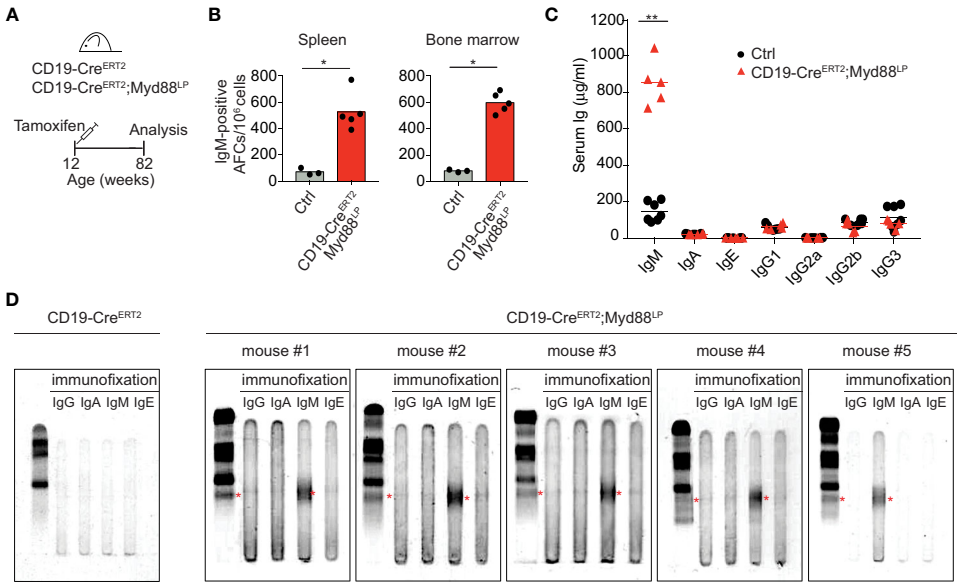

FIGURE 4 | Myd88^{L252P}-expression in a small number of B cells leads to serum IgM paraproteins (M-spikes). **(A)** CD19-Cre^{ERT2};Myd88^{L252P} animals were fed one time with tamoxifen and analyzed after 70 weeks. **(B)** ELISPOT analysis in spleen and bone marrow. IgM-secreting, antibody-forming cells are five to six times elevated in CD19-Cre^{ERT2};Myd88^{L252P} mice. **(C)** ELISA measurement of immunoglobulin serum titers. Only IgM was elevated in CD19-Cre^{ERT2};Myd88^{L252P} mice. **(B, C)** Each symbol represents one mouse (n ≥ 3). *p ≤ 0.05, **p ≤ 0.01. **(D)** Serum protein electrophoresis and immunofixation of serum from five CD19-Cre^{ERT2};Myd88^{L252P} mice. Each mouse showed a paraprotein band within the γ-globulin fraction (red stars) that was positive for IgM. Mouse #4 had an additional paraprotein band that was negative for IgM. (See also **Supplementary Figures 7** and **8**).

Thus, our data show that chronic activation of Myd88 in a small fraction of B cells can lead to the development of IgM M-spikes in the serum of aged, but otherwise healthy mice. They suggest a causal link between the Myd88^{L252P} mutation and IgM MGUS, the premalignant condition that precedes WM (23–26).

Myd88^{L252P} Expression in a Small Number of B Cells Leads to Clonal Expansions of Plasma Cells

In order to determine the extent of clonal expansions in the plasma cell compartment in the five aged CD19-Cre^{ERT2};Myd88^{L252P} mice, we analyzed rearranged V_H-region sequences in sorted plasma cells isolated from bone marrow and spleen. As read-out we examined the J558 family V genes which constitute about half of the expressed V_H gene repertoire in C57BL/6 mice (62–64). Amplification with a primer in the downstream J_H intron produced bands for all four J_H rearrangements in controls. By contrast, for four out of five CD19-Cre^{ERT2};Myd88^{L252P} mice, we only detected a single PCR band with J_H4 being used in each case (**Figure 5A**). Since only a limiting amount of sorted plasma cells was available for this analysis, we cannot exclude that the J_H4 bias may stem from preferential amplification of short VDJ rearrangements. (For the fifth mouse, we failed to obtain a PCR product.)

Subcloning and sequencing revealed that each of the four mice carried a different predominant J_H4 rearrangement involving a J558 family member and that this predominant clonotype was overrepresented in plasma cells from both, bone marrow and spleen (**Figure 5B**). Plasma cells from age-matched control and CD19-Cre;Myd88^{L252P} and Cγ1-Cre;Myd88^{L252P} mice also exhibited predominant clonotypes, but at a much lower frequency (12–25 versus 44–74% in mutants) and different ones in bone marrow and spleen (**Figure 5B** and **Supplementary Figure 9A**).

In striking contrast to the controls, the majority of plasma cells from CD19-Cre^{ERT2};Myd88^{L252P} mice expressed IgM (ranging from 68 and 88% in individual mice; **Supplementary Figure 9B**). Still, the overall extent of somatic mutation in GFP$^+$ bone marrow-derived plasma cells from CD19-Cre^{ERT2};Myd88^{L252P} mice was comparable to control plasma cells which predominantly expressed IgG (**Supplementary Figure 9B**). In three mice the most frequently detected VDJ genes showed a moderate number of somatic mutations of up to 5, 13, or 15, respectively, which allowed the reconstruction of genealogical trees on the basis of intraclonal variation (**Supplementary Figure 9C**). In one mouse (#4) the most frequent VDJ gene was unmutated.

In order to find out whether the IgM M-spikes observed in these four mice contained the same clonal VDJ rearrangements that were predominantly detected in spleen and bone marrow of the individual mice, we analyzed protein bands corresponding to the individual M-spikes by tandem mass spectrometry (**Supplementary Figure 10**). Proteomics confirmed in all cases that the predominant isotype in the M-spike was IgM, but did

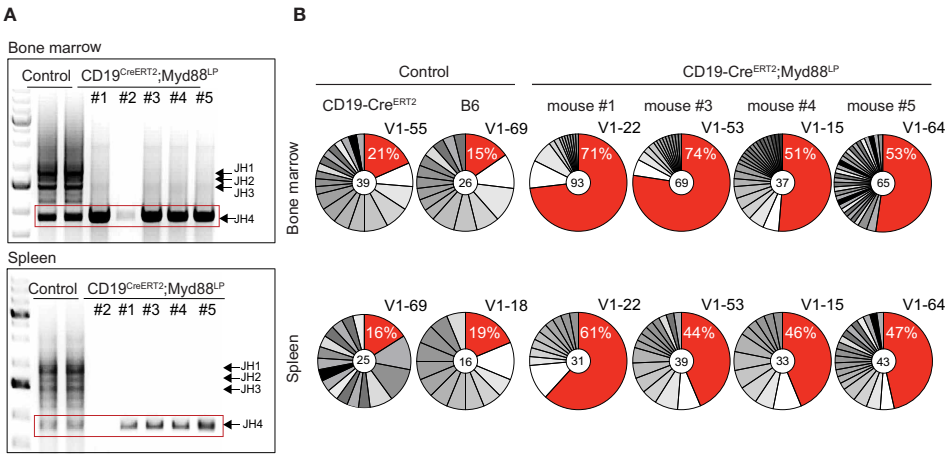

FIGURE 5 | CDR3 analysis of rearranged VDJ genes shows expansion of clonally related plasma cells in aged Cre^{ERT2};Myd88^{L252P} mice. Genomic DNA was purified from GFP-reporter-positive TACI^{+}CD138^{+} plasma cells isolated from bone marrow and spleen of CD19-Cre^{ERT2};Myd88^{L252P} mice 70 weeks after tamoxifen induction. **(A)** PCR amplification of rearranged J558 family V genes from bone marrow (upper panel) and spleen (lower panel). Bands corresponding to all four JH segments appeared in the controls, while in Cre^{ERT2};Myd88^{L252P} mice only J_H4 rearrangements could be detected. (No rearrangements were detected in mouse #2). **(B)** J_H4 bands (red rectangle shown in **A**) were cloned and sequenced. Clonal analysis based on CDR3 sequence revealed that in each mouse the same clones were most frequently detected in the bone marrow (upper panel) and spleen (lower panel). For the most frequently detected clonotype (red sector in pie chart), the % of sequences detected and the V_H J558 family member is given. V_H genes and VDJ rearrangements of the most frequent clonotypes were shared in bone marrow and spleen of each CD19-Cre^{ERT2};Myd88^{L252P} mouse, while they differed in bone marrow and spleen of controls and between the controls. Each pie chart represents one mouse. (See also **Supplementary Figures 9** and **10**).

not reveal clonotypic peptides corresponding to the VDJ regions that were most frequently detected by sequencing.

Notwithstanding the absence of a clear molecular link between the M-spikes and the most frequently detected plasma cell clones in bone marrow and spleen of the four CD19-Cre^{ERT2};Myd88^{L252P} mice, our clonal analysis suggests that—in a genetic scenario where introduction of Myd88^{L252P} mutation into CD19^{+} B cells is a rare event—Myd88^{L252P} mutation confers a survival and growth advantage to rare cells that over time produce clonal expansions of IgM-positive plasma cell progenitors (**Supplementary Figure 9C**).

DISCUSSION

IgM and non-IgM MGUS are different clinical entities that are both thought to arise from B cells at late stages of differentiation (23, 25, 65). While non-IgM MGUS mostly evolves to multiple myeloma (25, 66–68), IgM MGUS has been increasingly recognized as the premalignant precursor state for WM (23–26, 65). However, to date it has remained challenging to clinically or molecularly distinguish WM from smoldering WM and IgM MGUS (23, 69–71). Premalignant IgM MGUS and malignant WM cells were found to be phenotypically similar to each other (70).

The MYD88^{L265P} mutation is absent in multiple myeloma patients (27), but highly prevalent in both, WM and IgM-MGUS patients (27–33). It therefore may represent an early, unifying genetic event in WM pathogenesis. Here, we provide evidence that B-cell-specific expression of the mouse homolog of the human MYD88^{L265P} mutation (Myd88^{L252P}) is sufficient to cause a phenotype that resembles IgM MGUS. We thus establish a causal link between the Myd88^{L265P} mutation and the development of a phenotype resembling the WM precursor condition and shed new light on the etiology of WM.

Based on three different genetic scenarios, our results indicate that chronic activation of aberrant Myd88 signaling—by conditional mutagenesis of the endogenous Myd88 locus—confers a survival and low-grade proliferative advantage on IgM-expressing B cells. This advantage can manifest in different ways, depending on the number cells targeted by the mutation and the time window for progression: In a first scenario, activation of the mutation by CD19-Cre in early B cells caused a polyclonal, low-grade lymphoproliferative disease accompanied by polyclonal plasma cell expansion and progressively increasing serum IgM titers (up to 20-fold). In a second scenario, activation of the mutation at the initiation of the GC stage by Cγ1-Cre caused a similar, albeit weaker, phenotype, consistent with a lower number of mutated B cells. In a third scenario, a time-restricted activation of Myd88^{L252P} by CD19-Cre^{ERT2} in a small fraction of B cells led to clonal expansions of IgM-expressing plasma cells and the appearance of IgM M-spikes in the serum.

The latter scenario most closely mimics the *in vivo* situation in human patients, where Myd88 mutation presumably occurs as a rare event in a tumor progenitor B cell. It appears that IgM expressing Myd88^{L252P} mutated B cells can gain a competitive advantage over normal B cells over time resulting in an

outgrowth of clonally related, mutated cells and IgM M-spikes in the blood when the mutation is restricted to few or single progenitor B cells. Polyclonal activation of Myd88^{L252P} (as in the first and second scenario) may mask this effect, and indeed resulted in overall strongly elevated IgM levels (**Figure 1E** and **Supplementary Figure 6B**) (19). In support of this interpretation, we never detected IgM M-spikes when the mutation was activated by the CD19-Cre allele (causing recombination in most B cells) and only occasionally when the mutation was activated by the Cγ1-Cre allele (which is active in fewer B cells) (44).

The presence of IgM M-spikes in the blood of aged CD19-Cre^{ERT2};Myd88^{L252P} mice was accompanied by clonal expansions in the plasma cell compartment with the most frequently detected clonotype being identical in spleen and bone marrow. Clonally related plasma cells mostly carried somatically mutated VDJ regions, reminiscent of a molecular WM cell phenotype (6–11). We also observed intraclonal diversity with respect to somatic mutations (**Supplementary Figures 9B, C**), suggesting that the Myd88^{L252P} mutation drives IgM MGUS progenitors already at the GC stage, consistent with our finding that GC B cells rather than plasma cells are actively proliferating (**Supplementary Figures 6C, D**). However, our results do not exclude that the pro-proliferative activity of the Myd88^{L252P} mutation extends into later stages of B cell differentiation.

Our attempts to find a direct molecular link by proteomics between the IgM M-spikes and the most frequently detected clones were unsuccessful. This may be due to the low amount of starting material combined with the complexity of serum samples, the presence of multiple clonotypes in the isolated M-spike, the locally restricted area of the bone marrow biopsy (femur), or a combination of these factors. It is also possible that in CD19-Cre^{ERT2};Myd88^{L252P} mice the most frequently detected plasma cell clones form part of an early, dynamic clonal landscape in which several competing Myd88^{L252P} B cell clones are still present until secondary mutations help to establish dominance and long-term persistence of a single major clone.

Our study is in line with the prevailing view that the development of WM requires additional mutations besides MYD88^{L265P} (19, 20, 36, 39–41, 55). The observed B cell phenotypes are consistent with earlier work that assessed the effect of retroviral overexpression of mouse Myd88^{L252P} in B cells *ex vivo* (55) or B-cell-specific transgenic overexpression of human MYD88^{L265P} *in vivo* (20). Both approaches showed that the Myd88 mutation by itself is not sufficient to immortalize or neoplastically transform B cells. This appears plausible, because activation of pro-survival signaling by NF-κB entails negative feedback that limits B cell expansion (55). The need to remove negative feedback loops may explain the frequent occurrence of mutations that affect negative regulators of NF-κB in human WM or ABC-DLBCL patients (36, 37, 72–75). Our results (in genetic scenarios one and two) are also in line with the observation that human MYD88^{L265P} promotes in the mouse the development of a polyclonal, low-grade B cell lymphoproliferative disorder of lymphoplasmacytic appearance with increased serum IgM (20).

However, different from earlier studies, continuous activation of an endogenous Myd88^{L252P} mutation by CD19-Cre in our mouse cohort did not cause fulminant lymphoproliferative disease (19) or an increased transformation to B lymphoma or increased mortality (**Table 1**; **Supplementary Figure 3A**) (19, 20). Rather than owing to differences in the human and mouse Myd88 proteins, as proposed recently by Sewastianik et al. (20), these discrepancies may be caused by different external cues (such as TLR signaling induced by different microbial or mouse housing environments) (19) or the molecular effects of strong transgene overexpression (20), or both.

Our results suggest that IgM expression is specifically required for the pro-survival effect of the Myd88^{L252P} mutation, since mutated B cells showed normal Ig isotype switching in a wide range of experimental conditions, but only IgM-expressing, antigen-specific B cells were able to persist after immunization. In line with these results, Young et al. (76) proposed that cell surface IgM acts as an "initiator oncogene" for B cell lymphomas, with the IgM-BCR potently promoting B cell proliferation and IgG-BCRs preferentially promoting B-cell differentiation programs. In this view, the IgM-BCR acts "as an oncogene that initiates proto-malignant expansion of normal B cells", while the extended survival of pre-malignant cells would require additional cooperating oncogenic events.

One such event may be the MYD88^{L265P} mutation which transforms normal IgM-expressing proliferating B cells into premalignant cells that show prolonged survival and plasmacytic differentiation. This effect may be driven by external triggers through TLR signaling and be dependent on BCR surface expression. Enforced overexpression of Myd88^{L525P} in B cells under the control of a strong constitutive viral promoter (77) may overcome such a dependency on external triggers (13) and manifest directly in a Waldenstöm-like B cell lymphoma (77). In ABC-DLBCL cells, and in at least one WM-derived cell line, the MYD88^{L265P} mutation promotes the formation of an oncogenic signaling complex comprising Myd88, TLR9 and an IgM-BCR (My-T-BCR super complex) which enforces cooperative survival signaling through the BCR and TLR (16, 17, 76, 78, 79). It will be interesting to determine in this context whether a My-T-BCR super complex already forms in Myd88-mutated B or plasma cells expressing physiological levels of mutated Myd88, or whether super complex formation requires either additional oncogenic mutations or increased expression of mutated Myd88, or both.

DATA AVAILABILITY STATEMENT

All nucleotide datasets generated for this study can be found in the **Supplementary Material** (**Supplementary Tables 2** and **4**). The mass spectrometry proteomics data can be found in **Supplementary Material** (**Supplementary Table 3**) and raw data were deposited to the ProteomeXchange Consortium via the PRIDE (80) partner repository with the dataset identifier PXD017292 (Proteomics Identifications (PRIDE), RRID:SCR_003411).

ETHICS STATEMENT

The animal study was reviewed and approved by Landesamt für Gesundheit und Soziales Berlin (LaGeSo# G0263/15).

AUTHOR CONTRIBUTIONS

KS, US, CK, and KR designed research. US performed $Myd88^{L252P}$ gene targeting. KS performed all experiments except $Myd88^{L252P}$ gene targeting, prepared all figures, and a first manuscript draft. OP and PM carried out the proteomic analyses. KS, CK, KR, OP, and PM analyzed data. TS, RG, and WW provided expertise. CK wrote and KR edited the final manuscript with critical contributions from KS, TS, RG, and WW. All authors contributed to the article and approved the submitted version.

FUNDING

This work was supported by the European Research Council, Advanced Grant 268921 (to KR), the Helmholtz Association, Immunology & Inflammation ZT-0027 (to KR), the Deutsche Krebshilfe, Grant 70112800 (jointly to KR and M. Janz, Max Delbrück Center for Molecular Medicine in the Helmholtzgemeinschaft, Berlin, Germany), the Berlin School of Integrative Oncology and Charité Universitätsmedizin Berlin, Promotionsstipendium I (to KS) and the library of the Max Delbrück Center for Molecular Medicine in the Helmholtz Association, Open Access Fonds (to KR).

ACKNOWLEDGMENTS

We thank Kerstin Petsch, Jennifer Pempe and Mohamad Haji for technical assistance, Hans-Peter Rahn for FACS-related support, Andreas Zach for advice and Martin Janz for scientific discussions.

SUPPLEMENTARY MATERIAL

The Supplementary Material for this article can be found online at: https://www.frontiersin.org/articles/10.3389/fimmu.2020.602868/full#supplementary-material

REFERENCES

1. Dimopoulos MA, Panayiotidis P, Moulopoulos LA, Sfikakis P, Dalakas M. Waldenström's Macroglobulinemia: Clinical Features, Complications, and Management. *J Clin Oncol* (2000) 18:214–4. doi: 10.1200/jco.2000.18.1.214
2. Owen RG, Treon SP, Al-Katib A, Fonseca R, Greipp PR, McMaster ML, et al. Clinicopathological definition of Waldenstrom's macroglobulinemia: Consensus Panel Recommendations from the Second International Workshop on Waldenstrom's Macroglobulinemia. *Semin Oncol* (2003) 30:110–5. doi: 10.1053/sonc.2003.50082
3. Castillo JJ, Garcia-Sanz R, Hatjiharissi E, Kyle RA, Leleu X, McMaster M, et al. Recommendations for the diagnosis and initial evaluation of patients with Waldenström Macroglobulinaemia: A Task Force from the 8th International Workshop on Waldenström Macroglobulinaemia. *Brit J Haematol* (2016) 175:77–86. doi: 10.1111/bjh.14196
4. Swerdlow SH, Campo E, Pileri SA, Harris NL, Stein H, Siebert R, et al. The 2016 revision of the World Health Organization classification of lymphoid neoplasms. *Blood* (2016) 127:2375–90. doi: 10.1182/blood-2016-01-643569
5. Dimopoulos MA, Kastritis E. How I treat Waldenström macroglobulinemia. *Blood* (2019) 134:2022–35. doi: 10.1182/blood.2019000725
6. Ciric B, VanKeulen V, Rodriguez M, Kyle RA, Gertz MA, Pease LR. Clonal evolution in Waldenstrom macroglobulinemia highlights functional role of B-cell receptor. *Blood* (2001) 97:321–3. doi: 10.1182/blood.v97.1.321
7. Sahota SS, Forconi F, Ottensmeier CH, Provan D, Oscier DG, Hamblin TJ, et al. Typical Waldenstrom macroglobulinemia is derived from a B-cell arrested after cessation of somatic mutation but prior to isotype switch events. *Blood* (2002) 100:1505–7. doi: 10.1182/blood.V100.4.1505.h81602001505_1505_1507
8. Sahota SS, Forconi F, Ottensmeier CH, Stevenson FK. Origins of the malignant clone in typical Waldenstrom's macroglobulinemia. *Semin Oncol* (2003) 30:136–41. doi: 10.1053/sonc.2003.50072
9. Kriangkum J, Taylor BJ, Treon SP, Mant MJ, Belch AR, Pilarski LM. Clonotypic IgM V/D/J sequence analysis in Waldenstrom macroglobulinemia suggests an unusual B-cell origin and an expansion of polyclonal B cells in peripheral blood. *Blood* (2004) 104:2134–42. doi: 10.1182/blood-2003-11-4024
10. Janz S. Waldenström Macroglobulinemia: Clinical and Immunological Aspects, Natural History, Cell of Origin, and Emerging Mouse Models. *Isrn Hematol* (2013) 2013:1–25. doi: 10.1155/2013/815325
11. Varettoni M, Zibellini S, Capello D, Arcaini L, Rossi D, Pascutto C, et al. Clues to pathogenesis of Waldenström macroglobulinemia and immunoglobulin M monoclonal gammopathy of undetermined significance provided by analysis of immunoglobulin heavy chain gene rearrangement and clustering of B-cell receptors. *Leukemia Lymphoma* (2013) 54:2485–9. doi: 10.3109/10428194.2013.779689
12. Treon SP, Xu L, Yang G, Zhou Y, Liu X, Cao Y, et al. MYD88 L265P Somatic Mutation in Waldenström's Macroglobulinemia. *New Engl J Med* (2012) 367:826–33. doi: 10.1056/nejmoa1200710
13. Avbelj M, Wolz O-O, Fekonja O, Benčina M, Repič M, Mavri J, et al. Activation of lymphoma-associated MyD88 mutations via allostery-induced TIR-domain oligomerization. *Blood* (2014) 124:3896–904. doi: 10.1182/blood-2014-05-573188
14. Deguine J, Barton GM. MyD88: a central player in innate immune signaling. *F1000prime Rep* (2014) 6:97. doi: 10.12703/p6-97
15. Lee J-H, Jeong H, Choi J-W, Oh H, Kim Y-S. Clinicopathologic significance of MYD88 L265P mutation in diffuse large B-cell lymphoma: a meta-analysis. *Sci Rep UK* (2017) 7:1785. doi: 10.1038/s41598-017-01998-5
16. Ngo VN, Young RM, Schmitz R, Jhavar S, Xiao W, Lim K-H, et al. Oncogenically active MYD88 mutations in human lymphoma. *Nature* (2011) 470:115–9. doi: 10.1038/nature09671
17. Phelan JD, Young RM, Webster DE, Roulland S, Wright GW, Kasbekar M, et al. A multiprotein supercomplex controlling oncogenic signalling in lymphoma. *Nature* (2018) 560:387–91. doi: 10.1038/s41586-018-0290-0
18. Yang G, Zhou Y, Liu X, Xu L, Cao Y, Manning RJ, et al. A mutation in MYD88 (L265P) supports the survival of lymphoplasmacytic cells by activation of Bruton tyrosine kinase in Waldenström macroglobulinemia. *Blood* (2013) 122:1222–32. doi: 10.1182/blood-2012-12-475111
19. Knittel G, Liedgens P, Korovkina D, Seeger JM, Al-Baldawi Y, Al-Maarri M, et al. B-cell–specific conditional expression of Myd88p.L252P leads to the development of diffuse large B-cell lymphoma in mice. *Blood* (2016) 127:2732–41. doi: 10.1182/blood-2015-11-684183
20. Sewastianik T, Guerrera ML, Adler K, Dennis PS, Wright K, Shanmugam V, et al. Human MYD88L265P is insufficient by itself to drive neoplastic

transformation in mature mouse B cells. *Blood Adv* (2019) 3:3360–74. doi: 10.1182/bloodadvances.2019000588
21. Ailawadhi S, Kardosh A, Yang D, Cozen W, Patel G, Alamgir MA, et al. Outcome Disparities among Ethnic Subgroups of Waldenström's Macroglobulinemia: A Population-Based Study. *Oncology* (2014) 86:253–62. doi: 10.1159/000360992
22. Kyle RA, Benson JT, Larson DR, Therneau TM, Dispenzieri A, Kumar S, et al. Progression in smoldering Waldenström macroglobulinemia: long-term results. *Blood* (2012) 119:4462–6. doi: 10.1182/blood-2011-10-384768
23. Paludo J, Ansell SM. Advances in the understanding of IgM monoclonal gammopathy of undetermined significance. *F1000research* (2017) 6:2142. doi: 10.12688/f1000research.12880.1
24. Kapoor P, Ansell SM, Fonseca R, Chanan-Khan A, Kyle RA, Kumar SK, et al. Diagnosis and Management of Waldenström Macroglobulinemia: Mayo Stratification of Macroglobulinemia and Risk-Adapted Therapy (mSMART) Guidelines 2016. *JAMA Oncol* (2017) 3:1257–65. doi: 10.1001/jamaoncol.2016.5763
25. Kyle RA, Larson DR, Therneau TM, Dispenzieri A, Kumar S, Cerhan JR, et al. Long-Term Follow-up of Monoclonal Gammopathy of Undetermined Significance. *New Engl J Med* (2018) 378:241–9. doi: 10.1056/nejmoa1709974
26. Gertz MA. Waldenström macroglobulinemia: 2019 update on diagnosis, risk stratification, and management. *Am J Hematol* (2019) 94:266–76. doi: 10.1002/ajh.25292
27. Jiménez C, Sebastián E, Chillón MC, Giraldo P, Hernández JM, Escalante F, et al. MYD88 L265P is a marker highly characteristic of, but not restricted to, Waldenström's macroglobulinemia. *Leukemia* (2013) 27:1722–8. doi: 10.1038/leu.2013.62
28. Poulain S, Roumier C, Decambron A, Renneville A, Herbaux C, Bertrand E, et al. MYD88 L265P mutation in Waldenstrom macroglobulinemia. *Blood* (2013) 121:4504–11. doi: 10.1182/blood-2012-06-436329
29. Varettoni M, Arcaini L, Zibellini S, Boveri E, Rattotti S, Riboni R, et al. Prevalence and clinical significance of the MYD88 (L265P) somatic mutation in Waldenström's macroglobulinemia and related lymphoid neoplasms. *Blood* (2013) 121:2522–8. doi: 10.1182/blood-2012-09-457101
30. Varettoni M, Zibellini S, Arcaini L, Boveri E, Rattotti S, Pascutto C, et al. MYD88 (L265P) mutation is an independent risk factor for progression in patients with IgM monoclonal gammopathy of undetermined significance. *Blood* (2013) 122:2284–5. doi: 10.1182/blood-2013-07-513366
31. Xu L, Hunter ZR, Yang G, Zhou Y, Cao Y, Liu X, et al. MYD88 L265P in Waldenström macroglobulinemia, immunoglobulin M monoclonal gammopathy, and other B-cell lymphoproliferative disorders using conventional and quantitative allele-specific polymerase chain reaction. *Blood* (2013) 121:2051–8. doi: 10.1182/blood-2012-09-454355
32. Xu L, Hunter ZR, Yang G, Cao Y, Liu X, Manning R, et al. Detection of MYD88 L265P in peripheral blood of patients with Waldenström's Macroglobulinemia and IgM monoclonal gammopathy of undetermined significance. *Leukemia* (2014) 28:1698–704. doi: 10.1038/leu.2014.65
33. Nakamura A, Ohwada C, Takeuchi M, Takeda Y, Tsukamoto S, Mimura N, et al. Detection of MYD88 L265P mutation by next-generation deep sequencing in peripheral blood mononuclear cells of Waldenström's macroglobulinemia and IgM monoclonal gammopathy of undetermined significance. *PloS One* (2019) 14:e0221941. doi: 10.1371/journal.pone.0221941
34. Roccaro AM, Sacco A, Jimenez C, Maiso P, Moschetta M, Mishima Y, et al. C1013G/CXCR4 acts as a driver mutation of tumor progression and modulator of drug resistance in lymphoplasmacytic lymphoma. *Blood* (2014) 123:4120–31. doi: 10.1182/blood-2014-03-564583
35. Treon SP, Cao Y, Xu L, Yang G, Liu X, Hunter ZR. Somatic mutations in MYD88 and CXCR4 are determinants of clinical presentation and overall survival in Waldenström macroglobulinemia. *Blood* (2014) 123:2791–6. doi: 10.1182/blood-2014-01-550905
36. Hunter ZR, Xu L, Yang G, Zhou Y, Liu X, Cao Y, et al. The genomic landscape of Waldenström macroglobulinemia is characterized by highly recurring MYD88 and WHIM-like CXCR4 mutations, and small somatic deletions associated with B-cell lymphomagenesis. *Blood* (2014) 123:1637–46. doi: 10.1182/blood-2013-09-525808
37. Hunter ZR, Xu L, Yang G, Tsakmaklis N, Vos JM, Liu X, et al. Transcriptome sequencing reveals a profile that corresponds to genomic variants in Waldenström macroglobulinemia. *Blood* (2016) 128:827–38. doi: 10.1182/blood-2016-03-708263
38. Poulain S, Roumier C, Venet-Caillault A, Figeac M, Herbaux C, Marot G, et al. Genomic Landscape of CXCR4 Mutations in Waldenström Macroglobulinemia. *Clin Cancer Res* (2016) 22:1480–8. doi: 10.1158/1078-0432.ccr-15-0646
39. Schmidt J, Federmann B, Schindler N, Steinhilber J, Bonzheim I, Fend F, et al. MYD88 L265P and CXCR4 mutations in lymphoplasmacytic lymphoma identify cases with high disease activity. *Brit J Haematol* (2015) 169:795–803. doi: 10.1111/bjh.13361
40. Xu L, Hunter ZR, Tsakmaklis N, Cao Y, Yang G, Chen J, et al. Clonal architecture of CXCR4 WHIM-like mutations in Waldenström Macroglobulinaemia. *Brit J Haematol* (2016) 172:735–44. doi: 10.1111/bjh.13897
41. Varettoni M, Zibellini S, Defrancesco I, Ferretti VV, Rizzo E, Malcovati L, et al. Pattern of somatic mutations in patients with Waldenström macroglobulinemia or IgM monoclonal gammopathy of undetermined significance. *Haematologica* (2017) 102:2077–85. doi: 10.3324/haematol.2017.172718
42. Peitz M, Pfannkuche K, Rajewsky K, Edenhofer F. Ability of the hydrophobic FGF and basic TAT peptides to promote cellular uptake of recombinant Cre recombinase: A tool for efficient genetic engineering of mammalian genomes. *Proc Natl Acad Sci* (2002) 99:4489–94. doi: 10.1073/pnas.032068699
43. Otipoby KL, Waisman A, Derudder E, Srinivasan L, Franklin A, Rajewsky K. The B-cell antigen receptor integrates adaptive and innate immune signals. *Proc Natl Acad Sci* (2015) 112:12145–50. doi: 10.1073/pnas.1516428112
44. Casola S, Cattoretti G, Uyttersprot N, Koralov SB, Seagal J, Segal J, et al. Tracking germinal center B cells expressing germ-line immunoglobulin γ1 transcripts by conditional gene targeting. *Proc Natl Acad Sci* (2006) 103:7396–401. doi: 10.1073/pnas.0602353103
45. Srinivas S, Watanabe T, Lin C-S, William CM, Tanabe Y, Jessell TM, et al. Cre reporter strains produced by targeted insertion of EYFP and ECFP into the ROSA26 locus. *BMC Dev Biol* (2001) 1:4. doi: 10.1186/1471-213x-1-4
46. Rickert RC, Roes J, Rajewsky K. B Lymphocyte-Specific, Cre-mediated Mutagenesis in Mice. *Nucleic Acids Res* (1997) 25:1317–8. doi: 10.1093/nar/25.6.1317
47. Yasuda T, Wirtz T, Zhang B, Wunderlich T, Schmidt-Supprian M, Sommermann T, et al. Studying Epstein–Barr Virus Pathologies and Immune Surveillance by Reconstructing EBV Infection in Mice. *Cold Spring Harb Sym* (2013) 78:259–63. doi: 10.1101/sqb.2013.78.020222
48. Schenten D, Gerlach VL, Guo C, Velasco-Miguel S, Hladik CL, White CL, et al. DNA polymerase κ deficiency does not affect somatic hypermutation in mice. *Eur J Immunol* (2002) 32:3152–60. doi: 10.1002/1521-4141(200211)32:11<3152::aid-immu3152>3.0.co;2-2
49. Ye J, Ma N, Madden TL, Ostell JM. IgBLAST: an immunoglobulin variable domain sequence analysis tool. *Nucleic Acids Res* (2013) 41:W34–40. doi: 10.1093/nar/gkt382
50. Lefranc M-P, Pommié C, Ruiz M, Giudicelli V, Foulquier E, Truong L, et al. IMGT unique numbering for immunoglobulin and T cell receptor variable domains and Ig superfamily V-like domains. *Dev Comp Immunol* (2003) 27:55–77. doi: 10.1016/s0145-305x(02)00039-3
51. Shevchenko A, Tomas H, Havli J, Olsen JV, Mann M. In-gel digestion for mass spectrometric characterization of proteins and proteomes. *Nat Protoc* (2006) 1:2856–60. doi: 10.1038/nprot.2006.468
52. Rappsilber J, Mann M, Ishihama Y. Protocol for micro-purification, enrichment, pre-fractionation and storage of peptides for proteomics using StageTips. *Nat Protoc* (2007) 2:1896–906. doi: 10.1038/nprot.2007.261
53. Cox J, Neuhauser N, Michalski A, Scheltema RA, Olsen JV, Mann M. Andromeda: A Peptide Search Engine Integrated into the MaxQuant Environment. *J Proteome Res* (2011) 10:1794–805. doi: 10.1021/pr101065j
54. Cox J, Mann M. MaxQuant enables high peptide identification rates, individualized p.p.b.-range mass accuracies and proteome-wide protein quantification. *Nat Biotechnol* (2008) 26:1367–72. doi: 10.1038/nbt.1511
55. Wang JQ, Jeelall YS, Beutler B, Horikawa K, Goodnow CC. Consequences of the recurrent MYD88L265P somatic mutation for B cell tolerance. *J Exp Med* (2014) 211:413–26. doi: 10.1084/jem.20131424
56. Pradère J-P, Hernandez C, Koppe C, Friedman RA, Luedde T, Schwabe RF. Negative regulation of NF-κB p65 activity by serine 536 phosphorylation. *Sci Signal* (2016) 9:ra85–5. doi: 10.1126/scisignal.aab2820

57. Blackwell B-N, Bucci TJ, Hart RW, Turturro A. Longevity, Body Weight, and Neoplasia in Ad Libitum-Fed and Diet-Restricted C57BL6 Mice Fed NIH-31 Open Formula Diet. *Toxicol Pathol* (1995) 23:570–82. doi: 10.1177/019262339502300503
58. Kriangkum J, Taylor BJ, Strachan E, Mant MJ, Reiman T, Belch AR, et al. Impaired class switch recombination (CSR) in Waldenström macroglobulinemia (WM) despite apparently normal CSR machinery. *Blood* (2006) 107:2920–7. doi: 10.1182/blood-2005-09-3613
59. Babbage G, Townsend M, Zojer N, Mockridge IC, Garand R, Barlogie B, et al. IgM-expressing Waldenstrom's macroglobulinemia tumor cells reveal a potential for isotype switch events in vivo. *Leukemia* (2007) 21:827. doi: 10.1038/sj.leu.2404538
60. Kriangkum J, Taylor BJ, Treon SP, Mant MJ, Reiman T, Belch AR, et al. Molecular Characterization of Waldenstrom's Macroglobulinemia Reveals Frequent Occurrence of Two B-Cell Clones Having Distinct IgH VDJ Sequences. *Clin Cancer Res* (2007) 13:2005–13. doi: 10.1158/1078-0432.ccr-06-2788
61. Martín-Jiménez P, García-Sanz R, Sarasquete ME, Ocio E, Pérez JJ, González M, et al. Functional class switch recombination may occur 'in vivo' in Waldenström macroglobulinaemia. *Brit J Haematol* (2007) 136:114–6. doi: 10.1111/j.1365-2141.2006.06397.x
62. Jeong HD, Komisar JL, Kraig E, Teale JM. Strain-dependent expression of VH gene families. *J Immunol* (1988) 140:2436–41.
63. Yancopoulos GD, Malynn BA, Alt FW. Developmentally regulated and strain-specific expression of murine VH gene families. *J Exp Med* (1988) 168:417–35. doi: 10.1084/jem.168.1.417
64. Sheehan KM, Brodeur PH. Molecular cloning of the primary IgH repertoire: a quantitative analysis of VH gene usage in adult mice. *EMBO J* (1989) 8:2313–20. doi: 10.1002/j.1460-2075.1989.tb08358.x
65. Rajkumar SV, Dimopoulos MA, Palumbo A, Blade J, Merlini G, Mateos M-V, et al. International Myeloma Working Group updated criteria for the diagnosis of multiple myeloma. *Lancet Oncol* (2014) 15:e538–48. doi: 10.1016/s1470-2045(14)70442-5
66. Kyle RA, Therneau TM, Rajkumar SV, Offord JR, Larson DR, Plevak MF. Melton LJ. A Long-Term Study of Prognosis in Monoclonal Gammopathy of Undetermined Significance. *New Engl J Med* (2002) 346:564–9. doi: 10.1056/nejmoa01133202
67. Landgren O, Kyle RA, Pfeiffer RM, Katzmann JA, Caporaso NE, Hayes RB, et al. Monoclonal gammopathy of undetermined significance (MGUS) consistently precedes multiple myeloma: a prospective study. *Blood* (2009) 113:5412–7. doi: 10.1182/blood-2008-12-194241
68. Schuster SR, Rajkumar SV, Dispenzieri A, Morice W, Aspitia AM, Ansell S, et al. IgM multiple myeloma: Disease definition, prognosis, and differentiation from Waldenstrom's macroglobulinemia. *Am J Hematol* (2010) 85:853–5. doi: 10.1002/ajh.21845
69. Ocio EM, del CD, Caballero Á, Alonso J, Paiva B, Pesoa R, et al. Differential Diagnosis of IgM MGUS and WM According to B-Lymphoid Infiltration by Morphology and Flow Cytometry. *Clin Lymphoma Myeloma Leukemia* (2011) 11:93–5. doi: 10.3816/clml.2011.n.017
70. Paiva B, Corchete LA, Vidriales M-B, García-Sanz R, Perez JJ, Aires-Mejia I, et al. The cellular origin and malignant transformation of Waldenström macroglobulinemia. *Blood* (2015) 125:2370–80. doi: 10.1182/blood-2014-09-602565
71. Tedeschi A, Conticello C, Rizzi R, Benevolo G, Laurenti L, Petrucci MT, et al. Diagnostic framing of IgM monoclonal gammopathy: Focus on Waldenström macroglobulinemia. *Hematol Oncol* (2019) 37:117–28. doi: 10.1002/hon.2539
72. Braggio E, Keats JJ, Leleu X, Wier SV, Jimenez-Zepeda VH, Valdez R, et al. Identification of Copy Number Abnormalities and Inactivating Mutations in Two Negative Regulators of Nuclear Factor-κB Signaling Pathways in Waldenström's Macroglobulinemia. *Cancer Res* (2009) 69:3579–88. doi: 10.1158/0008-5472.can-08-3701
73. Wenzl K, Manske MK, Sarangi V, Asmann YW, Greipp PT, Schoon HR, et al. Loss of TNFAIP3 enhances MYD88L265P-driven signaling in non-Hodgkin lymphoma. *Blood Cancer J* (2018) 8:97. doi: 10.1038/s41408-018-0130-3
74. Schop RFJ, Wier SAV, Xu R, Ghobrial I, Ahmann GJ, Greipp PR, et al. 6q deletion discriminates Waldenström macroglobulinemia from IgM monoclonal gammopathy of undetermined significance. *Cancer Genet Cytogen* (2006) 169:150–3. doi: 10.1016/j.cancergencyto.2006.04.009
75. Ocio EM, Schop RFJ, Gonzalez B, Wier SAV, Hernandez-Rivas JM, Gutierrez NC, et al. 6q deletion in Waldenström macroglobulinemia is associated with features of adverse prognosis. *Brit J Haematol* (2007) 136:80–6. doi: 10.1111/j.1365-2141.2006.06389.x
76. Young RM, Phelan JD, Wilson WH, Staudt LM. Pathogenic B-cell receptor signaling in lymphoid malignancies: New insights to improve treatment. *Immunol Rev* (2019) 291:190–213. doi: 10.1111/imr.12792
77. Ouk C, Roland L, Saintamand A, Gachard N, Thomas M, Devéza M, et al. B-cell enforced expression of the mouse ortholog of MYD88L265P is responsible for Waldenström-like B-cell lymphoma. *bioRxiv* (2019) 794024. doi: 10.1101/794024
78. Yu X, Li W, Deng Q, Li L, Hsi ED, Young KH, et al. MYD88 L265P Mutation in Lymphoid Malignancies. *Cancer Res* (2018) 78:2457–62. doi: 10.1158/0008-5472.can-18-0215
79. Munshi M, Liu X, Chen JG, Xu L, Tsakmaklis N, Demos MG, et al. SYK is activated by mutated MYD88 and drives pro-survival signaling in MYD88 driven B-cell lymphomas. *Blood Cancer J* (2020) 10:12. doi: 10.1038/s41408-020-0277-6
80. Perez-Riverol Y, Csordas A, Bai J, Bernal-Llinares M, Hewapathirana S, Kundu DJ, et al. The PRIDE database and related tools and resources in 2019: improving support for quantification data. *Nucleic Acids Res* (2018) 47:D442–50. doi: 10.1093/nar/gky1106

Conflict of Interest: The authors declare that the research was conducted in the absence of any commercial or financial relationships that could be construed as a potential conflict of interest.

frontiers in Immunology

MINI REVIEW
published: 24 February 2021
doi: 10.3389/fimmu.2021.639844

Pathologically Relevant Mouse Models for Epstein–Barr Virus–Associated B Cell Lymphoma

*Shiyu Huang and Tomoharu Yasuda**

Department of Immunology, Graduate School of Biomedical and Health Sciences, Hiroshima University, Hiroshima, Japan

The Epstein–Barr virus (EBV) is endemic in humans and can efficiently transform infected B cells under some circumstances. If an EBV carrier experiences immune suppression, EBV^+ B cells can turn into lymphoblasts and exhibit growth expansion that may cause lymphoproliferative diseases which often develop into lymphoma. Our immune system conducts surveillance for EBV^+ B cells in order to block spontaneous tumor formation. Here, we summarize the EBV products involved in tumorigenesis, EBV-associated lymphomas, and pathologically relevant mouse models. Preclinical mouse models for a range of EBV-associated diseases not only clear the path to new therapeutic approaches but also aid in our understanding of the nature of lymphomagenesis and immune surveillance.

Keywords: Epstein-Barr virus, B cell lymphoma, immune surveillance, mouse model, lymphoproliferative disease

OPEN ACCESS

Edited by:
Gema Perez-Chacon, Spanish National Cancer Research Center (CNIO), Spain

Reviewed by:
Peter Daniel Burrows, University of Alabama at Birmingham, United States
Michael Hummel, Charité – Universitätsmedizin Berlin, Germany

***Correspondence:**
Tomoharu Yasuda
yasudat@hiroshima-u.ac.jp

Specialty section:
This article was submitted to B Cell Biology, a section of the journal Frontiers in Immunology

Received: *10 December 2020*
Accepted: *01 February 2021*
Published: *24 February 2021*

Citation:
Huang S and Yasuda T (2021) Pathologically Relevant Mouse Models for Epstein–Barr Virus–Associated B Cell Lymphoma. Front. Immunol. 12:639844. doi: 10.3389/fimmu.2021.639844

INTRODUCTION

Epstein–Barr virus (EBV), an oncogenic γ herpes virus, is widespread in all human populations and persists in the vast majority of individuals throughout their lifetime. EBV preferentially infects B cells through the CD21/CR2 receptor on the surface of B cells, which is an entry receptor for viral envelope glycoprotein gp350. Viral glycoprotein gp42 interacts with cellular human leukocyte antigen (HLA) Class II molecules as a co-receptor, triggering fusion of the viral envelope with the cell membrane (1). Primary infection in young children is usually asymptomatic, but if infection is delayed until adolescence, it can cause infectious mononucleosis (IM) accompanied by EBV-infected B cell expansion and enormous T cell activation (2). After the acute phase of infection, EBV persists in a small subset of memory B cells (0.0001–0.005% of peripheral blood B cells) throughout the patient's lifetime, and is maintained as silent because of the specifically established memory T cells (3–5). Although EBV is usually a harmless passenger, immunocompromised individuals can develop severe complications. Genetic defects that lead to impaired T cell function predispose individuals to EBV-driven lymphoproliferative diseases or hematological diseases such as X-linked lymphoproliferative disease (XLP) or familial hemophagocytic lymphohistiocytosis (FHL) (6, 7). Lymphomas associated with post-transplant lymphoproliferative diseases (PTLDs) arising in patients receiving immunosuppressive drug treatment after organ transplantation are usually positive for EBV. Human immunodeficiency virus (HIV) infection can also lead to the development of EBV^+ lymphoma called acquired immunodeficiency syndrome (AIDS)-related lymphoma. Thus, in immune suppression, B cells carrying the EBV episome turn into activated lymphoblasts, which later often develop into lymphoma. Furthermore, several escape mechanisms from EBV-specific immunity lead to EBV^+ lymphoma even in immunocompetent people, including Burkitt lymphoma (BL), Hodgkin's lymphoma (HL), and non-Hodgkin's lymphoma (NHL). EBV may

TABLE 1 | EBV latency programs and EBV-associated lymphomas.

Latent programs	Latency I	Latency II	Latency III
Expressed EBV non-coding RNAs	EBER1/2, BART miRNAs	EBER1/2, BART miRNAs	EBER1/2, BART miRNAs
Expressed EBV mRNAs	EBNA1	EBNA1 LMP1, LMP2A, LMP2B	EBNA1 LMP1, LMP2A, LMP2B EBNA2, EBNA3A EBNA3B, EBNA3C EBNA-LP
Sensitivity to CTL	Resistant	Resistant ∼ Sensitive	Sensitive
EBV-associated lymphomas (Association, %)	BL, endemic (95–100) BL, sporadic (20–30) AIDS-BL (55) AIDS-PEL (90–100) AIDS-DLBCL-CB (30)	HL, Western world (40) HL, Children in Central America (90) AIDS-HL (100) DLBCL (10–15)	PTLD (80) AIDS-PCNSL (100) AIDS-DLBCL-IB (90)

AIDS, Acquired immunodeficiency syndrome; BART, BamHI-A rightward reading frame transcript; BL, Burkitt lymphoma; CB, Centroblast; CTL, Cytotoxic T-lymphocyte; DLBCL, Diffuse large B-cell lymphoma; EBERs, EBV-encoded small RNAs; EBNA, EBV nuclear antigen; HL, Hodgkin's lymphoma; IB, Immunoblast; LMP, Latent membrane protein; PCNSL, Primary central nervous system lymphoma; PEL, Primary effusion lymphoma; PTLD, Post-transplant lymphoproliferative disease.

also act as a passenger in cases in which malignant transformation occurs in an EBV-infected B-lymphocyte. Although many B cell malignancies are associated with EBV infection, the precise roles of EBV in the tumorigenic process and immune escape remain largely unknown. Therefore, the development of preclinical mouse models for EBV infection and the pathogenesis of EBV-associated lymphoma is important as it could open up new therapeutic modalities.

EBV PRODUCTS IN LATENTLY INFECTED B CELLS

Upon EBV infection, each infected cell carries multiple extrachromosomal copies of viral episomes and constitutively expresses a limited set of viral gene products called latent proteins. Among EBV-encoded genes, nine viral proteins can be expressed from latently infected EBV episomes to maintain the viral genome and regulate host B cell properties: EBV-nuclear antigens EBNA1, EBNA2, EBNA3A, EBNA3B, EBNA3C, EBNA-LP, and latent membrane proteins LMP1, LMP2A, and LMP2B. Additionally, it also expresses non-coding RNAs EBER1, EBER2, BART miRNAs, and BHRF-1 miRNAs. EBV exhibits one of four latency programs, latency 0, I, II, or III, depending on the status of B cells and lymphoma types (**Table 1**). EBV can persist in resting B cells without expressing viral genes escaping from the immune system for a long period (latency 0) or they can express either latency I, II, or III depending on the disease type (8).

LATENT MEMBRANE PROTEINS (LMPs)

LMP1 is an important oncogene encoded by EBV that is expressed in many types of EBV-associated lymphomas (**Table 1**). LMP1 containing intracellular signals and transmembrane domains can promote self-aggregation in the plasma membrane that transmits constitutive intracellular signal mimicking CD40, an important costimulatory molecule for B cells. LMP1 mimics an active CD40 receptor and recruits tumor necrosis factor (TNF) receptor–associated factor (TRAF) in the COOH terminal cytoplasmic region. LMP1 expression induces NF-κB and MAPK activation, and upregulates anti-apoptotic factors A20, Bcl-2, and proto-oncogene c-Myc. The expression of LMP1 in B cells induces blastic change and massive proliferation, which eventually transform B cells. EBV lacking LMP1 is unable to transform B cells (9, 10). It is of note that LMP1 expression is known to be heterogenous in B-NHL. A meta-analysis demonstrated that LMP1 expression is an unfavorable prognostic factor for overall survival in NHL patients (11). LMP2A also contains signaling and transmembrane domains that transmit constitutive signals mimicking the B cell receptor (BCR). LMP2A enhances the expression of genes related to cell cycle induction and apoptosis inhibition, and changes the expression of genes related to cell metabolism. LMP2A transmits signals through Lyn and Syk, which can replace BCR in B cell development (12, 13). EBV-associated lymphomas originate from germinal center (GC) B cells. Although the BCR signal plays an important role in GC-derived lymphoma cells, GC B cells characteristically downregulate BCR expression and its signal, suggesting that EBV may replace BCR function. In addition, lymphoma derived from GC B cells such as HLs often lose BCR expression because of deleterious somatic mutations in their immunoglobulin genes. Importantly, the EBV-mediated transformation of both BCR^+ and BCR^- GC B cells is strictly dependent on LMP2A expression (14).

EBV NUCLEAR ANTIGENS AND NON-CODING RNA

EBNA1 is a DNA-binding nuclear phospho-protein that plays a central role in the replication and maintenance of the episomal EBV genome. Directing EBNA1 expression to B cells in transgenic mice results in B cell lymphomas, suggesting that EBNA1 might have a direct role in oncogenesis, although there is no evidence explaining the direct role of EBNA1 in the immortalization or transformation of B cells (15). EBNA2 is expressed early after infection and has an important role in the immortalization of B cells through the induction of viral genes such as LMP1 and LMP2A. EBNA2, which mimics Notch in binding to RBP-Jκ and activating cellular target genes (most notably Myc), is an essential molecule in human B cell growth transformation by EBV (8, 16). A recent study identified EBNA2 as a lead player in tampering with the immunogenicity of EBV^+ B cell lymphoma by altering PD-L1 expression (17). The EBNA3 family are transcriptional regulators controlling RBP-Jκ activity, and thereby regulate the activity of cellular and

viral promoters. Studies with EBV recombinants have shown that EBNA3A and EBNA3C are essential for human B cell transformation *in vitro* whereas EBNA3B is non-essential (18). Recently, EBNA3A was shown to promote LMP1- and LMP2A-induced lymphomagenesis in mice by inhibiting the terminal differentiation of lymphoma progenitors and cooperating with c-Myc expression (19). EBNA-LP is not required for human B cell transformation *in vitro*, but is required for the efficient outgrowth of LCLs (20). EBNA-LP promotes the cell cycle through the induction of Cyclin D2 together with EBNA2 (21). The ability of EBNA-LP to enhance EBNA2-mediated transactivation suggests its importance in EBV-driven lymphomagenesis. In addition to the latent proteins, non-coding RNA, EBER1, and EBER2 are consistently expressed in all forms of latent EBV infection (**Table 1**). EBER blocks IFN-induced apoptosis by binding to dsRNA-activated protein kinase (PKR). The role of EBER in IL-10 production in BL cells has been shown. EBER promotes the induction of autocrine growth factors IL-10, IL-9, and insulin-like growth factor-1 (22). The transgenic expression of EBER1 in the mouse B cell compartment promotes hyperplasia and Myc-induced lymphoma development (23). Therefore, EBERs may contribute to tumor growth or escape from the immune system. BART miRNAs (encoding 44 mature BART miRNAs) are expressed in all latency types whereas BHRF1 miRNAs (encoding 4 mature BHRF1 miRNAs) are only expressed in type III latency. Although the aberrant expression of these miRNAs may be involved in transformation and tumor growth, the precise role has not yet been established (24).

BURKITT LYMPHOMA

BL was the first B cell lymphoma discovered to be associated with EBV. BL is characterized by c-Myc chromosomal translocation and is subdivided into three types, endemic, sporadic, and immunodeficiency, all of which are associated with EBV. Endemic and sporadic BL account for 95–100 and 20–30% of EBV-associated lymphomas, respectively (**Table 1**). Nearly all BL carries c-Myc/Ig translocation $t_{(8;14)}$, $t_{(2;8)}$, or $t_{(8;22)}$ leading to dysregulated c-Myc proto-oncogene expression, indicating the critical role of c-Myc in Burkitt lymphomagenesis (25). In EBV-positive BLs, only EBNA1 is expressed besides EBERs and BART miRNAs (latency I). Other EBV latent genes are downregulated, and lymphoma cells are thus hidden from EBV-specific host memory T cells. Functional inhibition of EBNA1 eradicates the EBV episome and prevents the malignant phenotype of EBV^+ BL cells (26, 27). The constitutive expression of c-Myc together with the active form of phosphoinositide-3-kinase (PI3K) in germinal center B cells, an origin of BL, synergistically induces mouse B cell lymphoma similar to human BL (28). This study suggests that the anti-apoptotic survival signal coinciding with constitutive c-Myc expression is sufficient and critical to the development of BL. Transgenic expression of EBER1 in B cells (Eμ-EBER1) together with c-Myc- or N-Myc promoted Myc-dependent lymphomagenesis, suggesting the role of EBER1 in lymphomagenesis (23). Because the synergistic effect of Myc and EBER1 was relatively mild compared to Myc and active PI3K, however, additional events promoting cell survival might be required for BL tumor formation. Indeed, oncogenic mutations in the pro-survival genes, cell cycle regulator, and transcriptional regulators were found (29), and these additional mutations might be required for the lymphomagenesis from Myc-translocated EBV^+ GC B cells.

HODGKIN'S LYMPHOMA

HL is characterized by atypical, large tumor cells known as Hodgkin and Reed–Sternberg (HRS) cells. These cells usually represent <1% of the tumor tissue; most tumor cells are non-malignant T cells and other immune cells (8). In the Western world, EBV is detected in ∼40% of HRS cells in classical HL. In Latin America, nearly all cases of HL in children are EBV-positive. In EBV-positive cases, three EBV proteins, EBNA1, LMP1, and LMP2A, are expressed (latency II). HRS cells are equipped with mechanisms to escape immune surveillance, including the downregulation of MHC class I and II, and the overexpression of CTL suppressor molecules, such as PD-L1, PD-L2, TGF-β, IL-10, Gal-1, Fas-L, and Treg-attracting chemokines (30). HRS cells originate from GC B cells. The rearranged Ig V genes of HRS are somatically mutated but lack intra-clonal diversity, indicating that the SHM machinery is silenced in tumor cells. Interestingly, 25% of HRS cells carry non-sense or deleterious mutations in the functional immunoglobulin gene. GC B cells that acquire such crippling mutations are normally eliminated by apoptosis in the GC reaction, but the expression of LMP2A by EBV infection might allow the survival of GC B cells with crippling mutations as LMP2A could replace BCR (12, 13). To date, no mouse models relevant to HL disease have been successfully established.

DIFFUSE LARGE B CELL LYMPHOMA

Diffuse large B cell lymphoma (DLBCL) is the most common lymphoid malignant tumor, accounting for 30–40% of NHL derived from GC B cells. DLBCL occurs primarily in elderly adults, less frequently in young adults, and rarely in children. Approximately 10–15% of patients are EBV^+ DLBCL, and this is most prevalent in Asia (31, 32). The large B cells in EBV^+ DLBCL are clonal centroblastic B cells, which in most cases, express the latency II program (33). Several studies have reported how these EBV^+ lymphoma cells escape host immune surveillance. Senescence of the immune system related to the aging process that leads to the defective surveillance of EBV may play a role in pathogenesis (33). The dysregulated expression of PD-L1 and PD-L2 caused by a genetic truncation of 3′-UTR has also been identified in EBV^+ DLBCL, but not in EBV- DLBCL, which provides another explanation of why highly immunogenic EBV^+ DLBCL can escape immune surveillance in young adults (34).

POST-TRANSPLANT LYMPHOPROLIFERATIVE DISEASE

Post-transplant lymphoproliferative disease (PTLD) encompasses a heterogenous group of lymphocytic proliferations characterized by the proliferative expansion of lymphocytes, mostly EBV^+ B cells, in immunocompromised patients due to

treatment with immunosuppressive drugs after solid organ or hematopoietic stem cell transplantation. PTLD typically exhibits type III latency features. The World Health Organization (WHO) classification categorizes the disease into IM-like early lesions, polymorphic lymphomas (P-PTLD), and monomorphic lymphomas (M-PTLD). Virtually all early lesions are polyclonal and do not have any known molecular alterations. Many P-PTLDs and most M-PTLDs are clonal. Compared to P-PTLD, M-PTLDs harbor more karyotypic abnormalities. A murine PTLD model expressing LMP1 in B cells in which breaking immune surveillance results in rapid, fatal lymphoproliferation and lymphomagenesis has been established (35) (**Figure 1C**).

ACQUIRED IMMUNODEFICIENCY SYNDROME–RELATED LYMPHOMA

EBV-positive lymphomas are highly associated with immunocompromised patients who have AIDS caused by human immunodeficiency virus (HIV) infection (**Table 1**). In AIDS patients, the incidences of DLBCL, HL, BL, primary central nervous system lymphoma (PCNSL), and primary effusion lymphoma (PEL) are increased because of the lack of T cell–mediated immune surveillance, which suggests that $CD4^+$ T cells play central roles. EBV-positive rates in these lymphomas are extremely high (90–100% of PCNSL, HL, PEL, and immunoblastic DLBCL; 30–70% of BL and centroblastic DLBCL), indicating the important role of EBV in the development of lymphoma in AIDS patients (8, 36). The cellular origin of those lymphomas are thought to be mostly V gene–mutated GC B cells or post GC B cells.

EBV-SEROPOSITIVE HUMAN PERIPHERAL BLOOD B CELL TRANSFER MODEL

Injection of human peripheral blood lymphocytes (PBLs) from EBV-seropositive donors into severe combined immunodeficient (SCID) mice allows the development of EBV^+ B cell tumors within weeks that resemble the lymphoblastoid cell line (LCL) generated by EBV infection of normal B cells *in vitro* (**Figure 1A**). The PBL-derived tumors resembling EBV^+ large cell lymphoma in immunosuppressed patients formed monoclonal or oligoclonal foci (37). The remarkable efficiency of clonal tumor development in the human PBL-SCID model suggests that lymphomagenesis involves the direct outgrowth of EBV-transformed B cells without the requirement of secondary genetic alterations. This transfer model is unable to induce a host immune response to EBV^+ B cells, however, which should happen in lymphoproliferative diseases or lymphomas.

MOUSE MODELS OF EBV INFECTION AND ASSOCIATED MALIGNANCIES

Human beings are the only natural host of EBV. As only New World monkeys can be infected by EBV experimentally, there is a major limitation to using primates as an animal model of EBV-associated pathogenesis. Mice reconstituted with human immune cells, called humanized mice, have been developed to address the pathology of human hematopoietic cells, including EBV infection to human B cells (**Figure 1B**). Transplantation of human HSCs into severely immunocompromised mice such as $Rag2^{-/-}$ $\gamma c^{-/-}$, NOD-SCID, and NOD-SCID $\gamma c^{-/-}$ mice allows the reconstitution of a functional human immune system, including B cells, T cells, natural killer (NK) cells, dendritic cells (DCs), and macrophages. The administration of live EBV to those reconstituted mice successfully infected the reconstituted human B cells, developed $LMP1^+$ B cell proliferation, and mounted human MHC class I– and class II–restricted adaptive immune responses to EBV infection (38–40). Although this system has critical problems in human T cell selection on a mouse thymic background and the T cells generated a discriminated self from allogeneic MHC, this approach provides a tool with which to study pathogens that specifically target the human immune system and to test potential therapeutic interventions.

GENETICALLY ENGINEERED EBV MODELS

The reconstitution of EBV pathogenesis as well as lymphomagenesis through the conditional and timed expression of limited EBV molecules in mice without virus infection is challenging. We previously generated mice expressing LMP1 specifically in B cells in early development (CD19-Cre; R26LMP1 mouse, PTLD-like lymphoma model) (**Figure 1C**). Similar to EBV-infected human B cells, $LMP1^+$ mouse B cells were efficiently eliminated by T cells whereas disrupting immune surveillance resulted in rapid, fatal lymphoproliferation and lymphomagenesis (35). These results indicate the central role of LMP1 in the surveillance and transformation of EBV-infected B cells *in vivo*, and resulted in the establishment of the first preclinical mouse model for immune suppression-dependent lymphomagenesis.

The acute EBV infection of naïve B cells in mice can be modeled through the timed expression of LMP1 and LMP2A by tamoxifen-mediated Cre recombination (CD19-CreERT2; R26LMP1/LMP2A mouse) (**Figure 1D**). Although lethal when induced in all B cells, the induction of LMP1 and LMP2A in just a few naïve B cells initiated a phase of rapid B cell expansion followed by a proliferative T cell response that cleared the LMP-expressing B cells. Interfering with T cell activity prevented the clearance of LMP-expressing B cells (41, 42). Using this system, primary human immunodeficiency diseases can be reconstructed, such as perforin (Prf1)-deficient FHL (**Figure 1E**), which causes a life-threatening EBV-related immunoproliferative syndrome in humans (42). Thus, the timed expression of LMP1 together with LMP2A in subsets of mouse B cells allows the study of the major clinically relevant features of human EBV infection *in vivo,* thereby providing a unique animal model that may be useful for therapeutic testing.

As described above, although EBV infection in humanized mice has been successfully used to recapitulate virally driven B cell lymphomagenesis, this approach completely lacks the

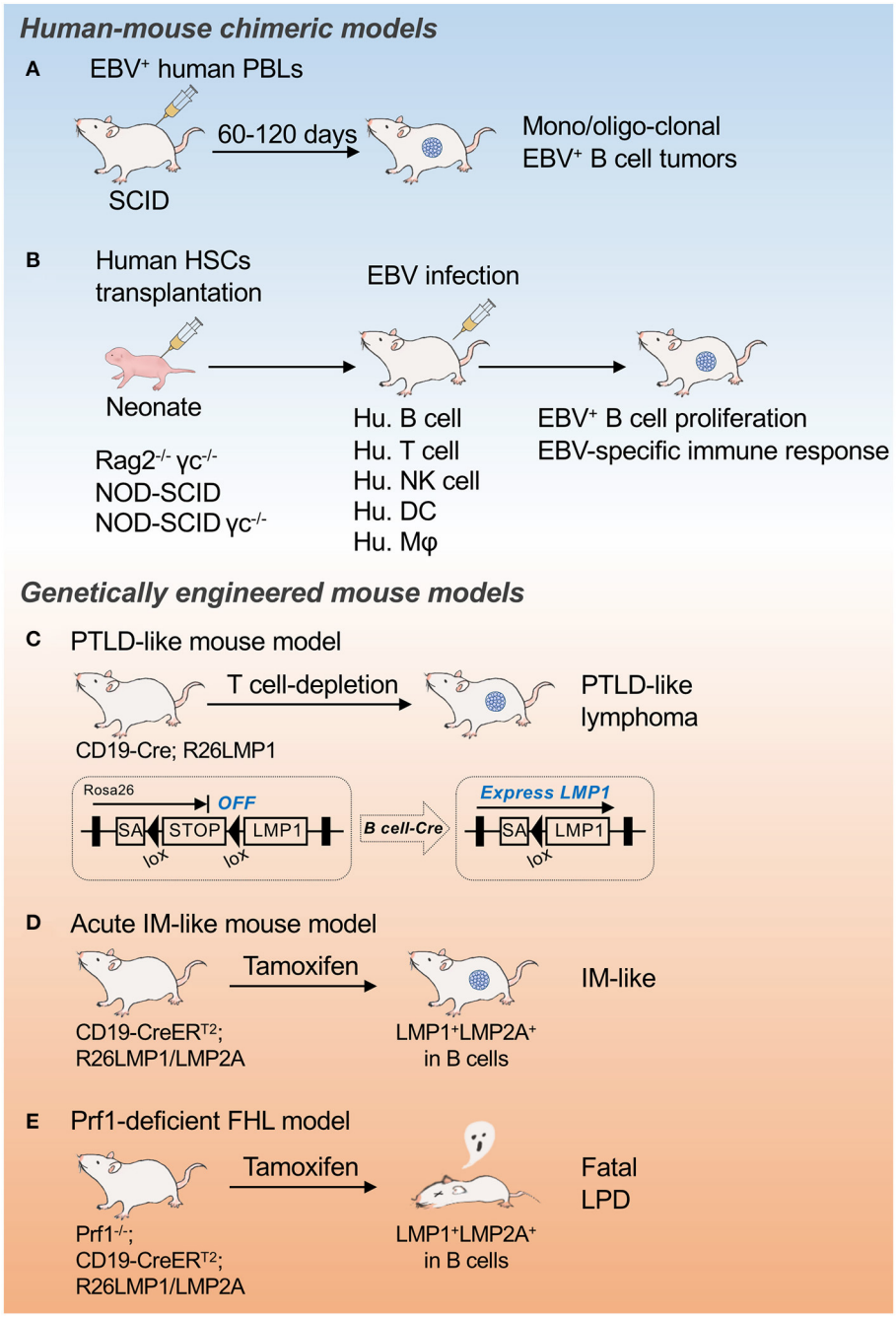

FIGURE 1 | Mouse models for EBV infection and associated malignancies. Schematic illustrations of EBV-seropositive human peripheral blood B cell transfer model **(A)**, Mouse models of EBV infection and associated malignancies **(B)**, PTLD-like mouse model **(C)**, Acute IM-like mouse model **(D)**, and Prf1-deficient FHL model **(E)**. SA, splice acceptor; PBL, peripheral blood lymphocytes; PTLD, post-transplant lymphoproliferative disease; IM, infectious mononucleosis; FHL, familial hemophagocytic lymphohistiocytosis; LPD, lymphoproliferative disease.

hematopoietic cell environment that should be generated normally (43). As such, it remains meaningful to study lymphomagenesis in mouse models that induce EBV-driven lymphoma in an *in vivo* environment that contains naturally occurring T cells after education and selection, and that also carries a normal set of innate and acquired immune cells with a uniform genetic background. Furthermore, mouse cytokines and chemokines cannot fully support human hematopoiesis and *in vivo* dynamics of human immune cells. A genetic engineering approach has been used to attempt an immunocompromised latency III-like lymphoma model in which EBNA3A, LMP1, and LMP2A are simultaneously

expressed in GC B cells. In immunocompetent mice, B cells expressing EBV genes are efficiently eliminated by T cells; however, in immunocompromised recipient mice, tumors similar to human EBV^+ lymphomas were formed. EBNA3A or a recurrent activating mutation of the B cell transcription factor EBF1, a functional proxy of EBNA3A, interplays with other EBV oncogenes in B cell transformation (19).

CONCLUSION

Genetic mouse models have shown that the expression of LMP1 is sufficient to model the major features of EBV infection in mice, namely, immunogenicity and tumorigenesis, despite the fact that EBV is endemic to humans. This is of particular interest because the T cell–mediated immune surveillance of $LMP1^+$ B cells stands in contrast to the belief that the human immune system has evolved to prevent the expansion of EBV-infected B cells. The virus might have evolved to be recognized by the mammalian immune system, likely because lifelong latent infection is advantageous over fatal infection. The development of preclinical mouse models for a range of EBV-associated pathologies is challenging but may open the path to the development of new therapeutic approaches.

AUTHOR CONTRIBUTIONS

SH wrote the manuscript and prepared the figure and table. TY conceptualized and wrote the manuscript and edited the figure and table. Both authors contributed to the article and approved the submitted version.

FUNDING

This work was supported by the Japan Society for the Promotion of Science (JSPS), Grant-in Aid for Research Activity Start-up 17H06937 (TY), Grant-in Aid for Scientific Research (B) 18H02669 (TY), Grant-in Aid for Challenging Research (Exploratory) 19K22538 TY, The Senshin Medical Research Foundation (TY), The Friends of Leukemia Research Fund (TY), and The Core Research for Organelle Diseases in Hiroshima University (the MEXT program for promoting the enhancement of research universities, Japan) (TY).

ACKNOWLEDGMENTS

We thank K. Rajewsky (Max Delbrück Center for Molecular Medicine, Germany) for critical discussion and support of the work. We thank N. Kikkawa for the secretarial help.

REFERENCES

1. Young LS, Rickinson AB. Epstein-Barr virus: 40 years on. *Nat Rev Cancer.* (2004) 4:757–68. doi: 10.1038/nrc1452
2. Cohen JI. Epstein–Barr virus infection. *N Engl J Med.* (2000) 343:481–92. doi: 10.1056/NEJM200008173430707
3. Khan G, Miyashita EM, Yang B, Babcock GJ, Thorley-Lawson DA. Is EBV persistence *in vivo* a model for B cell homeostasis? *Immunity.* (1996) 5:173–9. doi: 10.1016/S1074-7613(00)80493-8
4. Babcock GJ, Decker LL, Volk M, Thorley-Lawson DA. EBV persistence in memory B cells *in vivo*. *Immunity.* (1998) 9:395–404. doi: 10.1016/S1074-7613(00)80622-6
5. Hislop AD, Taylor GS, Sauce D, Rickinson AB. Cellular responses to viral infection in humans: lessons from Epstein-Barr virus. *Annu Rev Immunol.* (2007) 25:587–617. doi: 10.1146/annurev.immunol.25.022106.141553
6. Parvaneh N, Filipovich AH, Borkhardt A. Primary immunodeficiencies predisposed to Epstein-Barr virus-driven haematological diseases. *Br J Haematol.* (2013) 162:573–86. doi: 10.1111/bjh.12422
7. Sieni E, Cetica V, Hackmann Y, Coniglio ML, Da Ros M, Ciambotti B, et al. Familial hemophagocytic lymphohistiocytosis: when rare diseases shed light on immune system functioning. *Front Immunol.* (2014) 5:167. doi: 10.3389/fimmu.2014.00167
8. Küppers R. B cells under influence: transformation of B cells by Epstein-Barr virus. *Nat Rev Immunol.* (2003) 3:801–12. doi: 10.1038/nri1201
9. Young LS, Dawson CW, Eliopoulos AG. The expression and function of Epstein-Barr virus encoded latent genes. *Mol Pathol.* (2000) 53:238–47. doi: 10.1136/mp.53.5.238
10. Thorley-Lawson DA. Epstein-Barr virus: exploiting the immune system. *Nat Rev Immunol.* (2001) 1:75–82. doi: 10.1038/35095584
11. Mao Y, Lu MP, Lin H, Zhang DW, Liu Y, Li QD, et al. Prognostic significance of EBV latent membrane protein 1 expression in lymphomas: evidence from 15 studies. *PLoS ONE.* (2013) 8:e60313. doi: 10.1371/journal.pone.0060313
12. Caldwell RG, Wilson JB, Anderson SJ, Longnecker R. Epstein-Barr virus LMP2A drives B cell development and survival in the absence of normal B cell receptor signals. *Immunity.* (1998) 9:405–11. doi: 10.1016/S1074-7613(00)80623-8
13. Casola S, Otipoby KL, Alimzhanov M, Humme S, Uyttersprot N, Kutok JL, et al. B cell receptor signal strength determines B cell fate. *Nat Immunol.* (2004) 5:317–27. doi: 10.1038/ni1036
14. Mancao C, Hammerschmidt W. Epstein-Barr virus latent membrane protein 2A is a B-cell receptor mimic and essential for B-cell survival. *Blood.* (2007) 110:3715–21. doi: 10.1182/blood-2007-05-090142
15. Wilson JB, Bell JL, Levine AJ. Expression of Epstein-Barr virus nuclear antigen-1 induces B cell neoplasia in transgenic mice. *EMBO J.* (1996) 15:3117–26. doi: 10.1002/j.1460-2075.1996.tb00674.x
16. Cohen JI, Wang F, Mannick J, Kieff E. Epstein-Barr virus nuclear protein 2 is a key determinant of lymphocyte transformation. *Proc Natl Acad Sci USA.* (1989) 86:9558–62. doi: 10.1073/pnas.86.23.9558
17. Anastasiadou E, Stroopinsky D, Alimperti S, Jiao, AL, Pyzer AR, et al. Epstein–Barr virus-encoded EBNA2 alters immune checkpoint PD-L1 expression by downregulating miR-34a in B-cell lymphomas. *Leukemia.* (2019) 33:132–47. doi: 10.1038/s41375-018-0178-x
18. Rowe M, Young LS, Cadwallader K, Petti L, Kieff E, Rickinson AB. Distinction between Epstein-Barr virus type A (EBNA 2A) and type B (EBNA 2B) isolates extends to the EBNA 3 family of nuclear proteins. *J Virol.* (1989) 63:1031–9. doi: 10.1128/JVI.63.3.1031-1039.1989
19. Sommermann T, Yasuda T, Ronen J, Wirtz T, Weber T, Sack U, et al. Functional interplay of Epstein-Barr virus oncoproteins in a mouse model of B cell lymphomagenesis. *Proc Natl Acad Sci USA.* (2020) 117:14421–32. doi: 10.1073/pnas.1921139117
20. Mannick JB, Cohen JI, Birkenbach M, Marchini A, Kieff E. The Epstein-Barr virus nuclear protein encoded by the leader of the EBNA RNAs is important in B-lymphocyte transformation. *J Virol.* (1991) 65:6826–37. doi: 10.1128/JVI.65.12.6826-6837.1991
21. Sinclair AJ, Palmero I, Peters G, Farrell PJ. EBNA-2 and EBNA-LP cooperate to cause G0 to G1 transition during immortalization of resting human B lymphocytes by Epstein-Barr virus. *EMBO J.* (1994) 13:3321–8. doi: 10.1002/j.1460-2075.1994.tb06634.x
22. Iwakiri D, Takada K. Role of EBERs in the pathogenesis of EBV infection. *Adv Cancer Res.* (2010) 107:119–36. doi: 10.1016/S0065-230X(10)07004-1
23. Repellin CE, Tsimbouri PM, Philbey AW, Wilson JB. Lymphoid hyperplasia and lymphoma in transgenic mice expressing the small

non-coding RNA, EBER1 of Epstein-Barr virus. *PLoS ONE.* (2010) 5:e9092. doi: 10.1371/journal.pone.0009092
24. Kim H, Iizasa H, Kanehiro Y, Fekadu S, Yoshiyama H. Herpesviral microRNAs in cellular metabolism and immune responses. *Front Microbiol.* (2017) 8:1318. doi: 10.3389/fmicb.2017.01318
25. Hecht JL, Aster JC. Molecular biology of Burkitt's lymphoma. *J Clin Oncol.* (2000) 18:3707–21. doi: 10.1200/JCO.2000.18.21.3707
26. Nasimuzzaman M, Kuroda M, Dohno S, Yamamoto T, Iwatsuki K, Matsyzaki S, et al. Eradication of epstein-barr virus episome and associated inhibition of infected tumor cell growth by adenovirus vector-mediated transduction of dominant-negative EBNA1. *Mol Ther.* (2005) 11:578–90. doi: 10.1016/j.ymthe.2004.12.017
27. Vereide DT, Sugden B. Lymphomas differ in their dependence on Epstein-Barr virus. *Blood.* (2011) 117:1977–85. doi: 10.1182/blood-2010-05-285791
28. Sander S, Calado DP, Srinivasan L, Köchert K, Zhang B, Rosolowski M, et al. Synergy between PI3K signaling and MYC in Burkitt lymphomagenesis. *Cancer Cell.* (2012) 22:167–79. doi: 10.1016/j.ccr.2012.06.012
29. Schmitz R, Ceribelli M, Pittaluga S, Wright G, Staudt LM. Oncogenic mechanisms in Burkitt lymphoma. *Cold Spring Harb Perspect Med.* (2014) 4:a014282. doi: 10.1101/cshperspect.a014282
30. De Goycoechea D, Stalder G, Martins F, Duchosal MA. Immune checkpoint inhibition in classical Hodgkin lymphoma: from early achievements towards new perspectives. *J Oncol.* (2019) 7:9513701. doi: 10.1155/2019/9513701
31. Park S, Lee J, Ko YH, Han A, Jun HJ, Lee SC, et al. The impact of Epstein-Barr virus status on clinical outcome in diffuse large B-cell lymphoma. *Blood, J Am Soc Hematol.* (2007) 110:972–8. doi: 10.1182/blood-2007-01-067769
32. Zhou Y, Xu Z, Lin W, Duan Y, Lu C, Liu W, et al. Comprehensive genomic profiling of EBV-positive diffuse large B-cell lymphoma and the expression and clinicopathological correlations of some related genes. *Front Oncol.* (2019) 9:683. doi: 10.3389/fonc.2019.00683
33. Nicolae A, Pittaluga S, Abdullah S, Steinberg SM, Pham TA, Davies-Hill T, et al. EBV-positive large B-cell lymphomas in young patients: a nodal lymphoma with evidence for a tolerogenic immune environment. *Blood.* (2015) 126:863–72. doi: 10.1182/blood-2015-02-630632
34. Kataoka K, Miyoshi H, Sakata S, Dobashi A, Couronné L, Kogure Y, et al. Frequent structural variations involving programmed death ligands in Epstein-Barr virus-associated lymphomas. *Leukemia.* (2019) 33:1687–99. doi: 10.1038/s41375-019-0380-5
35. Zhang B, Kracker S, Yasuda T, Casola S, Vanneman M, Hömig-Hölzel C, et al. Immune surveillance and therapy of lymphomas driven by Epstein-Barr virus protein LMP1 in a mouse model. *Cell.* (2012) 148:739–51. doi: 10.1016/j.cell.2011.12.031
36. Bibas M, Antinori A. EBV and HIV-Related Lymphoma. *Mediterr J Hematol Infect Dis.* (2009) 1:e2009032. doi: 10.4084/MJHID.2009.032
37. Rowe M, Young LS, Crocker J, Stokes H, Henderson S, Rickinson AB. Epstein-Barr virus (EBV)-associated lymphoproliferative disease in the SCID mouse model: Implications for the pathogenesis of EBV-positive lymphomas in man. *J Exp Med.* (1991) 173:147–58. doi: 10.1084/jem.173.1.147
38. Traggiai E, Chicha L, Mazzucchelli L, Bronz L, Piffaretti JC, Lanzavecchia A, et al. Development of a human adaptive immune system in cord blood cell-transplanted mice. *Science.* (2004) 304:104–7. doi: 10.1126/science.1093933
39. Melkus MW, Estes JD, Padgett-Thomas A, Gatlin J, Denton PW, Othieno FA, et al. Humanized mice mount specific adaptive and innate immune responses to EBV and TSST-1. *Nat Med.* (2006) 12:1316–22. doi: 10.1038/nm1431
40. Yajima M, Imadome KI, Nakagawa A, Watanabe S, Terashima K, Nakamura H, et al. A new humanized mouse model of Epstein-Barr virus infection that reproduces persistent infection, lymphoproliferative disorder, and cell-mediated and humoral immune responses. *J Infect Dis.* (2008) 198:673–82. doi: 10.1086/590502
41. Yasuda T, Wirtz T, Zhang B, Wunderlich T, Schmidt-Supprian M, Sommermann T, et al. Studying Epstein-Barr virus pathologies and immune surveillance by reconstructing EBV infection in mice. *Cold Spring Harb Symp Quant Biol.* (2013) 78:259–63. doi: 10.1101/sqb.2013.78.020222
42. Wirtz T, Weber T, Kracker S, Sommermann T, Rajewsky K, Yasuda T. Mouse model for acute Epstein-Barr virus infection. *Proc Natl Acad Sci USA.* (2016) 113:13821–6. doi: 10.1073/pnas.1616574113
43. Christian M. Humanized mouse models for Epstein Barr virus infection. *Curr Opin Virol.* (2017) 25:113–8. doi: 10.1016/j.coviro.2017.07.026

Conflict of Interest: The authors declare that the research was conducted in the absence of any commercial or financial relationships that could be construed as a potential conflict of interest.

frontiers in Immunology

ORIGINAL RESEARCH
published: 09 March 2021
doi: 10.3389/fimmu.2021.627020

A Detailed Analysis of Parameters Supporting the Engraftment and Growth of Chronic Lymphocytic Leukemia Cells in Immune-Deficient Mice

*Piers E. M. Patten[1,2], Gerardo Ferrer[1], Shih-Shih Chen[1], Jonathan E. Kolitz[1,3], Kanti R. Rai[1,3], Steven L. Allen[1,3], Jacqueline C. Barrientos[1,3], Nikolaos Ioannou[2], Alan G. Ramsay[2] and Nicholas Chiorazzi[1,3,4]**

[1] Institute of Molecular Medicine, Karches Center for Oncology Research, The Feinstein Institutes for Medical Research, Northwell Health, Manhasset, NY, United States, [2] Faculty of Life Sciences & Medicine, School of Cancer & Pharmaceutical Sciences, Comprehensive Cancer Centre, Institute of Haematology, King's College London, London, United Kingdom, [3] Department of Medicine, Zucker School of Medicine at Hofstra/Northwell, Hempstead, NY, United States, [4] Department of Molecular Medicine, Zucker School of Medicine at Hofstra/Northwell, Hempstead, NY, United States

OPEN ACCESS

Edited by:
Juan M. Zapata, Consejo Superior de Investigaciones Científicas (CSIC), Spain

Reviewed by:
Carlos Cuesta-Mateos, Hospital de la Princesa, Spain
Silvia Deaglio, University of Turin, Italy

***Correspondence:**
Nicholas Chiorazzi
NChizzi@Northwell.edu

Specialty section:
This article was submitted to B Cell Biology, a section of the journal Frontiers in Immunology

Received: *07 November 2020*
Accepted: *11 January 2021*
Published: *09 March 2021*

Citation:
Patten PEM, Ferrer G, Chen S-S, Kolitz JE, Rai KR, Allen SL, Barrientos JC, Ioannou N, Ramsay AG and Chiorazzi N (2021) A Detailed Analysis of Parameters Supporting the Engraftment and Growth of Chronic Lymphocytic Leukemia Cells in Immune-Deficient Mice. Front. Immunol. 12:627020. doi: 10.3389/fimmu.2021.627020

Patient-derived xenograft models of chronic lymphocytic leukemia (CLL) can be created using highly immunodeficient animals, allowing analysis of primary tumor cells in an *in vivo* setting. However, unlike many other tumors, CLL B lymphocytes do not reproducibly grow in xenografts without manipulation, proliferating only when there is concomitant expansion of T cells. Here we show that *in vitro* pre-activation of CLL-derived T lymphocytes allows for a reliable and robust system for primary CLL cell growth within a fully autologous system that uses small numbers of cells and does not require pre-conditioning. In this system, growth of normal T and leukemic B cells follows four distinct temporal phases, each with characteristic blood and tissue findings. Phase 1 constitutes a period during which resting CLL B cells predominate, with cells aggregating at perivascular areas most often in the spleen. In Phase 2, T cells expand and provide T-cell help to promote B-cell division and expansion. Growth of CLL B and T cells persists in Phase 3, although some leukemic B cells undergo differentiation to more mature B-lineage cells (plasmablasts and plasma cells). By Phase 4, CLL B cells are for the most part lost with only T cells remaining. The required B-T cell interactions are not dependent on other human hematopoietic cells nor on murine macrophages or follicular dendritic cells, which appear to be relatively excluded from the perivascular lymphoid aggregates. Notably, the growth kinetics and degree of anatomic localization of CLL B and T cells is significantly influenced by intravenous versus intraperitoneal administration. Importantly, B cells delivered intraperitoneally either remain within the peritoneal cavity in a quiescent state, despite the presence of dividing T cells, or migrate to lymphoid tissues where they actively divide; this dichotomy mimics the human condition in that cells in primary lymphoid tissues and the blood are predominately resting, whereas those in secondary lymphoid tissues

proliferate. Finally, the utility of this approach is illustrated by documenting the effects of a bispecific antibody reactive with B and T cells. Collectively, this model represents a powerful tool to evaluate CLL biology and novel therapeutics *in vivo*.

Keywords: chronic lymphocytic leukemia, patient-derived xenograft, engraftment, growth, T cells, B cells

INTRODUCTION

Patient-derived xenograft (PDX) models of chronic lymphocytic leukemia (CLL) can help analyze the biology of primary leukemic B and T cells in an *in vivo* setting (1–7). However, creating successful xenografts requires surmounting several inherent barriers, the most significant being the transfer and growth for a relatively long period of time of cells of one species into recipients of another. This difficulty has been obviated to a great degree by using severely immune-deficient mice lacking mature T cells, B cells and NK cells ("alymphoid mice"). A commonly used recipient strain of such mice is the NOD-*scid* IL2Rgamma^{null} animal, referred to as the "NSG" mouse. Another major barrier to successful xenografting is pulling together sufficient environmental cues, from the donor and/or the host, to allow not only the survival but also the growth of the transferred cell population.

We previously used NSG animals to develop a PDX model in which transfer of CLL peripheral blood mononuclear cells (PBMCs) along with allogeneic antigen-presenting cells (APCs) led to *in vivo* CLL-derived T-cell activation that promoted survival and growth of the leukemic cells (4). In this model, the presence of activated T cells was essential for successful CLL B-cell proliferation since CLL B-cell growth was only found when concomitant expansion of autologous T cells was observed. Moreover, elimination of T lymphocytes, in particular CD4$^+$ cells, at the initiation of engraftment prevented growth of the leukemic B cells (4).

This approach has advantages and disadvantages. Positive aspects include the simplicity of the technique, the relatively small numbers of CLL B and T cells needed to achieve a productive outcome, and the ready promotion of CLL-cell growth *in vivo*. The major negative feature is the dependence on T-cell activation taking place *in vivo* as a consequence of the donor T cells recognizing the foreign histocompatibility antigens of the provoking, co-administered human APCs. Although effective in most instances, the level of histocompatibility difference between the antigen-presenting cell of the normal donor and the T lymphocytes from the CLL-cell donor is rarely, if ever known. Therefore, the extent and degree of CLL T-cell activation that can occur in the recipient animals differs and is not readily predictable and quantifiable in advance of cell transfer. Consequently, the extent of T-cell help provided for leukemic B-cell proliferation cannot be foretold and controlled to make robust comparisons between experiments involving a diverse set of donors.

Here we address the hypothesis that *in vitro* pre-activation of CLL-derived T lymphocytes prior to xenografting with autologous CLL cells provides a more reliable and constant source, on a per cell basis, of T-cell help for the growth of leukemic B cells in NSG recipients. We show that this approach leads to reproducible growth of primary CLL cells within a fully autologous system using limited numbers of leukemic cells from a broad range of patients. We also detail extensive studies of CLL-cell proliferation and how these relate to CLL-derived human T cells, murine hematopoietic and non-hematopoietic cells, route of administration, and the need to pre-condition recipients. An example of the utility of these improvements in testing the efficacy of a novel therapeutic is provided.

MATERIALS AND METHODS

Chronic Lymphocytic Leukemia Patient Samples and Characterization

In accordance with the Declaration of Helsinki and as approved by the Institutional Review Board of Northwell Health, after obtaining informed consent, blood was collected from 19 CLL patients for whom clinical information, laboratory data, and *IGHV-IGHD-IGHJ* DNA sequences [**Table 1** and (8)] were available. PBMCs were separated by density gradient centrifugation using Ficoll Paque Plus (GE Healthcare Life Sciences) and cryopreserved until use in RPMI-1640 medium (Invitrogen) supplemented with 10% heat-inactivated fetal bovine serum (FBS, Atlanta Biologicals).

Xenogeneic Transplantation

Four to 8 week old NOD-scid IL2Rgamma^{null} ("NSG^{TM}", Jackson Laboratory) mice were used as xenograft recipients for cryopreserved CLL cells from only a single donor. If a sample had reduced viability, it was centrifuged through a Ficoll gradient to remove excess dead cells. For those experiments where extent of cell division was determined *in vivo*, cells were incubated 10 minutes at 37°C with CFSE (2.5μM; Invitrogen) and washed with cold culture medium just before transfer.

For those experiment requiring activated autologous T lymphocytes, CD3$^+$ cells from a single CLL patient were enriched from PBMCs using anti-CD3 microbeads (Miltenyi Biotec) by following the manufacturer's recommended protocol. Then, 1 × 10^6 CD3$^+$cells per mL were cultured for 3–14 days with 25 μl of human T-Activator CD3/CD28 Dynabeads (Invitrogen) and 30 units of IL-2 (R&D) per mL of cells in culture medium (RPMI-1640 supplemented with 10% heat-inactivated FBS and antibiotics (GE Healthcare Life Sciences)) at 37°C, 95% humidity and 5% of CO_2. Cultures were maintained at 1 × 10^6 cells/mL with fresh culture medium containing IL-2. In those instances when cells were cultured for > 7 days, beads were removed using a magnet, and the CD3$^+$cells were re-exposed to new anti-CD3/

TABLE 1 | Characteristics of the patients used in this study.

Patient ID #	Ig Isotype	*IGHV*	*IGHV* mutation status	Cytogenetics							
				6q23.3	11q13	11q22.3	12 centromere	13q14.3	13q34	14q32	17p13
0515	IgM	4-39	U	N	N	N	N	A	N	N	N
0545	IgM	3-30	M	N	N	N	N	N	N	N	N
0854	IgM	1-03	M	ND	ND	N	N	A	N	ND	N
1083	IgM	4-b	U	N	N	A	N	A	N	N	N
1122	IgM	3-09	U	ND	N	N	A	N	N	N	N
1164	IgM	4-34	M	N	N	N	N	N	N	N	N
1279	IgM	1-02	U	ND	ND	N	N	A	N	N	N
1301	IgM	4-31	U	N	N	N	A	N	N	N	N
1429	IgG	3-48	M	N	ND	N	N	A	N	ND	N
1435	IgM	1-08	M	N	N	N	N	N	N	N	N
1463	IgM	3-21	M	N	N	N	N	A	N	N	N
1493	ND	33-03	M	N	N	N	N	A	N	N	N
1523	IgM	3-48	U	ND	N	N	N	A	N	N	N
1539	IgM	3-30	M	ND	ND	N	N	A	ND	ND	A
1552	ND	1-18	M	N	N	N	N	A	N	N	N
1623	IgM	2-70	M	ND	ND	ND	ND	ND	ND	ND	ND
1925	ND	3-11	U	N	N	A	N	A	N	N	N
2030	ND	3-30	U	A	A	N	N	A	A	A	N
2156	IgM	V5-51	U	N	N	A	N	A	N	N	N

IGHV mutation status is mutated (M) if the expressed IGHV sequence is >2% different from germline; otherwise it is considered IGHV-unmutated (U).
Cytogenetics was assigned as abnormal (A) or normal (N) by FISH.
ND, Not done.

28 beads and fresh culture medium. At the end of the T-cell activation period, autologous CLL PBMCs from the same patient (all experiments) were thawed and evaluated by trypan blue (Thermo Fischer Scientific).

Then 20×10^6 viable PBMCs were mixed with $CD3^+$ (at a 1:40 ratio of $CD3^+$ cells: PBMCs) or without $CD3^+$ activated cells and injected.

Each individual NSG mouse then received 20 million live cells resuspended in 50-100 ml PBS transferred either intravenously (iv) *via* the retro-orbital plexus or intraperitoneally (ip) by percutaneous injection. Additionally, in a subset of studies, mice received 25 mg/kg busulfan ip for microenvironmental preconditioning 24 h prior to xenografting. Following injection, mice were bled and sacrificed as described for each experiment. Human cells and murine sera were evaluated as indicated below.

Assessment of Blood, Bone Marrow, and Splenic Tissue At Euthanasia

At euthanasia, spleens were bisected in order to prepare single cell suspensions for flow cytometry (FC) studies and tissue blocks were made for microscopy studies. Antibodies used for FC studies are listed in **Table S1** and primary antibodies for microscopy studies in **Table S2**. All FC data were acquired with a BD LSRII flow cytometer (Becton Dickinson Immunocytometry Systems) and analyzed by FlowJo V10.6.2 software (TreeStar). Absolute numbers of human cells were calculated using the cell count from the single cell suspension obtained at the time of processing, and the percentage was identified by FC. The VECTASTAIN® ABC system (Vector Laboratories) was used to visualize primary antibodies for light microscopy studies. Primary antibodies for immunofluorescent microscopy were visualized with affinity purified donkey IgG antibodies (Jackson Immunoresearch). Confocal microscopy was performed using either an Olympus IX70 microscope or a Nikon A1R confocal microscope. All images obtained were edited for optimal color contrast using Adobe Creative Cloud v5.1.0.407 (Adobe Systems).

Measurement of Secreted Human IgG

Human IgG concentrations in murine plasma were measured by ELISA. 96-well flat-bottom microplates (Corning) were coated with 100 µl/well of 5 µg/ml goat $F(ab)'_2$ anti-human IgG polyclonal antibodies (pAbs) (Southern Biotech). After overnight incubation, blocking and washing, wells were incubated with 80 µl/well dilutions of samples and standards (IgG from human serum; Sigma), again washed, and then mixed with 100 µl/well of a 1:8,000 dilution of a 1:1 mixture of goat anti-human Ig kappa and anti-human Ig lambda pAbs conjugated with horseradish peroxidase (Southern Biotech). Finally, plates were incubated with TMB Sure Blue (KPL), reactions stopped with 60 µl/well of 1N HCl (Fisher Scientific), and absorption at 450 nm measured on an ELx808 absorbance microplate reader (BioTek Instruments, Inc). IgG concentrations were calculated based on standard curves using the instrument's KCjunior (v1.22) software. Human IgG detection limit varied from 0.3 to 37.8 µg/ml.

Assessment of Plasma IFNγ

Plasma was collected at the time of animal sacrifice and stored at -80°C until use. Levels of IFNγ were measured by cytometric bead array (BD Biosciences). Results were correlated with the sum of the numbers of human $CD45^+CD4^+CD5^+$, $CD45^+CD8^+CD5^+$, and $CD45^+CD4^+CD8^+CD5^+$ cells expressed as a ratio over the number of $mCD45^+hCD45^-$ cells obtained

using identical FSC and SSC gates from FACS analysis of single cell splenic suspensions obtained at the same time point.

Statistical Analyses

All statistical tests were performed using Prism v8 (GraphPad Software, Inc). Normality was assessed using the D'Agostino-Pearson Omnibus Test, and appropriate parametric and non-parametric analyses performed thereafter. Mann-Whitney U tests were used for analyses of CLL T- and B-cell numbers in comparison experiments using PBMCs alone, PBMCS plus activated T cells, and the different injection routes (iv versus ip). For the experiments using DART molecules, Kruskal-Wallis multiple comparison tests were performed for analysis of plasma IFNγ and IgG levels and the percent of $CD5^+CD19^+$ cells obtained from the 3 groups of animals.

RESULTS

Transfer of Unmanipulated Chronic Lymphocytic Leukemia Peripheral Blood Mononuclear Cells Into NSG Mice Leads To Inefficient CLL B-Cell Growth That Is Only Substantial When Autologous T-Cell Expansion Spontaneously Occurs

The transfer of solely unmanipulated primary CLL PBMCs intravenously into alymphoid mice can result in CLL recovery from the spleen after a period of 3–4 weeks (1, 5, 7). We performed such experiments transferring CLL PBMCs into unconditioned NSG animals to assess the frequency of successful xenografting, spontaneous *in vivo* T-cell activation, and growth of CLL B and T cells. In two thirds of the animals, such transfers led to the detection of none or only scanty, apparently resting CLL B cells (**Figure 1A**); in the remaining mice, CLL B-cell expansion was found (**Figure 1B**). Notably, in all those animals with CLL B-cell expansion, there was concomitant autologous T-cell growth. Moreover, evidence for cellular proliferation, based on the presence of $Ki67^+$ cells, was also found only in those animals with T-cell expansion (**Figure 1B**).

Collectively, these findings confirm that primary CLL B cells grow in alymphoid mice only when there is a concurrent expansion of T cells (4). The frequency that T-cell activation spontaneously occurs and consequently leads to CLL B-cell growth when transferring unmanipulated CLL PBMCs is low (~33% in these experiments).

Co-Transfer of Autologous T Cells, Activated Polyclonally *In Vitro*, Leads To Much Greater and More Reproducible Growth of Chronic Lymphocytic Leukemia B Cells in NSG Mice

To overcome the above variability, we tested if co-transfer of a fixed numbers of pre-activated autologous T cells with CLL B cells would reproducibly lead to a greater and more prolonged proliferation of leukemic B cells than transferring PBMCs alone. To do so, we injected into NSG mice 20×10^6 PBMCs alone or in combination with 0.5×10^6 pre-activated T cells (1:40 T:B) from 4 CLL patients (2 *IGHV*-mutated, M-CLL cases 1493 and 1521, and 2 *IGHV*-unmutated, U-CLL cases 2030 and 2156), and recipient animals were bled weekly for 3 weeks. Finally, mice were randomly assorted into groups of 5 mice per patient sample and euthanized at weeks 4, 5, 7 and 9; blood, spleen and bone marrow (BM) samples were collected at each time point. For each group of animals, we calculated the absolute numbers of different cell types present at each site (**Figure 2**). We refer to the combination of CLL PBMCs plus *in vitro* autologous, activated T cells (aT) hereafter as "PBMCs + aT".

Upon analyzing blood samples, human CD45-expressing cells were identified from days 7 through 63 (**Figure 2**). When

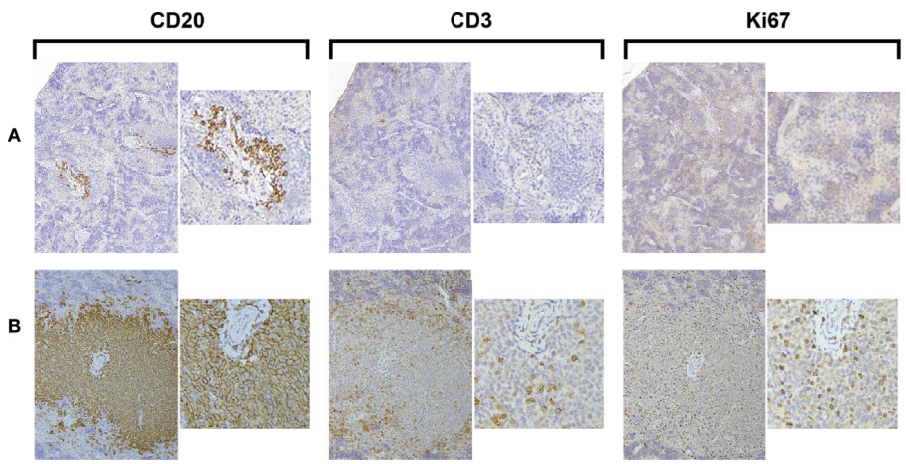

FIGURE 1 | Growth of CLL B cells only occurs when there is associated expansion of autologous T cells. Representative × 10 original magnification IH images of splenic tissue obtained at euthanasia **(A)** Few $CD20^+$ cells with no $CD3^+$ cells or $Ki67^+$ cells are present (CLL1083, representative result from 10/15 animals). **(B)** Aggregates of $CD20^+$ and $CD3^+$ cells with $Ki67^+$ cells are apparent around blood vessels (perivascular aggregates, PVAs) (CLL1279, representative of 5/15 animals).

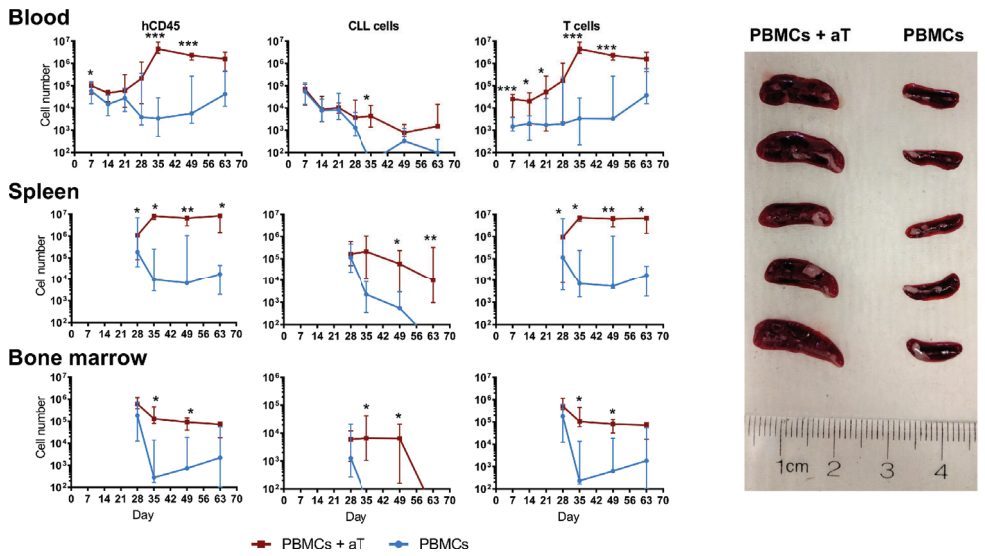

FIGURE 2 | Co-injection of autologous activated T cells with CLL PBMCs leads to more effective engraftment and growth in NSG mice. Time course quantification by FC of human CD45$^+$ cells, CLL B cells and autologous CLL T cells from single cell suspensions in the peripheral blood, spleen and bone marrow of 4 different patients evaluated independently. PBMCs with or without aT were injected into 5 mice per group and bled weekly up to euthanasia at week 4 (n = 40 mice); for two of the patients, additional groups of mice were injected, and these were euthanized at weeks 5, 7 and 9. Points represent the median and the interquartile range. * corresponds to Mann-Whitney U test P values < 0.05, ** $P < 0.01$, and *** $P < 0.001$. On the right, spleens of 10 mice at week 5 post injection of 20 × 10^6 CLL PBMCs with (Left; n = 5) and without (Right; n = 5) 0.5 × 10^6 activated T cells (aT).

focusing on CLL B cells, the numbers in the blood diminished progressively from the time of injection through week 3 for both the PBMC only and the PBMC + aT groups (**Figure 2**); this is consistent with B lymphocytes recirculating less and being more tissue resident (9, 10). However, the degree of change between the two groups differed with a lesser fall in the PBMC + aT groups than PBMCs alone. For the PBMC alone group, B cells were no longer detectable after day 56.

In contrast, T-cell counts behaved differently. At the time of the first blood sampling (day 7), the PBMC + aT group had a significantly higher number of T cells, possibly influenced by the higher number of T lymphocytes transferred initially (**Figure 2**). However, between days 14 and 35, T-cell counts between the two groups diverged appreciably due to *in vivo* expansion. This numerical superiority reached a peak at day 35 and continued to be maximally divergent until the last bleeding (day 63) (**Figure 2**).

These differences in the numbers of CD45$^+$ and CLL B and T cells in the blood were mirrored temporally in the spleens (**Figure 2**) and BMs (**Figure 2**) of the two groups of animals, with day 35 being the critical point at which the groups significantly diverged. This disparity was reflected by the clear dominance in spleen sizes for the PBMC + aT group at each time that euthanasia was carried out (**Figure 2**).

Finally, it is notable that T cell numbers remained relatively constant from day 35 until the end of the experiment (day 63) (**Figure 2**). In contrast, the numbers of CLL B cells started to decline beginning at day 49. As will be addressed below, the time points at which individual patient samples reach maximal and minimal numbers of CLL B and T cells differ for specific samples.

No Clear Advantage To Pre-Conditioning NSG Recipients For Xenografting Mature Chronic Lymphocytic Leukemia Cells

Busulfan pre-conditioning can support the transfer of unmanipulated CLL PBMCs (5). Therefore, we tested if this type of pre-conditioning improved engraftment and growth in the PBMC + aT model. To do so, we injected busulfan ip into 50% of NSG recipients and then transferring iv, into all animals, PBMCs from 4 (2 U-CLL and 2 M-CLL) patients alone (**Supplementary Figure 1**) or with pre-activated T cells (**Figure 3**). All animals were sacrificed 5 weeks later, and the numbers of CLL-derived B and T cells in the blood, spleen, and BM evaluated. Busulfan administration did not alter the numbers of CLL B or T cells found at any of the examined sites (**Figure 3A**). Hence, there was not an advantage to busulfan preconditioning NSG recipients when transferring mature CLL B and T cells using the PBMC + aT system.

Additionally, although human hematopoietic cells engraft best in NSG mice after low dose irradiation (11) and this has been successfully employed in transfers of CLL cells (2–4), others (7) and we (not shown) have not found this to enhance xenografting CLL PBMCs.

Identification of Distinct Temporal Phases of Engraftment and Growth of Chronic Lymphocytic Leukemia B and T Cells In NSG Mice

Since the above indicated that the PBMC + aT approach optimized leukemia-cell growth without a need for preconditioning and that the greatest numbers of cells were found in murine spleens, we

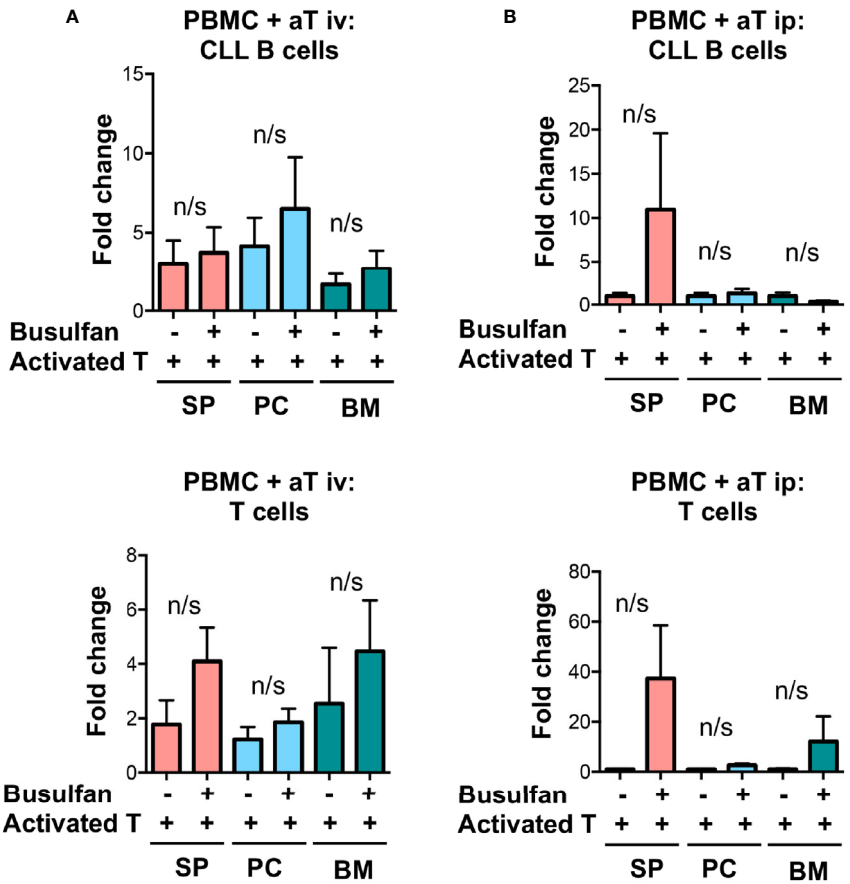

FIGURE 3 | Busulfan preconditioning does not provide a clear advantage for the xenografting of primary CLL cells in the PBMC + aT model. **(A)** Five NSG mice did not or did receive 25mg/kg busulfan ip 24 h prior to xenografting. Then, 20 × 10^6 CLL PBMCs with 0.5 × 10^6 activated T cells (aT) were injected iv into NSG mice. Five weeks after cell injection, mice were sacrificed and single cell suspensions from blood, spleen, bone marrow (BM) and peritoneum were analyzed by flow cytometry. Busulfan did not significantly improve CLL B-cell (top) and T-cell (bottom) engraftment. Data represent a composite of experiments involving cells from 4 patients, 2 U-CLL and 2 M-CLL. **(B)** Similar busulfan preconditioning was given or not to two other sets of 5 NSG mice that received samples from 4 different patients (2 U-CLL and 2 M-CLL). Twenty-four h after, 20 × 10^6 CLL PBMCs with 0.5 × 10^6 activated T cells (aT) were injected ip into each recipient mouse. Although there is a trend for better engraftment of CLL B and T cells in busulfan-pretreated mice, there are no significant differences between the numbers of CLL B and T cells in any of the groups. Bar graphs represent the mean fold change (after setting the average cell counts obtained from PBMC mouse spleens as 1); S.E.M. determined by Mann-Whitney U test. n/s: no statistically significant difference.

categorized the temporal relationships of B- and T-cell expansion in the system. This was done by associating IH studies of tissues and FC analyses of cells from the blood and spleen with the presence of plasma Ig and cytokines over time. This exercise defined 4 distinct, albeit interconnected phases of T- and B-cell growth in NSG recipients. **Table 2** presents the comprehensive analysis after transfers using CLL 1122 and M-CLL 1164; features of the timings of the plasma, FC findings and pertinent findings of IH studies from these and other representative patient samples are shown in **Figure 4**. Of note, since these studies use primary CLL cells, whose biological characteristics vary between patients, the exact timing of each phase between different patient samples is not necessarily temporally identical.

Phase 1 is characterized by a predominance of CLL B cells in the peripheral blood and spleen. At this point, leukemic cells are resting, as indicated by the lack of CFSE dilution determined by flow cytometry (3 and 7 days post transfer of cells; **Figure 4A** and **Table 2**). Consistent with this, CLL B-cell numbers in the blood did not significantly change between days 7-21 (**Figure 2**). In addition, transferred cells localizing around blood vessels at this time are virtually all B lymphocytes (as exemplified by CD20 expression), with very few, if any $CD3^+$ cells detectable by IH (**Figure 4B**, top panel). Studies using a larger series of CLL cases indicate that these initially leukemic, B-cell restricted perivascular aggregates (PVAs) form between 24 – 72 h after transfer (not shown). The lack of leukemic B-cell division in Phase 1 might result from not yet reaching the numbers of activated T cells needed to provide the requisite levels of human cytokines or the necessary numbers of T-B cell contacts in recipient mice.

Phase 2 is defined by increasing T-cell proliferation and the consequent initiation of substantial CLL B-cell division. This is

TABLE 2 | Phases of engraftment in the PDX model.

Phase	Circulating hCD45$^+$ cells	Human Plasma IFNγ	Human Plasma Ig	CFSE pattern of spleen-residing CD4$^+$ cells	CFSE pattern of spleen-residing CD5$^+$CD19$^+$ cells	CD5$^+$CD19$^+$: CD4$^+$ spleen-residing ratio as determined by flow cytometry	Observed ratio of CD20$^+$ to CD3$^+$ cells seen in splenic tissue by IH	Morphologic description of splenic tissue
Phase 1	Present	Absent	Absent	CFSE dilution patterns show CD4$^+$ cells at all stages of division	CFSE dilution patterns show that the majority of cells have undergone <1 division	>1	>1	hCD45$^+$ cells localized to perivascular areas, principally CD20$^+$. Very low CD3$^+$ numbers
Phase 2	Present	Present	Absent	CFSE dilution patterns show >6 division in 90% or more cells	CFSE dilution patterns show CD5$^+$CD19$^+$ cells at all stages of division	1:1	>1	hCD45$^+$ cells localized to perivascular areas, principally CD20$^+$, CD3$^+$ more obvious
Phase 3	Present	Present	Present	CFSE dilution patterns show >6 division in 90% or more cells	CFSE dilution patterns show >6 division in 90% or more cells	<1	>1	hCD45$^+$ present throughout spleen. CD20$^+$ cells remain in aggregates intermingled with CD3$^+$ cells, red pulp may be infiltrated with CD3$^+$ cells and Ig^{++} cells
Phase 4	Present	Present	Present	CFSE shows >6 division in 90% or more cells	Minimal cells	<1	<1	hCD45$^+$ throughout spleen. Very few CD20$^+$ cells in aggregates, replaced by Ig^{++} cells, red pulp infiltrated with CD3$^+$ cells and Ig^{++} cells

evidenced by dilution of CFSE intensity in both cell types (T >> B cells) (**Figure 4A** and **Table 2**), increased numbers of CD3$^+$ cells as shown by IH (**Figure 4B**, second panel), the presence of Ki67$^+$CD20$^+$ and Ki67$^+$CD3$^+$ cells in splenic PVAs (**Figure 4C**), and detection of human IFNγ in the plasma (**Figure 4A and Table 2**). Note that leukemic B cells outnumber autologous T cells when analyzed by IHC, whereas FC of single cell suspensions prepared from the same spleens reveal a more equal ratio of B and T cells. We speculate this represents the loss of dividing CD20$^+$ cells during processing or the inability to mechanically dissociate activated CD20$^+$ cells from the tissue (**Figure 4D**); the loss of proliferating B cells upon dissociation of lymphoid tissue is encountered in other settings (12). In this Phase, human Ig is not yet detectable in plasma (**Figure 4A** and **Table 2**).

In Phase 3, a proportion of the spleen-residing CD5$^+$CD19$^+$ cells have undergone multiple cell divisions (≥ 6) as indicated by complete absence of CFSE as measured by FC, with the degree of CLL B-cell replication varying among patients. In addition, leukemic B cells start to show features of plasmablast/plasma cell differentiation, consistent with the detection of circulating human IgG [**Figure 4A**, 21 days onwards, **Table 2** and (6)]. Importantly, splenic histology continued to show aggregates of CD20$^+$ cells, intermingled with CD3$^+$ cells as before, with some evidence of plasmablasts/plasma cells at the peripheral margins [as shown by CD38 expression (13)]; this suggested that terminal differentiation of leukemic B cells to CD20$^-$ antibody secreting cells was an ongoing process and was not yet complete (**Figure 4B**, third panel).

Phase 4 is defined by the virtual complete loss of CD20$^+$ cells by IHC, along with an overabundance of cells bearing CD3 and other cells with intense intracellular Ig expression (**Figure 4B**, fourth panel). This is especially the case in animals transferred with higher T:B cell ratios. Serial analyses showed a predominance of CD4$^+$ over CD8$^+$ T cells with no significant differences in this percentage at all time points (**Figure 5A**, upper). Examining all euthanized animals from 13 different CLL transfers indicated that CD4$^+$ cells were the dominant T-cell subpopulation (mean 83.1%); in some animals this was as high as 99% of all T cells (**Figure 5A**, lower). In comparison, based on IHC studies of different CLL transfers, we found that CD4$^+$ cells aggregated around and occasionally moved into the PVAs, whereas CD8$^+$ cells (when present) showed no particular pattern of localization in splenic tissue (**Figure 5B**).

Analyses of The Types Of Non-Lymphoid Human Cells and Of Hematopoietic and Non-Hematopoietic Murine Cells in and Around Chronic Lymphocytic Leukemia B Cells Growing in NSG Mice

Next, we examined the presence of other human hematopoietic cells in and around the PVAs; such cells would have been contained in the initial cellular inoculum and have engrafted and persisted in the murine recipients. These searches, however, were fruitless, with no human myeloid cells being found in the peripheral blood or other tissues of recipient mice. This

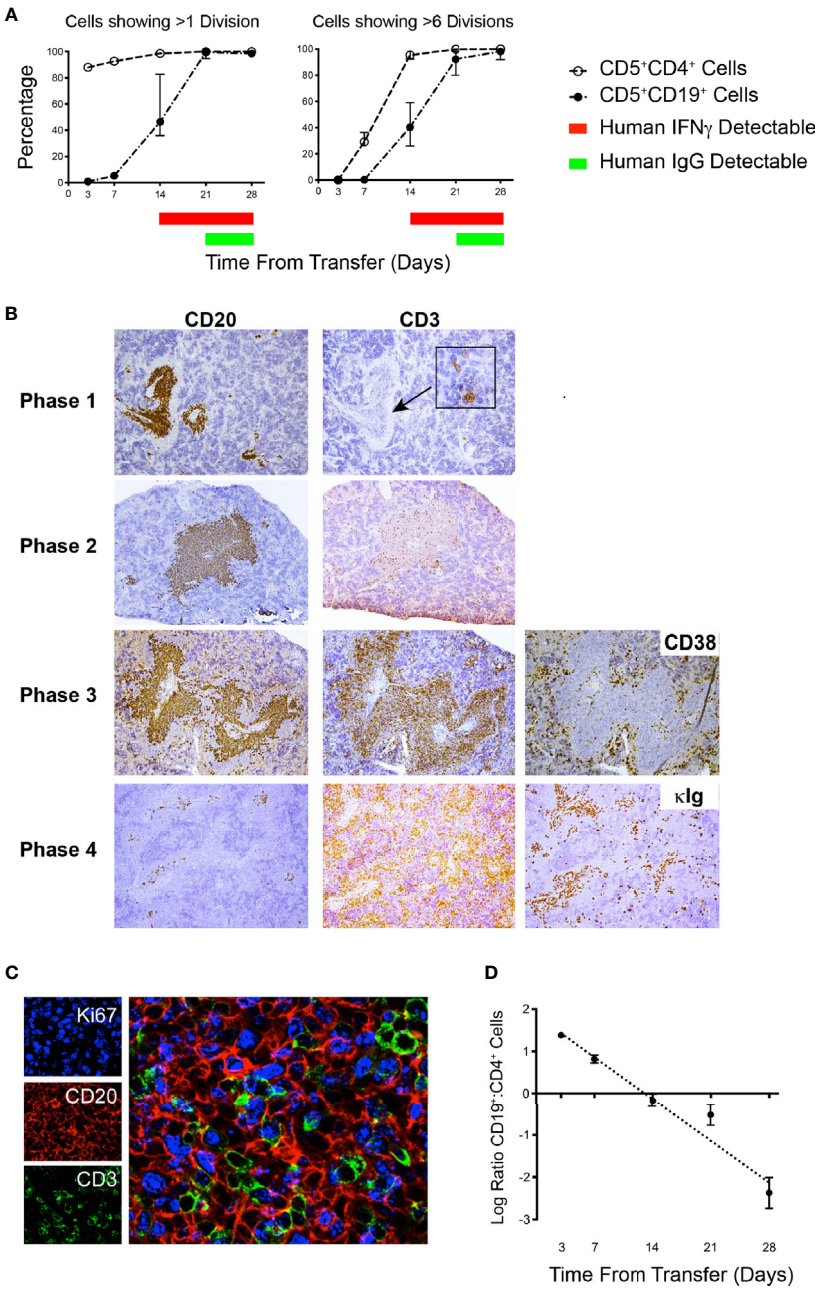

FIGURE 4 | Flow cytometry and IH analyses together with plasma findings over time help define phases of CLL B- and T-cell engraftment and growth. **(A)** Percentage of human $CD5^+CD4^+$ and $CD5^+CD19^+$ spleen-residing cells that have undergone >1 division and >6 divisions as indicated by CFSE dilution (Top) and time of appearance of detectable human IFNγ and human IgG in plasma over 28 days. Data derived from 25 animals using U-CLL1122, with euthanasia performed on 5 animals at each time point. Similar results were obtained using M-CLL1164. **(B)** Representative × 10 original magnification IH of splenic tissue showing typical CD20 and CD3 findings at each phase of engraftment. In Phase 1 the human cells identified are almost exclusively $CD20^+$ with virtually no $CD3^+$ cells detectable. With progression to Phases 2 and 3, $CD3^+$ staining density becomes increased. Beginning in Phase 3 and continuing to Phase 4, $CD38^+$ cells (used to identify plasmablasts/plasma cells) appear outside the $CD20^+$PVAs. Ultimately, by Phase 4 very few $CD20^+$ cells are seen in aggregates, but cytoplasmic Ig^{++} cells are now present (far right hand panel). Representative images obtained from spleens obtained from cases U-CLL1122 (top 2 rows), U-CLL1523 (third row) and U-CLL1083 (bottom row). **(C)** PVAs are strongly $Ki67^+$ once both B- and T-cell division occurs. 40x original magnification view using immunofluorescence showing that both $CD20^+$ (red) and $CD3^+$ (green) cells express Ki67 (blue). Images obtained from U-CLL1301. **(D)** Flow cytometry findings from the experiment in **(A)** indicating the ratio of $CD5^+CD19^+$ cells to $CD5^+CD4^+$ cells.

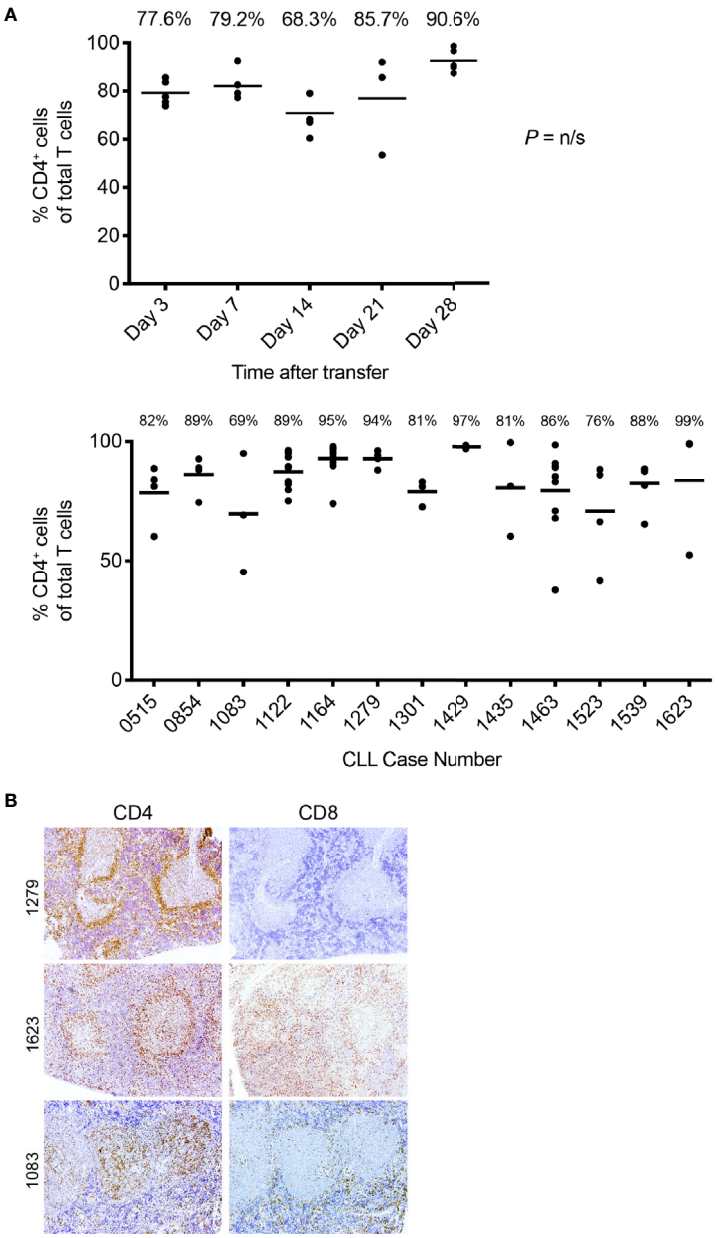

FIGURE 5 | T-cell findings in the PBMC + aT PDX model. **(A)** T cells residing in NSG spleens following transfer are principally $CD4^+$. Top. The percentage of $CD5^+CD4^+$as a total of all T cells obtained by flow cytometry analysis of spleen at euthanasia at the time points shown. Data obtained from transfer of cells into 25 mice with euthanasia of 5 animals at each time point. Median percentage $CD5^+CD4^+$ cells indicated by bar and percentage figure. Bottom. The percentage of $CD5^+CD4^+$as a total of all T cells obtained by flow cytometry analysis of spleen at euthanasia. Data obtained from 13 independent experiments (each corresponding to a different CLL case number) where transfer had been made at least 28 days earlier. Median percentage $CD5^+CD4^+$ cells indicated by bar and percentage figure. n/s: no statistically significant differences. **(B)** Representative FC and IH findings of $CD4^+$ and $CD8^+$ staining in spleen. Images at × 10 original magnification. Pale central areas correspond to $CD20^+$PVAs. For CLL1279, $CD4^+$ cells are located especially around the rim of the known location of CD20 cells; a minimal number of $CD8^+$ cells are present. CLL1623 has both $CD4^+$ and $CD8^+$ cells; $CD4^+$ cells again locate around and within $CD20^+$ aggregates. In CLL1083, $CD4^+$ cells are densely present within the $CD20^+$PVAs with less at the outer margin.

conclusion is based on the absence of cells reactive with CD11b, CD11c, CD33, CD14, and CD15 mAbs identified by FC and IHC (not shown). Notably, we did identify $CD68^+$ cells in the spleen by FC and IHC (**Figure 6A**). However, these proved to be human CLL B cells as indicated by co-localization with $PAX5^+$ cells by IH and evidence for upregulation of CD68 by $CD5^+CD19^+$ cells by FC following transfer into animals (**Figure 6A**).

Next, we explored the presence and identity of murine non-lymphoid and non-hematopoietic cells and their proximity to human B and T cells. As expected, staining for murine

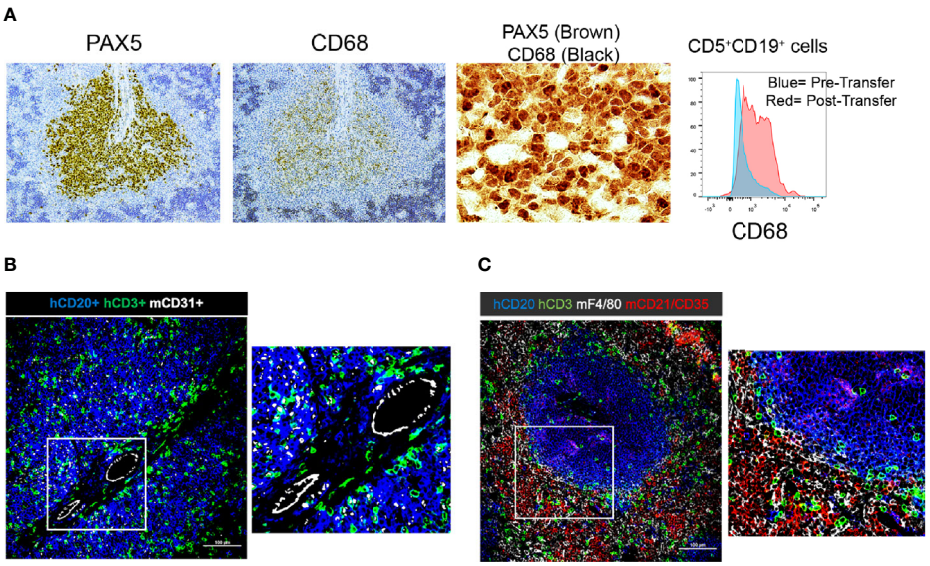

FIGURE 6 | Immunohistochemistry demonstrating the presence and localization of non-B and non-T cells of donor or recipient origin in engrafted spleens. **(A)** 20x (single color PAX5 and CD68) and 60x (dual color) IH images of representative spleens aggregated from 5 independent experiments; results with CLL1279 are demonstrated here. Aggregates contain CD68$^+$ cells that are B lymphocytes as indicated by co-localization with PAX5 in dual color staining. Flow cytometry further demonstrates that CD5$^+$CD19$^+$ cells express CD68 upon transfer into NSG mice. **(B)** 20x and 40x magnification view of human CD20$^+$ and CD3$^+$ cells and mouse CD31$^+$ cells by immunofluorescence of CLL-engrafted spleens; staining from a representative case of at least 10 independent experiments. **(C)** 20x and 40x magnification view of human CD20$^+$ and CD3$^+$ cells and mouse F4/80$^+$ and CD21$^+$/35$^+$ cells after immunofluorescence staining of the same case.

endothelial cells (CD31$^+$) confirmed that the CLL cells localized around blood vessels (**Figure 6B**). In addition, we did find murine macrophages (F4/80$^+$ cells). However, strikingly, none were located within the CLL B-cell areas; all resided exclusively at the periphery of the PVAs (**Figure 6C**). Similarly, the majority of murine follicular dendritic cells (FDCs; CD21$^+$CD35$^+$) were located outside the PVAs, although a few were observed within (**Figure 6C**).

Effects of Route of Administration of Chronic Lymphocytic Leukemia Cells on Engraftment and Growth

Finally, we questioned if the route of cell injection—ip vs. iv—affected the level, localization, and expansion of CLL B and T cells in the blood, spleen, BM and peritoneum (**Figure 7**). PBMCs + aT from 4 patients were injected ip or iv, and engraftment and growth followed for 28 days. Of interest, regardless of the route of administration, equal numbers of human CD45$^+$ cells were found in the blood at day 7. However, when analyzing CD3$^+$ or CD19$^+$ cells in the circulation, there were significantly more CLL T cells after iv than ip injection, and more CLL B cells after ip than iv injection (**Figure 7A**). Notably, there were no differences in the numbers of CLL B cells in the spleen, BM, and peripheral blood at day 28 between the types of administration, except for the virtual absence of B cells in the peritoneal cavity if the inoculum was given iv (**Figure 7B**). In contrast, CLL T cells placed initially in the peritoneum were found in greater numbers at day 28 in the spleen than those introduced iv (**Figure 7B**).

When analyzing the populations in the peritoneal cavity and spleen for the extent of cell proliferation, we observed that only a very small fraction of B cells in the peritoneum had divided through day 28 (**Figure 7C**). This was quite different for those CLL B cells that had taken residence in the spleen, regardless of their site of initial transfer, as B lymphocytes at that location divided robustly. The disparity of CLL B-cell division between the peritoneal cavity and the spleen is especially striking in lieu of the high numbers of dividing T cells at both sites (**Figure 7C**).

To assure that these differences would not change if the tissue microenvironments of the NSG recipients were preconditioned, we administered busulfan to the animals 24 h prior to ip injection of CLL B and T cells and then analyzed 5 weeks later the numbers of cells in the spleen, peritoneum and BM in 4 CLL patients (2 M-CLL, and 2 U-CLL) (**Figures 3A, B**). No significant differences in engraftment, localization and proliferation of CLL B cells were found in animals with or without busulfan pre-conditioning. There was, however, a trend for better engraftment of CLL B cells in the spleen and T cells at these sites after preconditioning.

Utility of the Peripheral Blood Mononuclear Cell + aT Model To Test Therapeutics

To investigate the value of this revised technique in testing the efficacy of therapeutics in a preclinical setting, we used a bispecific retargeted antibody based DART® molecule that engages CD19 on leukemia/lymphoma B cells and the TCR on T lymphocytes (14). This CD19xTCR antibody (hereafter referred to as "DART molecule") is effective in clearing transplanted lymphoma cell

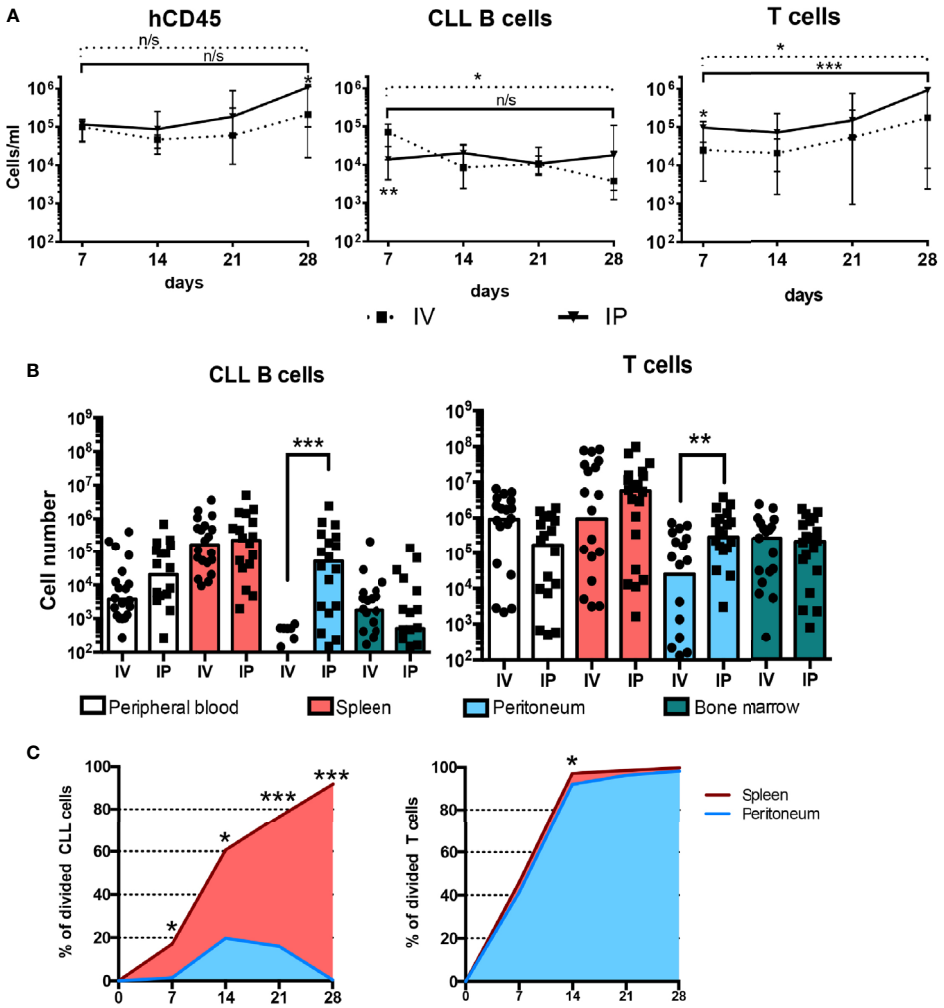

FIGURE 7 | IP administration of CLL B and T cells gives rise to different distributions and activation states. **(A)** Time course quantification of human CD45-expressing cells, CLL B cells and human T cells evaluated by FC in the peripheral blood of mice injected with 20 × 10^6 CLL PBMCs with 0.5 × 10^6 activated T cells either iv or ip (4 patients' samples, 5 mice per patient and condition). Points represent the median and the interquartile range. **(B)** CLL B and T cell absolute counts at day 28 post injection in peripheral blood, spleen, peritoneum and bone marrow from mice injected iv (n = 20) or ip (n = 20). **(C)** Percentage of divided CLL B cells evaluated by CFSE dilution by FC in the spleen and the peritoneum over time. * corresponds to Mann-Whitney U test *P* values < 0.05, ***P* < 0.01, and ****P* < 0.001. n/s: no statistically significant difference.

lines co-administered with human PBMCs in a NOD/SCID model and primary patient material from cases of acute lymphoblastic leukemia and diffuse large B cell lymphoma (15). Using the PBMC + aT model, we compared the effects of the DART molecule and of a FITCxTcR antibody that cannot target B cells (referred to as "DART control molecule") and of saline. **Figure 8A** illustrates the experimental protocol followed.

Each animal in 3 groups (5/group) received iv 20 × 10^6 CLL B cells with 0.5 × 10^6 activated autologous T cells from the U-CLL1539 clone. Twenty five days following transfer (Phase 3 of engraftment for this sample), plasma levels of IFNγ and IgG were comparable between the 3 groups of mice (**Figure 8B**, Pre DART Molecule Injection), indicating the comparable nature of CLL B- and T-cell growth among the groups. After receiving the DART molecule, DART control molecule, or saline ip on 5 consecutive days, the animals in each group were euthanized 10 days after the last injection. Plasma levels of IFNγ remained comparable, with the amounts of IFNγ increasing in each group by ~1 log over time (median pre- and post-injection: 70.9 vs. 830.2 pg/ml); this indicated a continued expansion of T cells in all animals regardless of their treatment group (**Figure 8B**).

However plasma IgG levels from the same samples at the same time points from the PBS-treated animals and those receiving the DART control molecule exhibited similar or appreciably higher levels than at the pre-treatment assessment (median: Pre-treatment = 1558 µg/ml; Post-treatment = 9283 µg/ml). This reflected the unchecked growth and differentiation of CLL B cells.

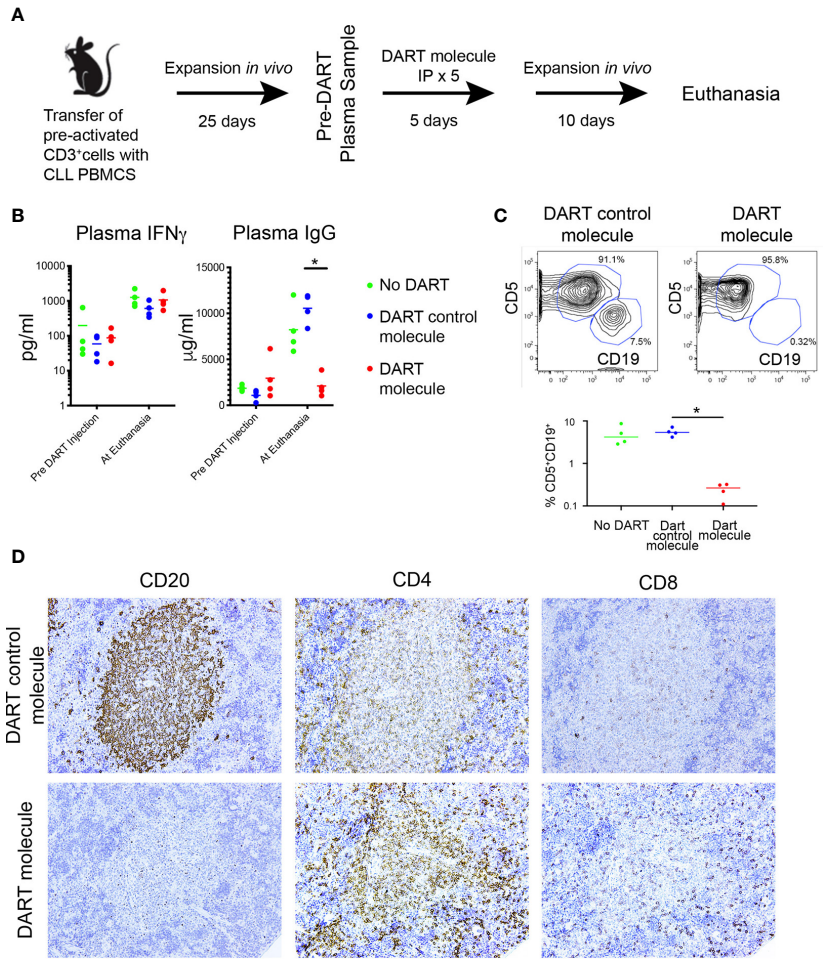

FIGURE 8 | The PBMC + aT PDX model demonstrates the activity of a CD19xTcR-specific DART. **(A)** Mice (n = 15) were injected with 0.5 × 10^6 anti-CD3/28 + IL-2 pre-activated CLL-derived T cells and 20 × 10^6 CLL PBMCs on Day 0. Expansion of both T and B cells was determined 25 days post transfer by detection of human IFNγ, and human IgG in murine plasma samples. DART bispecific antibodies (DART molecule, n = 4 animals; or DART control molecule, n = 4 animals) or saline were administered ip from Day 30 to Day 34. Plasma levels of human IFNγ and IgG were further determined at day 46 when euthanasia was performed. Animals with <10 pg/ml IFNγ at Day 25 were excluded from receiving DARTs and were not included in the analysis making 3 groups of 4 animals for each condition. **(B)** Plasma levels of IFNγ and IgG in the 3 groups of animals (n = 12, 4 per group), taken pre-DART injection at Day 25 and at euthanasia at Day 40. Results show no significant differences in IFNγ levels between the 3 groups before DART molecule injection and at euthanasia. In contrast, plasma Ig levels are significantly lower in CD19xTcR DART-treated animals (red dots), compared to the DART control molecule-treated control animals (blue dots). * corresponds to Kruskal-Wallis test *P* value < 0.05. **(C)** FC reveals absence of $CD5^+CD19^+$ cells in DART molecule-treated animals. Illustrative FC plots are representative of hCD45 single cell splenic suspensions obtained at euthanasia. Graph shows median $CD5^+CD19^+$ cells in each group as a percentage of total $hCD45^+$ cells isolated. Compared to DART control molecule-treated control animals (blue dots), there are significantly fewer $CD5^+CD19^+$ cells in DART molecule-treated animals (red dots). * corresponds to Kruskal-Wallis test *P* value < 0.05. **(D)** Representative IHC (x20 original magnification) of DART control molecule-treated animals (upper panel) compared to DART molecule-treated animals (lower panel). These results were apparent for both a U-CLL1539 (illustrated in Figure) and M-CLL0545.

In contrast, plasma IgG levels were significantly lower in the DART molecule-treated animals (**Figure 8B**). In fact, Ig levels in the animals receiving the DART molecule were also lower than those 15 days earlier at the time of initiation of treatment (median: Pre-treatment = 2288 µg/ml, Post-treatment = 1781 µg/ml), further supporting that CLL B-cell numbers were substantially reduced (**Figure 8B**). Consistent with this, flow cytometric analyses of spleen cells from the 3 groups showed that $CD5^+CD19^+$ cells were virtually absent in all animals treated with the DART molecule, whereas those in animals treated with saline or the DART control molecule were sizeable and very similar (**Figure 8C**). Additionally, there were equal numbers of $CD5^+CD4^+$ and $CD5^+CD8^+$ cells in all 3 groups, with the predominant type being $CD4^+$; no expansion of the $CD8^+$ subset was seen in the DART molecule-treated animals (not shown).

Companion IHC studies indicated the presence of splenic $hCD45^+$ cells in all groups, and clearly showed typical $CD20^+$ PVAs in untreated (not shown) and DART control molecule-treated animals (**Figure 8D**, upper panel). However, $CD20^+$ cells and PVAs were completely absent in 3 of 4 DART molecule-

treated animals (**Figure 8D**, lower panel); in the fourth animal, only patchy staining for such cells/structures (estimated as 20% of that seen in untreated animals) was detected. All animals showed dense staining for $CD4^+$ cells within PVAs, which was more marked in those animals treated with the DART molecule (**Figure 8D**). $CD8^+$ cells did not show any particular localization pattern. Results were replicated in a subsequent experiment using the CLL 0545 clone.

DISCUSSION

In this study we optimized the engraftment and growth of primary CLL B cells in NSG mice using limited numbers of cryopreserved, primary, peripheral blood patient samples. This was achieved by providing a constant number of polyclonally-activated autologous T cells, pre-stimulated *in vitro*, at the time of transfer into recipient mice.

This approach (PBMCs + aT) has several advantages. First, it increases significantly the percentage of animals that are successfully engrafted when compared to the transfer of PBMCs alone.

Second, the approach eliminates the need to rely on autologous T-cell activation *in vivo*. Moreover, the approach does away with the use of allogeneic antigen-presenting cells (APC) to initiate T-cell activation *in vivo*. As stated previously, the former approach can be suboptimal because the level of histocompatibility disparity between the APC and the CLL cell donor is usually unknown, and hence the extent and degree of CLL T-cell activation occurring in recipient mice differs and is not be predictable nor quantifiable in advance.

Another advantage of the PBMCs + aT approach is the relatively small number of PBMCs needed to carry out the engraftment process (20×10^6). Durig *et al.* have shown that injecting animals, ip and then iv, with larger numbers of PBMCs alone (100×10^6 on each occasion) helps engraftment (1); this is certainly an improvement on a single injection of 100×10^6 PBMCs alone (2, 3, 5, 7). The PBMC + aT method, however, obviates the need for 2 injections and reduces the numbers of cells needed (200×10^6 vs. 20×10^6 cells).

Additionally, all the experiments reported here used cryopreserved patient cells. Although the use of fresh cells can be advantageous (7), this requirement makes answering questions about the biology of CLL cells much more difficult. For example, it would be very cumbersome to compare cells from two types of patients if only fresh cells had to be used, since this would require knowing in advance the existence of the variable to be studied between individual patients and arranging for patients, differing in this variable, to donate the same amount of blood on the same day and at approximately the same time. Furthermore, the use of fresh cells does not allow simultaneous analysis of samples taken at several points in time, making comparisons more restricted and much less rigorous. The capacity to use cryopreserved material removes these and other restrictions.

Finally, the PBMC + aT approach does not require chemical (busulfan) or X-ray preconditioning for effective engraftment of mature CLL cells. This, again, makes the method more convenient and less laborious.

It is important to point out that we assign engraftment as being successful when CLL cells not only survive but also divide in recipient mice. Leukemia-cell survival is a measure of the capacity of CLL cells to accept and benefit from murine microenvironmental signals, actions that a good model should be able to examine. Importantly and additionally, the PBMC + aT method measures the ability of CLL cells to receive and respond to activation signals *in vivo*. Thus, having the transferred cells multiply in recipient animals allows measurement of leukemic-cell birth *in vivo*, a parameter intimately linked to CLL-patient clinical courses (16).

Having a reproducible model for the engraftment and growth of CLL cells *in vivo* allowed us to perform detailed IHC and FC analyses of the kinetics of B-cell proliferation and its relationship with T-cell expansion. We identified 4 phases that a successful transfer traverses. The first phase is characterized by the deposition of quiescent leukemic B cells around blood vessels shortly after cell transfer, hence the term perivascular aggregates (PVAs). During this phase and in Phase 2, activated T cells start and continue to expand at the PVAs, initiating CLL B-cell activation and growth. The majority of T cells are $CD4^+$. Anatomically, the few $CD8^+$ cells present are interspersed with CLL B cells in the PVAs, whereas the $CD4^+$ T cells are more often found at the margins of the PVAs and less so distributed throughout the structures. We have not defined a parameter that associates with the apparent different geographic localization of the $CD4^+$cells. By the time of Phase 3, CLL B-cell division is robust, with some cells dividing 6 or more times. Among the latter are cells that phenotypically resemble plasmablasts or plasma cells and secrete CLL Ig. Phase 4 is characterized by the almost complete absence of cells bearing a B-cell phenotype and the predominance of $CD4^+$ T cells. In this regard, it is noteworthy that T-cell numbers reach a plateau during Phase 3 and remain constant through Phase 4. The capping of T-cell numbers at a defined level, often at or near day 35 after transfer, is consistent with attaining full occupancy of available lymphoid niches (17). Moreover, the rise in T cell numbers is likely due to the greater rate of proliferation for T cells than B cells and the higher likelihood that T cells recirculate throughout the entire experimental period.

We could not find evidence for human non-lymphoid cells engrafting in this system, indicating that the myeloid and other lineages are inherently not transferrable as mature cells or that the murine microenvironment of NSG mice cannot support their survival and growth. However this finding strongly implies that murine non-B and non-T cells within the NSG microenvironment are capable of providing necessary non-lymphoid support that xenografted CLL cells require; this is compatible with human and murine stromal cells providing supportive cues in *in vitro* (18) and *in vivo* (4). However, it was striking to find that murine macrophages and FDCs, albeit the latter at a somewhat lesser degree were not found within the CLL PVAs, suggesting an active

exclusion of these cells from those areas and a lack of their requirement for leukemic-cell proliferation. The reason for this is obscure at this point. However since both of these cell types are APCs (macrophages for T cells and FDCs for B cells), their absence would suggest that the T-B interactions occurring in PVAs are not cognate, but more likely mediated by cytokines (6), and that selection for higher affinity B-cell receptors might not occur, even though B-cell differentiation and BCR diversification along apparent genealogies can occur within these structures (6). The latter findings might reflect selection for non-IG genetic changes, not changes that enhance BCR binding of (auto)antigens.

A full understanding of the kinetics of B- and T-cell engraftment in NSG mice is essential for the analysis of novel therapeutics. We here demonstrate the efficacy of a bispecific antibody (14) whose beneficial effects require the ability to engage autologous T cells in the cytolytic process. As well as being an example of the utility of the PBMC + aT method, these studies highlight and provide an assay whereby the cell interactions between CLL B and T cells and the antibody needed to achieve the therapeutic result can be observed and studied further. Hence, therapeutic agents requiring T-cell participation should take into account that soon after engraftment (end of Phase 1 and beginning of Phase 2) only T cells are dividing, as indicated by the presence of human IFNγ in the blood. Similarly, T-cell numbers are generally limited within PVAs until at least Phase 2. Therefore investigations regarding the utility of agents that exploit T cells (for example, the DART molecule used here) would be expected to have maximal effects only if introduced at or after this phase of engraftment.

Finally, we would like to highlight the biologic insights as well as the technical advantages that our studies of the route of administration of CLL B cells and autologous, activated T cells provide. First, these findings indicate that the (micro) environment that the cells encounter at the time of initial transfer has a substantial effect on migration, cell interactions, and subsequent cell division. Specifically, when activated T and resting CLL B cells are administered iv, the majority of cells leave the blood (B > T) and track to the spleen and BM and not to the peritoneal cavity. In the spleen and BM, both B and T cells undergo vigorous cell division, so much so that CLL B cells are eventually lost, probably for a variety of reasons, including exhaustion because of [1] the numbers of divisions that occur, [2] unsuccessful competition with T cells for survival niches and nutrient cytokines, and [3] elimination T-cell mediated cytolysis.

In contrast when the same cells are deposited in the peritoneal cavity, the vast majority of CLL B cells remaining at that anatomic site are quiescent, despite being among rapidly dividing T cells that one would expect would provide help for B-cell proliferation as occurs when the same cells exit the peritoneum and enter the spleen. Indeed, sufficient numbers of B and T cells migrate to the spleen and BM and undergo robust division at those sites such that B cells achieve the same levels as animals receiving the inoculum ip and in fact T cell numbers exceed that of animals given the same cells iv. So either T cells continue to emerge from the peritoneal cavity into the blood, or they divide in the cavity (or elsewhere) and (re)enter the circulation in higher numbers (**Figure 6B**).

The discrepancies in B-cell division in the peritoneal cavity versus the spleen are reminiscent of normal murine B-1 cells (19) and murine CLL-like TCL1 cells (20). The precise mechanisms responsible for these striking differences in B-cell growth and survival at these anatomic sites are not known, although experiments with murine B-1 cells suggest that soluble factors in the peritoneal cavity might be involved (19).

Regardless, the ability to have quiescent and proliferating subpopulations of human CLL cells in the same animals provides a considerable experimental advantage since this more closely resembles human CLL where there are both dividing and non-dividing pools of leukemic cells (21, 22). In addition, these findings suggest that within this model, the peritoneal cavity resembles the blood and BM of patients, where cells are primarily resting, and the spleen resembles human lymph nodes, where most CLL-cell division occurs (5, 23).

Finally, it is important to recognize that despite the many advantages of this model, the recipient animals do not develop obvious CLL disease. Thus, the model is best used to evaluate the biologic properties of CLL cells and how interactions with autologous T cells modify these properties. Experiments designed to modify the system to model the pathology of CLL are in progress.

In conclusion, we demonstrate here that by using *in vitro* activated autologous T cells in the PBMC + aT PDX model, more reproducible and enhanced engraftment and growth of CLL B cells is achieved using a limited initial inoculum of cryopreserved cells. The system allows comprehensive studies of how CLL B and T cells behave in a xenogeneic setting as well as how these cells interact with and are influenced by their surrounding microenvironment in different tissues and how that might reflect the human leukemic process. Finally, the method provides a robust system for the study of new therapeutic agents.

DATA AVAILABILITY STATEMENT

The raw data supporting the conclusions of this article will be made available by the authors, without undue reservation.

ETHICS STATEMENT

The studies involving human participants were reviewed and approved by The Institutional Review Board of Northwell Health. The patients/participants provided their written informed consent to participate in this study. The animal study was reviewed and approved by The Institutional Animal Care and Use Committee of Northwell Health.

AUTHOR CONTRIBUTIONS

PP and GF conceived the study, performed the experiments, wrote the first draft, and performed the revisions. S-SC conceived

the study, performed the experiments, and performed the revisions. JK, KR, SA, and JB provided patient material and reviewed the manuscript. NI and AR performed the experiments and performed the revisions. NC conceived the study, wrote the first draft, and performed the revisions. PP and GF contributed equally to the study. All authors contributed to the article and approved the submitted version.

FUNDING

NC received funding for a portion of these studies from Janssen Pharmaceuticals, Inc. NC and KR received philanthropic support from The Nash Family Foundation, the Karches Foundation, The Marks Foundation, and the Jean Walton Fund for Leukemia, Lymphoma, & Myeloma Research. PEMP was funded in part by Blood Cancer UK (Blood Cancer UK grant numbers 11039 and 09011).

SUPPLEMENTARY MATERIAL

The Supplementary Material for this article can be found online at: https://www.frontiersin.org/articles/10.3389/fimmu.2021.627020/full#supplementary-material

Supplementary Table 1 | Antibodies for flow cytometry.

Supplementary Table 2 | Antibodies used for microscopy studies.

Supplementary Figure 1 | Busulfan preconditioning does not provide a clear advantage for xenografting primary CLL cells in the PBMC model. Five NSG mice did not and 5 did receive 25mg/kg busulfan ip 24 h prior to xenografting (10 mice per patient, total 4 patients). Then, 20×10^6 CLL PBMCs were injected iv into NSG mice. Five weeks after cell injection, mice were sacrificed and single cell suspensions from spleen, bone marrow (BM) and peritoneum were analyzed by flow cytometry. Busulfan did not significantly improve the numbers of CLL B cells (top) and T cells (bottom) found at the three anatomic sites. Bar graphs represent the mean fold change (after setting the average cell counts obtained from PBMC mouse spleens as 1); S.E.M. determined by Mann-Whitney U test. n/s: no statistically significant difference.

REFERENCES

1. Durig J, Ebeling P, Grabellus F, Sorg UR, Mollmann M, Schutt P, et al. A novel nonobese diabetic/severe combined immunodeficient xenograft model for chronic lymphocytic leukemia reflects important clinical characteristics of the disease. *Cancer Res* (2007) 67(18):8653–61. doi: 10.1158/0008-5472.CAN-07-1198
2. Aydin S, Grabellus F, Eisele L, Mollmann M, Hanoun M, Ebeling P, et al. Investigating the role of CD38 and functionally related molecular risk factors in the CLL NOD/SCID xenograft model. *Eur J Haematol* (2011) 87(1):10–9. doi: 10.1111/j.1600-0609.2011.01626.x
3. Oldreive CE, Skowronska A, Davies NJ, Parry H, Agathanggelou A, Krysov S, et al. T-cell number and subtype influence the disease course of primary chronic lymphocytic leukaemia xenografts in alymphoid mice. *Dis Model Mech* (2015) 8(11):1401–12. doi: 10.1242/dmm.021147
4. Bagnara D, Kaufman MS, Calissano C, Marsilio S, Patten PE, Simone R, et al. A novel adoptive transfer model of chronic lymphocytic leukemia suggests a key role for T lymphocytes in the disease. *Blood* (2011) 117(20):5463–72. doi: 10.1182/blood-2010-12-324210
5. Herman SE, Sun X, McAuley EM, Hsieh MM, Pittaluga S, Raffeld M, et al. Modeling tumor-host interactions of chronic lymphocytic leukemia in xenografted mice to study tumor biology and evaluate targeted therapy. *Leukemia* (2013) 27:2311–21. doi: 10.1038/leu.2013.131
6. Patten PE, Ferrer G, Chen SS, Simone R, Marsilio S, Yan XJ, et al. Chronic lymphocytic leukemia cells diversify and differentiate in vivo via a nonclassical Th1-dependent, Bcl-6-deficient process. *JCI Insight* (2016) 1 (4):e86288. doi: 10.1172/jci.insight.86288
7. Decker S, Zwick A, Khaja Saleem S, Kissel S, Rettig A, Aumann K, et al. Optimized Xenograft Protocol for Chronic Lymphocytic Leukemia Results in High Engraftment Efficiency for All CLL Subgroups. *Int J Mol Sci* (2019) 20 (24):6277–94. doi: 10.3390/ijms20246277
8. Fais F, Ghiotto F, Hashimoto S, Sellars B, Valetto A, Allen SL, et al. Chronic lymphocytic leukemia B cells express restricted sets of mutated and unmutated antigen receptors. *J Clin Invest* (1998) 102(8):1515–25. doi: 10.1172/JCI3009
9. Westermann J, Puskas Z, Pabst R. Blood transit and recirculation kinetics of lymphocyte subsets in normal rats. *Scand J Immunol* (1988) 28(2):203–10. doi: 10.1111/j.1365-3083.1988.tb02432.x
10. Young AJ, Marston WL, Dessing M, Dudler L, Hein WR. Distinct recirculating and non-recirculating B-lymphocyte pools in the peripheral blood are defined by coordinated expression of CD21 and L-selectin. *Blood* (1997) 90(12):4865–75. doi: 10.1182/blood.V90.12.4865
11. Wiekmeijer AS, Pike-Overzet K, Brugman MH, Salvatori DC, Egeler RM, Bredius RG, et al. Sustained Engraftment of Cryopreserved Human Bone Marrow CD34(+) Cells in Young Adult NSG Mice. *Biores Open Access* (2014) 3(3):110–6. doi: 10.1089/biores.2014.0008
12. Papa I, Vinuesa CG. Synaptic Interactions in Germinal Centers. *Front Immunol* (2018) 9:1858. doi: 10.3389/fimmu.2018.01858
13. Rawstron AC. Immunophenotyping of plasma cells. *Curr Protoc Cytom* (2006) 6.23.1–6.23.14. doi: 10.1002/0471142956.cy0623s36
14. Moore PA, Zhang W, Rainey GJ, Burke S, Li H, Huang L, et al. Application of dual affinity retargeting molecules to achieve optimal redirected T-cell killing of B-cell lymphoma. *Blood* (2011) 117(17):4542–51. doi: 10.1182/blood-2010-09-306449
15. Circosta P, Elia AR, Landra I, Machiorlatti R, Todaro M, Aliberti S, et al. Tailoring CD19xCD3-DART exposure enhances T-cells to eradication of B-cell neoplasms. *Oncoimmunology* (2018) 7(4):e1341032. doi: 10.1080/2162402X.2017.1341032
16. Murphy EJ, Neuberg DS, Rassenti LZ, Hayes G, Redd R, Emson C, et al. Leukemia-cell proliferation and disease progression in patients with early stage chronic lymphocytic leukemia. *Leukemia* (2017) 31(6):1348–54. doi: 10.1038/leu.2017.34
17. Naradikian MS, Perate AR, Cancro MP. BAFF receptors and ligands create independent homeostatic niches for B cell subsets. *Curr Opin Immunol* (2015) 34:126–9. doi: 10.1016/j.coi.2015.03.005
18. Kurtova AV, Balakrishnan K, Chen R, Ding W, Schnabl S, Quiroga MP, et al. Diverse marrow stromal cells protect CLL cells from spontaneous and drug-induced apoptosis: development of a reliable and reproducible system to assess stromal cell adhesion-mediated drug resistance. *Blood* (2009) 114 (20):4441–50. doi: 10.1182/blood-2009-07-233718
19. Chumley MJ, Dal Porto JM, Cambier JC. The unique antigen receptor signaling phenotype of B-1 cells is influenced by locale but induced by antigen. *J Immunol* (2002) 169(4):1735–43. doi: 10.4049/jimmunol.169.4.1735
20. Chen SS, Batliwalla F, Holodick NE, Yan XJ, Yancopoulos S, Croce CM, et al. Autoantigen can promote progression to a more aggressive TCL1 leukemia by selecting variants with enhanced B-cell receptor signaling. *Proc Natl Acad Sci USA* (2013) 110(16):E1500–E7. doi: 10.1073/pnas.1300616110
21. Messmer BT, Messmer D, Allen SL, Kolitz JE, Kudalkar P, Cesar D, et al. In vivo measurements document the dynamic cellular kinetics of chronic lymphocytic leukemia B cells. *J Clin Invest* (2005) 115(3):755–64. doi: 10.1172/JCI23409
22. Calissano C, Damle RN, Marsilio S, Yan XJ, Yancopoulos S, Hayes G, et al. Intra-clonal complexity in chronic lymphocytic leukemia: fractions enriched in recently born/divided and older/quiescent cells. *Mol Med (Cambridge Mass* (2011) 17(11-12):1374–82. doi: 10.2119/molmed.2011.00360
23. Herndon TM, Chen SS, Saba NS, Valdez J, Emson C, Gatmaitan M, et al. Direct in vivo evidence for increased proliferation of CLL cells in lymph nodes compared to bone marrow and peripheral blood. *Leukemia* (2017) 31 (6):1340–7. doi: 10.1038/leu.2017.11

Conflict of Interest: NC received the DART molecule, the DART control molecule, and financial support to carry out the studies in **Figure 8** from Janssen Pharmaceuticals, Inc.

The remaining authors declare that the research was conducted in the absence of any commercial or financial relationships that could be construed as a potential conflict of interest.

frontiers in Immunology

REVIEW
published: 12 April 2021
doi: 10.3389/fimmu.2021.634584

The Eμ-hnRNP K Murine Model of Lymphoma: Novel Insights into the Role of hnRNP K in B-Cell Malignancies

Prerna Malaney[1†], María Velasco-Estevez[2†], Pedro Aguilar-Garrido[2†], Marisa J. L. Aitken[1], Lauren E. Chan[1], Xiaorui Zhang[1], Sean M. Post[1] and Miguel Gallardo[2]*

[1] Department of Leukemia, MD Anderson Cancer Center, Houston, TX, United States, [2] H12O–CNIO Haematological Malignancies Clinical Research Unit, CNIO, Madrid, Spain

OPEN ACCESS

Edited by:
Christelle Vincent-Fabert, UMR7276 Contrôle des réponses immunes B et des lymphoprolifération (CRIBL), France

Reviewed by:
Michel Cogne, University of Limoges, France
Rachel Maurie Gerstein, University of Massachusetts Medical School, United States

***Correspondence:**
Miguel Gallardo
mgallardod@cnio.es;
miguelgallardodelgado@gmail.com

[†]These authors have contributed equally to this work

Specialty section:
This article was submitted to B Cell Biology, a section of the journal Frontiers in Immunology

Received: 28 November 2020
Accepted: 23 March 2021
Published: 12 April 2021

Citation:
Malaney P, Velasco-Estevez M, Aguilar-Garrido P, Aitken MJL, Chan LE, Zhang X, Post SM and Gallardo M (2021) The Eμ-hnRNP K Murine Model of Lymphoma: Novel Insights into the Role of hnRNP K in B-Cell Malignancies. Front. Immunol. 12:634584. doi: 10.3389/fimmu.2021.634584

B-cell lymphomas are one of the most biologically and molecularly heterogeneous group of malignancies. The inherent complexity of this cancer subtype necessitates the development of appropriate animal model systems to characterize the disease with the ultimate objective of identifying effective therapies. In this article, we discuss a new driver of B-cell lymphomas – hnRNP K (heterogenous nuclear ribonucleoprotein K)—an RNA-binding protein. We introduce the *Eμ-Hnrnpk* mouse model, a murine model characterized by hnRNP K overexpression in B cells, which develops B-cell lymphomas with high penetrance. Molecular analysis of the disease developed in this model reveals an upregulation of the *c-Myc* oncogene *via* post-transcriptional and translational mechanisms underscoring the impact of non-genomic *MYC* activation in B-cell lymphomas. Finally, the transplantability of the disease developed in *Eμ-Hnrnpk* mice makes it a valuable pre-clinical platform for the assessment of novel therapeutics.

Keywords: B-cell malignancies, lymphoma, diffuse large B cell lymphoma, mouse model, hnRNP K, *Eμ-Hnrnpk*, RNA-binding protein, *MYC*

INTRODUCTION TO B-CELL MALIGNANCIES

B-cell neoplasms comprise a heterogeneous cohort of hematological malignancies originating from B cells. They are classified, according to WHO criteria, into precursor B-cell neoplasms (B-lymphoblastic leukemia) and mature B-cell neoplasms (1). Mature B-cell neoplasms encompass a plethora of malignancies, such as leukemias (chronic lymphocytic leukemia, small lymphocytic lymphoma), plasma cell malignancies (e.g. myeloma), and lymphomas. Specifically, lymphomas are classified as Hodgkin's and non-Hodgkin's lymphomas, which account for 10% and 90% of cases, respectively (2). Nearly half of all non-Hodgkin's lymphomas are diffuse large B-cell lymphomas (DLBCL), making them the most commonly diagnosed lymphoma sub-type. Other non-Hodgkin's

Abbreviations: DLBCL, diffuse large B-cell lymphoma; hnRNP K, heterogeneous nuclear ribonucleoprotein K; VDJ, variability, diversity, and joining; PDX, patient-derived xenograft; IgH, immunoglobulin heavy; RBP, RNA-binding protein; GC, germinal center; SHM, somatic hypermutation; CSR, class-switch recombination.

lymphomas include follicular lymphomas, marginal zone lymphoma, mantle cell lymphoma and Burkitt's lymphoma (3).

B cells are part of the adaptive immune system and play a vital role in the production of antigen-specific immunoglobulins (antibodies) in response to invasive pathogens. In order to do so, B cells must maintain an extensive array of antigen receptors. B cells must also demonstrate high variability in antigen recognition sites in order to protect organisms against a plethora of pathogens. To achieve this, B cells employ a complex mechanism called VDJ recombination, which enables the generation of an almost unlimited repertoire of antigenic B-cell receptors. The VDJ recombination process involves the formation and repair of several highly regulated DNA breaks. Aberrations in this intricate process along with spontaneous mutations and breaks in the DNA lead to alterations that in turn promote the malignant transformation of B cells (4, 5).

Aberrant VDJ recombination often results in chromosomal translocations. A clear example of this is Burkitt's lymphoma wherein a chromosomal translocation results in constitutive activation of the *MYC* oncogene (6–8). Other examples include the t(14;18) translocation in follicular lymphoma, resulting in constitutive expression of *BCL2* (4) and the t(11;14) translocation involving the cyclin D1 gene in mantle-cell lymphoma (9, 10). In addition to translocations, somatic mutations in various genes have also been implicated in the pathogenesis of other non-Hodgkin's lymphomas (11). Beyond mutations, overexpression of oncogenes and loss of tumor suppressor genes have also been identified as driver events for lymphomagenesis (12–14). Well-defined genetic basis of disease has helped establish several genetically defined transgenic models of B-cell malignancies, as discussed below.

Microscopic analysis of lymphomas show that tumors contain not only cancerous cells, but also host immune cells, stromal cells, blood vessels and the extracellular matrix, comprising the *tumor microenvironment* (15). Tumor cells create this microenvironment by first homing to sites that promote or help their growth, and later recruiting support cells and/or causing cells in their microenvironment to differentiate to their benefit (3). In recent years, it has become clear that the tumor microenvironment is a key player in the onset and progression of cancer, as well as therapy resistance, underscoring the need for better understanding in this area. Investigating B-cell lymphomas using *in vitro* systems is an important initial approach, but its predictive value is limited as it leaves out other factors such as the host immune system and the tumor microenvironment. Therefore, the use of more complex tools such as genetically engineered mouse models are needed to more fully study B-cell malignancies.

Need for the Development of New Murine Models for B-Cell Malignancies

Murine models of hematological malignancies can be classified as genetically modified models or patient-derived xenograft (PDX) models. The former can be used to investigate the onset, progression and therapeutic approaches for leukemia and lymphomas, while the latter is a valuable platform for drug testing and pre-clinical research.

PDX models are ideal for preclinical studies, wherein a heterogeneous population of tumor cells extracted from a patient is implanted into an immunocompromised mouse, thereby facilitating studies that assess the response or resistance of the disease to existing and novel therapeutic agents (16). Despite the caveat of lacking the tumor-immune cell component, B-cell lymphoma PDX mouse models can show biological, histopathological and clinical features of the original patient tumor, making it an ideal platform for preclinical studies (17). The use of humanized mice for transplantation is gaining popularity and allows for the assessment of immunotherapies as well as the study of the interactions between the tumor and the immune system (18). However, PDX models cannot be used to investigate the onset and progression of tumors. They are also not amenable for the identification of novel oncogenes or tumor suppressor genes, making transgenic and knockout mouse models the preferred platform for this aim. While PDX models enable the assessment of developed disease, transgenic animal models can be used to investigate the origin and onset of disease. Moreover, PDX models carry the diversity of the patients they are derived from and are therefore diverse in their pathology and drug responses, complicating interpretation of data. Transgenic models, however, have a common background allowing for a replicable and controlled phenotype for research. Taken together, the research hypotheses and objectives must be taken into consideration while selecting an appropriate animal model.

There are several well-defined genetic alterations observed in human patients that give rise to B-cell lymphomas due to uncontrolled B-cell proliferation and/or maturation. Some of these genetic alterations have already been recreated in transgenic mice to study the spontaneous onset and progression of lymphomas and leukemia-like phenotypes. Notable models include a *BCL6* knock-in which results in a DLBCL-like phenotype (19), *VavP-Bcl2* mice, mimicking the t(14; 18) chromosomal translocation, which develop follicular lymphomas, a targeted deletion of *Trp53 – CD21-Tp53lox* – that develops non-germinal center B-cell lymphomas, and *Eμ-Tcl1* mice which develop aggressive chronic lymphocytic leukemia (20–22).

However, the most recurrent and extensively investigated genetic alterations are translocations of the *MYC* oncogene. In the 1980s, *MYC* was identified as the first proto-oncogene in B-cell lymphomas. Transgenic mouse models with translocations in the *Myc* gene were first introduced in 1985 (23). Of these models, the most extensively used is the *Eμ-Myc* model. This mouse obtained by the translocation of *Myc* to the Ig Heavy chain (IgH) locus, causing overexpression of c-Myc and abnormal B-cell proliferation (24). Similar to humans, *Eμ-Myc* mice develop B-cell lymphoma-like malignancies with a >90% penetrance and variable onset. These *Eμ-Myc* mice exhibit either a DLBCL phenotype or a Burkitt's lymphoma phenotype depending on the time of development (25, 26). Another model of c-Myc driven Burkitt's lymphoma is one driven solely by the 3' regulatory region of the IgH locus rather than the *Eμ* enhancer. This model results in the development of B-cell malignancies with a mature B-cell phenotype in contrast to the *Eμ* model wherein a pro-B phenotype is predominant (27, 28).

However, multiple mouse models with other *Myc* translocations develop different B-cell malignancies, such as *Vκ-Myc* mice for myeloma (29), *λ-Myc* for Burkitt's lymphoma (30), iMycEμ for endemic Burkitt's lymphoma (31), and iMycCμ mice for sporadic and immunodeficiency-associated Burkitt's lymphoma (32), demonstrating the critical role of c-Myc in B cell biology.

NEW DRIVER OF B-CELL LYMPHOMAS: HNRNP K

Altered genes have historically been designated as either tumor suppressors or oncogenes. However, recent studies have shown that some genes can have dual oncogenic and tumor-suppressive functions in different contexts (33). One such example of a dual regulator is heterogeneous nuclear ribonucleoprotein K (*HNRNPK*) (34).

hnRNP K is an ss-DNA and RNA-binding protein that regulates a myriad of cellular processes *via* transcriptional, posttranscriptional and translational mechanisms. It contains three K homology (KH) domains – responsible for nucleic acid binding – one K-protein-interactive domain (KI), and one nuclear-cytoplasmic shuttling domain (KNS) (35, 36). Due to hnRNP K's pleiotropic nature, both its over- and under-expression can be pathogenic (37–41), likely by deregulating the transcription and/or translation of multiple cellular oncogenes or tumor suppressors. For instance, there is a clinical correlation between high levels of hnRNP K and the onset and treatment resistance of various tumors types in patients, such as lung (42), breast (43), rectal adenocarcinoma (44), and melanoma (45). In the context of hematological malignancies, ~2% of acute myeloid leukemia patients have a 9q21.32 deletion that encompasses the *HNRNPK* gene, resulting in loss of one copy of *HNRNPK*. Consequently, haploinsufficiency of *HNRNPK* was shown to be pathogenic in mice, as an *Hnrnpk*$^{+/-}$ mouse model showed a myeloproliferative phenotype and reduced survival. In addition, *Hnrnpk* haploinsufficiency also triggered B-cell lymphoma phenotypes in 30% of the animals. This role of hnRNP K as a tumor suppressor is partially due to its regulation of the p53/p21 pathway (40, 46). However, it is of note that hnRNP K acts not only as a tumor suppressor, but also an oncogene. It has been shown that hnRNP K promotes the expression of classical oncogenes such *c-Myc*, resulting in the development of B-cell malignancies (39, 45), as well as c-Src (47) and eIF4E (38). As an ss-DNA and RNA-binding protein, hnRNP K can regulate both the transcription and translation of certain genes, as it does in the case of *MYC*. It has been observed that hnRNP K binds to the CT-rich regions of the *MYC* promoter, enhancing transcription of this gene (48–50). Additionally, hnRNP K positively regulates translation of *MYC* mRNA by binding to the IRES (Internal Ribosome Entry Site) sequence, aiding its entry to the ribosome through a cap-independent mechanism (37, 51). Control of *MYC* translation *via* this mechanism through hnRNP K is significant in the context of tumorigenesis, as it has been observed that even a single CT mutation in the IRES sequence – present in 42% of myeloma multiple patients – could enhance the binding of hnRNP K to this sequence and promote an increased aberrant expression of c-Myc (52). In fact, hnRNP K has been described as an (IRES)-trans-acting factors (ITAF) and can potentially regulating cap-independent translation of several oncogenes resulting in the systemic activation of an oncogenic program (53, 54).

Given the role of hnRNP K in regulating the expression levels of oncogenic molecules, elevated hnRNP K levels are observed in several solid and hematological malignancies (42, 44, 45). Specific to B-cell lymphomas, as we have previously described in Gallardo et al., hnRNP K is overexpressed in human patients with diffuse large B-cell lymphoma and is associated with poor clinical outcomes and non-responsiveness to chemotherapy (39). Overexpression of hnRNP K is also observed in Burkitt's lymphoma where sumoylated hnRNP K is elevated, which regulates the expression of c-Myc at the translational level (55). Taken together, a dual role of hnRNP K has been observed in the formation of hematological malignancies, wherein an under-expression of the protein leads to a deficit in its role inducing the expression of tumor suppressors p53/p21, thus leading to a myeloproliferative phenotype and lymphoma in rodents (40), while on the other hand, an increment in the levels of hnRNP K has been related to higher levels of c-Myc and the formation of lymphomas (39, 55).

Critically, with respect to B-cell malignancies, we observe an oncogenic function for hnRNP K. Our data showed that hnRNP K is overexpressed in DLBCL patients and higher expression of hnRNP K correlates with poor clinical outcomes and lack of response to chemotherapy in these patients. Interestingly, we observed that hnRNP K is overexpressed in patients who do not harbor any *MYC* genomic alterations. The regulation of *MYC* by hnRNP K occurs at the post-transcriptional and translational level, indicating that hnRNP K over-expression represents a key non-genomic mechanism of *MYC* regulation in B-cell lymphomas (37).

The role of hnRNP K is especially critical given the increasing clinical relevance of RNA-binding proteins (RBPs) and splicing factors in hematological malignancies. Mutations and aberrant expression of RBPs is increasingly being observed in leukemia, myelodysplastic disease, and lymphomas (56–60). Moreover, taking into consideration the critical role of c-Myc not only in B-cell biology and B-cell malignancies, but also in other heme malignancies, hnRNP K-mediated regulation of c-Myc warrants extensive study. The B-cell specific murine model of hnRNP K, *Eμ-Hnrnpk*, described below, is therefore crucial for unraveling the complex and nuanced role of this protein in B-cell malignancies.

Eμ-HNRNPK MURINE MODEL AS A PLATFORM TO STUDY B-CELL MALIGNANCIES

We previously generated the *Eμ-Hnrnpk* mouse model by placing the *Hnrnpk* cDNA downstream of the extensively characterized immunoglobulin heavy-chain (*Igh*) enhancer Eμ. The resulting mice specifically overexpress hnRNP K in B cells, have reduced survival, and develop B-cell malignancies (39). The *Eμ-Hnrnpk* model has several utilities and applications. First, the

model helps establish the RNA-binding protein, hnRNP K, as a *bona fide* oncogene. To the best of our knowledge, this is the first published transgenic mouse model that demonstrates the oncogenicity of hnRNP K over-expression. Second, the model provides an *in-vivo* system to assay the role of hnRNP K in B-cell biology and malignancy. Third, the mice provide a pre-clinical platform to test existing and experimental therapeutics.

Phenotype of the *Eμ-Hnrnpk* Mouse Model

The *Eμ-Hnrnpk* mice develop B-cell malignancies with a high latency. Roughly 70% of mice survived the first year but only 20% survived until the end of the second year. This accelerated mortality between years one and two may be due to yet-unknown secondary genomic aberrations or epigenetic changes warranting further in-depth analyses of this disease model. In contrast with the slow generation of the phenotype, the disease penetrance is incredibly high – almost 100% of the mice developed some type of B-cell malignancy.

Gross analyses revealed that *Eμ-Hnrnpk* mice have marked hepatosplenomegaly, a 12-fold increase in spleen weight, and a 3.5-fold increase in the hepatic weight. The splenomegaly is accompanied by loss of splenic architecture, expansion of B-cell lineages as evidenced by increased PAX5 staining, and the presence of highly proliferative Ki67+ cells. In addition to their proliferative nature, the malignant cells have invasive properties as well. Livers of tumor-burdened mice showed extensive B-cell (B220+) infiltration and minimal T-cell (CD3+) infiltration.

The malignancy of *Eμ-Hnrnpk* cells was confirmed through transplantation assays. Immunodeficient mice injected with cells from *Eμ-Hnrnpk* mice bearing disease recapitulate the same phenotypes (reduced survival, B cell proliferation), confirming the cell-autonomous nature of *Eμ-Hnrnpk* cells.

The preponderance of large malignant cells observed in hematopoietic tissues of the *Eμ-Hnrnpk* mice and clinical data from DLBCL patients pinpoint the role of hnRNP K overexpression in this disease. However, a small proportion (2-5%) of the *Eμ-Hnrnpk* mice developed other types of B-cell malignancies, not described herein, consistent with plasma cell-like malignancy. This observation falls in line with some late-arising tumors seen in *Eμ-Myc* mice that tend to develop lymphomas derived from plasma cells or with plasma cell differentiation (25).

Molecular Mechanism of hnRNP K-Mediated Lymphomagenesis

Due to the plurality of hnRNP K's cellular roles, the molecular mechanism of hnRNP K-mediated lymphomagenesis is likely to be multifaceted and complex. However, hnRNP K has been previously demonstrated to bind to C-rich regions in DNA and RNA (38, 61). Data obtained from RIP-Seq (RNA immunoprecipitation followed by sequencing) and its formaldehyde-fixed molecular cousin (fRIP-seq) (62) experiments, previously published in Gallardo et al., revealed that one of the top targets of hnRNP K is the *MYC* transcript, and that this interaction enhances its stability and translation (39). We confirmed a direct interaction between hnRNP K protein and the *MYC* transcript using fluorescence anisotropy assays. Actinomycin-chase experiments revealed an increased stability of the *MYC* transcript associated with hnRNP K overexpression. Finally, polysome profiling assays revealed the essential role of hnRNP K in regulating *MYC* translation and that knockdown of hnRNP K adversely affected the loading of the *MYC* transcript onto monosomes. Taken together, our biochemical and molecular assays establish a physical and functional link between hnRNP K and *MYC* (**Figure 1**). This finding is borne out in the *in vivo* model: lymphomas derived from *Eμ-Hnrnpk* mice show elevated c-Myc levels. These findings are particularly relevant when coupled with the observation that hnRNP K expression levels are elevated in DLBCL patients without *MYC* genomic alterations, suggesting that hnRNP K can drive c-Myc signaling in the absence of *MYC* mutations. Therefore, hnRNP K overexpression represents an alternate mechanism of c-Myc pathway activation in B-cell malignancies. Interestingly, *Smurf2* ablation in mice also results in the development of B-cell tumors due to transcriptional upregulation of the c-Myc protein representing yet another non-genomic mechanism of aberrant c-Myc

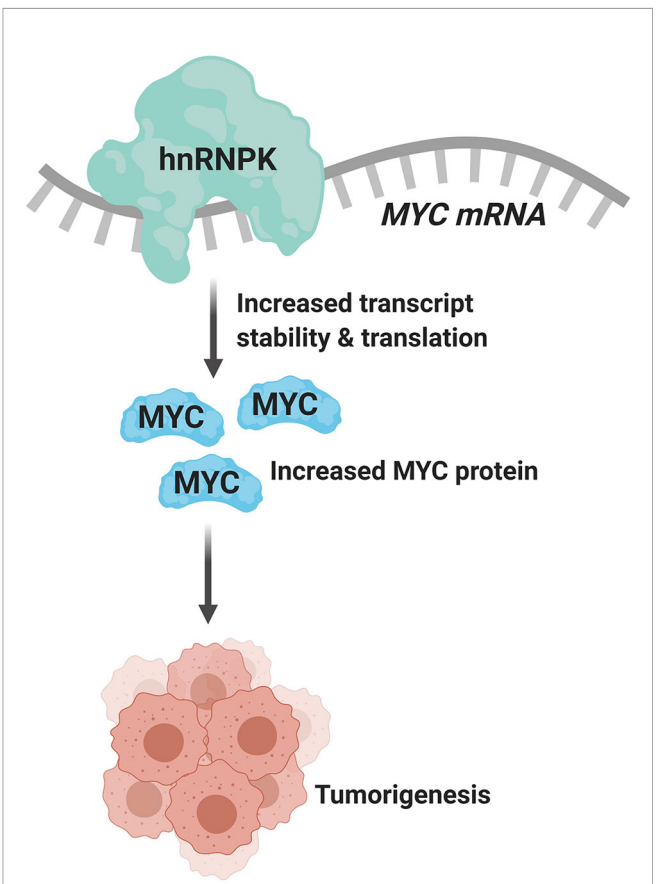

FIGURE 1 | hnRNP K binds to and regulates the stability and translation of the *MYC* transcript (created with BioRender.com).

expression in tumors (63). Considering the fact that hnRNP K binds to a multitude of transcripts, it would be reasonable to assume that it causes lymphomagenesis *via* several mechanisms and not just *via* regulation of c-Myc. An overlap of RIP-Seq data from two hematological cell lines (K562 and OCI-AML3) with a set of genes implicated in lymphomas reveal several interesting candidates for further study (**Figure 2**) (19, 64).

Beyond its RNA-binding functions, hnRNP K also interacts with a host of proteins *via* its KI domain. Therefore, it is entirely plausible that the protein interactome of hnRNP K contributes to its oncogenicity. Immunoprecipitation of hnRNP K followed by mass spectrometry, as described in Gallardo et al., revealed that hnRNP K associates with a host of ribosomal and RNA processing proteins (39). Given the preponderance of ribosomal subunits in the hnRNP K interactome, the impact that hnRNP K has on global translational profiles and its relationship to p53 allude to the possibility that aberrations in hnRNP K are likely to contribute to a nucleolar stress response (NSR). In fact, IP/MS experiments reveal a physical interaction between hnRNP K and the NSR sensor Nucleolin (NCL). The impact of hnRNP K on ribosome biogenesis and nucleolar stress pathways and their relevance to disease is currently under investigation in our laboratories.

In conclusion, the *Eμ-Hnrnpk* mice demonstrate a level of biological heterogeneity that is also seen in human disease. Consequently, the model represents a valuable tool for the assessment of existing and novel drugs and therapies. The transplantability of malignant cells from this model and the aggressive nature of the transplanted disease allow for a rapid evaluation of therapeutic modalities. Although current transplantation studies with the *Eμ-Hnrnpk* are limited to immunodeficient mice, future research with syngeneic models may be of value, particularly to test immunotherapeutic agents.

DISCUSSION

The generation, maturation, and genetic reprogramming of B-cell lymphocytes represent some of the most complex biological processes outside of development. The maturation process occurs in a bevy of host hematologic tissues. Germinal centers (GCs) – specific structures in secondary lymphoid organs, such as lymph nodes and the spleen – are where the generation and selection of B cells occurs. GCs are typically divided into the dark and the light zone. In the dark zone, B cells undergo rapid and mutative cell division called immunoglobulin somatic hypermutation (SHM), while in the light zone, B cells are selected based on antigen affinity. The whole process of GC initiation, dark zone formation, and the passage of B cells between the dark and light zones to final differentiation is a concatenated process involving the participation of a plethora of proteins such as BCL6, BCL2, TCL1, PAX5, IRF4, NFKB, MLL2 and c-Myc (65). All of these molecules are differentially expressed based on areas within the GC and/or stage of B-cell differentiation and are intricately balanced *via* multiple feedback loops. The inherent process of B-cell maturation and function relies on the inaccuracy of targeted DNA breaks and subsequent repair during VDJ recombination, SHM, and class-switch recombination (CSR). The rapid mutative divisions in B cells therefore put their genomic integrity in jeopardy. When an error occurs, the two most common genomic sequelae are chromosomal translocations and aberrant SHMs (ASHMs) (66). These alterations are due to mistakes in recombination activating gene (RAG) mediated VDJ recombination process, mistakes in the activation-induced cytidine deaminase (AID) dependent-CSR process, or translocations involving IGH (66). The result of these aberrancies is commonly the juxtaposition of strong promoters/enhancers (e.g. IGH) in front of oncogenes related with B-cell biology. The dysregulation of these oncogenes

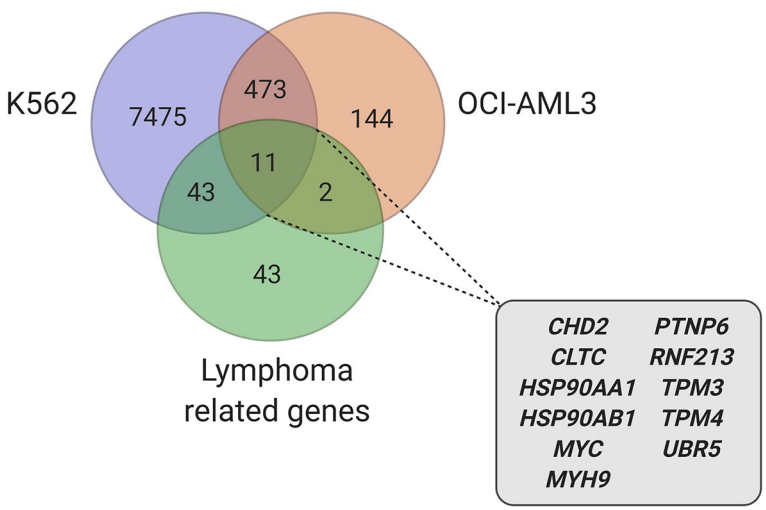

FIGURE 2 | Candidate genes, involved in lymphoma, identified in hnRNP K RIP-Seq datasets (39, 64) (created with BioRender.com).

drives B-cell hematological malignancies such as follicular lymphoma (*BCL2* translocation, MLL2 inactivation) (11, 67) DLBCL (e.g. *BCL6*, *BCL2* and *MYC* translocation) (8, 68, 69) or Burkitt's lymphoma (*MYC* translocation) (70, 71).

In the last 40 years, researchers have tried to reproduce the same genetic alterations and translocations found in human B-cell malignancies in animal models in order to develop tools to study the pathophysiology of the disease and develop pre-clinical therapeutic platforms. However, there are some challenges involved in the creation of these models. The vast majority of models of B-cell disease – such as *Eμ-Myc*, *VavP-Bcl2* or *Iμ-Bcl6* – are not "clean" models, i.e. they do not perfectly recapitulate human disease or often result in the development of multiple phenotypes due to two main reasons. First, "timing" and "location" in B-cell development plays a pivotal role in its biology, and heavily impact the development of B-cell malignancies. Thus, expression of the oncogenes in a more mature or immature B-cell subtype could result in completely different phenotypes than those observed in human disease. Consequently, the use of universal B-cell promoters that are common to multiple B-cell subtypes will often result in mixed phenotypes (25). Second, most drivers of B-cell malignancies are master regulators of a slew of different biological processes. Therefore, dysregulation of these molecules inhibits DNA damage response, increases genomic instability, or promotes other biological phenomena that enhance the accumulation of genomic aberrations in lymphoma cells. These genetic alterations will likely be different in each individual mouse, and its relationship with the driver alteration could explain the diversity of phenotypes. As an example, Lefebure et al. studied the genetic landscape of *Eμ-Myc* mice and observed multiple single nucleotide variants, deletions, or indels in *Bcor*, *Trp53*, *Cdkn2a, Kras* or *Nras*, suggesting that genomic instability driven by the genetic modification i.e., *Myc*, and the collaboration of other oncogenes and tumor suppressors contribute to the final malignant phenotype (72). The *Eμ-Hnrnpk* mouse model is not an exception to these problems. The limitations of the model are in fact consistent with other B-cell malignancy models. hnRNP K is also a master regulator of multiple biological process, as it regulates transcription, translation, DNA damage response, and splicing (36), which may contribute to the diversity of phenotypes observed in the *Eμ-Hnrnpk* model. Moreover, hnRNP K, as an RNA-binding protein, governs the expression of other master regulators beyond c-Myc (39). There are also multiple lines of evidence that suggest hnRNP K can function as a master cancer switch, driving not only hematological neoplasms, but also solid tumors (42–45).

One of the most common lymphomagenesis mouse models used is the *Eμ-Myc* mouse model. The extensive use of the *Eμ-Myc* model is not only due to historical reasons (model was developed in 1985), but also due to the biological mechanisms of lymphomagenesis. c-Myc is the most widely studied master regulator of B-cell malignancies and is altered in follicular lymphoma, DLBCL, Burkitt's lymphoma, and myeloma. However, dysregulation of the c-Myc pathway is observed more frequently than can be explained *via MYC* genomic aberrations. Thus, it is critical to identify c-Myc regulators that contribute to its non-genomic regulation. To this end, hnRNP K as an RNA-binding protein emerged as an idyllic candidate, and the *Eμ-Hnrnpk* mouse model allows exploration of B-cell malignancies in the absence of *MYC* alterations. Moreover, we recently found that hnRNP K is overexpressed in DLBCL patients, suggesting its direct role in B-cell malignancies and thereby making the *Eμ-Hnrnpk* model relevant beyond its function as a genetic and mechanistic tool. However, hnRNP K is a relatively under-studied molecule in cancer, particularly in B-cell neoplasms. Our studies with *Hnrnpk* haploinsufficient mice demonstrated that hnRNP K plays a vital role in lymphomagenesis beyond its role as a c-Myc regulator (40). Rigorous experimentation is required to better determine the role of hnRNP K in lymphocyte biology and its implications in development of DLBCL and other B-cell malignancies. Further work also needs to be done to identify the mechanisms underlying hnRNP K overexpression in human disease.

Perhaps the biggest drawback of most common B-cell malignancy mouse models is the diversity in phenotype development that makes them divergent from human disease. As previously discussed, the nature of the oncogenic drivers and their relationship with other cancer regulators combined with the spatio-temporal expression of the genetic modifications contributes to these divergences. Thus, more selective and specific mouse models, using promoters of one-stage/one-grade of B-cell maturation could help to surpass these limitations. Moreover, the generation of more complex mouse models that could recapitulate human diseases more precisely, with a combination of different genetic alterations, could guarantee more consistent models. In fact, complex models, such as *Eμ-Myc/BCR^{HEL}/sHEL* to mimic Burkitt's lymphoma, or *IL-14α TG × c-Myc TG (DTG)* mice for blastoid-variant mantle-cell lymphoma (MCL-BV) are good examples (73, 74).

The ability of a murine model to accurately mimic human disease is more relevant when animal models are used as therapeutic platforms. The selection of a model that does not accurately recapitulate human disease could contribute to the low correlation between results observed in pre-clinical and clinical trials. Indeed, only 8% of pre-clinical animal model research successfully advances to clinical trials, and of the experimental agents that are successful in preclinical models, 85% of them fail in early stages of human trials (75). Hence, a battery of B-cell malignancies drivers and promoters is needed to more precisely mimic the spatio-temporal compartmentalization of alterations to ensure better clinical correlations. To this end, the *Eμ-Hnrnpk* model adds to the catalog of mouse models available to study B-cell malignancies and establish therapeutic platforms, alone or in combination with other drivers.

ETHICS STATEMENT

The animal study was reviewed and approved by Institutional Animal Care and Use Committee at MD Anderson under protocol 0000787-RN02.

AUTHOR CONTRIBUTIONS

PM, MV-E, and PA-G: conceptualized, organized, and wrote the manuscript and generated figures. MJLA, LEC, and XZ: critically revised the manuscript. SMP and MG supervised and critically revised the manuscript. All authors contributed to the article and approved the submitted version.

FUNDING

This study has been supported a National Cancer Institute/ National Institutes of Health Award (R01CA207204) and Leukemia and Lymphoma Society (6577–19) to SMP. PM is a Jane Coffin Childs Memorial Fund for Medical Research Fellow and MA is a recipient of the Dr. John J. Kopchick Fellowship. MG is supported by financial support from the Cris contra el Cancer association and Instituto de Salud Carlos III (Ministry of Economy, Industry and Competitiveness) and cofunded by the European Regional Development Fund with Miguel Servet (CP19/00140) and PI (PI18/00295).

ACKNOWLEDGMENTS

The authors would like to thank Carmen Delgado for her support in cytopathologic analysis.

REFERENCES

1. Swerdlow SH, Campo E, Pileri SA, Harris NL, Stein H, Siebert R, et al. The 2016 revision of the World Health Organization classification of lymphoid neoplasms. *Blood* (2016) 127(20):2375–90. doi: 10.1182/blood-2016-01-643569
2. Mugnaini EN, Ghosh N. Lymphoma. *Prim Care* (2016) 43(4):661–75. doi: 10.1016/j.pop.2016.07.012
3. Scott DW, Gascoyne RD. The tumour microenvironment in B cell lymphomas. *Nat Rev Cancer* (2014) 14(8):517–34. doi: 10.1038/nrc3774
4. Tsujimoto Y, Cossman J, Jaffe E, Croce CM. Involvement of the bcl-2 gene in human follicular lymphoma. *Science (New York NY)* (1985) 228(4706):1440–3. doi: 10.1126/science.3874430
5. Tsujimoto Y, Jaffe E, Cossman J, Gorham J, Nowell PC, Croce CM. Clustering of breakpoints on chromosome 11 in human B-cell neoplasms with the t(11 ; 14) chromosome translocation. *Nature* (1985) 315(6017):340–3. doi: 10.1038/315340a0
6. Dalla-Favera R, Bregni M, Erikson J, Patterson D, Gallo RC, Croce CM. Human c-myc onc gene is located on the region of chromosome 8 that is translocated in Burkitt lymphoma cells. *Proc Natl Acad Sci* (1982) 79 (24):7824–7. doi: 10.1073/pnas.79.24.7824
7. Taub R, Kirsch I, Morton C, Lenoir G, Swan D, Tronick S, et al. Translocation of the c-myc gene into the immunoglobulin heavy chain locus in human Burkitt lymphoma and murine plasmacytoma cells. *Proc Natl Acad Sci U S A* (1982) 79(24):7837–41. doi: 10.1073/pnas.79.24.7837
8. Hummel M, Bentink S, Berger H, Klapper W, Wessendorf S, Barth TF, et al. A biologic definition of Burkitt's lymphoma from transcriptional and genomic profiling. *N Engl J Med* (2006) 354(23):2419–30. doi: 10.1056/NEJMoa055351
9. Leroux D, Le Marc'Hadour F, Gressin R, Jacob MC, Keddari E, Monteil M, et al. Non-Hodgkin's lymphomas with t(11;14)(q13;q32): a subset of mantle zone/intermediate lymphocytic lymphoma? *Br J Haematol* (1991) 77(3):346–53. doi: 10.1111/j.1365-2141.1991.tb08582.x
10. Rimokh R, Berger F, Cornillet P, Wahbi K, Rouault J-P, Ffrench M, et al. Break in the BCL1 locus is closely associated with intermediate lymphocytic lymphoma subtype. *Genes Chromosomes Cancer* (1990) 2(3):223–6. doi: 10.1002/gcc.2870020310
11. Morin RD, Mendez-Lago M, Mungall AJ, Goya R, Mungall KL, Corbett RD, et al. Frequent mutation of histone-modifying genes in non-Hodgkin lymphoma. *Nature* (2011) 476(7360):298–303. doi: 10.1038/nature10351
12. Watanabe T, Hotta T, Ichikawa A, Kinoshita T, Nagai H, Uchida T, et al. The MDM2 oncogene overexpression in chronic lymphocytic leukemia and low-grade lymphoma of B-cell origin. *Blood* (1994) 84(9):3158–65. doi: 10.1182/blood.V84.9.3158.bloodjournal8493158
13. Hachem A, Gartenhaus RB. Oncogenes as molecular targets in lymphoma. *Blood* (2005) 106(6):1911–23. doi: 10.1182/blood-2004-12-4621
14. Geradts J, Andriko JW, Abbondanzo SL. Loss of Tumor Suppressor Gene Expression in High-Grade But Not Low-Grade Non-Hodgkin's Lymphomas. *Am J Clin Pathol* (1998) 109(6):669–74. doi: 10.1093/ajcp/109.6.669
15. Cioroianu AI, Stinga PI, Sticlaru L, Cioplea MD, Nichita L, Popp C, et al. Tumor Microenvironment in Diffuse Large B-Cell Lymphoma: Role and Prognosis. *Anal Cell Pathol* (2019) 2019:8586354. doi: 10.1155/2019/8586354
16. Hidalgo M, Amant F, Biankin AV, Budinská E, Byrne AT, Caldas C, et al. Patient-derived xenograft models: an emerging platform for translational cancer research. *Cancer Discov* (2014) 4(9):998–1013. doi: 10.1158/2159-8290.Cd-14-0001
17. Zhang L, Nomie K, Zhang H, Bell T, Pham L, Kadri S, et al. B-Cell Lymphoma Patient-Derived Xenograft Models Enable Drug Discovery and Are a Platform for Personalized Therapy. *Clin Cancer Res* (2017) 23(15):4212–23. doi: 10.1158/1078-0432.Ccr-16-2703
18. Morton JJ, Bird G, Refaeli Y, Jimeno A. Humanized Mouse Xenograft Models: Narrowing the Tumor-Microenvironment Gap. *Cancer Res* (2016) 76 (21):6153–8. doi: 10.1158/0008-5472.CAN-16-1260
19. Cattoretti G, Pasqualucci L, Ballon G, Tam W, Nandula SV, Shen Q, et al. Deregulated BCL6 expression recapitulates the pathogenesis of human diffuse large B cell lymphomas in mice. *Cancer Cell* (2005) 7(5):445–55. doi: 10.1016/j.ccr.2005.03.037
20. Gostissa M, Bianco JM, Malkin DJ, Kutok JL, Rodig SJ, Morse HC,3, et al. Conditional inactivation of p53 in mature B cells promotes generation of nongerminal center-derived B-cell lymphomas. *Proc Natl Acad Sci U S A* (2013) 110(8):2934–9. doi: 10.1073/pnas.1222570110
21. Egle A, Harris AW, Bath ML, O'Reilly L, Cory S. VavP-Bcl2 transgenic mice develop follicular lymphoma preceded by germinal center hyperplasia. *Blood* (2004) 103(6):2276–83. doi: 10.1182/blood-2003-07-2469
22. Lee HJ, Gallardo M, Ma H, Zhang X, Larsson CA, Mejia A, et al. p53-independent ibrutinib responses in an Eμ-TCL1 mouse model demonstrates efficacy in high-risk CLL. *Blood Cancer J* (2016) 6(6):e434. doi: 10.1038/bcj.2016.41
23. Adams JM, Harris AW, Pinkert CA, Corcoran LM, Alexander WS, Cory S, et al. The c-myc oncogene driven by immunoglobulin enhancers induces lymphoid malignancy in transgenic mice. *Nature* (1985) 318(6046):533–8. doi: 10.1038/318533a0
24. Harris AW, Pinkert CA, Crawford M, Langdon WY, Brinster RL, Adams JM. The E mu-myc transgenic mouse. A model for high-incidence spontaneous lymphoma and leukemia of early B cells. *J Exp Med* (1988) 167(2):353–71. doi: 10.1084/jem.167.2.353
25. Mori S, Rempel RE, Chang JT, Yao G, Lagoo AS, Potti A, et al. Utilization of pathway signatures to reveal distinct types of B lymphoma in the Emicro-myc model and human diffuse large B-cell lymphoma. *Cancer Res* (2008) 68 (20):8525–34. doi: 10.1158/0008-5472.Can-08-1329
26. Donnou S, Galand C, Touitou V, Sautès-Fridman C, Fabry Z, Fisson S. Murine Models of B-Cell Lymphomas: Promising Tools for Designing Cancer Therapies. *Adv Hematol* (2012) 2012:701704. doi: 10.1155/2012/701704
27. Ghazzaui N, Issaoui H, Ferrad M, Carrion C, Cook-Moreau J, Denizot Y, et al. Eμ and 3'RR transcriptional enhancers of the IgH locus cooperate to promote c-myc–induced mature B-cell lymphomas. *Blood Adv* (2020) 4(1):28–39. doi: 10.1182/bloodadvances.2019000845

28. Ghazzaui N, Saintamand A, Issaoui H, Vincent-Fabert C, Denizot Y. The IgH 3' regulatory region and c-myc-induced B-cell lymphomagenesis. *Oncotarget* (2017) 8(4):7059–67. doi: 10.18632/oncotarget.12535
29. Chesi M, Robbiani DF, Sebag M, Chng WJ, Affer M, Tiedemann R, et al. AID-dependent activation of a MYC transgene induces multiple myeloma in a conditional mouse model of post-germinal center malignancies. *Cancer Cell* (2008) 13(2):167–80. doi: 10.1016/j.ccr.2008.01.007
30. Kovalchuk AL, Qi CF, Torrey TA, Taddesse-Heath L, Feigenbaum L, Park SS, et al. Burkitt lymphoma in the mouse. *J Exp Med* (2000) 192(8):1183–90. doi: 10.1084/jem.192.8.1183
31. Park SS, Kim JS, Tessarollo L, Owens JD, Peng L, Han SS, et al. Insertion of c-Myc into Igh induces B-cell and plasma-cell neoplasms in mice. *Cancer Res* (2005) 65(4):1306–15. doi: 10.1158/0008-5472.Can-04-0268
32. Cheung WC, Kim JS, Linden M, Peng L, Van Ness B, Polakiewicz RD, et al. Novel targeted deregulation of c-Myc cooperates with Bcl-X(L) to cause plasma cell neoplasms in mice. *J Clin Invest* (2004) 113(12):1763–73. doi: 10.1172/jci20369
33. Manfredi JJ. The Mdm2–p53 relationship evolves: Mdm2 swings both ways as an oncogene and a tumor suppressor. *Genes Dev* (2010) 24(15):1580–9. doi: 10.1101/gad.1941710
34. Gallardo M, Hornbaker MJ, Zhang X, Hu P, Bueso-Ramos C, Post SM. Aberrant hnRNP K expression: All roads lead to cancer. *Cell Cycle (Georgetown Tex)* (2016) 15(12):1552–7. doi: 10.1080/15384101.2016.1164372
35. Barboro P, Ferrari N, Balbi C. Emerging roles of heterogeneous nuclear ribonucleoprotein K (hnRNP K) in cancer progression. *Cancer Lett* (2014) 352 (2):152–9. doi: 10.1016/j.canlet.2014.06.019
36. Bomsztyk K, Denisenko O, Ostrowski J. hnRNP K: one protein multiple processes. *BioEssays* (2004) 26(6):629–38. doi: 10.1002/bies.20048
37. Notari M, Neviani P, Santhanam R, Blaser BW, Chang JS, Galietta A, et al. A MAPK/HNRPK pathway controls BCR/ABL oncogenic potential by regulating MYC mRNA translation. *Blood* (2006) 107(6):2507–16. doi: 10.1182/blood-2005-09-3732
38. Lynch M, Chen L, Ravitz MJ, Mehtani S, Korenblat K, Pazin MJ, et al. hnRNP K binds a core polypyrimidine element in the eukaryotic translation initiation factor 4E (eIF4E) promoter, and its regulation of eIF4E contributes to neoplastic transformation. *Mol Cell Biol* (2005) 25(15):6436–53. doi: 10.1128/mcb.25.15.6436-6453.2005
39. Gallardo M, Malaney P, Aitken MJL, Zhang X, Link TM, Shah V, et al. Uncovering the Role of RNA-Binding Protein hnRNP K in B-Cell Lymphomas. *J Natl Cancer Inst* (2020) 112(1):95–106. doi: 10.1093/jnci/djz078
40. Gallardo M, Lee HJ, Zhang X, Bueso-Ramos C, Pageon LR, McArthur M, et al. hnRNP K Is a Haploinsufficient Tumor Suppressor that Regulates Proliferation and Differentiation Programs in Hematologic Malignancies. *Cancer Cell* (2015) 28(4):486–99. doi: 10.1016/j.ccell.2015.09.001
41. Enge M, Bao W, Hedström E, Jackson SP, Moumen A, Selivanova G. MDM2-dependent downregulation of p21 and hnRNP K provides a switch between apoptosis and growth arrest induced by pharmacologically activated p53. *Cancer Cell* (2009) 15(3):171–83. doi: 10.1016/j.ccr.2009.01.019
42. Tang F, Li W, Chen Y, Wang D, Han J, Liu D. Downregulation of hnRNP K by RNAi inhibits growth of human lung carcinoma cells. *Oncol Lett* (2014) 7 (4):1073–7. doi: 10.3892/ol.2014.1832
43. Mandal M, Vadlamudi R, Nguyen D, Wang R-A, Costa L, Bagheri-Yarmand R, et al. Growth Factors Regulate Heterogeneous Nuclear Ribonucleoprotein K Expression and Function. *J Biol Chem* (2001) 276(13):9699–704. doi: 10.1074/jbc.M008514200
44. Daskalaki W, Wardelmann E, Port M, Stock K, Steinestel J, Huss S, et al. Expression levels of hnRNP K and p21WAF1/CIP1 are associated with resistance to radiochemotherapy independent of p53 pathway activation in rectal adenocarcinoma. *Int J Mol Med* (2018) 42(6):3269–77. doi: 10.3892/ijmm.2018.3898
45. Wen F, Shen A, Shanas R, Bhattacharyya A, Lian F, Hostetter G, et al. Higher expression of the heterogeneous nuclear ribonucleoprotein k in melanoma. *Ann Surg Oncol* (2010) 17(10):2619–27. doi: 10.1245/s10434-010-1121-1
46. Moumen A, Masterson P, O'Connor MJ, Jackson SP. hnRNP K: an HDM2 target and transcriptional coactivator of p53 in response to DNA damage. *Cell* (2005) 123(6):1065–78. doi: 10.1016/j.cell.2005.09.032
47. Ritchie SA, Pasha MK, Batten DJ, Sharma RK, Olson DJ, Ross AR, et al. Identification of the SRC pyrimidine-binding protein (SPy) as hnRNP K: implications in the regulation of SRC1A transcription. *Nucleic Acids Res* (2003) 31(5):1502–13. doi: 10.1093/nar/gkg246
48. Lee MH, Mori S, Raychaudhuri P. trans-Activation by the hnRNP K protein involves an increase in RNA synthesis from the reporter genes. *J Biol Chem* (1996) 271(7):3420–7. doi: 10.1074/jbc.271.7.3420
49. Michelotti EF, Michelotti GA, Aronsohn AI, Levens D. Heterogeneous nuclear ribonucleoprotein K is a transcription factor. *Mol Cell Biol* (1996) 16(5):2350–60. doi: 10.1128/mcb.16.5.2350
50. Michelotti EF, Tomonaga T, Krutzsch H, Levens D. Cellular nucleic acid binding protein regulates the CT element of the human c-myc protooncogene. *J Biol Chem* (1995) 270(16):9494–9. doi: 10.1074/jbc.270.16.9494
51. Evans JR, Mitchell SA, Spriggs KA, Ostrowski J, Bomsztyk K, Ostarek D, et al. Members of the poly (rC) binding protein family stimulate the activity of the c-myc internal ribosome entry segment in vitro and in vivo. *Oncogene* (2003) 22(39):8012–20. doi: 10.1038/sj.onc.1206645
52. Chappell SA, LeQuesne JP, Paulin FE, deSchoolmeester ML, Stoneley M, Soutar RL, et al. A mutation in the c-myc-IRES leads to enhanced internal ribosome entry in multiple myeloma: a novel mechanism of oncogene de-regulation. *Oncogene* (2000) 19(38):4437–40. doi: 10.1038/sj.onc.1203791
53. Horvilleur E, Wilson LA, Bastide A, Piñeiro D, Pöyry TAA, Willis AE. Cap-Independent Translation in Hematological Malignancies. *Front Oncol* (2015) 5:293. doi: 10.3389/fonc.2015.00293
54. Spriggs KA, Bushell M, Mitchell SA, Willis AE. Internal ribosome entry segment-mediated translation during apoptosis: the role of IRES-trans-acting factors. *Cell Death Differ* (2005) 12(6):585–91. doi: 10.1038/sj.cdd.4401642
55. Suk FM, Lin SY, Lin RJ, Hsine YH, Liao YJ, Fang SU, et al. Bortezomib inhibits Burkitt's lymphoma cell proliferation by downregulating sumoylated hnRNP K and c-Myc expression. *Oncotarget* (2015) 6(28):25988–6001. doi: 10.18632/oncotarget.4620
56. Ilagan JO, Ramakrishnan A, Hayes B, Murphy ME, Zebari AS, Bradley P, et al. U2AF1 mutations alter splice site recognition in hematological malignancies. *Genome Res* (2015) 25(1):14–26. doi: 10.1101/gr.181016.114
57. Zhang J, Ali AM, Lieu YK, Liu Z, Gao J, Rabadan R, et al. Disease-Causing Mutations in SF3B1 Alter Splicing by Disrupting Interaction with SUGP1. *Mol Cell* (2019) 76(1):82–95.e7. doi: 10.1016/j.molcel.2019.07.017
58. Kim E, Ilagan JO, Liang Y, Daubner GM, Lee SC, Ramakrishnan A, et al. SRSF2 Mutations Contribute to Myelodysplasia by Mutant-Specific Effects on Exon Recognition. *Cancer Cell* (2015) 27(5):617–30. doi: 10.1016/j.ccell.2015.04.006
59. Kharas MG, Lengner CJ, Al-Shahrour F, Bullinger L, Ball B, Zaidi S, et al. Musashi-2 regulates normal hematopoiesis and promotes aggressive myeloid leukemia. *Nat Med* (2010) 16(8):903–8. doi: 10.1038/nm.2187
60. Palanichamy JK, Tran TM, Howard JM, Contreras JR, Fernando TR, Sterne-Weiler T, et al. RNA-binding protein IGF2BP3 targeting of oncogenic transcripts promotes hematopoietic progenitor proliferation. *J Clin Invest* (2016) 126(4):1495–511. doi: 10.1172/JCI80046
61. Paziewska A, Wyrwicz LS, Bujnicki JM, Bomsztyk K, Ostrowski J. Cooperative binding of the hnRNP K three KH domains to mRNA targets. *FEBS Lett* (2004) 577(1):134–40. doi: 10.1016/j.febslet.2004.08.086
62. G Hendrickson D, Kelley DR, Tenen D, Bernstein B, Rinn JL. Widespread RNA binding by chromatin-associated proteins. *Genome Biol* (2016) 17(1):28. doi: 10.1186/s13059-016-0878-3
63. Ramkumar C, Cui H, Kong Y, Jones SN, Gerstein RM, Zhang H. Smurf2 suppresses B-cell proliferation and lymphomagenesis by mediating ubiquitination and degradation of YY1. *Nat Commun* (2013) 4:2598–. doi: 10.1038/ncomms3598
64. Van Nostrand EL, Freese P, Pratt GA, Wang X, Wei X, Xiao R, et al. A large-scale binding and functional map of human RNA-binding proteins. *Nature* (2020) 583(7818):711–9. doi: 10.1038/s41586-020-2077-3
65. McHeyzer-Williams M, Okitsu S, Wang N, McHeyzer-Williams L. Molecular programming of B cell memory. *Nat Rev Immunol* (2011) 12(1):24–34. doi: 10.1038/nri3128
66. Shaffer AL, Rosenwald A, Staudt LM. Lymphoid malignancies: the dark side of B-cell differentiation. *Nat Rev Immunol* (2002) 2(12):920–32. doi: 10.1038/nri953

67. Yunis JJ, Oken MM, Kaplan ME, Ensrud KM, Howe RR, Theologides A. Distinctive chromosomal abnormalities in histologic subtypes of non-Hodgkin's lymphoma. *N Engl J Med* (1982) 307(20):1231–6. doi: 10.1056/nejm198211113072002
68. Huang JZ, Sanger WG, Greiner TC, Staudt LM, Weisenburger DD, Pickering DL, et al. The t(14;18) defines a unique subset of diffuse large B-cell lymphoma with a germinal center B-cell gene expression profile. *Blood* (2002) 99 (7):2285–90. doi: 10.1182/blood.v99.7.2285
69. Iqbal J, Greiner TC, Patel K, Dave BJ, Smith L, Ji J, et al. Distinctive patterns of BCL6 molecular alterations and their functional consequences in different subgroups of diffuse large B-cell lymphoma. *Leukemia* (2007) 21(11):2332–43. doi: 10.1038/sj.leu.2404856
70. Zech L, Haglund U, Nilsson K, Klein G. Characteristic chromosomal abnormalities in biopsies and lymphoid-cell lines from patients with Burkitt and non-Burkitt lymphomas. *Int J Cancer* (1976) 17(1):47–56. doi: 10.1002/ijc.2910170108
71. Manolov G, Manolova Y. Marker Band in One Chromosome 14 from Burkitt Lymphomas. *Nature* (1972) 237(5349):33–4. doi: 10.1038/237033a0
72. Lefebure M, Tothill RW, Kruse E, Hawkins ED, Shortt J, Matthews GM, et al. Genomic characterisation of Eμ-Myc mouse lymphomas identifies Bcor as a Myc co-operative tumour-suppressor gene. *Nat Commun* (2017) 8(1):14581. doi: 10.1038/ncomms14581
73. Ford RJ, Shen L, Lin-Lee YC, Pham LV, Multani A, Zhou HJ, et al. Development of a murine model for blastoid variant mantle-cell lymphoma. *Blood* (2007) 109(11):4899–906. doi: 10.1182/blood-2006-08-038497
74. Refaeli Y, Young RM, Turner BC, Duda J, Field KA, Bishop JM. The B cell antigen receptor and overexpression of MYC can cooperate in the genesis of B cell lymphomas. *PloS Biol* (2008) 6(6):e152. doi: 10.1371/journal.pbio.0060152
75. Mak IW, Evaniew N, Ghert M. Lost in translation: animal models and clinical trials in cancer treatment. *Am J Trans Res* (2014) 6(2):114–8.

Conflict of Interest: The authors declare that the research was conducted in the absence of any commercial or financial relationships that could be construed as a potential conflict of interest.

frontiers in Immunology

ORIGINAL RESEARCH
published: 12 April 2021
doi: 10.3389/fimmu.2021.627602

The *Traf2*DNx*BCL2-tg* Mouse Model of Chronic Lymphocytic Leukemia/ Small Lymphocytic Lymphoma Recapitulates the Biased IGHV Gene Usage, Stereotypy, and Antigen-Specific HCDR3 Selection of Its Human Counterpart

Gema Perez-Chacon [1,2†] *and Juan M. Zapata* [1,2*]

[1] *Instituto de Investigaciones Biomédicas "Alberto Sols", CSIC-UAM, Madrid, Spain,* [2] *Instituto de Investigación Hospital Universitario La Paz (IDIPAZ), Madrid, Spain*

OPEN ACCESS

Edited by:
Harry W. Schroeder, University of Alabama at Birmingham, United States

Reviewed by:
Andreas Agathangelidis, Institute of Applied Biosciences (INAB), Greece
Shiv Pillai, Harvard Medical School, United States

***Correspondence:**
Juan M. Zapata
jmzapata@iib.uam.es

†Present Address:
Gema Perez-Chacon, Centro Nacional de Investigaciones Oncológicas (CNIO), Madrid, Spain

Specialty section:
This article was submitted to B Cell Biology, a section of the journal Frontiers in Immunology

Received: *09 November 2020*
Accepted: *08 March 2021*
Published: *12 April 2021*

Citation:
Perez-Chacon G and Zapata JM (2021) The Traf2DNxBCL2-tg Mouse Model of Chronic Lymphocytic Leukemia/Small Lymphocytic Lymphoma Recapitulates the Biased IGHV Gene Usage, Stereotypy, and Antigen-Specific HCDR3 Selection of Its Human Counterpart. Front. Immunol. 12:627602. doi: 10.3389/fimmu.2021.627602

Chronic lymphocytic leukemia (CLL)/Small lymphocytic lymphoma (SLL) is a heterogeneous disease consisting of at least two separate subtypes, based on the mutation status of the immunoglobulin heavy chain variable gene (IGHV) sequence. Exposure to antigens seems to play a role in malignant transformation and in the selection and expansion of more aggressive CLL clones. Furthermore, a biased usage of particular IGHV gene subgroups and the existence of stereotyped B-cell receptors (BCRs) are distinctive characteristics of human CLL. We have previously described that *Traf2*DN/*BCL2* double-transgenic (tg, $^{+/+}$) mice develop CLL/SLL with high incidence with aging. In this model, TNF-Receptor Associated Factor (TRAF)-2 deficiency cooperates with B cell lymphoma (BCL)-2 in promoting CLL/SLL in mice by specifically enforcing marginal zone (MZ) B cell differentiation and rendering B cells independent of BAFF for survival. In this report, we have performed the sequencing of the IGHV-D-J rearrangements of B cell clones from the *Traf2*DN/*BCL2*-tg$^{+/+}$ mice with CLL/SLL. The results indicate that these mice develop oligoclonal and monoclonal B cell expansions. Allotransplantation of the oligoclonal populations into immunodeficient mice resulted in the preferential expansion of one of the parental clones. The analysis of the IGHV sequences indicated that 15% were mutated (M) and 85% unmutated (UM). Furthermore, while the *Traf2*DN/*BCL2*-tg$^{-/-}$ (wild-type), $^{-/+}$ (*BCL2* single-tg) and $^{+/-}$ (*Traf2DN*DN single-tg) littermates showed the expression of various IGHV gene subgroups, the CLL/SLL expanded clones from the *Traf2*DN/*BCL2*-tg$^{+/+}$ (double-transgenic) mice showed a more restricted IGHV gene subgroup usage and an overrepresentation of particular IGHV genes. In addition, the HCDR3-encoded protein sequence indicates the existence of stereotyped immunoglobulin (Ig) in the BCRs and strong similarities with BCR recognizing autoantigens and pathogen-associated antigens. Altogether, these results

highlight the remarkable similarities between the CLL/SLL developed by the *Traf2*DN/*BCL2*-tg$^{+/+}$ mice and its human counterpart.

Keywords: TRAF2, BCL2, chronic lymphocytic leukemia, CLL, small lymphocytic lymphoma, IGHV, BCR stereotipy

INTRODUCTION

Chronic lymphocytic leukemia (CLL) is the most common adult leukemia in the Western world. CLL and small lymphocytic lymphoma (SLL) are two manifestations of the same B cell neoplasia and are characterized by the accumulation of slowly proliferating CD5^{+}CD23^{+} B lymphocytes with dysregulated apoptosis (1–3).

It is well established that CLL is a heterogeneous disease consisting of at least two separate subtypes, based on phenotypic and clinical behavior. Approximately 55% of CLL patients have mutated (M) immunoglobulin heavy chain variable (IGHV) genes (4–6), which have a better prognosis than patients with unmutated (UM)- IGHV genes (6–8). According to phenotypic analysis and gene expression profiling both M- and UM-CLL are antigen-experienced B cells (9, 10). The differences in clinical outcome and biological characteristics between CLL patients with M- and UM-IGHV genes could be related to distinct differences in mutation incidence and distribution reflecting specific underlying mutagenic mechanisms between these two groups (11). As a result, M- and UM-CLL show differences in BCR reactivity profile (12) and signaling (13).

In addition, CLL can also be classified according to the expression of stereotyped HCDR3, which are found in a 41% of CLL patients (14, 15). Indeed, the remarkable similarity of HCDR3 regions within sets of patients strongly supports the notion that B cell receptor (BCR) recognition of particular antigens is a driving force in clonal selection, expansion and evolution in CLL [reviewed in (16, 17)].

CLL cells are low proliferating cells, mostly quiescent and with dysregulated apoptosis. Only a small percentage are proliferating cells, which makes difficult their expansion in immunodeficient mice. Besides, human CLL cell xenotransplantation may results in the expansion of B cell clones that do not recapitulate the IGHV-D-J rearrangements of the parental clone [reviewed in (18)]. In addition, it has been shown that donor T cells are required to support CLL implantation (19). However, proliferating T cells could result in a graft *versus* host disease that hampers the utility of CLL xenotransplanted mice.

Mouse models of CLL are useful tools for the study of CLL etiology and as preclinical platforms for new drug testing. Several CLL mouse models are currently available, which recapitulate key aspects of the human disease [reviewed in (20)]. However, a majority of these CLL mouse models, including the profusely studied E*μ-T Cell Leukemia-1* (E*μ-TCL-1*)-tg mice [reviewed in (21)], only produce UM-CLL clones, thus implying that M-CLL etiology is not properly represented in these mice.

We previously described that B cell-specific *Traf2*DN/*BCL2*-double-tg ($^{+/+}$) mice develop CLL/SLL with high incidence (22, 23). In this mouse model, expression of TRAF2DN causes the depletion of endogenous TRAF2, resulting in unbridled BAFF signaling and constitutive NFKB2 activation, causing the expansion of marginal zone (MZ) B cells (24). BCL2 overexpression, which is a CLL trademark (25), would provide MZ B cells with non-redundant and complementary protection against apoptosis that predisposes these cells to CLL/SLL.

In this report we show that the CLL/SLL arising in the *Traf2*DN/*BCL2*-tg$^{+/+}$ mice consists of expanded M- and UM-CLL/SLL clones. Expanded clones show a biased IGHV gene usage, stereotypy and express HCDR3 that are similar to those recognizing autoantigens and pathogen antigens, thus closely resembling human CLL.

MATERIALS AND METHODS

Transgenic Mice

Lymphocyte-specific *Traf2*DN-tg expressing a 1D4-epitope–tagged TRAF2 deletion mutant lacking the N-terminal 240 amino acids (AA) encompassing the RING and zinc finger domains (TRAF2DN) (26) and B cell-specific *BCL2*-tg mice mimicking the t(14;18)(q32;21) translocation involving *BCL2* and *IgH* found in human follicular lymphoma (27) have been previously described. *Traf2*DN-tg (FVB/N) and *BCL2*-tg (BALB/c) heterozygous mice were bred to produce F1 litters with progeny of the four possible genotypes ((wild-type $^{-/-}$; *Traf2*DN-tg (single-positive, $^{+/-}$); *BCL2*-tg (single-positive, $^{-/+}$); and *Traf2*DN/*BCL2* (double-positive, $^{+/+}$)) expressed on FVB/N x BALB/c mixed background as previously described (22). Analysis of the transgenic mouse genotypes was performed by polymerase chain reaction (PCR) using primers specific for *Traf2* (F) 5'-GACCAGGACAAGATTGAGGC-3' and (R) 5'-GCACATAGGAATTCTTGGCC-3') and *BCL2* (F) 5'-TTAGAGAGTTGCTTTACGTGGCCTG-3' and (R) 5'-ACCTGAGGAGACGGTGACC-3'. The animal protocols were approved by the Bioethics Committee of the hosting institution. Mice showing symptoms of distress and pain (heavy breath, weight loss, distended belly, respiratory distress, lethargy, etc) were euthanized. All transgenic mice in the study were heterozygotes for each transgene.

Isolation of Mononuclear Cells

Spleens, lymph nodes and blood from *Traf2*DN/*BCL2*-tg mice of the different genotypes were collected and mononuclear cells were isolated by Ficoll density centrifugation (Lympholyte-M; Cedarlane Laboratories, Burlington, NC).

Flow Cytometry Analysis

Mononuclear cells were incubated with 50 μg/ml human γ-globulin for 10 minutes at 4°C. Then, 10^6 cells were incubated with a combination of FITC-, PE-, or APC-conjugated antibodies against mouse CD45R/B220, CD21, CD23, IgM, IgD, CD5, and CD43

(all from BD Biosciences). After 30 minutes of incubation at 4°C, cells were washed with PBS and analyzed by flow cytometry in a FACSCanto II cytofluorimeter and the FACSDiVa 6.1.2 (BD Biosciences) flow cytometry analysis software.

Immunohistochemistry

Tissues and organs from transgenic mice were fixed in 10% formalin (Sigma-Aldrich) or in Bouin's solution (Sigma-Aldrich) for bone marrow analysis and embedded in paraffin. Tissue sections (5 μm) were deparaffinized and then stained with hematoxylin and eosin, dehydrated, and mounted in DPX (Fluka). Blood smears were stained with Wright-Giemsa (Sigma-Aldrich).

Immunoglobulin IGHV-D-J Sequence Analysis

Tissues and cells from *Traf2*DN*xBCL2* mice representative of all different genotypic combinations ($^{-/-}$; $^{+/-}$; $^{-/+}$ and $^{+/+}$) were extracted and total RNA was isolated using TRI_{ZOL} reagent and the PureLink™ RNA mini kit (Life Technologies, Carlsbad, CA), following the manufacturer's instructions. The obtained RNA was reverse transcribed into cDNA using 2 U Superscript II reverse transcriptase (Life Technologies). The IGHV-D-J regions were amplified following a modified protocol (28), using the following primers: IGHV primer (F) 5'-SARGTBMAGCTGSAGSAGTCWGG-3'; CHμ primer (R) 5'-CAGATCTCTGTTTTTGCCTCGTA-3'; CHγ primer (R) 5'-ATGCAAGGCTTACACCACAATCC-3' and CHα primer (R) 5'-TAATAGGAGGAGGAGGAGTAGGAC-3' (S: G/C; R: A/G; B: C/G/T; M: A/C; W: A/T). The conditions of the PCR reaction were: one cycle of denaturing at 94°C for 10 minutes, followed by 38 cycles of denaturing at 94°C for 1 minute, annealing at 52°C for 1 minute and extension at 68°C for 1 minute, with a final extension step at 68°C for 10 minutes. The PCR products were then analyzed by gel electrophoresis on a 2% agarose gel, excised and purified (Qiagen). Purified products were cloned using the pGEM®-T Vector System (Promega, Madison, WI, USA), following the manufacturer's instructions. From 5 to 15 colonies of each sample were grown up in culture overnight and the plasmids were extracted using the Wizard® Plus SV Minipreps DNA Purification System (Promega). Miniprep products were sequenced in a capillary sequencer by GATC Biotech (Konstanz, Germany). Nucleotide sequences were analyzed by means of Chromas 2.4.3 software (Technelysium, Queensland, Australia) and compared with those mouse germ line (GL) sequences available in the IMGT repertoire IG database using the IMGT/V-QUEST analysis tool (29). Since our mice are FVB/N x BALB/c F1 hybrids and the GL of these strains are underrepresented (BALB/c) or absent (FVB/N) in the IMGT repertoire IG database, to discriminate between *bona fide* somatic hypermutation (SHM) and strain-specific IGHV gene polymorphism (SSP), a clustal W multiple sequence analysis of the IGHV sequences from the clones with identical IGHV genes ($n \geq 3$) found in the *Traf2*DN*xBCL2*-tg and *Traf3*x*BCL2*-tg mice irrespective of their genotype (both FVB/N x BALB/c F1 hybrids) was made. A detailed description of the criteria used to discriminate between SSP and SHM is provided in **Supplementary Materials and Methods**. Sequences ≥ 98% identity to the corresponding GL IGHV gene sequence were considered unmutated (UM). Isolectric point (pI) of HCDR3 region was calculated with the Compute pI/Mw tool (ExPASy Bioinformatics Resource Portal, http://web.expasy.org/compute_pi/). HCDR3 analysis was carried out comparing the sequence in the protein BLAST database.

Statistics

IBM SPSS statistics v.26 (SPSS, Chicago, IL) and Graph Pad Prism 5 were used for statistical analysis. Statistical significance for HCDR3 length and isoelectric point (pI) was determined using the *t*-Student test. Pearson Chi-Square and likelihood ratio tests with Monte Carlo correction were applied for assessing the significance of the IGHV-D-J subgroups distribution among genotypes. Proportion test was used to determine the significance of IGHV gene expression frequency.

RESULTS

Characteristics of BCRs Expressed by CLL/SLL B Cells From the *TRAF2*DN*xBCL2*-tg$^{+/+}$ Mice

As stated above, *Traf2*DN*xBCL2*-tg$^{+/+}$ mice develop CLL/SLL with high incidence as they age (22). In most mice, SLL arises first, involving splenomegaly, lymphadenopathy and infiltration of different tissues and organs, later progressing to CLL (22, 23). An example of the histology features of the bone marrow, blood, spleen and lung of a representative *Traf2*DN*xBCL2*-tg$^{+/+}$ mouse with CLL/SLL is shown in **Figure 1A**. In addition, flow cytometry analysis of the B cell populations in this mouse (**Figure 1B**) identified two B cell populations. One majority population, with larger cells based on their forward scatter (FSC) profile and expressing low levels of B220, IgD, CD21 and CD23 and high levels of IgM (**Figure 1B**), corresponds to the CLL/SLL expanded cells (blue). These cells were CD43^{high} and CD5$^{low\ or\ null}$ (not shown). The other population (FSC^{small}) is composed by seemingly normal B2 cells expressing B220^{high}, IgM^{low}, IgD^{high}, CD21^{high}, and CD23^{middle} (green) (**Figure 1B**). These cells were CD43^{null} and CD5^{null} (not shown). The expanded CLL/SLL population is found in blood, spleen and in pleural effusion (**Figure 1B**).

To ascertain the BCR characteristics of these CLL/SLL cells, we have analyzed the sequences of the HCDR3 of these mice. **Table 1** shows the HCDR3 features and frequency of the expanded clones isolated from *Traf2*DN*xBCL2*-tg$^{+/+}$ mice with CLL/SLL. Based on the HCDR3 sequences, these mice develop oligoclonal (mice: #13, #16, #65, #72 and #74) and monoclonal (mice: #29, #40, #45, #50 and #51) B cell expansions (**Table 1**). Interestingly, when spleen and blood were compared, we have examples of mice with identical expanded clones in both sources (mice: #16, #40 and #65) but also a mouse (#55) with different clones in spleen and blood.

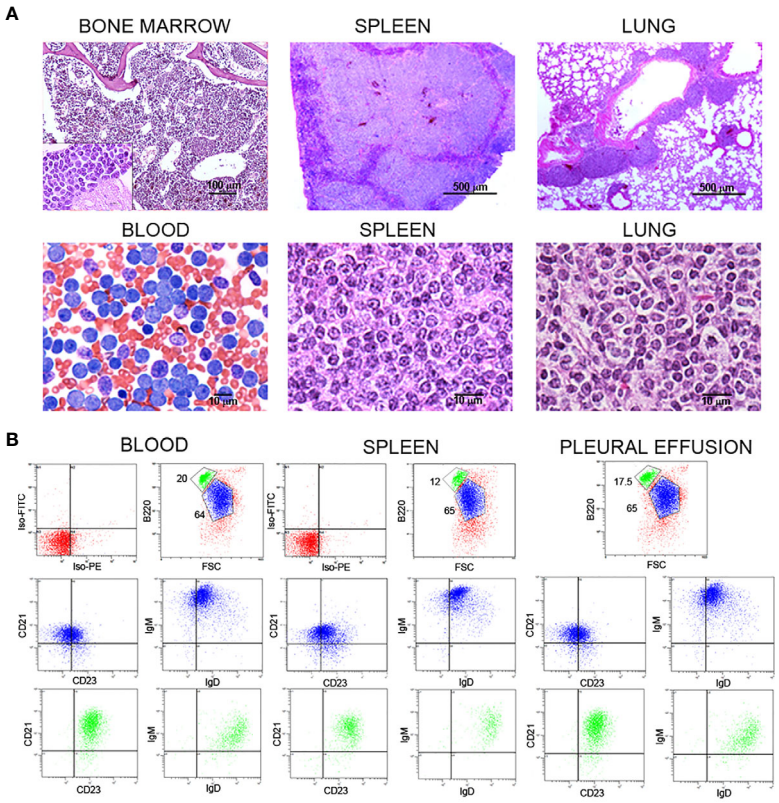

FIGURE 1 | Histochemical and flow cytometry analysis of B cell populations and tissues from representative *Traf2*DNx*BCL2*-tg$^{+/+}$ mice with CLL/SLL. **(A)** Histochemical analysis of bone marrow, spleen, lung and blood from one representative *Traf2*DNx*BCL2*-tg$^{+/+}$ mouse that had developed CLL/SLL is shown. H&E staining was used for bone marrow (x10 and x100), spleen (x4 and x100) and lung (x4 and x100), and Wright-Giemsa staining for the blood smear (x60). Scale bars are shown. **(B)** Three-color flow cytometry analysis was performed to determine the phenotype of expanded B lymphocyte populations. Gating of the expanded population was based on the CD45R/B220 and FSC plot of each sample analyzed and is indicated in the figure. Plots show CD21/CD23 and IgM/IgD expression for the expanded B cell population (FSC^{large}/B220^{low}, blue) and of the normal B2 population (FSC^{small}/B220^{high}, green). The quadrants settings were selected based on the staining of isotype controls. The tissue source of the analyzed lymphocytes is indicated in the figure.

In addition, blood lymphocytes or splenocytes (40-60 x 10^6) from representative *Traf2*DN*xBCL2*-tg$^{+/+}$ mice (#55, #72 and #74) were allotransplanted into immunodeficient SCID/NOD mice. Animals were euthanized when they develop any sign of illness (distended belly, respiratory distress, lethargy, etc). As shown in **Table 1**, only one of the expanded CLL/SLL clones found in each of the parental mice was selectively expanded in the immunodeficient allotransplanted mice.

IGHV-D-J Subgroups and Gene Usage by the Expanded CLL/SLL Cells From the *TRAF2*DNx*BCL2*-tg$^{+/+}$ Mice

CLL clones from human CLL patients express mostly IgM and have a biased usage of IGHV genes compared to normal B cells [reviewed in (30)]. These characteristics are also shared by the Eμ-*TCL-1*-tg (28, 31) and the *MDR*$^{-/-}$ and *miR-15a/16-1*$^{-/-}$ (32) mouse models of CLL. Thus, to ascertain whether B cells from the *Traf2*DNx*BCL2*-tg$^{+/+}$ mice with CLL/SLL have similar characteristics, we have analyzed the Ig isotypes and IGHV-D-J rearrangements expressed by B cells from these mice and compared them with those found in mice representing all other genotype combinations. For this purpose, *Traf2*DN-tg (FVB/N background) and *BCL2*-tg (BALB/c background) mice were crossed to produce F1 litters with mice harboring the different transgene combinations, *Traf2*DN*xBCL2*-tg$^{-/-}$, $^{+/-}$, $^{-/+}$ and $^{+/+}$. The analyses were performed when the *Traf2*DNx*BCL2*-tg$^{+/+}$ mice developed CLL/SLL, using for comparison age- and sex-matched mice representing all genotypes and genders. As shown in **Figure 2A**, retrotranscription and amplification of the mRNAs encoding for IgM, IgG and IgA shows that B cells from *Traf2*DNx*BCL2*-tg$^{+/+}$ mice with CLL/SLL almost exclusively express IgM, while all three Igs (M, G and A) mRNAs could be readily detected in B cells from representative mice of all the other genotypes. The relative expression of IgM, IgG and IgA in the *Traf2*DNx*BCL2*-tg with the different genotypes and in the expanded CLL/SLL clones is shown in **Figure 2B**.

Next, we studied whether a biased IGHV gene usage was also a feature of the CLL/SLL developed by the *Traf2*DNx*BCL2*-tg$^{+/+}$ mice. The IGHV, IGHD and IGHJ genes and the HCDR3 sequences expressed in the expanded B cell clones from the

TABLE 1 | Characteristics of the expanded CLL/SLL clones from the *Traf2*DNx*BCL2*-tg +/+ mice.

Animal no.	Age (months)	Sex	Tissue	IGHV Family IMGT	IGHV gene IMGT	IGHV gene Vbase2	IGD family IMGT	IGD gene	IGHJ gene	SHM %	SHM status	Frequency	%	HCDR3	HCDR3 lenght	pI
13	**13**	**F**	**Spleen**	VH14	IGHV14-2*02 F	VHSM7.a2psi.88	D2	DSP2.9	JH4	1.1	UM	5/13	38	**GRDDGYYYAMDY**	12	3.93
				VH5	IGHV5-17*02 F	VH7183.a47.76	D3	DST4.3	JH4	2.1	M	3/13	23	AREGPRRDYYAMDY	14	6.16
16	**12**	**M**	**Spleen**	VH1	IGHV1-85*01 F	VHJ558.88.194	D1	DFL16.1	JH3	0.35	UM	6/10	60	ASYAFAY	7	5.57
				VH5	IGHV5-17*02 F	VH7183.a47.76	D2	DSP2.2	JH4	0.35	UM	3/10	30	ASRSTMIIMDY	11	5.88
			Blood	VH5	IGHV5-17*02 F	VH7183.a47.76	D2	DSP2.2	JH4	0.35	UM	7/10	70	ASRSTMIIMDY	11	5.88
				VH1	IGHV1-85*01 F	VHJ558.88.194	D1	DFL16.1	JH3	0.7	UM	3/10	30	ASYAFAY	7	5.57
29	**20**	**F**	**Spleen**	VH1	IGHV1-80*01 F	VHJ558.83.189	D2	DSP2.2	JH4	2.1	M	8/10	80	ASPSYDYPYYYAMDY	15	3.56
40	**11**	**F**	**Spleen**	VH5	IGHV5-17*02 F	VH7183.a47.76	D2	DSP2.6	JH4	0	UM	8/10	80	ATYYGYDRVYYYAMDY	16	4.21
			Blood	VH5	IGHV5-17*02 F	VH7183.a47.76	D2	DSP2.6	JH4	0.35	UM	9/10	90	ATYYGYDRVYYYAMDY	16	4.21
45	**20**	**F**	**Spleen**	VH1	IGHV1-9*01 F	VHJ558.b9	D2	DSP2.2	JH3	0.7	UM	8/10	80	ARGDYDGEFAY	11	4.03
50	**18**	**M**	**Spleen**	VH1	IGHV1-74*04 F	V102	D2	DSP2.4	JH4	0.35	UM	10/10	100	**ASGYDYAMDY**	10	3.56
51	**18**	**M**	**Spleen**	VH1	IGHV1-9*01 F	VHJ558.b9	D4	DQ52	JH4	0.7	UM	10/10	100	ARGNWDFYYAMDY	13	4.21
55 P	**16**	**F**	**Spleen**	VH1	IGHV1-74*04 F	V102	D2	DSP2.4	JH4	0	UM	10/10	100	**ASGYDYAMDY**	10	3.56
			Blood	VH5	IGHV5-17*02 F	VH7183.a47.76	D2	DSP2.9	JH4	0.35	UM	5/10	50	AVYVIYDGYYGAMDY	15	3.56
				VH1	IGHV1-77*01 F	VHJ558.80.186	D1	DFL16.1e	JH2	1.4	UM	5/10	50	ARGGDY	6	5.88
55 F1	**-**		**Node**	VH1	IGHV1-77*01 F	VHJ558.80.186	D1	DFL16.1e	JH2	0.7	UM	9/10	90	ARGGDY	6	5.88
65	**12**	**M**	**Spleen**	VH5	IGHV5-17*02 F	VH7183.a47.76	D3	DST4.3	JH2	0	UM	2/9	22,2	ALGAGYFDY	9	3.8
				VH1	IGHV1-69*02 F	VH124	D2	DSP2.9	JH1	4.9	M	2/9	22,2	ARGNDGSYWYFDV	13	4.21
				VH3	IGHV3-5*02 F	VH36-60.a5.112	D3	DST4	JH4	1.0	UM	2/9	22,2	ARIRGGAMDY	10	8.79
			Blood	VH14	IGHV14-2*02 P	VHSM7.a2psi.88	D2	DSP2.9	JH4	0.35	UM	3/10	30	**GRDDGYYYAMDY**	12	3.93
				VH5	IGHV5-17*02 F	VH7183.a47.76	D3	DST4.3	JH2	0.7	UM	7/10	70	ALGAGYFDY	9	3.8
72 P	**15**	**F**	**Spleen**	VH14	IGHV14-2*02 P	VHSM7.a2psi.88	D2	DSP2.9	JH4	0.7	UM	4/14	29	**GRDDGYYYAMDY**	12	3.93
				VH1	IGHV1S130*01 [F]	Unknown	D2	DSP2.2	JH2	0.35	UM	4/14	29	ARVRNWDFEDY	11	4.56
72 F1	**-**		**Spleen**	VH1	IGHV1S130*01 [F]	Unknown	D2	DSP2.2	JH2	0	UM	7/10	70	ARVRNWDFEDY	11	4.56
74 P	**15**	**F**	**Spleen**	VH1	IGHV1S130*01 [F]	Unknown	D1	DFL16.1	JH2	0	UM	6/10	60	ASGPDFDY	8	3.56
				VH1	IGHV1-9*01 F	VHJ558.b9	D2	DSP2.4	JH4	0	UM	3/10	30	ARGGYYGYDGDYYAMDY	17	3.93
74 F1	**-**		**Spleen**	VH1	IGHV1-9*01 F	VHJ558.b9	D2	DSP2.4	JH4	0.7	UM	8/8	100	ARGGYYGYDGDYYAMDY	17	3.93

Table shows the mouse ID number, the tissue source of the mRNA sample, the age and the sex of the mice. The immunoglobulin IGHV, IGHD and IGHJ subgroups and genes found recombined in each CLL B cell clone are indicated, according to IMGT/V-QUEST and Vbase2 analysis tools. SHM status indicates whether the IGHV region is unmutated (UM; ≤ 2% difference from the GL sequence) or mutated (M; >2% difference from the GL sequence) after correcting for SSP as described in ***Supplementary Materials and Methods****. The frequency and % of occurrence of the B cell clones isolated from the indicated tissues of each mouse is also shown. All clones encoded a productive Ig and the HCDR3 sequence is also provided. Basic (red) and acid (green) AAs are highlighted and stereotyped HCDR3 are shown in bold. The length and isoelectric point (pI) of the HCDR3 sequence are shown. Additional information pertaining to these CLL clones is provided in* ***Supplementary Table 4****.*

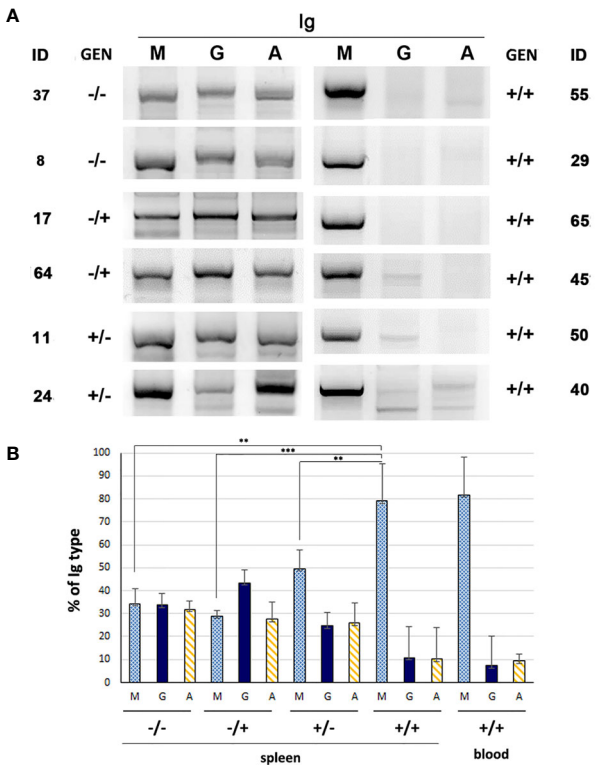

FIGURE 2 | Immunoglobulin subtypes found in *Traf2*DN*xBCL2*-tg mice representative of all different genotypic combinations ($^{-/-}$; $^{+/-}$; $^{-/+}$ and $^{+/+}$). **(A)** mRNA from the indicated mice was extracted and retrotranscribed into cDNA using random primers. Then, PCR was performed using specific primers for the IGHV-D-J region of IgM, IgG or IgA, as described in Materials and Methods. The amplified PCR fragments were analyzed in 2% agarose gels and staining with SYBR Safe and UV light. **(B)** IgM, IgG and IgA cDNAs from mice of the various genotypes ($^{-/-}$, n = 5; $^{-/+}$, n = 3; $^{+/-}$, n = 4; $^{+/+}$, spleen, n = 8, blood, n = 3) were analyzed as indicated in A and the resulting bands were quantified. The results show the percentage of each Ig (M, G and A) found in mice of the various genotypes (average ± SD), Statistical significance: **p < 0.005; ***p < 0.0005).

*Traf2*DN*xBCL2*-tg$^{+/+}$ mice with CLL/SLL are shown in **Table 1**. In addition, similar information from the *Traf2*DN*xBCL2*-tg mice with $^{-/-}$, $^{+/-}$, $^{-/+}$ genotypes and the whole list of clones isolated from the *Traf2*DN*xBCL2*-tg$^{+/+}$ mice are shown in **Supplementary Tables 1–4**, respectively. A schematic representation of the IGHV, IGHD and IGHJ subgroups expressed in B cells from mice of each genotype and those used by the expanded B cell clones of the *Traf2*DN*xBCL2*-tg$^{+/+}$ mice with CLL/SLL are shown in **Figure 3** and **Supplementary Figure 1**. B cell clones isolated from the *Traf2*DN*xBCL2*-tg$^{-/-}$ (wild-type) mice demonstrated the usage of various IGHV subgroups, with a larger representation of IGHV1 (37%) followed by IGHV2 (13%), IGHV5 (13%), IGHV10 (10%) and IGHV14 (10%) subgroup genes. A similar picture emerges from the analysis of the *Traf2*DN*xBCL2*-tg mice of $^{+/-}$ and $^{-/+}$ genotypes, also showing the usage of various IGHV subgroups, with IGHV1 being the most prominently used in all of them, consistent with the larger representation of this subgroup in the murine GL repertoire (33). In contrast, IGHV1 (51%), IGHV5 (19%), IGHV14 (14%) and IGHV3 (9%) are the subgroup genes most conspicuously used by B cells from the *Traf2*DN*xBCL2*-tg$^{+/+}$ mice and also by the expanded CLL/SLL clones (**Figure 3** and **Supplementary Table 5**). Interestingly, the IGHV subgroup expression frequency observed in other CLL mouse models is seemingly different to that of the *Traf2*DN*xBCL2*-tg$^{+/+}$ expanded CLL/SLL clones, with the exception of IGHV1, which is the most expressed IGHV gene subgroup in all of them (**Supplementary Table 5**) (see discussion).

Pearson Chi-square and likelihood ratio (LR) test with the Monte Carlo correction showed that the distribution of IGHV subgroups expressed in the *Traf2*DN*xBCL2*-tg$^{+/+}$ B cell clones compare to those expressed in the $^{-/-}$, $^{+/-}$ and $^{-/+}$ mice was statistically significant (p = 0.069) at 90% confidence, but not at 95% confidence, with a significant LR (0.015).

To determine whether this restricted IGHV gene subgroup usage was a distinctive characteristic of the *Traf2*DN*xBCL2*-tg$^{+/+}$ CLL/SLL model or was instead a general feature that could also be found in the expanded B cell clones of other types of B cell malignancies, we analyzed the IGHV subgroup repertoire used by the mature non-Hodgkin lymphomas (NHL) developed by the *TRAF3*x*BCL2*-tg$^{+/+}$ mice (34). These mice are also F1 hybrids of FBV/N x BALB/c background, and therefore are genetically equivalent to the *Traf2*DN*xBCL2*-tg mice. As shown in **Supplementary Figure 2**, in B cells from the *TRAF3*x*BCL2*-tg$^{+/+}$ mice the IGHV subgroup usage (IGHV1 (43%), IGHV5 (13%), IGHV14 (11.8%), IGHV2 (10.5%) is similar to that found in the wild-type (*Traf2*DN*xBCL2*-tg$^{-/-}$) mice. The expanded B cell clones from the *TRAF3*x*BCL2*-tg$^{+/+}$ mice that have developed post-germinal center (GC) NHL malignancies used more frequently genes from the IGHV1 subgroup genes (56%), similar to the *Traf2*DNx*BCL2*-tg$^{+/+}$ CLL/SLL clones, but the usage of IGHV5 (12.5%) and IGHV14 (6.3%) genes is much reduced compared to the latter. Expression of IGHV2 genes is also found in the *TRAF3*x*BCL2*-tg$^{+/+}$ mice, while it is absent in the *Traf2*DN*xBCL2*-tg$^{+/+}$ mice.

Regarding the usage of the IGHD genes, B cell clones of all genotypes preferentially used IGHD2 subgroup gene members (**Figure 3** and **Supplementary Figure 1**) and no statistical significance was observed in the IGHD subgroup distribution among the various *Traf2*DNx*BCL2* genotypes (p = 0.275; LR = 0.327). In contrast, there is a favored usage of the IGHJ4 gene by the *Traf2*DNx*BCL2*-tg$^{+/+}$ mice (all clones, 58%; expanded CLL clones, 63%) compared to the mice with the other *Traf2*DNx*BCL2* genotype combinations (p = 0.024; LR = 0.024) (**Figure 3**) and also compared to the average IGHJ4 gene usage in mice (21.5%) (35).

Next, we assessed whether *Traf2*DNx*BCL2*-tg$^{+/+}$ CLL/SLL clones show any preferential usage of particular IGHV genes similar to what has been described in human CLL [reviewed in (30)] and the Eμ-*TCL-1*-tg mice (28). Indeed, as shown in **Table 2**, we observed that 3 genes are overrepresented in the *Traf2*DNx*BCL2*-tg$^{+/+}$ CLL/SLL clones compared to the B cells from mice of all other genotypes and in the *TRAF3*x*BCL2*-tg$^{+/+}$

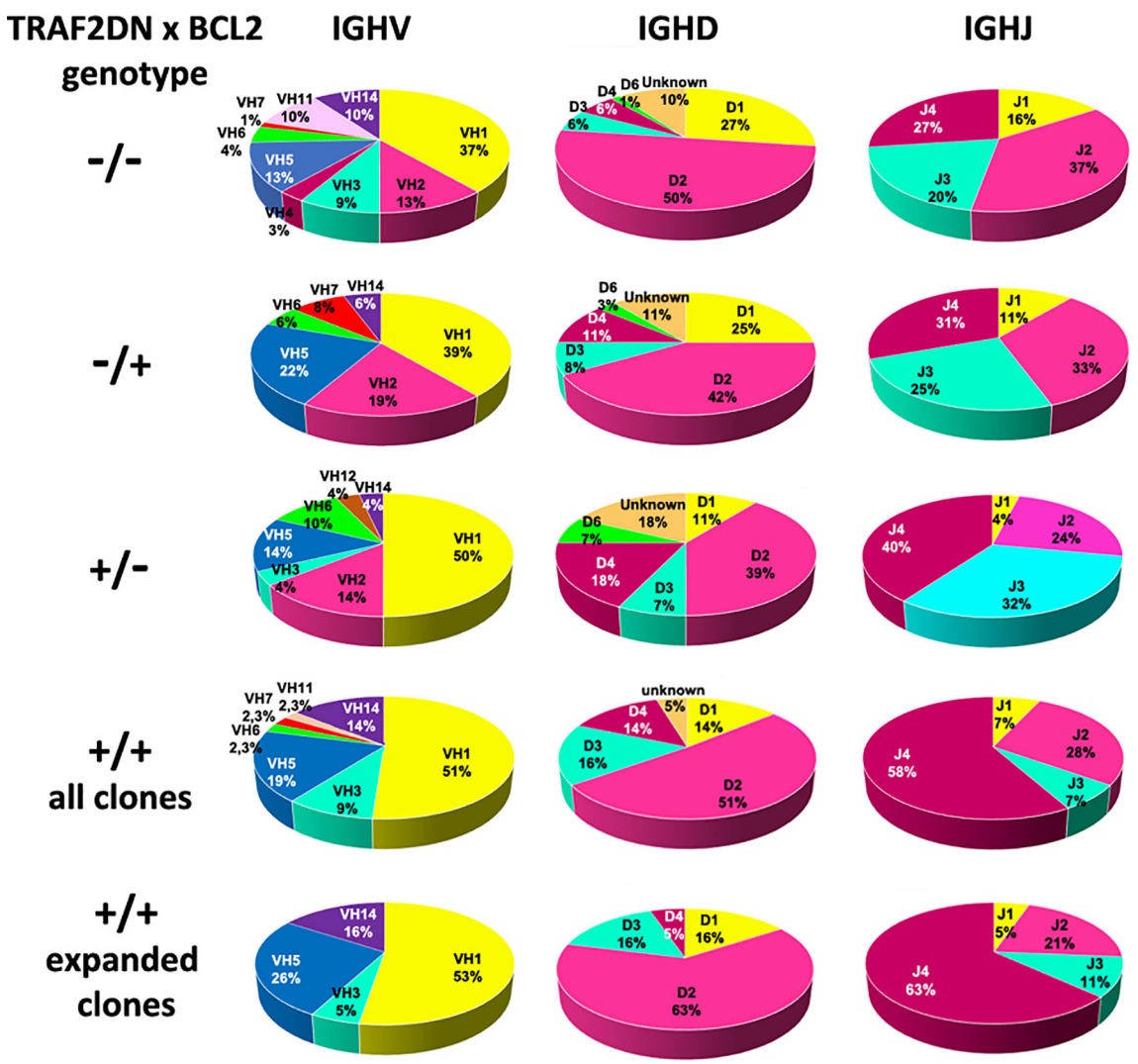

FIGURE 3 | Analysis of the IGHV, IGHD and IGHJ genes subgroup usage in *Traf2*DN*xBCL2*-tg. Circle diagrams representing the percentage of the IGHV, IGHD and IGHJ subgroup usage of mice representative of all different genotypic combinations ($^{-/-}$; $^{+/-}$; $^{-/+}$ and $^{+/+}$), including those found in the *Traf2*DN*xBCL2*-tg$^{+/+}$ expanded CLL/SLL clones are shown.

mice. Thus, VH7183.a47.76 (IGHV5) is found in 25% of the *Traf2*DN*xBCL2*-tg$^{+/+}$ CLL/SLL clones. It is found recombined to a wide variety of IGHD and IGHJ genes producing distinct HCDR3 sequences (**Table 1**). The expression of this gene is also overrepresented in B cell clones from the *Traf2*DN*xBCL2*-tg$^{+/+}$ (18%) and the *Traf2*DN*xBCL2*-tg$^{-/+}$ (14.3%) mice compared to the 1.86% rearrangement frequency found in the BALB/c strain (33). Proportion test shows that these differences are statistically significant (P>0.0001) (**Table 2**). The expression of these gene in the *TRAF3*x*BCL2*-tg$^{+/+}$ B cell lymphoma clones is not significantly different to the expression in the normal population. Another gene, VHJ558.b9 (IGHV1) is found in 15% of the *Traf2*DN*xBCL2*-tg$^{+/+}$ CLL/SLL clones (13.3% of all *Traf2*DN*xBCL2*-tg$^{+/+}$ B cell clones), a statistically significant difference (P<0.0001) compared to the 1.18% rearrangement frequency found in the C57BL/6 strain (33). It is also overrepresented in the *TRAF3*x*BCL2*-tg$^{+/+}$ B cell clones but not in the expanded B cell lymphoma clones. Finally, VHSM7.a2psi.88 (IGHV14) is rarely or not found in BALB/c and C57BL/6 strains (33), but it was found in 15% of the expanded CLL/SLL clones and in 8.9% of all *Traf2*DN*xBCL2*-tg$^{+/+}$ B cell clones (P<0.0001) (**Table 2**). Interestingly, this VHSM7.a2psi.88 was found recombined to DSP2.9 and IGHJ4 genes in expanded clones from 3 different *Traf2*DN*xBCL2*-tg$^{+/+}$ mice with CLL/SLL, producing an identical HCDR3 sequence (see below).

Altogether, these results suggest that a preferential usage of IGHV subgroups and genes by the expanded CLL/SLL clones from the *Traf2*DN*xBCL2*-tg$^{+/+}$ mice is occurring, similar to what has been previously observed in human CLL patients and in the Eμ-*TCL-1*-tg mouse model of CLL.

TABLE 2 | A restricted set of IGHV genes predominates in the expanded *Traf2*DNx*BCL2*-tg$^{+/+}$ CLL/SLL clones.

Mouse tg-line	Genotype	IGVH genes (% usage)					
		IGHV5 VH7183.a47.76	*P*	IGHV1 VH558.b9	*P*	IGHV14 VHSM7.a2psi88	*P*
Traf2*DNx*BCL2	**-/-**	**4.3**	0.12	**1.4**	0.86	**nf**	0.9
	+/-	**4**	0.48	**4**	0.004	**nf**	0.87
	-/+	**14.3**	**<0.0001**	**6**	0.014	**nf**	0.85
	+/+	**18**	**<0.0001**	**13**	**<0.0001**	**2**	**<0.0001**
	+/+ *	**25**	**<0.0001**	**15**	**<0.0001**	**15**	**<0.0001**
TRAF3xBCL2	**+/+**	**2.5**	0.5	**8.1**	**<0.0001**	**nf**	0.69
	+/+ *	**6.2**	0.18	**nf**	0.66	**nf**	0.9
% in mouse (Ref 33)	**wt**	**1.9**	**-**	**1.2**	**-**	**<0.1**	**-**

The IGHV subgroup, gene and its frequency (%) in the B cell clones isolated from the Traf2DNxBCL2-tg and TRAF3xBCL2-tg mice of the indicated genotypes, as well as the expression frequency (%) of these genes in mice (33) is shown. Statistical significance was calculated using proportion test and significant results are highlighted in bold. Clones from different tissues of the same mouse are only counted once. Clones found in parental and F1 mice are only counted once. +/+ indicated the expanded B cell clones (CLL/SLL in the Traf2DNxBCL2-tg$^{+/+}$ mice and mature non-Hodgkin lymphoma in the TRAF3xBCL2-tg$^{+/+}$ mice). nf, not found.*

Analysis of the IGHV Somatic Hypermutation Status and HCDR3 Features of the CLL/SLL Clones From the *Traf2*DNx*BCL2*-tg$^{+/+}$ Mice

Patients with CLL segregate into two groups based on the number of SHMs in the rearranged IGHV genes of the transformed clones. Approximately 55% of CLL patients have transformed B cells with mutations in IGHV genes (M) (4–6). The rest of the patients have UM IGHV CLL clones, which correlates with poor disease prognosis (6–8).

To determine the frequency of M *vs.* UM IGHV regions in the expanded CLL/SLL clones of the *Traf2*DNx*BCL2*-tg$^{+/+}$ mice we first compared the IGHV sequence of the transformed clones with the available GL sequences stored in the IMGT repertoire IG database [mostly based on the C57BL/6, with scattered presence of 129/sv and BALB/c lines GL sequences (33)]. The results obtained using the IMGT/V-QUEST analysis tool showed that many sequences have considerable variations with their respective GL IGHV genes. A similar result was obtained when the IGHV sequences from the B cell clones isolated from mice with the other genotypes ($^{-/-}$, $^{+/-}$, $^{-/+}$ and all $^{+/+}$) was compared. Since our mice are FVB/N x BALB/c hybrids and because it has been shown that the IGHV GL repertoire and sequence is highly variable among inbred mouse strains (33, 36), these variations might reflect the reported differences among strains and the absence of IGHV GL sequences from the FVB/N mouse line in the IMGT repertoire IG database.

To determine whether some of these variations with the GL sequences may be the result of SSPs, we have performed a clustal W sequence comparison of the IGHV region of *Traf2*DNx*BCL2*-tg B cell clones with identical IGHV alleles, irrespective of their genotype. Indeed, we have observed the existence of nucleotide mismatches compared to the IMGT referenced IGHV gene that are conserved in most of the corresponding IGHV gene from different *Traf2*DNx*BCL2*-tg individuals and genotypes. Since SHM randomly introduces any of the 4 nucleotides in a given spot, a mismatch of the same nucleotide in the same position of several identical alleles compared to the GL sequence strongly suggest the existence of a polymorphism. The number of SSPs found in the IGHV rearranged sequences from the *Traf2*DNx*BCL2*-tg B cell clones ranges from 1 (0.35% of the IGHV sequence) to 24 (9.375%), averaging a 2.54% SSPs, consistent with previously reported IGHV GL differences among mouse strains (36). The criteria for discriminating between SSP and SHM and examples of the IGHV gene sequence comparisons are shown in supplementary materials and methods and **Supplementary Figure 3**, respectively.

The estimation of SHM events (%) according to the criteria described above found in the expanded CLL/SLL B cell clones is shown in **Table 1**. In addition, the percentage of similarity of the IGHV region of the analyzed B cell clones with the GL and the SPP and SHM estimated events for the B cell clones from all the *Traf2*DNx*BCL2*-tg genotypes, is shown in **Supplementary Tables 1–4**. A standard 2% difference with the GL was applied to categorize UM or M IGHV clones (4, 28, 37). As shown in **Supplementary Table 6**, the CLL/SLL expanded clones from the *Traf2*DNx*BCL2*-tg$^{+/+}$ mice were 85% UM and 15% M (identical clones found in a different tissue of the same mouse as well as identical clones found in parental and allotransplanted F1 mice were only counted once). Similar UM and M percentages were found in *Traf2*DNx*BCL2*-tg$^{+/-}$ (78.6% UM *vs.* 21.4% M), and *Traf2*DNx*BCL2*-tg$^{+/+}$ (all clones) (80% UM *vs.* 20% M) mice and a larger population of UM B cell clones was also found in *Traf2*DNx*BCL2*-tg$^{-/+}$ (60% UM *vs.* 40% M). In contrast, *Traf2*DNx*BCL2*-tg$^{-/-}$ B cell clones are split in half (46% UM *vs.* 54% M). This result is consistent with the fact that *Traf2*-deficiency causes the expansion of MZ B cells (24, 38), which are mostly UM (39). In addition, *Bcl2* overexpression has been shown to reduce the SHM rate (40).

It has been reported in human CLL patients that UM- and M-CLL clones have a biased usage of IGHV subgroups. Thus, IGHV1 genes predominate in the rearrangements of UM-CLL cells while IGHV3 and IGHV4 genes are more frequently found in M-CLL cells (5, 6, 41). A larger percentage of IGHV1 genes are also found in UM-CLL clones from the E*μ-TCL-1*-tg mice (28) and the *MDR*$^{-/-}$ and *miR15a/16-1*$^{-/-}$ mice (32). A comparison between the IGHV, IGHD and IGHJ subgroup usage between M- and UM-clones from the *Traf2*DNx*BCL2*-tg$^{+/+}$ is shown in **Figure 4**. Our analyses showed that UM-B cell clones from the *Traf2*DNx*BCL2*-tg$^{+/+}$ used more frequently IGHV1 (46%), IGHV14 (20%), IGHV5 (17%) and IGHV3 (11%), while M-B

cell clones used IGHV1 (70%), IGHV5 (20%) and IGHV11 (10%). A similar trend was observed in UM- and M-CLL/SLL clones, although the reduced number of M-CLL/SLL clones (n=3) avoid any conclusion. In addition, IGHD2 and IGHJ4 genes were overrepresented in both UM- and M-*Traf2*DNx*BCL2*-tg$^{+/+}$ B cell clones and in expanded CLL/SLL clones (**Figure 4**).

Other HCDR3 features, such as length, charge and AA sequence are intrinsic HCDR3 characteristics. HCDR3 sequences vary in their AA composition, charge and length depending on how the IGHV, IGHD and IGHJ genes recombine (5, 42, 43). A summary of the analysis of these HCDR3 features in the expanded *Traf2*DNx*BCL2*-tg$^{+/+}$ B cell clones and of B cells from the other genotypes is shown in **Supplementary Table 6**. The analysis of the HCDR3 AA sequence of the expanded *Traf2*DNx*BCL2*-tg$^{+/+}$ CLL/SLL clones shows an average length of 11.6 ± 2.9 AAs, which is similar to the HCDR3 length in all other genotypes ($^{-/-}$, 11.92 ± 2.7; $^{+/-}$, 10.71 ± 2.6; $^{-/+}$, 12.11 ± 3.3; $^{+/+}$, 11.44 ± 2.8) and in accordance with the HCDR3 average length in mice (11.5 ± 1.9 AAs) (44). Moreover, no remarkable differences were observed between the HCDR3 average length of M *vs.* UM clones in any of the genotypes, including the expanded CLL/SLL clones (**Supplementary Table 6**). Although long HCDR3 have been proposed to be a characteristic of UM-CLL HCDR3 in humans (5, 42), long HCDR3 were found in both M- and UM-clones from mice of the different genotypes, including the expanded CLL/SLL clones. It is noteworthy that the HCDR3 average length of the *Traf2*DNx*BCL2*-tg$^{+/+}$ UM-CLL/SLL clones (11.18 ± 2.9 AAs) is similar to the HCDR3 average length of the UM-CLL clones from the E*μ-TCL-1*-tg mice [11.6 ± 2.3 AAs (28) and 10.6 ± 2.4 AAs (31)] and from the *IgH-TEμ* mice [11.4 ± 2.32 (45)]. The average length of the UM-CLL/SLL clones developed by the *MDR*$^{-/-}$ and *miR15a/16-1*$^{-/-}$ is slightly longer [12.87 ± 2.17 AAs (32)], but compared to that of the *Traf2*DNx*BCL2*-tg$^{+/+}$ UM-CLL/SLL clones these differences did not reach statistical significance (P = 0.073).

The average isoelectric point (pI) of the HCDR3 expressed in the analyzed B cell clones from the *Traf2*DNx*BCL2*-tg mice of the distinct genotypes is also shown in **Supplementary Table 6**. The *Traf2*DNx*BCL2*-tg$^{+/+}$ expanded CLL/SLL clones have the most acidic HCDR3 (4.54 ± 1.31) compared to that of *Traf2*DNx*BCL2*-tg mice with the other genotypes. Indeed, only one *Traf2*DNx*BCL2*-tg$^{+/+}$ CLL/SLL clone had a HCDR3 with a basic pI. Aspartic acid and arginine are the most frequently found acidic and basic AAs, respectively. In addition, tyrosine is frequently overrepresented, with some HCDR3 containing as much as 44% of tyrosine, compared to the average 25% frequency for this AA found in the mouse HCDR3 (44). Of note is that the average pI of the HCDR3 of UM-CLL/SLL clones from the *Traf2*DNx*BCL2*-tg$^{+/+}$ is significantly more acidic than the average pI of the HCDR3 from the E*μ-TCL-1*-tg UM-CLL clones (4.5 ± 1.4 *vs.* 5.9 ± 1.9) (P=0.02).

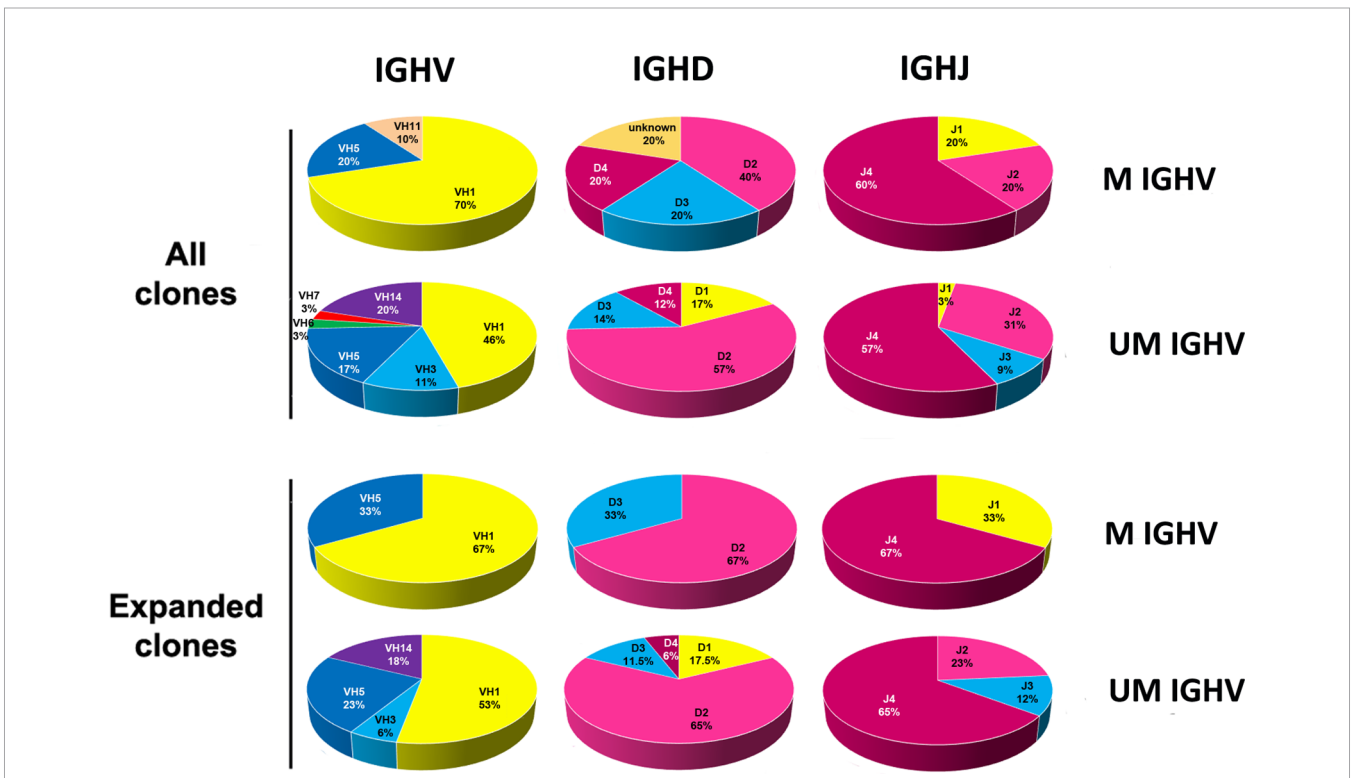

FIGURE 4 | Analysis of the IGHV, IGHD and IGHJ genes subgroup usage in the CLL/SLL clones from the *Traf2*DNx*BCL2*-tg$^{+/+}$ mice according to the SHM status (UM and M). The percentage of usage of the various IGHV, IGHD and IGHJ subgroups found in B cell clones isolated from the *Traf2*DNx*BCL2*-tg$^{+/+}$ mice (all) and those found in the expanded CLL/SLL clones, distributed according to the SHM status (UM and M), are indicated and represented in circle diagrams. A given IGHV gene was considered UM if there was ≤ 2% variation from the GL once corrected for the presence of SSPs.

Identical HCDR3 Are Expressed in *Traf2*DNx*BCL2*-tg$^{+/+}$ CLL/SLL Clones From Distinct Mice

A distinctive characteristic of human CLL is the expression of structurally identical or highly similar HCDR3 between unrelated individuals producing structurally similar BCRs (14, 15, 46). This occurrence is known as HCDR3 stereotypy and points out toward the role of antigens in the clonal selection and pathogenesis of the disease [reviewed in (17, 30, 47)]. Stereotyped HCDR3 rearrangements account for 41% of human CLL clones (15). BCR stereotypes are also found in CLL clones from the Eμ-*TCL-1*-tg (28, 31) and from the *MDR*$^{-/-}$ and *miR-15a/16-1*$^{-/-}$ (32) mice, among others.

Our results also demonstrate the existence of two identical HCDR3 sequences in the *Traf2*DNx*BCL2*-tg$^{+/+}$ expanded CLL/SLL clones. One is found in mice #50 and #55 (ASGYDYAMDY) and the other in mice #13, #65 and #72 (GRDDGYYYAMDY) (**Table 1**), accounting for the 25% of the CLL/SLL clones. These *Traf2*DNx*BCL2*-tg$^{+/+}$ CLL/SLL stereotyped HCDR3 sequences are found in UM clones, in agreement with the findings in stereotyped HCDR3 sequences from human CLL (17) and from the above mentioned CLL mouse models (28, 32), that are also found in UM-CLL clones. In addition, it is worth noting that other stereotyped sequences are also found in seemingly not expanded clones from the *Traf2*DNx*BCL2*-tg$^{+/+}$ mice (**Supplementary Table 7**). These stereotyped sequences might belong to low represented CLL/SLL clones. Including these low represented clones, we found 18 stereotyped HCDR3 account (31% of all *Traf2*DNx*BCL2*-tg$^{+/+}$ B cell clones), of which 16 of them are UM and 2 are M.

Interestingly, stereotyped HCDR3 sequences were also found in a few B cell clones from the *Traf2*DNx*BCL2*-tg$^{-/-}$, $^{+/-}$ and $^{-/+}$ mice (**Supplementary Table 7**). Of note is that some of these stereotyped sequences are found in clones expressing distinct IGHV genes, although always from the same IGHV subgroup. In addition, **Supplementary Figure 4** shows a Clustal W analysis of the IGHV regions from representative clones producing identical HCDR3. Even though these IGHV regions are UM, they differ in their SHM pattern.

It is also worth mentioning that HCDR3 expressed in CLL clones from the Eμ-*TCL-1*-tg (28), the *MDR*$^{-/-}$ and *miR-15a/16-1*$^{-/-}$ (32) and the *IgH-TE*μ (45) mice were also found in *Traf2*DNx*BCL2*-tg$^{-/-,+/-,+/+}$ and in *TRAF3*x*BCL2*-tg$^{+/+}$ mice, although none of these were expanded clones (**Supplementary Table 8**).This result is consistent with the existence of CLL-biased stereotyped BCR in healthy individuals (48, 49).

Putative Antigens Recognized by the HCDR3 Sequences of the CLL/SLL Clones From the *Traf2*DNx*BCL2*-tg$^{+/+}$ by Comparison With Those in Public Databases

As stated above, CLL cells frequently express BCR recognizing autoantigens and pathogen-associated antigens [reviewed in (16, 17)] that are involved in the clonal selection and progression of the disease (31, 50–54).

The comparison of the BCR HCDR3 sequences of the expanded *Traf2*DNx*Bcl2*-tg$^{+/+}$ CLL/SLL clones with similar sequences found in public databases showed high homology with HCDR3 recognizing autoantigens, such as phosphatidylcholine (82 and 75% homology), cardiolipin (86% homology), dsDNA (80% homology), as well as to pathogen antigens, such as hepatitis C virus E2 protein (81% homology), CMV glycoprotein B (76% homology), *Bordetella* (75% homology) and Vaccinia protein A3 (80% homology) (**Table 3** and **Supplementary Table 9**). Many of these antigens were already described as being recognized by the BCR of human and mouse CLL clones, including phosphatidylcholine (28), cardiolipin (55, 56), dsDNA (55, 57) and CMV (58, 59), further supporting the role of these types of antigens in the etiology of *Traf2*DNx*Bcl2*-tg$^{+/+}$ CLL/SLL.

DISCUSSION

Characteristics of the HCDR3 of the *Traf2*DNx*BCL2*-tg Mice

The results presented herein underscore the similarities between the CLL/SLL developed by the *Traf2*DNx*BCL2*-tg$^{+/+}$ mice and the CLL developed by human patients. This includes a biased usage of IGHV genes, the existence of CLL/SLL clones with stereotyped HCDR3 and the expansion of CLL/SLL clones with HCDR3 similar to those recognizing autoantigens and bacteria antigenic determinants (1, 30, 60, 61). Furthermore, compared to other CLL mouse models, such as the Eμ-*TCL-1*-tg (28) and the *MDR*$^{-/-}$ and the *miR-15a/16-1*$^{-/-}$ (32) that only generate UM-CLL clones, the CLL/SLL developed by the *Traf2*DNx*BCL2*-tg$^{+/+}$ mice produce both UM- and M-CLL/SLL clones, similar to human CLL, albeit a vast majority of them are UM.

In this report we have compared the IGHV, IGHD and IGHJ gene usage and the HCDR3 sequences expressed in B cells from mice representing all the different genotypes obtained by crossing heterozygous *Traf2*DN-tg and *BCL2*-tg mice, that is, *Traf2*DNx*BCL2*-tg$^{-/-}$ (wild-type), $^{+/-}$ (expressing only TRAF2DN), $^{-/+}$ (expressing only BCL2) and $^{+/+}$ (expressing both TRAF2DN and BCL2). Our results further demonstrate that monoclonal and oligoclonal B expansions are only observed in the *Traf2*DNx*BCL2*-tg$^{+/+}$ mice that developed CLL/SLL, thus confirming that the expression of both transgenes is necessary to trigger CLL/SLL in these mice (22). In addition, the comparison of B cell clones isolated from *Traf2*DNx*BCL2*-tg mice with all possible transgene combinations reveal a more restricted set of IGHV subgroup and IGHV gene usage by the expanded *Traf2*DNx*BCL2*-tg$^{+/+}$ CLL/SLL clones compared to B cells from mice of the other genotypes. In all genotypes, IGHV1 genes are the most frequently used by B cells from all the different genotypes, in accordance with the fact that IGHV1 is the gene subgroup most prominently used in mice (33). Of note is the lack of IGHV2 genes found in *Traf2*DNx*BCL2*-tg$^{+/+}$ B cells, while this subgroup is readily represented in B cells from mice with the other genotypes and is also found in lymphoma B cell clones from the *TRAF3*x*BCL2*-tg$^{+/+}$ mice. In this regard, it is

TABLE 3 | HCDR3 sequence alignments of the *Traf2*DNx*BCL2*-tg+/+ CLL/SLL clones and their putative target antigens.

DENDROGRAM	MOUSE NUMBER AND CLONE SOURCE	CLUSTALW ALIGNMENT HCDR3	SHM	POSSIBLE ANTIGEN (% HOMOLOGY HCDR3)	GeneBank ID
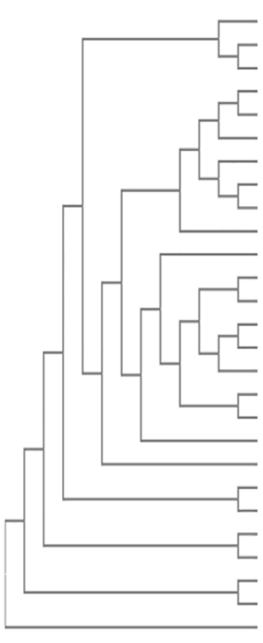	45_spleen_1(8/10)	--------ARGD--YDGEF-AY	UM	**hepatitis C virus (81%)**	**4Q0X.H**
	65_blood_1(7/10)	------ALGAG---YF----DY	UM	ANA (66%)	AAS00801.1
	65_spleen_1(2/9)	------ALGAG---YF----DY	UM	ANA (66%)	AAS00801.1
	55_blood_2(5/10)	--------ARG---G-----DY	UM	Not found	
	55_F1_1(9/10)	--------ARG---G-----DY	UM	Not found	
	51_spleen_1(10/10)	--------ARGNWDFYYAM-DY	UM	Friends virus (69%)	AHZ94470.1
	74_spleen_1(6/10)	--------ASG-PDFD----DY	UM	Not found	
	50_spleen_1(10/10)	--------ASG---YDYAM-DY	UM	lipoteichoic acid (71%)	AAX56286.1
	55_spleen_1(10/10)	--------ASG---YDYAM-DY	UM	lipoteichoic acid (71%)	AAX56286.1
	65_spleen_3(2/9)	--------ARI---RGGAM-DY	UM	**vaccinia protein A33 (80%)**	**AHB38924.1**
	55_blood_1(5/10)	---AVYVIYDG---YYGAM-DY	UM	GMB autoantigen (71%)	AAL92851.1
	74_spleen_2(3/10)	ARGGYYG-YGY---DYYAM-DY	UM	**Phosphatidylcholine (82%)**	**AAB07432.1**
	74_F1_1(8/8)	ARGGYYG-YGY---DYYAM-DY	UM	**Phosphatidylcholine (82%)**	**AAB07432.1**
	13_spleen_1(5/13)	------GRDDG---YYYAM-DY	UM	**glycoprotein B(CMV) (76%)**	**AAB26953.1**
	65_blood_2(3/10)	------GRDDG---YYYAM-DY	UM	glycoprotein B(CMV) (69%)	AAB26953.1
	72_spleen_1(4/14)	------GRDDG---YYYAM-DY	UM	glycoprotein B(CMV) (69%)	AAB26953.1
	40_blood_1(9/10)	--ATYYGYDRV---YYYAM-DY	UM	**Phosphatidylcholine (75%)**	**AAB07432.1**
	40_spleen_1(8/10)	--ATYYGYDRV---YYYAM-DY	UM	**Phosphatidylcholine (75%)**	**AAB07432.1**
	29_spleen_1(9/10)	--AS-PSYDYP---YYYAM-DY	M	***Bordetella pertussis*(75%)**	**ABB13479.1**
	13_spleen_2(3/10)	----AREGPRR---DYYAM-DY	M	**DsDNA (80%)**	**BAB87185.1**
	16_blood_2(3/10)	--------------ASYAF-AY	UM	Not found	
	16_spleen_1(6/10)	--------------ASYAF-AY	UM	Not found	
	72_spleen_2(4/14)	--------ARV---RNWDFEDY	UM	Not found	
	72_F1_1(7/10)	--------ARV---RNWDFEDY	UM	Not found	
	16_blood_1(7/10)	--------ASR---STMIIMDY	UM	Not found	
	16_spleen_2(3/10)	--------ASR---STMIIMDY	UM	Not found	
	65_spleen_2(2/9)	-----ARGNDG---SYWYF-DV	M	**Cardiolipin (86%)**	**AAB71184.1**

A clustal W alignment and dendrogram comparing the HCDR3 from the expanded Traf2DNxBCL2-tg+/+ CLL/SLL clones is shown. The ID number of the mouse, the source of the tissue, the frequency of occurrence for each clone and the SHM status of the clone (M or UM) are indicated. The putative antigens recognized by the CLL/SLL HCDR3 were determined using NCBI protein Blast (non-redundant sequences restricted to Mus musculus, taxid. 10090) and selecting the antigen recognized by antibodies encoding HCDR3 with the highest similarities to the HCDR3 expressed by the CLL/SLL clones (the antigen candidate and the % of HCDR3 similarities is indicated). Those HCDR3 with ≥ 75% similarities are highlighted. The GenBank accession code for the referred antibodies is provided. Alignment was performed using the clustal W muscle tree method UPGM https://www.ebi.ac.uk/Tools/phylogeny/simple_phylogeny/.

worth noting that *Traf2*DNx*BCL2*-tg$^{+/+}$ CLL/SLL clones have a MZ origin (24) and that the IGHV2 gene subgroup is underrepresented in transformed B cells of a MZ origin (62, 63)

As described above, the analysis of the IGHV subgroup usage of the expanded *Traf2*DNx*BCL2*-tg$^{+/+}$ CLL/SLL clones indicates a preponderance of certain gene subgroups (IGHV1 > IGHV5 > IGHV14 > IGHV3) (**Supplementary Table 5**). In contrast, the expression of IGHV subgroups found in other CLL mouse models described in the literature is seemingly different. This includes the Eμ-*TCL-1*-tg [IGHV1 > IGHV11 = IGHV12 > IGHV4, calculated from (28)], the *MDR*$^{-/-}$ and *miR-15a/16-1*$^{-/-}$ [IGHV1 > IGHV11 > IGHV12, calculated from (32)] and the *IgH-TE*μ-tg [IGHV1 = IGHV11, calculated from (45)] mice (**Supplementary Table 5**). Although IGHV1 is most frequently found in the CLL clones from all these mouse models, the preferential use of IGHV5 and IGHV14 by the *Traf2*DNx*BCL2*-tg$^{+/+}$ CLL/SLL clones instead of the use of IGHV11 and IGHV12 seen in the other CLL mouse models might indicate that the CLL/SLL developed by the *Traf2*DNx*BCL2*-tg$^{+/+}$ mice arises from a B cell subset different to that of the other CLL mouse models (see below). These differences might also underlie the reported differences in IGHV-D-J usage by mice of different strains (33, 36). In this regard, differences in IGHV subgroup usage have been also observed in CLL from distinct human populations [(64, 65) and references therein]. However, it is noteworthy that mouse IGHV5 and IGHV11 belong to the IGHV clan whose human counterpart is IGHV3, mouse IGHV1 and IGHV14 share clan with human IGHV1, and mouse IGHV3 and IGHV12 are in the same clan than human IGHV4 (66). Interestingly, IGHV3, IGHV1 and IGHV4 are the subgroups most frequently represented in human CLL [(64) and references therein], further stressing the similarities between these CLL mouse models and the human disease. However, it is worth noting human IGHV3, 1 and 4 subgroups contain the larger number of genes and also dominate the repertoire in other physiological and pathological contexts.

Although some mouse CLL clones may have longer HCDR3 than normal B cells, as it has been shown in sets of UM-CLL in humans (5, 42), a comparison of the HCDR3 average length of the *Traf2*DNx*BCL2*-tg$^{+/+}$ UM-CLL/SLL clones and those from the Eμ-*TCL-1*-tg, the *MDR*$^{-/-}$, the *miR-15a/16-1*$^{-/-}$ and the *IgH-TE*μ-tg mice showed no significant differences among them and, in all cases, it was similar to the HCDR3 average length of normal mouse B cells. However, even though this result suggests that this feature of human UM-CLL is not shared by its mouse counterparts, an analysis of a large cohort of CLL samples from 2662 patients have shown that the stereotyped HCDR3 sequences seem to cluster in discrete groups of 9, 13, 20 and 22 AAs (14), thus suggesting that long HCDR3 are not a general feature of human UM-CLL but rather of some stereotype subtypes. Thus, due to the limited number of mouse CLL

HCDR3 sequences available, it remains an open question whether a similar distribution could be observed in mouse CLL.

It is important to note that the *Traf2*DNx*BCL2*-tg mice are in a FVB/NxBALB/c mixed background. This is relevant considering that the vast majority of the IGHV sequences available at the IMGT repertoire IG database are from C57BL/6 mice and that IGHV from FVB/N mice are not represented in this database. As stated above, there is a large sequence GL IGHV variation between mouse strains (33, 36). Therefore, a direct comparison of the IGHV sequences from the *Traf2*DNx*BCL2*-tg mice with those GL stored at IMGT would not be representative of the actual percentage of variation of the analyzed IGHV sequences with the GL. To provide a more precise analysis, we have compared all available sequences of the same IGHV gene from the *Traf2*DNx*BCL2*-tg mice (irrespective of their genotype) and *TRAF3*x*BCL2*-tg mice (also in a FVB/NxBALB/c mixed background), as well as with available FVB/N IGHV sequences available in public databases. These comparisons allowed discriminating what differences with the GL sequence were more likely SSP or SHM. Our results indicate that a majority of the IGHV sequences of the *Traf2*DNx*BCL2*-tg -/+; +/- and ++ have ≤ 2% differences with the GL and are categorized as UM. However, it is important to state that these results are an estimation of SHM events and that a comparison with the GL of the mouse strain analyzed is required for an accurate assessment of SHM events.

Insights Into the Cellular Origins on Mouse CLL

CLL ontogeny is still a matter of intense study and discussion (2, 67, 68). This also applies to the identification of the cellular source of mouse CLL, notwithstanding our deeper knowledge on mouse B cell ontogeny and differentiation compared to that of humans. Questions still remain even on whether human and mouse CLL arises from a single or multiple cell types.

MZ B cells are IgM^+ cells responding to T-independent antigens. They have a limited IGHV-D-J repertoire usage often producing polyreactive BCR recognizing autoantigens and pathogen antigens (69). MZ B cells are mostly UM but they can go through extra-germinal center SHMs producing also M-MZ B cells (70). Our studies on the mechanisms causing CLL/SLL development in the *Traf2*DNx*BCL2*-$tg^{+/+}$ mice showed that B cell-specific TRAF2DN expression caused proteasome-dependent degradation of endogenous TRAF2, thus rendering B cell-specific *Traf2*DN-tg mice into *bona fide* B cell-specific *Traf2*-deficient mice (24). Confirming previous results (38, 71), we showed that the lack of functional TRAF2 enforces MZ B cell accumulation and releases B cells from the need of BAFF for survival (24). BCL2 overexpression, a defining characteristic of human CLL cells (25) would provide in this model a necessary additional level of protection against apoptosis, likely through a similar mechanism to that described in human CLL (72). Altogether, our results would be consistent with a role for *Traf2*-deficiency and BCL2 overexpression in promoting MZ B cells expansion and predisposing MZ B cells to CLL/SLL transformation (24).

A role for MZ B cells as the source of the CLL/SLL arising in the *Traf2*DNx*BCL2*-$tg^{+/+}$ mice might explain why in this mouse model SLL arises first, later progressing to CLL (22). This would be in line with the ability of MZ B cells to move into circulation (73). Moreover, since the CLL/SLL developed by the *Traf2*DNx*BCL2*-$tg^{+/+}$ mice may express or not CD5 on their surface (22), this could reflect that MZ B cells were at different activation stage at the time of transformation [reviewed in (2)].

On the other hand, various lines of evidence suggest that the CLL developed by other mouse models might arise from a different B cell type. In this regard, there is evidence pointing out to a B1a cell origin for UM-CLL developed by some of the available CLL mouse models [reviewed in (2)]. First, the preferential usage of IGHV1 and IGHV11 genes by the E*μ-TCL-1*-tg (28, 51, 74) and by the $MDR^{-/-}$ and *miR-15a/16-1*$^{-/-}$ mice (32) is similar to the preferential IGHV subgroup usage of mouse splenic B1a cells (75). Second, the most frequently expressed clones in B1a cells (both, peritoneal and splenic) have HCDR3 with the sequences MRYGNYWYFDV, MRYSNYWYFDV, MRYGSYWYFDV and MRYGSSYWYFDV (75) found in BCRs that are reactive to phosphatidylcholine (28). These HCDR3 are commonly found in expanded CLL clones from the E*μ-TCL-1*-tg mice (28) the $MDR^{-/-}$ and *miR-15a/16-1*$^{-/-}$ mice (32) and the *IgH-TEμ* mice (45) (**Supplementary Table 8**). Third, Hayakawa and coworkers (52) have shown that allotransplantation of B1 cells, but not of other B cell subtypes, from the Eμ-*TCL1*-tg mice resulted in CLL with a biased repertoire, including stereotyped BCRs, thus recapitulating the CLL developed by the Eμ-*TCL1*-tg mice.

Of note is that both MZ B cells and B1 cells have been proposed as a possible source for CLL cells [reviewed in (2)]. However, there is conflicting evidence for MZ B cells as the source of human CLL (2, 67) and we are still lacking clear evidence on the existence of a human counterpart of mouse B1 cells. Therefore, despite the high similarities of the CLL developed by humans and the available mouse CLL models, including the *Traf2*DNx*BCL2*-$tg^{+/+}$ mice, additional research is needed to elucidate whether mouse and human CLL have a similar ontogeny and cell type origin.

Possible Role of Autoantigens and Pathogen Antigens in the CLL/SLL Developed by the *Traf2*DNx*BCL2*-$tg^{+/+}$ Mice

Although CLL cells relying on antigen-independent, cell-autonomous BCR signaling have been described (76), there is ample evidence for the role of autoantigen-stimulated BCR in CLL clonal selection, expansion and clonal evolution (31, 50–54). Our results showing the similarities of the HCDR3 expressed by the expanded *Traf2*DNx*BCL2*-$tg^{+/+}$ CLL/SLL clones to those recognizing autoantigens and pathogens suggest that antigen-stimulation would also drive disease progression in our CLL/SLL mouse model, similarly to what has been demonstrated in the E*μ-TCL-1*-tg mice (31, 51).

Stereotyped HCDR3 sequences are mostly found in UM-CLL clones in humans and produce BCRs that frequently recognized

autoantigens [reviewed in (16, 17)]. In agreement with these findings, the identical HCDR3 found in the *Traf2*DNx*BCL2*-tg$^{+/+}$ mice were also UM-CLL/SLL clones. Moreover, we found several *Traf2*DNx*BCL2*-tg$^{+/+}$ UM-CLL/SLL clones expressing HCDR3 highly similar to HCDR3 recognizing autoantigens (phosphatidylcholine) and pathogen antigens (CMV, hepatitis C virus, and lipoteichoic acid). However, HCDR3 with similar antigen specificities were also found in M-CLL/SLL clones, recognizing autoantigens, such as cardiolipin and dsDNA, and pathogen antigens (*Bordetella*) (**Table 3**). In this regard, Herve and coworkers (12) have shown that both M- and UM-CLL clones derived from self-reactive B cell precursors and our data would be in agreement with those results.

Finally, the presence of B cell clones with similar HCDR3 sequence in mice with different genotypes (*Traf2*DNx*BCL2*-tg$^{-/-}$; $^{+/-}$, $^{-/+}$ and $^{+/+}$) suggests that all mice are exposed to similar antigens and have similar immune responses to them. Exposure to the same antigens should be expected considering that mice in this study are littermates and are housed together. The fact that only the *Traf2*DNx*BCL2*-tg$^{+/+}$ mice develop CLL/SLL highlights the need of both *Traf2* deficiency and BCL2 overexpression for promoting CLL development in this mouse model and underlines a role for autoantigens- and pathogen antigens-specific HCDR3 in driving disease progression.

DATA AVAILABILITY STATEMENT

The raw data supporting the conclusions of this article will be made available by the authors, without undue reservation.

ETHICS STATEMENT

The animal study was reviewed and approved by Bioethics Committee of the Consejo Superior de Investigaciones Científicas (CSIC).

AUTHOR CONTRIBUTIONS

GP-C designed, performed, and analyzed the experiments and helped writing the paper. JZ designed and analyzed the experiments and wrote the paper. All authors contributed to the article and approved the submitted version.

FUNDING

This work was supported by grants from the Agencia Estatal de Investigacion (PID2019-110405RB-I00/AEI/10.13039/501100011033) and from the Instituto de Salud Carlos III (PI16/000895). We acknowledge support of the publication fee by the CSIC Open Access Publication Support Initiative through its Unit of Information Resources for Research (URICI). The cost of this publication was paid in part by FEDER funds.

ACKNOWLEDGMENTS

We are indebted to Laura Barrios (Scientific Calculation Center, SGAI, CSIC) for statistical analyses. We are thankful to Maria G. Gonzalez-Bueno for excellent technical support. We are grateful to the personnel of the Animal facility and Genomics facilities at Instituto de Investigaciones Biomedicas "Alberto Sols". We also thank Dr. Paloma Perez-Aciego (Fundacion LAIR, Madrid) for kindly providing reagents and helpful discussions. Pablo Carr, Andrea de Andrés and Blanca Jiménez are acknowledged for helpful technical assistance.

SUPPLEMENTARY MATERIAL

The Supplementary Material for this article can be found online at: https://www.frontiersin.org/articles/10.3389/fimmu.2021.627602/full#supplementary-material

REFERENCES

1. Chiorazzi N, Rai KR, Ferrarini M. Chronic lymphocytic leukemia. *N Engl J Med* (2005) 352(8):804–15. doi: 10.1056/NEJMra041720
2. Chiorazzi N, Ferrarini M. Cellular origin(s) of chronic lymphocytic leukemia: cautionary notes and additional considerations and possibilities. *Blood* (2011) 117(6):1781–91. doi: 10.1182/blood-2010-07-155663
3. Kipps TJ, Stevenson FK, Wu CJ, Croce CM, Packham G, Wierda WG, et al. Chronic lymphocytic leukaemia. *Nat Rev Dis Primers* (2017) 3:16096. doi: 10.1038/nrdp.2016.96
4. Schroeder HW Jr, Dighiero G. The pathogenesis of chronic lymphocytic leukemia: analysis of the antibody repertoire. *Immunol Today* (1994) 15 (6):288–94. doi: 10.1016/0167-5699(94)90009-4
5. Fais F, Ghiotto F, Hashimoto S, Sellars B, Valetto A, Allen SL, et al. Chronic lymphocytic leukemia B cells express restricted sets of mutated and unmutated antigen receptors. *J Clin Invest* (1998) 102(8):1515–25. doi: 10.1172/JCI3009
6. Hamblin TJ, Davis Z, Gardiner A, Oscier DG, Stevenson FK. Unmutated Ig V(H) genes are associated with a more aggressive form of chronic lymphocytic leukemia. *Blood* (1999) 94(6):1848–54. doi: 10.1182/blood.V94.6.1848.418k05_1848_1854
7. Damle RN, Wasil T, Fais F, Ghiotto F, Valetto A, Allen SL, et al. Ig V gene mutation status and CD38 expression as novel prognostic indicators in chronic lymphocytic leukemia. *Blood* (1999) 94(6):1840–7. doi: 10.1182/blood.V94.6.1840
8. Maloum K, Davi F, Merle-Beral H, Pritsch O, Magnac C, Vuillier F, et al. Expression of unmutated VH genes is a detrimental prognostic factor in chronic lymphocytic leukemia. *Blood* (2000) 96(1):377–9. doi: 10.1182/blood.V96.1.377.013k56f_377_379
9. Damle RN, Ghiotto F, Valetto A, Albesiano E, Fais F, Yan XJ, et al. B-cell chronic lymphocytic leukemia cells express a surface membrane phenotype of activated, antigen-experienced B lymphocytes. *Blood* (2002) 99(11):4087–93. doi: 10.1182/blood.V99.11.4087
10. Klein U, Tu Y, Stolovitzky GA, Mattioli M, Cattoretti G, Husson H, et al. Gene expression profiling of B cell chronic lymphocytic leukemia reveals a homogeneous phenotype related to memory B cells. *J Exp Med* (2001) 194 (11):1625–38. doi: 10.1084/jem.194.11.1625

11. Burns A, Alsolami R, Becq J, Stamatopoulos B, Timbs A, Bruce D, et al. Whole-genome sequencing of chronic lymphocytic leukaemia reveals distinct differences in the mutational landscape between IgHV(mut) and IgHV (unmut) subgroups. *Leukemia* (2018) 32(2):573. doi: 10.1038/leu.2017.311
12. Herve M, Xu K, Ng YS, Wardemann H, Albesiano E, Messmer BT, et al. Unmutated and mutated chronic lymphocytic leukemias derive from self-reactive B cell precursors despite expressing different antibody reactivity. *J Clin Invest* (2005) 115(6):1636–43. doi: 10.1172/JCI24387
13. Allsup DJ, Kamiguti AS, Lin K, Sherrington PD, Matrai Z, Slupsky JR, et al. B-cell receptor translocation to lipid rafts and associated signaling differ between prognostically important subgroups of chronic lymphocytic leukemia. *Cancer Res* (2005) 65(16):7328–37. doi: 10.1158/0008-5472.CAN-03-1563
14. Darzentas N, Hadzidimitriou A, Murray F, Hatzi K, Josefsson P, Laoutaris N, et al. A different ontogenesis for chronic lymphocytic leukemia cases carrying stereotyped antigen receptors: molecular and computational evidence. *Leukemia* (2010) 24(1):125–32. doi: 10.1038/leu.2009.186
15. Agathangelidis A, Chatzidimitriou A, Gemenetzi K, Giudicelli V, Karypidou M, Plevova K, et al. Higher-order connections between stereotyped subsets: implications for improved patient classification in CLL. *Blood* (2020) 137 (10):1365–76. doi: 10.1182/blood.2020007039
16. Chiorazzi N, Hatzi K, Albesiano E. B-cell chronic lymphocytic leukemia, a clonal disease of B lymphocytes with receptors that vary in specificity for (auto)antigens. *Ann N Y Acad Sci* (2005) 1062:1–12. doi: 10.1196/annals.1358.002
17. Ghia P, Chiorazzi N, Stamatopoulos K. Microenvironmental influences in chronic lymphocytic leukaemia: the role of antigen stimulation. *J Intern Med* (2008) 264(6):549–62. doi: 10.1111/j.1365-2796.2008.02030.x
18. Bertilaccio MT, Scielzo C, Simonetti G, Ten Hacken E, Apollonio B, Ghia P, et al. Xenograft models of chronic lymphocytic leukemia: problems, pitfalls and future directions. *Leukemia* (2013) 27(3):534–40. doi: 10.1038/leu.2012.268
19. Bagnara D, Kaufman MS, Calissano C, Marsilio S, Patten PE, Simone R, et al. A novel adoptive transfer model of chronic lymphocytic leukemia suggests a key role for T lymphocytes in the disease. *Blood* (2011) 117(20):5463–72. doi: 10.1182/blood-2010-12-324210
20. Perez-Chacon G, Zapata JM. Mouse Models of Chronic Lymphocytic Leukemia. In: P Oppezzo, editor. *Chronic Lymphocytic Leukemia*. Rijeka, Croatia: InTech (2012). p. 203–28.
21. Bresin A, D'Abundo L, Narducci MG, Fiorenza MT, Croce CM, Negrini M, et al. TCL1 transgenic mouse model as a tool for the study of therapeutic targets and microenvironment in human B-cell chronic lymphocytic leukemia. *Cell Death Dis* (2016) 7:e2071. doi: 10.1038/cddis.2015.419
22. Zapata JM, Krajewska M, Morse HC,3, Choi Y, Reed JC. TNF receptor-associated factor (TRAF) domain and Bcl-2 cooperate to induce small B cell lymphoma/chronic lymphocytic leukemia in transgenic mice. *Proc Natl Acad Sci USA* (2004) 101(47):16600–5. doi: 10.1073/pnas.0407541101
23. Kress CL, Konopleva M, Martinez-Garcia V, Krajewska M, Lefebvre S, Hyer M, et al. Triterpenoids display single agent anti-tumor activity in a transgenic mouse model of chronic lymphocytic leukemia and small lymphocytic lymphoma. *PLoS One* (2007) 2(6):e559. doi: 10.1371/journal.pone.0000559
24. Perez-Chacon G, Llobet D, Pardo C, Pindado J, Choi Y, Reed JC, et al. TNFR-associated factor 2 deficiency in B lymphocytes predisposes to chronic lymphocytic leukemia/small lymphocytic lymphoma in mice. *J Immunol* (2012) 189(2):1053–61. doi: 10.4049/jimmunol.1200814
25. Robertson LE, Plunkett W, McConnell K, Keating MJ, McDonnell TJ. Bcl-2 expression in chronic lymphocytic leukemia and its correlation with the induction of apoptosis and clinical outcome. *Leukemia* (1996) 10(3):456–9.
26. Lee SY, Reichlin A, Santana A, Sokol KA, Nussenzweig MC, Choi Y. TRAF2 is essential for JNK but not NF-$_K$B activation and regulates lymphocyte proliferation and survival. *Immunity* (1997) 7:703–13. doi: 10.1016/S1074-7613(00)80390-8
27. Katsumata M, Siegel RM, Louie DC, Miyashita T, Tsujimoto Y, Nowell PC, et al. Differential effects of Bcl-2 on B and T lymphocytes in transgenic mice. *Proc Natl Acad Sci USA* (1992) 89:11376–80. doi: 10.1073/pnas.89.23.11376
28. Yan XJ, Albesiano E, Zanesi N, Yancopoulos S, Sawyer A, Romano E, et al. B cell receptors in TCL1 transgenic mice resemble those of aggressive, treatment-resistant human chronic lymphocytic leukemia. *Proc Natl Acad Sci USA* (2006) 103(31):11713–8. doi: 10.1073/pnas.0604564103
29. Brochet X, Lefranc MP, Giudicelli V. IMGT/V-QUEST: the highly customized and integrated system for IG and TR standardized V-J and V-D-J sequence analysis. *Nucleic Acids Res* (2008) 36(Web Server issue):W503–8. doi: 10.1093/nar/gkn316
30. Karan-Djurasevic T, Pavlovic S. Somatic Hypermutational Status and Gene Repertoire of Immunoglobulin Rearrangements in Chronic Lymphocytic Leukemia. In: I Gheorghita, editor. *Lymphocyte Updates - Cancer, Autoimmunity and Infection*. Rijeka, Croatia: InTech (2017). p. 49–78. (Chapter 3).
31. Iacovelli S, Hug E, Bennardo S, Duehren-von Minden M, Gobessi S, Rinaldi A, et al. Two types of BCR interactions are positively selected during leukemia development in the Emu-TCL1 transgenic mouse model of CLL. *Blood* (2015) 125(10):1578–88. doi: 10.1182/blood-2014-07-587790
32. Klein U, Lia M, Crespo M, Siegel R, Shen Q, Mo T, et al. The DLEU2/miR-15a/16-1 cluster controls B cell proliferation and its deletion leads to chronic lymphocytic leukemia. *Cancer Cell* (2010) 17(1):28–40. doi: 10.1016/j.ccr.2009.11.019
33. Collins AM, Wang Y, Roskin KM, Marquis CP, Jackson KJ. The mouse antibody heavy chain repertoire is germline-focused and highly variable between inbred strains. Philosophical transactions of the Royal Society of London Series B. *Biol Sci* (2015) 370(1676):20140236. doi: 10.1098/rstb.2014.0236
34. Perez-Chacon G, Adrados M, Vallejo-Cremades MT, Lefebvre S, Reed JC, Zapata JM. Dysregulated TRAF3 and BCL2 Expression Promotes Multiple Classes of Mature Non-hodgkin B Cell Lymphoma in Mice. *Front Immunol* (2019) 9:3114. doi: 10.3389/fimmu.2018.03114
35. Rettig TA, Ward C, Bye BA, Pecaut MJ, Chapes SK. Characterization of the naive murine antibody repertoire using unamplified high-throughput sequencing. *PLoS One* (2018) 13(1):e0190982. doi: 10.1371/journal.pone.0190982
36. Watson CT, Kos JT, Gibson WS, Newman L, Deikus G, Busse CE, et al. A comparison of immunoglobulin IGHV, IGHD and IGHJ genes in wild-derived and classical inbred mouse strains. *Immunol Cell Biol* (2019) 97 (10):888–901. doi: 10.1111/imcb.12288
37. Tobin G, Thunberg U, Laurell A, Karlsson K, Aleskog A, Willander K, et al. Patients with chronic lymphocytic leukemia with mutated VH genes presenting with Binet stage B or C form a subgroup with a poor outcome. *Haematologica* (2005) 90(4):465–9.
38. Gardam S, Sierro F, Basten A, Mackay F, Brink R. TRAF2 and TRAF3 signal adapters act cooperatively to control the maturation and survival signals delivered to B cells by the BAFF receptor. *Immunity* (2008) 28(3):391–401. doi: 10.1016/j.immuni.2008.01.009
39. Martin F, Kearney JF. Marginal-zone B cells. *Nat Rev Immunol* (2002) 2 (5):323–35. doi: 10.1038/nri799
40. Mastache EF, Lindroth K, Fernandez C, Gonzalez-Fernandez A. Somatic hypermutation of Ig genes is affected differently by failures in apoptosis caused by disruption of Fas (lpr mutation) or by overexpression of Bcl-2. *Scandinavian J Immunol* (2006) 63(6):420–9. doi: 10.1111/j.1365-3083.2006.001758.x
41. Mauerer K, Zahrieh D, Gorgun G, Li A, Zhou J, Ansen S, et al. Immunoglobulin gene segment usage, location and immunogenicity in mutated and unmutated chronic lymphocytic leukaemia. *Br J Haematol* (2005) 129(4):499–510. doi: 10.1111/j.1365-2141.2005.05480.x
42. Johnson TA, Rassenti LZ, Kipps TJ. Ig VH1 genes expressed in B cell chronic lymphocytic leukemia exhibit distinctive molecular features. *J Immunol* (1997) 158(1):235–46.
43. Widhopf GF,2, Kipps TJ. Normal B cells express 51p1-encoded Ig heavy chains that are distinct from those expressed by chronic lymphocytic leukemia B cells. *J Immunol* (2001) 166(1):95–102. doi: 10.4049/jimmunol.166.1.95
44. Shi B, Ma L, He X, Wang X, Wang P, Zhou L, et al. Comparative analysis of human and mouse immunoglobulin variable heavy regions from IMGT/LIGM-DB with IMGT/HighV-QUEST. *Theor Biol Med Model* (2014) 11 (1):30. doi: 10.1186/1742-4682-11-30
45. Pal Singh S, de Bruijn MJW, de Almeida MP, Meijers RWJ, Nitschke L, Langerak AW, et al. Identification of Distinct Unmutated Chronic Lymphocytic Leukemia Subsets in Mice Based on Their T Cell Dependency. *Front Immunol* (2018) 9:1996. doi: 10.3389/fimmu.2018.01996
46. Agathangelidis A, Darzentas N, Hadzidimitriou A, Brochet X, Murray F, Yan XJ, et al. Stereotyped B-cell receptors in one-third of chronic lymphocytic

leukemia: a molecular classification with implications for targeted therapies. *Blood* (2012) 119(19):4467–75. doi: 10.1182/blood-2011-11-393694
47. Agathangelidis A, Vardi A, Baliakas P, Stamatopoulos K. Stereotyped B-cell receptors in chronic lymphocytic leukemia. *Leuk Lymphoma* (2014) 55 (10):2252–61. doi: 10.3109/10428194.2013.879715
48. Colombo M, Bagnara D, Reverberi D, Matis S, Cardillo M, Massara R, et al. Tracing CLL-biased stereotyped immunoglobulin gene rearrangements in normal B cell subsets using a high-throughput immunogenetic approach. *Mol Med* (2020) 26(1):25. doi: 10.1186/s10020-020-00151-9
49. Muggen AF, de Jong M, Wolvers-Tettero ILM, Kallemeijn MJ, Teodosio C, Darzentas N, et al. The presence of CLL-associated stereotypic B cell receptors in the normal BCR repertoire from healthy individuals increases with age. *Immun Ageing* (2019) 16:22. doi: 10.1186/s12979-019-0163-x
50. Zwick C, Fadle N, Regitz E, Kemele M, Stilgenbauer S, Buhler A, et al. Autoantigenic targets of B-cell receptors derived from chronic lymphocytic leukemias bind to and induce proliferation of leukemic cells. *Blood* (2013) 121 (23):4708–17. doi: 10.1182/blood-2012-08-447904
51. Chen SS, Batliwalla F, Holodick NE, Yan XJ, Yancopoulos S, Croce CM, et al. Autoantigen can promote progression to a more aggressive TCL1 leukemia by selecting variants with enhanced B-cell receptor signaling. *Proc Natl Acad Sci USA* (2013) 110(16):E1500–7. doi: 10.1073/pnas.1300616110
52. Hayakawa K, Formica AM, Brill-Dashoff J, Shinton SA, Ichikawa D, Zhou Y, et al. Early generated B1 B cells with restricted BCRs become chronic lymphocytic leukemia with continued c-Myc and low Bmf expression. *J Exp Med* (2016) 213(13):3007–24. doi: 10.1084/jem.20160712
53. Hayakawa K, Formica AM, Colombo MJ, Shinton SA, Brill-Dashoff J, Morse Iii HC, et al. Loss of a chromosomal region with synteny to human 13q14 occurs in mouse chronic lymphocytic leukemia that originates from early-generated B-1 B cells. *Leukemia* (2016) 30(7):1510–9. doi: 10.1038/leu.2016.61
54. Jimenez de Oya N, De Giovanni M, Fioravanti J, Ubelhart R, Di Lucia P, Fiocchi A, et al. Pathogen-specific B-cell receptors drive chronic lymphocytic leukemia by light-chain-dependent cross-reaction with autoantigens. *EMBO Mol Med* (2017) 9(11):1482–90. doi: 10.15252/emmm.201707732
55. Broker BM, Klajman A, Youinou P, Jouquan J, Worman CP, Murphy J, et al. Chronic lymphocytic leukemic (CLL) cells secrete multispecific autoantibodies. *J Autoimmun* (1988) 1(5):469–81. doi: 10.1016/0896-8411(88)90068-6
56. Lanemo Myhrinder A, Hellqvist E, Sidorova E, Soderberg A, Baxendale H, Dahle C, et al. A new perspective: molecular motifs on oxidized LDL, apoptotic cells, and bacteria are targets for chronic lymphocytic leukemia antibodies. *Blood* (2008) 111(7):3838–48. doi: 10.1182/blood-2007-11-125450
57. Sthoeger ZM, Wakai M, Tse DB, Vinciguerra VP, Allen SL, Budman DR, et al. Production of autoantibodies by CD5-expressing B lymphocytes from patients with chronic lymphocytic leukemia. *J Exp Med* (1989) 169(1):255–68. doi: 10.1084/jem.169.1.255
58. Kostareli E, Hadzidimitriou A, Stavroyianni N, Darzentas N, Athanasiadou A, Gounari M, et al. Molecular evidence for EBV and CMV persistence in a subset of patients with chronic lymphocytic leukemia expressing stereotyped IGHV4-34 B-cell receptors. *Leukemia* (2009) 23(5):919–24. doi: 10.1038/leu.2008.379
59. Steininger C, Rassenti LZ, Vanura K, Eigenberger K, Jager U, Kipps TJ, et al. Relative seroprevalence of human herpes viruses in patients with chronic lymphocytic leukaemia. *Eur J Clin Invest* (2009) 39(6):497–506. doi: 10.1111/j.1365-2362.2009.02131.x
60. Chiorazzi N, Ferrarini M. B cell chronic lymphocytic leukemia: lessons learned from studies of the B cell antigen receptor. *Annu Rev Immunol* (2003) 21:841–94. doi: 10.1146/annurev.immunol.21.120601.141018
61. Ten Hacken E, Gounari M, Ghia P, Burger JA. The importance of B cell receptor isotypes and stereotypes in chronic lymphocytic leukemia. *Leukemia* (2019) 33(2):287–98. doi: 10.1038/s41375-018-0303-x
62. Traverse-Glehen A, Davi F, Ben Simon E, Callet-Bauchu E, Felman P, Baseggio L, et al. Analysis of VH genes in marginal zone lymphoma reveals marked heterogeneity between splenic and nodal tumors and suggests the existence of clonal selection. *Haematologica* (2005) 90(4):470–8.
63. Granai M, Amato T, Di Napoli A, Santi R, Vergoni F, Di Stefano G, et al. IGHV mutational status of nodal marginal zone lymphoma by NGS reveals distinct pathogenic pathways with different prognostic implications. *Virchows Arch* (2020) 477(1):143–50. doi: 10.1007/s00428-019-02712-8
64. Hojjat-Farsangi M, Jeddi-Tehrani M, Razavi SM, Sharifian RA, Mellstedt H, Shokri F, et al. Immunoglobulin heavy chain variable region gene usage and mutational status of the leukemic B cells in Iranian patients with chronic lymphocytic leukemia. *Cancer Sci* (2009) 100(12):2346–53. doi: 10.1111/j.1349-7006.2009.01341.x
65. Marinelli M, Ilari C, Xia Y, Del Giudice I, Cafforio L, Della Starza I, et al. Immunoglobulin gene rearrangements in Chinese and Italian patients with chronic lymphocytic leukemia. *Oncotarget* (2016) 7(15):20520–31. doi: 10.18632/oncotarget.7819
66. Elemento O, Lefranc MP. IMGT/PhyloGene: an on-line tool for comparative analysis of immunoglobulin and T cell receptor genes. *Dev Comp Immunol* (2003) 27(9):763–79. doi: 10.1016/S0145-305X(03)00078-8
67. Seifert M, Sellmann L, Bloehdorn J, Wein F, Stilgenbauer S, Durig J, et al. Cellular origin and pathophysiology of chronic lymphocytic leukemia. *J Exp Med* (2012) 209(12):2183–98. doi: 10.1084/jem.20120833
68. Darwiche W, Gubler B, Marolleau JP, Ghamlouch H. Chronic Lymphocytic Leukemia B-Cell Normal Cellular Counterpart: Clues From a Functional Perspective. *Front Immunol* (2018) 9:683. doi: 10.3389/fimmu.2018.00683
69. Cerutti A, Cols M, Puga I. Marginal zone B cells: virtues of innate-like antibody-producing lymphocytes. *Nat Rev Immunol* (2013) 13(2):118–32. doi: 10.1038/nri3383
70. Hendricks J, Bos NA, Kroese FGM. Heterogeneity of Memory Marginal Zone B Cells. *Crit Rev Immunol* (2018) 38(2):145–58. doi: 10.1615/CritRevImmunol.2018024985
71. Grech AP, Amesbury M, Chan T, Gardam S, Basten A, Brink R. TRAF2 differentially regulates the canonical and noncanonical pathways of NF-kappaB activation in mature B cells. *Immunity* (2004) 21(5):629–42. doi: 10.1016/j.immuni.2004.09.011
72. Del Gaizo Moore V, Brown JR, Certo M, Love TM, Novina CD, Letai A. Chronic lymphocytic leukemia requires BCL2 to sequester prodeath BIM, explaining sensitivity to BCL2 antagonist ABT-737. *J Clin Invest* (2007) 117 (1):112–21. doi: 10.1172/JCI28281
73. Weill JC, Weller S, Reynaud CA. Human marginal zone B cells. *Annu Rev Immunol* (2009) 27:267–85. doi: 10.1146/annurev.immunol.021908.132607
74. Bichi R, Shinton SA, Martin ES, Koval A, Calin GA, Cesari R, et al. Human chronic lymphocytic leukemia modeled in mouse by targeted TCL1 expression. *Proc Natl Acad Sci USA* (2002) 99(10):6955–60. doi: 10.1073/pnas.102181599
75. Prohaska TA, Que X, Diehl CJ, Hendrikx S, Chang MW, Jepsen K, et al. Massively Parallel Sequencing of Peritoneal and Splenic B Cell Repertoires Highlights Unique Properties of B-1 Cell Antibodies. *J Immunol* (2018) 200 (5):1702–17. doi: 10.4049/jimmunol.1700568
76. Duhren-von Minden M, Ubelhart R, Schneider D, Wossning T, Bach MP, Buchner M, et al. Chronic lymphocytic leukaemia is driven by antigen-independent cell-autonomous signalling. *Nature* (2012) 489(7415):309–12. doi: 10.1038/nature11309

Conflict of Interest: The authors declare that the research was conducted in the absence of any commercial or financial relationships that could be construed as a potential conflict of interest.

frontiers in Immunology

ORIGINAL RESEARCH
published: 04 May 2021
doi: 10.3389/fimmu.2021.641692

Continuous MYD88 Activation Is Associated With Expansion and Then Transformation of IgM Differentiating Plasma Cells

Catherine Ouk[1†], Lilian Roland[1†], Nathalie Gachard[1‡], Stéphanie Poulain[2‡], Christelle Oblet[1], David Rizzo[1], Alexis Saintamand[1], Quentin Lemasson[1], Claire Carrion[1], Morgane Thomas[1], Karl Balabanian[3], Marion Espéli[3], Marie Parrens[4], Isabelle Soubeyran[5], Mélanie Boulin[1], Nathalie Faumont[1], Jean Feuillard[1] and Christelle Vincent-Fabert[1*]*

[1] UMR CNRS 7276/INSERM U1262 CRIBL, University of Limoges, and Hematology Laboratory of Dupuytren Hospital University Center (CHU) of Limoges, Limoges, France, [2] UMR CANTHER « CANcer Heterogeneity, Plasticity and Resistance to THERapies » INSERM 1277-CNRS 9020 UMRS 12, University of Lille, Hematology Laboratory, Biology and Pathology Center, CHU de Lille, Lille, France, [3] Institut de Recherche Saint-Louis, EMiLy, INSERM U1160, University of Paris, Paris, France, [4] Pathology Department, Hospital University Center of Bordeaux, Bordeaux, France, [5] Laboratory of Pathology, Institut Bergonié, Bordeaux, France

Activating mutations of *MYD88* (*MYD88*^{L265P} being the far most frequent) are found in most cases of Waldenström macroglobulinemia (WM) as well as in various aggressive B-cell lymphoma entities with features of plasma cell (PC) differentiation, such as activated B-cell type diffuse large B-cell lymphoma (DLBCL). To understand how MYD88 activation exerts its transformation potential, we developed a new mouse model in which the MYD88^{L252P} protein, the murine ortholog of human MYD88^{L265P}, is continuously expressed in CD19 positive B-cells together with the Yellow Fluorescent Protein (Myd88^{L252P} mice). In bone marrow, IgM B and plasma cells were expanded with a CD138 expression continuum from IgM^{high} CD138^{low} to IgM^{low} CD138^{high} cells and the progressive loss of the B220 marker. Serum protein electrophoresis (SPE) longitudinal analysis of 40 Myd88^{L252P} mice (16 to 56 weeks old) demonstrated that ageing was first associated with serum polyclonal hyper gammaglobulinemia (hyper Ig) and followed by a monoclonal immunoglobulin (Ig) peak related to a progressive increase in IgM serum levels. All Myd88^{L252P} mice exhibited spleen enlargement which was directly correlated with the SPE profile and was maximal for monoclonal Ig peaks. Myd88^{L252P} mice exhibited very early increased IgM PC differentiation. Most likely due to an early increase in the Ki67 proliferation index, IgM lymphoplasmacytic (LP) and plasma cells continuously expanded with age being first associated with hyper Ig and then with monoclonal Ig peak. This peak was consistently associated with a spleen LP-like B-cell lymphoma. Clonal expression of both membrane and secreted μ chain isoforms was demonstrated at the mRNA level by high throughput sequencing. The Myd88^{L252P} tumor transcriptomic signature identified both proliferation and canonical NF-κB p65/RelA activation. Comparison with *MYD88*^{L265P} WM showed that Myd88^{L252P} tumors also

OPEN ACCESS

Edited by:
Pablo Engel, University of Barcelona, Spain

Reviewed by:
Hiromi Kubagawa, German Rheumatism Research Center (DRFZ), Germany
Rachel Maurie Gerstein, University of Massachusetts Medical School, United States

***Correspondence:**
Christelle Vincent-Fabert
christelle.vincent-fabert@unilim.fr
Jean Feuillard
jean.feuillard@unilim.fr

[†]These authors have contributed equally to this work

[‡]These authors have contributed equally to this work

Specialty section:
This article was submitted to B Cell Biology, a section of the journal Frontiers in Immunology

Received: *14 December 2020*
Accepted: *14 April 2021*
Published: *04 May 2021*

Citation:
Ouk C, Roland L, Gachard N, Poulain S, Oblet C, Rizzo D, Saintamand A, Lemasson Q, Carrion C, Thomas M, Balabanian K, Espéli M, Parrens M, Soubeyran I, Boulin M, Faumont N, Feuillard J and Vincent-Fabert C (2021) Continuous MYD88 Activation Is Associated With Expansion and Then Transformation of IgM Differentiating Plasma Cells. Front. Immunol. 12:641692. doi: 10.3389/fimmu.2021.641692

shared the typical lymphoplasmacytic transcriptomic signature of WM bone marrow purified tumor B-cells. Altogether these results demonstrate for the first time that continuous MYD88 activation is specifically associated with clonal transformation of differentiating IgM B-cells. Since MYD88^{L252P} targets the IgM PC differentiation continuum, it provides an interesting preclinical model for development of new therapeutic approaches to both WM and aggressive MYD88 associated DLBCLs.

Keywords: MYD88 L265P mutation, lymphoplasmacytic lymphoma/Waldenstrom's macroglobulinemia, IgM secretion, monoclonal Ig peak, B-cell lymphoma, plasma cell

INTRODUCTION

Waldenström's macroglobulinemia (WM) is an incurable indolent B-cell lymphoma of the elderly accounting for less than 5% of B-cell lymphomas with, as unique characteristics, a serum IgM peak and primary medullary localization of lymphoplasmacytic cells that exhibit continuous differentiation from mature B lymphocytes to IgM secretory plasma cells (1). Secondary lymphoid organ infiltration and/or a leukemic phase is found in 20% cases. Other manifestations include neuropathy, cryoglobulinemia, skin rash, cold-agglutinin hemolytic anemia, and amyloidosis (2). The discovery of the activating mutation of *MYD88* (*MYD88^{L265P}* being the far most frequent) in more than 90% of WM cases contributed to the concept that this entity is genetically distinct from other B-cell lymphomas (3, 4). Being present in 50% of IgM monoclonal gammopathies of undetermined significance (MGUS), *MYD88* mutations are most likely a primary event in WM (5). Considered as secondary genetic events, activating mutations of *CXCR4* (CXCR4^{S338X} or CXCR4^{WHIM}), a receptor implicated in migration and bone marrow (BM) homing of leucocytes, are found in 30% of WM cases (6). Additional mutations of *CD79b*, *ARID1A* or *TP53* have been reported (7).

Despite these advances, WM pathophysiology is incompletely understood. Its treatment remains challenging and the exact role of *MYD88* mutations in the emergence of lymphoplasmacytic B-cell clones is not known (7, 8). Indeed, *MYD88* mutations are also found in 30% of activated B-cell type diffuse large B-cell lymphomas (ABC-DLBCL), more than half of primary cutaneous DLBCLs, leg type, and many DLBCLs at immune-privileged sites but not in plasma cell myelomas, even IgM types (9). It should be noted that IgM expression is a surrogate marker of ABC-DLBCLs (10). Moreover, all these aggressive B-cell tumors associated with MYD88, which often exhibit morphological features of plasma cell (PC) differentiation, are all associated with expression of the PC differentiation marker IRF4. MYD88 protein is the canonical adapter for inflammatory signaling pathways to downstream members of the Toll-like receptor (TLR) and interleukin-1 receptor (IL-1R) families. Forming the myddosome complex, MYD88 binds IL-1R or TLR family members to IRAK kinases family. IRAK activation leads to activation of the NF kappa B (NF-κB) transcription factor and interferon 3 and 7 regulatory factors (IRF3 and 7). MYD88^{L265P} constitutively increases formation of the myddosome complex with downstream NF-κB activation (3, 11, 12). Experimentally, MYD88^{L265P} is essential for survival of ABC-DLBCL and WM cell lines (3, 11). A recent publication suggests the involvement of HOIP and LUBAC-dependent NF-κB activation in the transformation potential of MYD88 activation in a mouse model (13). The current published mouse models with continuous MYD88 activation in the B-cell lineage develop aggressive clonal B-cell lymphomas that resemble human ABC-DLBCLs (13–15). Although discussed by Jo et al. in the HOIP/LUBAC activation context, no IgM peak was reported in these models. Therefore, the question of a direct role for MYD88 in the development of a lymphoplasmacytic lymphoma with monoclonal IgM secretion is still open. Recently, K Schmidt et al. reported a mouse model in which MYD88 activation was responsible for an indolent lymphoproliferative disorder resembling to IgM monoclonal gammopathy of unknown significance (IgM MGUS), the asymptomatic preclinical stage of WM (16).

Here, we present a new mouse model in which the MYD88^{L252P} protein, the murine ortholog of human MYD88^{L265P}, is continuously expressed in the B-cell lineage together with Yellow Fluorescent Protein (YFP) (Myd88^{L252P} mice). We show that these mice first developed early expansion of CD93^{neg} IgM PCs with an increase in both IgM secretion and bone marrow relocalization of IgM B-cells. Moreover, these mice also had increased percentages of IgM^{high} CD138^{low} and IgM^{low} CD138^{high} cells with a CD138 expression continuum between both cell types. Then, these mice developed an oligoclonal or clonal IgM lymphoplasmacytic-like B-cell lymphoma together with a serum IgM monoclonal peak. These tumors had marked transcriptomic similarities to WM but they were located in the spleen and exhibited significant increased proliferation. Despite differences between Myd88^{L252P} LP-like B-cell tumors and WM, our results demonstrate that the MYD88 transformation potential is strongly associated with a shift in B-cell peripheral differentiation toward plasma cells with IgM secretion. These results help explain why MYD88 activation is found in most WM and in various aggressive B-cell lymphomas with IgM PC differentiation engagement such as ABC DLBCLs.

MATERIALS AND METHODS

Generation of the Transgenic Mouse Line Myd88^{L252P}

The transgenes (cDNA) *Myd88^{WT}*-IRES-*Yfp* and *Myd88^{L252P}*-IRES-*Yfp* were synthetized (Genecust, Dudelange, Luxembourg)

and inserted into the pcDNA3.1 vector. Sequences of these transgenes are given in **Supplementary Materials and Methods**. The *Myd88^{L252P}*-IRES-*Yfp* insert was cloned into the pROSA26-1 vector (17) containing a LoxP-flanked region, consisting of a stop cassette and the *Neomycin* gene (18). The transgene *Myd88^{L252P}*-IRES-*Yfp* was inserted downstream from the stop cassette. JM8 embryonic stem (ES) cells were transfected with the targeting vector according to a previously described protocol (19). Targeted ES cells were screened for homologous recombination by PCR. Genomic DNA (gDNA) extraction was performed using an in house protocol and consisted of gDNA precipitation with absolute ethanol. Twenty nanograms gDNA were used for each PCR (primer sequences in **Supplementary Materials and Methods**) using LongAmp® *Taq* DNA Polymerase (New England Biolabs, Ipswich, MA) according to the manufacturer's recommendations. Recombined ES cells were injected into C57BL/6J blastocysts which were transferred into foster mothers to obtain chimeric mice (Myd88$^{L252P\text{-}flSTOP}$ mice).

Mice

Cd19^{Cre} mice (20) and mice carrying the *Myd88^{L252P}*-IRES-*Yfp* allele were crossed to induce the expression of the transgene in B cells (Myd88^{L252P} mice). Offspring were routinely screened by PCR using specific primers for insertion of the transgene (**Supplementary Materials and Methods**). Animals were housed at 21–23°C with a 12-hour light/dark cycle. All procedures were conducted under an approved protocol according to European guidelines for animal experimentation (French national authorization number: 8708503 and French ethics committee registration number APAFIS#14581-2018041009469362 v3).

Cell Transfection and NF-κB Dependent Dual-Luciferase Reporter Assay

A20 cells (5.10^6) were co-transfected with 5 µg of either empty pcDNA3.1, pcDNA3.1-*Myd88^{WT}* or pcDNA3.1-*Myd88^{L252P}* vectors, plus 100 ng pRL-TK *Renilla luciferase* expression vector (Promega Corporation, Madison, WI) and 5 µg of either the 3X-κB-L vector with three copies of the major histocompatibility complex (MHC) class I κB element or its mutated counterpart, the 3X-mutκB-L vector (21) using Amaxa L013 program (AMAXA Biosystems, Cologne, Germany). Twenty four hours after transfection, cells were lysed and luciferase activities were measured using the Dual-Luciferase Reporter Assay System and the Turner Designs TD-20/20 Luminometer (Promega Corporation, Madison, WI).

Sera Analyses

Serum was obtained from blood collected retro-orbitally. Specific ELISA and serum electrophoresis assay were performed as previously described (19, 22).

Flow Cytometry and *In Vivo* Proliferation Assays

In order to collect BM cells of Cd19^{Cre} and Myd88^{L252P} mice, femurs from both hind legs were rinsed with PBS and sternum was gently crushed and cells filtered on a nylon meshwork that was rinsed with PBS. Spleen cells from Cd19^{Cre} and Myd88^{L252P} were filtered through a sterile nylon membrane. Blood samples were collected retro-orbitally. Red cells were lysed by RBC Lysis Buffer (Biolegend, San Diego, CA). Cell suspensions were resuspended at 4°C in a labeling buffer (PBS, 1% BSA, 2mM EDTA) and labeled with fluorescent conjugated monoclonal antibodies listed in **Supplementary Materials and Methods**. Labeled cells were analyzed using a BD Fortessa SORP flow cytometer (BD Bioscience France, Le Pont de Claix, France). Results were analyzed using Kaluza Flow Cytometry software 1.2 (Beckman Coulter, Brea, CA).

Immunohistochemistry

Paraffin embedded tissue sections (5µm) were deparaffinized as follows: slides were immersed successively in xylene twice for 3 min, 3 times for 3 min in 100% ethanol, once for 3 min in 95% ethanol and 3 times in PBS for 5 min. Then, slides were immersed in citrate buffer pH7 and heated 4 times for 5 min 40 sec in a microwave at 800W. Image acquisition was performed with the Nanozoomer 2.0RS Hamamatsu and NDP.scan software (812 Joko-cho, Higashi-ku, Hamamatsu City, 431-3196, Japan). Quantification of Ki67 nuclear labelling was performed with the imageJS and the Ki67 module: http://imagejs.org/?http://module.imagejs.googlecode.com/git/mathbiol.chromomarkers.js&http://module.imagejs.googlecode.com/git/ki67 (23).

Gene Expression Profiling

A series of seven mice (three Cd19^{Cre} and four Myd88^{L252P}) was studied in parallel with bone marrow purified tumor B-cells from a series of 11 patients with *MYD88^{L265P}* WM (series 1) as well as lymph nodes from a series of 58 patients: 19 *MYD88^{WT}* chronic lymphocytic leukemia, 15 *MYD88^{L265P}* WM, 12 *MYD88^{wt}* Nodal marginal zone lymphoma, 5 *MYD88^{wt}* WM, 4 follicular lymphoma and 3 patients with benign follicular hyperplasia (series 2, **Supplementary Tables 1** and **2**). Approval of this protocol was obtained from the local IRB of the CHRU of Lille (CSTMT043). *MYD88* and *CXCR4* mutational status was determined as previously described (6). Total mRNA was extracted from whole infiltrated tissues and purified B-cells as reported (24). For humans and mice, RNA amplification and hybridization onto microarrays were performed on an Affymetrix Human Genome U133 Plus 2.0 Array and on an Affymetrix Gene Atlas system® with the MoGene-2_1-st-v1 Affymetrix chip (Affymetrix, Santa Clara, CA) respectively according to a previously described protocol (25) (GEO accession number GSE138273). Bioinformatic analyses are detailed in **Supplementary Materials and Methods**.

Repertoire Analysis

RNA was extracted from total spleen, and 1µg was used for sequencing. Transcripts were amplified by 5'RACE PCR using reverse primers hybridizing within either the membrane or secreted exon of the µ or γ genes. ProtoScript® II Reverse Transcriptase (New England Biolabs, Ipswich, MA) was used for reverse transcription and amplicons were obtained using

Phusion® High Fidelity DNA Polymerase (New England Biolabs, Ipswich, MA) according to the manufacturer's instructions. Primers used are listed in **Supplementary Materials and Methods**. Illumina sequencing adapter sequences were added by primer extension, and resulting amplicons were sequenced on an Illumina MiSeq sequencing system using MiSeq kit Reagent V2 500 cycles. Paired reads were merged using FLASH (26). Repertoire analysis was done using the IMGT/HighV-QUEST online tool (http://www.imgt.org/IMGT_vquest/vquest). The resulting output was parsed by in-house R script.

RESULTS

Generation of a Mouse Model With Insertion of the Mouse Mutation Myd88 L252P Into the Rosa26 Locus

To study the effect of continuous MYD88 activation on B-cell differentiation, we created a transgene containing the mutant murine cDNA sequence of *Myd88* (*Myd88^{L252P}*) which is orthologous to the human mutant sequence *MYD88^{L265P}*, in frame with the Yellow Fluorescent Protein (*Yfp*) sequence and separated by an Internal Ribosome Entry Site (IRES) sequence (*Myd88^{L252P}*-IRES-*Yfp*) (**Supplementary Figure 1A**). To validate this transgene, we checked that it induced expression of both MYD88^{L252P} and YFP proteins in the murine A20 B-cell line (**Supplementary Figures 1B, C**) and that it was responsible for constitutive NF-κB activation (**Supplementary Figure 1D**). The *Myd88^{L252P}*-IRES-*Yfp* insert was cloned into the pROSA26.1 vector (17) (**Supplementary Figure 1E**). In this construct, the insert was subcloned downstream from a *Neomycin*-STOP cassette flanked by LoxP sites. Chimeric mice were intercrossed to obtain stable germinal transmission of the *Myd88^{L252P}*-IRES-*Yfp* transgene (Myd88$^{L252P\text{-}flSTOP}$ mice). Myd88$^{L252P\text{-}flSTOP}$ and Cd19^{Cre} mice were crossed. Mice with both transgenes (Myd88^{L252P} mice) were then studied, with their age matched Cd19^{Cre} littermates as controls (Cd19^{Cre} LMC). Specific B-cell expression of the transgene was found in more than 90% of blood and spleen B cells compared to virtually no expression in the T-cell compartment (**Supplementary Figure 1F**). As expected and as evidence of NF-κB activation, Myd88^{L252P} splenocytes over-expressed the NF-κB target gene *Tnfaip3* at the mRNA level (**Supplementary Figure 1G**).

Serum Protein Electrophoresis Profiles Segregate Myd88^{L252P} Mice According to Age

As a first exploratory step, serum protein electrophoresis (SPE) was systematically performed on a series of 40 Myd88^{L252P} mice and 26 age matched Cd19^{Cre} LMCs. As shown in **Figure 1A** three SPE profiles were seen: normal, polyclonal hyper gammaglobulinemia (hyper Ig) and a monoclonal Ig peak. All Cd19^{Cre} LMCs exhibited normal SPE regardless of their age. In other words, SPEs with hyper Ig or Ig peaks were found only in Myd88^{L252P} mice (**Figures 1A, B**). **Figure 1B** shows the relationship between the age of Myd88^{L252P} mice and the SPE profile. Young Myd88^{L252P} mice (16-23 weeks) had a normal or hyper Ig SPE profile. In contrast, most mice older than 32 weeks had an Ig peak. In between these two groups, 24 to 31 week old mice (middle age) had a hyper Ig or an Ig peak in 65% and 35% cases respectively (Fisher test, $p=2.10^{-4}$). ELISA quantification of serum Ig revealed that young Myd88^{L252P} mice with a normal SPE exhibited a moderate IgM and IgG hyper Ig when compared to their Cd19^{Cre} LMC (**Figure 1C** and **Supplementary Figure 2**). Serum IgG levels of middle aged and old Myd88^{L252P} mice were variable when compared to their young counterparts. This was in contrast to serum IgM levels that were significantly increased in middle aged mice and even more so in old mice and correlated with the SPE profile and age (**Figure 1C** and **Supplementary Figure 2**).

These results first indicate that continuous MYD88 activation in B cells was associated with a global increase in Ig secretion. Second, age related occurrence of polyclonal hyper Ig and then monoclonal Ig peaks correlated with the increase in serum IgM levels. This suggests that, after a polyclonal expansion phase, aging of Myd88^{L252P} mice was associated with clonal restriction of IgM-secreting B-cells, very likely reflecting the MYD88^{L252P} B-cell transformation power in these cells. Therefore, these first results point to a strong relationship between MYD88^{L252P} and IgM-secreting B-cells.

Myd88^{L252P} Bone Marrow IgM Plasma Cell Content Was Increased and Displayed a CD138 Expression Continuum

As shown in **Figure 2A**, Myd88^{L252P} bone marrow global B-cell content was comparable to that of Cd19^{Cre} LMCs in terms of percentages in 16 week old mice with normal SPE. Transgene expression was mainly found in Myd88^{L252P} CD19^{high} B-cells. Indeed, with an on/off effect, percentages of YFP positive cells (*i.e* of LoxP rearranged cells) was directly correlated with CD19 mean fluorescence intensity (**Figure 2B**). Comparison of CD19^{cre} LMC and Myd88^{L252P} mice did not reveal any significant bone marrow B-cell increase with age. However older Myd88^{L252P} mice had increased levels of IgM^{Pos} CD19^{high} B-cells (**Figures 3A, B**, left panel and **Supplementary Figure 3** for the gating strategy). Strikingly, a CD138 expression continuum was clearly evident in a triple parametric B220/CD138/IgM histogram gated on mature B-cells and/or PCs in Myd88^{L252P} mice only (**Figure 3A**, lower panel see in red the decrease in B220 and the increase in CD138 expression). This CD138 expression continuum, that we recently showed to be characteristics of MYD88^{L265P} WM bone marrow tumor B-cells (Gayet et al, Cytometry B 2021), started from IgM^{high} CD138^{low} and ended at IgM^{low} CD138^{high} cells (**Figure 3A**, lower panel). This CD138 expression continuum was absent in Cd19^{Cre} LMCs. Consequently, Myd88^{L252P} mice showed increased percentages of both IgM^{high} CD138^{low} B-cells (most likely precursors of IgM PCs) and total bone marrow PCs (**Figure 3B**, right panel). Moreover, the proportion of bone marrow IgM PCs was significantly increased in young Myd88^{L252P} mice and even more in older Myd88^{L252P} mice (**Figure 3C**). Indeed, Myd88^{L252P} CD19^{Pos}/YFP^{Pos} B cells tended to accumulate in the

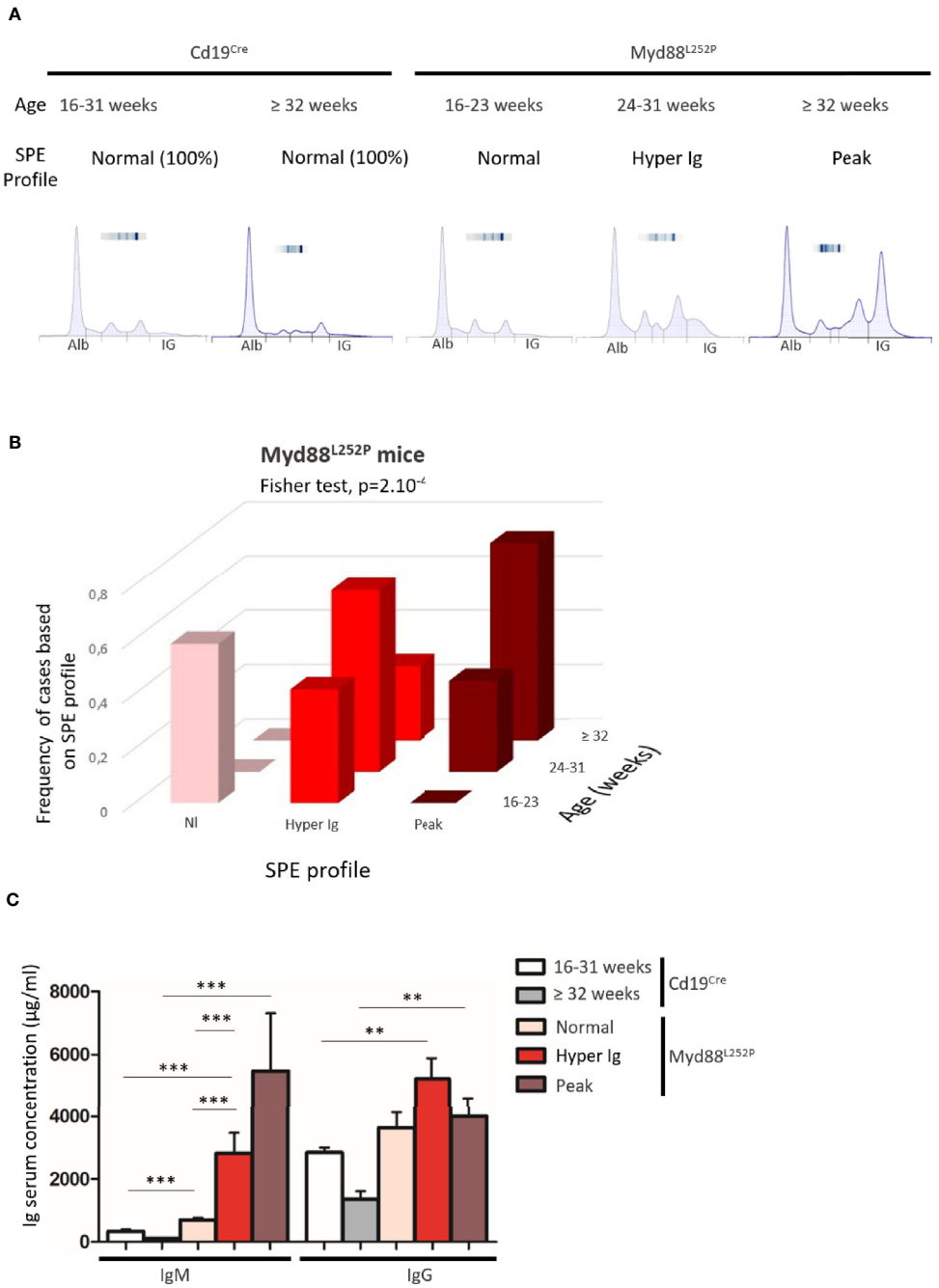

FIGURE 1 | Myd88^{L252P} transgenic mice exhibited serum IgM hypergammaglobulinemia and then monoclonal IgM peaks when ageing. **(A)** Examples of serum protein electrophoresis of Cd19^{Cre} mice (respectively 16 and 36 weeks-old) and three Myd88^{L252P} mice (16, 24 and 36 week-old) with normal, polyclonal hypergammaglobulinemia (hyper Ig) and monoclonal Ig peaks respectively. **(B)** Frequencies of cases according to SPE profile and age for Myd88^{L252P} mice (n = 40). **(C)** IgM and IgG serum levels in Cd19^{Cre} and Myd88^{L252P} mice. For Cd19^{Cre} (n = 15), Myd88^{L252P} (n = 36). Results are expressed as the mean ± SEM. Mann Whitney test p-value < 0.01 and < 0.001 are symbolized by ** and *** respectively.

IgM^{high} B-cell compartment when compared to its Myd88^{L252P} CD19^{pos}/YFP^{neg} counterpart (**Supplementary Figure 4**).

Altogether, these results indicate that transgene expression started in a minority of CD19^{weak} B-cell precursors and was mainly expressed at the latest stages of B-cell lymphopoiesis when CD19 expression was high. Evidence for bone marrow increase in both IgM^{high} CD138^{low} and PCs with the characteristic CD138 expression continuum may either suggest

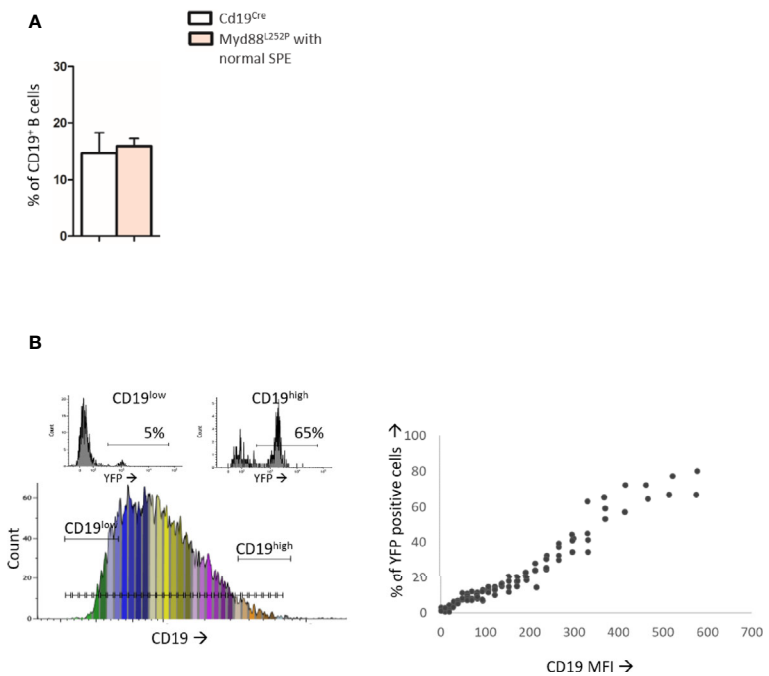

FIGURE 2 | Analysis of B-cell differentiation in bone marrow from 16 week-old Cd19^{Cre} and Myd88^{L252P} mice. **(A)**: Percentage of CD19^{pos} and/or B220^{pos} B-cells in bone marrow from 16 week-old Cd19^{Cre} (n =9) and Myd88^{L252P} mice (n = 9). Results are expressed as the mean ± SEM. **(B)**: Flow cytometry analysis of the transgene expression according to CD19 expression levels (n=9). Left panel: CD19 monoparametric histogram sliced according to CD19 MFI intervals. For each CD19 MFI interval, the percentage of bone marrow B220^{pos} YFP positive cells was noted. Two examples of YFP monoparametric histograms are presented in the upper part, one for CD19^{low} B220^{pos} B-cells and one for CD19^{high} B220^{pos} B-cells with their respective percentages of YFP^{pos} cells Right panel: percentage of YFP^{pos} B220^{pos} B-cells (Y axis) according to CD19 MFI (X axis).

that the bone marrow of Myd88^{L252P} mice had the ability to home IgM PC precursors and PCs and/or a shift in peripheral B-cell differentiation toward IgM PC in Myd88^{L252P} mice.

MYD88^{L252P} First Induced Peripheral Early Lymphoplasmacytic and Plasma Cells Expansion and Then B-Cell Transformation Into a Lymphoplasmacytic-Like Lymphoma

Extended white blood cell differential was not altered and mice did not exhibit any palpable/visible peripheral lymphadenopathy (data not shown) regardless of the SPE profile. Young Myd88^{L252P} mice with normal SPE tended to have spleen enlargement when compared to their age related Cd19^{Cre} LMCs (**Figure 4**). Spleen enlargement was dramatically increased in Myd88^{L252P} mice with hyper Ig and even more so in those with an IgM peak, a feature that was most likely to related to B-cell transformation. Indeed, the B/T cell ratio was markedly increased in these latter mice (**Supplementary Figure 5**).

While spleen histology of young Myd88^{L252P} mice was comparable to that of their Cd19^{Cre} LMCs, with an apparent normal spleen architecture, Myd88^{L252P} mice with hyper Ig or an Ig peak exhibited enlarged and congruent lymphoid nodules (**Figures 5A–E**). At high magnification, a marked lymphoplasmacytic aspect consisting of a mixture of small to large lymphocytes with numerous lymphoplasmacytic cells (LP cells) and PCs was noted in all Myd88^{L252P} mice whatever their SPE profile (**Figures 5F–J**). This spleen aspect was particularly striking for mice with Ig peaks, and was characterized by massive and diffuse infiltration of lymphoplasmacytic cells that evoked human B-cell lymphomas with features of PC differentiation, further called "LP-like lymphoma" or "LP-like tumors". (see also the cytological imprint in **Supplementary Figure 6**). Presence of LP cells and PCs in Myd88^{L252P} spleen was invariably confirmed by immunohistochemistry after intracellular Ig labeling regardless of SPE status, with numerous LP cells and terminally differentiated PCs (cells with intermediate or strong intracytoplasmic Ig labeling respectively). Noteworthy, cell densities were markedly increased in Myd88^{L252P} mice with hyper Ig or with an Ig peak (**Figures 5K–O**).

Based on B-cell expression of CD21 and CD23, frequencies of CD21^{pos} CD23^{high} follicular B-cells were not significantly altered in Myd88^{L252P} mice regardless of their SPE status (**Figure 6A** and **Supplementary Figure 7**). In contrast, a decrease of CD21^{high} CD23^{pos} marginal zone B-cells was observed. This cell content nearly disappeared in Myd88^{L252P} mice with an Ig peak. Only total PCs were increased in these mice (**Figure 6B**). However, among total spleen PCs, percentages of IgM PCs were increased in a similar manner in all Myd88^{L252P} mice no matter what their SPE status was (**Figure 6C** and **Supplementary**

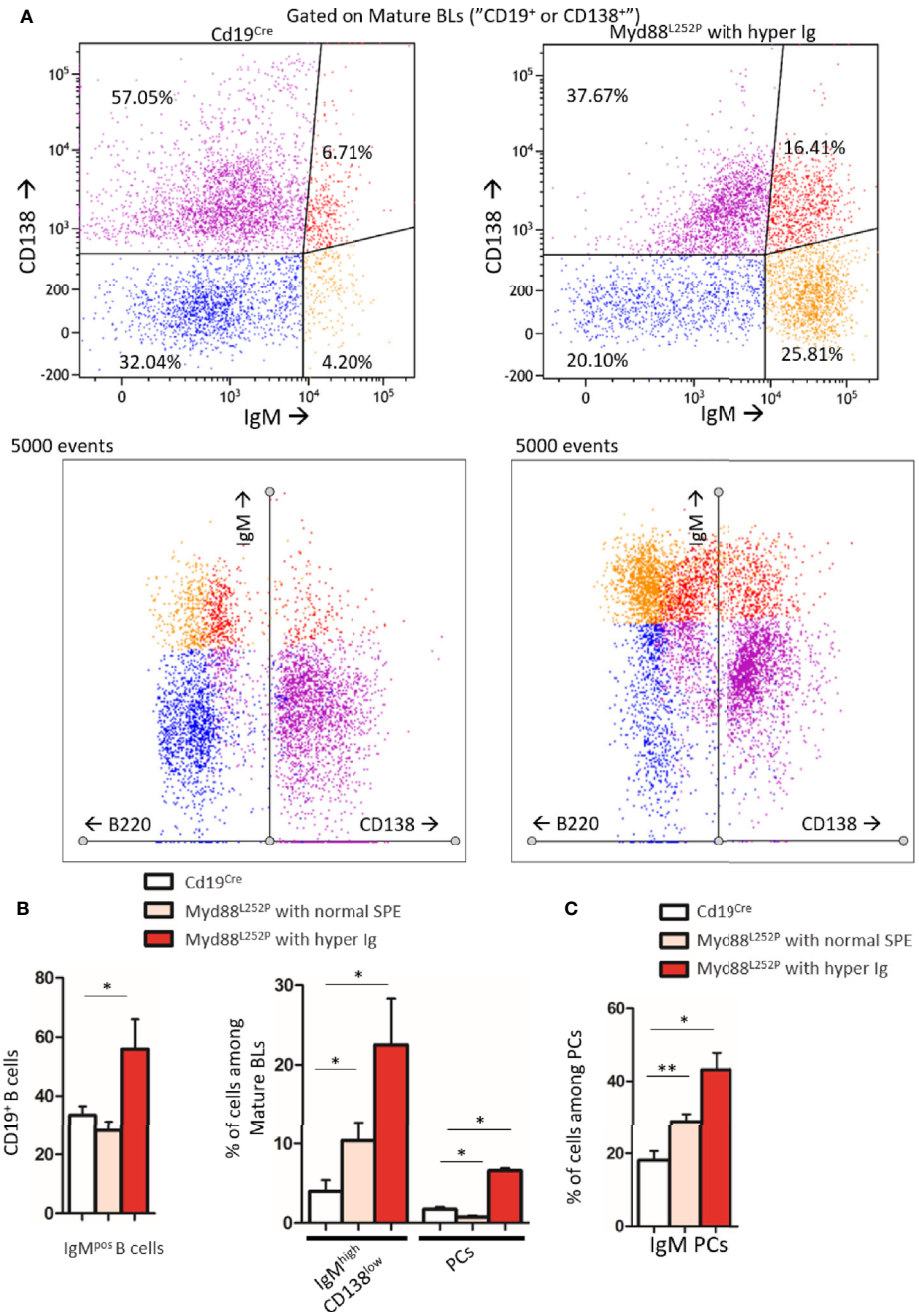

FIGURE 3 | Increase in the IgM PC compartment in bone marrow from Myd88^{L252P} transgenic mice. **(A)** Example of bi and triple parametric flow cytometry histograms gated on mature B or plasma cells for expression of IgM, B220 and CD138 for Cd19^{Cre} and Myd88^{L252P} mice (left and right panels respectively). Upper panels: IgM$^{low\ or\ neg}$ CD138^{neg}, IgM^{high} CD138^{low}, IgM^{high} CD138^{high} and IgM^{low} CD138^{high} cells are colored in blue, orange, red and purple respectively using a hinged quadstat of the Kaluza software and an IgM/CD138 2-dimensional plot. The hinged quadstat was set-up for one Cd19^{Cre} mouse. Lower panels: triple parametric histograms using the radar function of the Kaluza software. Note the CD138 expression continuum on Myd88^{L252P} bone marrow B-cells that correlated with a progressive decrease in B220 expression. This CD138 expression continuum was virtually absent in Cd19^{Cre} mice. **(B)** Percentages of total IgM^{pos} B cells and IgM^{high} CD138^{low} pre PCs and B220^{low} CD138^{high} PCs in bone marrow from 16-24 week-old Cd19^{Cre} (n =6) and Myd88^{L252P} mice with normal SPE or hyper Ig (n = 6 and n = 3 respectively). Results are shown as the mean ± SEM. Mann Whitney test p-value < 0.05 is symbolized by *. **(C)** Percentages of IgM^{pos} CD138^{high} PCs among total PCs in bone marrow from 16-31 week-old Cd19^{Cre} (n =6) and Myd88^{L252P} mice with normal SPE or hyper Ig (n = 6 and n = 3 respectively). Results are shown as the mean ± SEM. Mann Whitney test p-value < 0.05 and < 0.01 are symbolized by * and ** respectively.

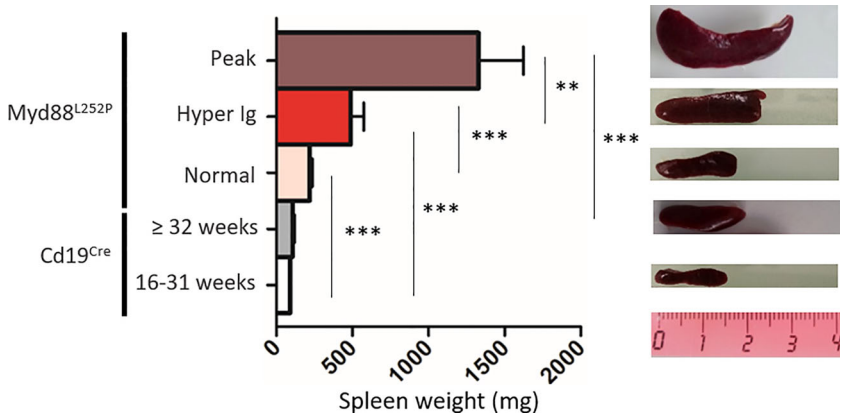

FIGURE 4 | Myd88^{L252P} mice exhibited a progressively increasing splenomegaly consistently related to the SPE profile. Spleen size of Cd19^{Cre} and Myd88^{L252P} age-paired mice. Myd88^{L252P} mice were sacrificed together with at least one Cd19^{Cre} mouse of the same age. Left panel: distribution of spleen weights; right panel: examples of spleen macroscopy (Cd19^{Cre} n = 9 for 16-31 weeks-old and n = 16 for ≥ 32 weeks; Myd88^{L252P} with normal SPE: n = 9; with hyper Ig: n = 13; with Ig peak: n = 19). Results are given as the mean ± SEM. Mann Whitney test p-value < 0.01 and p-value < 0.001 are symbolized by ** and *** respectively.

Figure 7). Moreover IgM PCs were predominantly CD93^{neg} suggesting that they belonged to the proliferating PC compartment (27) (**Figure 6C** and **Supplementary Figure 7**).

Therefore, morphological and immunophenotypic results indicated that continuous MYD88 activation was associated with continuous peripheral IgM PC differentiation very early on and that these LP and PC subsets continuously expanded with age first being associated with hyper Ig and then with an Ig monoclonal peak and a LP-like lymphoma aspect in the spleen.

Proliferation Index of Myd88^{L252P} LP-Like Tumors Was Moderately Increased in Myd88^{L252P} Tumors With an LP-Aspect

To better study these Myd88^{L252P} LP-like tumors, we compared their Ki67 proliferation index to that their of Cd19^{Cre} LMCs as well as to L.CD40, L.CD40/Λ*c-MYC* mice as controls. L.CD40 mice are a model of marginal zone spleen B cell indolent lymphomas without plasma cell differentiation but with NF-κB activation (28). L.CD40/Λ*c-MYC* mice are a model of ABC-DLBCLs with both c-Myc and NF-κB activation in B-cells (24). Very few Ki67 positive cells were seen outside germinal centers in spleen sections from Cd19^{Cre} mice (**Figure 7A** panel A). The Ki67 index was weak in L.CD40 mice (**Figure 7A** panel B). By contrast, the vast majority of cells from L.CD40/Λ*c-MYC* tumors were Ki67 positive (**Figure 7A** panel C). Being moderately increased in young mice with a normal SPE, the Ki67 proliferative index was further enhanced in mice with hyper Ig and even higher in those with an Ig peak, but never reached the proliferation index levels of L.CD40/Λ*c-MYC* tumors (**Figures 7A**, panels D–7 and **7B**). *In vivo* incorporation of BrdU was tested for four mice with an Ig peak and one with polyclonal hyper Ig. Results confirmed that the proliferation index was consistently increased (**Supplementary Figure 8**) albeit always less than 30% with this technique.

Altogether, these results show that MYD88^{L252P} expression in B-cells was responsible for progressive peripheral B-cell expansion related to an early increase in B-cell proliferation. Mice with an Ig peak clearly exhibited a lymphoproliferative disease with a marked increase in proliferation index but with features of an LP-like lymphoma such as the presence of numerous LP cells and PCs.

Myd88^{L252P} Mice With Ig Peaks Developed IgM but Not Igg Monoclonal or Oligoclonal B-Cell Lymphomas With Expression of Both Membrane and Secretory Heavy Chain mRNA

Since Myd88^{L252P} mice had a global hyper Ig even if predominantly IgM, it was important to assess μ or γ chain clonality of tumor surface and secreted immunoglobulins at the molecular level. Six LP-like cases with monoclonal Ig peaks and five Cd19^{Cre} mice were studied. mRNA reverse transcription followed by RACE PCR with primers specific for either the membrane or secreted forms of mouse μ or γ heavy chains was performed, followed by high throughput sequencing (HTS) of the VDJ-Cμ or VDJ-Cγ region (**Figure 8A**). **Figures 8B, C** show the relative frequency of the five most abundant mRNA clones for the μ or γ heavy chains respectively. RACE PCR and HTS results indicate that Myd88^{L252P} mice developed clonal or oligoclonal B-cell expansion with expression of both secreted and membrane forms of the μ heavy chain that had the same VDJ-Cμ clonal rearrangement (**Figure 8B**), without any bias in terms of V segment usage (not shown). The same RACE PCR technique with primers specific for either the membrane or secreted form of the mouse γ heavy chain did not identify any significant B-cell clonal expansion in Myd88^{L252P} tumors (**Figure 8C**).

These results indicate that, despite initial IgM and IgG hyper Ig in young Myd88^{L252P} mice, MYD88^{L252P} specifically promoted IgM B-cell lymphomagenesis with clonal expression of both membrane and secreted μ chain isoforms identical VDJ gene rearrangements. These results are in full agreement with the

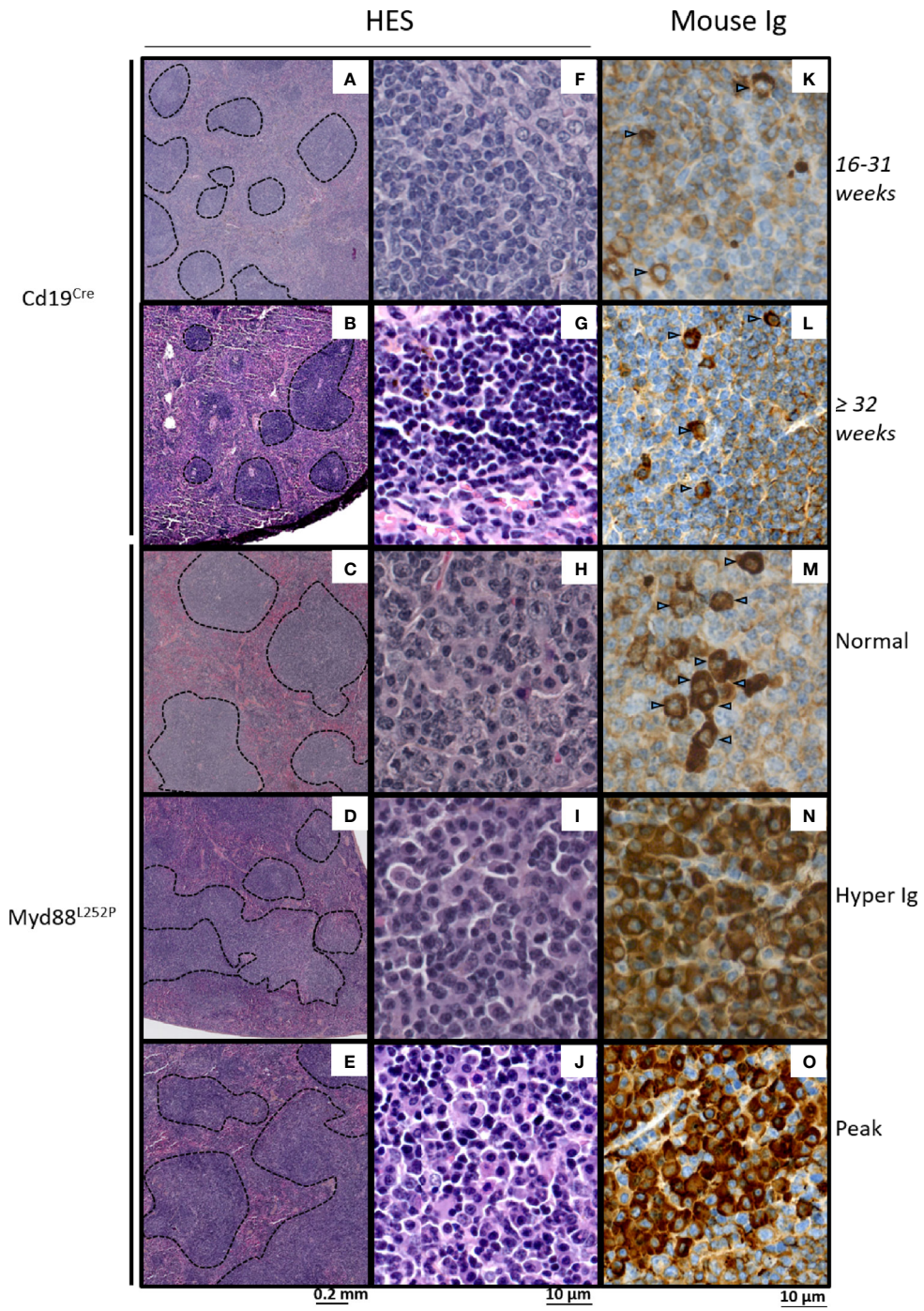

FIGURE 5 | Morphological and immunophenotypic plasma cell engagement of Myd88^{L252P} tumors. Hematein eosin morphological aspect **(A–J)** and intracytoplasmic Ig labeling **(K–O)** of Cd19^{Cre} and Myd88^{L252P} spleens: one 16-31 week-old Cd19^{Cre} **(A, F, K)**, one ≥ 32 week-old Cd19^{Cre} **(B, G, L)** and three Myd88^{L252P} **(C, H, M)** for Normal group, **(D, I, N)** for Hyper Ig group and **E, J, O** for Peak group) mice are shown. Panels **(A–E)** at low magnification, Myd88^{L252P} tumors often exhibited a nodular pattern **(C–E)**. Panels **(F–J)**: at high magnification, most Myd88^{L252P} tumors had small B-cell aspects with marked lymphoplasmacytic engagement (panels **H–J)**. Panels **(K–O)** Myd88^{L252P} tumors with a lymphoplasmacytic aspect exhibited marked plasma cell differentiation as revealed by the presence of intracytoplasmic Ig in numerous cells (arrows) with various labeling intensities **(M–O)**.

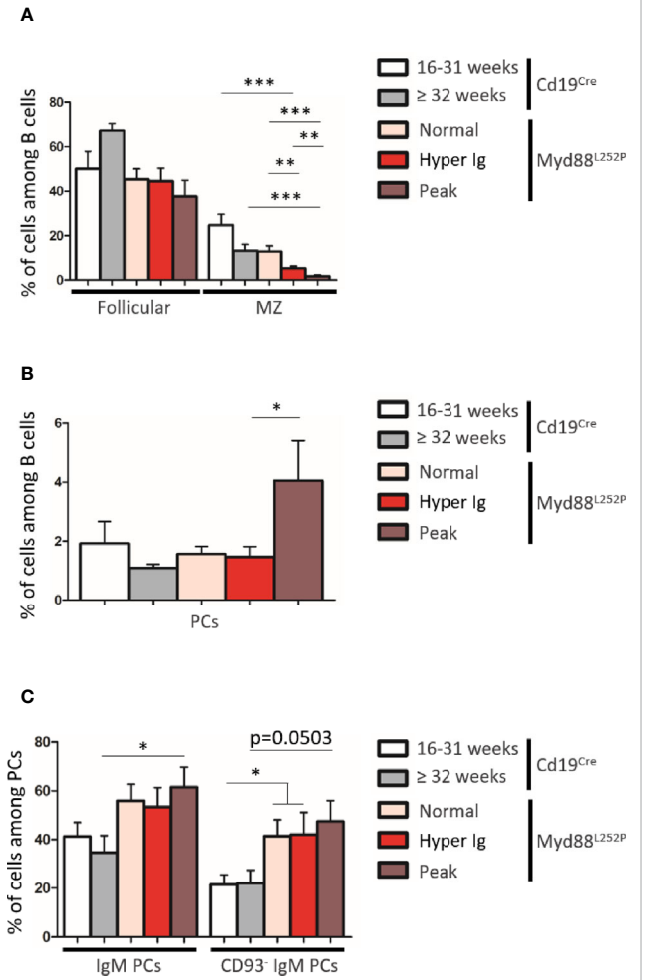

FIGURE 6 | B-cell differentiation in spleens from Cd19^{Cre} and Myd88^{L252P} mice. **(A)** Percentage of Follicular B cells (CD21^{pos} CD23^{high}) and marginal zone (MZ) B cells (CD21^{high} CD23^{pos}). **(B)** Percentage of plasma cells (PCs, B220^{low} CD138^{high}). **(C)** Percentage of IgM^{+} PCs and CD93^{neg} IgM PCs. Myd88^{L252P} mice (with normal SPE: n = 7; with hyper Ig: n = 10; with Ig peak: n = 9) were compared to Cd19^{Cre} mice LMCs (16-31 week and ≥ 32 week-old mice; n = 9 for each group) Results are presented as the mean ± SEM. Mann Whitney test p-value < 0.05, p-value < 0.01 and p-value < 0.001 are symbolized by *, ** and ***.

lymphoplasmacytic aspect Myd88^{L252P} tumors and the persistent IgM plasma cell differentiation continuum.

Transcriptomic Signature of Myd88^{L252P} LP-like Tumors Revealed NF-κB RelA Activation, Proliferation and Plasma Cell Differentiation and Overlapped With Waldenström's Macroglobulinemia Gene Expression Profile (GEP)

To explore the transcriptomic signature of Myd88^{L252P} LP-like tumors in conditions similar to those of most studies on human B-cell lymphomas and to look for common features with WM, we selected a short series of massively invaded Myd88^{L252P} spleen tumors with monoclonal Ig peaks. Comparisons were first done with their Cd19^{Cre} LMCs, and then with WM patients.

With a fold change of 2, a set of 1515 differentially expressed genes were found in Myd88^{L252P} spleen tumors when compared to spleens from Cd19^{Cre} LMCs (**Supplementary Table 3**). To analyze this set of genes, we combined both K-mean and hierarchical clustering and principal component analysis, as already published (29). Following this methodology, deregulated genes in Myd88^{L252P} spleen tumors could be segmented into 14 classes of co-regulated genes (**Figure 9** with methodological details in **Supplementary Materials** and **Methods**, **Supplementary Figure 9** and **Supplementary Table 4**). Consistent with increased B/T ratios in Myd88^{L252P} LP-like tumors, expression of genes belonging to the T-cell lineage, as well as T-cell signaling and activation signatures was down-regulated in Myd88^{L252P} spleen tumors (**Figure 9**, see clusters I, K and L). Of note, RelB signature was associated with that of T-cells and was decreased in Myd88^{L252P} spleen tumors. In contrast, expression of genes belonging to the proliferation, *RelA* NF-κB activation pathway and plasma cell differentiation signatures were up-regulated (**Figure 9**, cluster J mainly as well as cluster B, G and M for proliferation).

To identify MYD88^{L252P} deregulated genes in common with those of WM patients having the *MYD88^{L265P}* mutation, transcriptomes of Myd88^{L252P} tumors were compared to those of purified WM bone marrow B-cells from a series of 11 *MYD88^{L265P}* WM patients. A subset of 319 coherently dysregulated genes in both Myd88^{L252P} LP-like tumors and WM tumor B-cells (163 up and 156 down, **Supplementary Tables 5, 6**) was extracted from the 1515 differentially expressed genes in Myd88^{L252P} LP-like tumors. Unsupervised hierarchical clustering showed a 95% coherency between the branches of up and down regulated genes in both WM tumor B-cells and LP-like Myd88^{L252P} spleen tumors (**Figure 10A**, left and middle panels and **Supplementary Tables 5, 6**). To check whether this Myd88^{L252P}/WM signature could discriminate WM from other indolent NHLs, an independent series of 58 patients, including 15 *MYD88^{L265P}* WM, five *MYD88^{wt}* WM, 12 *MYD88^{wt}* NMZLs and 19 *MYD88^{wt}* CLL was analyzed (**Supplementary Tables 2, 7**). All *MYD88^{L265P}* WM patients clustered together after unsupervised hierarchical clustering (**Figure 10A**, right panel and **Supplementary Tables 7, 8**). Also belonging to the *MYD88^{L265P}* WM cluster were 3/5 (60%) *MYD88^{wt}* WM and 2/12 (17%) *MYD88^{wt}* NMZLs. We used the linear predicting score described by Wright et al. (31) to estimate the informativeness of the Myd88^{L252P}/WM signature for WM diagnosis. As shown in **Figure 10B**, as set of 174 genes (84 up and 90 down, **Figure 10B**) was found to predict WM with over 90% probability (**Supplementary Tables 9, 10**).

The plasma cell signature was the main component of the Myd88^{L252P}/WM GEP. Genes such as *EDEM1* and *2*, *IRF4* or *XBP1* were over-expressed while others such as *PAX5* or *BCL6* were markedly down-regulated (**Figure 10**). Consistently, functions revealed by Gene Set Enrichment analysis mainly corresponded to endoplasmic reticulum and Golgi apparatus

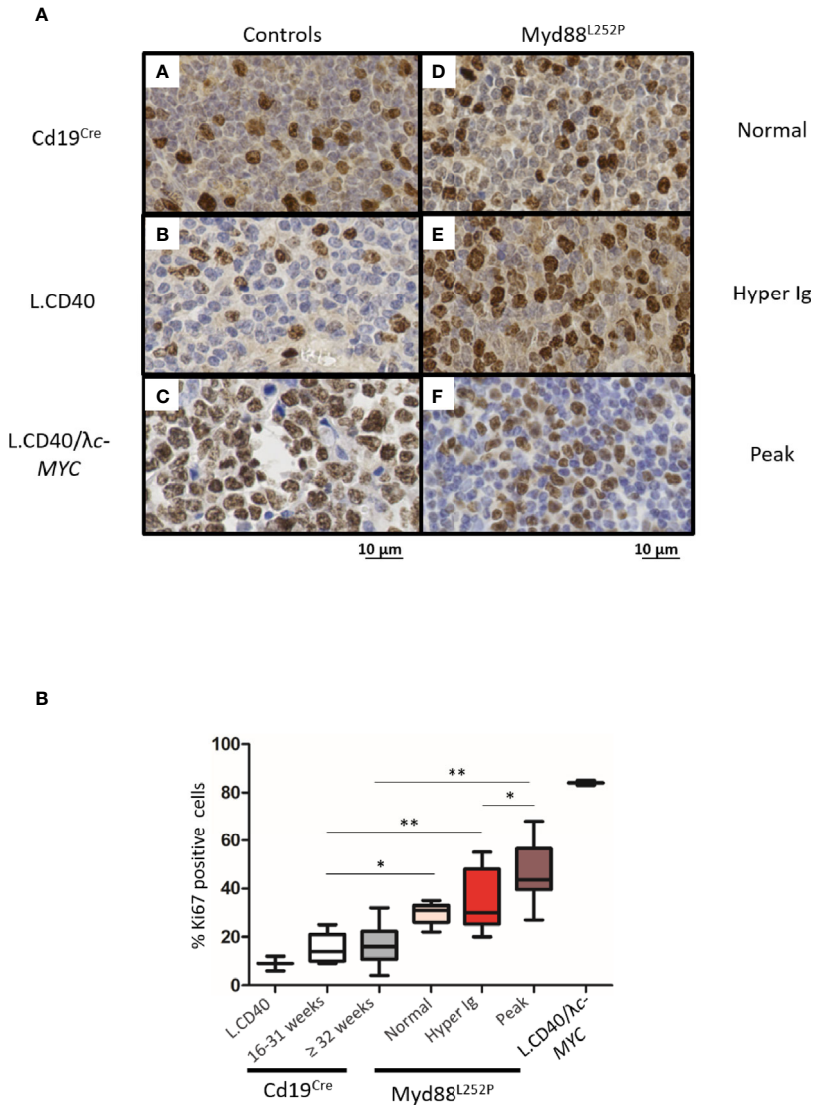

FIGURE 7 | Intermediate increase in Myd88^{L252P} tumor proliferation rate. **(A)** Examples of Ki67 labeling in spleen sections from three controls (panels A-C) and three Myd88^{L252P} mice (panels D-F, n=28). Controls were Cd19^{Cre} LMCs (panel A, n = 5 for 16-31 week-old mice and n = 8 for ≥ 32 week-old mice), L.CD40 mice (panel B) with indolent splenic lymphomas of marginal zone B-cells (n=2), as well as L.CD40/λc-Myc mice (panel C, n=2) with a ABC-DLBCL lymphomas (24, 28). The three Myd88^{L252P} tumors (panels D-F) are one representative example of each group defined according the SPE profile (normal n = 5, hyper Ig n = 8 and Ig peak n = 15). Here, L.CD40 mice were used as a model of indolent B-cell lymphoma with a low proliferation index while L.CD40/λc-Myc mice were a model of aggressive B-cell lymphoma with a high proliferation index. **(B)** Quantification of Ki67 labeling. Box plots represent the median and quartile of percentages of Ki67 positive cells. Mann Whitney test p-value < 0.05, p-value < 0.01 are symbolized by * and ** respectively.

(not shown). In accordance with results published by Hunter et al. (30), expression of genes such as *CXCR4*, *DUSP22*, *PIM1* and *2* or *TRAM1* was increased while expression of *SNED1* was decreased. Few genes of the Myd88^{L252P}/WM signature overlapped with those of ABC/GC DLBCLs published by Wright et al. (31). These overlapping genes, corresponding only to those that are overexpressed in ABC DLBCLs, were *IRF4, IGHM, CXCR4, P2RX5, PIM1* and *PIM2*. In other words, the Myd88^{L252P}/WM signature did not significantly overlap with that of GCB DLBCLs. Among other deregulated genes were cyclin kinase inhibitors *CDKN1B* (*p27^{kip1}*) and *CDKN2C* (*p18/INK4AC*), mutations of the former being found in hairy cell leukemias (32). *RASSF3* and *KRAS* were also up-regulated. *RASSF3* belongs to the Ras association domain family (RASSF).

Altogether, the Myd88^{L252P} tumor signature highlights proliferation as well as canonical NF-κB p65/RelA activation (but not RelB), which is in agreement with the known fact that MYD88 activates the classical NF-κB pathway. The Myd88^{L252P} tumor signature also strikingly confirms that lymphoplasmacytic differentiation is at the heart of MYD88 related B-cell transformation in mice, a feature shared with WM tumors with the *MYD88^{L265P}* mutation.

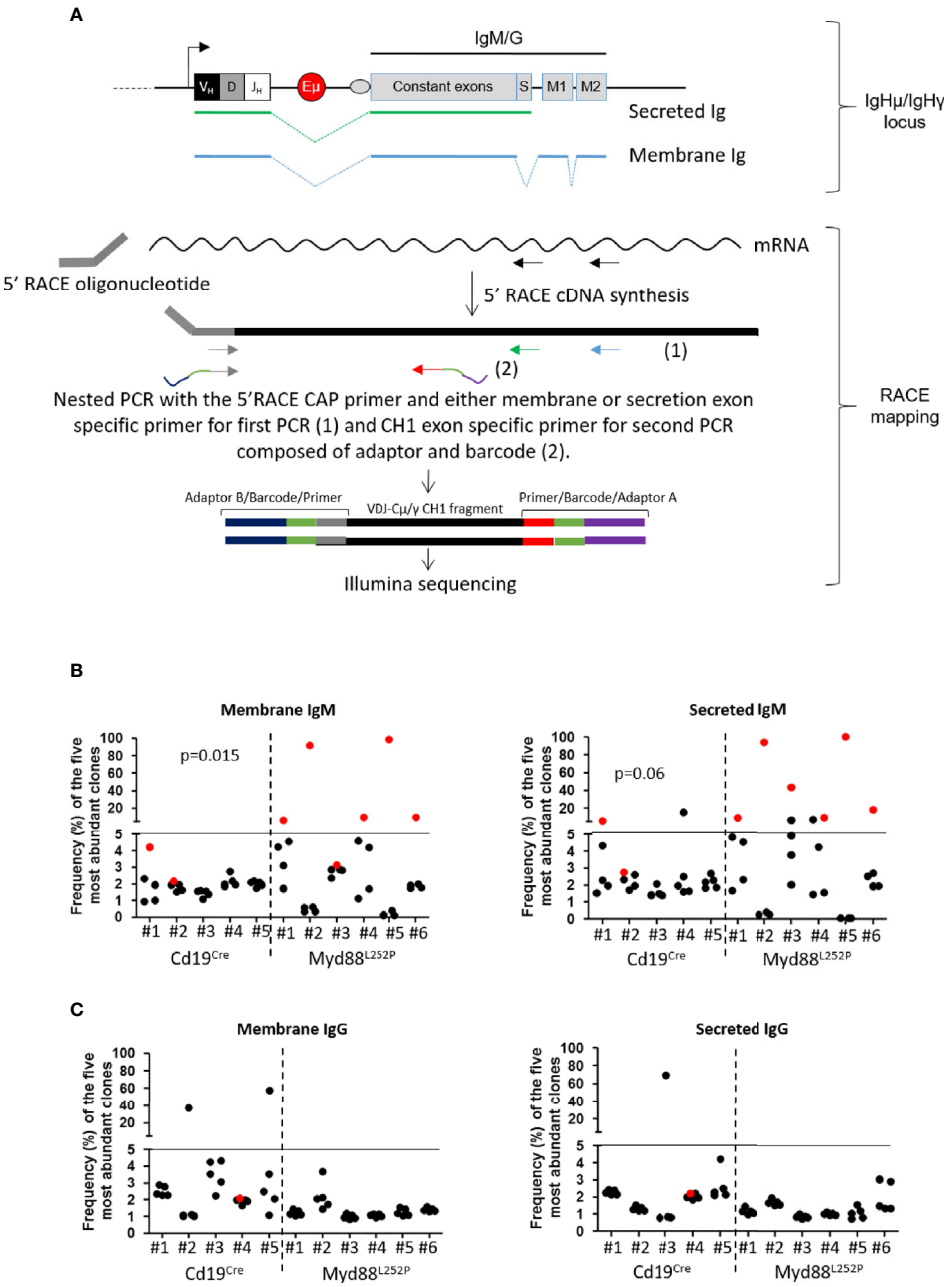

FIGURE 8 | μ and γ heavy chain mRNA clonal abundance: **(A)** RACE PCR technique quantifying clonal mRNA abundance of membrane and secreted forms of mouse μ and γ heavy chains. *Ighμ/Ighγ* locus (upper panel): *Igh* locus with variable regions (VDJ), the enhancer Eμ and constant genes (for IgM or IgG). Box "S" represents the secreted exon used for the secreted form of Ig, "M1 and M2" represent the membrane exons for the membrane form of Ig. Green or blue dotted lines show RNA splicing respectively for secreted and membrane Ig. RACE mapping (lower panel): 5'RACE PCR followed by preparation of libraries for Illumina sequencing. First, we amplified cDNA between the primer specific for the membrane or the secreted form (black arrows) and the 5'RACE oligonucleotide. Amplicons for Illumina sequencing were obtained after two nested PCRs; the first with the 5' Race CAP primer and either membrane (blue arrow) or secretion (green arrow) exon specific primer, and the second with the same 5' primer and a CH1 exon specific primer (grey arrow). For sequencing, forward (grey) and reverse (red) primers used for the second PCR contained adaptors (blue and purple) and a barcode (orange); each barcode sequence was specific for one sample only. **(B, C)** Relative frequency of the five most abundant mRNA clones coding for membrane (left) and secreted (right) forms of μ **(B)** and γ **(C)** heavy chains for Cd19^{Cre} (n = 5) and Myd88^{L252P} (n = 6) mice. The most abundant clones are highlighted in red when VDJ sequences of the dominant membrane and secreted clones were identical. Myd88^{L252P} mice exhibited IgM but not IgG clonal expansion with expression of both secreted and membrane form of the μ chain. Wilcoxon's test p-value are given in the figure.

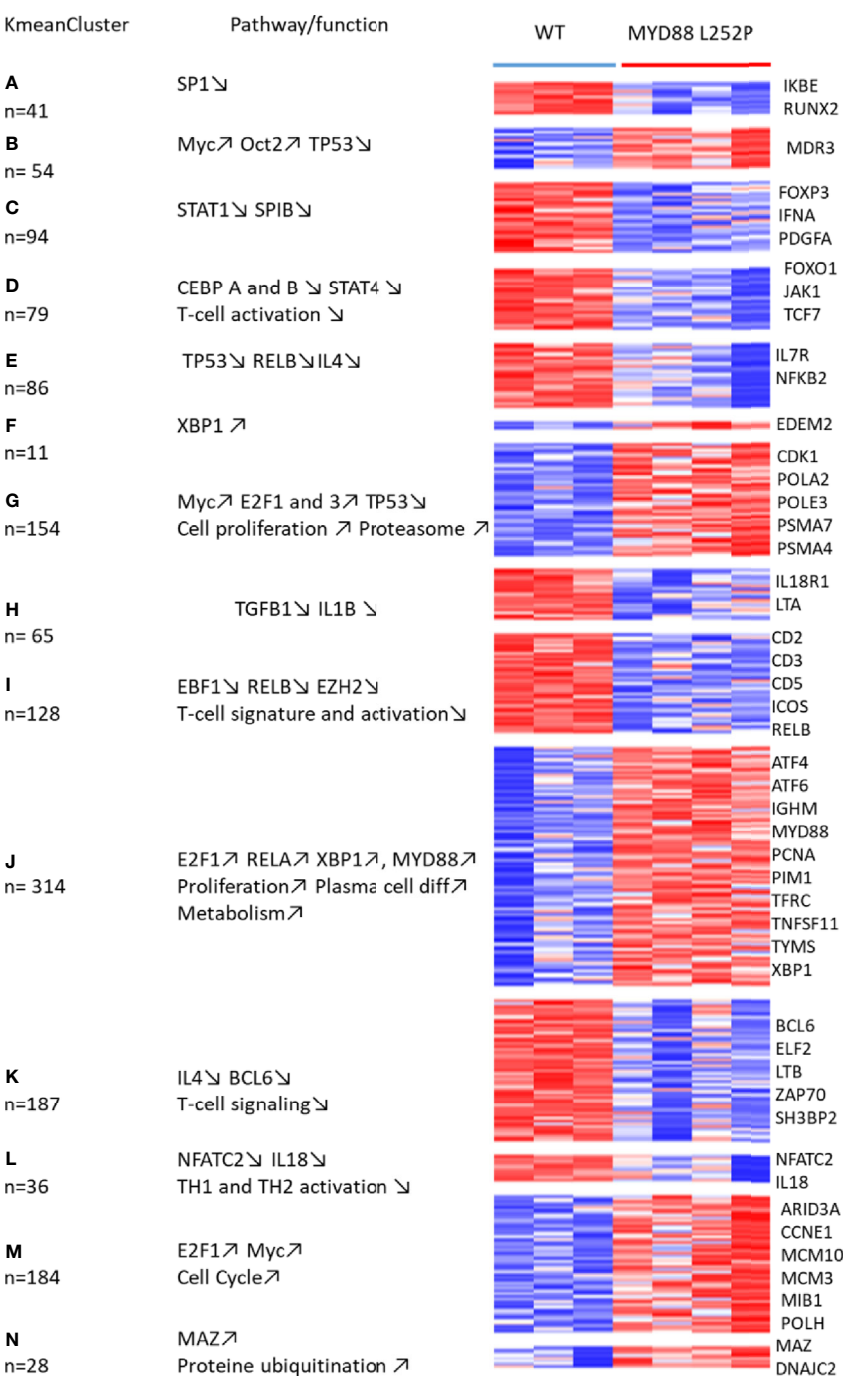

FIGURE 9 | Whole transcriptome analysis of Cd19^{Cre} and Myd88^{L252P} mice: total mRNA was extracted from whole spleen tissues. Gene expression profiles were obtained using the MoGene-2_1-st-v1 Affymetrix chip. mRNA transcripts (3236) were selected to be differentially expressed using the Limma R package. Expressed genes that were too heterogeneous were eliminated, resulting in a final selection of 1515 genes. These genes were segregated into 40 Kmean clusters. The closest Kmean clusters were merged 2 by 2 according to their proximity by principal component analysis of the mean vectors. This was repeated until maximization of the absolute value of Chi2 (29). This resulted in 14 aggregated clusters. Functional annotation of the aggregated Kmean clusters was performed using the Ingenuity Pathway Analysis (IPA) Software. Annotated heatmap of the 1515 genes are segregated into the 14 aggregated clusters. Left: the aggregated Kmean clusters with the corresponding number of genes; middle: main pathways and or function identified with the IPA software; right: some relevant genes.

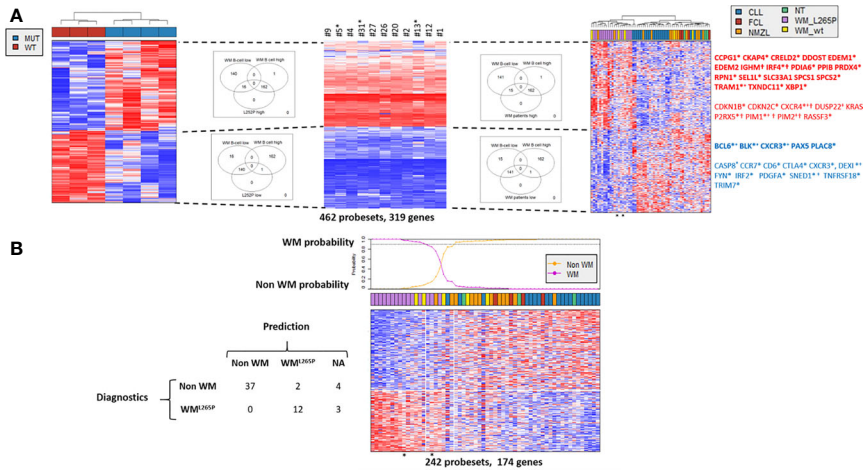

FIGURE 10 | Comparison of gene expression profile (GEP) of Myd88^{L252P} mice and patients with WM or other indolent B-cell NHL. Affymetrix differential gene expression profiles (GEP) between four Myd88^{L252P} mice (MUT, n=4) and three Cd19^{Cre} mice (WT, n=3) were compared to the Affymetrix GEP of purified bone marrow tumor B-cells from 11 WM patients with the *MYD88^{L265P}* mutation, resulting in selection of 462 probesets (319 genes). This selection was used on the Affymetrix transcriptome of an independent series of lymph node biopsies from 58 patients: 19 *MYD88^{wt}* chronic lymphocytic leukemias (CLL), 15 *MYD88^{L265P}* WM (WM_L265P), *12 MYD88^{wt}* nodal marginal zone lymphomas (NMZL), 5 *MYD88^{wt}* WM with IgM peaks (WM_WT), 4 follicular lymphomas (FCL) and 3 patients with follicular hyperplasia (NT). **(A)** Hierarchical clustering and heatmap of the 462 selected probesets for mice (left), purified bone marrow *MYD88^{L265P}* WM B-cells (middle) and lymph nodes (right). Down and up-regulated genes are in blue and red respectively. Branches of down and up regulated genes in Myd88^{L252P} mice, *MYD88^{L265P}* WM bone marrow B-cells and *MYD88^{L265P}* WM lymph nodes are delineated by dashed lines. Venn diagrams of the intersections between the branches are shown, highlighting the consistency between branches across the different clustering. Some genes of interest are noted on the right. In bold are those of the plasma cell signature; *: genes in the predictor (see **Figure 7B**); +: genes reported by Hunter et al. in WM (30); † : genes of the ABC/GC DLBCL signature (31). **(B)**: Informativeness of *MYD88^{L265P}* WM diagnosis using the 462 selected probesets defined in **Figure 8A**. The 462 probesets defined from MYD88^{L252P} mice and bone marrow tumor B-cells from *MYD88^{L265P}* WM patients were used to predict *MYD88^{L265P}* WM diagnosis (WM^{L265P} versus non WM) from other lymphomas within the series of 58 lymph node biopsies. Probabilities that each sample belongs to WM^{L265P} versus non WM group are indicated. The WM^{L265P} versus non WM or not attributed (NA) assignment is shown on the left.

DISCUSSION

Different mouse preclinical models with continuous MYD88 activation in B-cells have been published; All but one demonstrate the B-cell transformation potential of MYD88 but without presenting evidence for a correlation between IgM B-cell LP and PC differentiation (13–15).. The first report was published by Knittel et al. (14). The authors generated a mouse model that allows B-cell conditional expression of the *Myd88^{L252P}* allele from the endogenous *Myd88* locus. In this model, expression of *Myd88^{L252P}* would be regulated in a manner similar to that of the wild type allele. At least three regulatory levels of MYD88 activity have been reported. The MYD88 regulatory region harbors various transcription binding sites such as those for NF-κB, IRF1, SP1 or STAT factors and it was shown that this gene is regulated by IL-6 (33), which suggests a role for its expression in either plasma cell differentiation or inflammation. An alternative splice variant of *MYD88*, *MYD88s*, lacks exon 2 and is unable to activate NF-κB. This variant is also able to form a heterodimer with the full length MYD88 protein, resulting in decreased formation of the myddosome complex (34). MYD88s is increased during sepsis and is thought to ensure robust termination of MYD88 dependent inflammation (35, 36). As a third regulation mechanism, hypomethylation and upregulation of MYD88 are important for NF-κB activation (37). MYD88 promoter demethylation is important in glioblastoma and is associated with increased MYD88 protein expression in lung cancers (38, 39). Mice from Knittel's model occasionally developed DLBCLs when they aged. Therefore, the Knittel mouse model raises the question of the relationship between B-cell lymphomagenesis and regulation of the endogenous *Myd88* locus throughout B-cell life. In addition, this model also showed hyper Ig, even if polyclonal, which may suggest that expansion of Ig secreting B-cells could precede the lymphoma development. In that view, K Schmidt et al. recently published a mouse model with a transgene closed to the one of the Knittel's model. But, after exploring the effect of MYD88 activation in three different Cre context, Cd19-Cre, Cγ1-Cre and Cd19-Cre^{ERT2}, as well as analyzing the effect of NP-immunization, the authors concluded that MYD88 continuous activation promotes survival of long term IgM expressing B-cells with clonal restriction a monoclonal serum IgM paraprotein resulting in an IgM MGUS-like disorder (16).

To our knowledge, two papers, from Wang et al. and Sewastianik et al. reported the effect of the human MYD88^{L265P} protein in murine B-cells (15, 40). In the model of Wang et al, primary murine B-cells were retrovirally infected *ex vivo* before reinjection. In this model, an initial boost of B-cell proliferation was seen followed by B-cell apoptosis in a Bim-dependent manner. Importantly, no increase in immunoglobulin secretion was reported. Beside the fact that retroviral infection of B-cells may have its own interfering effects, this model raises the question of whether the human MYD88^{L265P} protein may have exactly the

same activation properties on a mouse B-cell background as in human B-lymphocytes. In the model of Sewastianik et al, the human loxP-flanked-stop-*MYD88^{L265P}* transgene was inserted downstream from the mouse *Collagen type I alpha 1 chain* (*Col1A1*) gene and MYD88^{L265P} expression was induced by crossing with *Aid^{Cre}* mice (15). In addition to focal skin rashes, some WM features were noted such as expansion of lymphoplasmacytic cells and increased IgM serum levels. However, only DLBCL clonal transformation was seen. Because AID is mainly expressed in germinal center B-cells and because the promoter of the *Col1A1* gene is highly active in fibroblasts and osteoblasts (41), this model raises the question whether temporality and/or expression pattern could be important in MYD88 driven B-cell lymphomagenesis.

The *Rosa26* locus has been solidly proven to be valuable for expression of numerous oncogenes in the B-cell lineage (see reference (42) for discussion as well as the literature of the K Rajewsky's group). By inserting our *Myd88^{L252P}*-IRES-*Yfp* transgene in this locus, we forced continuous expression of the mutated MYD88 protein in a heterozygous-like context while respecting the native MYD88 activation pathways of mouse B-cells. Moreover, we were able to monitor our transgene expression by flow cytometry due to YFP. Thereby, we created a conditional Myd88^{L252P} mouse model closed to the one published by Jo et al. (13). However, these authors mainly focused their work on the synergy between MYD88 and the catalytic subunit HOIP which increases LUBAC ligase activity that in turns promotes NF-κB canonical activation; only four so-called CD19-cre-MYD88LP have been studied at the tumor stage.

Here, a longitudinal analysis of a series of 40 Myd88^{L252P} mice compared to their age matched Cd19^{Cre} LMCs demonstrated that IgM plasma cell expansion is at the heart of MYD88 dependent B-cell transformation. Indeed, by examining clonal restriction of IgM secreting B-cells, we first showed that ageing of Myd88^{L252P} mice was associated with polyclonal hyper Ig followed by monoclonal Ig peak due to increased serum IgM. Second, we provide evidence indicating that bone marrow relocalization of IgM B-cells, IgM^{high} CD138^{low} cells and IgM PCs was increased in Myd88^{L252P} mice with a CD138 expression continuum, that is a characteristic of WM tumor B-cells. Third, analysis of spleen morphology and spleen B-cell subsets by flow cytometry indicated that continuous MYD88 activation was associated very early with peripheral LP cell and CD93^{neg} IgM PC expansion and that these cell subsets were markedly increased at the time of the Ig monoclonal peak. Fourth, appearance of a monoclonal Ig peak was constantly associated with a B-cell lymphoma with marked features of lymphoplasmacytic differentiation, so-called Myd88^{L252P} LP-like lymphoma. Fifth, at the molecular level, Myd88^{L252P} specifically promoted IgM B-cell lymphomagenesis with mRNA clonal expression of both membrane and secreted μ (but not γ) chain isoforms. Finally, the Myd88^{L252P} tumor gene expression profile not only highlights the canonical NF-κB p65/RelA activation pathway and proliferation, but also strikingly shares an *Xbp1* centered lymphoplasmacytic B-cell differentiation signature with MYD88^{L265P} WM. This signature differentiates MYD88^{L265P} WM from other indolent B-cell tumors including marginal zone lymphomas. Our results contradict the conclusions of Sewastianik et al. (15), and, being in line with those of K Schmidt et al. (16), firmly demonstrate the specific transforming effect of MYD88 activation in IgM PC differentiating B-cells.

To establish the gene expression signature from bulk Myd88^{L252P} spleen tumors rather than from purified B-cells is matter of discussion. The very obvious disadvantage of working on bulk tumors is certainly that all mRNA species from all cell types present in the tissue are mixed together. Even if massively invaded, both stromal and other residual immune cells (T-cells, macrophages, dendritic cells…) persist constantly in the tumor. In these conditions, specifically assigning a given mRNA expression pattern to tumor cells is always hazardous. However, because tumors were immediately snap-frozen, all mRNA species are supposed to be well preserved without any significant experimental bias. On the other hand, working on purified cells may also induce artefacts since the abundance of different mRNA species may vary during the time of purification which can also stress the cells. Above all, in the specific case of Myd88^{L252P} spleen tumors, which exhibit an LP aspect with continuous PC differentiation, the key question would have been to choose the right negative selection marker. Indeed, tumor cells are phenotypically heterogeneous with variable expression of B220, surface Ig or CD138 for example. Should we have selected B220^{high} versus B220^{low} B-cells or CD138^{low} versus CD138^{high} cells? Rather than make wrong or partial choices concerning which tumor cells to purify, we chose to work on bulk Myd88^{L252P} spleen tumors with well-preserved total mRNA and to compare this bulk signature to that of WM, including purified WM bone marrow tumor B-cells.

One characteristic feature of Myd88^{L252P} B-cells was the strong reduction of the marginal zone B-cell compartment. While also characterized by continuous activation of NF-κB, the L.CD40 mouse model published by Hömig-Hözel et al. (28), in which B-cells are submitted to continuous CD40 activation signaling, showed expansion of marginal zone B-lymphocytes. This points out the differences between TLRs and CD40 in terms of NF-κB activation. Indeed, CD40 is able to activate both the classical and alternative pathways, i.e. to induce the nuclear translocation of RelA and RelB NF-κB containing complexes while TLRs only activate the classical pathway. The effect of both pathways as well as the strength of NF-κB activation on B-cell fate has been extensively discussed by Pillai et al. (43). In this review, the authors also indicate that BTK activation blocks the Notch signaling pathway that is essential for marginal zone B-cell differentiation. It turns out that Hunter et al. have shown that Myd88 is able to activate BTK in a BCR independent manner (30), which consequently could repress B-cell maturation toward the marginal zone B-cell lineage.

Gene expression profiles of LP-like Myd88^{L252P} tumors distinctly suggest the involvement of RelA rather than RelB. RelA, but not RelB, is clearly associated with EBV-dependent B-cell immortalization and with EBV-associated DLBCL tumors, which exhibit a phenotype close to that of ABC-DLBCLs (25).

RelA is also essential for development of GC-derived PCs (44) and immunohistochemistry detected nuclear RelA in WM B-cells (45). Indeed, LP-like Myd88^{L252P} B-cell tumors shared strong overlaps with human WM in terms of gene expression profile. Even if a few genes were in common with the ABC-DBCL signature such as *IGHM, CXCR4* or *PIM1* and *PIM2*, the Myd88^{L252P}/WM signature points to dysregulation of plasma cell differentiation as the keystone of MYD88 transforming physiopathology. It also suggests that *KRAS* activation could be important. *RASSF3* and *KRAS* itself were up-regulated in both Myd88^{L252P} B-cell tumors and human WM. Consistently, and in agreement with results from the group of Treon (30), we also found *RASSF6* overexpression in WM patients (NG and JF unpublished results). CXCR4, whose expression is increased in WM, may activate the RAS pathway through RasGAP-associated proteins (46). The most frequent mutations involve *KRAS* and *NRAS* genes in multiple myeloma (47). Even if such mutations have not been reported in WM (6), our results highlight the putative role of the Ras activating pathway in WM, which may lead to the design of novel therapies.

Despite similarities between WM and Myd88^{L252P} LP-like tumors such as serum Ig monoclonal peak, increase in IgM prePCs, PC bone marrow relocalization and marked lymphoplasmacytic differentiation of tumor cells some major differences exist. The first difference, is the predominant site of tumor involvement. Even if splenomegaly is found in 20% of bona fide WM patients, it is largely admitted that bone marrow is the primary tumor site. In contrast, Myd88^{L252P} LP-like mouse tumors mainly developed in the spleen. Physiologically, IgM PCs tend to reside mainly in the spleen whereas switched IgG PCs migrate to the bone marrow (48). This raises the question of why WM IgM tumor B-cells migrate to bone marrow. In that view, it is largely suspected that *CXCR4* mutation could play a role in bone marrow homing. Further studies could also evaluate the transforming potential of Myd88 by adoptive transfer of LP-like tumor B-cells. Whether the transferred tumor will retain the lymphoplasmacytic aspect would also be interesting.

Another significant difference is the presence of large cells and increased proliferation in Myd88^{L252P} LP-like mouse tumors. The increased proliferation index was an early event since it was also found in young Myd88^{L252P} mice with normal SPE. As we previously discussed (24), only three mouse models for indolent lymphomas of the spleen have been published, one mimicking TRAF3 inactivation, the second with constitutive expression of BCL10 and the last one with continuous CD40 signaling (the L.CD40 model that we used as a control in **Figure 7**) (28, 49, 50). These three models are characterized by increased RelB activation. We previously demonstrated that immune surveillance may influence morphology and proliferation in the L.CD40 model. In this model, immunosuppression led to transformation of small indolent B-cell L.CD40 tumors into large B-cells with increased proliferation. Reactivating the anti-tumor response using anti-PD-L1 immunotherapy led to tumor regression (51, 52). These results on this mouse model suggest that the immunologically silent "indolent phenotype" of a B-cell tumor could be related to the immune pressure exerted on tumor B-cells. Whether and how activation of the alternative and canonical NF-κB pathways differently disturb immune surveillance remains to be determined, and comparison of both L.CD40 and Myd88^{L252P} mouse models could provide answers. However, as in the L.CD40 tumor model and in spleen marginal zone lymphomas (52, 53), the PD1/PD-L1 axis is most likely playing a role in the immune escape of aggressive tumor B-cells with MYD88 activation. Using Eμ-*MYC* transgenic hematopoietic stem cells (HSC) stably transduced with naturally occurring NF-κB mutants to generate various primary mouse lymphomas, Reimann et al. recently showed that MYD88 tumors express high levels of PD-L1 and that anti-PD-1 therapies induce T-cell dependent senescence of tumor cells (54). PD-L1 surface expression is weak or absent on WM tumor B-cells. However soluble PD-L1 serum levels are increased in WM patients and PD-L1 is upregulated by IL6 (55).

In summary, our longitudinal study of Myd88^{L252P} mice demonstrated that continuous MYD88 activation is able to promote early expansion of IgM LP cells and PCs with, first, serum polyclonal hyper Ig and then a monoclonal Ig peak. Ig peaks were constantly associated with B-cell lymphomas sharing characteristics with WM. Two major differences with WM were the spleen localization of Myd88^{L252P} tumors and increased proliferation. Here, we showed for the first time that IgM lymphoplasmacytic B-cell differentiation is at the heart of Myd88^{L252P} transforming potential. Thus, we also provide an interesting preclinical model for development of new therapeutic approaches or to study immune surveillance for example not only in WM but also in others B-cell lymphomas with features of plasma cell differentiation. Indeed, a better understanding of the underlying molecular mechanisms is necessary in order to develop new therapies for these incurable B-cell cancers.

DATA AVAILABILITY STATEMENT

The datasets presented in this study can be found in online repositories. The names of the repository/repositories and accession number(s) can be found below: https://www.ncbi.nlm.nih.gov/geo/, GSE138273.

ETHICS STATEMENT

The studies involving human participants were reviewed and approved by the local IRB of the CHRU of Lille (CSTMT043). The patients/participants provided their written informed consent to participate in this study. The animal study was reviewed and approved by French national authorization number: 8708503 and French ethics committee registration number APAFIS#14581-2018041009469362 v3.

AUTHOR CONTRIBUTIONS

COu and LR contributed equally to this work. COu and LR performed and analyzed experiments. AS helped to perform the

repertoire analysis. COb performed and analyzed ELISA. MD and NG performed the transcriptomic experiments. JF, SP, AS and LR performed the bioinformatics analyses. QL and CC performed flow cytometry analysis of bone marrow B-cell subsets. NF participated in the design of the project. KB and ME participated in the development of this study. CV-F created the mouse model, contributed to the experiments and analyzed the results. JF and CV-F directed the study and wrote the manuscript. All authors contributed to the article and approved the submitted version.

FUNDING

The group of JF is supported by grants from the Ligue Nationale Contre le Cancer (Equipe labellisée Ligue), the Comité Orientation Recherche Cancer (CORC), the France Lymphome Espoir association, the Nouvelle Aquitaine Region and the Haute-Vienne and Corrèze committees of the Ligue Nationale Contre le Cancer. CV-F was supported by the France Lymphome Espoir association of patients. SP is supported by the Septentrion committee of Ligue contre le Cancer. ME is supported by an ANR @RAction grant (ANR-14-ACHN-0008), an ANR JCJC grant (ANR-19-CE15-0019-01), an IDEX Université de Paris grant, a Fondation Arthritis grant and a Fondation ARC grant (PJA20181208173). KB is supported by an ANR PRC grant (ANR-17-CE14-0019), an INCa grant (PRT-K 2017) and the Association Saint Louis pour la Recherche sur les Leucémies.

ACKNOWLEDGMENTS

We thank the animal, histology and cytometry facilities of the BISCEm US 42 INSERM/UMS 2015 CNRS technological platform of the University of Limoges as well as the immunology laboratory of the Limoges University Hospital Center for their technical assistance. We thank Dr Jeanne Cook Moreau (UMR CNRS 7276/INSERM 1276) for careful English editing.

SUPPLEMENTARY MATERIAL

The Supplementary Material for this article can be found online at: https://www.frontiersin.org/articles/10.3389/fimmu.2021.641692/full#supplementary-material

REFERENCES

1. Preud'homme JL, Seligmann M. Immunoglobulins on the Surface of Lymphoid Cells in Waldenström's Macroglobulinemia. *J Clin Invest* (1972) 51(3):701–5. doi: 10.1172/JCI106858
2. Ghobrial IM. Are You Sure This is Waldenstrom Macroglobulinemia? *Hematol Am Soc Hematol Educ Prog* (2012) 2012:586–94. doi: 10.1182/asheducation.V2012.1.586.3798562
3. Treon SP, Xu L, Yang G, Zhou Y, Liu X, Cao Y, et al. Myd88 L265P Somatic Mutation in Waldenström's Macroglobulinemia. *N Engl J Med* (2012) 367 (9):826–33. doi: 10.1056/NEJMoa1200710
4. Gachard N, Parrens M, Soubeyran I, Petit B, Marfak A, Rizzo D, et al. IGHV Gene Features and MYD88 L265P Mutation Separate the Three Marginal Zone Lymphoma Entities and Waldenström Macroglobulinemia/Lymphoplasmacytic Lymphomas. *Leukemia* (2013) 27(1):183–9. doi: 10.1038/leu.2012.257
5. Jiménez C, Sebastián E, Chillón MC, Giraldo P, Mariano Hernández J, Escalante F, et al. Myd88 L265P is a Marker Highly Characteristic of, But Not Restricted to, Waldenström's Macroglobulinemia. *Leukemia* (2013) 27 (8):1722–8. doi: 10.1038/leu.2013.62
6. Poulain S, Roumier C, Venet-Caillault A, Figeac M, Herbaux C, Marot G, et al. Genomic Landscape of CXCR4 Mutations in Waldenström Macroglobulinemia. *Clin Cancer Res* (2016) 22(6):1480–8. doi: 10.1158/1078-0432.CCR-15-0646
7. Baron M, Simon L, Poulain S, Leblond V. How Recent Advances in Biology of Waldenström's Macroglobulinemia may Affect Therapy Strategy. *Curr Oncol Rep* (2019) 21(3):27. doi: 10.1007/s11912-019-0768-4
8. Leblond V, Kastritis E, Advani R, Ansell SM, Buske C, Castillo JJ, et al. Treatment Recommendations From the Eighth International Workshop on Waldenström's Macroglobulinemia. *Blood* (2016) 128(10):1321–8. doi: 10.1182/blood-2016-04-711234
9. Onaindia A, Medeiros LJ, Patel KP. Clinical Utility of Recently Identified Diagnostic, Prognostic, and Predictive Molecular Biomarkers in Mature B-cell Neoplasms. *Mod Pathol* (2017) 30(10):1338–66. doi: 10.1038/modpathol.2017.58
10. Ruminy P, Etancelin P, Couronné L, Parmentier F, Rainville V, Mareschal S, et al. The Isotype of the BCR as a Surrogate for the GCB and ABC Molecular Subtypes in Diffuse Large B-cell Lymphoma. *Leukemia* (2011) 25(4):681–8. doi: 10.1038/leu.2010.302
11. Ngo VN, Young RM, Schmitz R, Jhavar S, Xiao W, Lim K-H, et al. Oncogenically Active MYD88 Mutations in Human Lymphoma. *Nature* (2011) 470(7332):115–9. doi: 10.1038/nature09671
12. de Groen RAL, Schrader AMR, Kersten MJ, Pals ST, Vermaat JSP. MYD88 in the Driver's Seat of B-cell Lymphomagenesis: From Molecular Mechanisms to Clinical Implications. *Haematologica* (2019) 104(12):2337–48. doi: 10.3324/haematol.2019.227272
13. Jo T, Nishikori M, Kogure Y, Arima H, Sasaki K, Sasaki Y, et al. LUBAC Accelerates B-cell Lymphomagenesis by Conferring Resistance to Genotoxic Stress on B Cells. *Blood* (2020) 136(6):684–97. doi: 10.1182/blood.2019002654
14. Knittel G, Liedgens P, Korovkina D, Seeger JM, Al-Baldawi Y, Al-Maarri M, et al. B-Cell-Specific Conditional Expression of Myd88p.L252P Leads to the Development of Diffuse Large B-cell Lymphoma in Mice. *Blood* (2016) 127 (22):2732–41. doi: 10.1182/blood-2015-11-684183
15. Sewastianik T, Guerrera ML, Adler K, Dennis PS, Wright K, Shanmugam V, et al. Human MYD88L265P is Insufficient by Itself to Drive Neoplastic Transformation in Mature Mouse B Cells. *Blood Adv* (2019) 3(21):3360–74. doi: 10.1182/bloodadvances.2019000588
16. Schmidt K, Sack U, Graf R, Winkler W, Popp O, Mertins P, et al. B-Cell-Specific Myd88 L252p Expression Causes a Premalignant Gammopathy Resembling Igm MGUS. *Front Immunol* (2020) 11:602868. doi: 10.3389/fimmu.2020.602868
17. Soriano P. Generalized Lacz Expression With the ROSA26 Cre Reporter Strain. *Nat Genet* (1999) 21(1):70–1. doi: 10.1038/5007
18. Lakso M, Sauer B, Mosinger B, Lee EJ, Manning RW, Yu SH, et al. Targeted Oncogene Activation by Site-Specific Recombination in Transgenic Mice. *Proc Natl Acad Sci USA* (1992) 89(14):6232–6. doi: 10.1073/pnas.89.14.6232
19. Vincent-Fabert C, Fiancette R, Pinaud E, Truffinet V, Cogné N, Cogné M, et al. Genomic Deletion of the Whole IgH 3' Regulatory Region (hs3a, hs1,2, hs3b, and hs4) Dramatically Affects Class Switch Recombination and Ig Secretion to All Isotypes. *Blood* (2010) 116(11):1895–8. doi: 10.1182/blood-2010-01-264689
20. Rickert RC, Roes J, Rajewsky K. B Lymphocyte-Specific, Cre-mediated Mutagenesis in Mice. *Nucleic Acids Res* (1997) 25(6):1317–8. doi: 10.1093/nar/25.6.1317
21. Faumont N, Chanut A, Benard A, Cogne N, Delsol G, Feuillard J, et al. Comparative Analysis of Oncogenic Properties and Nuclear Factor-Kappab Activity of Latent Membrane Protein 1 Natural Variants From Hodgkin's Lymphoma's Reed-Sternberg Cells and Normal B-Lymphocytes. *Haematologica* (2009) 94(3):355–63. doi: 10.3324/haematol.13269

22. Chauzeix J, Laforêt M-P, Deveza M, Crowther L, Marcellaud E, Derouault P, et al. Normal Serum Protein Electrophoresis and Mutated IGHV Genes Detect Very Slowly Evolving Chronic Lymphocytic Leukemia Patients. *Cancer Med* (2018) 7(6):2621–8. doi: 10.1002/cam4.1510
23. Almeida JS, Iriabho EE, Gorrepati VL, Wilkinson SR, Grüneberg A, Robbins DE, et al. Imagejs: Personalized, Participated, Pervasive, and Reproducible Image Bioinformatics in the Web Browser. *J Pathol Inform* (2012) 3:25. doi: 10.4103/2153-3539.98813
24. David A, Arnaud N, Fradet M, Lascaux H, Ouk-Martin C, Gachard N, et al. c-Myc Dysregulation is a Co-Transforming Event for Nuclear Factor-κb Activated B Cells. *Haematologica* (2017) 102(5):883–94. doi: 10.3324/haematol.2016.156281
25. Chanut A, Duguet F, Marfak A, David A, Petit B, Parrens M, et al. Rela and RelB Cross-Talk and Function in Epstein-Barr Virus Transformed B Cells. *Leukemia* (2014) 28(4):871–9. doi: 10.1038/leu.2013.274
26. Magoč T, Salzberg SL. FLASH: Fast Length Adjustment of Short Reads to Improve Genome Assemblies. *Bioinformatics* (2011) 27(21):2957–63. doi: 10.1093/bioinformatics/btr507
27. Chevrier S, Genton C, Kallies A, Karnowski A, Otten LA, Malissen B, et al. CD93 is Required for Maintenance of Antibody Secretion and Persistence of Plasma Cells in the Bone Marrow Niche. *Proc Natl Acad Sci U S A* (2009) 106 (10):3895–900. doi: 10.1073/pnas.0809736106
28. Hömig-Hölzel C, Hojer C, Rastelli J, Casola S, Strobl LJ, Müller W, et al. Constitutive CD40 Signaling in B Cells Selectively Activates the Noncanonical NF-kappaB Pathway and Promotes Lymphomagenesis. *J Exp Med* (2008) 205 (6):1317–29. doi: 10.1084/jem.20080238
29. Faumont N, Durand-Panteix S, Schlee M, Grömminger S, Schuhmacher M, Hölzel M, et al. c-Myc and Rel/NF-kappaB are the Two Master Transcriptional Systems Activated in the Latency III Program of Epstein-Barr Virus-Immortalized B Cells. *J Virol* (2009) 83(10):5014–27. doi: 10.1128/JVI.02264-08
30. Hunter ZR, Xu L, Yang G, Tsakmaklis N, Vos JM, Liu X, et al. Transcriptome Sequencing Reveals a Profile That Corresponds to Genomic Variants in Waldenström Macroglobulinemia. *Blood* (2016) 128(6):827–38. doi: 10.1182/blood-2016-03-708263
31. Wright G, Tan B, Rosenwald A, Hurt EH, Wiestner A, Staudt LM. A Gene Expression-Based Method to Diagnose Clinically Distinct Subgroups of Diffuse Large B Cell Lymphoma. *Proc Natl Acad Sci USA* (2003) 100 (17):9991–6. doi: 10.1073/pnas.1732008100
32. Durham BH, Getta B, Dietrich S, Taylor J, Won H, Bogenberger JM, et al. Genomic Analysis of Hairy Cell Leukemia Identifies Novel Recurrent Genetic Alterations. *Blood* (2017) 130(14):1644–8. doi: 10.1182/blood-2017-01-765107
33. Harroch S, Gothelf Y, Revel M, Chebath J. 5' Upstream Sequences of MyD88, an IL-6 Primary Response Gene in M1 Cells: Detection of Functional IRF-1 and Stat Factors Binding Sites. *Nucleic Acids Res* (1995) 23(17):3539–46. doi: 10.1093/nar/23.17.3539
34. Janssens S, Burns K, Tschopp J, Beyaert R. Regulation of interleukin-1- and Lipopolysaccharide-Induced NF-kappaB Activation by Alternative Splicing of Myd88. *Curr Biol* (2002) 12(6):467–71. doi: 10.1016/S0960-9822(02)00712-1
35. Adib-Conquy M, Adrie C, Fitting C, Gattolliat O, Beyaert R, Cavaillon J-M. Up-Regulation of MyD88s and SIGIRR, Molecules Inhibiting Toll-like Receptor Signaling, in Monocytes From Septic Patients. *Crit Care Med* (2006) 34(9):2377–85. doi: 10.1097/01.CCM.0000233875.93866.88
36. Lee FF-Y, Davidson K, Harris C, McClendon J, Janssen WJ, Alper S. NF-κB mediates lipopolysaccharide-induced alternative pre-mRNA splicing of MyD88 in mouse macrophages. *J Biol Chem* (2020) 295(18):6236–48. doi: 10.1074/jbc.RA119.011495
37. Meng R, Li D, Feng Z, Xu Q. MyD88 Hypermethylation Mediated by DNMT1 is Associated With LTA-induced Inflammatory Response in Human Odontoblast-Like Cells. *Cell Tissue Res* (2019) 376(3):413–23. doi: 10.1007/s00441-019-02993-0
38. Šutić M, Motzek A, Bubanović G, Linke M, Sabol I, Vugrek O, et al. Promoter Methylation Status of ASC/TMS1/PYCARD is Associated With Decreased Overall Survival and TNM Status in Patients With Early Stage non-Small Cell Lung Cancer (NSCLC). *Transl Lung Cancer Res* (2019) 8(6):1000–15. doi: 10.21037/tlcr.2019.12.08
39. Wang W, Zhao Z, Wu F, Wang H, Wang J, Lan Q, et al. Bioinformatic Analysis of Gene Expression and Methylation Regulation in Glioblastoma. *J Neurooncol* (2018) 136(3):495–503. doi: 10.1007/s11060-017-2688-1
40. Wang JQ, Jeelall YS, Beutler B, Horikawa K, Goodnow CC. Consequences of the Recurrent MYD88(L265P) Somatic Mutation for B Cell Tolerance. *J Exp Med* (2014) 211(3):413–26. doi: 10.1084/jem.20131424
41. Komori T. Mouse Models for the Evaluation of Osteocyte Functions. *J Bone Metab* (2014) 21(1):55–60. doi: 10.11005/jbm.2014.21.1.55
42. Schmidt-Supprian M, Rajewsky K. Vagaries of Conditional Gene Targeting. *Nat Immunol* (2007) 8(7):665–8. doi: 10.1038/ni0707-665
43. Pillai S, Cariappa A. The Follicular Versus Marginal Zone B Lymphocyte Cell Fate Decision. *Nat Rev Immunol* (2009) 9(11):767–77. doi: 10.1038/nri2656
44. Heise N, De Silva NS, Silva K, Carette A, Simonetti G, Pasparakis M, et al. Germinal Center B Cell Maintenance and Differentiation are Controlled by Distinct NF-κb Transcription Factor Subunits. *J Exp Med* (2014) 211(10):2103–18. doi: 10.1084/jem.20132613
45. Merzianu M, Jiang L, Lin P, Wang X, Weber DM, Vadhan-Raj S, et al. Nuclear BCL-10 Expression is Common in Lymphoplasmacytic Lymphoma/Waldenström Macroglobulinemia and Does Not Correlate With P65 NF-kappaB Activation. *Mod Pathol* (2006) 19(7):891–8. doi: 10.1038/modpathol.3800609
46. Okabe S, Fukuda S, Kim Y-J, Niki M, Pelus LM, Ohyashiki K, et al. Stromal Cell-Derived factor-1alpha/CXCL12-induced Chemotaxis of T Cells Involves Activation of the RasGAP-associated Docking Protein p62Dok-1. *Blood* (2005) 105(2):474–80. doi: 10.1182/blood-2004-03-0843
47. Perrot A, Corre J, Avet-Loiseau H. Risk Stratification and Targets in Multiple Myeloma: From Genomics to the Bedside. *Am Soc Clin Oncol Educ Book* (2018) 38:675–80. doi: 10.1200/EDBK_200879
48. Bohannon C, Powers R, Satyabhama L, Cui A, Tipton C, Michaeli M, et al. Corrigendum: Long-lived Antigen-Induced IgM Plasma Cells Demonstrate Somatic Mutations and Contribute to Long-Term Protection. *Nat Commun* (2016) 7:12687. doi: 10.1038/ncomms12687
49. Li Z, Wang H, Xue L, Shin D-M, Roopenian D, Xu W, et al. Emu-BCL10 Mice Exhibit Constitutive Activation of Both Canonical and Noncanonical NF-kappaB Pathways Generating Marginal Zone (MZ) B-cell Expansion as a Precursor to Splenic MZ Lymphoma. *Blood* (2009) 114(19):4158–68. doi: 10.1182/blood-2008-12-192583
50. Moore CR, Liu Y, Shao C, Covey LR, Morse HC, Xie P. Specific Deletion of TRAF3 in B Lymphocytes Leads to B-lymphoma Development in Mice. *Leukemia* (2012) 26(5):1122–7. doi: 10.1038/leu.2011.309
51. Vincent-Fabert C, Saintamand A, David A, Alizadeh M, Boyer F, Arnaud N, et al. Reproducing Indolent B-cell Lymphoma Transformation With T-cell Immunosuppression in LMP1/CD40-expressing Mice. *Cell Mol Immunol* (2019) 16(4):412–4. doi: 10.1038/s41423-018-0197-6
52. Vincent-Fabert C, Roland L, Zimber-Strobl U, Feuillard J, Faumont N. Pre-Clinical Blocking of PD-L1 Molecule, Which Expression is Down Regulated by NF-κb, JAK1/JAK2 and BTK Inhibitors, Induces Regression of Activated B-cell Lymphoma. *Cell Commun Signal* (2019) 17(1):89. doi: 10.1186/s12964-019-0391-x
53. Vincent-Fabert C, Soubeyran I, Velasco V, Parrens M, Jeannet R, Lereclus E, et al. Inflamed Phenotype of Splenic Marginal Zone B-cell Lymphomas With Expression of PD-L1 by Intratumoral Monocytes/Macrophages and Dendritic Cells. *Cell Mol Immunol* (2019) 16(6):621–4. doi: 10.1038/s41423-019-0228-y
54. Reimann M, Schrezenmeier JF, Richter-Pechanska P, Dolnik A, Hick TP, Schleich K, et al. Adaptive T-cell Immunity Controls Senescence-Prone MyD88- or CARD11-mutant B-Cell Lymphomas. *Blood* (2020). doi: 10.1182/blood.2020005244
55. Jalali S, Price-Troska T, Paludo J, Villasboas J, Kim H-J, Yang Z-Z, et al. Soluble PD-1 Ligands Regulate T-cell Function in Waldenstrom Macroglobulinemia. *Blood Adv* (2018) 2(15):1985–97. doi: 10.1182/bloodadvances.2018021113

Conflict of Interest: The authors declare that the research was conducted in the absence of any commercial or financial relationships that could be construed as a potential conflict of interest.

frontiers in Immunology

MINI REVIEW
published: 25 May 2021
doi: 10.3389/fimmu.2021.669964

Genetically Engineered Mouse Models Support a Major Role of Immune Checkpoint-Dependent Immunosurveillance Escape in B-Cell Lymphomas

Quentin Lemasson[1,2], *Hussein Akil*[1,2], *Jean Feuillard*[1,2] *and Christelle Vincent-Fabert*[1,2]*

[1] UMR CNRS 7276/INSERM U1262 CRIBL, University of Limoges, Limoges, France, [2] Hematology Laboratory of Dupuytren Hospital University Center (CHU) of Limoges, Limoges, France

These last 20 years, research on immune tumor microenvironment led to identify some critical recurrent mechanisms used in cancer to escape immune response. Through immune checkpoints, which are cell surface molecules involved in the immune system control, it is now established that tumor cells are able to shutdown the immune response. Due to the complexity and heterogeneity of Non Hodgkin B-cell Lymphomas (NHBLs), it is difficult to understand the precise mechanisms of immune escape and to explain the mitigated effect of immune checkpoints blockade for their treatment. Because genetically engineered mouse models are very reliable tools to improve our understanding of molecular mechanisms involved in B-cell transformation and, at the same time, can be useful preclinical models to predict immune response, we reviewed hereafter some of these models that highlight the immune escape mechanisms of NHBLs and open perspectives on future therapies.

Keywords: B-cell lymphoma, immune surveillance, PD-1/PD-L1, CTLA-4, MHC-II, NKG2D

OPEN ACCESS

Edited by:
Hermann Eibel, University of Freiburg Medical Center, Germany

Reviewed by:
Christian Kosan, Friedrich Schiller University Jena, Germany
Stéphane J. C. Mancini, INSERM U1068 Centre de Recherche en Cancérologie de Marseille (CRCM), France

***Correspondence:**
Christelle Vincent-Fabert
christelle.vincent-fabert@unilim.fr

Specialty section:
This article was submitted to B Cell Biology, a section of the journal Frontiers in Immunology

Received: *19 February 2021*
Accepted: *11 May 2021*
Published: *25 May 2021*

Citation:
Lemasson Q, Akil H, Feuillard J and Vincent-Fabert C (2021) Genetically Engineered Mouse Models Support a Major Role of Immune Checkpoint-Dependent Immunosurveillance Escape in B-Cell Lymphomas. Front. Immunol. 12:669964. doi: 10.3389/fimmu.2021.669964

INTRODUCTION

Non Hodgkin B-cell Lymphomas (NHBLs) are malignant neoplasms characterized by an abnormal expansion of clonal B lymphocytes. Despite being subdivided in more than 50 entities (1), most of them can be ascribed as indolent (low grade) or aggressive forms (high grade). Immune escape, also called immunomodulation or immunoediting, is a way by which tumors neutralize and/or subvert the host's immune system to their advantage (2). The concept of host immune response against neoantigens has been demonstrated long time ago (3) and Tumor Infiltrated Lymphocytes (TILs) have been recognized very early as a biomarker of the immune response against cancer (4). However, tumor cells are able to evade immune response by developing an immunosuppressive microenvironment through the regulation of immune checkpoint protein expression, such proteins being essential in the negative control of activated immune cells. Various immunotherapy treatments aim to reactivate antitumor immune response by targeting specific immune-checkpoint proteins (5). Programmed cell-Death 1 (PD-1) and its ligand Programmed cell-Death Ligand 1 (PD-L1) are the most studied immune checkpoint proteins. If immune restoring therapies have given

spectacular results in some solid cancers such as those of the lung, colon or melanoma, effects on B-cell lymphomas are mitigated (6). There is an urgent need to understand how tumor B cells escape immune surveillance. Thanks to genetic engineering, mouse models are globally useful for phenocopying human B-cell lymphomas and investigating the emergence and progression of transformed B cells as well as their concomitant immune escape and for researching new therapeutic strategies.

Here, we discuss different mouse models that have been used to study the B-cell immune surveillance (**Figure 1** and **Table 1**). The human relevance of these models is first presented, and then, the experimental results are summarized and discussed. A large part of studies presented hereafter investigated the PD-1/PD-L1 axis. However, other molecules such as CTLA-4, MHC-II or NKG2D are discussed. Strikingly, these models provide functional clues to genetic abnormalities as well as immune evasion occurring in B-cell lymphomas, and recurrently highlight the role of NF-κB. Indeed, as reviewed recently, NF-κB plays a major role in immune checkpoint controls and directly regulates PD-L1 expression (17).

DEREGULATION OF PD-1/PD-L1 AXIS IN MOUSE MODELS OF B-CELL LYMPHOMAS

Discovered in the nineties, PD-1 and PD-L1 remain the most promising immune checkpoint targets for cancer immunotherapy (18, 19). PD-L1 (B7-H1 or CD274) binds to its receptor PD-1 (CD279) on T cells (20). PD-L1 first promotes naïve T-cell expansion through IL-10 stimulation (19). Then, PD-1/PD-L1 signaling induces effective inhibition/exhaustion of T cells in the context of chronic antigen stimulation (20). Among effects, PD-1/PD-L1 interaction leads to a drastic inhibition of the T-cell receptor (TCR) signaling as well as AKT, ERK and NF-κB signaling pathways. Essential for the immune response control, this mechanism is adopted by tumor cells to escape immune surveillance. PD-L1 expression by tumor B cells has been found in various lymphoma subtypes such as Diffuse Large B-Cell Lymphomas (DLBCL), associated or not with the Epstein Barr virus (EBV). This tumor phenotype is usually associated with an intratumoral infiltration of $PD1^+$ T-lymphocytes ($PD1^+$ TILs) (21, 22), thus exhibiting an inflamed phenotype according to classification of Chen (23). The selection pressure exerted by the immune surveillance is probably one of the drivers of the emergence of B-cell clones since chromosomal alterations in the 9p24.1 region which harbors the *PDL1* and *PDL2* loci are found in most classical Hodgkin lymphomas (HL) as well as in 27% of non Germinal Center B (GCB) DLBCLs, both B-cell cancers strongly associated with NF-κB activation (24). Anti-PD-1/PD-L1 therapy has given promising results in HL (25). PD-L1 expression is found in 26-75% (26) of patients with higher expression in Activated B-Cell (ABC) DLBCL, presumably due to the constitutively activated NF-κB as it is in Epstein Barr Virus (EBV)-positive DLBCL (27). However, correlation between PD-L1 expression and the response to PD-1/PD-L1 therapy in DLBCLs remains controversial (28).

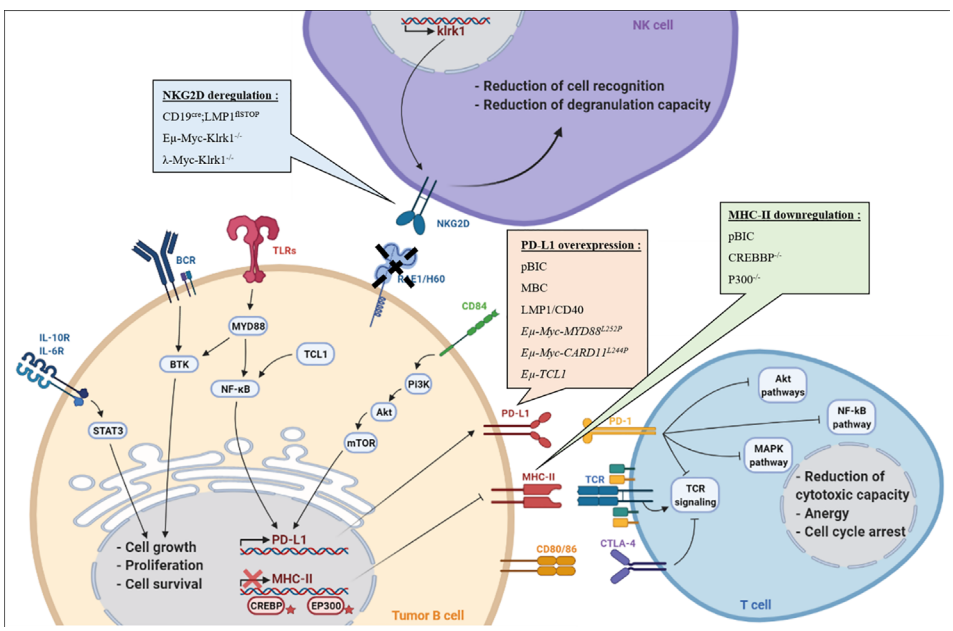

FIGURE 1 | B/T/NK cells in the immune escape context. Representation of different mechanisms exploited by tumor B-cell lymphomas to escape immune control during lymphomagenesis in each presented transgenic mouse models: (i) overexpression of PD-L1 associated with MHC-II downregulation to induce T-cell anergy, (ii) Reduction of RAE1/H60 expression to induce NK cells tolerance, (iii) CTLA-4 expressed by T-cells is targeted by lymphoma B cells, leading to T-cell inactivation.

TABLE 1 | Transgenic mouse models.

Model	Strategy	Expression/Induction	Phenocopy	Immune escape strategy	Reference
CRE regulated expression					
pBIC	NF-κB constitutive signaling *Blimp1* inactivation *p53* inactivation	GC-B cell compartment ($C\gamma1^{CRE}$)	ABC-DLBCL	PD-L1 overexpression MHC-II downregulation	(7)
MBC	endogenous $MYD88^{L252P}$ expression BCL2 overexpression	B-cell compartment ($Cd19^{CRE}$)	ABC-DLBCL	PD-L1 overexpression	(8)
$CREBBP^{-/-}$	CREBBP inactivation	GC-B cell compartment (AID^{CRE})	DLBCL	MHC-II deregulation	(9)
$P300^{-/-}$	p300 inactivation	GC-B cell compartment (AID^{CRE})	DLBCL	MHC-II deregulation	(9)
$CD19^{cre}$;$LMP1^{flSTOP}$	EBV's LMP1 expression	B-cell compartment ($Cd19^{CRE}$)	EBV driven lymphomas	NKG2D blocking	(10)
LMP1/CD40	CD40 constitutive signaling	B-cell compartment ($Cd19^{CRE}$)	SMZL	PD-L1 overexpression	(11)
EμMyc/λMyc regulated expression					
Eμ-Myc-$MYD88^{L252P}$	transplantation of Eμ-*Myc*-$MYD88^{L252P}$	B cell lineage	ABC-DLBCL	PD-L1/PD-L2 overexpression	(12)
Eμ-Myc-$CARD11^{L244P}$	transplantation of Eμ-*Myc*-$CARD11^{L244P}$ HSCs	B cell lineage	ABC-DLBCL	PD-L1/PD-L2 overexpression	(12)
hCTLA4-$Fc\gamma R^{-/-}$	Human CTLA4 expression FcγR inactivation	B cell lineage	CLL	CTLA4 deregulation	(13)
Eμ-Myc-$Klrk1^{-/-}$	NKG2D inactivation	B cell lineage	MYC driven lymphomas	Absence of NKG2D	(14)
λ-Myc-Klrk1-/-	NKG2D inactivation	B cell lineage	BL	Absence of NKG2D	(15)
Eμ-TCL1	TCL1 overexpression	B cell lineage	CLL	PD-L1/PD-L2 overexpression	(16)

(ABC-)DLBCL, (Activated B-Cell) Diffuse Large B-Cell Lymphoma; EBV, Epstein Barr Virus; SMZL, Splenic Marginal Zone Lymphoma; CLL, Chronic Lymphocytic Leukemia; BL, Burkitt Lymphoma.

Recently, two studies dealing with NF-κB associated DLBCLs showed similar results. The first one used the MBC model, developed by Knittel *et al.*, which develop aggressive DLBCL-like tumors (29). These mice harbor the $MYD88^{L252P}$ mutation and overexpress the anti-apoptotic factor BCL2, two features found in 29% and 40% of ABC-DLBCL cases respectively (30, 31). Flümann et al. found a striking resemblance of MBC tumors with human ABC-DLBCLs, with a similar gene expression profile (8). They also demonstrated overexpression of *Pdl1* on MBC lymphoma B cells associated with exhausted infiltrating $CD4^+$ and $CD8^+$ T cells, highlighting the immune escape strategy used by tumor cells.

In the second study, Reimann *et al.* engineered an original ABC-DLBCL model based on the demonstrated cooperation between c-MYC and NF-κB (32). Hematopoietic Stem Cells (HSC) from Eμ-*Myc* mice were stably transduced with naturally occurring NF-κB mutants, among them $MYD88^{L252P}$ or $CARD11^{L244P}$. Transduced Eμ-*Myc* cells were injected into lethally irradiated strain-matched C57BL/6 recipients. All these allograft models supported MYC-driven B-cell lymphomagenesis through increased protection against apoptosis, but only $MYD88^{L252P}$ or $CARD11^{L244P}$ Eμ-*Myc* tumors resembled to human ABC-DLBCL, including expression of PD-L1 which was responsible for an exhausted T-cell phenotype (12).

In both studies, the authors treated their mouse model with anti-PD-1 antibodies, leading to a significant increase in overall mouse survival and inducing phenotypic changes in infiltrating $CD4^+$ and $CD8^+$ T cells with a restored proliferation potential. The combination of anti-PD-1 antibody and BCL2 inhibitor showed an additive effect in the MBC model. The anti-PD-1 treatment seems to be really effective regarding these models. But recent human clinical trial showed a completely different reality (6), raising the question of resistance to these therapies. Some clues may have been given by the pBIC model. This model associates *Tp53* deletion, enhanced NF-κB signaling due to an activated IKK2 mutant, and *Blimp1* inactivation that blocks plasma-cell differentiation. Pascual *et al.* showed that, in these mice, DLBCL-like tumors exhibited an ABC-DLBCL phenotype with FOXP1 dysregulation and overexpression of PD-L1 by tumor cells. This phenotype was associated with intra-tumor infiltration of $PD\text{-}1^+$ $CD8^+$ T cells. Exhibiting an exhausted phenotype, these TILs also expressed other inhibitory molecules such as LAG-3 and 2B4 (7). In this model, anti-PD-1 treatment did not show any effect on mouse survival and anti-CD20 treatment alone had limited impact. But combining both antibodies markedly improved mouse survival and resulted in tumor regression with clearance of PD-1 TILs, strongly suggesting that therapies targeting the PD1/PD-L1 axis could be used in combination with other well established treatments in DLBCLs.

Taken together, these different mouse models for ABC-DLBCLs suggest that PD-1/PD-L1 immune checkpoint upregulation is one of the main mechanisms of immunosurveillance escape in ABC-DLBCL. It also indicates that, even when poorly effective alone, anti PD-1/PD-L1 therapies may very well be able to improve the effect of other molecules that directly target tumor B cells.

To our knowledge, only four mouse models of indolent B-cell lymphoma have been reported. One is related to Chronic Lymphocytic Leukemia (CLL) with *TCL1* (originally described in the former CD4 T-CLL, now called T-cell prolymphocytic leukemia) as a driver oncogene (33) and three others to marginal

zone lymphomas, involving *Traf3* deletion (34), *BCL10* deregulation (35) and CD40 signaling (11). The question of immune surveillance was addressed only in the TCL1 and CD40 mouse models. First, Hofbauher *et al*. demonstrated that development of a CLL-like disease was associated with a shift from naïve to memory phenotypes of both $CD4^+$ and $CD8^+$ T cells in Eμ-*TCL1* transgenic mice (16). In the context of aging, McClanahan *et al*. described in this model a PD-1 overexpression on $CD8^+$ T cells with a defect in immune synapse formation, associated with specific PD-L1 overexpression on B cells (36). In the same model, Lewinsky *et al*. demonstrated the role of CD84, a member of the Signaling Lymphocyte Activating Molecule (SLAM) family known to bridge between CLL cells and their microenvironment (37). CD84 (SLAMF5) activation upregulates PD-L1 expression on CLL cells and stroma cells, through the AKT/mTOR pathway, and promotes PD-1 expression on T cells resulting in their exhaustion (38). In an adoptive transfer of Eμ-*TCL1* CLLs, PD-L1 blockade restored the antitumor immune response, in conjunction with an enhanced pro-inflammatory microenvironment (39). However, the question of the tumor microenvironment arises with this strategy. Adoptive transfer of Eμ-*TCL1* leukemic cells proves their ability to invade and proliferate in a healthy microenvironment by their own, but this development is independent of the tumor microenvironment, and consequently a real immune escape mechanism remains hard to identify here.

Being also associated with NF-κB activating mutations, splenic marginal zone lymphomas exhibit an inflamed phenotype (40, 41). In the model of Hömig-Hözel *et al*., B-cell specific continuous CD40 signaling is due to specific B-cell expression of a chimeric LMP1/CD40 protein composed of the membrane moiety of the LMP1 protein of EBV and the intracytoplasmic transducing moiety of CD40 (11). LMP1/CD40 mice develop indolent lymphomas with clonal expansion of spleen marginal zone B cells. The indolent phenotype was shown to be associated with an overexpression of PD-L1 on B cells, such expression depending on NF-κB, STAT3 and BCR pathways (42). In this model, T-cell depletion resulted in progression toward an aggressive tumor, suggesting that some immune surveillance was still exerted on indolent B-cell lymphoma (43). Indeed, crossing the LMP1/CD40 and λ -*Myc* mice (in which *Myc* is under the control of the Ig lambda locus) led to the development of aggressive B-cell tumors with an immunoblast phenotype and further PD-L1 expression (32). This study suggests that the PD-1/PD-L1 axis is requested for emergence of an indolent lymphoma as well as for its progression towards an aggressive form. Concomitantly, our group demonstrated a beneficial effect of anti-PD-L1 therapy in the LMP1/CD40 model, resulting in tumor regression and T-cell reactivation. Interestingly, we also demonstrated that therapies targeting other pathways, such as NF-κB, JAK/STAT or BCR signaling, were also able to reduce PD-L1 surface expression of tumor B cells (42). Like in mouse DLBCL models, these results suggest that, as long as they are expressed, PD-1 and/or PD-L1 blockade in indolent B-cell lymphomas may synergize with other therapeutic molecules, for example, the specific inhibitors of JAK/STAT pathway, ruxolitinib, or, of BTK, ibrutinib.

In essence, these different transgenic mouse models highlight the major role of PD-1/PD-L1 axis deregulation in aggressive lymphomas development, but also showed the involvement of this immune checkpoint in the transformation of indolent lymphomas as long as they express PD-L1. They also indicate that the level of PD-L1 expression may be a critical parameter for immune evasion and tumor progression and point on the interest of combined therapies that include anti-tumor immune restoration.

DEREGULATION OF OTHER IMMUNE CHECKPOINTS IN MOUSE MODELS OF B-CELL LYMPHOMAS

CTLA-4

In Humans, a single nucleotide polymorphism located in the 3q13.33 region that harbors the CD80 and CD86 loci is associated with the risk of DLBCL, providing evidence for the role of immune function in the etiology of these lymphomas (44). The activating effects of CD80 and CD86 on CD28 are neutralized by the Cytotoxic T-Lymphocyte Antigen 4 (CTLA-4). CTLA-4, normally expressed on the surface of activated and regulatory T cells as well as B cells, even if weakly, is the second major immune checkpoint molecule. As CTLA-4 has a higher affinity to CD28 than for CD80 or CD86, it downregulates primary T-cell responses by interaction with B7 family members expressed on Antigen Presenting Cells (APCs) (45). CTLA-4 was shown to be abnormally expressed on B-cell lymphomas, and is notably a part of the CLL signature (46).

In the Eμ-*TCL1* mouse model, CTLA-4, which is expressed on CLL-like B cells, seems to promote STAT3 activation pathway through its dimerization with surface CD86 followed by its internalization, and thus acting as a costimulatory signal (47). By using the adoptive transfer strategy, Do *et al*. showed that specific CTLA4 blockade on tumor cells could affect leukemic progression (13).

MHC-II

Besides their direct role in antibody secretion, B cells express MHC-II and are also APCs. B-cells are able to improve T-cell activation and proliferation through a process called B/T-cell cooperation (48, 49). In B cell lymphomas, loss of MHC-II contributes to the immune evasion resulting in a decrease of T-cell activity. This loss of surface MHC-II may be due to genetic alterations of the *MHC-II* region, including homozygous deletions (50). Malignant B cells can also downregulate the expression of *MHC-II* by various mechanisms (7, 9, 51) such as the downregulation of the MHC-II transcriptional activators class II transactivator (*CIITA*). The consequence of *MHC-II* down-regulation in tumor B-cell escape has been exemplified in two KO models for the Histone Acetyl-Transferases (HAT) *Crebbp* or *Ep300* (which deletions are found in 50% of human DLBCLs). In these models, development of aggressive B-cell tumors was related to the fact that $CD4^+$ T cells were unable to interact with B cells because the latter had lost the expression of MHC-II which is normally up-regulated by these HAT (9).

In addition, loss of MHC-II was also demonstrated in the pBIC mouse lymphoma model, suggesting a cooperation with the PD-1/PD-L1 in immunosurveillance escape (7). If there is no current treatment allowing a direct restoration of MHC-II at the surface of tumor cells, McClanahan *et al.* showed a restoration of MHC-II surface expression after anti-PD-L1 treatment in the CLL model Eμ-*TCL1* (39).

Thereby, studies on pBIC and Eμ-*TCL1* models converge to show a striking correlation between PD-L1 and MHC-II deregulation in different types of lymphomas. Nevertheless, these findings deserve to be more closely investigated to improve the comprehension of immune checkpoints deregulation in lymphomas.

NKG2D

In Humans, cells infected by the EBV are under powerful immune surveillance by T and NK cells. Compromising this immune surveillance such as in AIDS or after organ transplantation, results in aggressive EBV-related B-cell lymphoproliferations. NK-cell functions could strongly be altered in DLBCLs that can be associated with resistance to rituximab-based therapies (52). Mouse Natural Killer Group 2 member D (NKG2D) is a receptor expressed by all cytotoxic lymphocytes, notably NK cells, activated $CD8^+$ T cells and activated macrophages (53). Two murine NKG2D ligands have been described (RAE-1 and H60) (53–56). Interaction between NKG2D and its ligands induces PI3K-AKT signaling, leading to an increase in target recognition, cytotoxic activity and a reduction in sensitivity to cell apoptosis (57). NKG2D ligands are normally expressed at the surface of any virally infected/tumorigenic cells. Both mouse and human studies suggest that tumor cells evade NKG2D recognition either by downregulating NKG2D ligands expression (14, 58) or by secreting massively circulating NKG2D ligands resulting in a downregulation of NKG2D expression on cytotoxic cells (59–61). The occurrence of B-cell lymphomas is accelerated in the absence of NKG2D. In mice, Guerra *et al.* showed, in 2008, that the deletion of *Klrk1*, the gene encoding NKG2D, in Eμ-*Myc* mice, accelerates the emergence of Eμ-*Myc*-induced lymphomas (14). A similar effect was shown on an EBV dependent mouse B-cell lymphoma (10), and also in a BL λ-*Myc-Klrk1*$^{-/-}$ mouse model (15). Belting *et al.* completed this observation by demonstrating the role of NKG2D in the control of B-cell lymphoma growth and observed another escape mechanism developed by lymphomas cells through downregulating NKG2DL during the NK cell activation through downregulating NKG2DL (15).

All these different studies demonstrate the importance to escape the recognition of NKG2D receptor in B-cell lymphomagenesis and suggest its implication in the aggressive phenotype of these diseases.

CONCLUSION

The pressure of the immune surveillance is certainly one of the major driving forces in the emergence of B-cell lymphomas. Together, results reported in the articles reviewed here, support the fact that mouse models are useful to analytically understand the immune escape in both aggressive and indolent B-cell lymphomas. Beyond PD-1/PD-L1 axis, roles of CTLA-4, of antigen presentation and of NK-cells is also highlighted. These models functionally explain and resume the role of the different actors of the immune surveillance in B-cell lymphomas. Engineered mouse models will contribute to better understand tumor microenvironment in the aim to identify novel mechanisms of B-cell immune escape, which may be the keystone of future therapies. Mouse models are also useful for the preclinical study of these therapies, evidencing the interest of combinations that include treatments able to restore the anti-tumor immune response. All the models presented here point out the major role of NF-κB activation, suggesting that this pathway should also be targeted together with immune restoration therapies. Before trying such strategies in Humans, this is testable in genetically engineered mouse models. Providing a strong support for the issue of immune escape in B-cell lymphomas, these models deserve to be widely used.

AUTHOR CONTRIBUTIONS

All authors contributed to the article and approved the submitted version. QL performed the literature review and prepared the figure and table. QL, HA, JF, and CVF wrote the manuscript.

FUNDING

The group of JF is supported by grants from the Ligue Nationale Contre le Cancer (Equipe labellisée Ligue), the Comité Orientation Recherche Cancer (CORC), the France Lymphome Espoir association, the Nouvelle Aquitaine Region and the Haute-Vienne and Corrèze committees of the Ligue Nationale Contre le Cancer. CVF was supported by the France Lymphome Espoir association of patients. QL was supported by the Fondation pour la Recherche Médicale (FRM, ECO202006011493).

ACKNOWLEDGMENTS

We thank Dr Jeanne Cook Moreau (UMR CNRS 7276/INSERM 1262) for careful English editing.

REFERENCES

1. Swerdlow SH, Campo E, Pileri SA, Harris NL, Stein H, Siebert R, et al. The 2016 Revision of the World Health Organization Classification of Lymphoid Neoplasms. *Blood* (2016) 127(20):2375–90. doi: 10.1182/blood-2016-01-643569
2. Menter T, Tzankov A. Mechanisms of Immune Evasion and Immune Modulation by Lymphoma Cells. *Front Oncol* (2018) 8:54. doi: 10.3389/fonc.2018.00054
3. Wortzel RD, Philipps C, Schreiber H. Multiple Tumour-Specific Antigens Expressed on a Single Tumour Cell. *Nature* (1983) 304(5922):165–7. doi: 10.1038/304165a0

4. Vose BM, Moore M. Human Tumor-Infiltrating Lymphocytes: A Marker of Host Response. *Semin Hematol* (1985) 22(1):27–40.
5. Witkowska M, Smolewski P. Immune Checkpoint Inhibitors to Treat Malignant Lymphomas. *J Immunol Res* (2018) 2018:1982423. doi: 10.1155/2018/1982423
6. Ansell SM, Minnema MC, Johnson P, Timmerman JM, Armand P, Shipp MA, et al. Nivolumab for Relapsed/Refractory Diffuse Large B-Cell Lymphoma in Patients Ineligible for or Having Failed Autologous Transplantation: A Single-Arm, Phase II Study. *J Clin Oncol Off J Am Soc Clin Oncol* (2019) 37(6):481–9. doi: 10.1200/JCO.18.00766
7. Pascual M, Mena-Varas M, Robles EF, Garcia-Barchino M-J, Panizo C, Hervas-Stubbs S, et al. PD-1/PD-L1 Immune Checkpoint and p53 Loss Facilitate Tumor Progression in Activated B-cell Diffuse Large B-cell Lymphomas. *Blood* (2019) 133(22):2401–12. doi: 10.1182/blood.2018889931
8. Flümann R, Rehkämper T, Nieper P, Pfeiffer P, Holzem A, Klein S, et al. An Autochthonous Mouse Model of Myd88- and BCL2-Driven Diffuse Large B-Cell Lymphoma Reveals Actionable Molecular Vulnerabilities. *Blood Cancer Discov* (2020) 2:70–91. doi: 10.1158/2643-3230.BCD-19-0059
9. Hashwah H, Schmid CA, Kasser S, Bertram K, Stelling A, Manz MG, et al. Inactivation of CREBBP Expands the Germinal Center B Cell Compartment, Down-Regulates MHCII Expression and Promotes DLBCL Growth. *Proc Natl Acad Sci USA* (2017) 114(36):9701–6. doi: 10.1073/pnas.1619555114
10. Zhang B, Kracker S, Yasuda T, Casola S, Vanneman M, Hömig-Hölzel C, et al. Immune Surveillance and Therapy of Lymphomas Driven by Epstein-Barr -Virus Protein LMP1 in a Mouse Model. *Cell* (2012) 148(4):739–51. doi: 10.1016/j.cell.2011.12.031
11. Hömig-Hölzel C, Hojer C, Rastelli J, Casola S, Strobl LJ, Müller W, et al. Constitutive CD40 Signaling in B Cells Selectively Activates the Noncanonical NF-κB Pathway and Promotes Lymphomagenesis. *J Exp Med* (2008) 205 (6):1317–29. doi: 10.1084/jem.20080238
12. Reimann M, Schrezenmeier JF, Richter-Pechanska P, Dolnik A, Hick TP, Schleich K, et al. Adaptive T-cell Immunity Controls Senescence-Prone MyD88- or CARD11-mutant B-Cell Lymphomas. *Blood* (2020). doi: 10.1182/blood.2020005244
13. Do P, Beckwith KA, Cheney C, Tran M, Beaver L, Griffin BG, et al. Leukemic B Cell CTLA-4 Suppresses Costimulation of T Cells. *J Immunol Baltim Md 1950* (2019) 202(9):2806–16. doi: 10.4049/jimmunol.1801359
14. Guerra N, Tan YX, Joncker NT, Choy A, Gallardo F, Xiong N, et al. NKG2D-Deficient Mice are Defective in Tumor Surveillance in Models of Spontaneous Malignancy. *Immunity* (2008) 28(4):571–80. doi: 10.1016/j.immuni.2008.02.016
15. Belting L, Hömberg N, Przewoznik M, Brenner C, Riedel T, Flatley A, et al. Critical Role of the NKG2D Receptor for NK Cell-Mediated Control and Immune Escape of B-Cell Lymphoma. *Eur J Immunol* (2015) 45(9):2593–601. doi: 10.1002/eji.201445375
16. Hofbauer JP, Heyder C, Denk U, Kocher T, Holler C, Trapin D, et al. Development of CLL in the TCL1 Transgenic Mouse Model Is Associated With Severe Skewing of the T-cell Compartment Homologous to Human CLL. *Leukemia* (2011) 25(9):1452–8. doi: 10.1038/leu.2011.111
17. Betzler AC, Theodoraki M-N, Schuler PJ, Döscher J, Laban S, Hoffmann TK, et al. NF-κB and Its Role in Checkpoint Control. *Int J Mol Sci* (2020) 21(11). doi: 10.3390/ijms21113949
18. Ishida Y, Agata Y, Shibahara K, Honjo T. Induced Expression of PD-1, a Novel Member of the Immunoglobulin Gene Superfamily, Upon Programmed Cell Death. *EMBO J* (1992) 11(11):3887–95. doi: 10.1002/j.1460-2075.1992.tb05481.x
19. Dong H, Zhu G, Tamada K, Chen L. B7-H1, A Third Member of the B7 Family, Co-Stimulates T-Cell Proliferation and Interleukin-10 Secretion. *Nat Med* (1999) 5(12):1365–9. doi: 10.1038/70932
20. Freeman GJ, Long AJ, Iwai Y, Bourque K, Chernova T, Nishimura H, et al. Engagement of the PD-1 Immunoinhibitory Receptor by a Novel B7 Family Member Leads to Negative Regulation of Lymphocyte Activation. *J Exp Med* (2000) 192(7):1027–34. doi: 10.1084/jem.192.7.1027
21. Menter T, Bodmer-Haecki A, Dirnhofer S, Tzankov A. Evaluation of the Diagnostic and Prognostic Value of PDL1 Expression in Hodgkin and B-Cell Lymphomas. *Hum Pathol* (2016) 54:17–24. doi: 10.1016/j.humpath.2016.03.005
22. Chen BJ, Chapuy B, Ouyang J, Sun HH, Roemer MGM, Xu ML, et al. PD-L1 Expression is Characteristic of a Subset of Aggressive B-Cell Lymphomas and Virus-Associated Malignancies. *Clin Cancer Res Off J Am Assoc Cancer Res* (2013) 19(13):3462–73. doi: 10.1158/1078-0432.CCR-13-0855
23. Chen DS, Mellman I. Elements of Cancer Immunity and the Cancer-Immune Set Point. *Nature* (2017) 541(7637):321–30. doi: 10.1038/nature21349
24. Godfrey J, Tumuluru S, Bao R, Leukam M, Venkataraman G, Phillip J, et al. PD-L1 Gene Alterations Identify a Subset of Diffuse Large B-Cell Lymphoma Harboring a T-Cell-Inflamed Phenotype. *Blood* (2019) 133(21):2279–90. doi: 10.1182/blood-2018-10-879015
25. Ansell SM. Nivolumab in the Treatment of Hodgkin Lymphoma. *Clin Cancer Res Off J Am Assoc Cancer Res* (2017) 23(7):1623–6. doi: 10.1158/1078-0432.CCR-16-1387
26. Xu-Monette ZY, Zhou J, Young KH. PD-1 Expression and Clinical PD-1 Blockade in B-Cell Lymphomas. *Blood* (2018) 131(1):68–83. doi: 10.1182/blood-2017-07-740993
27. Auclair H, Ouk-Martin C, Roland L, Santa P, Al Mohamad H, Faumont N, et al. EBV Latency III-Transformed B Cells Are Inducers of Conventional and Unconventional Regulatory T Cells in a PD-L1-Dependent Manner. *J Immunol Baltim Md 1950* (2019) 203(6):1665–74.
28. Zhang J, Medeiros LJ, Young KH. Cancer Immunotherapy in Diffuse Large B-Cell Lymphoma. *Front Oncol* (2018) 8:351. doi: 10.3389/fonc.2018.00351
29. Knittel G, Liedgens P, Korovkina D, Seeger JM, Al-Baldawi Y, Al-Maarri M, et al. B-Cell-Specific Conditional Expression of Myd88p.L252P Leads to the Development of Diffuse Large B-Cell Lymphoma in Mice. *Blood* (2016) 127 (22):2732–41. doi: 10.1182/blood-2015-11-684183
30. Ngo VN, Young RM, Schmitz R, Jhavar S, Xiao W, Lim K-H, et al. Oncogenically Active MYD88 Mutations in Human Lymphoma. *Nature* (2011) 470(7332):115–9. doi: 10.1038/nature09671
31. Lenz G, Wright GW, Emre NCT, Kohlhammer H, Dave SS, Davis RE, et al. Molecular Subtypes of Diffuse Large B-Cell Lymphoma Arise by Distinct Genetic Pathways. *Proc Natl Acad Sci USA* (2008) 105(36):13520–5. doi: 10.1073/pnas.0804295105
32. David A, Arnaud N, Fradet M, Lascaux H, Ouk-Martin C, Gachard N, et al. c-Myc Dysregulation is a Co-Transforming Event for Nuclear Factor-κB Activated B Cells. *Haematologica* (2017) 102(5):883–94. doi: 10.3324/haematol.2016.156281
33. Bichi R, Shinton SA, Martin ES, Koval A, Calin GA, Cesari R, et al. Human Chronic Lymphocytic Leukemia Modeled in Mouse by Targeted TCL1 Expression. *Proc Natl Acad Sci USA* (2002) 99(10):6955–60. doi: 10.1073/pnas.102181599
34. Moore CR, Liu Y, Shao C, Covey LR, Morse HC, Xie P. Specific Deletion of TRAF3 in B Lymphocytes Leads to B-Lymphoma Development in Mice. *Leukemia* (2012) 26(5):1122–7. doi: 10.1038/leu.2011.309
35. Li Z, Wang H, Xue L, Shin D-M, Roopenian D, Xu W, et al. Eμ-BCL10 Mice Exhibit Constitutive Activation of Both Canonical and Noncanonical NF-κB Pathways Generating Marginal Zone (MZ) B-Cell Expansion as a Precursor to Splenic MZ Lymphoma. *Blood* (2009) 114(19):4158–68. doi: 10.1182/blood-2008-12-192583
36. McClanahan F, Riches JC, Miller S, Day WP, Kotsiou E, Neuberg D, et al. Mechanisms of PD-L1/PD-1-Mediated CD8 T-Cell Dysfunction in the Context of Aging-Related Immune Defects in the Eμ-TCL1 CLL Mouse Model. *Blood* (2015) 126(2):212–21. doi: 10.1182/blood-2015-02-626754
37. Marom A, Barak AF, Kramer MP, Lewinsky H, Binsky-Ehrenreich I, Cohen S, et al. CD84 Mediates CLL-Microenvironment Interactions. *Oncogene* (2017) 36(5):628–38. doi: 10.1038/onc.2016.238
38. Lewinsky H, Barak AF, Huber V, Kramer MP, Radomir L, Sever L, et al. CD84 Regulates PD-1/PD-L1 Expression and Function in Chronic Lymphocytic Leukemia. *J Clin Invest* (2018) 128(12):5465–78. doi: 10.1172/JCI96610
39. McClanahan F, Hanna B, Miller S, Clear AJ, Lichter P, Gribben JG, et al. PD-L1 Checkpoint Blockade Prevents Immune Dysfunction and Leukemia Development in a Mouse Model of Chronic Lymphocytic Leukemia. *Blood* (2015) 126(2):203–11. doi: 10.1182/blood-2015-01-622936
40. Vincent-Fabert C, Soubeyran I, Velasco V, Parrens M, Jeannet R, Lereclus E, et al. Inflamed Phenotype of Splenic Marginal Zone B-Cell Lymphomas With Expression of PD-L1 by Intratumoral Monocytes/Macrophages and Dendritic Cells. *Cell Mol Immunol* (2019) 16(6):621–4. doi: 10.1038/s41423-019-0228-y
41. Spina V, Rossi D. NF-κB Deregulation in Splenic Marginal Zone Lymphoma. *Semin Cancer Biol* (2016) 39:61–7. doi: 10.1016/j.semcancer.2016.08.002

42. Vincent-Fabert C, Roland L, Zimber-Strobl U, Feuillard J, Faumont N. Pre-Clinical Blocking of PD-L1 Molecule, Which Expression Is Down Regulated by NF-κB, JAK1/JAK2 and BTK Inhibitors, Induces Regression of Activated B-Cell Lymphoma. *Cell Commun Signal CCS* (2019) 17(1):89. doi: 10.1186/s12964-019-0391-x
43. Vincent-Fabert C, Saintamand A, David A, Alizadeh M, Boyer F, Arnaud N, et al. Reproducing Indolent B-Cell Lymphoma Transformation With T-Cell Immunosuppression in LMP1/CD40-Expressing Mice. *Cell Mol Immunol* (2019) 16(4):412–4. doi: 10.1038/s41423-018-0197-6
44. Kleinstern G, Yan H, Hildebrandt MAT, Vijai J, Berndt SI, Ghesquières H, et al. Inherited Variants at 3q13.33 and 3p24.1 Are Associated With Risk of Diffuse Large B-Cell Lymphoma and Implicate Immune Pathways. *Hum Mol Genet* (2020) 29(1):70–9. doi: 10.1093/hmg/ddz228
45. Khailaie S, Rowshanravan B, Robert PA, Waters E, Halliday N, Badillo Herrera JD, et al. Characterization of CTLA4 Trafficking and Implications for Its Function. *Biophys J* (2018) 115(7):1330–43. doi: 10.1016/j.bpj.2018.08.020
46. Herishanu Y, Pérez-Galán P, Liu D, Biancotto A, Pittaluga S, Vire B, et al. The Lymph Node Microenvironment Promotes B-Cell Receptor Signaling, NF-kappaB Activation, and Tumor Proliferation in Chronic Lymphocytic Leukemia. *Blood* (2011) 117(2):563–74.
47. Herrmann A, Lahtz C, Nagao T, Song JY, Chan WC, Lee H, et al. CTLA4 Promotes Tyk2-STAT3-Dependent B-Cell Oncogenicity. *Cancer Res* (2017) 77(18):5118–28. doi: 10.1158/0008-5472.CAN-16-0342
48. Biram A, Davidzohn N, Shulman Z. T Cell Interactions With B Cells During Germinal Center Formation, A Three-Step Model. *Immunol Rev* (2019) 288 (1):37–48. doi: 10.1111/imr.12737
49. Luckheeram RV, Zhou R, Verma AD, Xia B. $CD4^+$T Cells: Differentiation and Functions. *Clin Dev Immunol* (2012) 2012:925135. doi: 10.1155/2012/925135
50. Riemersma SA, Jordanova ES, Schop RF, Philippo K, Looijenga LH, Schuuring E, et al. Extensive Genetic Alterations of the HLA Region, Including Homozygous Deletions of HLA Class II Genes in B-Cell Lymphomas Arising in Immune-Privileged Sites. *Blood* (2000) 96(10):3569–77. doi: 10.1182/blood.V96.10.3569
51. Brown PJ, Wong KK, Felce SL, Lyne L, Spearman H, Soilleux EJ, et al. FOXP1 Suppresses Immune Response Signatures and MHC Class II Expression in Activated B-Cell-Like Diffuse Large B-Cell Lymphomas. *Leukemia* (2016) 30 (3):605–16. doi: 10.1038/leu.2015.299
52. Cox MC, Battella S, La Scaleia R, Pelliccia S, Di Napoli A, Porzia A, et al. Tumor-Associated and Immunochemotherapy-Dependent Long-Term Alterations of the Peripheral Blood NK Cell Compartment in DLBCL Patients. *Oncoimmunology* (2015) 4(3):e990773. doi: 10.4161/2162402X.2014.990773
53. Diefenbach A, Jamieson AM, Liu SD, Shastri N, Raulet DH. Ligands for the Murine NKG2D Receptor: Expression by Tumor Cells and Activation of NK Cells and Macrophages. *Nat Immunol* (2000) 1(2):119–26. doi: 10.1038/77793
54. Malarkannan S, Shih PP, Eden PA, Horng T, Zuberi AR, Christianson G, et al. The Molecular and Functional Characterization of a Dominant Minor H Antigen, H60. *J Immunol Baltim Md 1950* (1998) 161(7):3501–9.
55. Cerwenka A, Bakker AB, McClanahan T, Wagner J, Wu J, Phillips JH, et al. Retinoic Acid Early Inducible Genes Define a Ligand Family for the Activating NKG2D Receptor in Mice. *Immunity* (2000) 12(6):721–7. doi: 10.1016/S1074-7613(00)80222-8
56. Nomura M, Zou Z, Joh T, Takihara Y, Matsuda Y, Shimada K. Genomic Structures and Characterization of Rae1 Family Members Encoding GPI-Anchored Cell Surface Proteins and Expressed Predominantly in Embryonic Mouse Brain. *J Biochem (Tokyo)* (1996) 120(5):987–95. doi: 10.1093/oxfordjournals.jbchem.a021517
57. Wu J, Song Y, Bakker AB, Bauer S, Spies T, Lanier LL, et al. An Activating Immunoreceptor Complex Formed by NKG2D and DAP10. *Science* (1999) 285(5428):730–2. doi: 10.1126/science.285.5428.730
58. Brenner CD, King S, Przewoznik M, Wolters I, Adam C, Bornkamm GW, et al. Requirements for Control of B-Cell Lymphoma by NK Cells. *Eur J Immunol* (2010) 40(2):494–504. doi: 10.1002/eji.200939937
59. Salih HR, Antropius H, Gieseke F, Lutz SZ, Kanz L, Rammensee H-G, et al. Functional Expression and Release of Ligands for the Activating Immunoreceptor NKG2D in Leukemia. *Blood* (2003) 102(4):1389–96. doi: 10.1182/blood-2003-01-0019
60. Hilpert J, Grosse-Hovest L, Grünebach F, Buechele C, Nuebling T, Raum T, et al. Comprehensive Analysis of NKG2D Ligand Expression and Release in Leukemia: Implications for NKG2D-Mediated NK Cell Responses. *J Immunol Baltim Md 1950* (2012) 189(3):1360–71. doi: 10.4049/jimmunol.1200796
61. Groh V, Wu J, Yee C, Spies T. Tumour-Derived Soluble MIC Ligands Impair Expression of NKG2D and T-Cell Activation. *Nature* (2002) 419(6908):734–8. doi: 10.1038/nature01112

Conflict of Interest: The authors declare that the research was conducted in the absence of any commercial or financial relationships that could be construed as a potential conflict of interest.

frontiers in Immunology

REVIEW
published: 02 June 2021
doi: 10.3389/fimmu.2021.667054

Laboratory Mice – A Driving Force in Immunopathology and Immunotherapy Studies of Human Multiple Myeloma

*Michael Pisano[1,2], Yan Cheng[1], Fumou Sun[1], Binod Dhakal[1], Anita D'Souza[1], Saurabh Chhabra[1], Jennifer M. Knight[3], Sridhar Rao[4,5], Fenghuang Zhan[6], Parameswaran Hari[1] and Siegfried Janz[1]**

[1] Division of Hematology and Oncology, Department of Medicine, Medical College of Wisconsin, Milwaukee, WI, United States, [2] Interdisciplinary Graduate Program in Immunology, University of Iowa, Iowa City, IA, United States, [3] Departments of Psychiatry, Medicine, and Microbiology & Immunology, Medical College of Wisconsin, Milwaukee, WI, United States, [4] Division of Hematology, Oncology and Marrow Transplant, Department of Pediatrics, Medical College of Wisconsin, Milwaukee, WI, United States, [5] Blood Research Institute, Versiti Wisconsin, Milwaukee, WI, United States, [6] Myeloma Center, Department of Internal Medicine and Winthrop P. Rockefeller Cancer Institute, University of Arkansas for Medical Sciences, Little Rock, AR, United States

OPEN ACCESS

Edited by:
Christelle Vincent-Fabert, UMR7276 Contrôle des réponses immunes B et des lymphoprolifération (CRIBL), France

Reviewed by:
Hans-Martin Jäck, University of Erlangen Nuremberg, Germany
Jerome Moreaux, Université de Montpellier, France

***Correspondence:**
Siegfried Janz
sjanz@mcw.edu

Specialty section:
This article was submitted to B Cell Biology, a section of the journal Frontiers in Immunology

Received: 11 February 2021
Accepted: 28 April 2021
Published: 02 June 2021

Citation:
Pisano M, Cheng Y, Sun F, Dhakal B, D'Souza A, Chhabra S, Knight JM, Rao S, Zhan F, Hari P and Janz S (2021) Laboratory Mice – A Driving Force in Immunopathology and Immunotherapy Studies of Human Multiple Myeloma. Front. Immunol. 12:667054. doi: 10.3389/fimmu.2021.667054

Mouse models of human cancer provide an important research tool for elucidating the natural history of neoplastic growth and developing new treatment and prevention approaches. This is particularly true for multiple myeloma (MM), a common and largely incurable neoplasm of post-germinal center, immunoglobulin-producing B lymphocytes, called plasma cells, that reside in the hematopoietic bone marrow (BM) and cause osteolytic lesions and kidney failure among other forms of end-organ damage. The most widely used mouse models used to aid drug and immunotherapy development rely on *in vivo* propagation of human myeloma cells in immunodeficient hosts (xenografting) or myeloma-like mouse plasma cells in immunocompetent hosts (autografting). Both strategies have made and continue to make valuable contributions to preclinical myeloma, including immune research, yet are ill-suited for studies on tumor development (oncogenesis). Genetically engineered mouse models (GEMMs), such as the widely known Vκ*MYC, may overcome this shortcoming because plasma cell tumors (PCTs) develop *de novo* (spontaneously) in a highly predictable fashion and accurately recapitulate many hallmarks of human myeloma. Moreover, PCTs arise in an intact organism able to mount a complete innate and adaptive immune response and tumor development reproduces the natural course of human myelomagenesis, beginning with monoclonal gammopathy of undetermined significance (MGUS), progressing to smoldering myeloma (SMM), and eventually transitioning to frank neoplasia. Here we review the utility of transplantation-based and transgenic mouse models of human MM for research on immunopathology and -therapy of plasma cell malignancies, discuss strengths and weaknesses of different experimental approaches, and outline opportunities for closing knowledge gaps, improving the outcome of patients with myeloma, and working towards a cure.

Keywords: genetically engineered mouse models of human cancer, auto- and xenografting, immune, immunodeficient mice models, immune pathogenesis, Myeloma

INTRODUCTION

Multiple myeloma (MM) is a neoplasm of terminally differentiated, post-germinal center, immunoglobulin (Ig)-producing B-lymphocytes, called plasma cells, that reside in the hematopoietic bone marrow (BM). Quintessential disease manifestations include a serum M-spike (monoclonal Ig, paraprotein) and signs of end-organ damage known as CRAB symptoms: hypercalcemia, renal insufficiency, anemia, and lytic bone lesions (1). The most recent estimate of the US National Cancer Institute SEER (Surveillance, Epidemiology, and End Results) Program predicts slightly more than 32 thousand cases of newly diagnosed myeloma (NDMM) and nearly 13 thousand disease-specific deaths in 2020. This renders MM the second most common and one of the deadliest blood cancers in the United States. Owing to newly developed myeloma agents, particularly proteasome inhibitors (PIs), immunomodulatory drugs (IMiDs) and monoclonal antibodies (mAbs), the outcome for patients with MM has significantly improved in recent years (2), making it possible, at long last, to cure a tangible number of patients (3). However, in the great majority of cases, following a period of successful therapy, myeloma relapses as a drug-refractory, aggressive disease that leaves few, if any, therapeutic options. The root causes of progression to relapsed and/or therapy-refractory myeloma (RRMM) include tumor cell-intrinsic changes such as point mutations in drug response genes (4), copy number alterations that may abrogate tumor suppressor pathways (5), epigenomic aberrations modifying gene expression (6), and increased cancer stemness, which may impact lineage fidelity and tumor dormancy to name but two changes (7). An equally important yet tumor cell-extrinsic driver of RRMM pathophysiology is the tumor microenvironment (TME), which provides myeloma-promoting interactions with resident BM cells, including specimens of the innate and adaptive immune system (8). Enhanced understanding of immune regulation of the BM microenvironment (BMME) has not only shed light on pathways of myeloma progression but also greatly advanced myeloma treatment over the past decade (9).

Mouse models of human myeloma have provided preclinical research tools for elucidating the role of the immune system in the natural history of plasma cell neoplasia and in assessing candidate immunotherapies for myeloma (10, 11). Numerous experimental model systems are available, however, none perfectly replicate human myeloma (**Figure 1**). The most widely used models rely on *in vivo* propagation of human myeloma cells in immunodeficient hosts (human-in-mouse xenografting) (12–14) or myeloma-like plasma cells from C57BL/6 (B6) (15) or BALB/c (C) mice (16) in genetically compatible (syngeneic) immunocompetent hosts (mouse-in-mouse autografting). Both strategies have made and continue to make important contributions to myeloma research (17, 18), but are hampered by the reality that *in vivo* transfer of malignant cells (tumor transplantation) is not suitable for studying tumor development (oncogenesis). In other words, xeno- and autografting of neoplastic plasma cells bypasses the natural course of human myelomagenesis that begins with monoclonal gammopathy of undetermined significance (MGUS) (19), progresses to smoldering myeloma (SMM) (20), and eventually transitions to frank neoplasia (NDMM). Laboratory mice, in which plasma cell tumors (PCT) arise *de novo* (spontaneously) in a fully immunocompetent microenvironment, may remedy this shortcoming yet are undermined by other limitations, including complex breeding schemes, cost and time. Here we review the contribution of mouse models to advances in immunopathology and -therapy of human myeloma, discuss strengths and weaknesses of different experimental approaches, and outline opportunities for closing knowledge gaps.

Abbreviations: BM, bone marrow; BMME, bone marrow microenvironment; B6, C57BL/6; C, BALB/c; Ig, immunoglobulin; IMiD, immunomodulatory drug; IP, intraperitoneal; IV, intravenous; mAb, monoclonal antibody; MGUS, monoclonal gammopathy of undetermined significance; MM, multiple myeloma; NDMM, newly diagnosed multiple myeloma; PI, proteasome inhibitor; RRMM, relapsed/refractory multiple myeloma; SC, subcutaneous; SMM, smoldering multiple myeloma; TME, tumor microenvironment.

IMMUNOPATHOLOGY AND -THERAPY OF MULTIPLE MYELOMA

Immune Editing and Immune Dysfunction in Myeloma

As mentioned above, frank myeloma is invariably preceded by the precursor conditions MGUS (19) and SMM (21). MGUS is, in most cases, asymptomatic (22) and is usually detected years before frank MM manifests. MGUS progresses to active myeloma at the slow and constant rate of approximately 1% per year (21, 23). Consistent with the more advanced stage of tumor development, the progression rate of SMM is higher: 10% per annum in the first 5 years and 3% thereafter (24). Notably, BM plasma cells of individuals with MGUS exhibit a gene expression profile that is highly similar to that of myeloma (25) and MGUS plasma cells contain many of the cytogenetic changes (chromosomal translocations, gains and deletions) typically seen in myeloma cells (26–28). These findings have long raised suspicion that MGUS may in fact be a malignancy that is suppressed by a strong, extrinsic force, such as a cognate cytotoxic immune response (immune surveillance). Because most cases of MGUS do not progress to MM, this surveillance mechanism must be effective and enduring, essentially covering the entire lifespan of most individuals harboring an aberrant plasma cell clone of this sort. A large body of recent work expertly reviewed elsewhere (29, 30) strongly suggests that the breakdown of immunologic surveillance is at the heart of the MGUS-to-MM transition. According to this theory, known as cancer immunoediting (**Figure 2A**), the immune system is initially highly successful in eliminating abnormal plasma cells (Elimination stage), but then switches to an impasse that permits a limited number of these cells to survive in a quiescent or dormant state (Equilibrium) that may last for many years in individuals with MGUS (34). For reasons that are not yet clear, the equilibrium is eventually disrupted in a subset of patients, allowing the aberrant cell clone to evade immune control (Escape) and fuel the malignant growth that underlies active

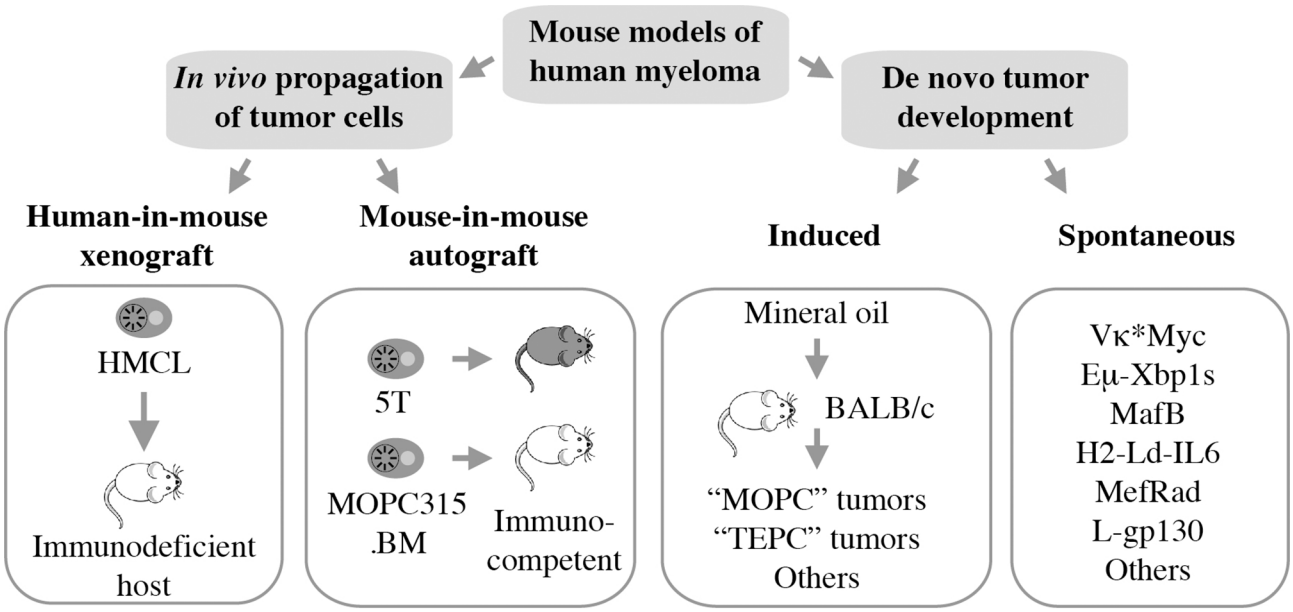

FIGURE 1 | Mouse models of human myeloma. Xeno- and autografting relies on *in vivo* propagation of fully transformed tumor cells. Models of tumor development include peritoneal plasmacytomas that can be readily induced in genetically susceptible BALB/c mice and myeloma-like tumors that arise spontaneously in a variety of transgenic mice.

myeloma. In sync with that scenario, immune suppression caused by regulatory T cells, myeloid derived suppressor cells (MDSC) and dysfunctional effector T lymphocytes, is a hallmark of NDMM (**Figure 2B**). Growth and survival support of myeloma cells by innate immune cells, including conventional and plasmacytoid dendritic cells (35, 36) and eosinophils (37), is the flip side of the same coin. Of practical relevance for patient care is the knowledge that immune dysfunction in patients with myeloma may lead to increased risk of infections (38) and lack of a vigorous vaccination response (39) – something to be mindful about in the midst of SARS-CoV-2 (40).

Immunotherapy of Myeloma

The past decade has witnessed tremendous progress in immunotherapeutic approaches to myeloma. Authoritative and up-to-date reviews are available (29, 41). Current FDA-approved interventions include monoclonal antibodies targeting CD38 [daratumumab (42), isatuximab (43)] or SLAMF7 [elotuzumab (44)] on the surface of tumor cells. An antibody-drug conjugate (ADC) that binds to BCMA [belantamab mafodotin (45)] has also been approved just recently. Additional BCMA-targeted therapies, in particular chimeric antigen receptor (CAR) T cells and bispecific T cell engagers (BITEs), are in advanced stages of clinical development. Immune modulation using small-drug inhibitors of cereblon, a component of an E2 ubiquitin ligase complex, is also approved for treatment of myeloma and is widely used for maintenance therapy internationally. Immunomodulatory drugs of this sort, dubbed IMIDs, include thalidomide (46), lenalidomide (47, 48), and pomalidomide (49). Next-generation cereblon-targeting agents that promise to overcome acquired resistance to IMIDs are in clinical trial (50). **Figure 2C** provides an overview of myeloma immunotherapies in clinical use. Not shown are proteasome inhibitors (PIs), a class of targeted myeloma agents that, in the past, have not been associated with immune-mediated myeloma-inhibiting effects. However, recent work demonstrates that modulating the immune microenvironment of myeloma, by virtue of inducing immunogenic cell death (51), primes a cytotoxic immune response to tumor cells, thereby contributing to disease control in a proteasome-independent manner.

XENOGRAFT MODELS OF MYELOMA

Propagating Human Myeloma Cell Lines (HMCLs) in NSG and NRG Hosts

Many advances in the field of myeloma biology, genetics, and therapy would not have been possible without preclinical investigations that relied on immunocompromised mice for hosting human myeloma cells. Human-in-mouse xenografting has a long and distinguished history in cancer, including myeloma research, beginning in the early 1960s with the discovery of the T lymphocyte-deficient nude mouse. This marked the inception of a developmental pipeline of mice that feature increasing levels of immunodeficiency. SCID (severe combined immunodeficiency) and Rag mice lack both T and B

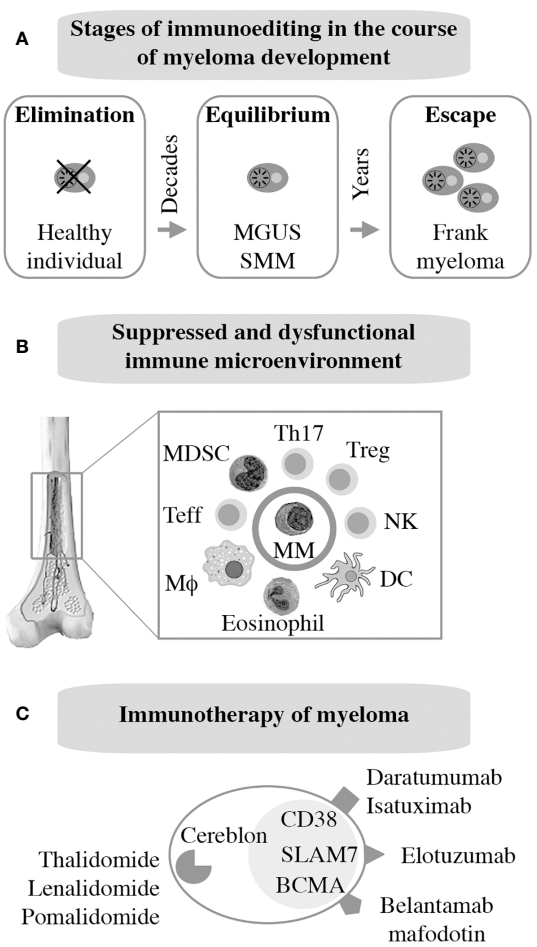

FIGURE 2 | Immunopathology and -therapy of myeloma. Evidence indicates that myeloma development is promoted, in part, by the gradual breakdown of immunosurveillance **(A)**. Consequently, patients with myeloma have a suppressed and dysfunctional immune microenvironment **(B)**. 2 subsets of Tregs that discriminate MGUS from MM (31); 2 subsets of terminal effector T cells (T_{TE}) are involved in MGUS to MM transition (32); Attrition of BM-resident T cells due to loss of "stem-like" TCF1/7hi T cells may underlie loss of immune surveillance in myeloma (33). Enhanced understanding of this microenvironment has been key for the development of immunotherapies of myeloma **(C)**.

lymphocytes. The underlying genetic defects are loss-of-function mutations in *Prkdc* (protein kinase, DNA activated, catalytic polypeptide) and *Rag1* or *Rag 2* (recombination activating gene 1 or 2), respectively. Transfer of the SCID and Rag mutations on the genetic background of NOD (non-obese diabetic) led to NOD-SCID and NOD-Rag mice, which exhibit a NK (natural killer) defect on top of T and B deficiency. In addition to diminished NK cell function, NOD leads to lack of circulating complement due to deletion of the C5-encoding *Hc* gene and proclivity to Type 1 diabetes mellitus due to autoimmune insulinitis (52). Further modification of NOD-SCID and NOD-Rag mice by crossing in IL2Rγ (interleukin-2 receptor subunit gamma) deficiency resulted in strains NSG and NRG, which are devoid of T, B and NK cells. Lack of IL2Rγ (a.k.a. CD132 or common gamma chain, γ_c) abrogates NK cells and compromises at least 6 interleukin signaling pathways: IL-2, 4, 7, 9, 15 and 21 (**Figure 3B**). NSG and NRG mice, which are commercially available and widely used in myeloma research, readily permit engraftment of human myeloma cells upon subcutaneous (SC), intravenous (IV), intraperitoneal (IP), or intratibial injection (53, 54). Strengths and limitations of myeloma xenografting have been reviewed in great depth elsewhere (55). Care must be taken to select the most appropriate HMCL for a given research question, as significant differences between cell lines exist (56, 57). 3D *in vitro* culture of myeloma cells using a variety of artificial scaffolds is an emerging technology that competes with xenografting and holds promise for drug testing for personalized myeloma therapy (58).

Engrafting Patient-Derived Myeloma Cells in Implanted Bone Chips

Major limitations of myeloma xenografting described above include the reality that tumor growth occurs mostly outside the BM and primary patient-derived tumors do not grow at all. The latter is a fundamental flaw caused by the stringent dependency of myeloma cells on support from the human BMME. HMCLs do not exhibit this dependency because they are derived from malignant plasma cells that circulated in the peripheral blood or occurred in body cavity effusions of patients with plasma cell leukemia, the end stage of myeloma progression. The derivation from leukemic cells is also in line with the extramedullary growth pattern (plasmacytoma) of HMCL-in-mouse xenografts mentioned above. To provide a TME that is more conducive for primary myeloma cells, investigators modified SCID mice by implanting small pieces of human or rabbit bone subcutaneously. Synthetic 3D scaffolds serving as surrogate bone provide an alternative approach. These experimental model systems have come to be known as SCID-hu (12, 59–61), SCID-rab (62), and SCID-syn (14) (**Figure 3A**). They are equally capable and have greatly enhanced preclinical myeloma research (10, 11) by addressing knowledge gaps in treatment and pathophysiology: SCID-hu (63–65), SCID-rab (66–68), and SCID-syn (69, 70). However, more widespread use of these models is hampered by ethical and practical limitations, such as reliable provision of fetal human bone and difficulties in administering human myeloma cells to small implants. The fact that fetal BM does not equate with adult BM in terms of cellular composition and immune milieu, and that rabbit or synthetic bone does not fully recapitulate the myeloma-supporting properties of human bone adds an additional biological limitation. This backdrop helps explain why the use of SCID-hu, SCID-rab, and SCID-syn has been declining in recent years and why researchers have been looking for alternative strategies to propagate myeloma in laboratory mice. The most promising development to date is the humanization of NRG mice, as described below.

Maintaining MGUS/SMM Plasma Cells in Humanized NRG Mice

Gene targeting in embryonic stem cells is a convenient research tool for substituting mouse genes with human counterparts and,

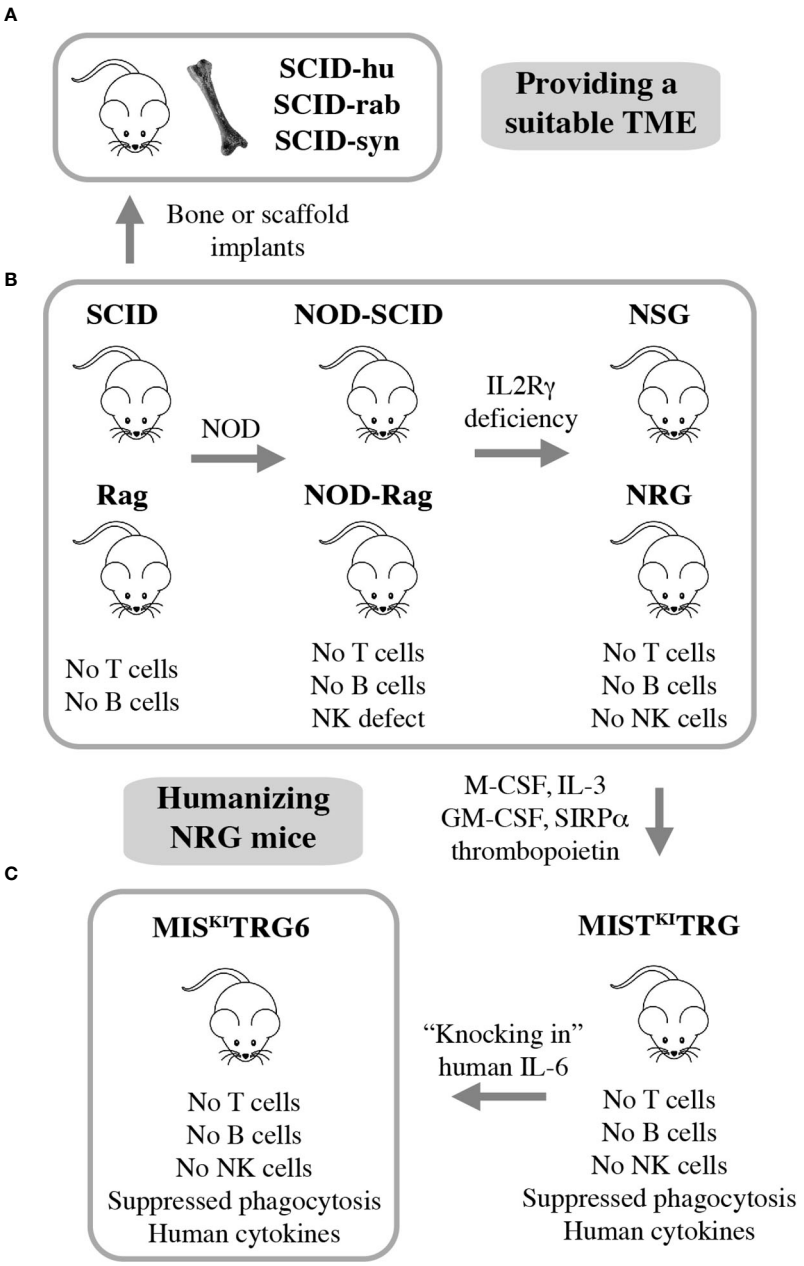

FIGURE 3 | Xenografting human myeloma in immunodeficient mice. NSG and NRG mice are widely employed for preclinical studies using human myeloma cell lines (HMCLs) but are limited in terms of hosting primary, patient-derived myeloma cells **(B)**. Implantation of bone chips or artificial scaffolds in SCID mice can overcome this limitation **(A)** but is faced with practical limitations and the inability to support MGUS and SMM plasma cells. Additional incremental steps in humanizing NSG and NRG mice may solve this problem. A promising step in this direction is the recent development of IL-6 transgenic MIS^{KI}TRG mice, which can support homing and survival of plasma cells not only from patients with frank and smoldering MM but also individuals with MGUS **(C)**.

thereby, humanizing laboratory mice. This approach has generated highly immunodeficient mice in which two major obstacles to engraftment of human cells have been largely overcome: innate immune rejection *via* phagocytosis and lack of activity of certain cytokines and growth factors across the human-mouse species barrier (71). Strain MIS$^{(KI)}$TRG is an excellent example of recent developments. It features, on the genetic background of NRG, the expression of 5 human "knock in" genes encoding M-CSF (macrophage colony-stimulating factor a.k.a. colony stimulating factor 1 or CSF1), IL-3 (interleukin-3), GM-CSF (granulocyte-macrophage colony-stimulating factor a.k.a. colony stimulating factor 2 or CSF2), SIRPα (signal regulatory protein α), and thrombopoietin (72). MIS$^{(KI)}$TRG mice exhibit improved engraftment of

hematopoietic stem and progenitor cells and lend themselves to hosting PDX (patient-derived xenograft) tumors from many human cancer types. However, these mice were still unsuitable for stable engraftment of primary myeloma cells. Cognizant of the critical role of IL-6 for growth and survival of neoplastic plasma cells (73), Madhav Dhodapkar and his associates added a human IL-6 allele to strain MIS$^{(KI)}$TRG, thus generating IL-6 transgenic MIS$^{(KI)}$TRG, or MIS$^{(KI)}$TRG6 mice (**Figure 3C**) (74). The introduction of human IL-6 resulted in a remarkable breakthrough for preclinical myeloma research, because for the first time it allowed engraftment and propagation of primary MM cells in a reliable and reproducible fashion. What is more, MIS$^{(KI)}$TRG6 supported engraftment of SMM and MGUS plasma cells upon transfer of CD3-depleted BM mononuclear cells to recipient bone. The finding that, unlike NDMM cells, RRMM cells actively homed to and expanded in other sites of the skeleton resembled the more advanced tumor progression stage of relapsed compared to new myeloma. Finally, while RRMM remained confined to bone, tumor samples from patients with plasma cell leukemia demonstrated the kind of systemic, extramedullary dissemination pattern that one might expect from a leukemic cell clone.

Utility of Myeloma Xenografting in Immunotherapy Research

Of the three principal model systems of myeloma xenografting described above, the HMCL-in-mouse approach, has probably had the greatest impact on immunotherapy research in myeloma. While MIS$^{(KI)}$TRG6 mice have not yet been used to that end, the implantation-based SCID models have largely been supplanted by HMCL-in-mouse xenografts, as mentioned above. Indeed, HMCL xenografting appears to lend itself readily to the complex requirements of experimental immunotherapy. Often this involves adoptive immune cell transfer to study mice and testing of new therapeutic antibodies or antibody-drug conjugates (ADCs) in mice co-treated with established myeloma drugs or candidate small-drug inhibitors. HMCL xenografts are often used as a first choice when the efficacy of cytotoxic T cells, NK cells, or engineered killer cells to remove myeloma in an intact organism *in vivo* is to be evaluated. To highlight but a few examples of their utility, HMCL xenografts have majorly contributed to the development of CAR-T treatments for BCMA (75) and newly emerging CAR-T targets such as CD229 (SLAMF3, LY9) (76). HMCL xenografts have been successfully employed to assess a monoclonal antibody to transferrin receptor 1, a newly emerging molecular target expressed on the surface of myeloma cells (77, 78). Similarly, HMCL xenografts have been used to evaluate AMG 701, a half-life extended BITE that binds to BCMA on myeloma cells and CD3 on T cells (79), and to demonstrate that the therapeutic efficacy of daratumumab in myeloma may be enhanced when CD38 in NK cells has been deleted (80). This body of work illustrates the rapid evolution of the myeloma immunotherapy landscape and that HMCL xenografting is poised to add further value to the field as we go forward.

AUTOGRAFT MODELS OF MYELOMA

5TMM

The 5T mouse model of human multiple myeloma, or 5TMM for short, is a versatile research tool for fundamental and applied studies on plasma cell malignancies. The model is based on the genetic proclivity of inbred C57BL/KaLwRij mice (closely related to the commonly used C57BL/6) (81) to spontaneously develop a benign monoclonal gammopathy (serum paraprotein) or MGUS-like condition (82) that can progress to frank myeloma (15, 83). Using serial *in vivo* propagation of bone marrow cells from independent C57BL/KaLwRij donors containing different paraproteins, a number of transplantable myeloma-like plasma cell tumors were generated (**Figure 4A**). Two of these, dubbed 5T2 and 5T33, were fully established and generously shared with qualified investigators in Europe, the United States, and elsewhere. 5TMM tumors cause osteolytic lesions (83) and recapitulate other features of human myeloma bone disease (84, 85). 5TMM tumors grow in a fully immunocompetent BMME and are easily tracked *in vivo* using radiological methods including X-ray and PET imaging (86). Unlike 5T2, which can only be maintained by passaging from mouse to mouse, two continuous cell lines were derived from 5T33: 5TGM1 (87, 88) and 5T33vt (89). The genetic differences between these cell lines and 5T2 have been recently determined using NGS (90). This revealed an additional strength of 5TMM in regard to modeling human myeloma; i.e., the significant overlap of patterns of somatic mutations across the human-mouse species barrier, particularly with respect to copy number changes of genes involved in gain of 1q and deletion of 13q in human myeloma (90). The availability of cell lines, 5TGM1 and 5T33vt, has greatly enhanced the flexibility and impact of the 5TMM model. For example, the cells can be easily modified by virtue of enforced up or down regulation of genes of interest or the introduction of reporter genes for whole-body fluorescence or bioluminescence imaging of tumor growth in a quantitative, objective manner (91). The cell lines have also facilitated the examination of myeloma-immune interactions *in vitro* and *in vivo*. For example, an early study using 5TGM1 demonstrated that myeloma cells inhibit the differentiation of BM-derived dendritic cells (DCs) and interfere with their function to induce cytotoxic and humeral immune responses (92). This is relevant for ongoing efforts in human myeloma to use DCs for vaccination approaches aimed at eliciting a robust T cell-dependent cytotoxic immu response (93).

5TMM as Research Tool for Immune Regulation of Myeloma

The broad utility of 5TMM for studies on the immunopathology and -therapy of myeloma was recognized soon after the first tumors were established. Initial investigations described the role of the paraprotein idiotype (Id) in immune regulation (94) and immune therapy (95) of plasma cell neoplasia. Follow-up studies relying on 5TGM1 demonstrated that the idiotype is a myeloma-specific antigen that can induce an Id-specific cytotoxic T cell (CTL), T helper 1 (Th1) and T helper 2 (Th2) response (96).

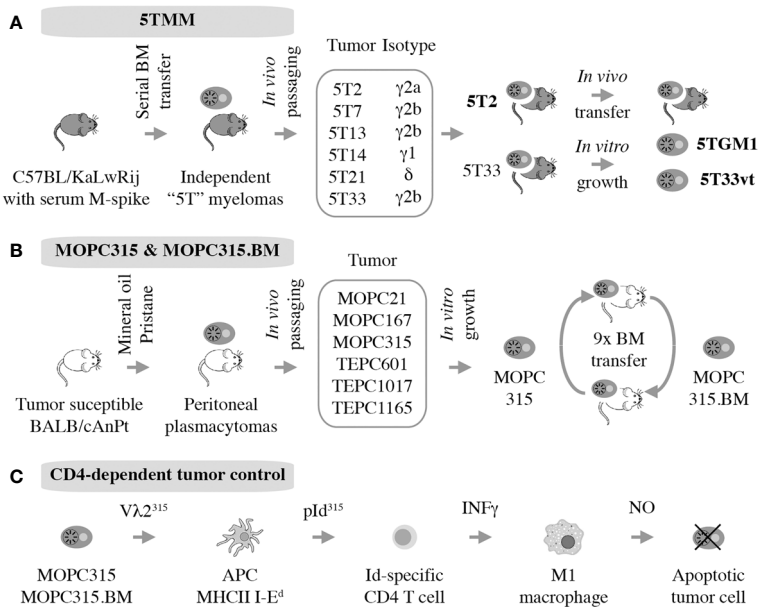

FIGURE 4 | Autografting mouse myeloma in immunocompetent mice. Two models have been established. 5TMM is on a genetic background that is highly similar to B6 and includes two continuous cell lines, 5TGM1 and 5T33vt, that are widely used **(A)**. MOPC315 is a peritoneal plasmacytoma on the genetic background of C that has given rise to a BM-seeking subline, MOPC315.BM, that holds great value for myeloma immunology research. **(B)** Decades of research by Bogen and colleagues have shown indirect CD4+ T cells mediated killing via interactions with cytotoxic macrophages, further demonstrating the utility of MOPC315.BM as an immunological research tool **(C)**.

CTLs and Th1s were found to suppress myeloma growth, whereas Id-specific Th2 cells promoted it (96) – a preclinical clue in support of the contention that modulation of the Th1:Th2 axis might have therapeutic benefits in myeloma. The finding that 5T-bearing mice exhibit an increase in the ratio of regulatory T cells (Tregs) to T effector cells (97) proved relevant for human myeloma when it became clear that patients with new disease contain elevated numbers of Tregs in the peripheral blood (98). With respect to myeloma immunotherapy, the 5T33 model made conceptual contributions to developing DC-based MM vaccines for idiotype protein (99). This included the design of more effective adjuvants based on CpG and IFN-α (100) and the realization that myeloma cell lysates provide a more powerful DC vaccine than idiotype protein and adjuvant, alone (101). These advances were confirmed in a clinical study a few years ago showing that a patient-derived DC-MM cell fusion (hybridoma) vaccine improved the therapeutic response in a quarter of myeloma patients post-ASCT from partial to (nearly) complete (102). 5TMM has also been used to examine immunomodulatory myeloma treatments at the preclinical level; e.g., investigators demonstrated that CD4 T cells were vital for lenalidomide's activity, while NK, B or CD8 T cells were not (103). Activation of innate-like invariant natural killer T (iNKT) cells, a cell type that has not yet been extensively examined in human myeloma, led to significantly increased survival of 5T33-bearing mice (104). The 5T33 model has also contributed early on to the CAR-T therapy field by showing that treatment using NKG2D-targeted CAR-T cells prolonged survival of tumor-bearing mice and induced a tumor-specific memory response (105). Furthermore, 5T33 not only demonstrated efficacy of immune checkpoint inhibitor (CPI) therapy using antibody to programmed death receptor-1 (PD-1) or its ligand (PDL-1), but also showed that $CD8^+$ T cells in tumor-bearing mice post-ASCT significantly upregulated PD-1 (106, 107). In summary, the practical limitation to *in vivo* studies using 5TMM requiring the genetic background of C57BL/KaLwRij (108) is a small inconvenience compared to the potential contribution of this model to aiding immunotherapy development for patients with myeloma.

MOPC315.BM

MOPC315 is an IgA-producing peritoneal plasmacytoma (PCT) that arose half a century ago (109) in a BALB/c (C) mouse treated with intraperitoneal injections of mineral oil (110). MOPC315 has been used for decades in studies on immune regulation of malignant plasma cell growth (111, 112) although it is not representative of human MM, which grows in the hematopoietic BM and depends on the BMME for survival. In a major step forward, this shortcoming was remedied by the development of a subline of MOPC315, dubbed MOPC315.BM, generated by serial IV autografting of BM-derived plasma cells for nine generations. In the course of *in vivo* propagation, tumor cell variants with exquisite affinity to the BM increased oncogenic potency (~1 month median survival of tumor-bearing mice), and capacity for BM homing and bone destruction were preferentially selected (**Figure 4B**). Transfection with a luciferase reporter further increased the utility the cell line (16). MOPC315.BM is now increasingly used in preclinical myeloma research. For example, it provided the foundation for recent studies on the involvement of IL-34 and notch signaling in

the pathophysiology of the focal and systemic bone loss in mice that mimics human myeloma bone disease (MBD) (113, 114). Additionally, MOPC315.BM has been employed to demonstrate that eosinophils and megakaryocytes support malignant plasma cell growth in the BM (115) and that oncolytic myxoma virus, in conjunction with ASCT, may be an effective treatment for PCT-bearing mice (116). Importantly, together with its parental line, MOPC315.BM has made major contributions to our appreciation of CD4 T cell responses in immunosurveillance and -therapy of myeloma (117), briefly summarized below.

Lesson on CD4-Dependent Control of Malignant Plasma Cell Growth

Strong evidence supports the significance of Id-specific CD4 T cells in clearance of MOPC315 plasma cells *in vivo* (118), confirming matching results in the 5TMM model described above. In a remarkable continuity of investigations that span more than 25 years, Bjarne Bogen and his colleagues have unequivocally shown that tumor cell-produced monoclonal Ig gives rise to a tumor-specific antigen (TSA) in the MOPC315 model system. The antigen is processed by professional antigen-presenting cells (APCs) that include tumor-infiltrating macrophages in the subcutaneous MOPC315 model and BM macrophages in the medullary MOPC315.BM model (119). With help of MHC class II-encoded I-E^d surface protein, APCs present the antigen to CD4 Th1 cells as a λ2 light-chain V region-derived idiotypic (Id) peptide; i.e., a neoepitope. This results in Th1-dependent production of IFN-γ, which activates bystander macrophages and promotes their polarization to the tumoricidal M1 phenotype. In turn, M1 macrophages upregulate inducible nitric oxide synthetase (iNOS) to produce and release nitric oxide (NO) into the extracellular milieu. NO then kills neighboring tumor cells using a mechanism that involves reactive nitrogen species (e.g., peroxynitrite) and activates the intrinsic pathway of programmed cell death (apoptosis). Thus, in the MOPC315 model system, $CD4^+$ T cells kill tumor cells indirectly with the assistance of cytotoxic macrophages (**Figure 4C**). MOPC315.BM has provided additional insights into myeloma immunology. Examples include the interaction of myeloid-derived suppressor cells and T cells *in vivo* (120), the development of allogeneic T cell treatments for myeloma that may circumvent GvHD (121, 122), and the evaluation of novel DNA vaccines for immunotherapeutic purposes (123). Similar to the inconvenience of the genetic background of 5TMM, MOPC315.BM is on the genetic background of BALB/c (C), which is not as widely used in cancer immunology as B6. However, this is a small price to pay considering the value MOPC315.BM can add to the immune revolution in myeloma treatment (124).

SPONTANEOUS PLASMA CELL TUMORS IN LABORATORY MICE

Inducible, Inflammation-Dependent Peritoneal Plasmacytoma

MOPC315 is but one representative of a large panel of peritoneal plasmacytomas that has been developed single handedly in the 1960s and 1970s by Dr. Michael Potter at the US National Cancer Institute, Bethesda, Maryland. He discovered that IP treatment of C mice using certain mineral oils (110) or a chemically defined component thereof, called pristane (2,6,10,14-tetramethylpentadecane) (125), induced development of MOPC (mineral oil induced plasmacytoma) and TEPC (tetramethylpentadecane induced plasmacytoma) tumors, respectively. Plasmacytomas induced in this fashion were crucial for basic research breakthroughs in antibody structure (126) and monoclonal antibody (hybridoma) technology, which began with MOPC21 (127). Unlike most inbred strains of mice, C is highly susceptible to plasmacytoma (128) due to a complex genetic trait that includes hypomorphic (weak efficiency) alleles of genes that encode the cell cycle inhibitor $p16^{INK4a}$ (129) and the FKBP12 rapamycin-associated protein Frap (130). Virtually all peritoneal PCTs harbor a *Myc*-activating chromosomal translocation (131) that takes the form of a balanced T(12;15) (*Igh-Myc*) in the majority (~85%) of cases. Plasmacytoma induction requires maintenance of mice in a non-SPF (specific pathogen-free) environment rich in antigenic stimuli including gut flora-derived antigens (132). Consistent with that, C mice raised under SPF or germ-free conditions exhibit a dramatically reduced tumor incidence (133) or fail to develop plasmacytoma altogether (134). Peritoneal plasmacytoma is the premier mouse model of inflammation-induced extramedullary myeloma has been used for decades to learn about immune regulation of malignant plasma cell growth (111, 112). However, BALB/c plasmacytomas are not widely used in myeloma research today because more accurate, transgenic mouse models of the disease have become available. These will be described in the following section.

Transgenic Mouse Models of Human Myeloma and Related Plasma Cell Neoplasms

Genetic modification of the mouse germline has been employed by several independent research groups to generate transgenic strains of mice that are prone to spontaneous plasma cell tumors (PCT) that replicate important features of human MM. Mice of this sort exhibit a predictable progression pattern from MGUS- and SMM-like precursor conditions to frank plasma cell neoplasia. This pattern is key for preclinical assessments of myeloma preventions, a hot topic in clinical myeloma research (135). PCT-prone mice feature a fully intact innate and adaptive immune system that is likely to adapt to tumor development much the same way as the human immune system adapts to myeloma (**Figure 2A**). Hence, trialing newly developed immunotherapeutics in mice that are genetically susceptible to PCT is poised to yield more complete and higher-quality information than one might get from mice that are immunocompetent but not undergoing tumorigenesis (136). The same argument can be made for the preclinical testing of complex treatment regimens that combine HSC transplantation and established myeloma drugs (PIs, IMiDs) with novel immunotherapies and small-compound inhibitors. Evaluating these types of treatment in PCT-susceptible mice may more

closely mimic the response of myeloma patients exposed to triplet and quadruplet drug regimens (137). **Figure 5** presents a developmental timeline of genetically engineered mouse models (GEMMs) of human myeloma and related malignancies. **Table 1** provides details on tumor incidence and phenotype, genetic drivers of tumor development, and genetic background of mice. An exhaustive discussion of individual models is beyond the scope of this review. To that end, the reader is referred to the primary literature and outstanding recent reviews from Tassone (55), Vlummens (138) and their associates. A general rule that may be gleaned from the table is that single-transgenic models exhibit delayed tumor onset and a relatively low tumor incidence. To accelerate plasma cell neoplasia, investigators have taken advantage of oncogene collaboration in double-transgenic mice, such as IL6Myc (139) and Bcl-X_LiMyc (140), that exhibit short tumor onset and full penetrance of the malignant phenotype (100% tumor incidence). Inducible transgenes such as L-gp130 (141) and models based on adoptive transfer of genetically modified B cells (142–144) serve the same purpose; i.e., faster and more consistent tumor development. Importantly, Vκ*MYC, developed by Marta Chesi and Leif Bergsagel at Mayo and generously shared with investigators in many countries, is the only model at this juncture for which robust immunology work is available. This is one of several reasons why Vκ*MYC is widely considered in the myeloma community as the gold standard of mouse models. Advances in immunosurveillance and immunotherapy of myeloma made possible by Vκ*MYC will be briefly discussed below.

Advances in Myeloma Immunology Made Possible by Vκ*MYC

The realization that Vκ*MYC-dependent myeloma causes changes in immune regulation in mice comparable to changes seen in patients with myeloma (145) laid the foundation for mechanistic studies describing role of specific pathways of immunity to Vκ*MYC-driven tumor development. The first investigation along this line revealed the importance of CD226 for immune surveillance of myeloma. Lack of CD226 reduced the anti-myeloma response of NK and CD8 T cells, resulting in quicker tumor progression and decreased overall survival of Vκ*MYC mice (146). Another insight afforded by Vκ*MYC concerned the intriguing link between microbial gut flora and IL-17-driven tumor progression. The underlying mechanism is complex but involves an increase in Th17 cells and activation of eosinophils. Not coincidentally, therapeutic control of these changes using antibodies to IL-17 and IL-5 delayed tumor progression (147). Vκ*MYC also provided definitive genetic evidence on the involvement of the pro-inflammatory cytokine IL-18 in myeloma progression (148). This was attributable to IL-18-dependent generation of myeloid-derived suppressor cells (MDSCs), an important driver of the dysfunctional immune environment in human myeloma (**Figure 2B**). Another study demonstrated that tumor progression and dissemination in Vκ*MYC is not under exclusive control of the TME. Insead, it is regulated, in part, by properties of tumor cells such as expression of CD138 (149) (**Figure 6A**). Vκ*MYC has also impacted the field of myeloma immunotherapy in more ways than one. One study showed that treatment of mice using IAP (inhibitor of apoptosis) antagonists activated an acute inflammatory response that led to enhanced tumor phagocytosis by macrophages. Interestingly, co-treatment using antibody to PD1 led to an additional increase in survival of mice (153). By implicating the upregulation of TIGIT (T-cell immunoglobulin and ITIM domain) on CD8 T cells, Vk*MYC has also contributed to our understanding of T cell exhaustion in myeloma. Checkpoint blockade of TIGIT prolonged survival of mice and reduced levels of immunosuppressive IL-10 produced by dendritic cells (154–156). Finally, studies using Vk*MYC demonstrated that: blocking type 1 interferon signaling may inhibit Treg expansion in myeloma (157), antibody to CD137 holds promise as a consolidation treatment in myeloma (158), and HSC transplantion may facilitate both a robust anti-MM CD8 T cell response and a myeloma-specific T cell memory (159)

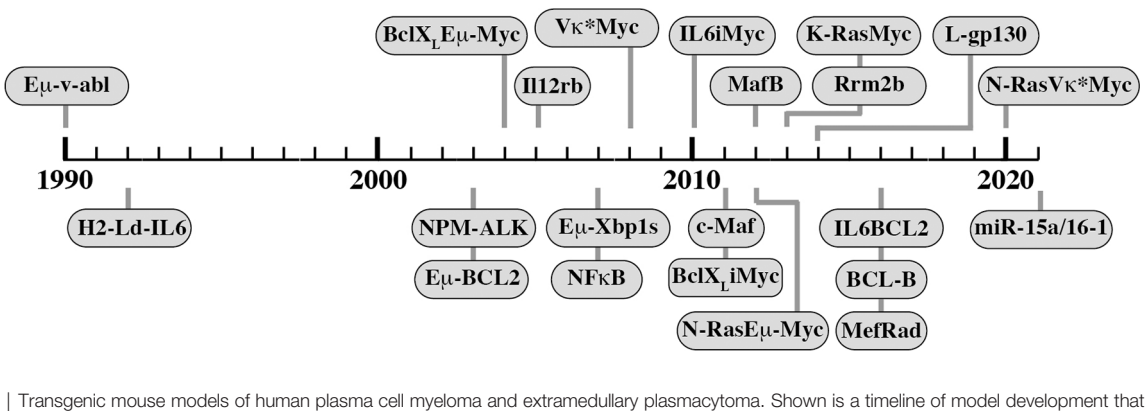

FIGURE 5 | Transgenic mouse models of human plasma cell myeloma and extramedullary plasmacytoma. Shown is a timeline of model development that begins with Eμ-v-abl developed by Susan Cory's group at WEHI and published in 1990. The H2-L^d-IL6 model of human plasmacytoma published in 2002 gave rise to the double-transgenic MycIL6 and BCL2IL6 models that take advantage of oncogene collaboration to accelerate neoplastic plasma cell development. Similarly, Vκ*MYC, the premier model of myeloma immunology research, was recently accelerated by breeding in a mutated *Ras* gene, leading to the highly promising VQ model published in 2020.

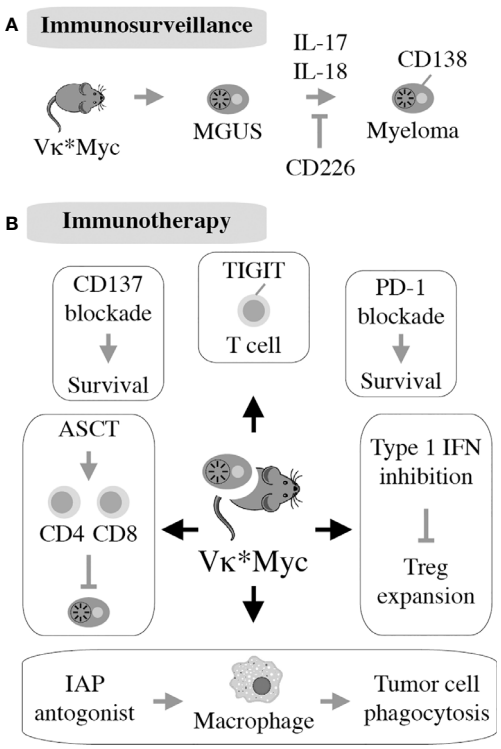

FIGURE 6 | First described in 2008, the Vk*MYC model takes advantage of AID-activated MYC to induce myeloma on the B6 background. All 122 mice in the original study had monoclonal plasma cell expansion in the BM resembling human MM. Eighty percent of mice had measurable M-spike by 50 weeks of age. Additionally, aged Vk*MYC mice displayed many hallmarks of human MM, including bone loss and protein deposition in the kidneys (150). This allows for thorough studies of the MGUS to MM transition in this model **(A)**. Vk*MYC mice accurately predict clinical efficacy of myeloma drugs (151) and provide a good model for experimental oncolytic immunotherapy (152) **(B)**.

(**Figure 6B**). The impressive body of work summarized above strongly suggests that Vk*MYC provides a valuable blueprint for immunological studies using other mouse myeloma models included in **Table 1**.

RESEARCH GAPS AND FUTURE DIRECTIONS

Following in the Footsteps of Vκ*MYC

One line of future investigation should be aimed at determining whether the immune changes seen in tumor bearing Vk*MYC mice also occur in other strains of mice prone to spontaneous PCT (**Table 1**). Independent confirmation would lend support to the contention that the observed changes represent bona fide biological sequelae of neoplastic plasma cell development rather than a special feature of this particular model. Uncovering significant differences in immune cell compartments or pathways of immunity between different mouse models may also be of value because it may help investigators match a particular type of human myeloma in terms of progression stage (e.g., NDMM vs RRMM), outcome risk (e.g., standard *vs* high risk), or molecular subgroup (184) with the most appropriate mouse counterpart. Since human myeloma exhibits a great deal of diversity in cytogenetic, gene expression, epigenetic, immunologic, and other features (185), MM should be represented by a collection of models that mirror that diversity. However, this goal has not yet been achieved as the models listed in **Table 1** represent but a narrow snapshot of the human myeloma landscape. With the exception of the most recently developed model that relies on a Cre recombinase effected loss of the microRNA-encoding tumor suppressor locus, *miR-15a/16-1*, malignant development is driven in these models by a limited set of oncogenes on the uniform, homogeneous genetic background of inbred mice (186). The overrepresentation of Myc, IL-6, and Bcl-2 family genes, particularly among the more thoroughly investigated models, underscores the narrowness and redundancy of the present situation.

Be this as it may, Vk*MYC and related models stand ready both to shed light on long-standing questions in myelomagenesis, such as the role of antigen and germinal center reentry of tumor precursors (187) and to revisit difficult issues in myeloma immunotherapy, such as the benefits of immune checkpoint inhibition (CPI) (188), which remain unclear at this juncture (189). Since Vk*MYC mice undergoing IAP inhibition responded to CPI with increased survival (153), in-depth analysis of that response may provide clues for how to incorporate CPI in human myeloma treatment protocols. Vk*MYC and other transgenics may also assist in validating novel immunotherapies that are emerging from exploratory studies using transplantation-based mouse models. Two recent advances that relied on 5TMM and HMCL, respectively, concerned the combination of vaccination and epigenetic therapies (190) and a neat strategy for enhancing the efficacy of daratumumab by genetic engineering of NK cells (191). Considering the increased interest of the clinical myeloma community in tumor prevention (192), Vk*MYC and related models may also afford opportunities for the preclinical evaluation of candidate interventions to block the progression of high-risk MGUS and SMM to frank myeloma.

Toward a Robust PDX Model of MM

Despite the breakthrough accomplishments of the MIS$^{(KI)}$TRG6 mouse described above, this xenograft model of human myeloma is still limited compared to well-established PDX (patient derived xenograft) models of solid cancer (193) and emerging PDX models of lymphoma (194). Biological limitations of MIS$^{(KI)}$TRG6 and the parental strain, MIS$^{(KI)}$TRG, include proclivity to anemia and quick exhaustion of human grafts after cell or tissue transfer (195). There are also some thorny non-biological limitations, including intellectual property rights that have prevented the wider distribution of the MIS$^{(KI)}$TRG6 thus far. Hence, additional work is warranted to improve upon this model and develop humanized laboratory mice that lend themselves to the preclinical evaluation of myeloma immunotherapy and precision medicine approaches. To that end, a fundamental conceptual consideration is the recognition that increasing

TABLE 1 | Transgenic mice prone to spontaneous plasma cell tumors recapitulating hallmarks of human plasma cell neoplasms including multiple myeloma.

Row	Mouse model [1]	TG [2]	Back-ground [3]	Year [4]	Ref. [5]	Survival of mice [6]	Percent tumors [7]	Tumor phenotype [8]
1	Eμ-v-abl	1	B6	1990	(160, 161)	>1 year	60	PC
2	H2-Ld-IL-6	1	C	1992	(162, 163)	250 days	60	PC > Ly
3	NPM-ALK	1	B6, C	2003	(164)	18 weeks	100	PC
4	Eμ–BCL2	1	B6, C	2003	(165)	120 days	100	PC > Ly
5	$BclX_L$EμMyc	2	Mixed [16]	2004	(166)	50 days	100	PC > MM
6	Eμ-Xbp1s	1	B6	2007	(167)	2 years	20	MM > PC
7	NFκB	1	Mixed [17]	2007	(168, 169)	50 weeks	80	PC > Ly
8	Vk*Myc	1	B6 [18]	2008	(170)	660 days	100	MM
9	Il12rb	1	B6	2005	(171)	2 years	30	PC
4	IL6Myc [9]	2	C	2010	(136, 172)	12 weeks	100	PC > MM
10	c-MAF	1	B6	2011	(173)	>2 years	30	Ly > PC
11	$BclX_L$iMyc [10]	2	Mixed [19]	2011	(174)	135 days	100	PC > MM
12	N-RasEμMyc [11]	1	Mixed [16]	2012	(175)	75 days	100	Ly > PC
13	MafB	1	B6	2012	(176)	1 year	45	MM > PC
14	Rrm2b	1	B6	2013	(177)	30 days	30	PC
15	K-RasMyc [12]	2	C	2013	(139, 140)	50 days	100	PC
16	L-gp130 [12]	1	B6	2014	(178)	200 days	100	MM
17	IL6BCL2 [9,12,13]	2	C	2016	(141)	5 months	100	MM > PC
18	BCL-B	1	B6	2016	(179)	500 days	100	MM
19	MefRad	2	B6	2016	(180)	480 days	70	MM > PC
20	L-gp130 [14]	1	B6	2019	(138)	5 months	50	MM
21	N-RasVk*Myc [15]	2	B6	2020	(181)	350 days	60	MM
22	miR15a/16-1 [16]	2	B6	2021	(182)	>1 year	45	Ly > PC

[1] *Mouse models in chronological order of development, as shown in* ***Figure 5****.*
[2] *Mouse models rely on one transgene or two transgenes to drive tumor development.*
[3] *Genetic background of mice is either C57BL/6 (B6), BALB/c (C) or mixed.*
[4] *Publication year.*
[5] *Original reference. A follow-up publication is included in some cases to provide more complete information on survival, tumor incidence, and tumor phenotypes.*
[6] *Median, mean, or estimated survival of mice, depending on results available. Surrogate of tumor onset.*
[7] *Percent tumor incidence (rounded).*
[8] *Phenotypes include plasma cell myeloma (MM), plasmacytoma (PC), and B lymphoma (Ly). The latter often exhibits plasmablastic features. The preponderance of a particular phenotype is indicated by a "larger than" symbol for models yielding different phenotypes.*
[9] *Using the same IL6 transgene as in row 2.*
[10] *Using the same Bcl-X_L encoding BCL2L1 transgene as in row 5.*
[11] *Using the same Myc transgene as in row 5.*
[12] *Model that relies on adoptive transfer of genetically modified B-lymphocytes to a preconditioned host in which neoplastic plasma cell development takes place.*
[13] *Using the same BCL2 transgene as in row 4.*
[14] *Using an inducible version of the transgene from row 16.*
[15] *Using the same Myc transgene as in row 8.*
[16] *Loss of microRNA in germinal center B cells effected by transgenic, AID-dependent Cre recombinase.*
[17] *(B6 x FVB/N) F1 hybrids*
[18] *B6 and SJL alleles.*
[19] *Transfer of Vκ*Myc onto background of C abolished cancer phenotype (183).*
[20] *B6, 129SvJ and FVB/N alleles.*

levels of immunodeficiency result in better engraftment of tumor cells (**Figure 3**) but diminished opportunities to assess the impact of the immune system on myeloma biology and treatment responses. One way to address this conundrum is a non-genetic form of humanizing mice by means of adoptive transfer of human hematopoietic stem and progenitor, T, NK, and other blood cells. All of these cells are easily obtained from patients with myeloma, particularly those undergoing SCT, and can be engrafted in mice together with BM-derived malignant plasma cells. Disadvantages of this approach include the small experimental window in the adoptively transferred mouse (on the order of a few days) and the high risk of GvHD that may distort study results (196).

A parallel way forward is to continue with the genetic humanization of laboratory mice. The aim is to generate humanized mouse PDX myeloma models that will be as promising for immunotherapy research as the new generation of mouse PDX carcinoma models is (197, 198). Molecular targets of humanization include components of the HSC niche (e.g., c-kit and Flt3) and biological pathways of myeloid and NK reconstitution (e.g., c-kit ligand and GM-CSF). Additional targets include the major histocompatibility complex (e.g., deletion of mouse beta-2 microglobulin) and, importantly, immune checkpoints such as CTLA-4, the CD47 "don't eat me" signal to macrophages, BTLA (CD272), TIM3, GITR, OX40 and others (199, 200). The long list of checkpoint genes underscores the elusiveness of humanizing the immune response of mice completely. The development of specialized, partially humanized mouse models dedicated to specific aspects of immunotherapy is therefore a viable compromise and a step in the right direction. A good example along this line is the generation of mice that contain a humanized form of cereblon (201), the molecular target of IMIDs. It renders the mice responsive to drugs of this sort, which are not active in normal mice. Three additional examples of humanized mouse models

relevant for myeloma research are NOG-hIL-6 (202), B6-hCD3E (170) and B6-hTIGIT (203), which facilitate preclinical studies on MDSCs, BITEs and CPI, respectively.

CONCLUSION

Although immunotherapy holds great promise for revolutionizing myeloma treatment (124), much remains to be learned. Currently, only a fraction of patients achieves a complete, long-lasting treatment response and a functional or definitive cure remains elusive for the great majority of patients. Accurate mouse models of myeloma are needed to close current knowledge gaps and accelerate the design and testing of new immunotherapies. The workhorses of preclinical myeloma research, HMCL-in-mouse xenografting and mouse-in-mouse autografting, will continue to be employed to that end, but we anticipate that humanized PDX models of myeloma (204) and transgenic mouse models of myeloma will become more important as we go forward. These models may elucidate the complex mechanisms underlying myeloma immunopathology and -therapy and minimize the risk of failure in challenging and expensive clinical trials. Sharing experimental model systems without strings attached, enhancing collaboration among regional core facilities and national reference centers, and establishing standards for high scientific rigor for the preclinical myeloma research will contribute to a future for patients with myeloma that is hopeful and bright.

AUTHOR CONTRIBUTIONS

MP performed the primary literature review and prepared the table. SJ edited the text, prepared the figures and formatted the final version. All authors contributed to the article and approved the submitted version.

FUNDING

This work was supported by the William G. Schuett, Jr., Multiple Myeloma Research Endowment. Additional support was provided by NCI R01CA204231 (to SR), NCI R01CA236814 and DOD CA180190 (to FZ) and NCI R01 CA151354 (to SJ).

REFERENCES

1. Rajkumar SV, Dimopoulos MA, Palumbo A, Blade J, Merlini G, Mateos MV, et al. International Myeloma Working Group Updated Criteria for the Diagnosis of Multiple Myeloma. *Lancet Oncol* (2014) 15:e538–48. doi: 10.1016/S1470-2045(14)70442-5
2. Rollig C, Knop S, Bornhauser M. Multiple Myeloma. *Lancet* (2015) 385:2197–208. doi: 10.1016/S0140-6736(14)60493-1
3. Barlogie B, Mitchell A, van Rhee F, Epstein J, Morgan GJ, Crowley J. Curing Myeloma At Last: Defining Criteria and Providing the Evidence. *Blood* (2014) 124:3043–51. doi: 10.1182/blood-2014-07-552059
4. Kortum KM, Mai EK, Hanafiah NH, Shi CX, Zhu YX, Bruins L, et al. Targeted Sequencing of Refractory Myeloma Reveals a High Incidence of Mutations in CRBN and Ras Pathway Genes. *Blood* (2016) 128:1226–33. doi: 10.1182/blood-2016-02-698092
5. Weinhold N, Ashby C, Rasche L, Chavan SS, Stein C, Stephens OW, et al. Clonal Selection and Double Hit Events Involving Tumor Suppressor Genes Underlie Relapse From Chemotherapy: Myeloma as a Model. *Blood* (2016) 128:1735–44. doi: 10.1182/blood-2016-06-723007
6. Agirre X, Castellano G, Pascual M, Heath S, Kulis M, Segura V, et al. Whole-Epigenome Analysis in Multiple Myeloma Reveals DNA Hypermethylation of B Cell-Specific Enhancers. *Genome Res* (2015) 25:478–87. doi: 10.1101/gr.180240.114
7. Nikesitch N, Ling SC. Molecular Mechanisms in Multiple Myeloma Drug Resistance. *J Clin Pathol* (2016) 69:97–101. doi: 10.1136/jclinpath-2015-203414
8. Gooding S, Edwards CM. New Approaches to Targeting the Bone Marrow Microenvironment in Multiple Myeloma. *Curr Opin Pharmacol* (2016) 28:43–9. doi: 10.1016/j.coph.2016.02.013
9. Gulla A, Anderson KC. Multiple Myeloma: The (R)Evolution of Current Therapy and a Glance Into Future. *Haematologica* (2020) 105(10):2358–67. doi: 10.3324/haematol.2020.247015
10. Paton-Hough J, Chantry AD, Lawson MA. A Review of Current Murine Models of Multiple Myeloma Used to Assess the Efficacy of Therapeutic Agents on Tumour Growth and Bone Disease. *Bone* (2015) 77:57–68. doi: 10.1016/j.bone.2015.04.004
11. Lwin ST, Edwards CM, Silbermann R. Preclinical Animal Models of Multiple Myeloma. *Bonekey Rep* (2016) 5:772. doi: 10.1038/bonekey.2015.142
12. Yaccoby S, Barlogie B, Epstein J. Primary Myeloma Cells Growing in SCID-hu Mice: A Model for Studying the Biology and Treatment of Myeloma and its Manifestations. *Blood* (1998) 92:2908–13. doi: 10.1182/blood.V92.8.2908.420a32_2908_2913
13. Miyakawa Y, Ohnishi Y, Tomisawa M, Monnai M, Kohmura K, Ueyama Y, et al. Establishment of a New Model of Human Multiple Myeloma Using NOD/SCID/gammac(null) (NOG) Mice. *Biochem Biophys Res Commun* (2004) 313:258–62. doi: 10.1016/j.bbrc.2003.11.120
14. Calimeri T, Battista E, Conforti F, Neri P, Di Martino MT, Rossi M, et al. A Unique Three-Dimensional SCID-polymeric Scaffold (SCID-Synth-Hu) Model for In Vivo Expansion of Human Primary Multiple Myeloma Cells. *Leukemia* (2011) 25:707–11. doi: 10.1038/leu.2010.300
15. Radl J, Croese JW, Zurcher C, Van den Enden-Vieveen MH, de Leeuw AM. Animal Model of Human Disease. *Multiple myeloma. Am J Pathol* (1988) 132:593–7.
16. Hofgaard PO, Jodal HC, Bommert K, Huard B, Caers J, Carlsen H, et al. A Novel Mouse Model for Multiple Myeloma (MOPC315.BM) That Allows Noninvasive Spatiotemporal Detection of Osteolytic Disease. *PloS One* (2012) 7:e51892. doi: 10.1371/journal.pone.0051892
17. Liu H, Liu Z, Du J, He J, Lin P, Amini B, et al. Thymidine Phosphorylase Exerts Complex Effects on Bone Resorption and Formation in Myeloma. *Sci Transl Med 8* (2016) 8(353):353ra113. doi: 10.1126/scitranslmed.aad8949
18. Higgs JT, Lee JH, Wang H, Ramani VC, Chanda D, Hardy CY, et al. Mesenchymal Stem Cells Expressing Osteoprotegerin Variants Inhibit Osteolysis in a Murine Model of Multiple Myeloma. *Blood Adv* (2017) 1:2375–85. doi: 10.1182/bloodadvances.2017007310
19. Weiss BM, Abadie J, Verma P, Howard RS, Kuehl WM. A Monoclonal Gammopathy Precedes Multiple Myeloma in Most Patients. *Blood* (2009) 113:5418–22. doi: 10.1182/blood-2008-12-195008
20. Muchtar E, Kumar SK, Magen H, Gertz MA. Diagnosis and Management of Smoldering Multiple Myeloma: The Razor's Edge Between Clonality and Cancer. *Leukemia lymphoma* (2018) 59:288–99. doi: 10.1080/10428194.2017.1334124
21. Kyle RA, Durie BG, Rajkumar SV, Landgren O, Blade J, Merlini G, et al. Monoclonal Gammopathy of Undetermined Significance (MGUS) and Smoldering (Asymptomatic) Multiple Myeloma: IMWG Consensus Perspectives Risk Factors for Progression and Guidelines for Monitoring and Management. *Leukemia* (2010) 24:1121–7. doi: 10.1038/leu.2010.60

22. Dispenzieri A. Monoclonal Gammopathies of Clinical Significance. *Hematol Am Soc Hematol Educ Program* (2020) 2020:380–8. doi: 10.1182/hematology.2020000122
23. Kyle RA. Monoclonal Gammopathy of Undetermined Significance and Smoldering Multiple Myeloma. *Eur J Haematol Suppl* (1989) 51:70–5. doi: 10.1111/j.1600-0609.1989.tb01496.x
24. Goyal G, Rajkumar SV, Lacy MQ, Gertz MA, Buadi FK, Dispenzieri A, et al. Impact of Prior Diagnosis of Monoclonal Gammopathy on Outcomes in Newly Diagnosed Multiple Myeloma. *Leukemia* (2019) 33:1273–7. doi: 10.1038/s41375-019-0419-7
25. Zhan F, Huang Y, Colla S, Stewart JP, Hanamura I, Gupta S, et al. The Molecular Classification of Multiple Myeloma. *Blood* (2006) 108:2020–8. doi: 10.1182/blood-2005-11-013458
26. Avet-Loiseau H, Facon T, Daviet A, Godon C, Rapp MJ, Harousseau JL, et al. 14q32 Translocations and Monosomy 13 Observed in Monoclonal Gammopathy of Undetermined Significance Delineate a Multistep Process for the Oncogenesis of Multiple Myeloma. *Intergroupe Francophone du Myelome. Cancer Res* (1999) 59:4546–50.
27. Kyle RA, Rajkumar SV. Monoclonal Gammopathy of Undetermined Significance. *Br J haematology* (2006) 134:573–89. doi: 10.1111/j.1365-2141.2006.06235.x
28. Lopez-Corral L, Gutierrez NC, Vidriales MB, Mateos MV, Rasillo A, Garcia-Sanz R, et al. The Progression From MGUS to Smoldering Myeloma and Eventually to Multiple Myeloma Involves a Clonal Expansion of Genetically Abnormal Plasma Cells. *Clin Cancer Res* (2011) 17:1692–700. doi: 10.1158/1078-0432.CCR-10-1066
29. Minnie SA, Hill GR. Immunotherapy of Multiple Myeloma. *J Clin Invest* (2020) 130:1565–75. doi: 10.1172/JCI129205
30. Nakamura K, Smyth MJ, Martinet L. Cancer Immunoediting and Immune Dysregulation in Multiple Myeloma. *Blood* (2020) 10;136(24):2731–40. doi: 10.1182/blood.2020006540
31. Marsh-Wakefield F, Kruzins A, McGuire HM, Yang S, Bryant C, Fazekas de St Groth B, et al. Mass Cytometry Discovers Two Discrete Subsets of CD39 (-)Treg Which Discriminate Mgus From Multiple Myeloma. *Front Immunol* (2019) 10:1596. doi: 10.3389/fimmu.2019.01596
32. Vuckovic S, Bryant CE, Lau KHA, Yang S, Favaloro J, McGuire HM, et al. Inverse Relationship Between Oligoclonal Expanded CD69- TTE and CD69+ TTE Cells in Bone Marrow of Multiple Myeloma Patients. *Blood Adv* (2020) 4:4593–604. doi: 10.1182/bloodadvances.2020002237
33. Bailur JK, McCachren SS, Doxie DB, Shrestha M, Pendleton K, Nooka AK, et al. Early Alterations in Stem-Like/Resident T Cells, Innate and Myeloid Cells in the Bone Marrow in Preneoplastic Gammopathy. *JCI Insight 5* (2019) 5(11). doi: 10.1172/jci.insight.127807
34. Phan TG, Croucher PI. The Dormant Cancer Cell Life Cycle. *Nat Rev Cancer* (2020) 20:398–411. doi: 10.1038/s41568-020-0263-0
35. Murray ME, Gavile CM, Nair JR, Koorella C, Carlson LM, Buac D, et al. CD28-Mediated Pro-Survival Signaling Induces Chemotherapeutic Resistance in Multiple Myeloma. *Blood* (2014) 123:3770–9. doi: 10.1182/blood-2013-10-530964
36. Ray A, Song Y, Chauhan D, Anderson KC. Blockade of Ubiquitin Receptor Rpn13 in Plasmacytoid Dendritic Cells Triggers Anti-Myeloma Immunity. *Blood Cancer J* (2019) 9:64. doi: 10.1038/s41408-019-0224-6
37. Wong TW, Kita H, Hanson CA, Walters DK, Arendt BK, Jelinek DF. Induction of Malignant Plasma Cell Proliferation by Eosinophils. *PloS One* (2013) 8:e70554. doi: 10.1371/journal.pone.0070554
38. Sorrig R, Klausen TW, Salomo M, Vangsted A, Gimsing P. Risk Factors for Infections in Newly Diagnosed Multiple Myeloma Patients: A Danish Retrospective Nationwide Cohort Study. *Eur J haematology* (2019) 102:182–90. doi: 10.1111/ejh.13190
39. Robertson JD, Nagesh K, Jowitt SN, Dougal M, Anderson H, Mutton K, et al. Immunogenicity of Vaccination Against Influenza, Streptococcus Pneumoniae and Haemophilus Influenzae Type B in Patients With Multiple Myeloma. *Br J Cancer* (2000) 82:1261–5. doi: 10.1054/bjoc.1999.1088
40. Isidori A, de Leval L, Gergis U, Musto P, Porcu P. Management of Patients With Hematologic Malignancies During the COVID-19 Pandemic: Practical Considerations and Lessons to Be Learned. *Front Oncol* (2020) 10:1439. doi: 10.3389/fonc.2020.01439
41. Nadeem O, Tai YT, Anderson KC. Immunotherapeutic and Targeted Approaches in Multiple Myeloma. *Immunotargets Ther* (2020) 9:201–15. doi: 10.2147/ITT.S240886
42. de Weers M, Tai YT, van der Veer MS, Bakker JM, Vink T, Jacobs DC, et al. Daratumumab, a Novel Therapeutic Human CD38 Monoclonal Antibody, Induces Killing of Multiple Myeloma and Other Hematological Tumors. *J Immunol* (2011) 186:1840–8. doi: 10.4049/jimmunol.1003032
43. Martin T, Baz R, Benson DM, Lendvai N, Wolf J, Munster P, et al. A Phase 1b Study of Isatuximab Plus Lenalidomide and Dexamethasone for Relapsed/Refractory Multiple Myeloma. *Blood* (2017) 129:3294–303. doi: 10.1182/blood-2016-09-740787
44. van de Donk NW, Moreau P, Plesner T, Palumbo A, Gay F, Laubach JP, et al. Clinical Efficacy and Management of Monoclonal Antibodies Targeting CD38 and SLAMF7 in Multiple Myeloma. *Blood* (2016) 127:681–95. doi: 10.1182/blood-2015-10-646810
45. Trudel S, Lendvai N, Popat R, Voorhees PM, Reeves B, Libby EN, et al. Targeting B-cell Maturation Antigen With GSK2857916 Antibody-Drug Conjugate in Relapsed or Refractory Multiple Myeloma (BMA117159): A Dose Escalation and Expansion Phase 1 Trial. *Lancet Oncol* (2018) 19:1641–53. doi: 10.1016/S1470-2045(18)30576-X
46. Singhal S, Mehta J, Desikan R, Ayers D, Roberson P, Eddlemon P, et al. Antitumor Activity of Thalidomide in Refractory Multiple Myeloma. *New Engl J Med* (1999) 341:1565–71. doi: 10.1056/NEJM199911183412102
47. Tai YT, Li XF, Catley L, Coffey R, Breitkreutz I, Bae J, et al. Immunomodulatory Drug Lenalidomide (CC-5013, IMiD3) Augments Anti-CD40 SGN-40-induced Cytotoxicity in Human Multiple Myeloma: Clinical Implications. *Cancer Res* (2005) 65:11712–20. doi: 10.1158/0008-5472.CAN-05-1657
48. Barlogie B, Shaughnessy J, Zangari M, Tricot G. High-Dose Therapy and Immunomodulatory Drugs in Multiple Myeloma. *Semin Oncol* (2002) 29:26–33. doi: 10.1016/S0093-7754(02)70058-4
49. Lacy MQ, Hayman SR, Gertz MA, Dispenzieri A, Buadi F, Kumar S, et al. Pomalidomide (CC4047) Plus Low-Dose Dexamethasone as Therapy for Relapsed Multiple Myeloma. *J Clin Oncol* (2009) 27:5008–14. doi: 10.1200/JCO.2009.23.6802
50. Bjorklund CC, Kang J, Amatangelo M, Polonskaia A, Katz M, Chiu H, et al. Iberdomide (Cc-220) Is a Potent Cereblon E3 Ligase Modulator With Antitumor and Immunostimulatory Activities in Lenalidomide- and Pomalidomide-Resistant Multiple Myeloma Cells With Dysregulated CRBN. *Leukemia* (2020) 34:1197–201. doi: 10.1038/s41375-019-0620-8
51. Galluzzi L, Buque A, Kepp O, Zitvogel L, Kroemer G. Immunogenic Cell Death in Cancer and Infectious Disease. *Nat Rev* (2017) 17:97–111. doi: 10.1038/nri.2016.107
52. Pearson JA, Wong FS, Wen L. The Importance of the Non Obese Diabetic (NOD) Mouse Model in Autoimmune Diabetes. *J Autoimmun* (2016) 66:76–88. doi: 10.1016/j.jaut.2015.08.019
53. Fryer RA, Graham TJ, Smith EM, Walker-Samuel S, Morgan GJ, Robinson SP, et al. Characterization of a Novel Mouse Model of Multiple Myeloma and its Use in Preclinical Therapeutic Assessment. *PloS One* (2013) 8:e57641. doi: 10.1371/journal.pone.0057641
54. Schueler J, Wider D, Klingner K, Siegers GM, May AM, Wasch R, et al. Intratibial Injection of Human Multiple Myeloma Cells in NOD/SCID Il-2Rgamma(null) Mice Mimics Human Myeloma and Serves as a Valuable Tool for the Development of Anticancer Strategies. *PloS One* (2013) 8:e79939. doi: 10.1371/journal.pone.0079939
55. Rossi M, Botta C, Arbitrio M, Grembiale RD, Tagliaferri P, Tassone P. Mouse Models of Multiple Myeloma: Technologic Platforms and Perspectives. *Oncotarget* (2018) 9:20119–33. doi: 10.18632/oncotarget.24614
56. Sarin V, Yu K, Ferguson ID, Gugliemini O, Nix MA, Hann B, et al. Evaluating the Efficacy of Multiple Myeloma Cell Lines as Models for Patient Tumors *Via* Transcriptomic Correlation Analysis. *Leukemia* (2020) 34(10):2754–65. doi: 10.1101/847368
57. Moreaux J, Klein B, Bataille R, Descamps G, Maiga S, Hose D, et al. A High-Risk Signature for Patients With Multiple Myeloma Established From the Molecular Classification of Human Myeloma Cell Lines. *Haematologica* (2011) 96:574–82. doi: 10.3324/haematol.2010.033456
58. Papadimitriou K, Kostopoulos IV, Tsopanidou A, Orologas-Stavrou N, Kastritis E, Tsitsilonis O, et al. Ex Vivo Models Simulating the Bone

Marrow Environment and Predicting Response to Therapy in Multiple Myeloma. *Cancers (Basel)* (2020) 12. doi: 10.3390/cancers12082006
59. Urashima M, Chen BP, Chen S, Pinkus GS, Bronson RT, Dedera DA, et al. The Development of a Model for the Homing of Multiple Myeloma Cells to Human Bone Marrow. *Blood* (1997) 90:754–65. doi: 10.1182/blood.V90.2.754.754_754_765
60. Kyoizumi S, Baum CM, Kaneshima H, McCune JM, Yee EJ, Namikawa R. Implantation and Maintenance of Functional Human Bone Marrow in SCID-hu Mice. *Blood* (1992) 79:1704–11. doi: 10.1182/blood.V79.7.1704.bloodjournal7971704
61. Epstein J, Yaccoby S. The SCID-hu Myeloma Model. *Methods Mol Med* (2005) 113:183–90. doi: 10.1385/1-59259-916-8:183
62. Yata K, Yaccoby S. The SCID-rab Model: A Novel In Vivo System for Primary Human Myeloma Demonstrating Growth of CD138-expressing Malignant Cells. *Leukemia* (2004) 18:1891–7. doi: 10.1038/sj.leu.2403513
63. Tassone P, Neri P, Burger R, Savino R, Shammas M, Catley L, et al. Combination Therapy With Interleukin-6 Receptor Superantagonist Sant7 and Dexamethasone Induces Antitumor Effects in a Novel SCID-hu In Vivo Model of Human Multiple Myeloma. *Clin Cancer Res* (2005) 11:4251–8. doi: 10.1158/1078-0432.CCR-04-2611
64. Yaccoby S, Pennisi A, Li X, Dillon SR, Zhan F, Barlogie B, et al. Atacicept (Taci-Ig) Inhibits Growth of TACI(high) Primary Myeloma Cells in SCID-hu Mice and in Coculture With Osteoclasts. *Leukemia* (2008) 22:406–13. doi: 10.1038/sj.leu.2405048
65. van Rhee F, Szmania SM, Dillon M, van Abbema AM, Li X, Stone MK, et al. Combinatorial Efficacy of anti-CS1 Monoclonal Antibody Elotuzumab (HuLuc63) and Bortezomib Against Multiple Myeloma. *Mol Cancer Ther* (2009) 8:2616–24. doi: 10.1158/1535-7163.MCT-09-0483
66. Pennisi A, Li X, Ling W, Khan S, Zangari M, Yaccoby S. The Proteasome Inhibitor, Bortezomib Suppresses Primary Myeloma and Stimulates Bone Formation in Myelomatous and Nonmyelomatous Bones In Vivo. *Am J Hematol* (2009) 84:6–14. doi: 10.1002/ajh.21310
67. Yaccoby S, Ling W, Zhan F, Walker R, Barlogie B, Shaughnessy JDJr. Antibody-Based Inhibition of DKK1 Suppresses Tumor-Induced Bone Resorption and Multiple Myeloma Growth In Vivo. *Blood* (2007) 109:2106–11. doi: 10.1182/blood-2006-09-047712
68. Li X, Ling W, Pennisi A, Wang Y, Khan S, Heidaran M, et al. Human Placenta-Derived Adherent Cells Prevent Bone Loss, Stimulate Bone Formation, and Suppress Growth of Multiple Myeloma in Bone. *Stem Cells* (2011) 29:263–73. doi: 10.1002/stem.572
69. Di Martino MT, Leone E, Amodio N, Foresta U, Lionetti M, Pitari MR, et al. Synthetic miR-34a Mimics as a Novel Therapeutic Agent for Multiple Myeloma: In Vitro and In Vivo Evidence. *Clin Cancer Res* (2012) 18:6260–70. doi: 10.1158/1078-0432.CCR-12-1708
70. Amodio N, Leotta M, Bellizzi D, Di Martino MT, D'Aquila P, Lionetti M, et al. DNA-Demethylating and Anti-Tumor Activity of Synthetic miR-29b Mimics in Multiple Myeloma. *Oncotarget* (2012) 3:1246–58. doi: 10.18632/oncotarget.675
71. Rongvaux A, Takizawa H, Strowig T, Willinger T, Eynon EE, Flavell RA, et al. Human Hemato-Lymphoid System Mice: Current Use and Future Potential for Medicine. *Annu Rev Immunol* (2013) 31:635–74. doi: 10.1146/annurev-immunol-032712-095921
72. Rongvaux A, Willinger T, Martinek J, Strowig T, Gearty SV, Teichmann LL, et al. Development and Function of Human Innate Immune Cells in a Humanized Mouse Model. *Nat Biotechnol* (2014) 32:364–72. doi: 10.1038/nbt.2858
73. Rosean TR, Tompkins VS, Tricot G, Holman CJ, Olivier AK, Zhan F, et al. Preclinical Validation of Interleukin 6 as a Therapeutic Target in Multiple Myeloma. *Immunol Res* (2014) 59:188–202. doi: 10.1007/s12026-014-8528-x
74. Das R, Strowig T, Verma R, Koduru S, Hafemann A, Hopf S, et al. Microenvironment-Dependent Growth of Preneoplastic and Malignant Plasma Cells in Humanized Mice. *Nat Med* (2016) 22:1351–7. doi: 10.1038/nm.4202
75. Lin L, Cho SF, Xing L, Wen K, Li Y, Yu T, et al. Preclinical Evaluation of CD8+ anti-BCMA mRNA Car T Cells for Treatment of Multiple Myeloma. *Leukemia* (2020) 35:752–63. doi: 10.1038/s41375-020-0951-5
76. Radhakrishnan SV, Luetkens T, Scherer SD, Davis P, Vander Mause ER, Olson ML, et al. Cd229 Car T Cells Eliminate Multiple Myeloma and Tumor Propagating Cells Without Fratricide. *Nat Commun* (2020) 11:798. doi: 10.1038/s41467-020-14619-z
77. Daniels-Wells TR, Candelaria PV, Leoh LS, Nava M, Martinez-Maza O, Penichet ML. An IgG1 Version of the Anti-transferrin Receptor 1 Antibody Ch128.1 Shows Significant Antitumor Activity Against Different Xenograft Models of Multiple Myeloma: A Brief Communication. *J Immunother* (2020) 43:48–52. doi: 10.1097/CJI.0000000000000304
78. Leoh LS, Kim YK, Candelaria PV, Martinez-Maza O, Daniels-Wells TR, Penichet ML. Efficacy and Mechanism of Antitumor Activity of an Antibody Targeting Transferrin Receptor 1 in Mouse Models of Human Multiple Myeloma. *J Immunol* (2018) 200:3485–94. doi: 10.4049/jimmunol.1700787
79. Goldstein RL, Goyos A, Li CM, Deegen P, Bogner P, Sternjak A, et al. AMG 701 Induces Cytotoxicity of Multiple Myeloma Cells and Depletes Plasma Cells in Cynomolgus Monkeys. *Blood Adv* (2020) 4:4180–94. doi: 10.1182/bloodadvances.2020002565
80. Naeimi Kararoudi M, Nagai Y, Elmas E, de Souza Fernandes Pereira M, Ali SA, Imus PH, et al. CD38 Deletion of Human Primary NK Cells Eliminates Daratumumab-Induced Fratricide and Boosts Their Effector Activity. *Blood* (2020) 136:2416–27. doi: 10.1182/blood.2020006200
81. Amend SR, Wilson WC, Chu L, Lu L, Liu P, Serie D, et al. Whole Genome Sequence of Multiple Myeloma-Prone C57BL/KaLwRij Mouse Strain Suggests the Origin of Disease Involves Multiple Cell Types. *PloS One* (2015) 10:e0127828. doi: 10.1371/journal.pone.0127828
82. Radl J, De Glopper ED, Schuit HR, Zurcher C. Idiopathic Paraproteinemia. II. Transplantation of the Paraprotein-Producing Clone From Old to Young C57BL/KaLwRij Mice. *J Immunol* (1979) 122:609–13.
83. Croese JW, Vas Nunes CM, Radl J, van den Enden-Vieveen MH, Brondijk RJ, Boersma WJ. The 5T2 Mouse Multiple Myeloma Model: Characterization of 5T2 Cells Within the Bone Marrow. *Br J Cancer* (1987) 56:555–60. doi: 10.1038/bjc.1987.241
84. Radl J, Croese JW, Zurcher C, van den Enden-Vieveen MH, Brondijk RJ, Kazil M, et al. Influence of Treatment With APD-bisphosphonate on the Bone Lesions in the Mouse 5T2 Multiple Myeloma. *Cancer* (1985) 55:1030–40. doi: 10.1002/1097-0142(19850301)55:5<1030::AID-CNCR2820550518>3.0.CO;2-Y
85. Vanderkerken K, Goes E, De Raeve H, Radl J, Van Camp B. Follow-Up of Bone Lesions in an Experimental Multiple Myeloma Mouse Model: Description of an In Vivo Technique Using Radiography Dedicated for Mammography. *Br J Cancer* (1996) 73:1463–5. doi: 10.1038/bjc.1996.277
86. Soodgupta D, Hurchla MA, Jiang M, Zheleznyak A, Weilbaecher KN, Anderson CJ, et al. Very Late Antigen-4 (Alpha(4)Beta(1) Integrin) Targeted PET Imaging of Multiple Myeloma. *PloS One* (2013) 8:e55841. doi: 10.1371/journal.pone.0055841
87. Manning LS, Berger JD, O'Donoghue HL, Sheridan GN, Claringbold PG, Turner JH. A Model of Multiple Myeloma: Culture of 5T33 Murine Myeloma Cells and Evaluation of Tumorigenicity in the C57BL/KaLwRij Mouse. *Br J Cancer* (1992) 66:1088–93. doi: 10.1038/bjc.1992.415
88. Dallas SL, Garrett IR, Oyajobi BO, Dallas MR, Boyce BF, Bauss F, et al. Ibandronate Reduces Osteolytic Lesions But Not Tumor Burden in a Murine Model of Myeloma Bone Disease. *Blood* (1999) 93:1697–706. doi: 10.1182/blood.V93.5.1697.405a17_1697_1706
89. De Smedt E, Lui H, Maes K, De Veirman K, Menu E, Vanderkerken K, et al. The Epigenome in Multiple Myeloma: Impact on Tumor Cell Plasticity and Drug Response. *Front Oncol* (2018) 8:566. doi: 10.3389/fonc.2018.00566
90. Maes K, Boeckx B, Vlummens P, De Veirman K, Menu E, Vanderkerken K, et al. The Genetic Landscape of 5T Models for Multiple Myeloma. *Sci Rep* (2018) 8:15030. doi: 10.1038/s41598-018-33396-w
91. Alici E, Konstantinidis KV, Aints A, Dilber MS, Abedi-Valugerdi M. Visualization of 5T33 Myeloma Cells in the C57BL/KaLwRij Mouse: Establishment of a New Syngeneic Murine Model of Multiple Myeloma. *Exp Hematol* (2004) 32:1064–72. doi: 10.1016/j.exphem.2004.07.019
92. Wang S, Yang J, Qian J, Wezeman M, Kwak LW, Yi Q. Tumor Evasion of the Immune System: Inhibiting P38 MAPK Signaling Restores the Function of Dendritic Cells in Multiple Myeloma. *Blood* (2006) 107:2432–9. doi: 10.1182/blood-2005-06-2486
93. Rosenblatt J, Avigan D. Cellular Immunotherapy for Multiple Myeloma. *Cancer J* (2019) 25:38–44. doi: 10.1097/PPO.0000000000000356

94. Croese JW, Vissinga CS, Boersma WJ, Radl J. Immune Regulation of Mouse 5T2 Multiple Myeloma. I. Immune Response to 5t2 MM Idiotype. *Neoplasma* (1991) 38:457–66.
95. Croese JW, Van den Enden-Vieveen MH, Radl J. Immune Regulation of 5T2 Mouse Multiple Myeloma. II. Immunological Treatment of 5t2 MM Residual Disease. *Neoplasma* (1991) 38:467–74.
96. Hong S, Qian J, Yang J, Li H, Kwak LW, Yi Q. Roles of Idiotype-Specific T Cells in Myeloma Cell Growth and Survival: Th1 and CTL Cells are Tumoricidal While Th2 Cells Promote Tumor Growth. *Cancer Res* (2008) 68:8456–64. doi: 10.1158/0008-5472.CAN-08-2213
97. Laronne-Bar-On A, Zipori D, Haran-Ghera N. Increased Regulatory Versus Effector T Cell Development Is Associated With Thymus Atrophy in Mouse Models of Multiple Myeloma. *J Immunol* (2008) 181:3714–24. doi: 10.4049/jimmunol.181.5.3714
98. Feyler S, von Lilienfeld-Toal M, Jarmin S, Marles L, Rawstron A, Ashcroft AJ, et al. Cd4(+)Cd25(+)FoxP3(+) Regulatory T Cells are Increased Whilst CD3(+)CD4(-)CD8(-)alphabetaTCR(+) Double Negative T Cells are Decreased in the Peripheral Blood of Patients With Multiple Myeloma Which Correlates With Disease Burden. *Br J Haematology* (2009) 144:686–95. doi: 10.1111/j.1365-2141.2008.07530.x
99. Savelyeva N, King CA, Vitetta ES, Stevenson FK. Inhibition of a Vaccine-Induced Anti-Tumor B Cell Response by Soluble Protein Antigen in the Absence of Continuing T Cell Help. *Proc Natl Acad Sci USA* (2005) 102:10987–92. doi: 10.1073/pnas.0505108102
100. Hong S, Qian J, Li H, Yang J, Lu Y, Zheng Y, et al. Cpg or IFN-alpha are More Potent Adjuvants Than GM-CSF to Promote Anti-Tumor Immunity Following Idiotype Vaccine in Multiple Myeloma. *Cancer Immunol Immunother* (2012) 61:561–71. doi: 10.1007/s00262-011-1123-2
101. Hong S, Li H, Qian J, Yang J, Lu Y, Yi Q. Optimizing Dendritic Cell Vaccine for Immunotherapy in Multiple Myeloma: Tumour Lysates are More Potent Tumour Antigens Than Idiotype Protein to Promote Anti-Tumour Immunity. *Clin Exp Immunol* (2012) 170:167–77. doi: 10.1111/j.1365-2249.2012.04642.x
102. Rosenblatt J, Avivi I, Vasir B, Uhl L, Munshi NC, Katz T, et al. Vaccination With Dendritic Cell/Tumor Fusions Following Autologous Stem Cell Transplant Induces Immunologic and Clinical Responses in Multiple Myeloma Patients. *Clin Cancer Res* (2013) 19:3640–8. doi: 10.1158/1078-0432.CCR-13-0282
103. Zhang L, Bi E, Hong S, Qian J, Zheng C, Wang M, et al. Cd4(+) T Cells Play a Crucial Role for Lenalidomide In Vivo Anti-Tumor Activity in Murine Multiple Myeloma. *Oncotarget* (2015) 6:36032–40. doi: 10.18632/oncotarget.5506
104. Nur H, Fostier K, Aspeslagh S, Renmans W, Bertrand E, Leleu X, et al. Preclinical Evaluation of Invariant Natural Killer T Cells in the 5T33 Multiple Myeloma Model. *PloS One* (2013) 8:e65075. doi: 10.1371/journal.pone.0065075
105. Barber A, Meehan KR, Sentman CL. Treatment of Multiple Myeloma With Adoptively Transferred Chimeric NKG2D Receptor-Expressing T Cells. *Gene Ther* (2011) 18:509–16. doi: 10.1038/gt.2010.174
106. Hallett WH, Jing W, Drobyski WR, Johnson BD. Immunosuppressive Effects of Multiple Myeloma are Overcome by PD-L1 Blockade. *Biol Blood Marrow Transplant* (2011) 17:1133–45. doi: 10.1016/j.bbmt.2011.03.011
107. Kearl TJ, Jing W, Gershan JA, Johnson BD. Programmed Death receptor-1/programmed Death Receptor Ligand-1 Blockade After Transient Lymphodepletion to Treat Myeloma. *J Immunol* (2013) 190:5620–8. doi: 10.4049/jimmunol.1202005
108. Fowler JA, Mundy GR, Lwin ST, Edwards CM. Bone Marrow Stromal Cells Create a Permissive Microenvironment for Myeloma Development: A New Stromal Role for Wnt Inhibitor Dkk1. *Cancer Res* (2012) 72:2183–9. doi: 10.1158/0008-5472.CAN-11-2067
109. Potter M. Neoplastic Development in Plasma Cells. *Immunol Rev* (2003) 194:177–95. doi: 10.1034/j.1600-065X.2003.00061.x
110. Potter M, Boyce C. Induction of Plasma Cell Neoplasms in Strain BALB/c Mice With Mineral Oil and Mineral Oil Adjuvants. *Nature* (1962) 193:1086. doi: 10.1038/1931086a0
111. Mokyr MB, Prokhorova A, Rubin M, Bluestone JA. Insight Into the Mechanism of TCR-V Beta 8+/CD8+ T Cell-Mediated MOPC-315 Tumor Eradication. *J Immunol* (1994) 153:3123–34.
112. Wang D, Floisand Y, Myklebust CV, Burgler S, Parente-Ribes A, Hofgaard PO, et al. Autologous Bone Marrow Th Cells can Support Multiple Myeloma Cell Proliferation In Vitro and in Xenografted Mice. *Leukemia* (2017) 31:2114–21. doi: 10.1038/leu.2017.69
113. Baghdadi M, Ishikawa K, Nakanishi S, Murata T, Umeyama Y, Kobayashi T, et al. A Role for IL-34 in Osteolytic Disease of Multiple Myeloma. *Blood Adv* (2019) 3:541–51. doi: 10.1182/bloodadvances.2018020008
114. Schwarzer R, Nickel N, Godau J, Willie BM, Duda GN, Schwarzer R, et al. Notch Pathway Inhibition Controls Myeloma Bone Disease in the Murine MOPC315. *BM Model Blood Cancer J* (2014) 4:e217. doi: 10.1038/bcj.2014.37
115. Wong D, Winter O, Hartig C, Siebels S, Szyska M, Tiburzy B, et al. Eosinophils and Megakaryocytes Support the Early Growth of Murine MOPC315 Myeloma Cells in Their Bone Marrow Niches. *PloS One* (2014) 9:e109018. doi: 10.1371/journal.pone.0109018
116. Villa NY, Rahman MM, Mamola J, D'Isabella J, Goras E, Kilbourne J, et al. Autologous Transplantation Using Donor Leukocytes Loaded Ex Vivo With Oncolytic Myxoma Virus can Eliminate Residual Multiple Myeloma. *Mol Ther Oncolytics* (2020) 18:171–88. doi: 10.1016/j.omto.2020.06.011
117. Bogen B, Fauskanger M, Haabeth OA, Tveita A. Cd4(+) T Cells Indirectly Kill Tumor Cells Via Induction of Cytotoxic Macrophages in Mouse Models. *Cancer Immunol Immunother* (2019) 68:1865–73. doi: 10.1007/s00262-019-02374-0
118. Haabeth OA, Tveita A, Fauskanger M, Hennig K, Hofgaard PO, Bogen B. Idiotype-Specific CD4(+) T Cells Eradicate Disseminated Myeloma. *Leukemia* (2016) 30:1216–20. doi: 10.1038/leu.2015.278
119. Haabeth OAW, Hennig K, Fauskanger M, Loset GA, Bogen B, Tveita A. Cd4+ T-cell Killing of Multiple Myeloma Cells is Mediated by Resident Bone Marrow Macrophages. *Blood Adv* (2020) 4:2595–605. doi: 10.1182/bloodadvances.2020001434
120. Binsfeld M, Muller J, Lamour V, De Veirman K, De Raeve H, Bellahcene A, et al. Granulocytic Myeloid-Derived Suppressor Cells Promote Angiogenesis in the Context of Multiple Myeloma. *Oncotarget* (2016) 7:37931–43. doi: 10.18632/oncotarget.9270
121. Binsfeld M, Beguin Y, Belle L, Otjacques E, Hannon M, Briquet A, et al. Establishment of a Murine Graft-Versus-Myeloma Model Using Allogeneic Stem Cell Transplantation. *PloS One* (2014) 9:e113764. doi: 10.1371/journal.pone.0113764
122. Yado S, Luboshits G, Hazan O, Or R, Firer MA. Long-Term Survival Without Graft-Versus-Host-Disease Following Infusion of Allogeneic Myeloma-Specific Vbeta T Cell Families. *J Immunother Cancer* (2019) 7:301. doi: 10.1186/s40425-019-0776-9
123. Braathen R, Spang HCL, Hinke DM, Blazevski J, Bobic S, Fossum E, et al. A DNA Vaccine That Encodes an Antigen-Presenting Cell-Specific Heterodimeric Protein Protects Against Cancer and Influenza. *Mol Ther Methods Clin Dev* (2020) 17:378–92. doi: 10.1016/j.omtm.2020.01.007
124. Rasche L, Hudecek M, Einsele H. What is the Future of Immunotherapy in Multiple Myeloma? *Blood* (2020) 136:2491–7. doi: 10.1182/blood.2019004176
125. Anderson PN, Potter M. Induction of Plasma Cell Tumours in BALB-c Mice With 2,6,10,14-Tetramethylpentadecane (Pristane). *Nature* (1969) 222:994–5. doi: 10.1038/222994a0
126. Stone MJ. Monoclonal Antibodies in the Prehybridoma Era: A Brief Historical Perspective and Personal Reminiscence. *Clin lymphoma* (2001) 2:148–54. doi: 10.3816/CLM.2001.n.020
127. Kohler G, Milstein C. Continuous Cultures of Fused Cells Secreting Antibody of Predefined Specificity. *Nature* (1975) 256:495–7. doi: 10.1038/256495a0
128. Potter M, Pumphrey JG, Bailey DW. Genetics of Susceptibility to Plasmacytoma Induction. I. Balb/cAnN (C), C57BL/6N (B6), C57BL/Ka (BK), (C Times B6)F1, (C Times BK)F1, and C Times B Recombinant-Inbred Strains. *J Natl Cancer Inst* (1975) 54:1413–7. doi: 10.1093/jnci/54.6.1413
129. Zhang SL, DuBois W, Ramsay ES, Bliskovski V, Morse HC, Taddesse-Heath L, et al. Efficiency Alleles of the Pctr1 Modifier Locus for Plasmacytoma Susceptibility. *Mol Cell Biol* (2001) 21:310–8. doi: 10.1128/MCB.21.1.310-318.2001
130. Bliskovsky V, Ramsay ES, Scott J, DuBois W, Shi W, Zhang S, et al. Frap, FKBP12 Rapamycin-Associated Protein, Is a Candidate Gene for the Plasmacytoma Resistance Locus Pctr2 and Can Act as a Tumor

Suppressor Gene. *Proc Natl Acad Sci USA* (2003) 100:14982–7. doi: 10.1073/pnas.2431627100
131. Shen-Ong GL, Keath EJ, Piccoli SP, Cole MD. Novel Myc Oncogene RNA From Abortive Immunoglobulin-Gene Recombination in Mouse Plasmacytomas. *Cell* (1982) 31:443–52. doi: 10.1016/0092-8674(82)90137-4
132. Niiro H, Clark EA. Regulation of B-Cell Fate by Antigen-Receptor Signals. *Nat Rev* (2002) 2:945–56. doi: 10.1038/nri955
133. Byrd LG, McDonald AH, Gold LG, Potter M. Specific Pathogen-Free BALB/cAn Mice are Refractory to Plasmacytoma Induction by Pristane. *J Immunol* (1991) 147:3632–7.
134. McIntire KR, Princler GL. Prolonged Adjuvant Stimulation in Germ-Free BALB-c Mice: Development of Plasma Cell Neoplasia. *Immunology* (1969) 17:481–7.
135. Lonial S, Jacobus S, Fonseca R, Weiss M, Kumar S, Orlowski RZ, et al. Randomized Trial of Lenalidomide Versus Observation in Smoldering Multiple Myeloma. *J Clin Oncol* (2020) 38:1126–37. doi: 10.1200/JCO.19.01740
136. Cooke RE, Koldej R, Ritchie D. Immunotherapeutics in Multiple Myeloma: How can Translational Mouse Models Help? *J Oncol* (2019) 2019:2186494. doi: 10.1155/2019/2186494
137. Rajkumar SV. Multiple Myeloma: Every Year a New Standard? *Hematol Oncol* (2019) 37 Suppl 1:62–5. doi: 10.1002/hon.2586
138. Vlummens P, De Veirman K, Menu E, De Bruyne E, Offner F, Vanderkerken K, et al. The Use of Murine Models for Studying Mechanistic Insights of Genomic Instability in Multiple Myeloma. *Front Genet* (2019) 10:740. doi: 10.3389/fgene.2019.00740
139. Rutsch S, Neppalli VT, Shin DM, DuBois W, Morse HC3, Goldschmidt H, et al. IL-6 and MYC Collaborate in Plasma Cell Tumor Formation in Mice. . *Blood* (2010) 115:1746–54. doi: 10.1182/blood-2009-08-237941
140. Boylan KL, Gosse MA, Staggs SE, Janz S, Grindle S, Kansas GS, et al. A Transgenic Mouse Model of Plasma Cell Malignancy Shows Phenotypic, Cytogenetic, and Gene Expression Heterogeneity Similar to Human Multiple Myeloma. *Cancer Res* (2007) 67:4069–78. doi: 10.1158/0008-5472.CAN-06-3699
141. Scherger AK, Al-Maarri M, Maurer HC, Schick M, Maurer S, Ollinger R, et al. Activated gp130 Signaling Selectively Targets B Cell Differentiation to Induce Mature Lymphoma and Plasmacytoma. *JCI Insight* (2019) 4(15). doi: 10.1172/jci.insight.128435
142. Hu Y, Zheng M, Gali R, Tian Z, Topal Gorgun G, Munshi NC, et al. A Novel Rapid-Onset High-Penetrance Plasmacytoma Mouse Model Driven by Deregulation of cMYC Cooperating With KRAS12V in BALB/c Mice. *Blood Cancer J* (2013) 3:e156. doi: 10.1038/bcj.2013.53
143. Hu Y, Song W, Cirstea D, Lu D, Munshi NC, Anderson KC. CSNK1alpha1 Mediates Malignant Plasma Cell Survival. *Leukemia* (2015) 29:474–82. doi: 10.1038/leu.2014.202
144. Tompkins VS, Rosean TR, Holman CJ, DeHoedt C, Olivier AK, Duncan KM, et al. Adoptive B-Cell Transfer Mouse Model of Human Myeloma. *Leukemia* (2016) 30:962–6. doi: 10.1038/leu.2015.197
145. Cooke RE, Gherardin NA, Harrison SJ, Quach H, Godfrey DI, Prince M, et al. Spontaneous Onset and Transplant Models of the Vk*MYC Mouse Show Immunological Sequelae Comparable to Human Multiple Myeloma. *J Transl Med* (2016) 14:259. doi: 10.1186/s12967-016-0994-6
146. Guillerey C, Ferrari de Andrade L, Vuckovic S, Miles K, Ngiow SF, Yong MC, et al. Immunosurveillance and Therapy of Multiple Myeloma Are CD226 Dependent. *J Clin Invest* (2015) 125:2904. doi: 10.1172/JCI82646
147. Calcinotto A, Brevi A, Chesi M, Ferrarese R, Garcia Perez L, Grioni M, et al. Microbiota-Driven Interleukin-17-Producing Cells and Eosinophils Synergize to Accelerate Multiple Myeloma Progression. *Nat Commun* (2018) 9:4832. doi: 10.1038/s41467-018-07305-8
148. Nakamura K, Kassem S, Cleynen A, Chretien ML, Guillerey C, Putz EM, et al. Dysregulated IL-18 is a Key Driver of Immunosuppression and a Possible Therapeutic Target in the Multiple Myeloma Microenvironment. *Cancer Cell* (2018) 33:634–48.e5. doi: 10.1016/j.ccell.2018.02.007
149. Akhmetzyanova I, McCarron MJ, Parekh S, Chesi M, Bergsagel PL, Fooksman DR. Dynamic CD138 Surface Expression Regulates Switch Between Myeloma Growth and Dissemination. *Leukemia* (2020) 34:245–56. doi: 10.1038/s41375-019-0519-4
150. Chesi M, Robbiani DF, Sebag M, Chng WJ, Affer M, Tiedemann R, et al. AID-Dependent Activation of a MYC Transgene Induces Multiple Myeloma in a Conditional Mouse Model of Post-Germinal Center Malignancies. *Cancer Cell* (2008) 13:167–80. doi: 10.1016/j.ccr.2008.01.007
151. Chesi M, Matthews GM, Garbitt VM, Palmer SE, Shortt J, Lefebure M, et al. Drug Response in a Genetically Engineered Mouse Model of Multiple Myeloma is Predictive of Clinical Efficacy. *Blood* (2012) 120:376–85. doi: 10.1182/blood-2012-02-412783
152. Thirukkumaran CM, Shi ZQ, Nuovo GJ, Luider J, Kopciuk KA, Dong Y, et al. Oncolytic Immunotherapy and Bortezomib Synergy Improves Survival of Refractory Multiple Myeloma in a Preclinical Model. *Blood Adv* (2019) 3:797–812. doi: 10.1182/bloodadvances.2018025593
153. Chesi M, Mirza NN, Garbitt VM, Sharik ME, Dueck AC, Asmann YW, et al. IAP Antagonists Induce Anti-Tumor Immunity in Multiple Myeloma. *Nat Med* (2016) 22:1411–20. doi: 10.1038/nm.4229
154. Minnie SA, Kuns RD, Gartlan KH, Zhang P, Wilkinson AN, Samson L, et al. Myeloma Escape After Stem Cell Transplantation is a Consequence of T-cell Exhaustion and is Prevented by TIGIT Blockade. *Blood* (2018) 132:1675–88. doi: 10.1182/blood-2018-01-825240
155. Guillerey C, Harjunpaa H, Carrie N, Kassem S, Teo T, Miles K, et al. TIGIT Immune Checkpoint Blockade Restores CD8(+) T-Cell Immunity Against Multiple Myeloma. *Blood* (2018) 132:1689–94. doi: 10.1182/blood-2018-01-825265
156. Asimakopoulos F. TIGIT Checkpoint Inhibition for Myeloma. *Blood* (2018) 132:1629–30. doi: 10.1182/blood-2018-08-864231
157. Kawano Y, Zavidij O, Park J, Moschetta M, Kokubun K, Mouhieddine TH, et al. Blocking IFNAR1 Inhibits Multiple Myeloma-Driven Treg Expansion and Immunosuppression. *J Clin Invest* (2018) 128:2487–99. doi: 10.1172/JCI88169
158. Guillerey C, Nakamura K, Pichler AC, Barkauskas D, Krumeich S, Stannard K, et al. Chemotherapy Followed by Anti-CD137 mAb Immunotherapy Improves Disease Control in a Mouse Myeloma Model. *JCI Insight* (2019) 5(14). doi: 10.1172/jci.insight.125932
159. Vuckovic S, Minnie SA, Smith D, Gartlan KH, Watkins TS, Markey KA, et al. Bone Marrow Transplantation Generates T Cell-Dependent Control of Myeloma in Mice. *J Clin Invest* (2019) 129:106–21. doi: 10.1172/JCI98888
160. Rosenbaum H, Harris AW, Bath ML, McNeall J, Webb E, Adams JM, et al. An E Mu-v-abl Transgene Elicits Plasmacytomas in Concert with An Activated Myc Gene. *EMBO J* (1990) 9:897–905.
161. Vandenberg CJ, Waring P, Strasser A, Cory S. Plasmacytomagenesis in Emu-v-abl Transgenic Mice Is Accelerated When Apoptosis Is Restrained. *Blood* (2014) 124:1099–109. doi: 10.1182/blood-2014-04-570770
162. Suematsu S, Matsusaka T, Matsuda T, Ohno S, Miyazaki J, Yamamura K, et al. Generation of Plasmacytomas With the Chromosomal Translocation t (12;15) in Interleukin 6 Transgenic Mice. *Proc Natl Acad Sci USA* (1992) 89:232–5. doi: 10.1073/pnas.89.1.232
163. Kovalchuk AL, Kim JS, Park SS, Coleman AE, Ward JM, Morse HC 3rd, et al. IL-6 Transgenic Mouse Model for Extraosseous Plasmacytoma. *Proc Natl Acad Sci USA* (2002) 99:1509–14. doi: 10.1073/pnas.022643999
164. Chiarle R, Gong JZ, Guasparri I, Pesci A, Cai J, Liu J, et al. NPM-ALK Transgenic Mice Spontaneously Develop T-Cell Lymphomas and Plasma Cell Tumors. *Blood* (2003) 101:1919–27. doi: 10.1182/blood-2002-05-1343
165. Silva S, Kovalchuk AL, Kim JS, Klein G, Janz S. BCL2 Accelerates Inflammation-Induced BALB/c Plasmacytomas and Promotes Novel Tumors with Coexisting T(12;15) and T(6;15) Translocations. *Cancer Res* (2003) 63:8656–63.
166. Linden M, Kirchhof N, Carlson C, Van Ness B. Targeted Overexpression of Bcl-XL in B-lymphoid Cells Results in Lymphoproliferative Disease and Plasma Cell Malignancies. *Blood* (2004) 103:2779–86. doi: 10.1182/blood-2003-10-3399
167. Carrasco DR, Sukhdeo K, Protopopova M, Sinha R, Enos M, Carrasco DE, et al. The Differentiation and Stress Response Factor XBP-1 Drives Multiple Myeloma Pathogenesis. *Cancer Cell* (2007) 11:349–60. doi: 10.1016/j.ccr.2007.02.015
168. Zhang B, Wang Z, Li T, Tsitsikov EN, Ding HF. NF-kappaB2 Mutation Targets TRAF1 to Induce Lymphomagenesis. *Blood* (2007) 110:743–51. doi: 10.1182/blood-2006-11-058446
169. McCarthy BA, Yang L, Ding J, Ren M, King W, ElSalanty M, et al. NF-kappaB2 Mutation Targets Survival, Proliferation and Differentiation Pathways in The Pathogenesis of Plasma Cell Tumors. *BMC Cancer* (2012) 12:203. doi: 10.1186/1471-2407-12-203

170. Ueda O, Wada NA, Kinoshita Y, Hino H, Kakefuda M, Ito T, et al. Delta, and Gamma Humanized Mouse to Evaluate Human CD3-mediated Therapeutics. *Sci Rep* (2017) 7:45839. doi: 10.1038/srep45839
171. Airoldi I, Di Carlo E, Cocco C, Sorrentino C, Fais F, Cilli M, et al. Lack of Il12rb2 Signaling Predisposes to Spontaneous Autoimmunity and Malignancy. *Blood* (2005) 106:3846–53. doi: 10.1182/blood-2005-05-2034
172. Sun F, Cheng Y, Walsh SA, Acevedo MR, Jing X, Han SS, et al. Osteolytic Disease in IL-6 and Myc Dependent Mouse Model of Human Myeloma. *Haematologica* (2020) 105:e111–5. doi: 10.3324/haematol.2019.221127
173. Morito N, Yoh K, Maeda A, Nakano T, Fujita A, Kusakabe M, et al. A Novel Transgenic Mouse Model of The Human Multiple Myeloma Chromosomal Translocation t(14;16)(q32;q23). *Cancer Res* (2011) 71:339–48. doi: 10.1158/0008-5472.CAN-10-1057
174. Cheung WC, Kim JS, Linden M, Peng L, Van Ness B, Polakiewicz RD, et al. Novel Targeted Deregulation of c-Myc Cooperates With Bcl-X(L) to Cause Plasma Cell Neoplasms in Mice. *J Clin Invest* (2004) 113:1763–73. doi: 10.1172/JCI20369
175. Linden MA, Kirchhof N, Carlson CS, Van Ness BG. Targeted Overexpression of an Activated N-ras Gene Results in B-cell And Plasma Cell Lymphoproliferation and Cooperates with c-myc to Induce Fatal B-cell Neoplasia. *Exp Hematol* (2012) 40:216–27. doi: 10.1016/j.exphem.2011.11.006
176. Vicente-Duenas C, Romero-Camarero I, Gonzalez-Herrero I, Alonso-Escudero E, Abollo-Jimenez F, Jiang X, et al. A Novel Molecular Mechanism Involved in Multiple Myeloma Development Revealed by Targeting MafB to Haematopoietic Progenitors. *EMBO J* (2012) 31:3704–17. doi: 10.1038/emboj.2012.227
177. Chang L, Guo R, Huang Q, Yen Y. Chromosomal Instability Triggered by Rrm2b Loss Leads to IL-6 Secretion and Plasmacytic Neoplasms. *Cell Rep* (2013) 3:1389–97. doi: 10.1016/j.celrep.2013.03.040
178. Dechow T, Steidle S, Gotze KS, Rudelius M, Behnke K, Pechloff K, et al. GP130 Activation Induces Myeloma and Collaborates with MYC. *J Clin Invest* (2014) 124:5263–74. doi: 10.1172/JCI69094
179. Hamouda MA, Jacquel A, Robert G, Puissant A, Richez V, Cassel R, et al. BCL-B (BCL2L10) is Overexpressed in Patients Suffering From Multiple Myeloma (MM) and Drives an MM-like Disease in Transgenic Mice. *J Exp Med* (2016) 213:1705–22. doi: 10.1084/jem.20150983
180. Asai T, Hatlen MA, Lossos C, Ndiaye-Lobry D, Deblasio A, Murata K, et al. Generation of a Novel, Multi-Stage, Progressive, and Transplantable Model of Plasma Cell Neoplasms. *Sci Rep* (2016) 6:22760. doi: 10.1038/srep22760
181. Wen Z, Rajagopalan A, Flietner E, Yun G, Chesi M, Furumo Q, et al. Expression of NrasQ61R and MYC Transgene in Germinal Center B Cells Induces a Highly Malignant Multiple Myeloma in Mice. *Blood* (2021). doi: 10.1182/blood.2020007156
182. Sewastianik T, Straubhaar JR, Zhao JJ, Samur MK, Adler K, Tanton HE, et al. miR-15a/16-1 Deletion in Activated B Cells Promotes Plasma Cell and Mature B-cell Neoplasms. *Blood* (2021) 137:1905–19. doi: 10.1182/blood.2020009088
183. Affer M, Chesi M, Chen WD, Keats JJ, Demchenko YN, Tamizhmani K, et al. Promiscuous MYC Locus Rearrangements Hijack Enhancers but Mostly Super-Enhancers to Dysregulate MYC Expression in Multiple Myeloma. *Leukemia* (2014). doi: 10.1038/leu.2014.70
184. Corre J, Munshi NC, Avet-Loiseau H. Risk Factors in MM: Is it Time for a Revision? *Blood* (2020) 137(1):16–19. doi: 10.1182/blood.2019004309
185. Kumar SK, Rajkumar V, Kyle RA, van Duin M, Sonneveld P, Mateos MV, et al. Multiple Myeloma. *Nat Rev Dis Primers* (2017) 3:17046. doi: 10.1038/nrdp.2017.46
186. Hunter KW. Mouse Models of Cancer: Does the Strain Matter? *Nat Rev Cancer* (2012) 12:144–9. doi: 10.1038/nrc3206
187. Rustad EH, Yellapantula V, Leongamornlert D, Bolli N, Ledergor G, Nadeu F, et al. Timing the Initiation of Multiple Myeloma. *Nat Commun* (2020) 11:1917. doi: 10.1038/s41467-020-15740-9
188. Costa F, Das R, Kini Bailur J, Dhodapkar K, Dhodapkar MV. Checkpoint Inhibition in Myeloma: Opportunities and Challenges. *Front Immunol* (2018) 9:2204. doi: 10.3389/fimmu.2018.02204
189. Cohen AD, Raje N, Fowler JA, Mezzi K, Scott EC, Dhodapkar MV. How to Train Your T Cells: Overcoming Immune Dysfunction in Multiple Myeloma. *Clin Cancer Res* (2020) 26:1541–54. doi: 10.1158/1078-0432.CCR-19-2111
190. De Beck L, Melhaoui S, De Veirman K, Menu E, De Bruyne E, Vanderkerken K, et al. Epigenetic Treatment of Multiple Myeloma Mediates Tumor Intrinsic and Extrinsic Immunomodulatory Effects. *Oncoimmunology* (2018) 7:e1484981. doi: 10.1080/2162402X.2018.1484981
191. Ochoa MC, Perez-Ruiz E, Minute L, Onate C, Perez G, Rodriguez I, et al. Daratumumab in Combination With Urelumab to Potentiate Anti-Myeloma Activity in Lymphocyte-Deficient Mice Reconstituted With Human NK Cells. *Oncoimmunology* (2019) 8:1599636. doi: 10.1080/2162402X.2019.1599636
192. Lomas OC, Ghobrial IM. Clinical Controversies in the Management of Smoldering Multiple Myeloma. *Am Soc Clin Oncol Educ Book* (2020) 40:1–6. doi: 10.1200/EDBK_278911
193. Invrea F, Rovito R, Torchiaro E, Petti C, Isella C, Medico E. Patient-Derived Xenografts (Pdxs) as Model Systems for Human Cancer. *Curr Opin Biotechnol* (2020) 63:151–6. doi: 10.1016/j.copbio.2020.01.003
194. Noble JN, Mishra A. Development and Significance of Mouse Models in Lymphoma Research. *Curr Hematol Malig Rep* (2019) 14:119–26. doi: 10.1007/s11899-019-00504-0
195. De La Rochere P, Guil-Luna S, Decaudin D, Azar G, Sidhu SS, Piaggio E. Humanized Mice for the Study of Immuno-Oncology. *Trends Immunol* (2018) 39:748–63. doi: 10.1016/j.it.2018.07.001
196. Tanaskovic O, Verga Falzacappa MV, Pelicci PG. Human Cord Blood (hCB)-CD34+ Humanized Mice Fail to Reject Human Acute Myeloid Leukemia Cells. *PloS One* (2019) 14:e0217345. doi: 10.1371/journal.pone.0217345
197. Tentler JJ, Lang J, Capasso A, Kim DJ, Benaim E, Lee YB, et al. Rx-5902, a Novel Beta-Catenin Modulator, Potentiates the Efficacy of Immune Checkpoint Inhibitors in Preclinical Models of Triple-Negative Breast Cancer. *BMC Cancer* (2020) 20:1063. doi: 10.1186/s12885-020-07500-1
198. Capasso A, Lang J, Pitts TM, Jordan KR, Lieu CH, Davis SL, et al. Characterization of Immune Responses to Anti-PD-1 Mono and Combination Immunotherapy in Hematopoietic Humanized Mice Implanted With Tumor Xenografts. *J Immunother Cancer* (2019) 7:37. doi: 10.1186/s40425-019-0518-z
199. Ito R, Takahashi T, Ito M. Humanized Mouse Models: Application to Human Diseases. *J Cell Physiol* (2018) 233:3723–8. doi: 10.1002/jcp.26045
200. Landgraf M, McGovern JA, Friedl P, Hutmacher DW. Rational Design of Mouse Models for Cancer Research. *Trends Biotechnol* (2018) 36:242–51. doi: 10.1016/j.tibtech.2017.12.001
201. Gemechu Y, Millrine D, Hashimoto S, Prakash J, Sanchenkova K, Metwally H, et al. Humanized Cereblon Mice Revealed Two Distinct Therapeutic Pathways of Immunomodulatory Drugs. *Proc Natl Acad Sci USA* (2018) 115:11802–7. doi: 10.1073/pnas.1814446115
202. Hanazawa A, Ito R, Katano I, Kawai K, Goto M, Suemizu H, et al. Generation of Human Immunosuppressive Myeloid Cell Populations in Human Interleukin-6 Transgenic Nog Mice. *Front Immunol* (2018) 9:152. doi: 10.3389/fimmu.2018.00152
203. Chauvin JM, Zarour HM. TIGIT in Cancer Immunotherapy. *J Immunother Cancer* (2020) 8(2). doi: 10.1136/jitc-2020-000957
204. Shultz LD, Keck J, Burzenski L, Jangalwe S, Vaidya S, Greiner DL, et al. Humanized Mouse Models of Immunological Diseases and Precision Medicine. *Mamm Genome* (2019) 30:123–42. doi: 10.1007/s00335-019-09796-2

Conflict of Interest: The authors declare that the research was conducted in the absence of any commercial or financial relationships that could be construed as a potential conflict of interest.

frontiers in Immunology

REVIEW
published: 16 July 2021
doi: 10.3389/fimmu.2021.683597

Human B Lymphomas Reveal Their Secrets Through Genetic Mouse Models

Noushin Mossadegh-Keller[1†], *Gabriel Brisou*[1,2†], *Alicia Beyou*[1], *Bertrand Nadel*[1] *and Sandrine Roulland*[1*]

[1] Aix Marseille Univ, CNRS, INSERM, CIML, Marseille, France, [2] Department of Hematology, Institut Paoli-Calmettes, Marseille, France

OPEN ACCESS

Edited by:
Juan M. Zapata, Instituto de Investigaciones Biomédicas Alberto Sols, Consejo Superior de Investigaciones Científicas (CSIC), Spain

Reviewed by:
Parham Ramezani-Rad, Sanford Burnham Prebys Medical Discovery Institute, United States
Miguel Gallardo, Spanish National Cancer Research Center (CNIO), Spain

***Correspondence:**
Sandrine Roulland
roulland@ciml.univ-mrs.fr

[†]These authors have contributed equally to this work

Specialty section:
This article was submitted to B Cell Biology, a section of the journal Frontiers in Immunology

Received: 21 March 2021
Accepted: 12 May 2021
Published: 16 July 2021

Citation:
Mossadegh-Keller N, Brisou G, Beyou A, Nadel B and Roulland S (2021) Human B Lymphomas Reveal Their Secrets Through Genetic Mouse Models. Front. Immunol. 12:683597. doi: 10.3389/fimmu.2021.683597

Lymphomas are cancers deriving from lymphocytes, arising preferentially in secondary lymphoid organs, and represent the 6th cancer worldwide and the most frequent blood cancer. The majority of B cell Non-Hodgkin lymphomas (B-NHL) develop from germinal center (GC) experienced mature B cells. GCs are transient structures that form in lymphoid organs in response to antigen exposure of naive B cells, and where B cell receptor (BCR) affinity maturation occurs to promote B cell differentiation into memory B and plasma cells producing high-affinity antibodies. Genomic instability associated with the somatic hypermutation (SHM) and class-switch recombination (CSR) processes during GC transit enhance susceptibility to malignant transformation. Most B cell differentiation steps in the GC are at the origin of frequent B cell malignant entities, namely Follicular Lymphoma (FL) and GCB diffuse large B cell lymphomas (GCB-DLBCL). Over the past decade, large sequencing efforts have provided a great boost in the identification of candidate oncogenes and tumor suppressors involved in FL and DLBCL oncogenesis. Mouse models have been instrumental to accurately mimic *in vivo* lymphoma-specific mutations and interrogate their normal function in the GC context and their oncogenic function leading to lymphoma onset. The limited access of biopsies during the initiating steps of the disease, the cellular and (epi)genetic heterogeneity of individual tumors across and within patients linked to perturbed dynamics of GC ecosystems make the development of genetically engineered mouse models crucial to decipher lymphomagenesis and disease progression and eventually to test the effects of novel targeted therapies. In this review, we provide an overview of some of the important genetically engineered mouse models that have been developed to recapitulate lymphoma-associated (epi)genetic alterations of two frequent GC-derived lymphoma entities: FL and GCB-DLCBL and describe how those mouse models have improved our knowledge of the molecular processes supporting GC B cell transformation.

Keywords: germinal center (GC), follicular lymphoma (FL), diffuse large B cell lymphoma (DLBCL), genetically engineered mouse (GEMs), epigenetic modifier mutations

INTRODUCTION

The germinal center (GC) is a specialized immune structure localized in secondary lymphoid organs—including lymph nodes, tonsils, and spleen—that forms upon antigenic challenge to support the B cell receptor (BCR) affinity maturation process. In this transient, highly dynamic structures, activated B cells undergo clonal expansion, somatic hypermutation (SHM) of immunoglobulin (Ig) variable genes, selection and eventual differentiation into memory B cells or long-lived plasma cells (PC) (1). The GC is canonically divided into two principal zones: the dark zone (DZ), where B cells undergo clonal expansion and accumulate SHM upon activation-induced-cytidine deaminase (AID) responsible of BCR diversification, and the light zone (LZ), where GC B cell will test their newly acquired mutated Ig for improved affinity to antigen through interaction with immune complex-coated follicular dendritic cells (FDCs) and selection by a limited number of CD4+ T follicular helper cells (T_{FH}) residing in the LZ (2). Within the LZ, B cells can have several fates: (i) a small subset of high-affinity GC B cells, selected in the LZ, will recycle back in the DZ to undergo further cycles of expansion/mutation/selection (3, 4), (ii) some selected LZ B cells can directly exit the GC differentiating into effectors such a memory B cells or plasma cells and (iii) LZ cells with low/no affinity BCRs following SHM due to a lack of antigen engagement and subsequent T cell help die by apoptosis (**Figure 1**). In the GC LZ, the strength and intensity of the signal received by B cells from T_{FH} cells, which is largely influenced by BCR affinity, mainly determines B cell fate. Recently, the dynamic transcriptional changes characterizing the GC cycle between LZ and DZ have been further refined through single cell gene expression approaches revealing a continuum of cell states between LZ and DZ and highly orchestrated group of molecular programs that co-evolve during the GC response (30–34).

T dependent humoral response proceeds in several steps triggered by multiple finely orchestrated cellular interactions that affect B cell response through the activation and repression of specific transcriptional programs. Molecular control of this highly dynamic process is complex and involves several transcriptional regulators such as transcription factors and epigenetic regulators that are frequently targeted by somatic mutations driving lymphomagenesis. After antigen encounter and T cell co-stimulation, B cells get activated through BCR, CD40 and toll like receptor (TLR) signalling, inducing NF-κB activation and the expression of genes involved in B cell activation and proliferation driving GC initiation (35, 36). BCL6 is a transcriptional repressor which play a central role in GC initiation and maintenance (37). Its expression is triggered by B–T interaction during the early initiation of the GC response, where it allows B cells to migrate into the center of B cell follicles through the downregulation of EBI2 and S1PR1 and induction of CXCR4. Once GCs are established, BCL6 coordinates the GC response by repressing thousands of genes involved in different cellular processes (T cell mediated B cell activation, BCR/CD40 signaling, apoptosis, DNA damage response, cellular cycle checkpoints,…) (38, 39). In this way, BCL6 allows DZ cells to establish a hyper-proliferative program while tolerating DNA damage caused by SHM without triggering proliferation arrest or apoptosis. In addition, BCL6 prevents signal transduction from several membrane receptors, thus preventing B cells from premature differentiation. BCL6 expression must be repressed to allow B cells to exit the GC. Two signals cooperate to repress BCL6: BCR activation *via* Ag presented by FDCs and CD40 activation *via* CD40L expressed by T_{FH} cells (38, 39). The transcription factor cMYC is also essential for GC initiation. Indeed, about 2 h after B cell activation, GC precursors transiently express c-MYC before expressing BCL6 and co-express c-MYC and BCL6 for a short period of time, allowing the initial proliferation phase leading to GC formation. Once the GC is established, c-MYC is then partially repressed by BCL6 (3, 4). Back in the LZ, high-affinity B cells that take up the Ag integrate signals from the BCR and additional signals through several receptors, including CD40, BAFF and TLRs which ultimately activate NF-κB. NF-κB signaling and CD40 costimulation result in cMYC re-expression in selected B cells that return to the DZ for further rounds of cell division (40). On the other hand, this activates IRF4 which, when highly expressed, represses BCL6 expression, thus promoting GC programme silencing and post-GC differentiation (35, 41). Indeed, at high concentration, IRF4 induces BLIMP1 expression which allows plasma cell differentiation (42). Memory B cell differentiation process is less understood but is thought to derive from B cells with low affinity BCR receiving a weak signal from T_{FH} cells, two transcription factors have been involved in this process: BACH2 and more recently HHEX (43, 44).

B cell lymphomas are cancers that develop from the malignant transformation of B lymphocytes at different stages of ontogeny (45). From naive to memory and plasma cells, most differentiation steps are associated with a malignant B cell counterpart defined historically as the cell-of-origin on the basis of histological definitions, phenotype and resemblance of transcriptomic profiles (46). Rapid clonal expansion, genomic instability, tolerance to DNA damage and metabolic reprogramming are physiological GC B cell-specific features that makes them permeable to lymphomagenesis (47, 48). Accordingly, GC B cells are considered at the origin of frequent B cell lymphomas—namely follicular lymphoma (FL), GC B cell-diffuse large B cell lymphoma (GCB-DLBCL), and Burkitt lymphoma (BL) (**Figure 1**). FL have a follicular growth pattern reminding normal GC architecture, with the presence of T_{FH} cells and FDC stromal cells, carries heavily mutated Ig genes known to occur in the GC primarily and retain a closely related signature to LZ B cells (49, 50). GCB-DLBCL is more transcriptionally reminiscent of LZ B cells while BL is more similar to DZ B cells (46, 51). Of note, single-cell gene expression analyses of mouse (16, 30, 44, 52) and human GC B cells (31–33) have revealed that GC B cell transcriptional states span a continuum from LZ to DZ, and that a large proportion (between 30 and 50%) of GC B cells are in an intermediate state between the two zones. Besides providing important datasets to understand GC transcriptional programs during the normal immune response, these studies offered a more granular survey of human GC B cells states that can serve as references for re-assessing and revisiting the concept of GC B cell lymphoma cell-of-origin (31, 32).

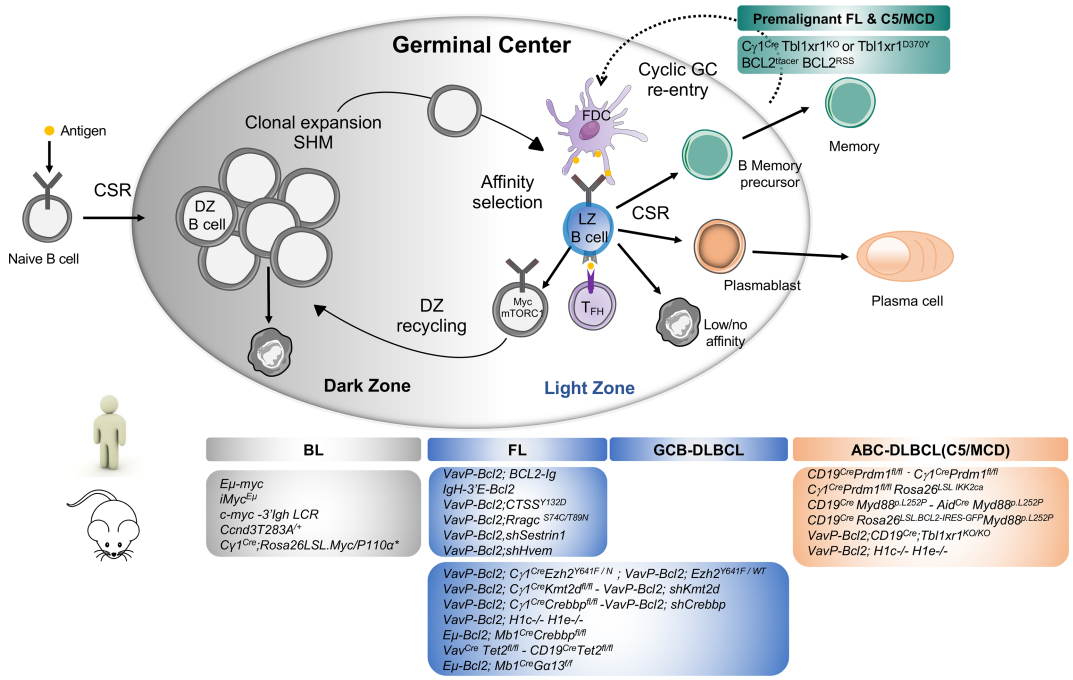

FIGURE 1 | Major mouse models of human B cell lymphomas linked to their putative normal B cell counterpart. Top Panel: Schematic representation of Germinal Center B cells. Activated B cells enter in the GC dark zone (DZ), the site of clonal expansion and somatic hypermutation. Only a subset of DZ B cells will be selected to pass in the GC light zone (LZ) while most DZ B cells undergo apoptosis. GC LZ is the site of affinity-based selection where high-affinity B cells tend to capture more antigen from FDC and receive more T cell help through CD40/CD40L interaction driving their re-entry into the DZ for defined rounds of proliferation and SHM. In the LZ, owing to the failure to receive T cell help and acquisition of damaging BCR mutations, most GC B cells will undergo apoptosis while some LZ B cells that gained productive BCR mutations and enhanced affinity will be selected and terminally differentiate into memory B or plasma cells depending on the strength of T cell help they received [recently reviewed in (5)]. In normal immune response, current models suggest that memory B cells tend to exit early the GC response following low level of T cell help and typically display less SHM and reduced levels of affinity maturation than plasma cells. A limited number of memory B cells can re-enter into secondary GC upon antigenic recall for additional rounds of mutations (6, 7). Cyclic memory cell reactivation of mutated B cells into the GC is however a driving mechanism leading to B cell transformation (8, 9). Bottom panel: The most important genetically-engineered mouse models are linked to the human lymphoma they intend to mimic distinguishing Burkitt Lymphoma (BL) arising from transformation of DZ cells, Follicular Lymphoma and GCB-DLBCL from LZ cells and ABC-DLBCL arising from Activated B/plasmablastic or memory B cells. BL is characterized by Myc translocations between the immunoglobulin heavy or light chain locus. Transgenic mice engineered to dysregulate MYC expression under proximal or distal enhancers Eμ-*Myc* (10), iMyc^{Eμ} (11) and *c-myc*3'LCR (12) led to the development of aggressive lymphomas with Burkitt-like phenotype with high penetrance and short latency *in vivo*. Conditional overexpression of Myc and PI3K signaling (*Cγ1*$^{Cre/wt}$;*Rosa26*$^{LSL.Myc/P110α*}$) in the GC cooperate to drive BL-like tumors identifying PI3K pathway activation as a key survival element in Myc-driven lymphomas (13). Modeling Cyclin D3 ^{T283A} gain-of-function mutations in B cells—which are recurrent event in DLBCL and sporadic BL (14, 15)—leads to increased DZ proliferation and occasional lymphoproliferative disease in older mice highlighting the need for additional events to exert its oncogenic function (16, 17). ABC-DLBCL are typically characterized by an enhanced activity of the NF-κB survival pathway and the co-occurrence of genomic aberrations in BCR (CD79B), MYD88, TBL1XR1, 18q gains affecting BCL2 and PRDM1 inactivation interfering with normal plasma cell differentiation, all defining features of the C5/MCD genetic subtype (18–20). Single conditional knockout of *Prdm1* in B cells or specifically in the GC reveal lymphoma lesions of post-GC origin (Bcl6^{-}, Irf4^{+}) indicative of a preplasmablastic stage in only 20% of animals and with a long latency (18, 21). Constitutive activation of NF-κB pathway with *Prdm1* disruption in the GC cooperate to drive DLBCL-like tumor development resembling human ABC-DLBCL (22, 23). Conditional expression in B cells of an oncogenic Myd88^{L252P} allele plus BCL2 overexpression (mimicking BCL2 copy number gains) result in the development of aggressive post-GC lymphomas recapitulating many genotypic, transcriptomic and signaling features of ABC-DLBCL pathogenesis (24, 25) notably the formation of the My-T-BCR (Myd88/TLR9/BCR) supercomplex driving NF-κB mediating survival signals (26) and detection of autoreactive antibodies suggesting a role for self-antigens in driving BCR stimulation as previously proposed in human and mouse models (27, 28). Somatic mutations in *TBL1XR1* are enriched in the MCD/C5 genetic subtype (18). Conditional deletion of *Tbl1xr1* or expression of TBL1XR1^{D370Y} mutant allele in B cells generates aberrant memory B cells which are more prone to cyclic re-entry into GC reaction thereby providing additional evidence on how skewed GC/Memory B cell dynamics act as a major pathogenic mechanism in lymphoma development (8, 9, 29). Combined with Bcl2 overexpression, *Tbl1xr1* mutant mice ultimately give rise to canonical post-GC extranodal ABC-like lymphomas with a proportion of B cells manifesting with a memory B cell phenotype consistent with a putative memory B cell origin of ABC-DLBCL tumors (21).

Yet, gene expression profiling only accounts for a portion of GC B cell lymphoma heterogeneity and the advent of next generation sequencing (NGS) has provided a great boost in the identification of genetic alterations (mutations, translocations, copy number alterations…) involved in FL and DLBCL oncogenesis, and has revealed an increased complexity of the lymphoma genetic landscape (14, 18, 19, 53–55). Although GCB-DLBCL and FL represent two clinically and histopathological distinct lymphoma entities, it has become apparent that these two subtypes are far more intricated from a genetic point of view as illustrated by shared multiple recurrent genetic lesions such as BCL2 alterations, mutations in epigenetic regulators (*KMT2D*,

CREBBP, *EZH2*, *EP300*…) and immune receptor signaling genes suggesting at least clonal evolution from a similar precursor cell and shared oncogenic pathways (53, 56). Accordingly, the recently defined EZB/C3 genetic subtype is composed by a majority of tumors with a GC B cell gene expression profile and is enriched for the most common genetic abnormalities such as BCL2 translocations and EZH2 mutations.

Among others, mouse models of lymphoid malignancies have advanced our understanding of lymphomagenesis [reviewed in (57–60)] and currently support the biological investigations on the most common putative driver mutations alone or in combination. The limited access to (pre)malignant biopsies during the initiating stage of lymphoma development, the difficulties to recapitulate in *in vitro* experimental systems the complexity of the GC reaction during an immune response (61), the spatial and (epi)genetic heterogeneity across and within human lymphomas make the development of genetically engineered mice models the most suitable tool i) to characterize the molecular mechanisms by which candidate lymphoma mutations contribute *in vivo* to lymphomagenesis either alone or in combination and ii) to trace how tumours grow and evolve over time by recapitulating the precise timing at which the genetic lesions happens in human settings iii) to test the effects of targeted pharmacological agents and iv) the synergy between co-occurring genetic alterations. In this review, we will present recent insights on FL and GCB-DLBCL lymphoma mouse models in which genetic alterations targeting the epigenome, immune signaling or metabolic pathways have been accurately recapitulated and for which mechanistic studies yielded new insights on how GC regulatory programs are hijacked by somatic mutations to prevent the resolution of 'pseudo-tumoral' GC B cell features and facilitate lymphomagenesis (**Table 1**). Starting with the founder BCL2 translocation common to the pathogenesis of most FL and GCB-DLBCL, we will focus on how genetically engineered mice (GEM) of (epi)genetic alterations shed new lights on the link between B 'cell-intrinsic' lesions and their cell-extrinsic functions to drive lymphoma development by promoting the remodeling of an aberrant immune niche and contributing to immune surveillance mechanisms.

MODELING T(14;18) TRANSLOCATION AND BCL2 OVEREXPRESSION

FL represents an attractive model to study the mechanisms by which lymphoid B cells undergo neoplastic initiation and progression in mouse models (50). While FL is considered as a disseminated GC-derived B cell neoplasia, acquisition of the t(14;18) translocation—that lays the *BCL2* gene under the transcriptional control of Ig heavy chain (*IGH*) regulatory regions—constitutes a critical early, likely primary, event in the natural history of the disease occurring in bone marrow (BM) pre B cells during illegitimate V(D)J recombination. It is now well established that t(14;18), although present in 85% of FL and about 30% of GCB-DLBCL patients, is not enough to transform B lymphocytes as t(14;18)-positive circulating B cells are detectable at low frequency (one in a million lymphocytes) in up to 70% of healthy adults who never develop the disease (85), indicating that complementary "hits" must further accumulate, presumably during the later phases of GC B cell maturation (86). Attempts to model the t(14;18) translocation and Bcl2 overexpression have started in the late 80's with first generation of Bcl2 transgenic mouse models (62).

Eμ-*BCL2* and *BCL2*-Ig

In 1989, to mimic the human *BCL2-IGH* translocated allele and assess the tumorigenic potential of BCL2 *in vivo*, Mc Donnell and colleagues developed the first *BCL2* transgenic mice bearing a human *BCL2*-Ig minigene where expression of BCL2 is restricted to B cells (62). The mice developed follicular hyperplasia made of small naive B cells—expressing markers such as B220, IgD, IgM and Igκ—with prolonged survival *in vitro*. In original studies, after 18 months of age these mice showed high-grade lymphomas although at a low penetrance and interestingly half of those mice harbored *c-myc* rearrangement. More recent follow-up studies showed that 40% of *BCL2*-Ig mice develop FL-like tumors expressing GC markers (PNA^+BCL6^+) by 17–18 months when chronically immunized with sheep red blood cells (SRBC) over 6 months (87). Strasser and colleagues similarly engineered a transgenic strain Eμ-*BCL2*, where *BCL2* is placed under the control of the 5' *IGH* enhancer Eμ (63). This model also showed an expansion of small B cells and plasma cells but did not yield tumor development, however an increased incidence of other B-lymphoid neoplasms was observed (64).

VavP-*BCL2* and IgH-3'E-*Bcl2*

The first experimental model that faithfully reproduced the human disease in term of localization, histology, phenotypic and genotypic features involved expression of Bcl2 in all hematopoietic cells. Egle and colleagues generated the VavP-*Bcl2* model where the *Bcl2* transgene is controlled by *Vav* gene regulatory sequences, which confer Bcl2 expression in multiple hematopoietic lineages (65). The mice developed, in 15–25% of cases, isotype-switched, somatically mutated Ig and disseminated lymphomas at 10 months of age. In contrast to Eμ-*BCL2* transgenic models of the same age, VavP-*Bcl2* mice develop spontaneous expansion of PNA^+ GC lesions in otherwise 'healthy' mice, a premalignant condition which is strongly dependent on CD4 T cell help as *in vivo* removal of CD4 cells almost abolished GC hyperplasia. In this model, CD4 T cells make a critical input into the exaggerated GC reactions and eventually the onset of FL. A second model developed by the group of Boxer (66) consisted of a IgH-3'E-*Bcl2* knock-in mice, where the *IgH* 3' enhancer regions was integrated 3' of *Bcl2* locus, thereby mimicking the effects of the long distance *IgH 3'* enhancer on Bcl2 expression and limiting Bcl2 expression to mature B cells. In addition to an altered B-cell differentiation and increased B cell numbers in the spleen, lymph node (LN) and BM, these mice recapitulated, between 7- and 14-months, typical histopathological features of GC-experienced FL-like tumors expressing the GC markers PNA and Bcl6 surrounded by FDC networks and $CD4^+$ T cells.

TABLE 1 | Relevant mouse models of follicular lymphoma and germinal center B cell diffuse large B cell lymphomas.

Target gene	Mouse Model	Model type	Target cells	Mutation type	Latency (mo)	Disease phenotype	References
Bcl2	*BCL2-Ig*	Transgenic (*BCL2-Ig* minigene)	B cells	Overexpression	18	Hyperplasia, FL	(62)
	Eμ-BCL2	Transgenic (driven by 5' Igh *Eμ* enhancer)	B cells	Overexpression	18	LPD	(63, 64)
	VavP-Bcl2	Transgenic (driven by *VavP* promoter)	All hematopoietic	Overexpression	10–18	FL	(65)
	IgH-3'E-Bcl2	Knock-in (driven by Igh *3'RR* enhancers)	Mature B	Overexpression	7–14	FL	(66)
	huBcl2^{RSS}	Transgenic (Inactive human *BCL2* locus flanked by RAG recombination sequence signals, RSS)	pre-B	Sporadic overexpression		no tumors	(8)
	huBcl2^{RSS};AID^{Cre} R26$^{LSL.YFP}$	BM chimera: HSPCs from AID^{Cre}Rosa26$^{LSL.YFP}$ transduced with *huBcl2^{RSS}* tracer	pre-B (BCL2) GC for EYFP	Sporadic overexpression	10	*In situ* Follicular Neoplasia	(8)
Crebbp; Bcl2	*Eμ-Bcl2; Mb1^{Cre}Crebbp$^{fl/fl}$*	Conditional knockout combined with *Bcl2* overexpression	pro-B	Loss of function	13	FL, GCB-DLBCL	(67)
	VavP-Bcl2; Cγ1^{Cre}Crebbp$^{fl/fl}$	Conditional knockout combined with *Bcl2* overexpression	GC	Loss of function	18	FL, GCB-DLBCL	(68)
	VavP-Bcl2; shCrebbp	BM chimera of HSPCs from *VavP-Bcl2* transduced with *shCrebbp*	All hematopoietic	Loss of function	2	FL, GCB-DLBCL	(69)
Kmt2d; Bcl2	*VavP-Bcl2; Cγ1^{Cre}Kmt2d$^{fl/fl}$*	Conditional knockout combined with *Bcl2* overexpression	GC	Loss of function	13	FL, GCB-DLBCL	(70)
	VavP-Bcl2; shKmt2d	BM chimera: HSPCs from *VavP-Bcl2* transduced with *shKmt2d*	All hematopoietic	Loss of function	5	FL, GCB-DLBCL	(71)
Ezh2	*Cd19^{Cre} Ezh2$^{Y641F/+}$*	Conditional knockin (endogenous promoter)	Pre-B	Gain of function	12	DLBCL	(72)
Ezh2; Bcl2	*VavP-Bcl2; Ezh2$^{Y641F/WT}$*	BM chimera: HSPCs from *VavP-Bcl2* transduced with *Ezh2^{Y641F}*	All Hematopoietic	Gain of function	3–4	GCB-DLBCL	(73, 74)
	Bcl2hi; Cd19^{Cre}Ezh2^{Y641F}	BM chimera: HSPCs from Cd19CreEzh2Y641F transduced with Bcl2	Pre-B	Gain of function	7	FL, GCB-DLBCL	(72)
	VavP-Bcl2; Cγ1^{Cre}Ezh2^{Y641F}	Conditional knockin combined with *Bcl2* overexpression	GC	Gain of function	–	GCB-DLBCL	(74)
Ezh2; Bcl6	*Cγ1^{Cre}Ezh2$^{Y641F/+;}$ IμBcl6*	Conditional knockin combined with *Bcl6* overexpression	GC	Gain of function	6–12	GCB-DLBCL	(75)
H1c/H1e	*VavP-Bcl2;H1c$^{-/-}$ H1e$^{-/-}$*	Non-conditional knockout with *Bcl2* overexpression	All hematopoietic	Loss of function		DLBCL	(76)
Tet1	*Tet1$^{KO/KO}$*	Non-conditional knockout	All hematopoietic	Loss of function	12	LPD, DLBCL	(77)
Tet2	*CD19^{Cre} Tet2$^{f/f}$*	Conditional knockout	Pre-B	Loss of function	4–18	CLL	(78)
	Vav^{Cre}Tet2$^{f/f}$	Conditional knockout	All hematopoietic	Loss of function	_	GCB-DLBCL	(79)
Hvem	*VavP-Bcl2; shHvem*	BM chimera: HSPCs from *VavP-Bcl2* transduced with *shHvem*	All hematopoietic	Loss of function	4	FL	(80)
Ctss	*Vav-Bcl2; CTSS^{Y132}*	BM chimera: HSPCs from *VavP-Bcl2* transduced with mutated human *CTSS^{Y132D}*	All hematopoietic	Gain of function	2	FL	(81)
	Vav-Bcl2; CTSS^{HIGH}	BM chimera: HSPCs from *VavP-Bcl2* transduced with overexpressed *CTSS*	All hematopoietic	Overexpression	2	FL	(81)
Gα13	*Mb1^{Cre}Gα13$^{f/f}$*	Conditional knockout	pro-B	Loss of function	>12	GCB-DLBCL	(82)
Gα13; Bcl2	*Eμ-Bcl2; Mb1^{Cre}Gα13$^{f/f}$*	Conditional knockout combined with *Bcl2* overexpression	pro-B	Loss of function	10	GCB-DLBCL	(82)
RragC^{mut}	*VavP-Bcl2;RragC$^{S74C/T89N}$*	Knock-in mice crossed with *VavP-Bcl2*	All hematopoietic	Gain of function	10	FL	(83)
Sestrin1	*VavP-Bcl2, shSestrin1*	BM chimera: HSPCs from *VavP-Bcl2* transduced with sh*Sestrin1*	All hematopoietic	Loss of function	–	FL	(84)

Despite its main limitations due to the unspecific Bcl2 deregulated expression in all hematopoietic cells, VavP-*Bcl2* is currently one of the most popular models to study *in vivo* the role of secondary genetic alterations that are frequently found in combination with BCL2 in FL and GCB-DLBCL genetically engineered mouse models.

These studies support the notion that despite a survival advantage conferred to B cells by BCL2, the lymphomagenic process requires additional hits (genetic and/or immunological) for transformation.

Modeling the Early Steps of FL Development: *BCL2^{tracer}* Model

Although several BCL2-engineered models have provided the initial proof-of-principle that BCL2 ectopic expression leads to FL and high-grade lymphomas, the expression of BCL2 in all B cells (and all

T cells for some models) do not represent a true premalignant intermediate stage seen during human lymphomagenesis, where the first t(14;18) event occur in a single B cell in the BM, and is carried on until its ectopic expression in the GC. Instead, pan-B cells BCL2 mouse models generate a polyclonal hyperplasia of naive B cells which is not a known progression step in human FL pathogenesis and as a consequence does not allow studying the early steps of clonal emergence and disease progression. The *BCL2*^{tracer} mouse model has been engineered to mimic "sporadic" t(14;18) translocation (8). This transgenic model relies on the introduction of potent RAG recombination sites at the vicinity of an inactivated human BCL2 transgenic minilocus. In this construct, recombination allows to turn on ectopic BCL2 expression in only few B cells, and at the appropriate window of B cell development in the BM pre-B cells. The recombination breakpoints provide unique PCR-based clonotypic markers to study early steps of clonal emergence and expansion in mouse blood/tissues at different time points, allowing a precise analysis of clonal progression kinetics. As expected, the emergence of BCL2$^+$ B cells was traced in various tissues at low frequency (1 in 10^5 to 10^6) recapitulating the "healthy human t(14;18) carrier" situation. At steady state or after acute immunization with a T-cell dependent antigen, BCL2 alone was not able to drive progression of BCL2-expressing cells into a tumor after 18 months of follow-up, confirming that lymphomagenesis is a stepwise process where premalignant B cells require the accumulation of secondary (epi)genetic alterations to progress into a tumor. However, a chronic immunization protocol with SRBC accelerated genomic instability by allowing BCL2-overexpressing B cells to give rise to memory cells that preferentially underwent iterative rounds of GC entry, allowing multiple rounds of AID-mediated mutagenesis over time to ultimately form premalignant *in situ* FL structures, the earliest known intermediate preceding human FL. Although this model alone does not form FL lesions, it has been instrumental to propose a revised model of early lymphomagenesis whereby cyclic reactivation of BCL2$^+$ memory B cells within new GC reactions would constitute a major pathogenic mechanism facilitating clonal expansion and accumulation of secondary mutations in FL precursors. It is likely that this reactivation in humans operates over decades before clinical manifestation (that we will never reach during the mouse lifespan) and ultimately contribute to the generation of a heterogeneous population of aberrant memory B cell intermediates resembling clonal FL evolving in asymptomatic patients years before diagnosis. Interestingly, this model also led to identify an "immunological 2nd hit" in FL, departing from the all-genetic, cell-intrinsic concept of lymphomagenesis.

MODELING EPIGENETIC ALTERATIONS

Recurrent mutations affecting histone modifying enzymes are a hallmark of GC-derived lymphomas, more particularly in FL. Within DLBCLs, these mutations are enriched within the GCB-DLBCL subtype, with further enrichment within the newly described EZB/C3 genetic subtype. Inactivating mutations of the H3K4 lysine methyltransferase *KMT2D* are found in 70 to 90% of FL cases and up to 30% of DLBCL cases representing the most frequently FL mutated genes in these lymphomas after t(14;18) translocations. Approximately 50 to 70% of FLs and ~25% of DLBCLs carry acquire inactivating mutations in *CREBBP*, whereas its paralog *EP300* is mutated in ~5% of cases. Activating mutations of the H3K27 histone methyltransferase *EZH2*, a component of the polycomb repressive complex 2, are found in 10 to 25% of FL cases and 20% of GCB-DLBCL cases (14, 18, 19, 53–55, 88–90). Overall, 95% of FL patients manifest with at least one chromatin modifier gene mutation. Thorough genomic inference analyses of the clonal evolution patterns in sequential pairs of FL at diagnosis *vs.* relapse/transformation showed that recurrent inactivating mutations in *CREBBP* and *KMT2D* represent early events in FL evolution and are likely to be present in the CPC pool supporting a founder role for these events.

CREBBP and *EP300* Inactivation

CREBBP and EP300 are highly homologous histone acetyltransferases (HAT) that modify gene expression through H3K27 acetylation at enhancer domains of both histone and non-histone substrates. In 50 to 75% of cases, mutations of *CREBBP* are missense inactivation of the acetyltransferase catalytic domain, the remaining mutant alleles causing truncation or loss of expression (54, 55, 69, 90). *CREBBP* and *EP300* mutations are usually detected only at one allele and exclusive fashion, which is thought to be explained by the compensatory and redundant role of these enzymes. The precise timing and location where *CREBBP* or *EP300* mutations happens during B cell transformation is still unclear in humans, but there is large agreement from clonal evolution studies and in premalignant FL conditions that CREBBP is an early event (91). Several groups have therefore attempted to investigate the role of hemizygous *vs.* homozygous *Crebbp* inactivation on mature B cell differentiation and lymphoma development *in vivo* using different strategies from early inactivation in all hematopoietic cells, early B-cell specific deletion or GC-specific deletion [Cγ1-Cre (92)], in combination or not with BCL2 transgenic models.

Horton and colleagues studied the consequences of *Crebbp* deletion in the hematopoietic stem cell compartment thanks to a pIpC-mediated Mx1-Cre recombinase system (93). Those animals developed B cell lymphoproliferative disorders accounting for 29% of all deaths. The B cell lesions localized mostly in the spleen and blood and stained with B220, CD19 and surface IgM indicating their mature B cell origin, however these tumors did not express GC markers. The occurrence of these lymphoproliferative disorders was preceded by the accumulation of lymphoid progenitors characterized by a hyperproliferative state and an altered DNA damage response linked to the loss of p53 activation in the absence of *Crebbp*. Interestingly, the authors found no enrichment for *Bcl6* targets among Crebbp binding sites in their system suggesting different epigenetic changes when *Crebbp* is deleted in hematopoietic stem cells (HSC). This data suggests that *CREBBP* mutations acquired early during hematopoiesis may contribute to the emergence of B cell lymphomas although this model might not be relevant for FL or DLBCL progression as the tumors do not exhibit GC features. It also indicates that the timing of mutation acquisition has an important impact on B cell development. In humans, detection of CREBBP mutations in HSCs remains a very rare event (93).

Three others groups investigated the B-cell deletion of *Crebbp* in combination with BCL2 overexpression to fit with the frequent co-occurrence of the two alterations in human FL and DLBCL (67–69). Jiang et al. recapitulated *Crebbp* downregulation and Bcl2 overexpression *in vivo* using a shRNA retroviral infection system of VavP-*Bcl2* hematopoietic stem progenitor cells (HSPCs) transplanted into lethally irradiated wild-type recipient mice. They observed an acceleration of lymphoma onset in double-mutant vs. *VavP-Bcl2* mice. Lymphoma cells expressed B220, CD19 and IgM and were characterized by somatically mutated Ig locus confirming their GC B cell origin. Importantly, a similar phenotype was observed with a shRNA targeting *Ep300*. The second model developed by Zhang and colleagues consisted in cohorts of Cγ1-Cre (92) and Cd19-Cre $Crebbp^{flox/flox}$ and $Crebbp^{flox/+}$ animals where inactivation of *Crebbp* was induced in GC or developing B cells respectively. After a follow-up of 18 months they did not observe any significant difference between *Crebbp* mutant mice and their littermate controls concluding that loss of *Crebbp* alone at early or late stages of B cell differentiation was not sufficient to induce lymphomagenesis. The generation of mice crossing Cγ1-Cre $Crebbp^{flox/flox}$ mice with VavP-*Bcl2* transgenic mice led to a significant increase in the incidence of B cell malignancies resembling human FL (92% in double mutant versus 61.5% in VavP-*Bcl2* controls). Furthermore, the tumors were characterized by a follicular architecture, were largely of GC origin with Bcl6 expression and presence of mutated Ig genes. In an extension of this study and to investigate in parallel how CREBBP and EP300 contribute to normal GC B cell physiology, Meyer et al. established mouse lines carrying single "floxed" HAT genes that are excised only in activated B cells in the GC (Cγ1-Cre) (94). In accordance with previous studies (95), Meyer et al. confirmed that loss of *Crebbp* in GC B cells led to increased GC formation while *Ep300* loss led to an opposite effect with decreased proportion of GC B cells in immunized mice (94). Transcriptomic analyses of purified GC B cells obtained from these two strains revealed that the set of genes modified by *Ep300* loss or *Crebbp* loss was different with expression of DZ transcripts preferentially repressed in *Ep300*-deleted GC B cells while LZ genes were preferentially decreased in *Crebbp*-deleted GC B cells providing a mechanistic explanation for the reduced numbers of GC B cells observed in the GC-deficient *Ep300* model. The most interesting phenotype comes from the drastic reduction of GC B cells observed when both HAT genes are deleted from the same GC cells. Indeed, the GC response was completely abrogated indicating that the ability of GC B cells to proliferate and differentiate relies on the combined activity of both acetyltransferases likely due to their overlapping and partially redundant functions. Interestingly, *CREBBP*-mutated lymphoma B cells maintained this dependency toward EP300 enzymatic activity which identify a unique vulnerability that provide exciting opportunities of targeting single mutant CREBBP or EP300 GC-derived lymphomas.

In a third model, Garcia-Ramirez et al. produced strains of Mb1-Cre $Crebbp^{flox/+}$ or $Crebbp^{flox/flox}$ mice where *Crebbp* was deleted at early pro-B cell stage in the BM. *Crebbp* deletion at early stages of B cell development led to reduced frequencies of B-cell subsets with reduced numbers of total $B220^+$ B cells in BM and spleen. When crossed with the Eμ-*BCL2* mouse model, these animals showed higher frequencies of GC B cells in the spleens after SRBC immunization and occasionally develop clonal B cell lymphoma with low penetrance and long latency (13 months). Histology was similar to human FL grade 3 or DLBCL and tumoral cells expressed Pax5 and Bcl6 and displayed SHMs consistent with a GC B cell origin (67).

Overall, these three independent *in vivo* models confirmed an oncogenic cooperation between *CREBBP* loss of functions and BCL2 overexpression to promote lymphomagenesis *in vivo*. Mechanistically, these studies showed that CREBBP, and likely EP300, maintain H3K27 acetylation at certain enhancer that are poised during GC reaction and whose reactivation is required for GC exit and terminal differentiation. This includes genes involved in immune synapse, downstream effectors of BCR and NF-κB or terminal differentiation (*Irf4*, *Nfkb2*, *Cd40*) and antigen presentation, the most notable being MHC class II molecules which are critical for B cell terminal differentiation. In normal GC cells, CREBBP targeted enhancers are direct targets of BCL6 and transiently repressed by BCL6/SMRT/HDAC3 complexes that deacetylate H3K27. Upon selection signals received in the LZ allowing GC exit, these enhancers recover H3K27ac state as CREBBP can directly acetylate BCL6 to inactivate its function by preventing the interaction with co-repressor complexes. By impairing the reactivation of these enhancers leaving unopposed BCL6 oncogenic activity, CREBBP loss of function disrupt the expression of immune synapse genes and their downstream signaling pathways, resulting in accumulation of aberrant GC B cells that fail to properly respond to exit signals from the GC microenvironment thereby promoting lymphoma progression. In human FL, decreased MHC II expression and reduced CD4 and CD8 T cell infiltrations have been described in *CREBBP*-mutant FL. A similar association between *CREBBP* inactivation and reduced expression of MHC class II is observed in murine lymphoma models which alters mutant GC cells ability to present antigen to $CD4^+$ cells. Interestingly, *CREBBP*-mutant lymphomas become dependent to HDAC3, the histone deacetylase opposing the effect of CREBBP, that has been identified as a relevant therapeutic target in these tumors (69). Mondello et al. recently showed that HDAC3-selective inhibitors have a dual effect by reversing CREBBP-mutant aberrant epigenetic programming limiting lymphoma growth inhibition while restoring antitumor immunity, notably antigen presenting-genes (96).

KMT2D Loss of Function

KMT2D is a component of the COMPASS complex involved in transcriptional activation through H3K4 monomethylation of gene enhancers in B cells. The majority of *KMT2D* mutations are nonsense events leading to a truncated protein lacking the enzymatic SET domain involved in H3K4 methylation resulting in a loss of function (90). To study the consequences of *Kmt2d* inactivation during B cell differentiation, Zhang and

colleagues generated a conditional *Kmt2d* knock-out model relying on a Cre-Lox system with conditional deletion of B cells early during B cell development (Cd19-Cre $Kmt2d^{flox/flox}$) or after GC initiation (Cγ1-Cre $Kmt2d^{flox/flox}$). Early deletion of *Kmt2d* lead to a higher number and enlarged GC formation while this effect was not seen with late GC deletion and *in vitro*, *Kmt2d*-deficient cells displayed a proliferative advantage compared to wild-type cells. However, *Kmt2d* deficiency in B cells alone upon early or late inactivation was not sufficient to induce FL or DLBCL *in vivo*. Kmt2d protein was mainly found on putative GC enhancers and global H3K4 methylation levels were diminished in *Kmt2d* mutant mice. Moreover, although GC-specific deletion was insufficient to initiate malignant transformation, $Kmt2d^{ko}$-VavP-*Bcl2* double-mutant mice developed B-cell lymphoproliferative disorders with an incidence of 78% (44% for VavP-*Bcl2* alone), with tumors expressing *BCL6* and *PAX5* consistent with a GC origin and recapitulating a spectrum of histopathological features ranging from early FL to DLBCL (40% early FL, 31% FL and 27% DLBCL) (70).

Using a different experimental system, Ortega-Molina and colleagues also explored cooperation between bcl2 and *Kmt2d* deletion in B cell lymphomagenesis. Using a retroviral infection system of shRNAs transduction to silence *Kmt2d* in HSPCs from VavP-*Bcl2* donor mice following transplantation into irradiated wild-type mice, an acceleration of the lymphomagenesis process as well as an increase in the incidence of FL-like tumors (from 30 to 60%) was observed in double-mutant mice compared to shRNA control vectors, validating the tumor suppressive role of *Kmt2d* in B lymphocytes. At preclinical stages of the disease, Ortega Molina et al. showed that after immunization, the number of GC B cells was increased when *Kmt2d* was suppressed. Moreover, GCs persisted for a longer period than in control mice. K*mt2d* loss was associated with a decrease in IgG1 production suggesting a dysfunction of the class switch recombination processes (71). Interestingly, the generation of $Kmt2d^{flox/flox}$Cd19-Cre crossed with a strain overexpressing AID led to the development of aggressive lymphomas resembling DLBCLs and confirms that, independently from BCL2 expression, genetic instability linked to AID overexpression cooperates with *Kmt2d* loss to promote lymphomagenesis.

Integrative genomic analyses from human samples carrying *KMT2D* mutations and *Kmt2d*-mouse FLs showed that genes differentially expressed in *Kmt2d*-mutated lymphomas were mostly repressed and affected a set of genes involved in terminal differentiation programs and GC exit, such as CD40 and BCR signaling, regulation of apoptosis, control of cell migration and proliferation. *KMT2D* mutations result in persistent demethylation of enhancers and failure of the respective genes to respond to signals, notably CD40 signaling from T_{FH}. Moreover, absence of *Kmt2d* affects negatively the expression of major B-cell tumor suppressors such as *Tnfaip3*, *Socs3*, *Tnfrsf14*, *Asxl1* or *Arid1a*. In conclusion, lack of *Kmt2d* leads to an aberrant repression of key genes normally required for GC exit, favoring an abnormal GC B cell outgrowth and failure to differentiate leading eventually to lymphoma development. Of note, these studies showed once more that the stage and/or the timing of a given (epi)genetic alteration has a strong influence on the transcriptional changes occurring in the GC. The developmental stage at which *Kmt2d* mutations are introduced in human precursor tumor cells is still unknown but it has been hypothesized that epigenetic reprogramming may require multiple rounds of cell divisions to allow the replacement of modified histones by non-modified histones explaining why *Kmt2d* inactivation after GC initiation may have a more modest phenotype than early inactivation.

EZH2 Gain of Function

EZH2 is a H3K27 methyltransferase part of the Polycomb Repressive complex-2 (PRC2). Heterozygous gain of function mutations, preferentially affecting the EZH2 SET domain at the Y641 residue and making EZH2 more efficient at H3K27 trimethylation (97), are found in up to 30% of GCB-DLBCL and FL and *de facto* enriched in EZB/C3 DLBCL subtype (18, 89, 98). Several groups have investigated the functional role of wild-type and mutant EZH2 during GC reaction and B cell lymphomagenesis (73, 75, 99, 100). Using a Cγ1-Cre $Ezh2^{flox/flox}$ strain, Béguelin et al. observed a marked reduction in GC B cells after immunization. They reproduced this phenotype in immunized wild-type mice treated with an EZH2 inhibitor targeting wild-type and mutant *EZH2*, establishing that EZH2 is required for GC formation (73). Similar observations were made by Caganova et al. underlining that under normal conditions, EZH2 enables GC formation at least in part by suppressing cell-cycle checkpoint genes like CDKN1A, impairing DNA damage responses to support centroblast proliferation and silencing essential plasma cell differentiation genes, particularly *Blimp1* and *Irf4* (99, 100).

To understand how $EZH2^{Y641}$ hotspot mutation perturbs GC development and drives lymphomagenesis, Béguelin and colleagues developed two mouse strains conditionally expressing the mutant $Ezh2^{Y641N}$ or $Ezh2^{Y641F}$ in GC B cells upon Cγ1-Cre recombinase (73, 75). Upon immunization, both models caused oversized GCs and displayed increased abundance of H3K27me3 mark at critical GC B cell bivalent promoter leading to permanent silencing of EZH2 target genes. The GC phenotype appears to be mediated through cooperative and mutually interdependent actions of EZH2 together with the transcriptional repressor BCL6 and BCOR repressive complex. These *Ezh2* mutant mice did not develop lymphomas. However, early activation (CD19-Cre) of mutant *Ezh2* in an independent study led to aggressive DLBCL in about 12 months (72). VavP-*Bcl2* HSPCs were transduced with retroviruses expressing $Ezh2^{Y641F}$, $Ezh2^{WT}$ or an empty vector and transplanted into lethally irradiated recipient mice subjected to SRBC immunization every 4 weeks to induce GC formation. $Ezh2^{Y641F}$ $Bcl2^{+}$ chimeric mice led to early lymphoma development in 70% of mice at 111 days (*vs* 20% in mice overexpressing $Ezh2^{WT}Bcl2^{+}$ and none in the *Bcl2* control at that stage), characterized by enlarged spleen and liver and resembling morphologically to DLBCL with centroblastic morphology (73, 74). These data demonstrate that *EZH2* gain of function mutations accelerate GC B cell lymphomagenesis in cooperation with Bcl2 overexpression, recapitulating features of

GCB-DLBCL. Similar results were obtained when transgenic and knock-in *Ezh2* strains engineered to express heterozygous mutant Ezh2 in GC B cells were crossed with VavP-*Bcl2*. Importantly, homozygous expression of mutant *Ezh2* phenocopies the *Ezh2* knock-out phenotype further attesting the requirement for the maintenance of the wild-type allele for *Ezh2* mutant enzymatic activity.

Recent studies questioned whether EZH2 mutation has additional and qualitatively distinct function in lymphomagenesis beyond simply being a more potent version of the wild-type enzyme. Along these lines, Ennishi et al. identified a strong enrichment of *EZH2* mutations in human DLBCL cases with loss of MHC-I and MHC-II expression linked to a reduced number of tumor-infiltrating lymphocytes and less T cell cytolytic activity (74). To investigate in detail the consequences of EZH2 mutations on MHC expression and immune microenvironment, the authors relied on two different mouse models. First, they used the *Ezh2*-mutant model developed by Béguelin et al. where VavP-*Bcl2* hematopoietic progenitors are infected with *Ezh2*-mutant containing retrovirus before re-injection into lethally irradiated recipient mice. Second, they used Cγ1-Cre $Ezh2^{Y641N}$ or $Ezh2^{Y641F}$ mice crossed with VavP-*Bcl2* strain which develops DLBCL-like tumors. In both experimental systems, MHC-I and MHC-II expression were significantly reduced in mutant *Ezh2* mice compared to wild-type mice, with reduced infiltration of CD3, CD4 and CD8 T cells in the tumor microenvironment, establishing *Ezh2* gain-of-function mutation as a driver of MHC downregulation in GC lymphomagenesis, and eventually favoring immune escape. Importantly they also showed that EZH2 epigenetic switch-off of MHC molecules, driven by transcriptional repression of MHC-I/II transactivators, could be reversed with EZH2 inhibitors. The ability to restore MHC expression provides an interesting proof of concept in combining epigenetic reprogramming small molecules with immunotherapeutic approaches.

More recently, Melnick and colleagues further strengthened the concept that *Ezh2* mutation initiate GC derived lymphomagenesis by escaping immune effector recognition and inducing a remodeling of the GC immunological niche (101). Using competitive BM chimera to track the cellular dynamics of $Ezh2^{Y641F}$ B cells during GC reaction, they found that *Ezh2* mutants manifested a competitive growth advantage in the GC. This competitive advantage led to GC hyperplasia characterized by an increase of a cycling LZ cell population, without maturation blockade, associated with the expansion of FDC network. Using droplet based single cell transcriptomics and advanced histone mass spectrometry technologies, they assessed how *Ezh2* mutation affected GC B cell cellular and histone methylation dynamics in an unbiased manner. They found that the epigenetic reprogramming imprinted by *Ezh2* mutation through the reinforcement of the repressive program induced by H3K27me3 accumulation led to the abolition of LZ B cells' dependence toward T_{FH} emanating signals. Indeed, DZ re-entry of *Ezh2*-mutated centrocytes was clearly diminished and these GC B cell escaped T_{FH}-mediated clonal selection. The ability of *Ezh2*-mutant GC B cells to proliferate within the LZ was linked to FDC interaction as this ability was impaired when FDC function was abolished through injection of soluble lymphotoxin receptor β. Remarkably, this study revealed how activating mutation of *EZH2* induces a premalignant FL-like niche allowing B cells to persist as slowly proliferative centrocytes without T_{FH} help and in a FDC dependent manner.

The above studies provide important insights on an emerging paradigm where one of the most critical function of epigenetic modifier mutations in promoting GC B cell transformation goes beyond the sole reprogramming of the GC epigenome, but instead arise from failure of GC exit signals to restore expression of genes that normally regulate immune signaling pathways and antigen presentation (47). Of therapeutic interest for the targeting of the FL common precursor cells, this remodeling of the immune synapse at least with *EZH2* mutations tends to occur early during lymphomagenesis.

Linker Histone Loss of Function

Linker histones (H1) are additional chromatin modifying genes involved in the organization and stabilization of the nucleosome structure, supporting the folding of chromatin into higher-order conformation, and regulating its epigenetic state through the recruitment of histone modifiers. Heterozygous H1 mutations, found in up to 44% of FL and 27% of GCB-DLBCL, are mostly missense events affecting the globular C-terminal domain which led to the loss of protein function with impaired chromatin binding (53). Among them, H1C and H1E are the most common affected H1 isoforms observed in B cell lymphomas (102, 103).

To investigate the functionality of these isoforms in lymphomagenesis, Yusufova and colleagues used the previously described $H1c^{-/-}$ $H1e^{-/-}$ mice model (104). At early time points after chronic SRBC immunization, those animals manifested lymphoproliferative disease with invasiveness of $B220^+$ B cells in extranodal tissues such as liver and lungs. Further analysis using competitive BM chimera revealed a competitive advantage for H1c/H1e-deficient B cells characterized by a specific increase of cycling LZ B cell population expressing Gl7, Fas and cd86 markers whereas no effect was found in other mature and immature B cell populations. Notably, H1 deficiency enables a chromatin decompaction in GC B cells with an enrichment in stem cell genes that become desilenced in H1-deficient GC cells. Given the frequent co-occurrence of *H1C* and *H1E* mutated genes with BCL2 overexpression in lymphomas, they crossed $H1c^{-/-}$ $H1e^{-/-}$ mice with *VavP-Bcl2* mice. Loss of H1 isoforms caused a more extensive disruption of lymph node architecture with diffuse infiltration of immunoblastic cells, along with an extensive invasion of $B220^+$ B cells and $CD3^+$ T cells in extranodal tissues establishing H1 proteins as *bona fide* tumor suppressors. RNA sequencing analysis of lymphoma-like tumors in mouse and humans revealed a significant enrichment for stem cell signature and serial transplantations confirms that loss of H1 conferred lymphoma cells with enhanced self-renewal potential. These findings enlighten the contribution of H1 linker deletion in driving malignant transformation where epigenetic marks changes favor a relaxed state chromatin in GC B cells, increasing B cell fitness advantage

by allowing self-renewal proprieties and may expose DNA to further AID-mediated additional hits.

TET1 and TET2 Loss

Besides chromatin modifiers genes, a number of studies have demonstrated methylation and disruption of cytosine methylation [5-methylcytosine (5mC)] patterning as another factor linked to the biology of B cell lymphoid malignancies (105). The methyl-cytosine dioxygenase *TET2* (ten-eleven translocation 2) missense or truncated mutation is present in 6–12% of GCB-DLBCL (14). *TET2* mutations are known to occur early in human HSCs and can be found in individuals with clonal haematopoiesis. Whether early *TET2* mutations has a driving role in DLBCL was explored in multiple models. 5mC is well established as an epigenetic mark associated with transcriptional silencing, notably of tumor suppressor genes. TET2 is involved in active DNA demethylation, catalysing the oxidation of 5mC to 5-hydroxymethylcytosine (5hmC). Recently, it has been appreciated that 5hmC also functions as an epigenetic mark, and when linked to gene enhancers, is associated with activation of nearby genes.

Conditional deletion of *Tet2* specifically in the B cell compartment with CD19-Cre Tet2$^{fl/fl}$ mice showed B cell transformation mimicking chronic lymphocytic leukemia (78). Programmed deletion of *Tet2* in hematopoietic cells (Vav-Cre) or B cells (CD19-Cre) in immunized animals disrupt the ability of GC B cells to undergo CSR and terminal differentiation. Furthermore, conditional deletion of *Tet2* at the GC stage results in a preneoplastic GC hyperplasia, blockage of GC exit and PC differentiation evolving in DLBCL-like tumors, confirming its role as a *bona fide* B cell tumor suppressor (79). Mechanistically, this phenotype is due to the focal loss of 5hmC at enhancers linked to B cell differentiation. Indeed, *Tet2*$^{-/-}$ GC B cells feature disruption of many enhancers linked to GC exit signaling pathways, antigen presentation, and terminal differentiation genes. This mechanism is conceptually similar to the functions of the histone modifiers in DLBCL which fails to restore the immune synapse. Interestingly, *TET2* and *CREBBP* mutations are mutually exclusive in DLBCL (106), thus a combined mouse model could be engineered to find a potential therapeutic vulnerability in DLBCL.

The methyl-cytosine dioxygenase *Tet1* (ten-eleven translocation 1) is also an important regulator of 5-hydroxymethylcytoine and interestingly transcriptionally silenced in FL. Cimmino and colleagues engineered *Tet1*-deficient mice where B cell lymphoma development was promoted resulting in a diminished survival compared to wild type mice (77). *Tet1*-deficient mice exhibited lymphadenopathy and hepato-splenomegaly. Splenic tumors were characterized by a massive infiltration of proliferating lymphocytes disrupting the normal architecture and expressing the GC markers Bcl6 and Irf4 but not the PC marker Cd138. When combined with Bcl2 overexpression, Tet1-deficient B cell lymphomagenesis was accelerated up to 10 weeks post-transplantation. Altogether, deletion of *Tet1* and *Tet2* in mice induces phenotypically predominant DLBCL tumors supporting a suppressor role in mature B cells.

MODELING EVASION FROM IMMUNE SURVEILLANCE AND DISSEMINATION

The influence of the GC microenvironment on B cell development which provides essential signals for the survival, selection and differentiation is well established with several actors residing in the GC LZ such as T follicular helper cells (T_{FH}), follicular dendritic cells (FDC), regulatory T cells (Treg), macrophages and stromal cells (19). FL is the paradigm of a B cell malignancy strongly dependent on direct interaction with a GC-like permissive microenvironment that co-evolves with malignant cell clones as a part of a dynamic interplay (49). Recent studies in both FL patients and genetically-engineered mouse models have started to highlight the link between B 'cell-intrinsic' tumor genetic alterations and their cell-extrinsic functions during lymphomagenesis by contributing to escape of immune surveillance mechanisms. We will discuss the latest studies showing how the *TNFRSF14 or CTSS* frequent alterations in FL modify the TME/malignant B cells crosstalk and contribute to lymphoma development either by affecting antigen processing and hiding from the immune system, or modifying its composition to become tumor-supportive.

Tnfrsf14 Loss in FL

TNFRSF14, the gene encoding the HVEM receptor located on 1p chromosome is one of the most frequent cell surface protein, deleted or mutated in >40% of FL cases and enriched in GCB-DLBCL (14, 18, 19). HVEM is expressed at the surface of B cells as well as other cell types and has multiple ligands including LIGHT or BTLA. Besides its role as a signaling receptor, HVEM can act as ligand and transmit signals into BTLA-expressing cells notably T_{FH} (107). How loss of *HVEM* contributes to lymphomagenesis has been the focus of two independent and complementary *in vivo* studies (80, 108). The first study took advantage of the well characterized VavP-*Bcl2* model that recapitulates key aspects of the genetics and pathology of human FLs to generate BM chimeras where knockdown of *Hvem* was mediated by transduction of shHvem into VavP-*Bcl2* HSCs followed by reconstitution of irradiated wild-type hosts. Knockdown of *Hvem* in all hematopoietic system caused a significant acceleration and increased penetrance of lymphoma development compared to VavP-*Bcl2 controls* with 90% of animals carrying tumors at 100 days. Despite the absence of B-cell specificity of the shRNA transduction strategy, only B cells were enriched with the short-hairpin construct indicating the *Hvem* knockdown in T cells was unlikely to participate to the lymphomagenic effect. Mechanistically, besides cell-autonomous activation of B cells, *Hvem* loss and the consequent loss of interaction with Btla triggers the amplification of T_{FH} producing high amounts of TNF and Lymphotoxin, the two non-redundant factors involved in lymphoid stromal cell differentiation and maintenance, and favors lymphoid stromal cell activation including FDC and FRC (Follicular Reticular Cells). This seminal study offers the first demonstration of a functional impact of a B-cell specific genetic alteration on the polarization of a FL-supportive microenvironment (80). Of therapeutic interest,

immunotherapeutic delivery of a soluble HVEM receptor, *via* modified CAR-T cells, inhibited the growth of lymphoma by restoring the BTLA-HVEM interaction highlighting the essential role of the tumor/microenvironment dialog in lymphomagenesis. In an independent study, Mintz et al. reported that in models of *Bcl2* overexpression in B cells, *Btla* deficiency in T cells led to a similar GC B cell outgrowth and accelerated lymphomagenesis than *Hvem* deficiency in B cells proposing an alternative mechanism by which the Btla-Hvem axis functions as an cell-extrinsic suppressor in lymphomagenesis (108). Using a chimeric mouse system, they identified that during a normal immune response, *Hvem* restrains B cell proliferation, differentiation and selection by reducing the delivery of signal in *trans* through the Btla-Hvem axis on T_{FH} cells. *Hvem* mutation in B cells would lead to a loss of negative signaling in T_{FH} cells and allows *Hvem*-mutant B cells to receive exaggerated helper signals that promote proliferation and accrual of AID-mediated mutations. Collectively, those data provide important evidence for a cell-extrinsic tumor suppressor role of *Hvem*. The ways in which increased signaling *via* CD40 and other T cell–derived helper factors cooperates with Bcl2-overexpression in lymphoma development remain to be fully elucidated.

CTSS Alterations in FL

Cathepsin S (CTSS) is part of a family of cysteine proteases whose role is essential in the regulation of normal immune response through its activity on antigen processing, B cell expansion and communication with $CD4^+$ T cells. By cleaving the CD74 chaperone protein bound on MHC class II molecules, CTSS enzymatic activity results in a smaller peptide CLIP that will be displaced and allow variable antigenic peptides to bond to MHCII and present at the cell surface. Recurrent hotspot mutations and gene amplifications of *CTSS* have been recently described in 6 and 13% of FL patients respectively (81, 109) and mechanistically, $CTSS^{Y132D}$ hotspot mutation promotes activation of the protein and increases its protease activity. To assess how the most common $CTSS^{Y132D}$ mutations or CTSS overexpression contribute to accelerate lymphoma development, Dheilly et al. generated a chimera mouse model of FL using the VavP-*Bcl2* mice as HSPC donor cells and expressing either mutated human CTSS or overexpressing human CTSS. Both models revealed an oncogenic role of CTSS over-activation with higher penetrance and decreased latency as compared to VavP-*Bcl2* tumors alone. Tumors with CTSS alterations were characterized by a remodeled tumor-prone microenvironment with an increased infiltration of $CD4^+$ T cells while limiting $CD8^+$ T cells recruitment. Depletion of $CD4^+$ T cells in *VavP-Bcl2*/CTSS chimera models confirm that CTSS is essential to support the communication and co-stimulatory signals between tumor B cells and $CD4^+$ cells in the GC context. Conversely, loss of CTSS activity in aggressive mouse lymphoma xenograft restrain lymphoma growth by recruiting and enhancing $CD8^+$ T cells cytotoxic activity while impairing communication with $CD4^+$ T_{FH} cells. These data show for the first time that by altering the processing of antigenic peptides, CTSS mutations or overexpression remodel the immune microenvironment to promote lymphoma growth and implies that targeting a regulator of antigen presentation such as CTSS could modulate the spectrum of processed antigens, promote activation of cytotoxic T cells, enhance tumor immunogenicity and improve response to anti-PD1 immunotherapies.

Disruption of Gα Migration Pathway

Another pathway frequently mutated in GC-derived lymphomas is the GC homing pathway involving *S1PR2* and *GNA13*. The guanine nucleotide binding protein *GNA13* (encoding *Gα13*), is a signaling mediator downstream of transmembrane G-protein-coupled receptors sphingosine-1-phosphate receptor-2 (S1PR2), that confines B cells in the GC and promotes growth regulation by suppressing both Akt and cell migration (110). In about 20% of GCB-DLBCL cases (38% in the EZB subtype), deleterious mutations affect one of the members of the *Gα13* homing pathways, namely *GNA13, S1PR2* and *P2RY8* (another S1P receptor expressed on GC B cells). To model *in vivo* the impact of *GNA13* loss during lymphomagenesis, Muppidi and colleagues utilized a mixed BM chimeric approach, deleting *Gα13* in all B-lineage using $Mb1^{Cre}$; $G\alpha13^{f/f}$ mice. Deficiency of *Gα13* favors the formation of enlarged mesenteric LN with GC B cells expansion associated with a marked disruption of the GC architecture and a loss of GC confinement due to the inability to suppress migration in response to S1P. Occasional transformation in B cell lymphomas displaying a GC-like phenotype ($Gl7^+CD138^-Bcl6^+Irf4^+IgD^-$) were observed at 1 year of age (82). One of the critical observations made in *Gα13* deficient cells is the loss of confinement which allows egress outside the GC, dissemination and seeding of these tumoral cells at distant sites such as blood and BM. As deficiency in S1PR2 did not phenocopy *Gα13* deficiency, the authors searched for additional Gα13 G protein coupled receptor that may be involved in GC B cell regulation and discovered that P2RY8, an orphan receptor also represses GC B cell growth promoting confinement *via* Gα13 and is mutated in GCB-DLBCL. Cooperation between Bcl2 overexpression and *Gna13* loss showed an exacerbated phenotype in double mutant mice leading to greater accumulation of GC B cells in spleen, wider dispersal throughout the follicles and more dissemination in blood and BM suggesting a combinatorial effect of Bcl2 in promoting abnormal B cell survival outside the GC niche. These findings shed new lights on an important mechanism by which disruption of Gα13 signaling exerts dual actions in promoting growth and favoring dissemination of GC B cell in GC-derived lymphomagenesis and offer a biological explanation for factors leading to systematic dissemination of tumoral GC B cells in multiple organs including the BM.

MODELING DYSREGULATION OF GC METABOLISM

During T-dependent adaptive immune responses, B cells undergo a quick anabolic shift that sustain the GC proliferative burst (111). Many B-cell lymphomas originating in the GC present an exceptionally high proliferation index. This implies massive metabolic requirements in order to generate sufficient energy and support anabolism for repeated growth and division cycles. Recurrent mutations in components of the nutrient sensing pathway that activates the mechanistic target of rapamycin complex 1 (mTORC1), a driver of cellular

anabolism are found in about 25% of FLs (112, 113). In response to growth factors and when there is sufficient intracellular amino acid concentration, mTORC1 promotes protein synthesis (114). Intracellular amino acid concentration is perceived through a protein complex present on lysosome surface comprising RAG GTPases, Ragulator complex, v-ATPase complex (vacuolar H^+-adenosine triphosphate ATPase) and SLC38A9 (sodium-coupled amino acid transporter 9). When amino acid concentration is sufficient, the RAG GTPases form heterodimers on lysosome surface allowing the recruitment of mTORC1 and downstream protein synthesis supporting cellular growth (114–116).

RRAGC Activating Mutations

The RRAGC gene encodes for Ras-related GTP-binding protein (RAGC), an essential activator of mTORC1 downstream of the sensing of cellular nutrients. Recurrent point mutations of *RRAGC* are found in 18% of FLs and are rare in other B cell lymphomas (112, 113). More than half of these events are associated with mutations of certain components of the v-ATPase complex (*ATP6V1B2* and *ATP6AP1*). To characterize the impact of recurrent *RRAGC* mutations on B cell function and lymphomagenesis, Ortega-Molina et al. used CRISPR/Cas9 genome editing techniques to engineer two independent murine *Rragc* knock-in mouse strains reproducing hotspot mutations recurrently found in human FL (S75C and T90N mutations) (83). Heterozygous $RagC^{S74C/+}$ and $RagC^{T89N/+}$ heterozygous mice showed no obvious phenotype. Lymphoid and myeloid cell populations frequencies were similar in mutant versus wild-type mice in the spleen and BM however RagC knock-in mutations conferred partial insensitivity to nutrient withdrawal. When bred to a VavP-*Bcl2* mice, RagC-$Bcl2^+$ double-mutant mice showed exacerbated B cell responses in response to immunization characterized by enlarged GCs, increased plasma cell production without impairment of high-affinity B cell selection and eventually acceleration of lymphoma development. This was observed both in the progeny of *VavP-Bcl2*-$RagC^{mut}$ mice but also using a BM chimeric system where VavP-*Bcl2*-$RagC^{mut}$ fetal liver cells were transplanted into lethally irradiated wild-type recipients. Histological analysis of these tumors revealed a follicular growth pattern of $Bcl6^+$ B cells with no difference according to genotype. Bulk RNA sequencing analysis of $B220^+$ cells obtained from $RagC^{mut}$ and $RagC^{WT}$ $Bcl2^+$ FL-like tumors revealed that the mTORC1 signaling signature was enriched in $RagC^{mut}$ FL. Furthermore, when transcriptional profiles from murine and human FL with or without RagC mutations were compared, upregulated genes in murine $RagC^{mut}$ FL were enriched in *RRAGC* mutated human FL. Interestingly, the mTOR inhibitor rapamycin, given orally to $RagC^{mut}$ and $RagC^{WT}$ $Bcl2^+$ mice during long term, inhibited proliferation selectively in $RagC^{mut}$ FL. Overall, this data shows that *RRAGC* mutations result in mTORC1 activation regardless of the intracellular amino acid concentration which confers a selective advantage to GC B cells. In addition, the presence of these mutations makes GC B cells less dependent to T_{FH} signals, as blockade of T cell help through anti-CD40L after GC induction makes RagCmut B cells intrinsically resistant to apoptosis despite T_{FH} suppression. Finally, when these mutations are associated with Bcl2 overexpression, the lymphomagenesis process is accelerated in a cell-intrinsic manner where mutant GC B cells with increased fitness could continue to undergo cycles of selection and proliferation favoring further acquisition of additional hits (83).

SESTRIN1 Loss of Function

SESTRIN1 has been identified as a target gene of the recurrent 6q deletion in FLs and it is also epigenetically inactivated by *EZH2* gain-of-function (84). SESTRIN1 is a mTORC1 regulator that inhibits cell growth when TP53 is activated in response to DNA damage. Inactivation of SESTRIN1, by del6q or by the *EZH2* mutation leads to mTORC1 activation. Therefore, SESTRIN1 loss represents an alternative to *RRAGC* mutations that maintain mTORC1 activity under nutrient starvation. To recapitulate *SESTRIN1* deficiency *in vivo*, in combination with BCL2 overexpression, Oricchio and colleagues retrovirally transduced *VavP-Bcl2* HSPCs with shRNAs targeting *Sestrin1*. *Sestrin1* deficiency led to an acceleration of the Bcl2-mediated lymphoma, establishing his tumor suppressive role in B cells. Morphologically, BCL2/Sestrin1-deficient tumors resembled FL with a follicular architecture, they displayed markers of a GC phenotype (PNA and BCL6), showed evidence of somatic hypermutation, an increased tumor proliferation based on Ki67 staining. Remarkably, pharmacological inhibition of EZH2 promotes SESTRIN1 re-expression and restores its tumor suppressive activity, suggesting the possibility to epigenetically control mTORC1 activity in lymphoma. Interestingly, *EZH2*/*RRAGC* gain of function mutations and *SESTRIN1* loss are mutually exclusive suggesting that these alterations are involved in mTORC1 activity maintenance allowing tumor cells to escape proliferation inhibition (84) also becoming less dependent to T_{FH} signals as shown in the context of *RRAGC* and *EZH2* mutations (83, 101). In summary, mTORC1 pathway activation, through various mutually exclusive molecular alterations, is clearly involved in B cell lymphomagenesis process and may be associated to a specific sensitivity to mTOR inhibitors.

CONCLUSIONS AND PERSPECTIVES

B cell lymphomas are among the most frequent hematopoietic malignancies and represent a molecularly heterogeneous group of diseases with different therapeutic vulnerabilities (26, 117) and clinical outcomes that largely depend on a complex interplay between a multitude of genomic alterations and heterogeneous tumor microenvironment signatures (118, 119). Sequencing studies allowed the identification of recurrently mutated genes that drive lymphomagenesis and led to refine DLBCL classification that pave the way for personalized therapeutic strategies (14, 19, 118). The latest large-scale genome sequencing studies identified up to seven different molecular subtypes of DLBCL (118) which represent an interesting framework for the development of models mimicking each molecular subtype. Now, recent DLBCL classifications based of TME composition revealed four distinct microenvironment compositions which provide independent contributions to clinical outcome regardless of the GCB/ABC

cell-of-origin or the genetic DLBCL subtype classification (119). The challenge of modeling future preclinical mouse models will be to recapitulate both the genomic features of the tumors and the parallel remodeling of the tumor microenvironment. Such tumors likely develop over decades in humans before clinical symptoms appear and rely on a complex combination of hits that have been accumulated in a stepwise and ordered manner leading to a spatially and temporally intra-tumor heterogeneity. Advanced technologies are emerging for a better characterization of the existing and future models and cellular heterogeneity in murine lymphomas can be resolved by measuring gene expression at a single cell resolution, allowing the study of B cells together with their microenvironment. Using those techniques, we and others have started to uncover and compare the underlying transcriptional and functional heterogeneity within FL malignant B cells and normal GC B cells in human and mice (31, 81, 101, 120, 121).

Another important feature of lymphoma biology that need to be properly addressed in mouse models is mimicking the kinetics and cellular context in which genetic hits accumulate overtime sometimes over years. The order of appearance of such hits and how it influences lymphomagenesis remains an area of active research. Mutations in *KMT2D*, *CREBBP* or *EZH2* represent early events during lymphomagenesis and have been proposed to occur in HSPCs. Mouse models reproducing these alterations do not induce lymphomagenesis on their own but accelerate GC B cell transformation when combined with BCL2 overexpression (68–71). Accordingly, recent genomic data obtained from prediagnostic samples formally demonstrate that BCL2 translocations systematically precede the acquisition of subsequent epigenetic mutations (122).

Murine models developed since several decades have been particularly useful to inform us on the biological mechanisms driving B cell lymphomagenesis, and helping to understand the functional consequences of genetic alterations. As one of the emerging functions of epigenetic modifier genes in GC B cell lymphoma is to favor disease initiation through the reprogramming of the immune niche, mouse models that faithfully recapitulate the complex interactions with the microenvironment will become valuable tools for the testing and development of novel, rationally designed therapeutic approaches (80, 101). In this line, it is remarkable that microenvironment remodeling seems to occur early in the context of *EZH2* mutations, suggesting that early epigenetic therapy may be useful to prevent disease progression (105).

GEM models may recapitulate the natural history and histological properties of human tumors. However, they display a limited mutational and immunological complexity compared to the human tumors they are intended to model (119). Novel sophisticated tools for engineering mouse models such as CRISPR-Cas9 gene editing techniques or patient-derived xenografts (especially those mimicking indolent lymphomas such as FL), including in humanized mice, will be useful to fill this gap and efficiently generate preclinical models that reflect the complex genetics of the human tumors (61, 123–125). The generation of transplantable lymphoma cell lines obtained from these GEM can be engineered to develop functional CRISPR screening *in vivo;* such an approach would also be useful to screen for therapeutic vulnerabilities in an unbiased manner. Now that most of the genetic drivers have been discovered in B cell lymphomas and that we are getting the tools for a more in-depth characterization of their functional consequences both on B cells and its microenvironment, we hope that studies using more complex GEM tumor models will serve to streamline the translation of targeted therapies with novel immunotherapies into the clinics.

AUTHOR CONTRIBUTIONS

All authors contribute to the writing of the review. All authors contributed to the article and approved the submitted version.

FUNDING

This work was supported by grants from Fondation pour La Recherche Médicale (GB), Fondation ARC, Institut National du Cancer, Canceropôle PACA and Institut Carnot Calym. We thank all the team members past and present that have contributed to some of the work described in this review.

REFERENCES

1. Cyster JG, Allen CDC. B Cell Responses: Cell Interaction Dynamics and Decisions. *Cell* (2019) 177:524–40. doi: 10.1016/j.cell.2019.03.016
2. Victora GD, Nussenzweig MC. Germinal Centers. *Annu Rev Immunol* (2012) 30:429–57. doi: 10.1146/annurev-immunol-020711-075032
3. Calado DP, Sasaki Y, Godinho SA, Pellerin A, Köchert K, Sleckman BP, et al. The Cell-Cycle Regulator c-Myc Is Essential for the Formation and Maintenance of Germinal Centers. *Nat Immunol* (2012) 13:1092–100. doi: 10.1038/ni.2418
4. Dominguez-Sola D, Victora GD, Ying CY, Phan RT, Saito M, Nussenzweig MC, et al. The Proto-Oncogene MYC Is Required for Selection in the Germinal Center and Cyclic Reentry. *Nat Immunol* (2012) 13:1083–91. doi: 10.1038/ni.2428
5. Laidlaw BJ, Cyster JG. Transcriptional Regulation of Memory B Cell Differentiation. *Nat Rev Immunol* (2020) 21:1–12. doi: 10.1038/s41577-020-00446-2
6. Dogan I, Bertocci B, Vilmont V, Delbos F, Mégret J, Storck S, et al. Multiple Layers of B Cell Memory With Different Effector Functions. *Nat Immunol* (2009) 10:1292–9. doi: 10.1038/ni.1814
7. Mesin L, Schiepers A, Ersching J, Barbulescu A, Cavazzoni CB, Angelini A, et al. Restricted Clonality and Limited Germinal Center Reentry Characterize Memory B Cell Reactivation by Boosting. *Cell* (2020) 180:92–106.e11. doi: 10.1016/j.cell.2019.11.032
8. Sungalee S, Mamessier E, Morgado E, Grégoire E, Brohawn PZ, Morehouse CA, et al. Germinal Center Reentries of BCL2-Overexpressing B Cells Drive Follicular Lymphoma Progression. *J Clin Invest* (2014) 124:5337–51. doi: 10.1172/JCI72415
9. Venturutti L, Melnick A. The Dangers of Déjà Vu: Memory B-Cells as the Cell-of-Origin of ABC-Dlbcls. *Blood* (2020) 136:2263–74. doi: 10.1182/blood.2020005857
10. Adams JM, Harris AW, Pinkert CA, Corcoran LM, Alexander WS, Cory S, et al. The C-Myc Oncogene Driven by Immunoglobulin Enhancers Induces Lymphoid Malignancy in Transgenic Mice. *Nature* (1985) 318:533–8. doi: 10.1038/318533a0
11. Park SS, Kim JS, Tessarollo L, Owens JD, Peng L, Han SS, et al. Insertion of C-Myc Into Igh Induces B-Cell and Plasma-Cell Neoplasms in Mice. *Cancer Res* (2005) 65:1306–15. doi: 10.1158/0008-5472.CAN-04-0268

12. Truffinet V, Pinaud E, Cogné N, Petit B, Guglielmi L, Cogné M, et al. The 3' IgH Locus Control Region Is Sufficient to Deregulate a C-Myc Transgene and Promote Mature B Cell Malignancies With a Predominant Burkitt-Like Phenotype. *J Immunol* (2007) 179:6033–42. doi: 10.4049/jimmunol.179.9.6033
13. Sander S, Calado DP, Srinivasan L, Köchert K, Zhang B, Rosolowski M, et al. Synergy Between Pi3k Signaling and MYC in Burkitt Lymphomagenesis. *Cancer Cell* (2012) 22:167–79. doi: 10.1016/j.ccr.2012.06.012
14. Reddy A, Zhang J, Davis NS, Moffitt AB, Love CL, Waldrop A, et al. Genetic and Functional Drivers of Diffuse Large B Cell Lymphoma. *Cell* (2017) 171:481–94. doi: 10.1016/j.cell.2017.09.027
15. Schmitz R, Young RM, Ceribelli M, Jhavar S, Xiao W, Zhang M, et al. Burkitt Lymphoma Pathogenesis and Therapeutic Targets From Structural and Functional Genomics. *Nature* (2012) 490:116–20. doi: 10.1038/nature11378
16. Pae J, Ersching J, Castro TBR, Schips M, Mesin L, Allon SJ, et al. Cyclin D3 Drives Inertial Cell Cycling in Dark Zone Germinal Center B Cells. *J Exp Med* (2021) 218:e20201699. doi: 10.1084/jem.20201699
17. Ramezani-Rad P, Chen C, Zhu Z, Rickert RC. Cyclin D3 Governs Clonal Expansion of Dark Zone Germinal Center B Cells. *Cell Rep* (2020) 33:108403. doi: 10.1016/j.celrep.2020.108403
18. Schmitz R, Wright GW, Huang DW, Johnson CA, Phelan JD, Wang JQ, et al. Genetics and Pathogenesis of Diffuse Large B-Cell Lymphoma. *New Engl J Med* (2018) 378:1396–407. doi: 10.1056/NEJMoa1801445
19. Chapuy B, Stewart C, Dunford AJ, Kim J, Kamburov A, Redd RA, et al. Molecular Subtypes of Diffuse Large B Cell Lymphoma Are Associated With Distinct Pathogenic Mechanisms and Outcomes. *Nat Med* (2018) 24:679–90. doi: 10.1038/s41591-018-0016-8
20. Young RM, Phelan JD, Shaffer AL, Wright GW, Huang DW, Schmitz R, et al. Taming the Heterogeneity of Aggressive Lymphomas for Precision Therapy. *Annu Rev Cancer Biol* (2019) 3:429–55. doi: 10.1146/annurev-cancerbio-030518-055734
21. Venturutti L, Teater M, Zhai A, Chadburn A, Babiker L, Kim D, et al. Tbl1xr1 Mutations Drive Extranodal Lymphoma by Inducing a Pro-Tumorigenic Memory Fate. *Cell* (2020) 182:297–316.e27. doi: 10.1016/j.cell.2020.05.049
22. Calado DP, Zhang B, Srinivasan L, Sasaki Y, Seagal J, Unitt C, et al. Constitutive Canonical Nf-κb Activation Cooperates With Disruption of BLIMP1 in the Pathogenesis of Activated B Cell-Like Diffuse Large Cell Lymphoma. *Cancer Cell* (2010) 18:580–9. doi: 10.1016/j.ccr.2010.11.024
23. Mandelbaum J, Bhagat G, Tang H, Mo T, Brahmachary M, Shen Q, et al. Blimp1 Is a Tumor Suppressor Gene Frequently Disrupted in Activated B Cell-Like Diffuse Large B Cell Lymphoma. *Cancer Cell* (2010) 18:568–79. doi: 10.1016/j.ccr.2010.10.030
24. Knittel G, Liedgens P, Korovkina D, Seeger JM, Al-Baldawi Y, Al-Maarri M, et al. B-Cell-Specific Conditional Expression of Myd88p.L252P Leads to the Development of Diffuse Large B-Cell Lymphoma in Mice. *Blood* (2016) 127:2732–41. doi: 10.1182/blood-2015-11-684183
25. Flümann R, Rehkämper T, Nieper P, Pfeiffer P, Holzem A, Klein S, et al. An Autochthonous Mouse Model of *Myd88* - and *BCL2* -Driven Diffuse Large B-Cell Lymphoma Reveals Actionable Molecular Vulnerabilities. *Blood Cancer Discov* (2021) 2:70–91. doi: 10.1158/2643-3230.BCD-19-0059
26. Phelan JD, Young RM, Webster DE, Roulland S, Wright GW, Kasbekar M, et al. A Multiprotein Supercomplex Controlling Oncogenic Signalling in Lymphoma. *Nature* (2018) 560:387–91. doi: 10.1038/s41586-018-0290-0
27. Young RM, Wu T, Schmitz R, Dawood M, Xiao W, Phelan JD, et al. Survival of Human Lymphoma Cells Requires B-Cell Receptor Engagement by Self-Antigens. *Proc Natl Acad Sci USA* (2015) 112:13447–54. doi: 10.1073/pnas.1514944112
28. Perez-Chacon G, Adrados M, Vallejo-Cremades MT, Lefebvre S, Reed JC, Zapata JM. Dysregulated TRAF3 and BCL2 Expression Promotes Multiple Classes of Mature Non-Hodgkin B Cell Lymphoma in Mice. *Front Immunol* (2018) 9:3114. doi: 10.3389/fimmu.2018.03114
29. Milpied P, Nadel B, Roulland S. Premalignant Cell Dynamics in Indolent B-Cell Malignancies. *Curr Opin Hematol* (2015) 22:388–96. doi: 10.1097/MOH.0000000000000159
30. McHeyzer-Williams LJ, Milpied PJ, Okitsu SL, McHeyzer-Williams MG. Class-Switched Memory B Cells Remodel Bcrs Within Secondary Germinal Centers. *Nat Immunol* (2015) 16:296–305. doi: 10.1038/ni.3095
31. Milpied P, Cervera-Marzal I, Mollichella M-L, Tesson B, Brisou G, Traverse-Glehen A, et al. Human Germinal Center Transcriptional Programs Are De-Synchronized in B Cell Lymphoma. *Nat Immunol* (2018) 19:1013–24. doi: 10.1038/s41590-018-0181-4
32. Holmes AB, Corinaldesi C, Shen Q, Kumar R, Compagno N, Wang Z, et al. Single-Cell Analysis of Germinal-Center B Cells Informs on Lymphoma Cell of Origin and Outcome. *J Exp Med* (2020) 217:e20200483. doi: 10.1084/jem.20200483
33. King HW, Orban N, Riches JC, Clear AJ, Warnes G, Teichmann SA, et al. Single-Cell Analysis of Human B Cell Maturation Predicts How Antibody Class Switching Shapes Selection Dynamics. *Sci Immunol* (2021) 6:eabe6291. doi: 10.1126/sciimmunol.abe6291
34. Kennedy DE, Okoreeh MK, Maienschein-Cline M, Ai J, Veselits M, McLean KC, et al. Novel Specialized Cell State and Spatial Compartments Within the Germinal Center. *Nat Immunol* (2020) 21:1–11. doi: 10.1038/s41590-020-0660-2
35. Ochiai K, Maienschein-Cline M, Simonetti G, Chen J, Rosenthal R, Brink R, et al. Transcriptional Regulation of Germinal Center B and Plasma Cell Fates by Dynamical Control of IRF4. *Immunity* (2013) 38:918–29. doi: 10.1016/j.immuni.2013.04.009
36. De Silva NS, Klein U. Dynamics of B Cells in Germinal Centres. *Nat Rev Immunol* (2015) 15:137–48. doi: 10.1038/nri3804
37. Basso K, Dalla-Favera R. Roles of BCL6 in Normal and Transformed Germinal Center B Cells. *Immunol Rev* (2012) 247:172–83. doi: 10.1111/j.1600-065X.2012.01112.x
38. Basso K, Dalla-Favera R. Bcl6: Master Regulator of the Germinal Center Reaction and Key Oncogene in B Cell Lymphomagenesis. *Adv Immunol* (2010) 105:193–210. doi: 10.1016/S0065-2776(10)05007-8
39. Hatzi K, Melnick A. Breaking Bad in the Germinal Center: How Deregulation of BCL6 Contributes to Lymphomagenesis. *Trends Mol Med* (2014) 20:343–52. doi: 10.1016/j.molmed.2014.03.001
40. Luo W, Weisel F, Shlomchik MJ. B Cell Receptor and CD40 Signaling Are Rewired for Synergistic Induction of the C-Myc Transcription Factor in Germinal Center B Cells. *Immunity* (2018) 48:313–26.e5. doi: 10.1016/j.immuni.2018.01.008
41. Saito M, Gao J, Basso K, Kitagawa Y, Smith PM, Bhagat G, et al. A Signaling Pathway Mediating Downregulation of BCL6 in Germinal Center B Cells Is Blocked by BCL6 Gene Alterations in B Cell Lymphoma. *Cancer Cell* (2007) 12:280–92. doi: 10.1016/j.ccr.2007.08.011
42. Klein U, Casola S, Cattoretti G, Shen Q, Lia M, Mo T, et al. Transcription Factor Irf4 Controls Plasma Cell Differentiation and Class-Switch Recombination. *Nat Immunol* (2006) 7:773–82. doi: 10.1038/ni1357
43. Shinnakasu R, Inoue T, Kometani K, Moriyama S, Adachi Y, Nakayama M, et al. Regulated Selection of Germinal-Center Cells Into the Memory B Cell Compartment. *Nat Immunol* (2016) 17:861–9. doi: 10.1038/ni.3460
44. Laidlaw BJ, Duan L, Xu Y, Vazquez SE, Cyster JG. The Transcription Factor Hhex Cooperates With the Corepressor Tle3 to Promote Memory B Cell Development. *Nat Immunol* (2020) 21:1–12. doi: 10.1038/s41590-020-0713-6
45. Basso K, Dalla-Favera R. Germinal Centres and B Cell Lymphomagenesis. *Nat Rev Immunol* (2015) 15:172–84. doi: 10.1038/nri3814
46. Alizadeh AA, Eisen MB, Davis RE, Ma C, Lossos IS, Rosenwald A, et al. Distinct Types of Diffuse Large B-Cell Lymphoma Identified by Gene Expression Profiling. *Nature* (2000) 403:503–11. doi: 10.1038/35000501
47. Mlynarczyk C, Fontán L, Melnick A. Germinal Center-Derived Lymphomas: The Darkest Side of Humoral Immunity. *Immunol Rev* (2019) 288:214–39. doi: 10.1111/imr.12755
48. Pasqualucci L. Molecular Pathogenesis of Germinal Center-Derived B Cell Lymphomas. *Immunol Rev* (2019) 288:240–61. doi: 10.1111/imr.12745
49. Verdière L, Mourcin F, Tarte K. Microenvironment Signaling Driving Lymphomagenesis. *Curr Opin Hematol* (2018) 25:335–45. doi: 10.1097/MOH.0000000000000440
50. Carbone A, Roulland S, Gloghini A, Younes A, von Keudell G, López-Guillermo A, et al. Follicular Lymphoma. *Nat Rev Dis Primers* (2019) 5:83. doi: 10.1038/s41572-019-0132-x
51. Victora GD, Dominguez-Sola D, Holmes AB, Deroubaix S, Dalla-Favera R, Nussenzweig MC. Identification of Human Germinal Center Light and Dark Zone Cells and Their Relationship to Human B-Cell Lymphomas. *Blood* (2012) 120:2240–8. doi: 10.1182/blood-2012-03-415380
52. Pikor NB, Mörbe U, Lütge M, Gil-Cruz C, Perez-Shibayama C, Novkovic M, et al. Remodeling of Light and Dark Zone Follicular Dendritic Cells Governs

Germinal Center Responses. *Nat Immunol* (2020) 21:1–11. doi: 10.1038/s41590-020-0672-y
53. Okosun J, Bödör C, Wang J, Araf S, Yang C-Y, Pan C, et al. Integrated Genomic Analysis Identifies Recurrent Mutations and Evolution Patterns Driving the Initiation and Progression of Follicular Lymphoma. *Nat Genet* (2014) 46:176–81. doi: 10.1038/ng.2856
54. Pasqualucci L, Dominguez-Sola D, Chiarenza A, Fabbri G, Grunn A, Trifonov V, et al. Inactivating Mutations of Acetyltransferase Genes in B-Cell Lymphoma. *Nature* (2011) 471:189–95. doi: 10.1038/nature09730
55. Green MR, Kihira S, Liu CL, Nair RV, Salari R, Gentles AJ, et al. Mutations in Early Follicular Lymphoma Progenitors Are Associated With Suppressed Antigen Presentation. *Proc Natl Acad Sci USA* (2015) 112:E1116–25. doi: 10.1073/pnas.1501199112
56. Pasqualucci L, Khiabanian H, Fangazio M, Vasishtha M, Messina M, Holmes AB, et al. Genetics of Follicular Lymphoma Transformation. *Cell Rep* (2014) 6:130–40. doi: 10.1016/j.celrep.2013.12.027
57. Ramezani-Rad P, Rickert RC. Murine Models of Germinal Center Derived-Lymphomas. *Curr Opin Immunol* (2017) 45:31–6. doi: 10.1016/j.coi.2016.12.002
58. Pasqualucci L, Klein U. Mouse Models in the Study of Mature B-Cell Malignancies. *Cold Spring Harb Perspect Med* (2021) 11:a034827. doi: 10.1101/cshperspect.a034827
59. Donnou S, Galand C, Touitou V, Sautès-Fridman C, Fabry Z, Fisson S. Murine Models of B-Cell Lymphomas: Promising Tools for Designing Cancer Therapies. *Adv Hematol* (2012) 2012:701704. doi: 10.1155/2012/701704
60. Flümann R, Nieper P, Reinhardt HC, Knittel G. New Murine Models of Aggressive Lymphoma. *Leukemia Lymphoma* (2020) 61:788–98. doi: 10.1080/10428194.2019.1691200
61. Purwada A, Shah SB, Béguelin W, August A, Melnick AM, Singh A. Ex Vivo Synthetic Immune Tissues With T Cell Signals for Differentiating Antigen-Specific, High Affinity Germinal Center B Cells. *Biomaterials* (2019) 198:27–36. doi: 10.1016/j.biomaterials.2018.06.034
62. McDonnell TJ, Deane N, Platt FM, Nunez G, Jaeger U, McKearn JP, et al. Bcl-2-Immunoglobulin Transgenic Mice Demonstrate Extended B Cell Survival and Follicular Lymphoproliferation. *Cell* (1989) 57:79–88. doi: 10.1016/0092-8674(89)90174-8
63. Strasser A, Whittingham S, Vaux DL, Bath ML, Adams JM, Cory S, et al. Enforced BCL2 Expression in B-Lymphoid Cells Prolongs Antibody Responses and Elicits Autoimmune Disease. *Proc Natl Acad Sci USA* (1991) 88:8661–5. doi: 10.1073/pnas.88.19.8661
64. Strasser A, Harris AW, Cory S. E Mu-Bcl-2 Transgene Facilitates Spontaneous Transformation of Early Pre-B and Immunoglobulin-Secreting Cells But Not T Cells. *Oncogene* (1993) 8:1–9.
65. Egle A, Harris AW, Bath ML, O'Reilly L, Cory S. Vavp-Bcl2 Transgenic Mice Develop Follicular Lymphoma Preceded by Germinal Center Hyperplasia. *Blood* (2004) 103:2276–83. doi: 10.1182/blood-2003-07-2469
66. Xiang H, Noonan EJ, Wang J, Duan H, Ma L, Michie S, et al. The Immunoglobulin Heavy Chain Gene 3' Enhancers Induce Bcl2 Deregulation and Lymphomagenesis in Murine B Cells. *Leukemia* (2011) 25:1484–93. doi: 10.1038/leu.2011.115
67. García-Ramírez I, Tadros S, González-Herrero I, Martín-Lorenzo A, Rodríguez-Hernández G, Moore D, et al. Crebbp Loss Cooperates With Bcl2 Overexpression to Promote Lymphoma in Mice. *Blood* (2017) 129:2645–56. doi: 10.1182/blood-2016-08-733469
68. Zhang J, Vlasevska S, Wells VA, Nataraj S, Holmes AB, Duval R, et al. The CREBBP Acetyltransferase Is a Haploinsufficient Tumor Suppressor in B-Cell Lymphoma. *Cancer Discov* (2017) 7:322–37. doi: 10.1158/2159-8290.CD-16-1417
69. Jiang Y, Ortega-Molina A, Geng H, Ying H-Y, Hatzi K, Parsa S, et al. Crebbp Inactivation Promotes the Development of HDAC3-Dependent Lymphomas. *Cancer Discov* (2017) 7:38–53. doi: 10.1158/2159-8290.CD-16-0975
70. Zhang J, Dominguez-Sola D, Hussein S, Lee J-E, Holmes AB, Bansal M, et al. Disruption of KMT2D Perturbs Germinal Center B Cell Development and Promotes Lymphomagenesis. *Nat Med* (2015) 21:1190–8. doi: 10.1038/nm.3940
71. Ortega-Molina A, Boss IW, Canela A, Pan H, Jiang Y, Zhao C, et al. The Histone Lysine Methyltransferase Kmt2d Sustains a Gene Expression Program That Represses B Cell Lymphoma Development. *Nat Med* (2015) 21:1199–208. doi: 10.1038/nm.3943
72. Souroullas GP, Jeck WR, Parker JS, Simon JM, Liu J-Y, Paulk J, et al. An Oncogenic Ezh2 Mutation Induces Tumors Through Global Redistribution of Histone 3 Lysine 27 Trimethylation. *Nat Med* (2016) 22:632–40. doi: 10.1038/nm.4092
73. Béguelin W, Popovic R, Teater M, Jiang Y, Bunting KL, Rosen M, et al. EZH2 Is Required for Germinal Center Formation and Somatic Ezh2 Mutations Promote Lymphoid Transformation. *Cancer Cell* (2013) 23:677–92. doi: 10.1016/j.ccr.2013.04.011
74. Ennishi D, Takata K, Béguelin W, Duns G, Mottok A, Farinha P, et al. Molecular and Genetic Characterization of MHC Deficiency Identifies EZH2 as Therapeutic Target for Enhancing Immune Recognition. *Cancer Discov* (2019) 9:546–63. doi: 10.1158/2159-8290.CD-18-1090
75. Béguelin W, Teater M, Gearhart MD, Calvo Fernández MT, Goldstein RL, Cárdenas MG, et al. EZH2 and BCL6 Cooperate to Assemble Cbx8-Bcor Complex to Repress Bivalent Promoters, Mediate Germinal Center Formation and Lymphomagenesis. *Cancer Cell* (2016) 30:197–213. doi: 10.1016/j.ccell.2016.07.006
76. Yusufova N, Kloetgen A, Teater M, Osunsade A, Camarillo JM, Chin CR, et al. Histone H1 Loss Drives Lymphoma by Disrupting 3d Chromatin Architecture. *Nature* (2020) 22:1–7. doi: 10.1038/s41586-020-3017-y
77. Cimmino L, Dawlaty MM, Ndiaye-Lobry D, Yap YS, Bakogianni S, Yu Y, et al. TET1 Is a Tumor Suppressor of Hematopoietic Malignancy. *Nat Immunol* (2015) 16:653–62. doi: 10.1038/ni.3148
78. Mouly E, Ghamlouch H, Della-Valle V, Scourzic L, Quivoron C, Roos-Weil D, et al. B-Cell Tumor Development in Tet2-Deficient Mice. *Blood Adv* (2018) 2:703–14. doi: 10.1182/bloodadvances.2017014118
79. Dominguez PM, Ghamlouch H, Rosikiewicz W, Kumar P, Béguelin W, Fontán L, et al. Tet2 Deficiency Causes Germinal Center Hyperplasia, Impairs Plasma Cell Differentiation, and Promotes B-Cell Lymphomagenesis. *Cancer Discov* (2018) 8:1632–53. doi: 10.1158/2159-8290.CD-18-0657
80. Boice M, Salloum D, Mourcin F, Sanghvi V, Amin R, Oricchio E, et al. Loss of the HVEM Tumor Suppressor in Lymphoma and Restoration by Modified Car-T Cells. *Cell* (2016) 167:405–18.e13. doi: 10.1016/j.cell.2016.08.032
81. Dheilly E, Battistello E, Katanayeva N, Sungalee S, Michaux J, Duns G, et al. Cathepsin S Regulates Antigen Processing and T Cell Activity in Non-Hodgkin Lymphoma. *Cancer Cell* (2020) 37:674–89. doi: 10.1016/j.ccell.2020.03.016
82. Muppidi JR, Schmitz R, Green JA, Xiao W, Larsen AB, Braun SE, et al. Loss of Signalling *Via* Gα13 in Germinal Centre B-Cell-Derived Lymphoma. *Nature* (2014) 516:254–8. doi: 10.1038/nature13765
83. Ortega-Molina A, Deleyto-Seldas N, Carreras J, Sanz A, Lebrero-Fernández C, Menéndez C, et al. Oncogenic Rag Gtpase Signalling Enhances B Cell Activation and Drives Follicular Lymphoma Sensitive to Pharmacological Inhibition of Mtor. *Nat Metab* (2019) 1:775–89. doi: 10.1038/s42255-019-0098-8
84. Oricchio E, Katanayeva N, Donaldson MC, Sungalee S, Pasion JP, Béguelin W, et al. Genetic and Epigenetic Inactivation of SESTRIN1 Controls mTORC1 and Response to EZH2 Inhibition in Follicular Lymphoma. *Sci Transl Med* (2017) 9:eaak9969. doi: 10.1126/scitranslmed.aak9969
85. Roulland S, Navarro J-M, Grenot P, Milili M, Agopian J, Montpellier B, et al. Follicular Lymphoma-Like B Cells in Healthy Individuals: A Novel Intermediate Step in Early Lymphomagenesis. *J Exp Med* (2006) 203:2425–31. doi: 10.1084/jem.20061292
86. Roulland S, Faroudi M, Mamessier E, Sungalee S, Salles G, Nadel B. Chapter 1 - Early Steps of Follicular Lymphoma Pathogenesis. In: Alt FW, editor. *Advances in Immunology*. Academic Press (2011). 111:1–46. doi: 10.1016/B978-0-12-385991-4.00001-5
87. Brescia P, Schneider C, Holmes AB, Shen Q, Hussein S, Pasqualucci L, et al. Mef2b Instructs Germinal Center Development and Acts as an Oncogene in B Cell Lymphomagenesis. *Cancer Cell* (2018) 34:453–65. doi: 10.1016/j.ccell.2018.08.006
88. Kridel R, Chan FC, Mottok A, Boyle M, Farinha P, Tan K, et al. Histological Transformation and Progression in Follicular Lymphoma: A Clonal Evolution Study. *PloS Med* (2016) 13:e1002197. doi: 10.1371/journal.pmed.1002197
89. Morin RD, Johnson NA, Severson TM, Mungall AJ, An J, Goya R, et al. Somatic Mutations Altering EZH2 (Tyr641) in Follicular and Diffuse Large B-Cell Lymphomas of Germinal-Center Origin. *Nat Genet* (2010) 42:181–5. doi: 10.1038/ng.518
90. Morin RD, Mendez-Lago M, Mungall AJ, Goya R, Mungall KL, Corbett RD, et al. Frequent Mutation of Histone-Modifying Genes in Non-Hodgkin Lymphoma. *Nature* (2011) 476:298–303. doi: 10.1038/nature10351

91. Schmidt J, Ramis-Zaldivar JE, Bonzheim I, Steinhilber J, Müller I, Haake A, et al. Crebbp Gene Mutations Are Frequently Detected in *In Situ* Follicular Neoplasia. *Blood* (2018) 132:2687–90. doi: 10.1182/blood-2018-03-837039
92. Casola S, Cattoretti G, Uyttersprot N, Koralov SB, Seagal J, Segal J, et al. Tracking Germinal Center B Cells Expressing Germ-Line Immunoglobulin Gamma1 Transcripts by Conditional Gene Targeting. *Proc Natl Acad Sci USA* (2006) 103:7396–401. doi: 10.1073/pnas.0602353103
93. Horton SJ, Giotopoulos G, Yun H, Vohra S, Sheppard O, Bashford-Rogers R, et al. Early Loss of *Crebbp* Confers Malignant Stem Cell Properties on Lymphoid Progenitors. *Nat Cell Biol* (2017) 19:1093–104. doi: 10.1038/ncb3597
94. Meyer SN, Scuoppo C, Vlasevska S, Bal E, Holmes AB, Holloman M, et al. Unique and Shared Epigenetic Programs of the CREBBP and EP300 Acetyltransferases in Germinal Center B Cells Reveal Targetable Dependencies in Lymphoma. *Immunity* (2019) 51:S1074761319303322. doi: 10.1016/j.immuni.2019.08.006
95. Hashwah H, Schmid CA, Kasser S, Bertram K, Stelling A, Manz MG, et al. Inactivation of CREBBP Expands the Germinal Center B Cell Compartment, Down-Regulates MHCII Expression and Promotes Dlbcl Growth. *Proc Natl Acad Sci USA* (2017) 114:9701–6. doi: 10.1073/pnas.1619555114
96. Mondello P, Tadros S, Teater M, Fontan L, Chang AY, Jain N, et al. Selective Inhibition of HDAC3 Targets Synthetic Vulnerabilities and Activates Immune Surveillance in Lymphoma. *Cancer Discov* (2020) 10:CD–19-0116. doi: 10.1158/2159-8290.CD-19-0116
97. McCabe MT, Graves AP, Ganji G, Diaz E, Halsey WS, Jiang Y, et al. Mutation of A677 in Histone Methyltransferase EZH2 in Human B-Cell Lymphoma Promotes Hypertrimethylation of Histone H3 on Lysine 27 (H3k27). *Proc Natl Acad Sci USA* (2012) 109:2989–94. doi: 10.1073/pnas.1116418109
98. Bödör C, Grossmann V, Popov N, Okosun J, O'Riain C, Tan K, et al. Ezh2 Mutations Are Frequent and Represent an Early Event in Follicular Lymphoma. *Blood* (2013) 122:3165–8. doi: 10.1182/blood-2013-04-496893
99. Caganova M, Carrisi C, Varano G, Mainoldi F, Zanardi F, Germain P-L, et al. Germinal Center Dysregulation by Histone Methyltransferase EZH2 Promotes Lymphomagenesis. *J Clin Invest* (2013) 123:5009–22. doi: 10.1172/JCI70626
100. Béguelin W, Rivas MA, Calvo Fernández MT, Teater M, Purwada A, Redmond D, et al. Ezh2 Enables Germinal Centre Formation Through Epigenetic Silencing of CDKN1A and an Rb-E2F1 Feedback Loop. *Nat Commun* (2017) 8:877. doi: 10.1038/s41467-017-01029-x
101. Béguelin W, Teater M, Meydan C, Hoehn KB, Phillip JM, Soshnev AA, et al. Mutant EZH2 Induces a Pre-Malignant Lymphoma Niche by Reprogramming the Immune Response. *Cancer Cell* (2020) 37:655–73.e11. doi: 10.1016/j.ccell.2020.04.004
102. Li H, Kaminski MS, Li Y, Yildiz M, Ouillette P, Jones S, et al. Mutations in Linker Histone Genes Hist1h1 B, C, D, and E; Oct2 (Pou2f2); IRF8; and ARID1A Underlying the Pathogenesis of Follicular Lymphoma. *Blood* (2014) 123:1487–98. doi: 10.1182/blood-2013-05-500264
103. Yusufova N, Kloetgen A, Teater M, Osunsade A, Camarillo JM, Chin CR, et al. Histone H1 Loss Drives Lymphoma by Disrupting 3d Chromatin Architecture. *Nature* (2021) 589:299–305. doi: 10.1038/s41586-020-3017-y
104. Fan Y, Nikitina T, Morin-Kensicki EM, Zhao J, Magnuson TR, Woodcock CL, et al. H1 Linker Histones Are Essential for Mouse Development and Affect Nucleosome Spacing *In Vivo*. *Mol Cell Biol* (2003) 23:4559–72. doi: 10.1128/mcb.23.13.4559-4572.2003
105. Duy C, Béguelin W, Melnick A. Epigenetic Mechanisms in Leukemias and Lymphomas. *Cold Spring Harb Perspect Med* (2020) 10:a034959. doi: 10.1101/cshperspect.a034959
106. Quivoron C, Couronné L, Della Valle V, Lopez CK, Plo I, Wagner-Ballon O, et al. Tet2 Inactivation Results in Pleiotropic Hematopoietic Abnormalities in Mouse and Is a Recurrent Event During Human Lymphomagenesis. *Cancer Cell* (2011) 20:25–38. doi: 10.1016/j.ccr.2011.06.003
107. Mintz MA, Cyster JG. T Follicular Helper Cells in Germinal Center B Cell Selection and Lymphomagenesis. *Immunol Rev* (2020) 296:48–61. doi: 10.1111/imr.12860
108. Mintz MA, Felce JH, Chou MY, Mayya V, Xu Y, Shui J-W, et al. The HVEM-BTLA Axis Restrains T Cell Help to Germinal Center B Cells and Functions as a Cell-Extrinsic Suppressor in Lymphomagenesis. *Immunity* (2019) 51:S1074761319302420. doi: 10.1016/j.immuni.2019.05.022
109. Bararia D, Hildebrand JA, Stolz S, Haebe S, Alig S, Trevisani CP, et al. Cathepsin S Alterations Induce a Tumor-Promoting Immune Microenvironment in Follicular Lymphoma. *Cell Rep* (2020) 3:107522. doi: 10.1016/j.celrep.2020.107522
110. Lu E, Cyster JG. G-Protein Coupled Receptors and Ligands That Organize Humoral Immune Responses. *Immunol Rev* (2019) 289:158–72. doi: 10.1111/imr.12743
111. Ersching J, Efeyan A, Mesin L, Jacobsen JT, Pasqual G, Grabiner BC, et al. Germinal Center Selection and Affinity Maturation Require Dynamic Regulation of mTORC1 Kinase. *Immunity* (2017) 46:1045–58.e6. doi: 10.1016/j.immuni.2017.06.005
112. Okosun J, Wolfson RL, Wang J, Araf S, Wilkins L, Castellano BM, et al. Recurrent mTORC1-Activating Rragc Mutations in Follicular Lymphoma. *Nat Genet* (2016) 48:183–8. doi: 10.1038/ng.3473
113. Ying ZX, Jin M, Peterson LF, Bernard D, Saiya-Cork K, Yildiz M, et al. Recurrent Mutations in the MTOR Regulator RRAGC in Follicular Lymphoma. *Clin Cancer Res* (2016) 22:5383–93. doi: 10.1158/1078-0432.CCR-16-0609
114. Zoncu R, Efeyan A, Sabatini DM. Mtor: From Growth Signal Integration to Cancer, Diabetes and Ageing. *Nat Rev Mol Cell Biol* (2011) 12:21–35. doi: 10.1038/nrm3025
115. Rebsamen M, Pochini L, Stasyk T, de Araújo MEG, Galluccio M, Kandasamy RK, et al. SLC38A9 Is a Component of the Lysosomal Amino Acid Sensing Machinery That Controls Mtorc1. *Nature* (2015) 519:477–81. doi: 10.1038/nature14107
116. Sancak Y, Bar-Peled L, Zoncu R, Markhard AL, Nada S, Sabatini DM. Ragulator-Rag Complex Targets mTORC1 to the Lysosomal Surface and Is Necessary for Its Activation by Amino Acids. *Cell* (2010) 141:290–303. doi: 10.1016/j.cell.2010.02.024
117. Young RM, Phelan JD, Wilson WH, Staudt LM. Pathogenic B-Cell Receptor Signaling in Lymphoid Malignancies: New Insights to Improve Treatment. *Immunol Rev* (2019) 291:190–213. doi: 10.1111/imr.12792
118. Wright GW, Huang DW, Phelan JD, Coulibaly ZA, Roulland S, Young RM, et al. A Probabilistic Classification Tool for Genetic Subtypes of Diffuse Large B Cell Lymphoma With Therapeutic Implications. *Cancer Cell* (2020) 37:551–68. doi: 10.1016/j.ccell.2020.03.015
119. Kotlov N, Bagaev A, Revuelta MV, Phillip JM, Cacciapuoti MT, Antysheva Z, et al. Clinical and Biological Subtypes of B-Cell Lymphoma Revealed by Microenvironmental Signatures. *Cancer Discov* (2021) 11:candisc.0839.2020. doi: 10.1158/2159-8290.CD-20-0839
120. Andor N, Simonds EF, Czerwinski DK, Chen J, Grimes SM, Wood-Bouwens C, et al. Single-Cell RNA-Seq of Follicular Lymphoma Reveals Malignant B-Cell Types and Coexpression of T-Cell Immune Checkpoints. *Blood* (2019) 133:1119–29. doi: 10.1182/blood-2018-08-862292
121. Brisou G, Zala M, Gil L, Pagano G, Bru A, Cervera-Marzal I, et al. Desynchronization of the Germinal Center Dynamics and Remodeling of the Tumor Microenvironment Characterize Kmt2d-Driven Lymphomagenesis. *Blood* (2018) 132:670–0. doi: 10.1182/blood-2018-99-116617
122. Schroers-Martin J. *Recurrent Crebbp Mutations in Follicular Lymphoma Appear Localized to the Committed B-Cell Lineage*. In (ASH). Available at: https://ash.confex.com/ash/2020/webprogram/Paper142761.html (Accessed March 21, 2021).
123. Townsend EC, Murakami MA, Christodoulou A, Christie AL, Köster J, DeSouza TA, et al. The Public Repository of Xenografts Enables Discovery and Randomized Phase II-Like Trials in Mice. *Cancer Cell* (2016) 29:574–86. doi: 10.1016/j.ccell.2016.03.008
124. Tothova Z, Krill-Burger JM, Popova KD, Landers CC, Sievers QL, Yudovich D, et al. Multiplex CRISPR/Cas9-Based Genome Editing in Human Hematopoietic Stem Cells Models Clonal Hematopoiesis and Myeloid Neoplasia. *Cell Stem Cell* (2017) 21:547–55. doi: 10.1016/j.stem.2017.07.015
125. Wang G, Chow RD, Zhu L, Bai Z, Ye L, Zhang F, et al. Crispr-GEMM Pooled Mutagenic Screening Identifies KMT2D as a Major Modulator of Immune Checkpoint Blockade. *Cancer Discov* (2020) 10:CD–19-1448. doi: 10.1158/2159-8290.CD-19-1448

Conflict of Interest: The authors declare that the research was conducted in the absence of any commercial or financial relationships that could be construed as a potential conflict of interest.

frontiers in Immunology

REVIEW
published: 12 August 2021
doi: 10.3389/fimmu.2021.710711

Mouse Models of Germinal Center Derived B-Cell Lymphomas

Stefanie N. Meyer[1], *Sanjay Koul*[2] *and Laura Pasqualucci*[1,3,4]*

[1] Institute for Cancer Genetics, Columbia University, New York, NY, United States, [2] Department of Biological Sciences & Geology, Queensborough Community College (City University of New York), Bayside, NY, United States, [3] Department of Pathology & Cell Biology, Columbia University, New York, NY, United States, [4] The Herbert Irving Comprehensive Cancer Center, Columbia University, New York, NY, United States

Over the last decades, the revolution in DNA sequencing has changed the way we understand the genetics and biology of B-cell lymphomas by uncovering a large number of recurrently mutated genes, whose aberrant function is likely to play an important role in the initiation and/or maintenance of these cancers. Dissecting how the involved genes contribute to the physiology and pathology of germinal center (GC) B cells –the origin of most B-cell lymphomas– will be key to advance our ability to diagnose and treat these patients. Genetically engineered mouse models (GEMM) that faithfully recapitulate lymphoma-associated genetic alterations offer a valuable platform to investigate the pathogenic roles of candidate oncogenes and tumor suppressors *in vivo*, and to pre-clinically develop new therapeutic principles in the context of an intact tumor immune microenvironment. In this review, we provide a summary of state-of-the art GEMMs obtained by accurately modelling the most common genetic alterations found in human GC B cell malignancies, with a focus on Burkitt lymphoma, follicular lymphoma, and diffuse large B-cell lymphoma, and we discuss how lessons learned from these models can help guide the design of novel therapeutic approaches for this disease.

Keywords: germinal center, lymphoma, genetics, mouse models, transgenic

OPEN ACCESS

Edited by:
Christelle Vincent-Fabert, UMR7276 Contrôle des réponses immunes B et des lymphoprolifération (CRIBL), France

Reviewed by:
Dinis Pedro Calado, Francis Crick Institute, United Kingdom
Jean Feuillard, University of Limoges, France

***Correspondence:**
Laura Pasqualucci
lp171@cumc.columbia.edu

Specialty section:
This article was submitted to B Cell Biology, a section of the journal Frontiers in Immunology

Received: *17 May 2021*
Accepted: *28 June 2021*
Published: *12 August 2021*

Citation:
Meyer SN, Koul S and Pasqualucci L (2021) Mouse Models of Germinal Center Derived B-Cell Lymphomas. Front. Immunol. 12:710711. doi: 10.3389/fimmu.2021.710711

INTRODUCTION

B-cell lymphomas are a spectrum of genetically, phenotypically and clinically diverse neoplasms that arise from the oncogenic transformation of B cells at various developmental stages and, in most cases, from germinal center (GC) B cells (1–3). Over the past two decades, studies aimed at charting the genetic landscape of these malignancies have uncovered a large number of recurrently mutated genes with potential pathogenic roles in these diseases (4–8). In order to understand the mechanisms by which these alterations contribute to lymphomagenesis, genetically engineered mouse models (GEMMs) have proven and will likely continue to prove instrumental, particularly in the case of GC-derived lymphomas, as an *in-vitro* system that faithfully recapitulates the complex biology of the GC reaction is still lacking. By mimicking genetic alterations that are found in the human disease, these models have allowed the detailed *in-vivo* investigation of several lymphoma-associated oncogenes and tumor suppressors, shedding light on their role in normal B cell development and tumorigenesis. It has to be said that each of the approaches used present specific advantages and disadvantages; for instance, GEMMs cannot reproduce the genetic

complexity and the heterogeneity of the human tumors, an aspect especially important when aiming at the discovery and pre-clinical testing of novel therapeutics. To overcome this hurdle, patient-derived xenografts have been introduced for the validation of candidate biomarkers and molecular targets (9–11). Moreover, the versatility of the clustered regularly interspersed short palindromic repeats (CRISPR)-Cas9 technology and its high efficiency for precise genome manipulation in mouse embryonic stem (ES) cells has opened the way to the construction of a new array of *in vivo* experimental models. Although no single model can individualy address the wide range of questions that remain to be investigated, access to the appropriate *in vivo* tools will greatly benefit the lymphoma community. In this review, we summarize the insights gained from modeling recurrent genetic lesions associated with human B cell malignancies, focusing on three common GC-derived non-Hodgkin lymphomas for which GEMMs that faithfully recapitulate key aspects of the human disease have been achieved: Burkitt lymphoma (BL), follicular lymphoma (FL), and diffuse large B-cell lymphoma (DLBCL). We refer the reader to the work of Huang and Yasuda for an overview on mouse models of EBV-driven lymphomas (12).

GERMINAL CENTERS: THE ORIGIN OF MOST B-CELL LYMPHOMAS

The development of mouse models that recapitulate with fidelity the human disease is intimately linked to a deep understanding of the pathogenesis of these tumors and particularly of their normal cellular counterpart, as the genetic lesion of interest should be targeted to the proper temporal and developmental stage context. For most B-cell lymphomas, this is represented by a GC B cell, as documented in the nineties by the analysis of clonally rearranged immunoglobulin genes in various lymphoma subtypes (1, 2). These studies invariably showed that BL, FL and DLBCL exhibit the imprinting of somatic hypermutation (SHM), an irreversible marker of GC transit. Thus, although the tumorigenesis process may be initiated at earlier stages of B cell differentiation (see the occurrence of BCL2 translocations in FL and DLBCL), the "tumor precursor cell" undergoes its final clonal expansion in the GC.

GCs are specialized structures that form transiently in secondary lymphoid organs upon encounter of a naïve B cell with its cognate antigen in the context of T cell-dependent, adaptive immune responses (13–15). The GC reaction serves one major purpose, that is to produce a population of cells capable of secreting high-affinity antibodies against the invading pathogen (i.e., plasma cells), or of maintaining the memory of that antigen for life (i.e., memory B cells), such that they can quickly differentiate into effector plasma cells upon recall responses against the same antigen (**Figure 1**) (16). Within the GC microenvironment, B cells cyclically recirculate between two anatomical areas known as the dark zone (DZ) and the light zone (LZ) (17). DZ B cells (also called centroblasts) proliferate at high rate and modify their immunoglobulin variable (*IgV*) region genes by the process of SHM, to generate antibody specificities with different affinity to the antigen. DZ B cells then cease proliferating and evolve into LZ B cells (also known as centrocytes), a more quiescent population that is again exposed to the antigen, retained on the surface of follicular dendritic cells (FDCs) in the form of immune complexes, and then compete for help by T-follicular helper (T_{FH}) cells in order to receive survival signals and undergo affinity-based selection (18). GC B cells that are not positively selected because the newly introduced somatic mutations led to a decrease in affinity, disrupted the antibody structure, or generated autoreactive antibodies, are destined to die by apoptosis. A subset of LZ B cells upregulate MYC and recycle to the DZ to undergo further rounds of SHM and selection (19, 20). Eventually, high affinity LZ B cells will differentiate into antibody secreting plasma cells or memory B cells. The GC LZ also supports the process of class switch recombination (CSR), a second AID-dependent B cell-specific DNA-modification that confers distinct effector functions to antibodies with identical specificities; however, recent work provided experimental evidence that CSR takes place predominantly in the early phases following antigen encounter, prior to the GC reaction and to SHM (21).

Consistent with this functional compartmentalization, GC DZ and LZ B cells are characterized by distinct epigenetic and transcriptional profiles that sustain diverse biological programs, with proliferation and DNA replication being enriched in DZ B cells, and a variety of signaling pathways downstream of surface receptor molecules being activated in LZ B cells, including the B-cell receptor (BCR) and the CD40 receptor (22). This oversimplified view of the GC reaction has been refined to higher granularity by recent single cell analyses of gene expression and somatically mutated *IgV* region genes in human GC B cells (23, 24). These studies revealed multiple subclusters of DZ and LZ B cells, along a continuum of transcriptional changes reflected in several intermediate subpopulations that bidirectionally recirculate between the DZ and LZ compartment, ultimately giving rise to precursor memory B cells and plasma blasts (**Figure 1**).

With the advent of genome-wide expression profile technologies, numerous studies have documented the close similarity between the phenotype of normal bulk GC B cell subsets and the transcriptional signature of various lymphoma entities, allowing a more refined assignment of BL, FL and DLBCL to their putative normal cellular counterpart, as well as the identification of functionally relevant disease subtypes (25, 26). For example, BL was found to show a gene expression profile that is closely related to the GC DZ signature, indicating a cellular origin from DZ B cells that are actively undergoing SHM (22). Conversely, FL closely resembles early LZ B cells representing an intermediate GC B cell stage, although at the single cell level tumor cells feature a desynchronization of the canonical gene expression programs found in their normal counterpart (23). Finally, at least two distinct phenotypic subtypes of DLBCL have been recognized by bulk gene expression profiling based on their similarity to distinct cellular counterparts within the GC: the so-called germinal center B cell

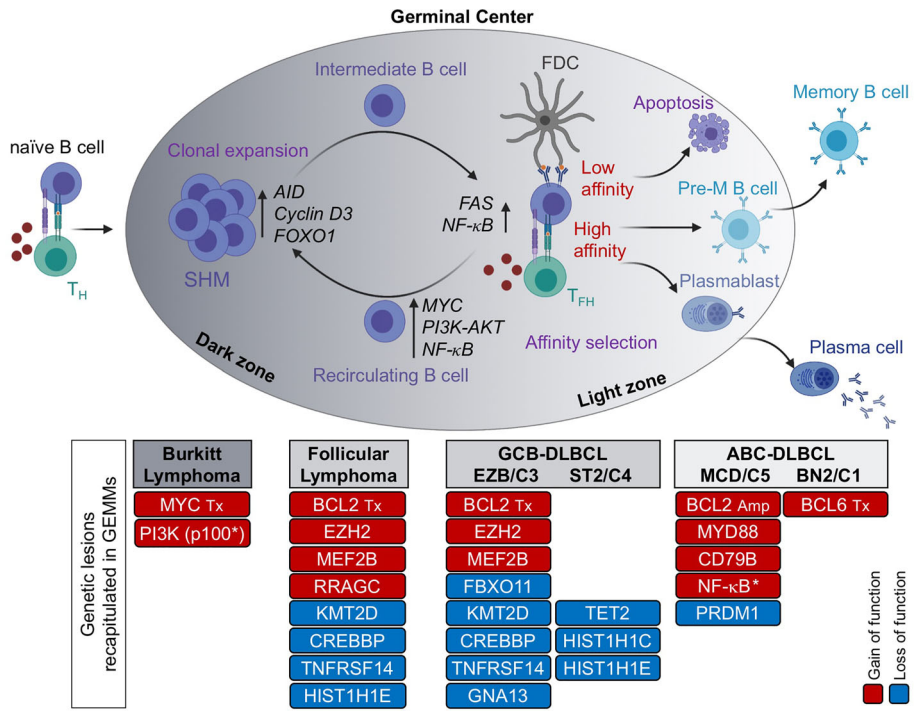

FIGURE 1 | The GC reaction as the normal counterpart of most B cell lymphomas. Formation of a GC begins when a naïve B cell encounters an antigen in the presence of co-stimulatory molecules, provided by a T helper cell. The GC is functionally and histologically divided into two main compartments, the dark zone (DZ) and the light zone (LZ). Within the DZ, cells undergo somatic hypermutation (SHM) of their immunoglobulin genes and rapid proliferation, whereas in the LZ, B cells are intermingled with follicular dendritic cells (FDCs) and T follicular helper (T_{FH}) cells, which provide positive selection signals to B cells with high affinity to the antigen. The LZ is also the site of CSR. By repeatedly cycling between the DZ and the LZ, B cells undergo several rounds of proliferation, SHM and affinity maturation before being positively selected. In contrast, B cells with low affinity for the antigen are eliminated by apoptosis. High affinity B cells that exit the GC differentiate into long-lived memory B cells or antibody-secreting plasma cells. Based on molecular profiling, Burkitt lymphoma is postulated to derive from DZ B cells, FL and GCB-DLBCL from LZ B cells, and ABC-DLBCL from B cells poised to undergo terminal differentiation (plasmablasts) or, in a subset of cases, pre-memory B cells. Genetic lesions that have been successfully modelled in the mouse and recapitulate key features of the human disease are indicated. Red, gain of function events; blue, loss of function events. M, mutation; Tx, translocation; Amp, copy number gain/amplification; *, pathway activation by use of a constitutively active protein.

like (GCB)-DLBCL, which is transcriptionally more similar to intermediate and LZ B cells (22, 27); and the activated B cell like (ABC)-DLBCL, which resembles *in vitro* activated B cells and corresponds *in vivo* to a small subset of LZ B cells poised to undergo plasma cell differentiation (27), but also includes, as recently suggested, cases with similarities to memory B cells (24, 28). The clinical relevance of the "cell-of-origin" (COO) classification is underscored by the association of GCB- and ABC-DLBCL with distinct prognostic categories, which supported its incorporation into the updated WHO classification of lymphoid malignancies (3). Nonetheless, it is likely that additional subgroups exist within and across this heterogeneous disease, where as many as 20% of cases remain unclassified. Confirming this notion, different genetic subsets were recently revealed based on genetic profiles, which also display separate clinical outcomes (29–31); moreover, two clinically relevant DLBCL subgroups exhibiting particularly favorable and poor prognosis, respectively, were identified by applying a single-cell based COO classification (24), warranting additional studies aimed at dissecting the complexity of this disease.

TYPES OF GEMMs

GEMMs represent a powerful tool for the study of human cancers as well as non-malignant diseases, because over 90% of the mouse and human genomes share regions of conserved synteny, and mouse ES cells are amenable to be genetically manipulated, allowing the construction of the mutation of interest in the context of an immune system that is comparable to the human counterpart. In the B-cell lymphoma field, a variety of mouse models have been generated for the overexpression or deletion of oncogenes and tumor-suppressor genes that are linked to the human condition, by using the following main strategies: i) classical transgenic approaches, ii) targeted approaches based on homologous recombination in ES cells (i.e., knock-in/knock-out mouse models, either constitutive

or conditional); and iii) adoptive transfer of manipulated hematopoietic stem cells (HSC) (**Figures 2A–C**) (32–34). More recently, the development of the CRISPR-Cas9 system, a genome-editing tool for efficient and precise genome engineering, has begun to transform the field by allowing to create virtually any mutation, thus expanding our possibilities to generate elaborate mouse-models.

The simplest *Transgenic Mouse Models* are obtained by random integration of a DNA construct into the genome upon injection into the pronucleus of fertilized eggs. These earlier models have provided critical information about the function of specific genes; however, transgenic approaches do not allow the control of the transgene copy number nor its integration site/s, which can be biased. Moreover, only a limited number of endogenous promoters are available to ensure the proper spatial and temporal control of gene expression. As such, most classical transgenic mouse models did not accurately mimic the type and/or the timing of the genetic lesion of interest, resulting in the development of tumors that do not always recapitulate the biology of the human disease. Accordingly, the field is moving away from using these lines, with few exceptions (e.g. the *VavP-Bcl2* and *Bcl2-Ig* mice discussed in the Follicular Lymphoma section) (35, 36).

Constitutive Knock-in/knock-out Mouse Models leverage on homologous recombination to modify endogenous genomic loci and introduce activating mutations in proto-oncogenes, disrupt tumor suppressor genes, or place a mutant cDNA under the control of a highly expressed heterologous promoter/enhancer element hijacked by chromosomal translocations in the human tumors (typically, the immunoglobulin genes). A successful example of the latter approach is represented by the Iμ-HABCL6 mouse model, where a BCL6 cDNA cassette was targeted downstream the endogenous immunoglobulin Iμ promoter to generate a chimeric transcriptional unit reproducing the outcome of a common *BCL6* chromosomal translocation variant found in DLBCL (37) (further discussed in the DLBCL section).

Conditional Knock-in/Knock-out Mouse Models. The generation of mouse strains where the Cre-recombinase enzyme is expressed under the control of spatially and temporally controlled promoters has greatly advanced our ability to construct faithful mouse models by directing the introduction of candidate mutations to various stages of B cell differentiation, thus allowing the conditional activation (via removal of a *loxP*-flanked "stop cassette") or inactivation of specific genes in the desired cell type. For instance, the crossing of floxed alleles to *mb1-Cre* (38) or *Cd19-Cre* (39) deleter strains permits gene recombination at early B-cell developmental stages and therefore throughout B cell development, whereas the *Cd21-Cre* recombinase is specifically active in peripheral B cells, from the transitional B cell stage (40).

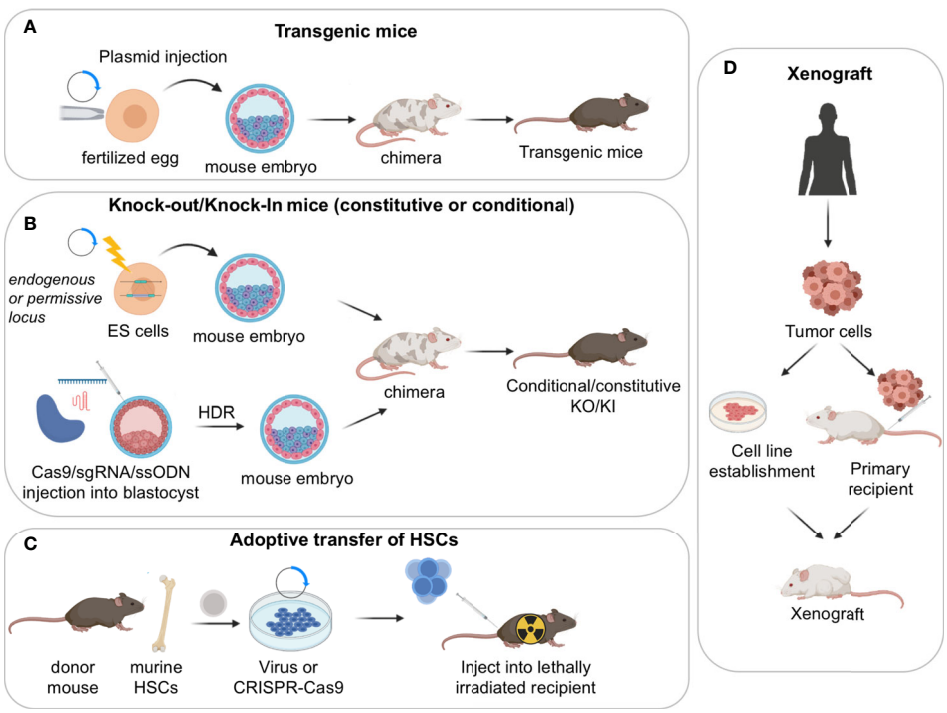

FIGURE 2 | Approaches used to generate mouse models of GC derived lymphomas. **(A)** Transgenic mouse models; **(B)** constitutive or conditional knock-out/knock-in mouse models, obtained *via* homologous recombination in ES cells or CRISPR-Cas9 mediated genome editing; **(C)** adoptive transfer of HSCs. **(D)** Xenograft mouse models of human lymphoma cells can be established by injection of stable cell lines or by direct implantation of primary tumor samples into recipient immunosuppressed or humanized mice. Serial passaging of the engrafted tumors may be necessary to achieve high xenotransplantation efficiency. These models are particularly useful for the pre-clinical evaluation of novel therapeutic combinations *in vivo*.

By far the most relevant Cre-recombinase alleles for the design of BL, FL and DLBCL mouse models are the *Cγ1-Cre* and *Aicda-Cre* knock-in alleles, which allow for precise Cre-mediated gene recombination in antigen-activated mature B cells, including GC B cells (**Figure 3A**) (42–44). Conditional knock-out alleles have been successfully employed to study the *in vivo* role of many lymphoma-associated tumor suppressor genes encoding for transcription factors (BLIMP1), epigenetic modifiers (EZH2, CREBBP, KMT2D, TET2), small G proteins (GNA13) and ubiquitin ligases (FBXO11). Likewise, conditional Cre-mediated activation of mutant gain-of-function alleles, under the control of the gene endogenous promoter (MEF2B-D83V) or in the context of the permissive ROSA26 locus (BCL2), allowed to investigate their contribution to tumor development *in vivo*.

Adoptive transfer approaches involve the isolation of hematopoietic progenitor cells (HPCs) from the bone marrow (BM) or fetal liver of a donor mouse and their subsequent genetic modification using retroviral vectors or the CRISPR-Cas9 tool, prior to BM transplantation into recipient animals. Typically, short-hairpin RNAs (shRNAs) are used for loss-of-function studies and cDNA cassettes are used to reproduce gain-of-function mutations, whereas the CRISPR-Cas9 editing approach can serve both purposes. These modified progenitor cells will then reconstitute the hematopoietic system of lethally or sub-lethally irradiated syngeneic animals, resulting in chimeric mice with a hematopoietic system derived from the donor cells (45). The adoptive transfer approach offers the advantage of being highly versatile and rapid, without the need for breeding with additional transgenic animals (34). It has however limits in the duration of the animal follow up and the potential effects of host irradiation. Mouse models obtained using this technique demonstrated that reduced dosage of *Kmt2d* or *Crebbp* accelerates Bcl2-driven lymphomagenesis by affecting the deposition of activating histone marks onto the regulatory domains of genes implicated in GC exit (discussed in the FL section) (46, 47).

CRISPR-Cas9 editing approaches. The advent of the CRISPR-Cas9 technology has transformed the approach to genome editing, as the Cas9 nuclease can be targeted to any specific, 20 nucleotide-long genomic sequence that is followed by a protospacer-adjacent motif (PAM), where it will cut the DNA (48). These DNA breaks can then be repaired by non-homologous end joining, leading to small insertions/deletions, or by homology-directed repair (HDR), which can be leveraged to generate precise DNA modifications by providing a DNA template. HDR can introduce point mutations, insertions of DNA sequences (e.g. protein tags, *LoxP* sites) or specific deletions. This approach, which is extensively reviewed elsewhere (49–51), bears the advantage of being rapid while maintaining the endogenous regulation of expression of the gene

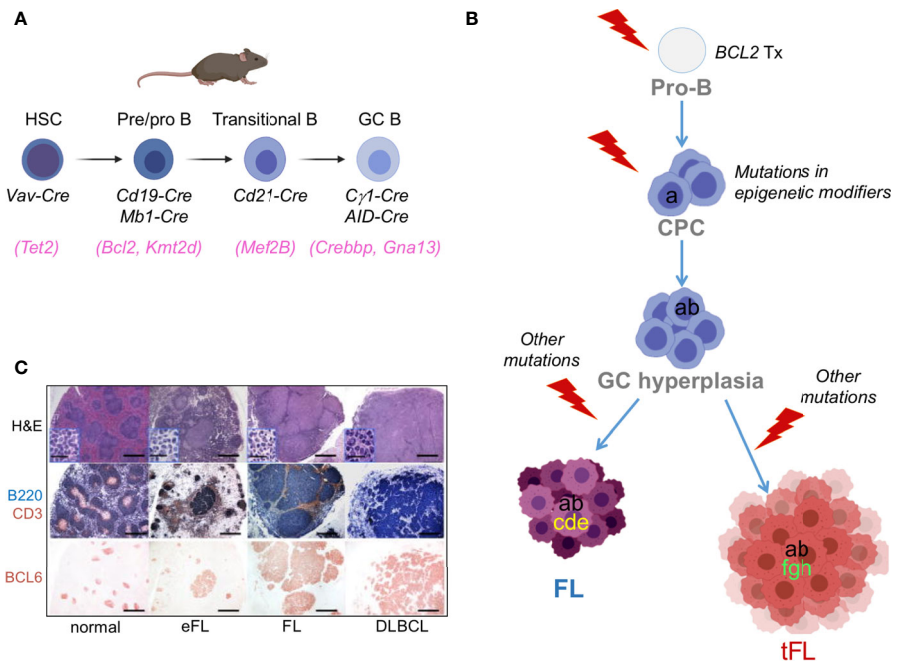

FIGURE 3 | Benchmarking GC-derived GEMMs. **(A)** Cre-drivers utilized to achieve deletion/mutation of lymphoma-associated genes at the appropriate stage of B cell development, namely a HSC (e.g. *TET2* mutations), an early B cell (e.g. *BCL2* translocations), a transitional/mature B cell (utilized for genes whose endogenous promoter is specifically induced in the GC, e.g. *MEF2B*), or a GC-B cell (e.g. *CREBBP/KMT2D*). **(B)** Divergent evolution model for the pathogenesis of FL and tFL inspiring the construction of compound GEMMs. The original B cell clone is on top; based on genetic evidence, *BCL2* translocations are thought to represent the earliest event, which takes place in a pro-B cell as a by-product of the VDJ recombination process. Subsequent gain of *CREBBP* and *KMT2D* mutations by a postulated common mutated precursor cell primes epigenetic reprogramming, favouring its persistence for years before the independent acquisition of distinct genetic alterations leads to final clonal expansion and malignant transformation into a FL or a tFL, through branching evolution. **(C)** Representative histo-pathological and immuno-phenotypic characterization of lymphoproliferative diseases developing in GEMMS of lymphoma [from (41)].

studied, and can allow complex manipulations involving multiple independently segregating alleles (52), although the construction of conditional alleles has been challenging. In the context of B cell lymphomas, a CRISPR-Cas9 based design was successfully utilized to engineer two activating mutations in the gene *RRAGC*, recurrently detected in FL patients (53) (see FL section). A lists of GEMMs recpitulating GC-derived lymphomas is reported in **Supplementary Table 1**.

PATIENT-DERIVED XENOGRAFT MODELS

Despite many advantages offered by GEMMs in understanding the basic mechanisms underpinning tumor development, conditional transgenic mice present some limits particularly in the context of preclinical oncology. First, they are expensive to generate, involve laborious techniques, and may require long time to establish a large animal cohort of the desired genotype, because many littermates will not carry the desired combination of alleles after crossing. Moreover, GEMMs are generated from inbred mouse strains and model only few mutations at a time; as a consequence, tumors developing in these animals may not recapitulate the genomic complexity of human lymphomas, and could thus be less clinically relevant. Finally, the variable onset and penetrance of disease makes them suboptimal models for drug development and testing.

To circumvent some of these problems, efforts have been made to directly implant tumor tissues or cells surgically dissected from cancer patients into immune-compromised recipient mice by subcutaneous, intravenous or orthotopic transplantation (**Figure 2D**). When successful, such model system, known as Patient Derived Tumor Xenografts (PDX), was shown to maintain the same genetic and histopathologic characteristics of the original tumor clone, and thus to better represent the genomic complexity of the human disease, in a way that is hard to achieve in GEMM (54, 55). However, more recent work has indicated that PDX models rapidly acquire copy number aberrations during passaging, most likely due to the expansion of minor clones present in the parental tumor, which could raise concerns about their role in cancer studies (56, 57). PDXs can be propagated without *in vitro* manipulation and have been used in several preclinical studies aimed at confirming findings obtained in *in vitro* cell lines and/or at assessing drug responses. Nonetheless, testing of multiple PDX models is necessary in order to obtain generalizable results, which quickly increases the complexity of the experiments. PDXs also require significant infrastructural support and may take several months before engraftment is achieved, which is why large repositories such as the Public Repository of Xenografts (ProXe) database or the Novartis Institutes for BioMedical Research PDX encyclopedia (NIBR PDXE) have been generated (10, 58). The establishment of several DLBCL and transformed FL PDXs has been reported, which can be stably propagated *in vivo* and reflect phenotypic and genetic features of the GCB- and ABC-DLBCL subtypes, while maintaining key genetic drivers of pathogenesis that were present at diagnosis (10, 59).

The major disadvantages of xenograft models are the lack of a physiological tumor microenvironment (unless in the context of orthotopic injections) and the lack of a functional immune response. The injection of tumor cells into the tissue of origin more closely mimics microenvironmental cues provided by the non-neoplastic cells, allowing the interaction between these components, even though differences in signaling pathways or cellular populations might be expected between the human and mouse microenvironment. The lack of a functional immune response can be partially addressed in NOD/SCID mice by addition of human peripheral blood lymphocytes, bone marrow, or fetal liver and thymus into irradiated or immunodeficient mice (60). However, due to the development of graft versus host disease, the observational window in these humanized mice is relatively short (61). Despite these issues, PDX models are expected to provide an improved platform for testing drug sensitivities and investigating the development of drug resistance, as well as for the validation of biomarkers (54), particularly when compared to cell line derived xenografts (62–65).

MOUSE MODELS OF BURKITT LYMPHOMA

The genetic hallmark of BL is a chromosomal translocation that brings the *MYC* gene under the control of one of the *IG* enhancers (66, 67), causing its ectopic transcription in the bulk GC population where MYC expression is otherwise limited to a small subset of cells primed for DZ re-entry (19, 20). Additionally, several genes were identified as recurrently mutated in this lymphoma. These include *ID3*, a negative regulator of TCF3/E2A that is inactivated in 35-58% of all BL subtypes, and *TCF3*, which encodes the transcription factor E2A and is targeted by gain-of-function mutations in 10-25% of cases (68–70). The TCF3-ID3 axis is predicted to promote antigen independent "tonic" BCR signaling, leading to the sustained activation of the phosphoinositide-3-kinase (PI3K) signaling pathway and therefore providing pro-survival signals to the tumor cell. Gain-of-function mutations of *CCND3* (5% of endemic BL and 38% of sporadic BL), which encodes for a D-type cyclin required for the proliferation of DZ B cells, and missense mutations of the FOXO1 transcription factor (20% of cases) are also recurrently found in different clinical variants of BL, highlighting a prominent oncogenic role for these two genes (69–73).

Mouse Models of Deregulated MYC Expression

As the first oncogenic translocation identified in B-cell lymphomas, several transgenic mouse models have been generated over the years to drive **MYC** overexpression throughout B-cell development under the control of different

IG enhancers, in an attempt to mimic the *IGH-MYC* translocation (74–77). At the time, it was not known that these lesions occur as by-products of the SHM or CSR process, that is, during the GC reaction. As a result of such early activation, most MYC-transgenic models develop pre-GC derived B-cell lymphomas that, while reproducing some histo-morphologic features of the human disease, lack surface *IG* expression (EμMYC mouse model) (74, 78) or retain transitional B cell markers (e.g. CD43) in the absence of somatically mutated *IGHV* regions (λ-MYC mouse model and 3' IgH LCR-driven Myc transgenics) (75, 77), an indication that the malignant transformation process occurred in transitional/pre-GC cells. Although these models have helped to investigate the role MYC plays in oncogenesis overall, or to elucidate the cooperativity among diverse oncogenes (79–82), they are not considered informative for dissecting the pathogenesis of BL; moreover, the nearly full penetrance of immature B-cell lymphomas in some of these models may complicate the study of the GC B cell response, as mice frequently die before becoming immunologically mature.

A mouse model that mimics all key aspects of BL was generated in the laboratory of Klaus Rajewsky in 2012 (83). This was achieved by inducing the overexpression of MYC specifically in GC B cells, in combination with a constitutive active form of the PI3K catalytic subunit (referred to as mutant P110*). Tumors developing in these mice closely resemble the human BL morphologically and histologically, as well as in their transcriptional profile, including the expression of BCL6. In addition, tertiary transforming events, such as mutations in *CCND3* and ongoing SHM, were observed in the developing tumors. Thus, the *Myc/P110** animal model could represent a valuable system to study the mechanisms underlying BL development, as well as the potential preclinical utility of targeted therapeutics. Using these mice, a pro-proliferative and anti-apoptotic function of FOXO1 was uncovered, which contributes to the transformation of GC B cells towards BL (84).

MOUSE MODELS OF FOLLICULAR LYMPHOMA AND GCB-DLBCL

FL is the second most common type of B-cell lymphoma (3). While typically an indolent disease, FL represents a continuing challenge for researchers and clinicians because it remains incurable. Moreover, a significant fraction of patients progress early or undergo histologic transformation to a more aggressive DLBCL, with poor long-term outcome (85, 86). A distinctive feature of this disease is the constitutive expression of the anti-apoptotic protein BCL2, due to the hallmark t(14;18) translocation that places the *BCL2* coding region under the control of the *IGH* enhancer (87). This genetic lesion is insufficient alone to drive lymphomagenesis in humans, as documented by the fact that *BCL2* translocations can be detected, at extremely low frequency, in the peripheral blood of most healthy individuals (88), yet the majority of these subjects will never develop a FL (89, 90). Thus, additional oncogenic events are required for the malignant transformation of these precursor cells. Indeed, whole exome sequencing analysis of large FL datasets revealed a plethora of additional, highly recurrent somatic mutations, with the majority of them targeting histone/chromatin modifying enzymes. These include the KMT2D methyltransferase, mutated in 70-80% of cases, the CREBBP acetyltransferase (65% of cases), and the EZH2 methyltransferase (22% of cases), but also multiple linker-histone family members (over 44% of cases) and, less commonly, the chromatin remodeler ARID1A (91–95). The nearly universal involvement of these genes in FL established aberrant epigenetic regulation as a central driving force in this lymphoma type, in addition to BCL2 deregulation.

Other common genetic alterations that have been successfully modeled in mice include gain-of-function mutations of *MEF2B* (15% of cases) (96), biallelic loss-of-function mutations and deletions of *TNFRSF14* (up to 40% of cases) (94, 97), and point mutations of the *RRAGC* gene. Of note, these same genes (with the exception of *RRAGC*) are also recurrently mutated in GCB-DLBCLs, and particularly in the recently identified EZB (for EZH2-BCL2)/C3 (Cluster 3) genetic subtype (29, 30). Accordingly, mouse models recapitulating these lesions develop both FL and DLBCL. We discuss them in this section because of the higher prevalence of these alterations in FL as compared to DLBCL, and the preferential development of FL-like diseases, with a smaller number of overt large B-cell lymphomas.

Mouse Models Engineered to Mimic the BCL2 Translocation

In order to study the impact of deregulated BCL2 expression *in vivo*, several attempts have been made to genetically engineer the t(14;18) translocation in mice. Of these models, two have successfully recapitulated FL-like tumors within their lifespan: the *VavP-Bcl2* mouse model and the *BCL2-Ig* mouse model (35, 98, 99). A third model, $BCL2^{tracer}$ mice, faithfully recapitulates the early stages of BCL2 deregulation, but does not advance to lymphomas. Similarly, Eμ-*BCL2* mice develop an expanded small B-lymphocyte population but they don't develop tumors spontaneously (100), unless combined with other oncogenes; nonetheless, this mouse model has been useful in revealing the cooperativity between *BCL2* and other candidate oncogenic events such as *CREBBP* loss (101). More recently, mice carrying a conditional *BCL2* knock-in allele in the Rosa26 locus (Rosa26LSL.BCL2.IRES.GFP) were reported to display enlarged spleens with an increase in follicular B cells and larger GCs, when BCL2 expression was induced in pre/pro B cells using the *Cd19-Cre* deleter strain (102). These mice were designed to mimic the *BCL2* copy number gains that are frequently associated with ABC-DLBCL, rather than the t(14;18) translocation. Consistently, the B cell lymphomas developing over time in roughly 50% of these animals are largely $B220^-$ and $CD138^+$, indicating a post-germinal center plasmablastic differentiation. Although recapitulating a more advanced stage than that from which ABC-DLBCLs presumably derive, this background was useful to study the

synergistic activity of mutations implicated in the pathogenesis of ABC-type DLBCL, and will be discussed in the DLBCL section (102).

In the ***VavP-Bcl2*** mouse model, the BCL2 oncogene was placed under the control of the pan-hematopoietic *Vav* promoter. Hence, BCL2 expression is enforced in the whole hematopoietic lineage, at an earlier developmental stage than when the human BCL2 translocation occurs (36). Despite this limitation, young *VavP-Bcl2* mice display spontaneous, antigen independent GC hyperplasia, and develop over time B-cell lymphomas that faithfully recapitulate the GC origin of the human FL, along with other critical aspects of its pathobiology such as the follicular pattern, the expression of peanut-agglutinin (PNA) and BCL6 in the absence of post-GC markers, and the presence of clonally rearranged *IGHV* genes that are somatically mutated (98). The *VavP-BCL2* model has served as an excellent experimental system for deciphering the cooperative role of other genetic lesions observed in the human condition concomitantly with *BCL2* translocations. To this end, *VavP-BCL2* mice were crossed with other GEMMs (e.g. $Crebbp^{fl/fl}$, $Kmt2d^{fl/fl}$, $Ezh2^{Y641N}$) or were used directly as a source of HPCs that were transduced with retroviral constructs carrying gain- or loss-of-function mutants before transplantation into irradiated mice (103). Nonetheless, the ubiquitous expression of BCL2 in the entire hematopoietic lineage and the dependency of *VavP-BCL2* GC B cells on BCL2-expressing $CD4^+$ T_{FH} cells could represent a drawback that investigators should carefully consider depending on the specific questions they wish to address.

Unlike the *VavP-Bcl2* mouse model, the ***BCL2-Ig*** model expresses a *Bcl2* minigene under the control of *IG* regulatory elements, and thus exclusively in B cells (35). This strain displays an excess of B lymphocytes (both small B cells and plasma cells) that were shown to survive for a prolonged period of time under *in vitro* conditions, providing the first *in vivo* evidence for the anti-apoptotic function of BCL2, independent of proliferation (35). Bcl2-Ig transgenic animals did not develop tumors in the original 12-month follow up study (35) but, when challenged by chronic immunization with a T cell dependent antigen, they were shown to accumulate GC B cells and, in 40% of cases, to develop $PAX5^+BCL6^+$ FLs, with a smaller fraction of plasmacytoid tumors ($PAX5^-BCL6^-IRF4^+$) (104).

Perhaps the model recapitulating with most fidelity the initial steps of FL genesis, though never progressing to overt FL, is the mosaic $\mathbf{BCL2^{Tracer}}$, where expression of a functional human *BCL2* (*hBCL2*) transgene is contingent on RAG dependent inversion of this cassette during the V(D)J recombination process (105). As such, this model mimics both the sporadic nature of the t(14;18) translocation and its induction at the appropriate developmental stage, i.e. a BM pro-/pre-B cell, as a byproduct of VDJ recombination (105, 106). In these mice, the recombination event leads to a unique coding joint; thus, the frequency of recombination can be confirmed at the genetic level by PCR and at the protein level by use of specific anti-hBCL2 antibodies. Although limited to the development of *in situ* FL, the $BCL2^{Tracer}$ model has helped in tracking the initial events leading to the accumulation and expansion of *BCL2*-translocated B cells, paving the framework for the current model of FL ontogenesis, based on three lines of evidence. First, as in the case of human *in situ* FL, when mice were challenged by T-cell dependent antigens, hBCL2-overexpressing B cells (but not the non-rearranged B cells) were triggered to make multiple GC re-entries and spread to an advanced pre-neoplastic stage. Second, while the fraction of $hBCL2^+$ cells in the naïve, GC and memory B-cell compartment was comparable upon a single immunization, their number was markedly enriched in the GC and memory B cell population, following chronic antigenic recall. Finally, $hBCL2^+$ cells were able to repopulate the GCs of immunized WT mice in adoptive transfer experiments (105). Together with the observation that t(14;18)-positive cells in healthy individuals harbor somatically mutated *IGHV* region genes, these data provide a plausible explanation for the origin of FL from a recirculating memory B cell requiring multiple transits through the GC, before the acquisition of additional genetic or epigenetic perturbations ultimately drives the development of clonal tumors.

Mouse Models Recapitulating Alterations in Histone Modification Genes

A second genetic hallmark of FL and EZB/C3 DLBCL is the presence of mutations in genes encoding histone/chromatin modifiers, collectively accounting for almost all FL cases and over 50% of DLBCL cases. These lesions constitute early events in the phylogenetic history of the disease, which in the context of FL transformation can be found in the dominant tumor clone of both the indolent FL and its transformed FL (tFL) counterpart, suggesting that they have been acquired by a putative common precursor cell (CPC), before divergent evolution and final clonal expansion (**Figure 3B**) (94, 107, 108). The exact developmental stage at which *KMT2D* and *CREBBP* mutations emerge remains to be determined; thus, hemizygous and homozygous loss of these genes has been modeled at different stages of B cell differentiation, by using Cre-drivers that are specifically active in HSC (109), early B cells (*Cd19-Cre* and *mb1-Cre*) (41, 47, 101, 110) and GC B cells (via the *Cγ1-Cre* recombinase) (41, 110, 111).

The Complex Of Proteins Associated with Set1 (**COMPASS**) plays a pivotal role in the process of mammalian transcription through mono- and di-methylation of histone 3 lysine 4 (H3K4) at enhancer/super-enhancer regions (112). This activity is executed through its catalytic subunit **KMT2D**, which is the most commonly mutated gene in FL and EZB/C3 DLBCL. *KMT2D* mutations are mainly truncating events, with few missense mutations in the SET domain, which all impair its enzymatic function, indicating that *KMT2D* acts as tumor suppressor gene in B cells. Interestingly, when *Kmt2d* was conditionally deleted in pre-B cells, that is, at a much earlier stage than when the final malignant transformation ensues, the GC B cell population expanded significantly in response to antigenic challenge, compared to wild-type littermates (41, 47). The same phenotype, but less pronounced, was observed when *Kmt2d* was disrupted at a later stage, after the initiation of the GC reaction (41). Analogously, changes in the transcriptional profile of GC B cells from *Cd19-Cre* compound mice were more robust

compared to GC B cells where deletion of *Kmt2d* was induced by *Cγ1-Cre* (41). The most prominent signature lost in *Kmt2d*-deficient GC B cells includes genes implicated in cytokine signaling, IFN responses and terminal differentiation programs. These data suggest an early role for *KMT2D* inactivation in FL, likely through epigenetic reprogramming. Consistent with this model, loss of *Kmt2d* alone in the GC was not sufficient to drive lymphomagenesis, but when combined with deregulated expression of *BCL2* (as observed in human FL and DLBCL) the two cooperate, leading to a significant increase in the percentage of *bona fide* FL and DLBCL characterized by clonally rearranged, mutated *IGHV* genes and the expression of GC-specific markers (**Figure 3C**) (41). The synergistic effect of *Kmt2d* loss and *BCL2* deregulation *in vivo* was independently confirmed in a mouse model of adoptive transfer where *Kmt2d* was knocked-down in *VavP-Bcl2* HPCs prior to reconstitution into lethally irradiated syngeneic mice (47).

Mutations inactivating the acetyltransferase ***CREBBP*** (either truncating or missense in the HAT domain) are the second most common epigenetic lesion in FL (95). Together with its paralog EP300, CREBBP belongs to the KAT3 family of histone and non-histone acetyl-transferases, which modulate transcription by acetylating H3K27 and H3K18 at gene enhancers and promoters. GEMMs mimicking the conditional loss of *Crebbp* share remarkable similarities with the *Kmt2d*-KO model, including: a) the increase in GC B cells with partially overlapping transcriptional changes; b) a more pronounced GC phenotype in *Cd19-Cre* background compared to *Cγ1-Cre* mice; c) the inability to drive full-blown tumor formation on their own, but a strong synergistic activity with *BCL2* deregulation, leading to acceleration of lymphoma onset and increased penetrance of FL (46, 110). In human GC B cells, CREBBP binds virtually all GC-specific super-enhancers; however, not all those genes are transcriptionally affected by its loss in purified murine GC B cells, as well as in DLBCL cell lines (46, 110). This might be partly due to the compensatory activity of its paralogue EP300 and, indeed, CREBBP and EP300 are rarely concurrently and biallelically mutated, indicating that GC B cells need a certain threshold of acetyltransferase activity for their survival (111). However, *CREBBP* deletion caused focal enhancer loss of H3K27Ac and reduced expression of specific genes that are involved in GC exit, such as downstream effectors of BCR and NF-κB signaling pathways, multiple cytokines, and antigen presenting molecules, with MHC class-II genes being the most notable among them (46, 110). These findings parallel the human FL, where *CREBBP* mutations are associated with decreased MHC-II expression and reduced frequency of tumor-infiltrating T-cell subsets (108). Notably, the chromatin domains occupied and acetylated by CREBBP are direct targets of the BCL6 oncorepressor in a complex with SMRT and HDAC3 (46, 110). Additionally, CREBBP directly acetylates several proteins that are relevant to B cell lymphoma biology, including the TP53 tumor suppressor, which requires acetylation for its activity, and the BCL6 protein, which instead is functionally impaired by acetylation due to the lost interaction with co-repressor complexes (95, 113). These GEMMs were critical to document a major role for CREBBP in GC B cells by opposing the oncogenic activity of BCL6 and thereby initiating the activation of terminal differentiation/antigen presentation program as LZ B cells engage T_{FH} cells and prepare to exit the GC. Consistent with these data, *CREBBP*-mutant lymphomas show reduced expression of genes that are antagonistically regulated by the BCL6-SMRT-HDAC3 complex and become dependent on HDAC3 for their survival. Conversely, when HDAC3 activity was inhibited, histone acetylation was restored at these enhancers and lymphoma growth was suppressed both *in vitro* and *in vivo* (46, 114). These studies identified HDAC3 and EP300 as vulnerabilities of *CREBBP*-mutant cells that may lead to potential therapeutic avenues for these lymphoma entities.

EZH2, a histone methyltransferase, catalyzes the addition of repressive H3K27me3 marks at selected, cell-context dependent regions that, in the GC, include proliferation checkpoint genes (e.g. *CDKN1A*, *CDKN1B*) and genes involved in plasma cell differentiation (e.g. *IRF4*, *PRDM1*), creating bivalent promoters that can be rapidly re-activated when B cells receive the signal to exit the GC (115). Indeed, EZH2 is required for GC formation (115, 116). Two hotspot gain-of-function mutations, Y646F (equivalent to the mouse residue Y641) and Y646N, have been observed in human lymphomas and were modeled in the mouse to study their role in lymphomagenesis. In these animals, expression of the conditional $Ezh2^{Y641F}$ allele is driven by the endogenous *Ezh2* promoter (117), whereas expression of the transgenic $Ezh2^{Y641N}$ allele is under the control of the CAG promoter (115). Both alleles, when selectively activated in the GC following the *Cγ1-Cre*-mediated excision of a lox-stop-lox cassette, led to massive GC hyperplasia, sustained by enhanced proliferation, blockade of terminal differentiation, and increased abundance of H3K27me3 levels at the promoters of Ezh2 target genes. A key element for this phenotype is the functional cooperation between EZH2 and the BCL6/BCOR repressor complex (117). In both models, expression of the mutant *Ezh2* knock-in allele did not lead to lymphomas; however, accelerated lymphomagenesis was observed when mice were crossed with *VavP-Bcl2* transgenics or upon adoptive transfer of *VavP-Bcl2* BM cells transduced with $Ezh2^{Y641F}$ vectors (115, 117, 118). *Ezh2* mutations were also shown to cooperate with deregulated BCL6 expression in a compound *IμHABCL6*;*Ezh2* knock-in mouse model, giving rise to a transplantable, GC-derived DLBCL-like disease. Comparatively, *Cd19-Cre* driven expression of a mutant Ezh2 protein under the control of the endogenous promoter induced B-cell lymphomas at high penetrance, but the phenotype of these tumors ($B220^+$, $CD19^+$, IgM^+, $CD43^+$, $CD5^+$ and $Mac1^+$) is not reminiscent of the human lymphomas, reinforcing the importance of achieving precise temporal and spatial control of the target genetic lesions (119). Besides documenting the oncogenic role of EZH2 mutations, the value of the *Ezh2;Cγ1-Cre* GEMMs is twofold: first, they revealed an additional function of Ezh2 in shaping the tumor microenvironment, providing an opportunity to study syngeneic immune responses (see following section); second, they proved to be a valuable tool for the preclinical testing of novel therapeutic approaches, as tumors developing in these mice replicate the human phenotype in

several aspects related to the tumor microenvironment. In particular, they display significantly lower expression of MHC-I and MHC-II, accompanied by an immunologically cold environment with reduced T-cell infiltrate, which could be restored upon treatment with EZH2 inhibitors (118).

FL and DLBCL also feature recurrent somatic mutations in histone genes, with the **linker Histone H1 family** being most commonly affected (up to 44% of FL and 26% of GCB-DLBCL cases), and the *HIST1H1C* and *HIST1H1E* family members accounting for the majority of mutations (94, 120). The cooperative role of inactivating *H1C* and *H1E* mutations, which are often concurrently found in the same case, was recently demonstrated in a double knock-out mouse model displaying an increase in both the size and number of GC structures that form upon T-cell dependent antigenic challenge. This phenotype was linked to the evidence of chromatin decompaction specifically at target genes of stem cell factors (e.g. NANOG, SOX2, and PRC2). Thus, *H1* mutations may impair proper chromatin compartmentalization and provide a fitness advantage to mature B cells by both preventing differentiation and activating stem cell like programs, including enhanced self-renewal. In line with this hypothesis, transplantation of *VavP-Bcl2;H1c*$^{-/+}$*H1e*$^{-/+}$ lymphoma cells into secondary and tertiary recipient mice yielded 100% engraftment, which was not observed with the *VavP-Bcl2* only tumors, consistent with the fact that *H1* mutant DLBCL are highly aggressive (120).

TET2 is a dioxygenase that converts 5-methylcytosine (5mC) to 5-hydroxymethylcytosine (5hmC), 5-formylcytosine and 5-carboxylcytosine, an important step in DNA demethylation (121). Oxidation of 5mC by TET2 has also been recognized as a modulator of enhancer activity during differentiation. Compared to myeloid neoplasms (122, 123), *TET2* inactivating mutations are detected at relatively low frequencies in FL/tFL (3-10% of cases) and DLBCL (6-12% of cases) (29, 30, 107, 124). Consistent with the observation that patients with *TET2* mutated lymphomas harbor the same mutation in their HSC (125), the contribution of these alterations to lymphomagenesis was studied *in vivo* by engineering the conditional loss of *Tet2* in HSCs or at later stages of B-cell development (126). *Tet2* deficiency facilitated the expansion of GC B cells in *Vav-Cre* and *Cd19-Cre* conditional KO mice, but not when directed to the GC stage, and led to promoter hypermethylation of genes implicated in GC LZ programs, with consequent transcriptional repression. However, these abnormal cells fail to advance to clonal DLBCL. When GC-specific *Tet2* deletion was combined with *BCL6* deregulation, effacement of the splenic architecture due to enlarged follicles or diffuse lymphoid infiltrates was observed. These tumors are negative for several mature B cell markers like CD23, CD21, IgM and IgD, and will require further detailed characterization. However, this work unraveled a potential link between TET2 and CREBBP in orchestrating the transcriptional program that sustains GC exit through CREBBP-dependent acetylation and stabilization of TET2, resulting in the activation of enhancer domains (126).

Together, the above studies were critical to demonstrate how mutations in epigenetic modifier genes initiate lymphomagenesis by reprogramming the epigenome of the CPC, leading to the activation of partially overlapping biological programs that, in cooperation with *BCL2* deregulation, cause malignant transformation. Identifying the specific stage at which these mutations are introduced, and the sequence of genetic or epigenetic events that cooperate with these lesions to drive full malignant transformation remains an open question that warrants further studies. Finally, the observation that MHC-II and other surface receptor molecules are regulated by epigenetic modifier genes suggests that epigenetic dysregulation may contribute to tumor immune escape by actively influencing the microenvironment.

Mutations Affecting the Cross-Talk With the Tumor Microenvironment

Normal GC B cell development, survival and differentiation is essentially dependent on pro survival signal transduction pathways that are engaged by the cross-talk with immune and accessory cells, including the secretion of multiple cytokines and chemokines. These micro-environmental interactions play an equally important role during FL development, as they create a permissive niche to support the malignant B cell population (127, 128). Interestingly, although LZ B cells –the normal counterpart of FL– are highly dependent on T cell help, augmenting the anti-tumor immune response by checkpoint blockade approaches has been disappointing in this disease (129). Such lack of success may be due in part to multiple genetic alterations that can affect the FL (and DLBCL) microenvironment directly and indirectly, allowing escape of immune surveillance, while creating a pre-lymphoma niche that fosters malignant transformation and growth. For instance, loss of MHC-I cell surface expression has been observed particularly during FL transformation to a more aggressive DLBCL, as the result of mutations in components of the MHC-I complex or to alterations in their transcription and transport, which may favor evasion from $CD8^+$ T cell immunosurveillance (118, 130, 131). Reduced MHC-II levels are also a feature of FL and DLBCL, which seems to be enriched in cases carrying mutations of CREBBP and EZH2. Together, these findings suggest a close link between epigenetic reprogramming and immune escape in these tumors, the study of which could ideally leverage on GEMMs.

TNFRSF14, which encodes the HVEM receptor, is mutated or deleted in 28% FL and 9% GCB-DLBCL (132, 133). *In vivo*, loss of function studies used an shRNA-knockdown strategy in the *VavP-Bcl2* HPC adoptive transfer system (132). Although this approach may not fully recapitulate the exact timing at which *TNFRSF14* mutations are presumably acquired in the human tumors, these mice showed an increased penetrance of Bcl2-driven FLs upon HVEM knockdown. Moreover, only a minority of T cells were found to express the *shHvem* hairpin construct, whereas *shHvem*-expressing B-lymphoma cells were significantly enriched. Mechanistically, this model revealed that HVEM loss stimulates BCR signaling and B cell proliferation both in cell-

autonomous and BTLA-dependent manner. Moreover, it demonstrated the ability of HVEM low expression to induce a tumor-supportive microenvironment through increased production of TNF-family cytokines that act as stroma-activating factors. Both murine and human *TNFRSF14*-deficient FLs show prominent lymphoid stroma activation. This research offered a new therapeutic avenue by demonstrating *in-vivo* that abnormal BCR signaling and cytokine production in FL can be normalized by injecting a soluble HVEM ectodomain protein, resulting in tumor growth delay.

As mentioned, a recent study has shown that mutant ***Ezh2*** can also affect the GC microenvironment, by attenuating the requirement of T_{FH} cells for GC B cell survival (134). In particular, single cell analysis showed an expansion of the LZ compartment that was not due to impaired differentiation, but to an increase in proliferation and a reduction in cells circulating back into the DZ. Genes downregulated in *Ezh2* mutant LZ cells are normally required for the interaction with T_{FH} cells (e.g. *Tnfrsf14*, *Cd69*, *Icos* and *Icam1*) and *Ezh2* mutant LZ cells showed impaired T_{FH} interactions, suggesting that they no longer need to compete for T cell help in order to survive and undergo selection. Instead, *Ezh2* mutant GC B cells upregulated genes involved in FDC signaling. Importantly, this study showed a significant association between *EZH2* mutated FLs and an extensive FDC network. Thus, lymphoma cells carrying *Ezh2* mutations may reprogram the GC niche to allow for their own aberrant expansion in an FDC-dependent manner, and remodel the interaction between B cells, T_{FH} and FDCs. These data also raise the possibility that one of the mechanisms underlying the activity of EZH2 inhibitors against *EZH2* mutant FLs (135) is their ability to restore proper interactions between the tumor cells and the microenvironment.

Modeling MEF2B Activating Mutations

MEF2B is a transcription factor that, within the B cell lineage, is exquisitely expressed in the GC (96). MEF2B instructs the GC transcriptional program by modulating a broad set of genes that are implicated in multiple biological functions and also include the BCL6 master regulator (104). This activity is hijacked in ~15% of FL and DLBCL due to a variety of somatic mutations that can be broadly classified into two groups: i) missense mutations in the protein amino-terminal portion, encoding the DNA-binding domain; and ii) truncating and missense mutations in the protein C-terminal portion, where post-translational modifications like sumoylation and phosphorylation have been mapped. While the consequences of the C-terminal group of mutations remain to be studied, the N-terminal mutations were found to prevent the physical interaction of MEF2B with components of the HUCA complex and HDAC genes, thus interfering with negative regulatory mechanisms of its activity. As MEF2B transcription is induced in the early stages of GC commitment, the role of the most common D83V N-terminal mutation was investigated in a conditional knock-in mouse model crossed with *Cd21-Cre* mice (104). *Mef2b*$^{+/D83V}$; *Cd21-Cre* mice display benchmark characteristics of GC-derived lymphomas, including a significantly enhanced GC response compared to their control littermates and the development of clonal FL and DLBCL in 20% of the animals, which became fully penetrant when mice were crossed with the *BCL2-Ig* allele.

Modeling Metabolic Reprogramming by *RRAGC* Mutations

RRAGC encodes a GTPase (RagC) involved in the activation of mammalian target of rapamycin complex 1 (mTORC1) that is responsible for the sensing and response to amino acid availability (136). Together with other components of this super-complex, *RRAGC* is mutated in ~17% of FL cases, implying an important pathogenetic role (137). A mouse model for the most common FL-associated *RRAGC* mutations was recently constructed by taking advantage of the CRISPR-Cas9 genome engineering technology to introduce the S74C and T89N sequence changes in the endogenous locus, followed by crossing with *VavP-Bcl2*-transgenic mice. These studies revealed that *Rragc*-mutant B cells show partial insensitivity to nutrient withdrawal, leading to accelerated FL tumorigenesis (53). The phenotype of *Rragc* mutant cells was not due to enhanced proliferation, but to reduced apoptosis, and was dependent on micro-environmental pro-survival signals normally provided by T_{FH} cells. Expression of the Rragc S74C and T89N protein increased GC B cell fitness by inducing mild activation of the mTORC1 pathway, consistent with a model whereby the mutation provides a competitive advantage to pre-malignant GC B cells, allowing them to undergo continuous cycles of selection and proliferation within the GC. This in turn could facilitate the acquisition of additional genetic alterations, and ultimately transformation into a *bone fide* FL. Interestingly, while mutations in *TNFRSF14* increased T_{FH} infiltration, *RRAGC* mutations decreased the GC dependency on T_{FH} signaling. Consistent with these opposing effects on the microenvironment, mutations in *RRAGC* and *TNFRSF14* are mutually exclusive. Targeting Rag GTPase signaling could thus represent a promising strategy against FL, warranting further efforts toward the development of specific inhibitors of nutrient signaling.

MOUSE MODELS OF DIFFUSE LARGE B-CELL LYMPHOMA

DLBCL, the most common type of lymphoma in adulthood, is a heterogeneous disease comprising a diverse group of phenotypically and molecularly distinct entities associated with different clinical responses to currently available first-line chemo-immunotherapeutic approaches (4). In addition to the phenotypic classification into GCB-DLBCL and ABC-DLBCL, as many as 8 distinct genetic subgroups have been recently identified based on the co-occurrence of specific mutational events (29–31). Among these, the EZB genetic subtype and the partially overlapping C3 DLBCL share significant similarities with FL in terms of mutational profile, as reviewed in the previous section. *MYC* translocations can also be found in ~12% of tumors with DLBCL morphology, generally in the

GCB type and largely in the presence of concurrent BCL2 rearrangements (~8% of cases) (see next section). Here, we summarize mouse models recapitulating other recurrent DLBCL-associated genetic lesions, including translocations of *BCL6*, loss-of-function mutations of *FBXO11* and *GNA13*, and a constellation of mutations targeting various components of the BCR, NF-κB, and terminal differentiation pathways, which represent a genetic hallmark of ABC-DLBCL.

Disruption of the Gα13 Signaling Pathway

Almost one third of GCB-DLBCL (and ~58% of BL) carry deleterious mutations in multiple components of the Gα13 pathway, which is responsible for the confinement of GC B cells and also feeds the AKT pathway. The mutated genes include *GNA13* and, more rarely, *S1PR2* and *ARHGEF1* (138), indicating that this signaling cascade might be playing an important role across lymphoma subtypes. The observation that lower expression of S1PR2 is associated with worse survival in DLBCL (139) further supports its functioning as a tumor suppressor. Two conditional knock-out mouse models have been created, in which *Gna13* was either specifically deleted in GC B cells *via* crossing with the *Aicda-Cre* transgenic strain (140), or ablated in all B cells by using a mixed BM chimera approach (*Gna13*$^{fl/fl}$*;mb1-Cre*) (138). Both models showed increased numbers of GC B cells with disordered GC architecture and altered DZ/LZ distribution, as well as higher levels of SHM activity and abnormal B-cell migration. Further supporting the critical role of the Gα13 pathway in lymphomagenesis, deletion of the *S1pr2* receptor led to the development of clonal B-cell lymphomas with morphologic, phenotypic and genetic characteristics resembling the human DLBCL in 50% of mice (141). Interestingly, lack of *Gna13* but not of *S1pr2* led to systemic dissemination of B cells in the lymph and blood, a finding that implies the existence of other G-protein coupled receptors regulating GC confinement. This observation led to the discovery of the P2RY8 receptor, which is also mutated in approximately 4% of GCB-DLBCL (138). Collectively, these studies provided insights into the mechanisms by which GNA13-deficient GC B cells leave the GC niche and spread systemically, and demonstrated a dual tumor-suppressor function for this signaling pathway *via* control of B-cell positioning and AKT activation.

Modeling BCL6 Chromosomal Translocations

BCL6 is a master regulator of the GC reaction and a common oncogene in both FL and DLBCL, where it constitutes a biological dependency. Deregulated expression of an intact BCL6 protein is induced in these tumors by a variety of genetic alterations that target the *BCL6* gene directly (e.g., chromosomal translocations or mutations in its 5' non-coding sequences) (142–146) and indirectly (e.g. mutations of CREBBP, MEF2B, FBXO11) (95, 96, 147, 148). The endogenous *BCL6* promoter contains a number of regulatory elements that are bound by transcriptional repressors to downregulate its transcription at the exit from the GC (e.g. IRF4), or to maintain homeostatic levels in the GC *via* an autoregulatory negative feedback loop. These regulatory sequences are lost as a consequence of "promoter substitution" (cases with chromosomal translocations) or of point mutations, thus disrupting the BCL6 tightly restricted expression pattern (142–146). By sustaining constitutive BCL6 expression and/or activity, these lesions prevent the terminal differentiation of GC B cells, which remain stuck in a highly proliferative and genetically unstable environment potentially conducive to malignant transformation. One of the most common translocations found in FL and DLBCL, t(3;14)(q27;q32), was mimicked in the first GEMM recapitulating the genetics and biology of DLBCL (37). This model was created by knocking in an HA-tagged *BCL6* allele into the murine *IG* heavy chain locus, for expression under the endogenous *Iμ* promoter (*Iμ.HA.BCL6*). *Iμ.HA.BCL6* mice show GC hyperplasia with increased DZ : LZ ratio also in the absence of antigenic stimulation, and develop over time clonal lymphomas that recapitulate key aspects of DLBCL, most notably the evidence of AID-dependent aberrant somatic hypermutation and the presence of stochastic Myc-IgH translocations (37, 79). Interestingly, *BCL6* translocations can be found in both GCB- and ABC-DLBCL, but are enriched in a subset of ABC-DLBCL belonging to the BN2/C1 genetic subgroup, for which a marginal zone B cell origin has been postulated (29, 30). In this subgroup, *BCL6* deregulation frequently co-occurs with *NOTCH2*, *SPEN* or *TNAFAIP3* mutations, for which conditional mouse models have been generated (149–152). One possibility is thus that ectopic expression of *BCL6* induced by the translocation in marginal zone B cells cooperates with other "marginal zone" genes to ultimately cause this type of lymphoma. Although individually none of these other mutations was sufficient to drive lymphomagenesis, compound mice involving the *Iμ.HA.BCL6* model could shed light on the specific oncogenic events induced by the combined deregulation of BCL6 and NOTCH2 signaling (153).

Biallelic Loss of *PRDM1/BLIMP1*

A distinctive feature of ABC-DLBCL, and particularly of the MCD/C5 genetic cluster, is the presence of genetic and epigenetic inactivation of the master plasma cell regulator **BLIMP1** (also known as PRDM1). In ~20% of cases, this is due to biallelic disruptive mutations and/or focal deletions of the *BLIMP1* locus, whereas in an additional subset of cases transcriptional silencing of BLIMP1 is achieved *via* deregulation of *BCL6* (154, 155). When engineered in the mouse, conditional B-cell specific *Blimp1* deletion (*Blimp1*$^{fl/fl}$; *Cd19-Cre* and *Blimp1*$^{fl/fl}$;*Cγ1-Cre*) induced a block in plasma cell differentiation and the development of DLBCLs, the majority harboring somatically hypermutated *IG* genes. These tumors typically express IRF4 and CD138 and are negative for BCL6, a molecular pattern closer to the human ABC-DLBCL (156). As in other lymphoma models, the long latency and the clonality of the DLBCLs in *Blimp1* conditional KO animals indicate that oncogenic events affecting other pathways collaborate with BLIMP1 inactivation during lymphomagenesis. One important contributor to this process is the NF-κB transcription complex, which is constitutively active in virtually all ABC-DLBCLs and is

targeted by genetic alterations at multiple levels in over half of the cases, frequently together with *BLIMP1* mutations (5, 157–160). Accordingly, DLBCLs developing in *Blimp1* conditional KO mice display nuclear active NF-κB (156), and a similar phenotype was reported in a conditional mouse model with combined disruption of *Blimp1* and enforced canonical NF-κB activation, obtained *via* a constitutively active IKK2 protein in GC B cells (*R26Stop*^{FL}*Ikk2ca*;Cγ1-Cre) (161).

Constitutive Activation of the NF-κB Signaling Pathway

The canonical (RELA/p50 and c-REL/p50) and non-canonical (RELB/p52) NF-κB signaling pathways have been shown to play distinct roles in the GC response (162, 163). In most ABC-DLBCL cases, the activity of the canonical NF-κB transcription complex is sustained by the presence of genetic alterations affecting multiple genes that encode for positive or negative regulators of the BCR, CD40 receptor, and TLR signaling cascades, with the TLR adaptor protein MYD88 being mutated in over 30% of patient samples (157–160). Consistently, both *Cd19-Cre* driven and Cγ1-Cre-driven expression of a ***Myd88***^{L252P} allele, corresponding to the most common activating mutation (L265P) in humans, promotes the occurrence of tumors that share several traits with the human ABC-DLBCL (164). *MYD88* mutations in the MCD/C5 ABC-DLBCL often occur in combination with *BCL2* copy number gains, and indeed, in the *Myd88*^{L252P} mouse model, the combination with *Cd19-Cre* driven overexpression of BCL2 led to a significant increase in ABC-DLBCL-like B cell lymphomas (102). These tumors were sensitive to combination therapies with immune checkpoint blockade and BCL2 inhibition, revealing potentially actionable molecular vulnerabilities (102). In addition, a synergistic crosstalk was observed between the *Myd88*^{L252P} hotspot mutation and ***CD79B*** mutations in a compound mouse model, exemplified by the accumulation of auto-reactive cells (165). Although these mice fail to develop overt lymphomas, their phenotype fits well with the suggested role of self-antigens in the survival of ABC-DLBCL cells *via* chronic activation of the BCR-signaling pathway (166). The *Myd88*^{L252P} model may also provide a system to further dissect the signals emanating from a recently described multiprotein supercomplex formed by MYD88, TLR9 and the BCR (167).

In a smaller subset of human DLBCL, the observation of nuclear p52 translocation implies that the non-canonical NF-κB signaling cascade is also activated (157). Part of these cases can be explained by the presence of truncating mutations/deletions of the ***TRAF3*** gene, often coexisting with *BCL6* translocations. *TRAF3* encodes for a negative regulator of the NF-κB non-canonical pathway, involved in the degradation of the NF-κB inducing kinase (NIK). Accordingly, enforced expression of NIK and BCL6 in the GC, as obtained by conditional mutagenesis in the IμHABcl6;*NikstopFL*;*Cγ1-Cre* mouse model, caused GC hyperplasia with blockade of terminal differentiation and development of IRF4-positive DLBCL (168). Notably, *NikstopFL*;*Cγ1-Cre* mice display overt plasma cell hyperplasia but do not succumb to tumors; thus, the oncogenic function of the alternative NF-κB pathway may require the concomitant disruption of terminal B-cell differentiation, which in this case was achieved by deregulated *BCL6* expression. An analogous synergistic phenotype was observed by combining constitutive NF-κB activation and Blimp1 loss in the compound *Blimp1*$^{fl/fl}$; *R26Stop*^{FL}*Ikk2ca*;*Cγ1-Cre* model (161).

Deletion of FBXO11

F-box protein 11 (**FBXO11**) is a member of the F-box protein family that functions in the protein degradation pathway. FBXO11 is a subunit of the substrate-recognition complex SKP1-cullin-1-F-box-protein (SCF) E3 ligase, which leads to ubiquitylation and degradation of numerous target proteins, including BCL6 and BLIMP1 (147, 169, 170). In DLBCL, *FBXO11* monoallelic mutations and/or deletions are present in 6% of cases and correlate with increased BCL6 expression (147). To recapitulate these events, a conditional *Fbxo11* knock-out mouse model was crossed with the GC specific *Cγ1-Cre* driver, documenting a direct link between Fbxo11 loss and the formation of enlarged GCs with increased BCL6 protein levels in response to antigenic challenge (148). Aged *Fbxo11*-deleted mice, when chronically immunized, develop various B-cell lymphoproliferative phenotypes including a low frequency of overt DLBCL. The low tumor penetrance indicates that additional alterations are required for full transformation, along with *FBXO11* inactivation. Nonetheless, this model confirmed a tumor-suppressor role for *FBXO11* in lymphomagenesis, and could be utilized to gain further insights into the mechanism underlying the pathogenetic process.

THE CHALLENGE OF DOUBLE HIT LYMPHOMAS AND tFL

High-grade large B cell lymphomas with concurrent MYC and BCL2 (or BCL6) translocations, previously known as double-hit (DHL)/triple-hit lymphomas, represent a rare category of tumors that is now recognized as a separate provisional entity in the revised WHO classification (3). DHLs typically display a GCB-like phenotype, different from tumors where these two genes are co-expressed in the absence of genetic alterations (171), and, although rare, constitute an area of intense research due to their poor clinical outcome, even though more recent studies suggest a certain degree of heterogeneity, with cases showing a more favorable prognosis (3, 172, 173). MYC translocations are also seen as a secondary genetic alteration occurring on a BCL2-rearranged genetic background during histologic transformation of FL to DLBCL, an adverse event denoted by an aggressive clinical course (85). As such, a faithful model recapitulating the genetics and phenotype of DHLs or tFL would be an invaluable tool for uncovering potential vulnerabilities and pre-clinically testing novel therapeutic principles. Efforts to understand the co-operation between BCL2 and MYC *in-vivo* have been conducted, for instance in transgenic mice expressing these two genes under the control of the Eμ enhancer (174, 175). However, the early timing of MYC deregulation invariably leads to the clonal

expansion of immature B cells. Thus, the construction of GEMMs that faithfully mimic the genetics and the pathobiology of these conditions with regard to both the developmental stage at which the translocations take place (for MYC, a GC B cell undergoing SHM or CSR) and the GC origin of the developing tumors (i.e., somatically mutated *IGHV* genes and immunophenotypic markers of GC B cells) remains a gap in the field.

CONCLUDING REMARKS

GEMMs have revolutionized the study of cancer biology and will remain an invaluable tool in biomedical research, by allowing to elucidate the *in vivo* consequences of novel mutational targets (including coding and non-coding regions of the genome), study the mechanisms underlying the development of B cell lymphomas, and test new therapeutic modalities in a pre-clinical setting. However, no single model can fully reproduce the complexity of the human tumors, which evolve through the sequential acquisition of multiple genetic and epigenetic changes, in concert with an adaptive microenvironment. Investigating the synergistic interactions that are implicated in the malignant transformation process and the plethora of novel therapeutic agents that are being considered for pre-clinical testing warrants the need for more rapid, high-throughput, and possibly less expensive approaches to modeling cancer. While the generation of lymphoma organoids, the expansion of PDX repositories, and the advent of increasingly sophisticated approaches such as the CRISPR-Cas9 editing technique may help to overcome some of the limitations, the judicious construction and study of GEMMs will likely continue to deliver advances that can greatly contribute to improving the management of B cell malignancies.

AUTHOR CONTRIBUTIONS

SM and SK wrote the first draft of the manuscript. LP supervised and finalized the work. All authors contributed to the article and approved the submitted version.

FUNDING

This work was supported in part by grants R01-CA172492 (to LP) and a Leukemia & Lymphoma Society Translational Research Project award (LP).

ACKNOWLEDGMENTS

We thank all members of the Pasqualucci and Dalla-Favera laboratories who have contributed to some of the work discussed in this review.

SUPPLEMENTARY MATERIAL

The Supplementary Material for this article can be found online at: https://www.frontiersin.org/articles/10.3389/fimmu.2021.710711/full#supplementary-material

REFERENCES

1. Kuppers R, Klein U, Hansmann ML, Rajewsky K. Cellular Origin of Human B-Cell Lymphomas. *New Engl J Med* (1999) 341(20):1520–9. doi: 10.1056/NEJM199911113412007
2. Stevenson F, Sahota S, Zhu D, Ottensmeier C, Chapman C, Oscier D, et al. Insight Into the Origin and Clonal History of B-Cell Tumors as Revealed by Analysis of Immunoglobulin Variable Region Genes. *Immunol Rev* (1998) 162:247–59. doi: 10.1111/j.1600-065X.1998.tb01446.x
3. Swerdlow SH, Campo E, Pileri SA, Harris NL, Stein H, Siebert R, et al. The 2016 Revision of the World Health Organization Classification of Lymphoid Neoplasms. *Blood* (2016) 127(20):2375–90. doi: 10.1182/blood-2016-01-643569
4. Pasqualucci L. Molecular Pathogenesis of Germinal Center-Derived B Cell Lymphomas. *Immunol Rev* (2019) 288(1):240–61. doi: 10.1111/imr.12745
5. Shaffer AL3rd, Young RM, Staudt LM. Pathogenesis of Human B Cell Lymphomas. *Annu Rev Immunol* (2012) 30:565–610. doi: 10.1146/annurev-immunol-020711-075027
6. Mottok A, Steidl C. Biology of Classical Hodgkin Lymphoma: Implications for Prognosis and Novel Therapies. *Blood* (2018) 131(15):1654–65. doi: 10.1182/blood-2017-09-772632
7. Weniger MA, Kuppers R. Molecular Biology of Hodgkin Lymphoma. *Leukemia* (2021) 35(4):968–81. doi: 10.1038/s41375-021-01204-6
8. Bea S, Valdes-Mas R, Navarro A, Salaverria I, Martin-Garcia D, Jares P, et al. Landscape of Somatic Mutations and Clonal Evolution in Mantle Cell Lymphoma. *Proc Natl Acad Sci USA* (2013) 110(45):18250–5. doi: 10.1073/pnas.1314608110
9. Richmond A, Su YJ. Mouse Xenograft Models vs GEM Models for Human Cancer Therapeutics. *Dis Model Mech* (2008) 1(2-3):78–82. doi: 10.1242/dmm.000976
10. Townsend EC, Murakami MA, Christodoulou A, Christie AL, Koster J, DeSouza TA, et al. The Public Repository of Xenografts Enables Discovery and Randomized Phase II-Like Trials in Mice. *Cancer Cell* (2016) 30(1):183. doi: 10.1016/j.ccell.2016.06.008
11. Pizzi M, Inghirami G. Patient-Derived Tumor Xenografts of Lymphoproliferative Disorders: Are They Surrogates for the Human Disease? *Curr Opin Hematol* (2017) 24(4):384–92. doi: 10.1097/MOH.0000000000000349
12. Huang S, Yasuda T. Pathologically Relevant Mouse Models for Epstein-Barr Virus-Associated B Cell Lymphoma. *Front Immunol* (2021) 12:639844. doi: 10.3389/fimmu.2021.639844
13. De Silva NS, Klein U. Dynamics of B Cells in Germinal Centres. *Nat Rev Immunol* (2015) 15(3):137–48. doi: 10.1038/nri3804
14. Mesin L, Ersching J, Victora GD. Germinal Center B Cell Dynamics. *Immunity* (2016) 45(3):471–82. doi: 10.1016/j.immuni.2016.09.001
15. Victora GD, Nussenzweig MC. Germinal Centers. *Annu Rev Immunol* (2012) 30:429–57. doi: 10.1146/annurev-immunol-020711-075032
16. Rajewsky K. Clonal Selection and Learning in the Antibody System. *Nature* (1996) 381(6585):751–8. doi: 10.1038/381751a0
17. Allen CD, Ansel KM, Low C, Lesley R, Tamamura H, Fujii N, et al. Germinal Center Dark and Light Zone Organization is Mediated by CXCR4 and CXCR5. *Nat Immunol* (2004) 5(9):943–52. doi: 10.1038/ni1100
18. Mintz MA, Cyster JG. T Follicular Helper Cells in Germinal Center B Cell Selection and Lymphomagenesis. *Immunol Rev* (2020) 296(1):48–61. doi: 10.1111/imr.12860
19. Dominguez-Sola D, Victora GD, Ying CY, Phan RT, Saito M, Nussenzweig MC, et al. The Proto-Oncogene MYC is Required for Selection in the Germinal Center and Cyclic Reentry. *Nat Immunol* (2012) 13(11):1083–91. doi: 10.1038/ni.2428
20. Calado DP, Sasaki Y, Godinho SA, Pellerin A, Kochert K, Sleckman BP, et al. The Cell-Cycle Regulator C-Myc is Essential for the Formation and

Maintenance of Germinal Centers. *Nat Immunol* (2012) 13(11):1092–100. doi: 10.1038/ni.2418
21. Roco JA, Mesin L, Binder SC, Nefzger C, Gonzalez-Figueroa P, Canete PF, et al. Class-Switch Recombination Occurs Infrequently in Germinal Centers. *Immunity* (2019) 51(2):337–50 e7. doi: 10.1016/j.immuni.2019.07.001
22. Victora GD, Dominguez-Sola D, Holmes AB, Deroubaix S, Dalla-Favera R, Nussenzweig MC. Identification of Human Germinal Center Light and Dark Zone Cells and Their Relationship to Human B-Cell Lymphomas. *Blood* (2012) 120(11):2240–8. doi: 10.1182/blood-2012-03-415380
23. Milpied P, Cervera-Marzal I, Mollichella ML, Tesson B, Brisou G, Traverse-Glehen A, et al. Human Germinal Center Transcriptional Programs are De-Synchronized in B Cell Lymphoma. *Nat Immunol* (2018) 19(9):1013–24. doi: 10.1038/s41590-018-0181-4
24. Holmes AB, Corinaldesi C, Shen Q, Kumar R, Compagno N, Wang Z, et al. Single-Cell Analysis of Germinal-Center B Cells Informs on Lymphoma Cell of Origin and Outcome. *J Exp Med* (2020) 217(10). doi: 10.1084/jem.20200483
25. Klein U, Dalla-Favera R. Germinal Centres: Role in B-Cell Physiology and Malignancy. *Nat Rev Immunol* (2008) 8(1):22–33. doi: 10.1038/nri2217
26. Shaffer AL, Wright G, Yang L, Powell J, Ngo V, Lamy L, et al. A Library of Gene Expression Signatures to Illuminate Normal and Pathological Lymphoid Biology. *Immunol Rev* (2006) 210:67–85. doi: 10.1111/j.0105-2896.2006.00373.x
27. Alizadeh AA, Eisen MB, Davis RE, Ma C, Lossos IS, Rosenwald A, et al. Distinct Types of Diffuse Large B-Cell Lymphoma Identified by Gene Expression Profiling. *Nature* (2000) 403(6769):503–11. doi: 10.1038/35000501
28. Venturutti L, Teater M, Zhai A, Chadburn A, Babiker L, Kim D, et al. TBL1XR1 Mutations Drive Extranodal Lymphoma by Inducing a Pro-Tumorigenic Memory Fate. *Cell* (2020) 182(2):297–316 e27. doi: 10.1016/j.cell.2020.05.049
29. Chapuy B, Stewart C, Dunford AJ, Kim J, Kamburov A, Redd RA, et al. Molecular Subtypes of Diffuse Large B Cell Lymphoma are Associated With Distinct Pathogenic Mechanisms and Outcomes. *Nat Med* (2018) 24(5):679–90. doi: 10.1038/s41591-018-0016-8
30. Schmitz R, Wright GW, Huang DW, Johnson CA, Phelan JD, Wang JQ, et al. Genetics and Pathogenesis of Diffuse Large B-Cell Lymphoma. *N Engl J Med* (2018) 378(15):1396–407. doi: 10.1056/NEJMoa1801445
31. Wright GW, Huang DW, Phelan JD, Coulibaly ZA, Roulland S, Young RM, et al. A Probabilistic Classification Tool for Genetic Subtypes of Diffuse Large B Cell Lymphoma With Therapeutic Implications. *Cancer Cell* (2020) 37(4):551–68.e14. doi: 10.1016/j.ccell.2020.03.015
32. Ramezani-Rad P, Rickert RC. Murine Models of Germinal Center Derived-Lymphomas. *Curr Opin Immunol* (2017) 45:31–6. doi: 10.1016/j.coi.2016.12.002
33. Pasqualucci L, Klein U. Mouse Models in the Study of Mature B-Cell Malignancies. Cold Spring Harbor perspectives in medicine. *Cold Spring Harb Perspect Med* (2021) 11(4). doi: 10.1101/cshperspect.a034827
34. Oricchio E, Wolfe AL, Schatz JH, Mavrakis KJ, Wendel HG. Mouse Models of Cancer as Biological Filters for Complex Genomic Data. *Dis Model Mech* (2010) 3(11-12):701–4. doi: 10.1242/dmm.006296
35. McDonnell TJ, Deane N, Platt FM, Nunez G, Jaeger U, McKearn JP, et al. Bcl-2-Immunoglobulin Transgenic Mice Demonstrate Extended B Cell Survival and Follicular Lymphoproliferation. *Cell* (1989) 57(1):79–88. doi: 10.1016/0092-8674(89)90174-8
36. Ogilvy S, Metcalf D, Print CG, Bath ML, Harris AW, Adams JM. Constitutive Bcl-2 Expression Throughout the Hematopoietic Compartment Affects Multiple Lineages and Enhances Progenitor Cell Survival. *Proc Natl Acad Sci USA* (1999) 96(26):14943–8. doi: 10.1073/pnas.96.26.14943
37. Cattoretti G, Pasqualucci L, Ballon G, Tam W, Nandula SV, Shen Q, et al. Deregulated BCL6 Expression Recapitulates the Pathogenesis of Human Diffuse Large B Cell Lymphomas in Mice. *Cancer Cell* (2005) 7(5):445–55. doi: 10.1016/j.ccr.2005.03.037
38. Hobeika E, Thiemann S, Storch B, Jumaa H, Nielsen PJ, Pelanda R, et al. Testing Gene Function Early in the B Cell Lineage in Mb1-Cre Mice. *Proc Natl Acad Sci USA* (2006) 103(37):13789–94. doi: 10.1073/pnas.0605944103
39. Rickert RC, Roes J, Rajewsky K. B lymphocyte-specific, Cre-Mediated Mutagenesis in Mice. *Nucleic Acids Res* (1997) 25(6):1317–8. doi: 10.1093/nar/25.6.1317
40. Kraus M, Alimzhanov MB, Rajewsky N, Rajewsky K. Survival of Resting Mature B Lymphocytes Depends on BCR Signaling *via* the Igalpha/Beta Heterodimer. *Cell* (2004) 117(6):787–800. doi: 10.1016/j.cell.2004.05.014
41. Zhang J, Dominguez-Sola D, Hussein S, Lee JE, Holmes AB, Bansal M, et al. Disruption of KMT2D Perturbs Germinal Center B Cell Development and Promotes Lymphomagenesis. *Nat Med* (2015) 21(10):1190–8. doi: 10.1038/nm.3940
42. Casola S, Cattoretti G, Uyttersprot N, Koralov SB, Seagal J, Hao Z, et al. Tracking Germinal Center B Cells Expressing Germ-Line Immunoglobulin Gamma1 Transcripts by Conditional Gene Targeting. *Proc Natl Acad Sci USA* (2006) 103(19):7396–401. doi: 10.1073/pnas.0602353103
43. Crouch EE, Li Z, Takizawa M, Fichtner-Feigl S, Gourzi P, Montano C, et al. Regulation of AID Expression in the Immune Response. *J Exp Med* (2007) 204(5):1145–56. doi: 10.1084/jem.20061952
44. Robbiani DF, Bothmer A, Callen E, Reina-San-Martin B, Dorsett Y, Difilippantonio S, et al. AID Is Required for the Chromosomal Breaks in C-Myc That Lead to C-Myc/IgH Translocations. *Cell* (2008) 135(6):1028–38. doi: 10.1016/j.cell.2008.09.062
45. Schmitt CA, Fridman JS, Yang M, Baranov E, Hoffman RM, Lowe SW. Dissecting P53 Tumor Suppressor Functions *In Vivo*. *Cancer Cell* (2002) 1 (3):289–98. doi: 10.1016/S1535-6108(02)00047-8
46. Jiang Y, Ortega-Molina A, Geng H, Ying HY, Hatzi K, Parsa S, et al. CREBBP Inactivation Promotes the Development of HDAC3-Dependent Lymphomas. *Cancer Discov* (2017) 7(1):38–53. doi: 10.1158/2159-8290.CD-16-0975
47. Ortega-Molina A, Boss IW, Canela A, Pan H, Jiang Y, Zhao C, et al. The Histone Lysine Methyltransferase KMT2D Sustains a Gene Expression Program That Represses B Cell Lymphoma Development. *Nat Med* (2015) 21(10):1199–208. doi: 10.1038/nm.3943
48. Jinek M, Chylinski K, Fonfara I, Hauer M, Doudna JA, Charpentier E. A Programmable Dual-RNA-Guided DNA Endonuclease in Adaptive Bacterial Immunity. *Science* (2012) 337(6096):816–21. doi: 10.1126/science.1225829
49. Mou H, Kennedy Z, Anderson DG, Yin H, Xue W. Precision Cancer Mouse Models Through Genome Editing With CRISPR-Cas9. *Genome Med* (2015) 7(1):53. doi: 10.1186/s13073-015-0178-7
50. Yang H, Wang H, Shivalila CS, Cheng AW, Shi L, Jaenisch R. One-Step Generation of Mice Carrying Reporter and Conditional Alleles by CRISPR/Cas-Mediated Genome Engineering. *Cell* (2013) 154(6):1370–9. doi: 10.1016/j.cell.2013.08.022
51. Wang H, Yang H, Shivalila CS, Dawlaty MM, Cheng AW, Zhang F, et al. One-Step Generation of Mice Carrying Mutations in Multiple Genes by CRISPR/Cas-Mediated Genome Engineering. *Cell* (2013) 153(4):910–8. doi: 10.1016/j.cell.2013.04.025
52. Ba Z, Meng FL, Gostissa M, Huang PY, Ke Q, Wang Z, et al. A Rapid Embryonic Stem Cell-Based Mouse Model for B-Cell Lymphomas Driven by Epstein-Barr Virus Protein LMP1. *Cancer Immunol Res* (2015) 3(6):641–9. doi: 10.1158/2326-6066.CIR-15-0058
53. Ortega-Molina A, Deleyto-Seldas N, Carreras J, Sanz A, Lebrero-Fernandez C, Menendez C, et al. Oncogenic Rag Gtpase Signaling Enhances B Cell Activation and Drives Follicular Lymphoma Sensitive to Pharmacological Inhibition of Mtor. *Nat Metab* (2019) 1(8):775–89. doi: 10.1038/s42255-019-0098-8
54. Zhang L, Nomie K, Zhang H, Bell T, Pham L, Kadri S, et al. B-Cell Lymphoma Patient-Derived Xenograft Models Enable Drug Discovery and are a Platform for Personalized Therapy. *Clin Cancer Research: An Off J Am Assoc Cancer Res* (2017) 23(15):4212–23. doi: 10.1158/1078-0432.CCR-16-2703
55. DeRose YS, Wang G, Lin YC, Bernard PS, Buys SS, Ebbert MT, et al. Tumor Grafts Derived From Women With Breast Cancer Authentically Reflect Tumor Pathology, Growth, Metastasis and Disease Outcomes. *Nat Med* (2011) 17(11):1514–20. doi: 10.1038/nm.2454
56. Ben-David U, Ha G, Tseng YY, Greenwald NF, Oh C, Shih J, et al. Patient-Derived Xenografts Undergo Mouse-Specific Tumor Evolution. *Nat Genet* (2017) 49(11):1567–75. doi: 10.1038/ng.3967

57. Shi J, Li Y, Jia R, Fan X. The Fidelity of Cancer Cells in PDX Models: Characteristics, Mechanism and Clinical Significance. *Int J Cancer* (2020) 146(8):2078–88. doi: 10.1002/ijc.32662
58. Gao H, Korn JM, Ferretti S, Monahan JE, Wang Y, Singh M, et al. High-Throughput Screening Using Patient-Derived Tumor Xenografts to Predict Clinical Trial Drug Response. *Nat Med* (2015) 21(11):1318–25. doi: 10.1038/nm.3954
59. Chapuy B, Cheng H, Watahiki A, Ducar MD, Tan Y, Chen L, et al. Diffuse Large B-Cell Lymphoma Patient-Derived Xenograft Models Capture the Molecular and Biological Heterogeneity of the Disease. *Blood* (2016) 127 (18):2203–13. doi: 10.1182/blood-2015-09-672352
60. Brehm MA, Wiles MV, Greiner DL, Shultz LD. Generation of Improved Humanized Mouse Models for Human Infectious Diseases. *J Immunol Methods* (2014) 410:3–17. doi: 10.1016/j.jim.2014.02.011
61. Shultz LD, Brehm MA, Garcia-Martinez JV, Greiner DL. Humanized Mice for Immune System Investigation: Progress, Promise and Challenges. *Nat Rev Immunol* (2012) 12(11):786–98. doi: 10.1038/nri3311
62. Scuoppo C, Wang J, Persaud M, Mittan SK, Basso K, Pasqualucci L, et al. Repurposing Dasatinib for Diffuse Large B Cell Lymphoma. *Proc Natl Acad Sci USA* (2019) 116(34):16981–6. doi: 10.1073/pnas.1905239116
63. Hidalgo M, Amant F, Biankin AV, Budinska E, Byrne AT, Caldas C, et al. Patient-Derived Xenograft Models: An Emerging Platform for Translational Cancer Research. *Cancer Discov* (2014) 4(9):998–1013. doi: 10.1158/2159-8290.CD-14-0001
64. Bertotti A, Migliardi G, Galimi F, Sassi F, Torti D, Isella C, et al. A Molecularly Annotated Platform of Patient-Derived Xenografts ("Xenopatients") Identifies HER2 as an Effective Therapeutic Target in Cetuximab-Resistant Colorectal Cancer. *Cancer Discov* (2011) 1(6):508–23. doi: 10.1158/2159-8290.CD-11-0109
65. Culjkovic-Kraljacic B, Fernando TM, Marullo R, Calvo-Vidal N, Verma A, Yang S, et al. Combinatorial Targeting of Nuclear Export and Translation of RNA Inhibits Aggressive B-Cell Lymphomas. *Blood* (2016) 127(7):858–68. doi: 10.1182/blood-2015-05-645069
66. Dalla-Favera R, Bregni M, Erikson J, Patterson D, Gallo RC, Croce CM. Human C-Myc Onc Gene Is Located on the Region of Chromosome 8 That Is Translocated in Burkitt Lymphoma Cells. *Proc Natl Acad Sci USA* (1982) 79(24):7824–7. doi: 10.1073/pnas.79.24.7824
67. Taub R, Kirsch I, Morton C, Lenoir G, Swan D, Tronick S, et al. Translocation of the C-Myc Gene Into the Immunoglobulin Heavy Chain Locus in Human Burkitt Lymphoma and Murine Plasmacytoma Cells. *Proc Natl Acad Sci USA* (1982) 79(24):7837–41. doi: 10.1073/pnas.79.24.7837
68. Lin CY, Loven J, Rahl PB, Paranal RM, Burge CB, Bradner JE, et al. Transcriptional Amplification in Tumor Cells With Elevated C-Myc. *Cell* (2012) 151(1):56–67. doi: 10.1016/j.cell.2012.08.026
69. Richter J, Schlesner M, Hoffmann S, Kreuz M, Leich E, Burkhardt B, et al. Recurrent Mutation of the ID3 Gene in Burkitt Lymphoma Identified by Integrated Genome, Exome and Transcriptome Sequencing. *Nat Genet* (2012) 44(12):1316–20. doi: 10.1038/ng.2469
70. Schmitz R, Young RM, Ceribelli M, Jhavar S, Xiao W, Zhang M, et al. Burkitt Lymphoma Pathogenesis and Therapeutic Targets From Structural and Functional Genomics. *Nature* (2012) 490(7418):116–20. doi: 10.1038/nature11378
71. Cato MH, Chintalapati SK, Yau IW, Omori SA, Rickert RC. Cyclin D3 is Selectively Required for Proliferative Expansion of Germinal Center B Cells. *Mol Cell Biol* (2011) 31(1):127–37. doi: 10.1128/MCB.00650-10
72. Peled JU, Yu JJ, Venkatesh J, Bi E, Ding BB, Krupski-Downs M, et al. Requirement for Cyclin D3 in Germinal Center Formation and Function. *Cell Res* (2010) 20(6):631–46. doi: 10.1038/cr.2010.55
73. Schmitz R, Ceribelli M, Pittaluga S, Wright G, Staudt LM. Oncogenic Mechanisms in Burkitt Lymphoma. *Cold Spring Harbor Perspect Med* (2014) 4(2). doi: 10.1101/cshperspect.a014282
74. Adams JM, Harris AW, Pinkert CA, Corcoran LM, Alexander WS, Cory S, et al. The C-Myc Oncogene Driven by Immunoglobulin Enhancers Induces Lymphoid Malignancy in Transgenic Mice. *Nature* (1985) 318(6046):533–8. doi: 10.1038/318533a0
75. Kovalchuk AL, Qi CF, Torrey TA, Taddesse-Heath L, Feigenbaum L, Park SS, et al. Burkitt Lymphoma in the Mouse. *J Exp Med* (2000) 192(8):1183–90. doi: 10.1084/jem.192.8.1183
76. Butzler C, Zou X, Popov AV, Bruggemann M. Rapid Induction of B-Cell Lymphomas in Mice Carrying a Human IgH/C-MycYAC. *Oncogene* (1997) 14(11):1383–8. doi: 10.1038/sj.onc.1200968
77. Truffinet V, Pinaud E, Cogne N, Petit B, Guglielmi L, Cogne M, et al. The 3' Igh Locus Control Region is Sufficient to Deregulate a C-Myc Transgene and Promote Mature B Cell Malignancies With a Predominant Burkitt-Like Phenotype. *J Immunol* (2007) 179(9):6033–42. doi: 10.4049/jimmunol.179.9.6033
78. Harris AW, Pinkert CA, Crawford M, Langdon WY, Brinster RL, Adams JM. The E Mu-Myc Transgenic Mouse. A Model for High-Incidence Spontaneous Lymphoma and Leukemia of Early B Cells. *J Exp Med* (1988) 167(2):353–71. doi: 10.1084/jem.167.2.353
79. Pasqualucci L, Bhagat G, Jankovic M, Compagno M, Smith P, Muramatsu M, et al. AID is Required for Germinal Center-Derived Lymphomagenesis. *Nat Genet* (2008) 40(1):108–12. doi: 10.1038/ng.2007.35
80. Varano G, Raffel S, Sormani M, Zanardi F, Lonardi S, Zasada C, et al. The B-Cell Receptor Controls Fitness of MYC-Driven Lymphoma Cells *via* GSK3beta Inhibition. *Nature* (2017) 546(7657):302–6. doi: 10.1038/nature22353
81. Hemann MT, Bric A, Teruya-Feldstein J, Herbst A, Nilsson JA, Cordon-Cardo C, et al. Evasion of the P53 Tumour Surveillance Network by Tumour-Derived MYC Mutants. *Nature* (2005) 436(7052):807–11. doi: 10.1038/nature03845
82. Rava M, D'Andrea A, Nicoli P, Gritti I, Donati G, Doni M, et al. Therapeutic synergy between tigecycline and venetoclax in a preclinical model of MYC/BCL2 double-hit B cell lymphoma. *Sci Transl Med* (2018) 10(426). doi: 10.1126/scitranslmed.aan8723
83. Sander S, Calado DP, Srinivasan L, Kochert K, Zhang B, Rosolowski M, et al. Synergy Between PI3K Signaling and MYC in Burkitt Lymphomagenesis. *Cancer Cell* (2012) 22(2):167–79. doi: 10.1016/j.ccr.2012.06.012
84. Kabrani E, Chu VT, Tasouri E, Sommermann T, Bassler K, Ulas T, et al. Nuclear FOXO1 Promotes Lymphomagenesis in Germinal Center B Cells. *Blood* (2018) 132(25):2670–83. doi: 10.1182/blood-2018-06-856203
85. Casulo C, Burack WR, Friedberg JW. Transformed Follicular Non-Hodgkin Lymphoma. *Blood* (2015) 125(1):40–7. doi: 10.1182/blood-2014-04-516815
86. Lossos IS, Gascoyne RD. Transformation of Follicular Lymphoma. *Best Pract Res Clin Haematol* (2011) 24(2):147–63. doi: 10.1016/j.beha.2011.02.006
87. Kridel R, Sehn LH, Gascoyne RD. Pathogenesis of Follicular Lymphoma. *J Clin Invest* (2012) 122(10):3424–31. doi: 10.1172/JCI63186
88. Limpens J, Stad R, Vos C, de Vlaam C, de Jong D, van Ommen GJ, et al. Lymphoma-Associated Translocation T(14;18) in Blood B Cells of Normal Individuals. *Blood* (1995) 85(9):2528–36. doi: 10.1182/blood.V85.9.2528.bloodjournal8592528
89. Roulland S, Navarro JM, Grenot P, Milili M, Agopian J, Montpellier B, et al. Follicular Lymphoma-Like B Cells in Healthy Individuals: A Novel Intermediate Step in Early Lymphomagenesis. *J Exp Med* (2006) 203 (11):2425–31. doi: 10.1084/jem.20061292
90. Roulland S, Faroudi M, Mamessier E, Sungalee S, Salles G, Nadel B. Early Steps of Follicular Lymphoma Pathogenesis. *Adv Immunol* (2011) 111:1–46. doi: 10.1016/B978-0-12-385991-4.00001-5
91. Li H, Kaminski MS, Li Y, Yildiz M, Ouillette P, Jones S, et al. Mutations in Linker Histone Genes HIST1H1 B, C, D, and E; OCT2 (POU2F2); IRF8; and ARID1A Underlying the Pathogenesis of Follicular Lymphoma. *Blood* (2014) 123(10):1487–98. doi: 10.1182/blood-2013-05-500264
92. Morin RD, Johnson NA, Severson TM, Mungall AJ, An J, Goya R, et al. Somatic Mutations Altering EZH2 (Tyr641) in Follicular and Diffuse Large B-Cell Lymphomas of Germinal-Center Origin. *Nat Genet* (2010) 42 (2):181–5. doi: 10.1038/ng.518
93. Morin RD, Mendez-Lago M, Mungall AJ, Goya R, Mungall KL, Corbett RD, et al. Frequent Mutation of Histone-Modifying Genes in Non-Hodgkin Lymphoma. *Nature* (2011) 476(7360):298–303. doi: 10.1038/nature10351
94. Okosun J, Bodor C, Wang J, Araf S, Yang CY, Pan C, et al. Integrated Genomic Analysis Identifies Recurrent Mutations and Evolution Patterns Driving the Initiation and Progression of Follicular Lymphoma. *Nat Genet* (2014) 46(2):176–81. doi: 10.1038/ng.2856
95. Pasqualucci L, Dominguez-Sola D, Chiarenza A, Fabbri G, Grunn A, Trifonov V, et al. Inactivating Mutations of Acetyltransferase Genes in B-

Cell Lymphoma. *Nature* (2011) 471(7337):189–95. doi: 10.1038/nature09730
96. Ying CY, Dominguez-Sola D, Fabi M, Lorenz IC, Hussein S, Bansal M, et al. MEF2B Mutations Lead to Deregulated Expression of the Oncogene BCL6 in Diffuse Large B Cell Lymphoma. *Nat Immunol* (2013) 14(10):1084–92. doi: 10.1038/ni.2688
97. Cheung KJ, Johnson NA, Affleck JG, Severson T, Steidl C, Ben-Neriah S, et al. Acquired TNFRSF14 Mutations in Follicular Lymphoma are Associated With Worse Prognosis. *Cancer Res* (2010) 70(22):9166–74. doi: 10.1158/0008-5472.CAN-10-2460
98. Egle A, Harris AW, Bath ML, O'Reilly L, Cory S. VavP-Bcl2 Transgenic Mice Develop Follicular Lymphoma Preceded by Germinal Center Hyperplasia. *Blood* (2004) 103(6):2276–83. doi: 10.1182/blood-2003-07-2469
99. McDonnell TJ, Korsmeyer SJ. Progression From Lymphoid Hyperplasia to High-Grade Malignant Lymphoma in Mice Transgenic for the T(14; 18). *Nature* (1991) 349(6306):254–6. doi: 10.1038/349254a0
100. Strasser A, Whittingham S, Vaux DL, Bath ML, Adams JM, Cory S, et al. Enforced BCL2 Expression in B-Lymphoid Cells Prolongs Antibody Responses and Elicits Autoimmune Disease. *Proc Natl Acad Sci USA* (1991) 88(19):8661–5. doi: 10.1073/pnas.88.19.8661
101. Garcia-Ramirez I, Tadros S, Gonzalez-Herrero I, Martin-Lorenzo A, Rodriguez-Hernandez G, Moore D, et al. Crebbp Loss Cooperates With Bcl2 Overexpression to Promote Lymphoma in Mice. *Blood* (2017) 129 (19):2645–56. doi: 10.1182/blood-2016-08-733469
102. Flumann R, Rehkamper T, Nieper P, Pfeiffer P, Holzem A, Klein S, et al. An Autochthonous Mouse Model of Myd88- and BCL2-Driven Diffuse Large B-Cell Lymphoma Reveals Actionable Molecular Vulnerabilities. *Blood Cancer Discov* (2021) 2(1):70–91. doi: 10.1158/2643-3230.BCD-19-0059
103. Oricchio E, Papapetrou EP, Lafaille F, Ganat YM, Kriks S, Ortega-Molina A, et al. A Cell Engineering Strategy to Enhance the Safety of Stem Cell Therapies. *Cell Rep* (2014) 8(6):1677–85. doi: 10.1016/j.celrep.2014.08.039
104. Brescia P, Schneider C, Holmes AB, Shen Q, Hussein S, Pasqualucci L, et al. MEF2B Instructs Germinal Center Development and Acts as an Oncogene in B Cell Lymphomagenesis. *Cancer Cell* (2018) 34(3):453–65.e9. doi: 10.1016/j.ccell.2018.08.006
105. Sungalee S, Mamessier E, Morgado E, Gregoire E, Brohawn PZ, Morehouse CA, et al. Germinal Center Reentries of BCL2-Overexpressing B Cells Drive Follicular Lymphoma Progression. *J Clin Invest* (2014) 124(12):5337–51. doi: 10.1172/JCI72415
106. Kuppers R, Dalla-Favera R. Mechanisms of Chromosomal Translocations in B Cell Lymphomas. *Oncogene* (2001) 20(40):5580–94. doi: 10.1038/sj.onc.1204640
107. Pasqualucci L, Khiabanian H, Fangazio M, Vasishtha M, Messina M, Holmes AB, et al. Genetics of Follicular Lymphoma Transformation. *Cell Rep* (2014) 6(1):130–40. doi: 10.1016/j.celrep.2013.12.027
108. Green MR, Kihira S, Liu CL, Nair RV, Salari R, Gentles AJ, et al. Mutations in Early Follicular Lymphoma Progenitors Are Associated With Suppressed Antigen Presentation. *Proc Natl Acad Sci USA* (2015) 112(10):E1116–25. doi: 10.1073/pnas.1501199112
109. Horton SJ, Giotopoulos G, Yun H, Vohra S, Sheppard O, Bashford-Rogers R, et al. Early Loss of Crebbp Confers Malignant Stem Cell Properties on Lymphoid Progenitors. *Nat Cell Biol* (2017) 19(9):1093–104. doi: 10.1038/ncb3597
110. Zhang J, Vlasevska S, Wells VA, Nataraj S, Holmes AB, Duval R, et al. The CREBBP Acetyltransferase Is a Haploinsufficient Tumor Suppressor in B-Cell Lymphoma. *Cancer Discov* (2017) 7(3):322–37. doi: 10.1158/2159-8290.CD-16-1417
111. Meyer SN, Scuoppo C, Vlasevska S, Bal E, Holmes AB, Holloman M, et al. Unique and Shared Epigenetic Programs of the CREBBP and EP300 Acetyltransferases in Germinal Center B Cells Reveal Targetable Dependencies in Lymphoma. *Immunity* (2019) 51(3):535–+. doi: 10.1016/j.immuni.2019.08.006
112. Sze CC, Shilatifard A. MLL3/MLL4/COMPASS Family on Epigenetic Regulation of Enhancer Function and Cancer. *Cold Spring Harbor Perspect Med* (2016) 6(11). doi: 10.1101/cshperspect.a026427
113. Bereshchenko OR, Gu W, Dalla-Favera R. Acetylation Inactivates the Transcriptional Repressor BCL6. *Nat Genet* (2002) 32(4):606–13. doi: 10.1038/ng1018
114. Mondello P, Tadros S, Teater M, Fontan L, Chang AY, Jain N, et al. Selective Inhibition of HDAC3 Targets Synthetic Vulnerabilities and Activates Immune Surveillance in Lymphoma. *Cancer Discov* (2020) 10(3):440–59. doi: 10.1101/531954
115. Beguelin W, Popovic R, Teater M, Jiang Y, Bunting KL, Rosen M, et al. EZH2 Is Required for Germinal Center Formation and Somatic EZH2 Mutations Promote Lymphoid Transformation. *Cancer Cell* (2013) 23(5):677–92. doi: 10.1016/j.ccr.2013.04.011
116. Caganova M, Carrisi C, Varano G, Mainoldi F, Zanardi F, Germain PL, et al. Germinal Center Dysregulation by Histone Methyltransferase EZH2 Promotes Lymphomagenesis. *J Clin Invest* (2013) 123(12):5009–22. doi: 10.1172/JCI70626
117. Beguelin W, Teater M, Gearhart MD, Calvo Fernandez MT, Goldstein RL, Cardenas MG, et al. EZH2 and BCL6 Cooperate to Assemble CBX8-BCOR Complex to Repress Bivalent Promoters, Mediate Germinal Center Formation and Lymphomagenesis. *Cancer Cell* (2016) 30(2):197–213. doi: 10.1016/j.ccell.2016.07.006
118. Ennishi D, Takata K, Beguelin W, Duns G, Mottok A, Farinha P, et al. Molecular and Genetic Characterization of MHC Deficiency Identifies EZH2 as Therapeutic Target for Enhancing Immune Recognition. *Cancer Discov* (2019) 9(4):546–63. doi: 10.1158/2159-8290.CD-18-1090
119. Souroullas GP, Jeck WR, Parker JS, Simon JM, Liu JY, Paulk J, et al. An Oncogenic Ezh2 Mutation Induces Tumors Through Global Redistribution of Histone 3 Lysine 27 Trimethylation. *Nat Med* (2016) 22(6):632–40. doi: 10.1038/nm.4092
120. Yusufova N, Kloetgen A, Teater M, Osunsade A, Camarillo JM, Chin CR, et al. Histone H1 Loss Drives Lymphoma by Disrupting 3D Chromatin Architecture. *Nature* (2020) 589(7841):299–305. doi: 10.1038/s41586-020-3017-y
121. Ito S, Shen L, Dai Q, Wu SC, Collins LB, Swenberg JA, et al. Tet Proteins can Convert 5-Methylcytosine to 5-Formylcytosine and 5-Carboxylcytosine. *Science* (2011) 333(6047):1300–3. doi: 10.1126/science.1210597
122. Busque L, Patel JP, Figueroa ME, Vasanthakumar A, Provost S, Hamilou Z, et al. Recurrent Somatic TET2 Mutations in Normal Elderly Individuals With Clonal Hematopoiesis. *Nat Genet* (2012) 44(11):1179–81. doi: 10.1038/ng.2413
123. Moran-Crusio K, Reavie L, Shih A, Abdel-Wahab O, Ndiaye-Lobry D, Lobry C, et al. Tet2 Loss Leads to Increased Hematopoietic Stem Cell Self-Renewal and Myeloid Transformation. *Cancer Cell* (2011) 20(1):11–24. doi: 10.1016/j.ccr.2011.06.001
124. Reddy A, Zhang J, Davis NS, Moffitt AB, Love CL, Waldrop A, et al. Genetic and Functional Drivers of Diffuse Large B Cell Lymphoma. *Cell* (2017) 171 (2):481–94.e15. doi: 10.1016/j.cell.2017.09.027
125. Quivoron C, Couronne L, Della Valle V, Lopez CK, Plo I, Wagner-Ballon O, et al. TET2 Inactivation Results in Pleiotropic Hematopoietic Abnormalities in Mouse and is a Recurrent Event During Human Lymphomagenesis. *Cancer Cell* (2011) 20(1):25–38. doi: 10.1016/j.ccr.2011.06.003
126. Dominguez PM, Ghamlouch H, Rosikiewicz W, Kumar P, Beguelin W, Fontan L, et al. TET2 Deficiency Causes Germinal Center Hyperplasia, Impairs Plasma Cell Differentiation, and Promotes B-Cell Lymphomagenesis. *Cancer Discov* (2018) 8(12):1632–53. doi: 10.1158/2159-8290.CD-18-0657
127. Scott DW, Gascoyne RD. The Tumour Microenvironment in B Cell Lymphomas. *Nat Rev Cancer* (2014) 14(8):517–34. doi: 10.1038/nrc3774
128. Lamaison C, Tarte K. Impact of B Cell/Lymphoid Stromal Cell Crosstalk in B-Cell Physiology and Malignancy. *Immunol Lett* (2019) 215:12–8. doi: 10.1016/j.imlet.2019.02.005
129. Kline J, Godfrey J, Ansell SM. The Immune Landscape and Response to Immune Checkpoint Blockade Therapy in Lymphoma. *Blood* (2020) 135 (8):523–33. doi: 10.1182/blood.2019000847
130. Challa-Malladi M, Lieu YK, Califano O, Holmes AB, Bhagat G, Murty VV, et al. Combined Genetic Inactivation of Beta2-Microglobulin and CD58 Reveals Frequent Escape From Immune Recognition in Diffuse Large B Cell Lymphoma. *Cancer Cell* (2011) 20(6):728–40. doi: 10.1016/j.ccr.2011.11.006
131. Fangazio M, Ladewig E, Gomez K, Garcia-Ibanez L, Kumar R, Teruya Feldstein J, et al. Genetic Mechanisms of HLA-I Loss and Immune Escape in Diffuse Large B Cell Lymphoma. *Proc Natl Acad Sci USA* (2021) 118(22). doi: 10.1073/pnas.2104504118

132. Boice M, Salloum D, Mourcin F, Sanghvi V, Amin R, Oricchio E, et al. Loss of the HVEM Tumor Suppressor in Lymphoma and Restoration by Modified CAR-T Cells. *Cell* (2016) 167(2):405–18 e13. doi: 10.1016/j.cell.2016.08.032
133. Karube K, Enjuanes A, Dlouhy I, Jares P, Martin-Garcia D, Nadeu F, et al. Integrating Genomic Alterations in Diffuse Large B-Cell Lymphoma Identifies New Relevant Pathways and Potential Therapeutic Targets. *Leukemia* (2018) 32(3):675–84. doi: 10.1038/leu.2017.251
134. Beguelin W, Teater M, Meydan C, Hoehn KB, Phillip JM, Soshnev AA, et al. Mutant EZH2 Induces a Pre-Malignant Lymphoma Niche by Reprogramming the Immune Response. *Cancer Cell* (2020) 37(5):655–73 e11. doi: 10.1016/j.ccell.2020.04.004
135. McCabe MT, Ott HM, Ganji G, Korenchuk S, Thompson C, Van Aller GS, et al. EZH2 Inhibition as a Therapeutic Strategy for Lymphoma With EZH2-Activating Mutations. *Nature* (2012) 492(7427):108–12. doi: 10.1038/nature11606
136. Efeyan A, Comb WC, Sabatini DM. Nutrient-Sensing Mechanisms and Pathways. *Nature* (2015) 517(7534):302–10. doi: 10.1038/nature14190
137. Okosun J, Wolfson RL, Wang J, Araf S, Wilkins L, Castellano BM, et al. Recurrent Mtorc1-Activating RRAGC Mutations in Follicular Lymphoma. *Nat Genet* (2016) 48(2):183–8. doi: 10.1038/ng.3473
138. Muppidi JR, Schmitz R, Green JA, Xiao W, Larsen AB, Braun SE, et al. Loss of signalling *via* Galpha13 in germinal centre B-cell-derived lymphoma. *Nature* (2014) 516(7530):254–8. doi: 10.1038/nature13765
139. Flori M, Schmid CA, Sumrall ET, Tzankov A, Law CW, Robinson MD, et al. The Hematopoietic Oncoprotein FOXP1 Promotes Tumor Cell Survival in Diffuse Large B-Cell Lymphoma by Repressing S1PR2 Signaling. *Blood* (2016) 127(11):1438–48. doi: 10.1182/blood-2015-08-662635
140. Healy JA, Nugent A, Rempel RE, Moffitt AB, Davis NS, Jiang X, et al. GNA13 Loss in Germinal Center B Cells Leads to Impaired Apoptosis and Promotes Lymphoma In Vivo. *Blood* (2016) 127(22):2723–31. doi: 10.1182/blood-2015-07-659938
141. Cattoretti G, Mandelbaum J, Lee N, Chaves AH, Mahler AM, Chadburn A, et al. Targeted Disruption of the S1P2 Sphingosine 1-Phosphate Receptor Gene Leads to Diffuse Large B-Cell Lymphoma Formation. *Cancer Res* (2009) 69(22):8686–92. doi: 10.1158/0008-5472.CAN-09-1110
142. Saito M, Gao J, Basso K, Kitagawa Y, Smith PM, Bhagat G, et al. A Signaling Pathway Mediating Downregulation of BCL6 in Germinal Center B Cells is Blocked by BCL6 Gene Alterations in B Cell Lymphoma. *Cancer Cell* (2007) 12(3):280–92. doi: 10.1016/j.ccr.2007.08.011
143. Wang X, Li Z, Naganuma A, Ye BH. Negative Autoregulation of BCL-6 Is Bypassed by Genetic Alterations in Diffuse Large B Cell Lymphomas. *Proc Natl Acad Sci United States America* (2002) 99(23):15018–23. doi: 10.1073/pnas.232581199
144. Pasqualucci L, Migliazza A, Basso K, Houldsworth J, Chaganti RS, Dalla-Favera R. Mutations of the BCL6 Proto-Oncogene Disrupt its Negative Autoregulation in Diffuse Large B-Cell Lymphoma. *Blood* (2003) 101(8):2914–23. doi: 10.1182/blood-2002-11-3387
145. Pasqualucci L, Migliazza A, Fracchiolla N, William C, Neri A, Baldini L, et al. BCL-6 Mutations in Normal Germinal Center B Cells: Evidence of Somatic Hypermutation Acting Outside Ig Loci. *Proc Natl Acad Sci USA* (1998) 95(20):11816–21. doi: 10.1073/pnas.95.20.11816
146. Ye BH, Lista F, Lo Coco F, Knowles DM, Offit K, Chaganti RS, et al. Alterations of a Zinc Finger-Encoding Gene, BCL-6, in Diffuse Large-Cell Lymphoma. *Science* (1993) 262(5134):747–50. doi: 10.1126/science.8235596
147. Duan S, Cermak L, Pagan JK, Rossi M, Martinengo C, di Celle PF, et al. FBXO11 Targets BCL6 for Degradation and Is Inactivated in Diffuse Large B-Cell Lymphomas. *Nature* (2012) 481(7379):90–3. doi: 10.1038/nature10688
148. Schneider C, Kon N, Amadori L, Shen Q, Schwartz FH, Tischler B, et al. FBXO11 Inactivation Leads to Abnormal Germinal-Center Formation and Lymphoproliferative Disease. *Blood* (2016) 128(5):660–6. doi: 10.1182/blood-2015-11-684357
149. Yabe D, Fukuda H, Aoki M, Yamada S, Takebayashi S, Shinkura R, et al. Generation of a Conditional Knockout Allele for Mammalian Spen Protein Mint/SHARP. *Genesis* (2007) 45(5):300–6. doi: 10.1002/dvg.20296
150. Fujimura S, Jiang Q, Kobayashi C, Nishinakamura R. Notch2 Activation in the Embryonic Kidney Depletes Nephron Progenitors. *J Am Soc Nephrol* (2010) 21(5):803–10. doi: 10.1681/ASN.2009040353
151. Hampel F, Ehrenberg S, Hojer C, Draeseke A, Marschall-Schroter G, Kuhn R, et al. CD19-Independent Instruction of Murine Marginal Zone B-Cell Development by Constitutive Notch2 Signaling. *Blood* (2011) 118(24):6321–31. doi: 10.1182/blood-2010-12-325944
152. Nakagawa MM, Thummar K, Mandelbaum J, Pasqualucci L, Rathinam CV. Lack of the Ubiquitin-Editing Enzyme A20 Results in Loss of Hematopoietic Stem Cell Quiescence. *J Exp Med* (2015) 212(2):203–16. doi: 10.1084/jem.20132544
153. Valls E, Lobry C, Geng H, Wang L, Cardenas M, Rivas M, et al. BCL6 Antagonizes NOTCH2 to Maintain Survival of Human Follicular Lymphoma Cells. *Cancer Discov* (2017) 7(5):506–21. doi: 10.1158/2159-8290.CD-16-1189
154. Tam W, Gomez M, Chadburn A, Lee JW, Chan WC, Knowles DM. Mutational Analysis of PRDM1 Indicates a Tumor-Suppressor Role in Diffuse Large B-Cell Lymphomas. *Blood* (2006) 107(10):4090–100. doi: 10.1182/blood-2005-09-3778
155. Pasqualucci L, Compagno M, Houldsworth J, Monti S, Grunn A, Nandula SV, et al. Inactivation of the PRDM1/BLIMP1 Gene in Diffuse Large B Cell Lymphoma. *J Exp Med* (2006) 203(2):311–7. doi: 10.1084/jem.20052204
156. Mandelbaum J, Bhagat G, Tang H, Mo T, Brahmachary M, Shen Q, et al. BLIMP1 is a Tumor Suppressor Gene Frequently Disrupted in Activated B Cell-Like Diffuse Large B Cell Lymphoma. *Cancer Cell* (2010) 18(6):568–79. doi: 10.1016/j.ccr.2010.10.030
157. Compagno M, Lim WK, Grunn A, Nandula SV, Brahmachary M, Shen Q, et al. Mutations of Multiple Genes Cause Deregulation of NF-KappaB in Diffuse Large B-Cell Lymphoma. *Nature* (2009) 459(7247):717–21. doi: 10.1038/nature07968
158. Lenz G, Davis RE, Ngo VN, Lam L, George TC, Wright GW, et al. Oncogenic CARD11 Mutations in Human Diffuse Large B Cell Lymphoma. *Science* (2008) 319(5870):1676–9. doi: 10.1126/science.1153629
159. Ngo VN, Young RM, Schmitz R, Jhavar S, Xiao W, Lim KH, et al. Oncogenically Active MYD88 Mutations in Human Lymphoma. *Nature* (2011) 470(7332):115–9. doi: 10.1038/nature09671
160. Davis RE, Ngo VN, Lenz G, Tolar P, Young RM, Romesser PB, et al. Chronic Active B-Cell-Receptor Signalling in Diffuse Large B-Cell Lymphoma. *Nature* (2010) 463(7277):88–92. doi: 10.1038/nature08638
161. Calado DP, Zhang B, Srinivasan L, Sasaki Y, Seagal J, Unitt C, et al. Constitutive Canonical NF-Kappab Activation Cooperates With Disruption of BLIMP1 in the Pathogenesis of Activated B Cell-Like Diffuse Large Cell Lymphoma. *Cancer Cell* (2010) 18(6):580–9. doi: 10.1016/j.ccr.2010.11.024
162. De Silva NS, Anderson MM, Carette A, Silva K, Heise N, Bhagat G, et al. Transcription Factors of the Alternative NF-KappaB Pathway are Required for Germinal Center B-Cell Development. *Proc Natl Acad Sci USA* (2016) 113(32):9063–8. doi: 10.1073/pnas.1602728113
163. Heise N, De Silva NS, Silva K, Carette A, Simonetti G, Pasparakis M, et al. Germinal Center B Cell Maintenance and Differentiation Are Controlled by Distinct NF-KappaB Transcription Factor Subunits. *J Exp Med* (2014) 211(10):2103–18. doi: 10.1084/jem.20132613
164. Knittel G, Liedgens P, Korovkina D, Seeger JM, Al-Baldawi Y, Al-Maarri M, et al. B-Cell-Specific Conditional Expression of Myd88p.L252P Leads to the Development of Diffuse Large B-Cell Lymphoma in Mice. *Blood* (2016) 127(22):2732–41. doi: 10.1182/blood-2015-11-684183
165. Wang JQ, Jeelall YS, Humburg P, Batchelor EL, Kaya SM, Yoo HM, et al. Synergistic Cooperation and Crosstalk Between MYD88(L265P) and Mutations That Dysregulate CD79B and Surface IgM. *J Exp Med* (2017) 214(9):2759–76. doi: 10.1084/jem.20161454
166. Young RM, Wu T, Schmitz R, Dawood M, Xiao W, Phelan JD, et al. Survival of Human Lymphoma Cells Requires B-Cell Receptor Engagement by Self-Antigens. *Proc Natl Acad Sci USA* (2015) 112(44):13447–54. doi: 10.1073/pnas.1514944112
167. Phelan JD, Young RM, Webster DE, Roulland S, Wright GW, Kasbekar M, et al. A Multiprotein Supercomplex Controlling Oncogenic Signalling in Lymphoma. *Nature* (2018) 560(7718):387–91. doi: 10.1038/s41586-018-0290-0
168. Zhang B, Calado DP, Wang Z, Frohler S, Kochert K, Qian Y, et al. An Oncogenic Role for Alternative NF-KappaB Signaling in DLBCL Revealed Upon Deregulated BCL6 Expression. *Cell Rep* (2015) 11(5):715–26. doi: 10.1016/j.celrep.2015.03.059

169. Skaar JR, Pagan JK, Pagano M. Mechanisms and Function of Substrate Recruitment by F-Box Proteins. *Nat Rev Mol Cell Biol* (2013) 14(6):369–81. doi: 10.1038/nrm3582
170. Horn M, Geisen C, Cermak L, Becker B, Nakamura S, Klein C, et al. DRE-1/FBXO11-Dependent Degradation of BLMP-1/BLIMP-1 Governs C. *Elegans Dev Timing Maturation Dev Cell* (2014) 28(6):697–710. doi: 10.1016/j.devcel.2014.01.028
171. Johnson NA, Slack GW, Savage KJ, Connors JM, Ben-Neriah S, Rogic S, et al. Concurrent Expression of MYC and BCL2 in Diffuse Large B-Cell Lymphoma Treated With Rituximab Plus Cyclophosphamide, Doxorubicin, Vincristine, and Prednisone. *J Clin Oncol: Off J Am Soc Clin Oncol* (2012) 30(28):3452–9. doi: 10.1200/JCO.2011.41.0985
172. Sesques P, Johnson NA. Approach to the Diagnosis and Treatment of High-Grade B-Cell Lymphomas With MYC and BCL2 and/or BCL6 Rearrangements. *Blood* (2017) 129(3):280–8. doi: 10.1182/blood-2016-02-636316
173. Sarkozy C, Traverse-Glehen A, Coiffier B. Double-Hit and Double-Protein-Expression Lymphomas: Aggressive and Refractory Lymphomas. *Lancet Oncol* (2015) 16(15):e555–67. doi: 10.1016/S1470-2045(15)00005-4
174. Strasser A, Harris AW, Bath ML, Cory S. Novel Primitive Lymphoid Tumours Induced in Transgenic Mice by Cooperation Between Myc and Bcl-2. *Nature* (1990) 348(6299):331–3. doi: 10.1038/348331a0
175. Sewastianik T, Prochorec-Sobieszek M, Chapuy B, Juszczynski P. MYC Deregulation in Lymphoid Tumors: Molecular Mechanisms, Clinical Consequences and Therapeutic Implications. *Biochim Biophys Acta* (2014) 1846(2):457–67. doi: 10.1016/j.bbcan.2014.08.006

Conflict of Interest: The authors declare that the research was conducted in the absence of any commercial or financial relationships that could be construed as a potential conflict of interest.

frontiers in Immunology

REVIEW
published: 13 August 2021
doi: 10.3389/fimmu.2021.670280

Forward and Reverse Genetics of B Cell Malignancies: From Insertional Mutagenesis to CRISPR-Cas

Joanna C. Dawes [1,2*] *and Anthony G. Uren* [1,2*]

[1] *Medical Research Council, London Institute of Medical Sciences, London, United Kingdom,* [2] *Institute of Clinical Sciences (ICS), Faculty of Medicine, Imperial College London, London, United Kingdom*

Cancer genome sequencing has identified dozens of mutations with a putative role in lymphomagenesis and leukemogenesis. Validation of driver mutations responsible for B cell neoplasms is complicated by the volume of mutations worthy of investigation and by the complex ways that multiple mutations arising from different stages of B cell development can cooperate. Forward and reverse genetic strategies in mice can provide complementary validation of human driver genes and in some cases comparative genomics of these models with human tumors has directed the identification of new drivers in human malignancies. We review a collection of forward genetic screens performed using insertional mutagenesis, chemical mutagenesis and exome sequencing and discuss how the high coverage of subclonal mutations in insertional mutagenesis screens can identify cooperating mutations at rates not possible using human tumor genomes. We also compare a set of independently conducted screens from *Pax5* mutant mice that converge upon a common set of mutations observed in human acute lymphoblastic leukemia (ALL). We also discuss reverse genetic models and screens that use CRISPR-Cas, ORFs and shRNAs to provide high throughput *in vivo* proof of oncogenic function, with an emphasis on models using adoptive transfer of *ex vivo* cultured cells. Finally, we summarize mouse models that offer temporal regulation of candidate genes in an *in vivo* setting to demonstrate the potential of their encoded proteins as therapeutic targets.

Keywords: B cell leukemia, B cell lymphoma, mouse models, insertional mutagenesis, exome sequencing, reverse genetics, CRISPR-Cas, shRNA

OPEN ACCESS

Edited by:
Christelle Vincent-Fabert, UMR7276 Contrôle des réponses immunes B et des lymphoprolifération (CRIBL), France

Reviewed by:
Rodney P. DeKoter, Western University, Canada
Cyril Broccardo, INSERM U1037 Centre de Recherche en Cancérologie de Toulouse, France

***Correspondence:**
Anthony G. Uren
anthony.uren@gmail.com
Joanna C. Dawes
dawesjoanna@gmail.com

Specialty section:
This article was submitted to B Cell Biology, a section of the journal Frontiers in Immunology

Received: *20 February 2021*
Accepted: *09 July 2021*
Published: *13 August 2021*

Citation:
Dawes JC and Uren AG (2021) Forward and Reverse Genetics of B Cell Malignancies: From Insertional Mutagenesis to CRISPR-Cas. Front. Immunol. 12:670280. doi: 10.3389/fimmu.2021.670280

INTRODUCTION

B cell neoplasms can be categorized by their cell of origin, each subtype being representative of a discrete stage in differentiation with characteristic phenotypes and genetic lesions (**Table 1**, **Figure 1**) [reviewed in (1, 2)]. Accurate modelling of these diseases in mice requires alteration of various biological processes at different stages of B cell development including differentiation, migration, rearrangement of immunoglobulin genes, T helper interactions, positive selection for antigen and negative selection against autoreactivity. Like most tumors, B cell malignancies accumulate amplifications, deletions, rearrangements, deregulation of methylation and non-synonymous point mutations. Additionally, B

TABLE 1 | Major subtypes of B cell malignancies.

Subtype	Nearest normal B cell phenotype
Burkitt lymphoma (BL)	Germinal Center B cell
B-cell acute lymphoblastic leukaemia (B ALL)	Pre B cell, Pro B cell, Mature B cell
Chronic Lymphocytic Leukemia (CLL), Small Lymphocyte Lymphoma (SLL)	Mature B cell or Post–germinal center B cells
Diffuse large B-cell lymphoma (DLBCL)	Activated B cell or Germinal Center B cell
Follicular Lymphoma (FL)	Germinal center B cell
Hairy cell leukemia (HZL), variant hairy cell leukemia (HZL-v)	Marginal zone/memory B cells
Hodgkin lymphoma (HL)	Germinal Center B cell
Lymphoplasmacytic Lymphoma (LPL), Morbus Waldenström	Plasma cells
Mantle cell lymphoma (MCL)	Mantle B cell
MALT lymphoma (MALT)	Post Germinal Center B cells
Marginal zone lymphoma (MZL)	Marginal zone B cells
Monoclonal B-cell lymphocytosis (MBL)	Germinal Center B cell
Plasma cell myeloma (PCM), Multiple Myeloma (MM), Monoclonal Gammopathy of undetermined significance (MGUS)	Plasma cells
Prolymphocytic leukemia (B-PLL)	Pro B cells (aggressive CLL variant)

cells are characterized by remodeling of the immunoglobulin loci by recombinase activating gene (RAG) mediated V(D)J recombination of immunoglobulin variable regions and by activation induced cytidine deaminase (AID) mediated class switch recombination. Errors of these processes mean immunoglobulin loci are the most frequent translocation partners of B cell malignancies, often placing oncogenes under the control of the highly expressed immunoglobulin promoters and enhancers and causing deregulated and constitutive expression (3–6) (**Figure 2**). Somatic hypermutation by AID is also a known source of oncogenic mutations in B neoplasms as evidenced by the mutation fingerprint of commonly mutated genes, and aberrant somatic hypermutation of non-immunoglobulin genes at hotspots located throughout the genome also contributes to lymphomagenesis (4, 7–9).

Speculation on the developmental stage that each malignancy is derived from is based on a combination of genetic lesions and phenotypic characteristics [reviewed in (1, 2)]. The cell of origin suggested by translocation breakpoints does not always match the cell of origin suggested by somatic hypermutations and/or markers expressed on the cell surface. Follicular lymphoma (FL) and diffuse large B cell lymphoma (DLBCL) appear to have a

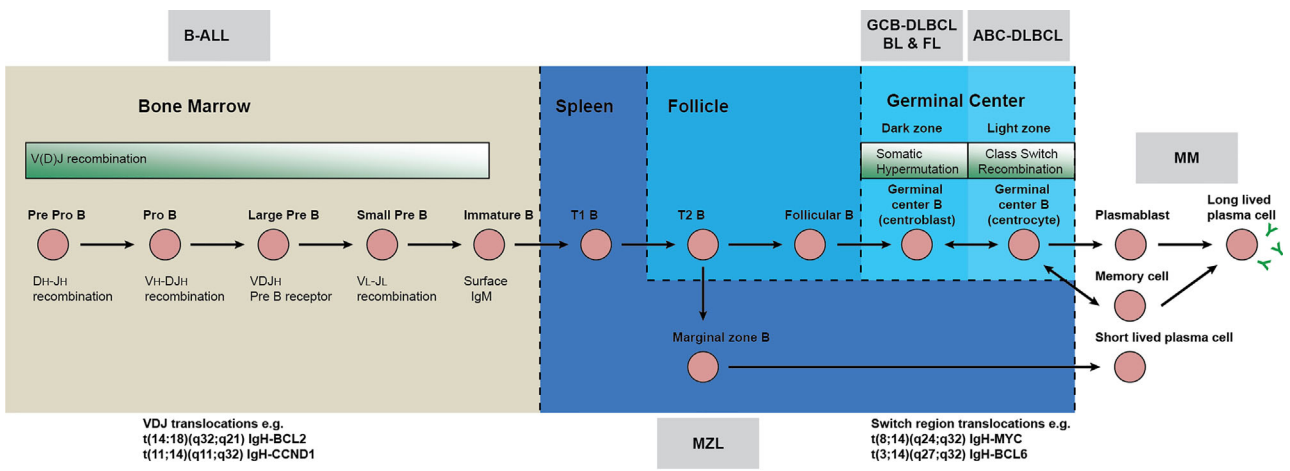

FIGURE 1 | Neoplastic mechanisms throughout B cell development. Early B-cell development in adult bone marrow is characterized by generation of the B-cell receptor (BCR). Immunoglobulin heavy chain (IgH) gene rearrangements (V_H, D_H and J_H), together with the V_L-J_L rearrangements of light chain (IgL) gene segments generate a B-cell repertoire of antibodies that recognize a variety of antigens. If the BCR does not form correctly, or is autoreactive, the cell undergoes apoptosis or receptor editing. Immature B-cells with functional BCRs, migrate to secondary lymphoid organs like the spleen and lymph nodes where they form follicles during the T-cell dependent immune response. Within the follicle, B-cells undergo two further remodeling steps in the germinal centers (GC): somatic hypermutation (SHM) and class switch recombination (CSR). SHM introduces point mutations, deletions or duplications into the variable region of the immunoglobulin genes. CSR replaces the IgH chain constant region, altering the effector response but not the antigen binding domain. GC B-cells that have undergone CSR and have high affinity IgG BCRs are selected for and differentiate into plasma cells and long-lived plasma cells, the effectors of adaptive immunity. The assignment of translocations to either V(D)J recombination in pro/pre B cells in the marrow or class switch recombination in the germinal center is based on the location and sequences of junctions present in each translocation. For instance, V(D)J derived translocations typically give rise to *BCL2* or *CCND1* translocations to the Ig variable regions whereas class switching frequently results in translocations between *BCL6* or *MYC* and Ig constant regions.

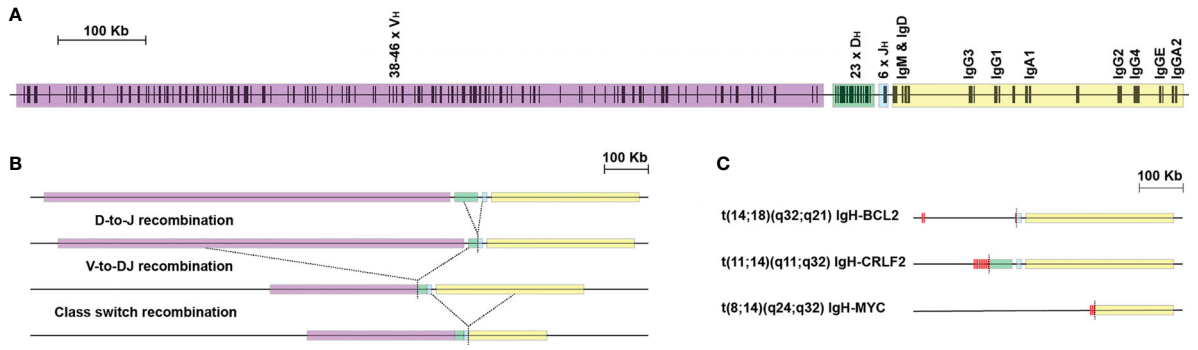

FIGURE 2 | Aberrent V(D)J & class switch recombination creates oncogenic translocations. Immunoglobulin variable region rearrangement and class switch recombination are error prone processes. **(A)** The immunoglobulin heavy chain locus is divided into different repetitive elements including variable segments (VH purple), diversity segments (DH green), joining segments (JH blue) and constant regions (yellow). Vertical bars depict both functional gene segments (typical numbers are indicated), non-functional pseudogenes (numbers not indicated) and repetitive elements (adapted from imgt.org). **(B)** Expression of recombinase activating genes (RAG) during pre pro, pro and pre B stages creates breaks between V(D)J segments, which are resolved by excision of intervening DNA. Activation induced cytidine deaminase (AID) deaminates cytosine residues of single stranded DNA which are exposed during transcription. The resulting mismatch is processed by error prone DNA repair mechanisms (including endonuclease G) resulting in excision of the default IgM/IgD constant region and fusion of the joining segments with constant regions of other isotypes. **(C)** Errors in resolving breaks initiated by RAG and AID can resolve as translocations with non-immunoglobulin loci. Break points adjacent to the heavy chain J_H or D_H segments indicate that translocations occur at the pre pro B cell stage in the bone marrow (*IgH/BCL2* or *IgH/CRLF2*). Similar translocations also originate from immunoglobulin light chain loci. Translocations may also result from class-switch recombination in the light zone of the germinal center, evidenced by breakpoints in the immunoglobulin constant region (*IgH/Myc*). Breakpoints adjacent to successfully rearranged V(D)J segments with somatically mutated variable portions indicate that an AID mediated translocation has occurred later in development in the germinal center dark zone.

mature B cell phenotype. Nonetheless, they share a common translocation *IgH/BCL2* t(14;18)(q32;q21) which occurs early in B cell development during V(D)J recombination mediated by RAG in the primary lymphoid organs (10). This translocation places the anti-apoptotic *BCL2* gene under control of the immunoglobulin heavy chain (*IgH*) enhancer and plays a causal role in germinal center derived malignancies. Though this translocation is commonly an initiating event in development of FL, it alone is not sufficient to initiate lymphomagenesis and similar translocations can be detected in the peripheral blood and lymph nodes of healthy individuals (11). Similarly, whilst chronic lymphocytic leukemia (CLL) is also considered a mature B cell malignancy, the propensity for cells to become malignant appears to arise as early as the hematopoietic stem cell (HSC) stage and driver lesions are detectable in the hematopoietic progenitors of some patients (12–14). CLL is also characterized by distinct subtypes that either have unmutated variable regions or hypermutated post germinal center variable regions. Mantle cell lymphoma (MCL) has a similar bifurcation between mutated/unmutated variable regions.

Further complicating matters, some B cell neoplasms result from the transformation of non-malignant monoclonal outgrowths or from other neoplasm subtypes. DLBCL can arise from the transformation of CLL, small lymphocytic leukemia (SLL) or FL (15) or less commonly from mucosa associated lymphoid tissue (MALT) lymphoma (16, 17) or Hodgkin lymphoma (HL) (18). CLL can itself develop from the precursor condition monoclonal B cell lymphocytosis (19) and a high proportion of multiple myeloma (MM) arise from monoclonal gammopathy of undetermined significance (20, 21).

Recent genomic studies of B cell malignancies implicate a handful of well-characterized, commonly mutated or translocated genes as well as a long tail of genes that have limited or no experimental evidence to support a role in disease. Since it is unlikely that all these mutations are driving oncogenesis there is need for validation methods such as functional genomic screens, forward genetic screens and comparative genomics to scrutinize driver mutations and better prioritize candidates for further study. The diverse mechanisms by which mutations contribute to disease means that many can only be tested within the context of specific developmental stages, predisposing mutations and optimal antigen receptor stimulation. For secondary/later stage mutations, oncogenic function and selection may only occur within a specific context of germline variants and/or early stage initiating mutations. This exponentially expanding set of parameters for validation experiments therefore requires prioritization by analysis of mutation profiles and higher throughput testing methods.

In some respects, sequencing human tumors can be viewed as a special case of forward genetics, i.e. surveying genetic diversity under selection in order to identify which genetic changes drive a biological process. Forward genetic screens can also be targeted to the somatic cells of mice using either chemical or insertional mutagens. In the context of mouse cancer models, reverse genetics is the introduction of variation known to be associated with cancer in order to study the function of that variation. This variation can be introduced to the germline or targeted to specific populations of somatic cells.

The benefit of using mouse models to study hematologic malignancies is that the major genes and biological processes

driving hematopoiesis and immunity are sufficiently conserved such that human malignancies can be recapitulated by the introduction of equivalent mutations. Mice also allow the complexity of immune system biology to be recapitulated *in vivo* in ways not yet possible with cultured cells or organoids.

This review covers mouse models used to rapidly screen for and validate large numbers of candidate genes driving B cell malignancies and is aimed at readers seeking to understand various techniques for targeting different developmental stages and disease subtypes. We provide a history of forward and reverse genetic approaches in mice that balance the trade-offs between fidelity, precision, and throughput. In the first half we discuss how forward genetics in mice can independently validate the oncogenic function of rarely mutated genes from human studies, and in some cases is a tool leading to discovery of human cancer genes. In the second half we cover reverse genetic screens and validation experiments where throughput is increased through the use of transplantation of primary cells transduced with ORF, shRNA and CRISPR-Cas viral constructs. Throughout we also emphasize strategies to direct models toward specific malignancy subtypes by a combination of germline lesions, targeted cell populations and temporal control of gene expression.

FORWARD GENETIC MODELS

Many driver genes are difficult to identify because they are subject to deregulation by non-coding mutations, copy number changes or epigenetic modification. Comparative genomic analyses of human tumors with the findings from forward genetic screens in mouse models can narrow down the identity of these driver genes. Mice with germline mutations that sensitize them to a specific disease subtypes are subjected to mutagenesis of their somatic cells and the resultant tumors are sequenced. We discuss here the combined use of genetically modified mice, insertional mutagens and exome sequencing as tools to perform forward genetic screens in B cell neoplasms (summarized in **Table 2**). Observing which mutations are present in both mouse and human cohorts, or which mutation combinations are selected to co-occur more or less frequently than expected by chance can prioritize validation experiments.

Insertional Mutagenesis Screens in Somatic Cells

Somatic insertional mutagenesis screens are one of the most efficient tools for performing forward genetic screens in mouse models of cancer. When insertional mutagens are integrated randomly throughout the genome of somatic cells, they can deregulate and disrupt genes in a manner analogous to chromosomal rearrangements, deletions, non-coding mutations and truncating coding mutations. Mouse tissues are typically mutagenized by replicative retroviruses or germline copies of transposons mobilized in different tissues. Under optimal conditions a subset of these mutagenized cells eventually give rise to malignancies.

The primary benefit of analyzing integration mutations is the ease with which they can be mapped to the genome by amplifying sequences that flank the integration using various ligation mediated PCR methods. In analyzing cohorts of tumors in these screens, loci found to have insertion sites in independent tumors, more frequently than expected by chance, are defined as common insertion sites or common integration sites (CISs). Selection of mutations at these CIS loci indicates that they cause changes in expression levels or cause disruption/truncation of cancer drivers. There can be substantial phenotypic and genetic variability between malignancies of a single cohort and driving specificity toward B cells rather than T or myeloid lineages has been achieved through a combination of limiting mutagenesis to B lineages, screening mice with a predisposition toward B malignancy subtypes and curating uniform subsets of B lineage tumors from mixed cohorts.

Retroviral Mutagenesis in the Hematopoietic Compartment

Slow transforming retroviruses have an extensive history of use as insertional mutagens in the hematopoietic compartment [reviewed in (62)]. When newborn mice are infected with slow transforming retroviruses, they fail to mount an immune response and consequently develop a viremia that lasts the lifetime of the animal. Successive rounds of reinfection lead to an accumulation of insertion mutations in cells of the hematopoietic compartment, where the high rate of proliferation during early postnatal development makes them the preferred host cells for virus propagation. In some strains the spontaneous activation of endogenous ecotropic retroviruses gives rise to disease by a similar process. Over time, mutations providing a selective advantage will lead to the clonal expansion of cells with multiple oncogenic insertion mutations.

These viruses induce a range of hematologic malignancies. B cell tumor cohorts have been generated by choosing specific combinations of virus strain and host mouse strain. Sequences within the virus LTRs are responsible for cell type-specific expression and alterations can skew tumors toward B cell subtypes (63, 64). Akv is an endogenous, ecotropic murine leukemia virus isolated from the AKR strain which causes mature B cell lymphomas with an FL and DLBCL phenotype (65). Mutation of the Akv LTR enhancer sequences causes plasmacytoma like disease (66) and mutation of splice sites broadens the diversity of B malignancy subtypes (32). Somatic reactivation of endogenous ecotropic proviruses can also give rise to B lineage malignancies in inbred mouse strains (SJL/J mice, CWD/LeAgl, SEA/GnJ, SL/Hk) (67, 68), recombinant inbred strains (AKXD) (69) and the NFS.V+ congenic mice (bearing ecotropic MuLV loci from AKXD or C58/Lw) (70, 71). When integration sites from B malignancies of these models were cloned, many were found recurrently at sites that were known or have subsequently been found to be drivers of B cell malignancies (27, 30–39, 41, 42) (**Table 2**).

Retroviral integrations tend to increase the expression of oncogenes although occasionally intragenic integrations cause loss of function of tumor suppressors. One of the more

TABLE 2 | Forward genetic screens in mouse models of B cell malignancies.

Publication	Study type	Mutagen	Mouse strains	B cell malignancies
van Lohuizen et al. (22)	MuLV mutagenesis	Mo-MuLV	Eμ-Myc	pre B cell lymphoma
Haupt et al. (23)	MuLV mutagenesis	Mo-MuLV	Eμ-Myc	pre B & mature B cell lymphoma
Shinto et al. (24)	MuLV mutagenesis	Mo-MuLV	Eμ-BCL2	pre B & B cell lymphoma
van der Lugt et al. (25)	MuLV mutagenesis	Mo-MuLV	Eμ-Myc Pim1-/-	pre B cell lymphoma
Sheppard et al. (26)	MuLV mutagenesis	Mo-MuLV	Eμ-Mycn	pre B cell lymphoma
Mikkers et al. (27)	MuLV mutagenesis	Mo-MuLV	Eμ-Myc; Pim1-/-; Pim2-/-	pre B cell lymphoma
Dang et al. (28)	MuLV/ENU mutagenesis/exome sequencing	Mo-MuLV or ENU	thymectomized Pax5+/- & Pax5-/-	pre B leukemia / B cell leukemia
Webster et al. (29)	MuLV mutagenesis	Mo-MuLV	Eμ-BCL2, Vav-BCL2	mature B cell lymphoma
Martín-Hernández et al. (30)	MuLV mutagenesis	Akv1-99 MuLV	NMRI mice	B cell lymphoma
Ma et al. (31)	MuLV mutagenesis	Akv MuLV & derivatives	NMRI mice	DLBCL and plasmacytoma
Sorensen et al. (32)	MuLV mutagenesis	Akv MuLV & derivatives	NMRI mice	B cell lymphoma, plasmacytoma
Liu et al. (33)	MuLV mutagenesis	Akv MuLV & derivatives	NMRI mice	B cell lymphoma, plasmacytoma
Pyrz et al. (34)	MuLV mutagenesis	Akv MuLV & derivatives	NMRI mice	B cell lymphoma
Hartley et al. (35)	MuLV mutagenesis	endogenous ecotropic MuLV	NFS.V+ mice	DLBCL, BL, MZL, FL, SLL & Immunoblastic lymphoma
Suzuki et al. (36)	MuLV mutagenesis	endogenous ecotropic MuLV	AKXD mice	DLBCL, BL, MZL, FL, Pre B & Immunoblastic lymphoma
Tsuruyama et al. (37)	MuLV mutagenesis	endogenous ecotropic MuLV	SL/Kh mice	pre B cell lymphoma / B cell lymphoblastic lymphoma
Jin et al. (38)	MuLV mutagenesis	endogenous ecotropic MuLV	SL/Kh mice	pre B cell lymphoma / B cell lymphoblastic lymphoma
Shin et al. (39)	MuLV mutagenesis	endogenous ecotropic MuLV	NFS.V+ mice	Splenic marginal zone lymphoma
Suzuki et al. (40)	MuLV mutagenesis	endogenous ecotropic MuLV	AKXD-Blm m3 mice	B cell lymphoma
Weiser et al. (41)	MuLV mutagenesis	endogenous ecotropic MuLV	AKXD mice	pre B cell & B cell leukemia/lymphoma
Tsuruyama et al. (42)	MuLV mutagenesis	endogenous ecotropic MuLV	SL/Kh mice	pre B cell lymphoma / B cell lymphoblastic lymphoma
Van Der Weyden et al. (43)	SB mutagenesis	ETV6 knock in SB	ETV6-RUNX1-SB knock in	B cell precursor ALL
Zanesi et al. (44)	SB mutagenesis	SB	Emu-Tcl1	CLL
Van Der Weyden et al. (45)	SB mutagenesis/exome	ETV6 knock in SB	ETV6-RUNX1-SB knock in; Pax5+/-	B cell precursor ALL
Heltemes-Harris et al. (46)	SB mutagenesis	SB	Stat5b-CA	B ALL
Rahrmann et al. (47)	SB mutagenesis	SB	$Trp53^{R270H}$ or Pten +/-	FL and DLBCL
Weber et al. (48)	PB mutagenesis	Rosa26 knock in PB	*Blm*m3 mice	DLBCL
Sander et al. (49)	exome	none	Myc and PI3K conditional	BL
Sungalee et al. (50)	exome of premalignant cells	none	Eμ-hBCL2 transduced mice	FL & FL in situ
Gough et al. (51)	exome	none	Vav-NUP98-PHF23	progenitor B-1 ALL
Martin-Lorenzo et al. (52)	exome	none	Pax5 +/-	precursor B ALL
Dang et al. (28)	MuLV/ENU mutagenesis/exome sequencing	Mo-MuLV or ENU	Pax5 +/-	pre B leukemia / B cell leukemia
Van Der Weyden et al. (45)	SB mutagenesis/exome	ETV6 knock in SB	ETV6-RUNX1-SB knock in; Pax5+/-	B cell precursor ALL
Duque-Afonso et al. (53)	exome	none	E2A-PBX1 conditional	B ALL
Lefebure et al. (54)	exome	none	Eμ-Myc	BL
Rodríguez-Hernández et al. (55)	exome	none	Sca1-*ETV6-RUNX1*	precursor B ALL
Gough et al. (56)	exome	none	Vav-NUP98-PHF23	progenitor B-1 ALL
Mouly et al. (57)	exome	none	Tet2 +/- and Tet2 -/-	B cell lymphoma
Jamrog et al. (58)	exome	none	PAX5-ENL knockin	B ALL
Zaborsky et al. (59)	exome	none	Emu-TCL1	CLL
Flümann et al. (60)	exome	none	Myd88 & Bcl2 conditional	DLBCL
Vicente-Duenãs et al. (61)	exome	none	Pax5+/-	B ALL

innovative strategies to increase the proportion of tumor suppressors identified is the screening of mice on a *Blm* hypomorphic background (40). *Blm* encodes a recQ DNA helicase the loss of which creates genomic instability. This encourages DNA repair by homologous recombination, which in turn leads to increased sister chromatid exchange and large stretches of loss of heterozygosity. When integration of a virus disrupts a tumor suppressor gene, any subsequent deletions or loss of heterozygosity that removes the wild type copy will increase selection of tumor suppressor mutations.

Enforced expression of B cell lymphoma oncogenes such as *MYC*, *NMYC* or *BCL2*, in the B cell compartment or loss of tumor suppressors can also skew MuLV driven malignancies toward B cell lymphoma and leukemias (22–26). Recent large scale analyses of the common integration sites of two *BCL2* transgenic strains infected with Moloney MuLV (MoMuLV) shows a statistically significant bias toward verified drivers of human B lymphoma and leukemia (*Pou2f2*, *Pax5*, *Ikzf3*, *Ebf1*) in addition to dozens of other candidate loci (29).

Transposon Mutagenesis in the Hematopoietic Compartment

The use of DNA transposons as somatic insertional mutagens in mice has led to dozens of tissue and cell type specific screens [reviewed in (72–74)]. The Sleeping Beauty (SB) transposon isolated from salmonid fish and the piggyBac (PB) transposon isolated from the cabbage looper moth have both been adapted for use in mammalian cells. When mice bearing a concatemer of a transposon as a germline transgene are crossed to mice that express the cognate transposase, this causes mobilization of the transposon in somatic cells. By controlling expression of the transposase and the cargo of the transposon (typically a promoter trap and/or gene trap) this technique generates a wider spectrum of tumor types than slow transforming retroviruses, although this versatility is tempered by several caveats. Transposons have a tendency to hop in *cis* which can complicate analysis of integrations near the initial concatemer. Furthermore, remobilization of the transposon during tumor development can cause local hopping around the region of tumor initiating mutations and there is typically a higher level of background non-CIS mutations that provide no selective advantage to tumor cells. The screens discussed in detail below have successfully targeted transposon mutagenesis to the B cell compartment using a combination of predisposing mutations combined with tissue specific transposase expression.

Weakly oncogenic mutations observed in human tumors do not always lead to tumor development in mouse models due to a lack of cooperating mutations. One of the first B cell malignancy SB screens used a mouse model of the t(12;21)(p13;q22) *ETV6/RUNX1* (*TEL/AML1*) fusion transcript, seen frequently in B cell acute lymphoblastic leukemia (ALL). Mice expressing the *ETV6/RUNX1* fusion and the SB transposase variant HSB5 from the endogenous *Etv6* locus had a background of long latency hematologic malignancies similar to wild type controls i.e. the fusion itself caused only slightly higher rates of lymphomagenesis (43). When this allele was combined with a gene trap/promoter trap transposon the mice developed a spectrum of acute myeloid leukemia (AML), T cell ALL and B cell precursor ALL. By sequencing the integrations of B ALL samples, recurrent truncating mutations were observed in *Ebf1*, a tumor suppressor of B ALL (75, 76) which encodes a transcriptional activator of another B cell ALL tumor suppressor *Pax5*.

STAT5 activating mutations are observed in a small proportion of B ALL, however mice expressing a constitutively active form of *STAT5B* (*STAT5*-CA N642H) do not develop ALL (46). Combining this allele with a transposon gene/promoter trap concatemer, a Cre-inducible SB and *Cd79a*-Cre (switching in developing B cells) induced progenitor B cell leukemias thereby verifying *STAT5B* N642H as an oncogene in B ALL. Integrations of 65 mice identified 12 CIS, the most commonly mutated genes suggesting three major mechanisms for *STAT5* mediated transformation: disruption of B-cell development (*Sos1*, *Kdm2a, Ikzf1, Klf3)*, enhanced *JAK/STAT5* signaling (*Jak1*) and modification of the *CDKN2A* tumor-suppressor pathway (*Bmi1*, *Cdkn2a*).

The exomes of CLL samples average less than one coding driver mutation per sample, making mechanisms of transformation difficult to identify. The Eμ-*TCL1* transgenic model develops a disease that is phenotypically similar to CLL. The B cells of these mice were mutagenized using a conditional SB transposase switched by *CD19*-Cre (pan B cell) (44, 59). Transposon mobilization decreased latency of Eμ-*TCL* leukemias and integrations of 15 mice yielded 8 CIS loci, four of which implicate Nf-kappaB signaling (*Nfkb1*, *Tab2*, *Map3K14*, and *Nfkbid*). NF-kappaB activating mutations are rare in the coding regions of human CLL however it has been shown that CLL cells are frequently dependent on extracellular signaling pathways that activate Nf-kappaB (77) and several mouse models of CLL/SLL have constitutive activation of NF-kappaB pathways (78–80).

The Cre strains used to switch conditional SB alleles need not be entirely B cell specific in order to generate B cell malignancies. The *Cnp*-Cre strain expresses Cre in the nervous system and splenic germinal centers (47). Combining *Cnp*-Cre with an SB11 conditional allele, a transposon concatemer and a conditional oncogenic point mutation of tumor suppressor *Trp53* ($Trp53^{R270H}$) generated a mixture of solid tumors as well as lymphoid malignancies with an FL/DLBCL like phenotype. Integrations from 23 samples identified *Bach2* as the most frequently mutated locus. *Pten* disrupting mutations were also identified and the authors verified *Pten* as a tumor suppressor in the *Cnp*-Cre driven model. These results are consistent with human germinal center B cell DLBCL where *PTEN* is mutated or deleted (81) and reduced expression correlates with AKT activation (82).

More recently the piggyBac transposon has also been adapted for somatic insertional mutagenesis. Mice expressing constitutive piggyBac transposase were crossed with a gene trap piggyBac transposon concatemer allele onto a $Blm^{m3/m3}$ hypomorph background (48). Gene trap transposons are more likely to generate intragenic loss of function mutations which are in turn more likely to be selected if they occur in tumor

suppressors. The use of a *Blm* hypomorph background to enhance loss of heterozygosity events is the same strategy used to enrich for tumor suppressors in the retroviral screen of AKXD $Blm^{m3/m3}$ mice cited in the previous section (40). A spectrum of solid and hematological tumors were generated, with the majority of mice having DLBCL like B lymphoid malignancies. These had recurrent amplification of *Bcl11a* and *Rel*, this region also being amplified in human DLBCL. Integration site cloning using the semiquantitative QiSeq insert cloning protocol (83) on 43 samples identified nearly 300,000 integrations. Inactivating/disrupting mutations were observed in tumor suppressors known to be mutated in human DLBCL and there was significant overlap between the orthologs of CIS genes and the set of genes that are down regulated in human DLBCL *vs* non-malignant B cells. This suggests CIS genes may inform the identification of genes that are down regulated in human DLBCL by epigenetic variation and/or large-scale deletions.

Quantitative Analyses of Subclonal Integration Mutations

Improvement in next generation sequencing platforms and ligation mediated PCR methods have increased the throughput and sensitivity of integration site cloning. Ligation mediated-PCR methods such as vectorette and splinkerette-PCR use a non-complimentary adaptor that facilitates enrichment of integrated sequences separately from the remainder of the genome (84–86). Shearing of tumor DNA prior to construction of sequencing libraries allows the abundance of each integration within a sample to be quantitated by counting the number of unique read fragment lengths mapping to each integration (83, 87–89). This approach to quantitation minimizes sequence and amplification biases particularly when compared to libraries prepared by non-random digestion at restriction enzymes recognition sites. Other studies have quantitated integrations through analyses of whole genome amplification of single cells (SBCapSeq) (90, 91) or using unique molecular identifiers (LUMI-PCR) (92).

Collectively, these recent methods allow affordable, genome wide identification of thousands of subclonal mutations with a sensitivity spanning more than two orders of magnitude. This quantitative coverage in turn allows estimation of the order in which lesions occurred (93) and cloning large numbers of subclonal mutations provides the statistical power needed to derive genetic associations between early-stage clonal mutations and late-stage subclonal mutations (29). Translating these types of analyses to human tumors is currently limited by depth of sequencing coverage. Currently whole genome sequencing of human tumors rarely exceeds 100x coverage and therefore offers less sensitive detection of subclonal mutations than recent integration site cloning studies. Nonetheless, recent studies of single cell sequencing of human tumors include thousands of cells which can therefore identify subclonal mutations within limited/targeted regions of the genome (94–97).

The scale of these datasets requires innovations in statistical methodology, both to identify selected mutations and to demonstrate associations between them. For density based estimates of mutation selection (98–100) the background integration biases of insertional mutagens can be compensated for by the use of unselected cell populations for comparison with tumor mutation distributions (29, 93, 101). Alternatively, identifying local ratios of forward/reverse strand mutations throughout the genome is analogous to using ratios of synonymous and non-synonymous coding mutations in that it does not require correction for integration site biases of the mutagen (29, 93). Strand bias analyses requires a higher density of integrations to reach statistical significance and will only identify loci with a strong bias in one direction or the other.

Analyses of concurrent mutations is complicated by the inclusion of subclonal mutations. When sequencing coverage is deep enough to include very subclonal mutations, some of the most frequently mutated loci can be found mutated in 100% of samples. Any two loci found to have subclonal mutations in all samples will appear to be 100% concomitant, even when these mutations are not found within the same subclones of each sample. For this reason, quantifying the significance of concurrent mutations requires the use of contingency table tests that exclusively use clonal mutations i.e. mutations with a high likelihood of occurring within the same cells. Alternatively it is possible to use asymmetrical contingency tables that classify all tumors on the basis of their early stage "trunk" clonal mutations and/or germline mutations at one locus and then test for the distribution of all mutations (both clonal and subclonal) at other loci (29, 102, 103). The number of genome-wide pairwise tests that can be performed on these cohorts can number in the thousands and this in turn requires stringent multiple testing correction to limit false positive associations. Nonetheless, with high coverage of subclonal mutations it is now possible to identify hundreds of significantly co-mutated loci pairs from a cohort of several hundred mice infected with MoMuLV (29).

Forward Genetic Screens by Exome Sequencing

The expense of exome and whole genome sequencing is generally reserved for the study of human tumors however, an increasing number of mouse tumor exomes have also been sequenced, albeit with cohort sizes that are far smaller than their human counterparts. In most cases this sequencing is to verify that the model accurately recapitulates human disease, however, some studies also suggest or verify candidate drivers where coding mutations in human cohorts fail to reach statistical significance. Several examples are discussed below.

Combining Cre recombinase inducible alleles of mutant *Myd88* (L252P) and *Rosa-26* expressed *Bcl2* with germinal center specific *Cγ1-Cre* generated a human ABC-DLBCL like model (60). Sequencing samples from 17 mice confirmed mutation of human DLBCL drivers including *Pim1*, *Myc*, *Kmt2d*, *Nfkbia*, *Stat3*, *Pou2f2*, and *Hist1h1e*. In a similar study, conditional expression in germinal center B cells of *Myc* and constitutively activated *Akt* (fusing p85 to p110) gave rise to Burkitt's lymphoma (BL) like disease with recurrent mutations in *Ccnd3*, which is mutated in BL and known to regulate germinal center B cell proliferation (49).

TET1 and *TET2* encode methylcytosine dioxygenase enzymes that are thought to play a role in demethylation of DNA by catalyzing conversion of 5-methylcytosine to 5-hydroxymethylcytosine. *TET2* is mutated in a range of hematopoietic malignancies including a subset of DLBCL where mutations can be traced back to HSC populations, suggesting *TET2* mutation is an early event in lymphomagenesis (104). Mice lacking *Tet2* globally or in B cell subpopulations (*CD19*-Cre or *Vav*-Cre) develop B cell lymphoma (57, 105). One study sequencing six B cell tumors matched to germline counterparts revealed thirty-four acquired mutations, albeit not recurrently mutated, presumably due to the limited cohort size. Nonetheless, more than half of these genes are also mutated in either DLBCL, CLL or both.

TET1 is not mutated in human B malignancies however it is downregulated in human DLBCL and FL which inconclusively suggests a role for *TET1* in human B lymphoma. *Tet1* deficient mice develop mature B cell malignancies which when sequenced were found to have missense mutations in the mouse homologues of known human B cell malignancy drivers including *Gna13*, *Kmt2d*, *Myd88, Cd83*, *Pim1, Cd79B* and *Fas* (106). Additional mutations were observed in linker histone genes, histone variants and histone modifying enzymes. Histone linker mutations are a feature of FL (107). These mutations corroborate a role for *TET1* down regulation in human B cell malignancies.

Mouse models that accurately recapitulate human disease can also identify novel drivers. The Eμ -*Myc* model is a mainstay of B cell leukemia/lymphoma research but exomes from this model have only recently been sequenced (54). Sequencing of 23 lymphoma exomes revealed recurrent mutations in known drivers such as *Trp53*, *Cdkn2a* and *Kras*, but also the "*BCL6* corepressor" gene *Bcor*. Inactivating mutations in *Bcor* accelerated Eμ-*Myc* driven lymphomas in transplantation assays. An independent study sequenced *NUP98/PHF23* transgenic mice which primarily develop T cell lymphoma but in a minority of cases also develop progenitor B-1 type ALL. This study also identified *Bcor* mutations in addition to mutations of *Jak1*, *Jak2*, *Jak3* and *Stat5a* (51, 56). *Bcor* loss of function mutations were subsequently found to cause B-1 progenitor ALL in mice (108).

Aside from driver detection, exome sequencing can also be a powerful tool to examine the mutagenic processes of early premalignant states under defined experimental conditions. Sungalee *et al.* developed an innovative model of t(14;18) translocation where human *BCL2* expression from an Eμ enhancer is sporadically induced by RAG recombinase in pro/pre B cells (50). Repeat immunization demonstrated a survival advantage for *hBCL2* expressing cells after multiple rounds of germinal center reentry. Exome sequencing was performed on *BCL2*-enriched germinal center and memory cell fractions from three chronically immunized mice and a control (empty vector) mouse. B cell subsets of the *BCL2*-transduced mice had between 111 and 2,565 nonsilent SNVs compared with 63 to 70 SNVs in the control mouse, despite the absence of overt morphological differences between *hBCL2* and control animals. This model demonstrates a role for *BCL2* in enhanced survival of cells that accumulate potentially oncogenic off target mutations of AID.

Pax5 Driven Models of B ALL; A Case Study of Multimodal Screens Converging on Common Findings

PAX5 encodes a B cell development transcription factor that activates B cell specific genes and represses genes of alternative lineages. It is one of the most frequently altered genes in B ALL and a varied spectrum of somatic rearrangements, translocations, mutations and deletions have been observed at this locus (76, 109–111). Karyotypic analysis indicates translocations are early events whereas deletion of a second allele appears to be a secondary later event. Germline point mutations that inhibit *PAX5* function also increase the likelihood of B ALL and some are accompanied by somatic deletion of the other *PAX5* allele or cooperating *PAX5* mutations (112–115). The discovery of frequent *PAX5* deletion and translocations in human ALL was rapidly followed by a large number of studies using some form of *Pax5* deletion or translocation in mice to model B ALL. To date six independent studies have included exome sequencing and/or insertional mutagenesis of mouse B ALL samples generated by mutation of *Pax5*. The convergence of findings of these studies demonstrates the value of multimodal screening in mice to validate mutation profiles of human tumors.

Pax5 heterozygosity combined with thymectomy skews ENU and MoMuLV driven lymphomas toward a B lineage disease since thymectomy removes competing T cell malignancies (28). Array-CGH copy number analyses of these malignancies identified amplification of chromosome 15 (and consequently *Myc*) and focal deletions of the second allele of *Pax5*. Exome sequencing revealed B ALL samples from ENU treated mice had 5-fold more exonic mutations than MuLV infected mice and identified recurrent mutations in the human ALL mutated genes: *Pax5*, *Jak3*, *Ptpn11*, *Jak1*, and *Nras*. *Pax5* mutations were almost exclusively within the DNA-binding paired domain and equivalent to mutations observed in human B ALL. *Jak1* and *Jak3* mutations were located in the pseudokinase domains of *JAK1* and *JAK3*, and are known to induce cytokine-independent proliferation and activation of downstream signaling pathways sensitive to JAK inhibitors. MoMuLV CIS included an overlapping set of B ALL drivers including *Myc*, *Stat5b*, *Zeb2*, *Jak1*, *Jak3*, *Ikzf1*, *Gsdmc*, *Ebf1* and *Ptpn11*.

In another study multiple Cre strains (*Cd19*, *Mb1(Cd79a)* or *Mx1*) were used to induce conditional expression of a *E2A/PBX1* fusion, resulting in B cell precursor ALLs, which arrested at the pro B/large pre B II stages in a manner similar to human *E2A/PBX1* ALL (53). Copy number analyses and exome sequencing of leukemia samples revealed that 30% harbored inactivating mutations or deletion of *Pax5* that resulted in decreased expression. Combining *E2A/PBX1* with *Pax5* deletion increased the penetrance and shortened the latency of leukemia. Other mutated loci from *E2A/PBX1* tumors included *Cdkn2a*, *Jak1*, *Jak3*, *Ptpn11* and *Kras*.

The *ETV6/RUNX1*-SB model described in the previous section (43) was subsequently combined with heterozygous deletion of *Pax5* which increased the incidence of B-cell precursor (BCP)-ALL (45). Targeted exome sequencing identified recurrent mutations in *Jak3*, *Trp53* and *Jak1*, with *Jak1/3* mutations again being found in the pseudokinase domain. Insertional mutagenesis identified 6 CIS,

four of which (*Zfp423, Cblb, Stat5b and Foxp1*) have well-characterized roles in B cell maturation. Increased *ZNF423* expression is associated with *ETV6/RUNX1*+ B ALL and *Pax5* or *Ebf1* mutations synergize with *STAT5* in B ALL. It is worth noting this mutation profile is more likely a function of *Pax5* loss since a different model of *ETV6/RUNX1* with wild type *Pax5* primarily identified loss of function mutations in the KDM lysine demethylase family (55).

B ALL models have also been used to study the relationship between gut microbiota and leukemia incidence (52, 55, 61). *Pax5* heterozygous mice do not develop leukemia when housed in specific pathogen free (SPF) conditions however they are prone to precursor B ALL when exposed to common pathogens and sequencing of these leukemias identified recurrent *Jak3* mutations (52). In an independent study it was also shown that *Pax5* heterozygous mice or mice bearing a *Sca1-ETV6/RUNX1* transgene also do not develop B ALL when housed in SPF conditions. Nonetheless both mouse strains had sufficiently altered immune responses to alter the gut microbiome composition when housed in a non-SPF facility and *Pax5* heterozygous mice in SPF conditions treated with antibiotics developed B ALL (61). The authors hypothesize that dysbiosis caused by non-SPF housing or the absence a normal gut biome in SPF conditions with antibiotics drives disease on this background, however secondary mutations were also required. Exome sequencing of 17 B ALL cases from non-SPF conditions identified recurrent mutations affecting the JAK/STAT and RAS signaling pathways (*Jak1*, *Jak3*, and *Ptpn11*). Non-SPF mice treated with antibiotics also harbored recurrent mutations in *Kit*, *Flt3*, and *Cbl* that have not been observed in other $Pax5^{+/-}$ cohorts. This may suggest that selection of secondary mutations reflects differences in gut biome.

PAX5 is frequently mutated by translocation events creating fusion proteins in human tumors and some of these have been shown to cause B ALL in mice (58, 116). In one of these studies exome sequencing of five leukemic mice expressing a *PAX5/ENL* fusion identified mutations in *Ptpn11*, *Kras*, *Pax5*, and *Jak3* genes (58). Of these genes *PAX5, PTPN11*, *KRAS* and its homologue *NRAS* were found recurrently mutated across a panel of human B ALL samples from diverse subtypes.

These six independent studies using complementary experimental designs all identify mutations in *Jak3* by exome sequencing and in some cases also by insertional mutagenesis. Furthermore, four studies identified mutations in *Jak1*, three studies identified Ras family member mutations (albeit through different mechanisms) and four had *Ptpn11* mutations. Collectively this work demonstrates how mutagenesis and exome sequencing of mouse models with defined lesions can reliably and reproducibly reveal cooperating mutations in independent cohorts, and that *Pax5* heterozygosity in mice faithfully reproduces mutational profiles observed in human B ALL.

REVERSE GENETIC MODELS

Over the past decade the expanding number of candidate mutations associated with B cell malignancies has increased the requirement for medium to high throughput methods of validation. There is an extensive literature of transgenes, knockouts and conditional alleles for B cell lymphomas [reviewed in (117–121)]. Although tissue specific switching of conditional alleles is arguably the gold standard for mouse tumor models, the obvious drawback of this approach is the time taken to generate strains and cohorts of multiallelic models. In this section we discuss higher throughput reverse genetic models including transplantation/adoptive transfer models with an emphasis on models using primary cells transduced with viral constructs. We also summarize recently developed methods for rapid generation of multiallelic strains and several approaches to temporal control of gene expression.

B Cell Malignancy Models From Transplantation of Virus Transduced Cells

Early transplantation-based B cell malignancy models used cell lines derived from spontaneous malignancies injected into syngeneic hosts and/or human malignant cell lines injected as xenografts into immunocompromised mouse strains [reviewed in (122)]. More recently primary B cell malignancies have been transduced with viral constructs prior to transplantation, either to overexpress oncogenes (123–125) or to express shRNAs/sgRNAs that validate essential genes, therapeutic targets and tumor suppressors (126–134) (**Table 3**).

Primary B lymphomas have also been used to perform *in vivo* shRNA screens. In one study shRNAs against 1000 candidate cancer genes were selected to identify genes that are required for B lymphoma growth *in vivo* and this identified regulators of actin dynamics and cell motility (136). In a more targeted study, combining an *in vitro* screen with *in vivo* verification, conditional deletion of the *miR-17∼92* cluster was found to cause apoptosis in Eμ-*Myc* lymphomas. *In vitro* screening of shRNAs against targets of these microRNAs identified *Pten* suppression as a mediator of *miR-17∼92* survival signals which was verified when shRNAs against *Pten* rescued *in vivo* lymphoma growth of *miR-17∼92* deleted Eμ-*Myc* lymphoma cells (137).

Studying the transition of non-malignant cells into lymphomas and leukemias requires the use of untransformed primary cells. Retroviral transduction of primary cell suspensions from spleen, bone marrow and fetal liver can reveal the transforming potential of candidate genes and mutations. In early experiments both viral and cellular genes were found to facilitate colony formation in agar, clonal outgrowth of cell lines and development of malignancies from adoptive transfer into irradiated or immuno-compromised recipients [reviewed in (139, 140)]. The malignancy subtypes generated are a function of the genes being transduced and the lineage of infected cells, with B cell malignancies being successfully generated from wild type donor cells by using cellular genes (141, 142), acute transforming retrovirus oncogenes (143–147) and the fusion transcripts of oncogenic translocations (145, 148–152) (summarized in **Table 4**). Experiments using the mixed populations of cell types from whole bone marrow as donor cells can yield a mixture of malignancy subtypes from a single cohort. The use of purified

TABLE 3 | Reverse genetic B cell malignancy transplantation assays using primary lymphomas.

Publication	Donor lymphoma genotype	Recepient	Donor cell type	Genes delivered	Malignancy type
Schmitt CA et al. (123)	Eμ-Myc	syngeneic	primary B lymphoma	*Bcl2* ORF virus	B lymphoma
Schmitt CA et al. (124)	Eμ-Myc	syngeneic	primary B lymphoma	*Bcl2* ORF virus	B lymphoma
Schmitt CA et al. (125)	Eμ-Myc, Eμ-Myc;Trp53$^{+/-}$, Eμ-Myc;p19$^{ARF+/-}$ & Eμ-Myc;Cdkn2a/p19 $^{ARF+/-}$	syngeneic	primary B lymphoma & fetal liver derived HSPCs	*Bcl2*, Casp9 dominant negative *Cdkn2a* & *p19ARF* ORF viruses	B lymphoma
Schmitt CA et al. (135)	Eμ-Myc or Eμ-Myc;Trp53$^{+/-}$	syngeneic	primary B lymphoma & fetal liver derived HSPCs	*Bcl2* & *Casp9* dominant negative ORF viruses	B lymphoma
Refaeli Y et al. (126)	Eμ-Myc;BCR^{HEL} & Eμ-Myc;BCR^{HEL};sHEL	syngeneic	primary B lymphoma	Cd79a (Igα) & Cd79b (Igβ) shRNA virus	B lymphoma
Young RM et al. (127)	Eμ-Myc;BCR^{HEL} & Eμ-Myc;BCR^{HEL};sHEL	syngeneic	primary B lymphoma	*Syk* shRNA virus	B lymphoma
Meacham CE et al. (136)	Eμ-Myc;p19$^{ARF-/-}$	syngeneic	primary B lymphoma	1000 gene shRNA virus library	B lymphoma
Mu P et al. (137)	Eμ-Myc;miR-17~92$^{ff/ff}$;Rosa26-Cre-ER	athymic nude mice	primary B lymphoma	*Pten* shRNA & *miR-17~92* viruses	B lymphoma
Zuber J et al. (128)	Eμ-Myc;Trp53$^{-/-}$	syngeneic	primary B lymphoma	*Rpa3* shRNA viruses	B lymphoma
Malina A et al (138)	Eμ-Myc;p19$^{ARF-/-}$	syngeneic	primary B lymphoma	*Trp53* & *Rosa26* sgRNA viruses	B lymphoma
Cao Z et al. (129)	Eμ-Myc, B6RV2 leukemia cells, primary human Burkitt's lymphoma	syngeneic or NSG	primary B lymphoma or B leukemia cell line	*Notch1 Notch2 Hey1* & *Jag1* shRNA viruses	B lymphoma
Hoellein A et al. (130)	Eμ-Myc	syngeneic	primary B lymphoma	*Sae2* shRNA viruses	B lymphoma
Matthews GM et al. (131)	Eμ-Myc & Eμ-Myc;Hdac1$^{-/-}$	syngeneic	primary B lymphoma	*Hdac2* & *Hdac3* shRNA viruses	B lymphoma
Duque-Afonso et al. (132)	E2A-PBX1;CD19.Cre & E2A-PBX1;Mx1.Cre	syngeneic	primary B ALL	*Plcg2* shRNA virus	B ALL
Braun CJ et al. (134)	Eμ-Myc;p19$^{ARF-/-}$ & Bcr-Abl	syngeneic	primary B lymphoma	*Trp53*, *Chek2* & 25 gene library sgRNAs & dCas9/dCas9-VP64 viruses	B lymphoma & B ALL
Li X et al. (133)	Eμ-Myc;p19$^{ARF-/-}$	syngeneic	primary B lymphoma	*Utx* shRNA & *Efnb1* ORF virus	B lymphoma

TABLE 4 | Reverse genetic B cell malignancy transplantation assays using primary cells.

Publication	Donor primary cell genotype	Recipient	Donor cell type	Genes delivered	Malignancy type
Schwartz et al. (143)	wild type	syngeneic	bone marrow derived pre B cells & sIg+ B cells	v-*myc* & v-*H-ras* ORF viruses	B lymphoma
McLaughlin et al. (148)	wild type	syngeneic	bone marrow derived immature B cells	*BCR-ABL1* p210 ORF virus	B lymphoma
Heard et al. (144)	wild type	syngeneic	bone marrow	v-*fms* ORF virus	B cell lymphoma & erythroleukemia
Alexander et al. (153)	Eμ-*Myc*	nude mice	bone marrow	v-*H-ras* & v-*raf* ORF virus	B lineage subcutaneous tumors
Keliher et al. (145)	wild type	syngeneic	bone marrow	Abelson MuLV (v-*abl*) & *BCR-ABL1* p210 ORF virus	pre B cell lymphoma & myeloproliferative disease
Daley et al. (149)	wild type	syngeneic	bone marrow	*BCR-ABL1* p210 ORF virus	CML, B/T ALL & macrophage tumors
Elefanty et al. (150)	wild type	syngeneic	bone marrow	*BCR-ABL1* ORF virus	pre-B lymphoid, T lymphoid, macrophage, erythroid & mast cell tumors
Hawley et al. (146)	wild type	syngeneic	bone marrow	v-*H-Ras* ORF virus	pre-T-cell thymic lymphomas & pre-B-cell lymphoblastic leukemia/lymphomas
Kitayama et al. (141)	wild type ($Kit^{+/+}$)	$Kit^{W/W\text{-}v}$	bone marrow	Kit^{G599} & Kit^{V814} ORF viruses	B cell leukemia
Thome et al. (147)	wild type	syngeneic	bone marrow derived pre B cells	Abelson MuLV (v-*abl*)	B lymphoma
Kuefer et al. (151)	wild type	syngeneic	bone marrow	*NPM-ALK* fusion ORF virus	B lineage large-cell lymphoma
Hawley et al. (142)	wild type	syngeneic	bone marrow (5-FU-treated)	*Flt3* ORF virus	B cell and/or myeloid hematologic malignancies
Li et al. (152)	wild type	syngeneic	bone marrow (5-FU treated & untreated)	*BCR-ABL1* p190, p210 & p230 ORF viruses	CML, B ALL & macrophage tumors
Sexl et al. (154)	*wild type & Stat5a/b*$^{DeltaN/DeltaN}$	syngeneic	bone marrow	*BCR-ABL1*p210 & p185 ORF viruses	B cell & myeloid leukemia
Schmitt et al. (125)	Eμ-*Myc*, Eμ-*Myc*;*Trp53*$^{+/-}$, Eμ-*Myc*;*p19*$^{ARF+/-}$ & Eμ-*Myc*;*Cdkn2a/p19*$^{ARF+/-}$	syngeneic	primary B lymphoma & fetal liver derived HSPCs	*Bcl2*, Casp9 dominant negative *Cdkn2a* & *p19ARF* ORF viruses	B lymphoma
Schmitt et al. (135)	Eμ-*Myc* & Eμ-*Myc*;*Trp53*$^{+/-}$	syngeneic	primary B lymphoma & fetal liver derived HSPCs	*Bcl2 & Casp9* dominant negative ORF viruses	B lymphoma
Hemann et al. (155)	Eμ-*Myc*	syngeneic	fetal liver derived HSCs	*Trp53* shRNAs	B lymphoma
Hemann et al. (156)	Eμ-*Myc* & wild type	syngeneic	fetal liver derived HSCs	*Puma/Bbc3* shRNA virus	B lymphoma
Wendel et al. (157)	Eμ-*Myc*, Eμ-*Myc*;*p19*$^{ARF+/-}$ & Eμ-*Myc*;*Trp53*$^{+/-}$	syngeneic	fetal liver derived HSCs & primary B lymphoma	*Bcl2*, *Eif4e*, constitutive *Akt* & dominant negative *Casp9* ORF viruses	B lymphoma
Hu et al. (158)	wild type & *Lyn*$^{-/-}$;*Hck*$^{-/-}$;*Fgr*$^{-/-}$	syngeneic	bone marrow (5-FU-treated & untreated)	*BCR-ABL1* p210 ORF virus	CML & B ALL
Hemann et al. (159)	wild type, *Bim*$^{-/-}$, *Trp53*$^{+/-}$ & *Trp53*$^{-/-}$	syngeneic	fetal liver derived HSCs	*Myc* & *Myc* mutant ORF viruses	B lymphoma
He et al. (160)	Eμ-*Myc*	syngeneic	fetal liver derived HSCs	*mir-17–19b* microRNA virus	B lymphoma
Herbst et al. (161)	*Trp53*$^{+/-}$	syngeneic	fetal liver derived HSCs	*Myc* & *Myc* mutant ORF viruses	B lymphoma
Williams et al. (162)	wild type, *p19*$^{ARF+/-}$ & *p19*$^{ARF-/-}$	syngeneic	bone marrow derived pre B cells	*BCR-ABL1*p210 & p185 ORF viruses	B lympholeukemia
Hoelbl et al. (163)	wild type & *Stat5a/b*$^{-/-}$	*Rag2*$^{-/-}$	fetal liver cells & bone marrow	*BCR-ABL1* p185 ORF virus & Abelson MuLV (v-*abl*)	B lymphoid leukemia
Barabé et al. (164)	wild type (human)	NSG & B-NOD/SCID	human umbilical cord blood stem and progenitor cells (Lin– CB)	*MLL-ENL* (*KMT2A-MLLT1*) & *MLL-AF9* (*KMT2A-MLLT3*) ORF viruses	B precursor acute lymphomblastic leukemia & AML
Wang etal (165)	wild type, *Cdkn2a/p19*$^{ARF+/-}$ & *p19*$^{ARF-/-}$	syngeneic	bone marrow HSCs, common lymphoid progenitors, pro/pre B cells	*BCR-ABL1*p210 ORF virus	B ALL & CML
Bric et al. (166)	Eμ-*Myc*	syngeneic	fetal liver derived HSPCs	1000 gene shRNA virus library	B lymphoma
Hoelbl et al. (167)	*Stat5*$^{fl/fl}$ & *Mx1Cre*$^{+}$;*Stat5*$^{fl/fl}$	*Rag2*$^{-/-}$ $\gamma c^{-/-}$	bone marrow (5-FU treated & untreated)	*BCR-ABL1* p210 ORF virus & Abelson MuLV (v-abl)	B lymphoid leukemia & CML
Nakagawa et al. (168)	wild type	SCID	fetal liver derived pro B cells	*Bcl2*, *Myc* & *Ccnd1* ORF viruses & human ORF virus library	immature B cell lymphoma

(Continued)

TABLE 4 | Continued

Publication	Donor primary cell genotype	Recipient	Donor cell type	Genes delivered	Malignancy type
Bouquet et al. (169)	wild type	*Rag1*$^{-/-}$	fetal liver derived pre B cell lines	*Myc* & *Pim1* ORF viruses	pre B cell hyperplasia
Kovacic et al. (170)	wild type, *Mx1Cre*$^{+}$;*Stat5*$^{+/+}$ & Mx1Cre^{+}; *Stat5*$^{fl/fl}$	syngeneic	bone marrow, long-term HSCs, lymphoid-myeloid progenitors & HSC-depleted marrow	*BCR-ABL1*p210 & p185 ORF viruses	B acute lymphomblastic leukemia & CML
Leskov et al. (171)	wild type (human)	NSG	human umbilical cord blood derived CD133+ HSCs	*MYC* & *BCL2* ORF viruses	pre B cell lymphoma/leukemia
Arita et al. (172)	wild type	NSG	spleen derived induced germinal centre B cells	*Bcl2l1 (Bcl-xl)* & *Myc* ORF viruses	mature B cell lymphoma
Aubrey et al. (173)	Eμ-*Myc*	syngeneic	fetal liver derived HSPCs	*Trp53* sgRNA virus	B lymphoma
Ortega-Molina et al. (174)	VavP-*BCL2*	syngeneic	fetal liver derived HSCs	*Kmt2d* shRNA virus	B lymphoma
Scheicher et al. (175)	wild type & *Cdk6*$^{-/-}$	NSG	bone marrow	*BCR-ABL1*p210 ORF virus	B leukemia
Jiang et al. (176)	VavP-*BCL2*	syngeneic	fetal liver derived HSCs	*Crebbp* shRNA virus	B lymphoma
Katigbak et al. (177)	Eμ-*Myc*	syngeneic	fetal liver derived HSPCs	sgRNA virus library	B lymphoma
Wolf et al. (178)	*Myc*-GFP	*Rag1*$^{-/-}$	fetal liver derived pre B cell line	ORF virus library	B lymphoma
Wolf et al. (179)	GFP-rtTA	*Rag1*$^{-/-}$	fetal liver pre BI cells	*Myc* & *Bcl-xl* ORF viruses	plasmablast/plasma cell hyperplasia
van Oosterwijk et al. (180)	*wild type, p19*$^{ARF-/-}$, *p15*$^{smARF+/+}$ & *p15*$^{smArf-/-}$	syngeneic	bone marrow derived pre B cells	*BCR-ABL1* p185 ORF	B ALL
McHugh et al. (181)	wild type (human)	NSG	human fetal liver derived derived CD34+ hematopoietic progenitor cells	EBV & KSHV infection	B lymphoma
Reimer et al. (182)	wild type (human)	NSG	human cord blood derived HSPCs	*MLL*(*KMT2A*) & *ENL*(*MLLT1*) sgRNA viruses	B ALL & MLL
Lefebure et al. (54)	Eμ-*Myc*	syngeneic	fetal liver cells	*Trp53* & *Bcor* shRNA/sgRNA viruses	B lymphoma
Katigbak et al. (183)	Eμ-*Myc*;*Rosa26*-rtTA;*Col1A1*-TRE-Cas9-IRES-GFP/CAG-rtTA	syngeneic	fetal liver derived HSPCs	*Trp53* sgRNA virus	B lymphoma
Janic et al. (184)	Eμ-*Myc*, Eμ-*Myc;Bbc3*$^{-/-}$ & *Bbc3*$^{-/-}$; *Cdkn1a*$^{-/-}$	syngeneic	fetal liver derived HSPCs	*Trp53* sgRNA viruses & shRNA library viruses	B lymphoma
Jeong et al. (185)	wild type (human)	NSG	human cord blood derived HSPCs	*AF9*(*MLLT3*) & *MLL*(*KMT2A*) sgRNAs	B ALL, AML, or MPAL
Yin et al. (108)	*NUP98-PHF23*	syngeneic	fetal liver cells & bone marrow	*Bcor* shRNA/sgRNA viruses	progeniotor B1 acute lymphomblastic leukemia
Weber et al. (48)	Eμ-*Myc*;*Rosa26*-Cas9	syngeneic	fetal liver derived HSPCs	*Rfx7* & *Phip* sgRNA viruses	B lymphoma
Rajan et al. (186)	wild type	syngeneic	fetal liver derived HSCs	*Npm1* & *Alk* sgRNA plasmids	T & B anaplastic large cell lymphoma
Verma et al. (187)	wild type	syngeneic & *Mmp9*$^{-/-}$	bone marrow	*BCR-ABL1* ORF & *TNF* shRNA viruses	B acute lymphomblastic leukemia

target cells offers greater control of malignancy subtype, and protocols for the culture and transduction of purified HSCs, hematopoietic stem and precursor cells (HSPCs), B lineage precursors/progenitors and splenic B cells (188–190) have all been adapted to generate B lineage malignancies.

Combining both sensitized germline alleles with transduction of retroviruses also influences the cell type and developmental stage of the disease being modelled. One of the most frequently used strain to derive B cell malignancies by adoptive transfer of transduced cells is the Eμ-*Myc* model of Burkitt lymphoma (191). When bone marrow derived pre B cells from Eμ-*Myc* transgenic mice were transformed by transduction with v-*H-ras* or v-*raf*, the resulting clones forming subcutaneous tumors in nude mice (153). Later protocols using transplanted Eμ-*Myc* fetal liver cells (typically HSCs and HSPCs) yielded B cell lymphomas that could be accelerated by loss of tumor suppressors in the germline (e.g. *Trp53*, *Cdkn2a, p19^{ARF}*) and by retroviral expression of cooperating ORFs (125, 135, 157, 162). The use of fetal liver cells is particularly useful for the generation of lymphomas where one or more germline alleles prevent normal development after E17. This approach has been used to demonstrate that deletion of the essential mediators of apoptosis *Apaf1* and *Casp9* does not affect reconstitution by fetal liver HSCs (192) or alter the phenotype or latency of lymphomas derived from reconstitution by Eμ-*Myc* fetal liver HSCs (193).

Viral constructs capable of robust expression of short RNAs have facilitated rapid verification of putative tumor suppressors and oncogenic microRNAs. In an early study a series of *Trp53* shRNAs introduced into Eμ-*Myc* HSCs were found to accelerate lymphomagenesis in a manner that correlated with the strength of knockdown (155) and similar results were obtained for the *mir-17–19b* microRNA (160) and for shRNAs against *Puma* (*Bbc3*, a proapoptotic downstream target of *Trp53)* (156) and *Bcor* (a tumor suppressor of Burkitt lymphoma) (54). The Eμ-*Myc* model has also been used to screen pools of shRNAs against a set of 1000 known and putative cancer genes for tumor suppressor activity. Infecting fetal liver HSCs and transplanting them into recipients identified *Sfrp1*, *Numb*, *Mek1*, *Ang2* as tumor suppressors, as well as identifying known components of the DNA damage response machinery including *Rad17 (*166). A more focused shRNA screen of known targets of *Trp53* was conducted using fetal liver HSCs of mice that were either Eμ-*Myc Puma*-/- or *Cdkn1a*(*p21)*-/-*Puma*-/- in order to identify targets of p53 that were responsible for its tumor suppressor role independently of *Cdkn1a* or *Puma* (184). This identified a spectrum of shRNAs against DNA damage repair genes including *Mlh1*, *Msh2*, *Rnf144b*, *Cav1* and *Ddit4* which were capable of accelerating Eμ-*Myc* fetal liver HSC transplant lymphomas.

The most common strains used in these transplantation experiments are wild type mice, Eμ-*Myc* transgenics, *Trp53* mutants and *Cdkn2a*/*p19^{ARF}* mutants however many other strains have also been used to probe the cooperative or epistatic relationships of transduced genes with germline alleles (108, 158, 159, 161, 162, 165, 174–176, 180, 187) (summarized in **Table 4**). HSCs transduced with *Myc* retroviruses develop into aggressive pre B cell lymphomas when transplanted (159), and point mutants of *Myc* typically found in Burkitt's lymphoma increased penetrance and accelerated latency. Replacing wild type donor cells with *Trp53$^{-/+}$*, *Trp53$^{-/-}$* or *Bim$^{-/-}$* donor HSCs accelerates latency of wild type *Myc* more than *Myc* mutants, suggesting these mutations reduce *Myc* induced apoptosis mediated by *Trp53*/*Bim* and reduce selection for *Trp53* inactivation. Thus, epistatic effects and mutation redundancy can be rapidly investigated using germline alleles that predispose animals to disease.

Modelling the Genetics and Cell of Origin of *BCR/ABL* Leukemias

The "Philadelphia chromosome" translocation, t(9;22)(q34;q11), that expresses the *BCR/ABL1* translocation product is observed in both human CML and B ALL. Retroviral transduction of hematopoietic cells with the *BCR/ABL1* fusion transcript and transplantation into syngeneic recipients is one of the most extensively studied transplantation models in the literature. *BCR/ABL1* transduced bone marrow gives rise to various lineages of malignancies including, B lineage, myeloid and mixed lineage leukemias. Disease subtype and latency can be altered by varying donor cell lineage, genotype, culture protocols and the use of different *BCR/ABL1* isoforms. B lineage disease is particularly promoted by culture conditions that enhance pro/pre B differentiation and the use of the p185(p190) isoform (152, 170). Myeloid disease can be promoted by the p210 isoform and by pre-treating donor mice with 5-fluorouracil which depletes bone marrow of cycling cells and prompts cycling of quiescent HSCs (152, 170).

Mutations that determine which cell lineages can form different malignancy subtypes have been extensively studied using this model. Transplantation of purified HSCs transduced with *BCR/ABL1* retrovirus typically gives rise to CML, however loss of both *Cdkn2a/p19^{ARF}* or only *p19^{ARF}* in donor cells gives rise to B ALL (165). This is consistent with the observation of concomitant deletion of the *CDKN2A/p14^{ARF}* locus in human B ALL but not in CML. *p19^{ARF}* loss also enables B ALL to develop rapidly from *BCR/ABL1* transduced common lymphoid progenitors, pro B cells and pre B cells. Furthermore, *p19^{ARF}* null pro B cell derived disease was phenotypically different from wild type pro B cell derived disease which had substantially lower penetrance and delayed kinetics. When compared to *p19^{ARF}* null pro B cell derived disease, *p19^{ARF}* null HSC derived B ALL had greater colony forming potential in methylcellulose, greater resistance to dexamethasone and reduced resistance to the kinase inhibitor imatinib mesylate (Gleevec) (162, 165). Germline truncations of *p19^{ARF}* have also identified a specific region responsible for *Trp53* induction and suppression of *BCR/ABL1* leukemias (180).

These differences of *BCR/ABL1* driven disease in different lineages might suggest a separate cell of origin for B cell and myeloid disease, however using purified HSCs as donor cells suggests both CML and B ALL can arise from a long-term HSC cell of origin (170). In this model disease subtype is primarily

influenced by the use of different isoforms of *BCR/ABL1*, with the longer p210 isoform giving rise to CML whereas a shorter isoform p185 causes B ALL. Despite this common cell of origin, the cancer-propagating "cancer stem cell" populations responsible for maintaining these diseases appear to be distinct. The CML disease was maintained by a long-term HSC population whereas B ALL was maintained by a differentiated pro B population.

The interactions of *BCR/ABL1* with other donor cell lesions has also identified additional essential mediators of disease. *Stat5a* and *Stat5b* are necessary for establishment and maintenance of malignancies derived from *BCR/ABL1* infected bone marrow (163, 167) and N-terminal truncation of *Stat5a* and *Stat5b* skews *BCR/ABL1* p210 transplants toward a B cell lineage but *BCR/ABL1* p185 transplants are unaffected (154). *BCR/ABL* p210 fails to induce disease when using *Cdk6*$^{-/-}$ bone marrow, possibly due to defects in HSC cycling in these mice (175). *BCR/ABL1* transduced bone marrow lacking three Src kinases (*Lyn*$^{-/-}$;*Hck*$^{-/-}$;*Fgr*$^{-/-}$) resulted in delayed onset of B ALL compared with wild type donors however this delay was not seen for the onset of CML derived using 5-fluorouracil treated donors (158). This demonstrates a B lineage specific requirement of Src kinases for *BRC/ABL1* driven malignancies, and is consistent with synergy of pan Src kinase inhibitor CGP76030 with imatinib mesylate in treating *BCR/ABL1*-induced B ALL but not CML.

Collectively the above literature of *BCR/ABL1* malignancy models demonstrate how the genotype and developmental stage of transduced donor cells can alter disease subtype, clonogenicity and treatment response. These studies also demonstrate the value of transplantation models in defining the tumor initiating cell types of genetically similar (if not identical) but phenotypically distinct diseases.

Modelling Disease Derived From Specific Stages of B Cell Development

One disadvantage of using HSCs or mixed populations of bone marrow as donor cells is their potential to develop a wide spectrum of malignancy lineages from undefined developmental stages. Culture systems for *in vitro* expansion of B cell progenitors (189, 194, 195) have been further refined to use B220+Kit+ fetal liver cells cultured with IL-7 on ST-2 stromal cells (168) and more recently stroma free pro B cell culture conditions have also been developed using IL-7, SCF and FLT3 ligand (196). These systems allow expansion and transduction of progenitor/precursor B cells for use in transplantation studies. In one study, pro B cells were transduced with combinations of *Bcl2*, *Myc* and *Ccnd1*, and transplanted into severe combined immunodeficient (SCID) mice. The recipients develop an immature B cell lymphoma/leukemia which infiltrated the lymph nodes, spleen, thymus and bone marrow. *Ex vivo* cultured pro B cells transduced with *Bcl2* and *Myc* were also transduced with a cDNA library and selected for continued growth in the absence of IL-7 and ST-2 stromal cells. *CCND3* and *NRAS* both rendered these cultures independent of IL-7 and ST-2 cells and accelerated *Myc/Bcl2* driven disease when transplanted into SCID mice.

Long term proliferative pre B cell lines derived from fetal liver have also been used to identify and characterize genes that cooperate with *Myc* in an *in vivo* setting (195). Tetracycline inducible vectors expressing both *Myc* and *Pim1* have demonstrated an interdependent role of these genes in allowing *in vivo* expansion of pre B cell lines, and this expansion is dependent upon continued expression of both genes (169). In a similar study, doxycycline inducible *Myc* and *Bcl2l1* (*Bcl-xL*) pre BI cells were differentiated to immature B1 cells *in vitro*, and timed CpG stimulation generated either pre BII-like or mature B1-cell lines and IgM-secreting B1 cells. Introduction of these pre BI cells into *Rag1*$^{-/-}$ mice gives rise to plasmablast and plasma cell hyperplasia that was reversible when doxycycline was removed (179).

This model was also used to screen a library of cDNAs in pre B cell lines to identify genes that cooperate with *Myc* (178). Cells were selected *in vitro* in the absence of stromal cells and IL7 and *in vivo* by transplantation into *Rag1*$^{-/-}$ immunocompromised recipients. These screens identified multiple *Myc* cooperating genes including *Exosc1*, *Rpl18a*, *Rpl35a Ndufs7*, *Cacybp*, and *Ptprcap*. Overexpression of both a full length and truncated form of *Exosc1* (a component of the RNA exosome) were validated as cooperating with *Myc* and the authors proposed the mechanism is a function of global inhibition of mRNA degradation.

Later stages of B cell development can also be reproduced *in vitro*. Propagating naïve splenic B cells on a layer of 3T3 fibroblasts expressing both *CD40L* and *BAFF* causes them to proliferate into germinal center B cell like cells called *in-vitro*-induced germinal center B (iGB) cells (190). When iGB cells were cultured with IL-4 they differentiated toward memory B cell precursors and IL-21 steered differentiation to a long-lived plasma cell phenotype. Retroviral transduction of these iGB cells with *Myc* and *Bcl2* and transplantation into sublethally irradiated syngeneic recipients led to development of aggressive DLBCL like disease (172).

It is worth noting that *in vivo* library based screens of B cell biology need not be strictly limited to readouts of malignancy. Various models of B cell development and positive/negative selection of B cells are also relevant to malignancy. The IgMb-macroself mouse strain ubiquitously expresses a superantigen that causes deletion of immature B cells through reaction of surface IgM with a "self" superantigen. Transduction of bone marrow HSPCs with retroviruses encoding a miRNA expression library, and reconstitution of macroself recipients led to selection of cells expressing *miR-148a*, which was then verified to prevent deletion of self-reactive B cells (197).

The heavy chain of the B1-8^{hi} transgenic strain has an increased affinity to the 4-Hydroxy-3-nitrophenylacetyl (NP) hapten after immunization and this model has been used to screen for modifiers of germinal center formation. Splenic B cells from B1-8^{hi} transgenic mice were stimulated with anti-CD180 antibody, transduced with a library of shRNAs and transplanted into wild-type C57BL/6 mice (198). Recipients were then immunized with NP-chicken gamma globulin and alum to stimulate germinal center formation by the transplanted cells. Comparing the ratio of shRNA transduced B cells from germinal

centers to non-germinal center cells revealed selection against *Zdhhc2* shRNA, thereby demonstrating a role for this gene in productive germinal center formation. *Zdhhc2* shRNA also inhibited development of iGB cells *ex vivo*. Although these two studies do not model tumor development, they demonstrate how specific stages of B cell development can be probed using adoptive transfer of primary B cells to perform reverse genetic screens.

CRISPR-Cas Gene Editing in B Cell Malignancy Models

Various site-specific nucleases such as zinc finger nucleases, transcription activator-like effector nucleases (TALENs) and Cas endonucleases have been adapted to targeted editing of mammalian genomes (199). Since the proof of concept of CRISPR-Cas editing in mammalian cells (200, 201) this system has gained popularity primarily because the target site specificity is determined by a short guide RNA (sgRNA) sequence that includes a ~20 nucleotide segment that is complementary to the target site sequence. This property makes CRISPR-Cas targeting constructs easier to use than zinc finger nuclease and TALEN constructs which express large open reading frames and require longer sequences of protein encoded DNA binding motifs to determine target site specificity. There can also be gene/locus specific differences between the technologies, with TALENs demonstrating greater activity in heterochromatin and Cas9 greater activity in euchromatin (202).

The short targeting sequence of CRISPR-Cas endonucleases facilitates functional genomics experiments with a similar throughput to shRNA vectors, with the additional benefit of editing target alleles permanently rather than changing gene expression by lowering mRNA levels. Like shRNAs, sgRNAs can vary in their efficiency and off target effects. Double stranded DNA breaks created by SpCas9 are primarily repaired by nonhomologous end joining (NHEJ) which is an error prone process. Consequently, some earlier versions of CRISPR-Cas editing have been shown to create imprecise lesions. Depending on the delivery system used, a subset of target sites may generate deletions of thousands of bases, complex rearrangements and crossover events (203–207). Nonetheless, technical innovations including novel Cas variants and fusions, improved sgRNA design, optimized delivery methods and allele replacement by homologous recombination have reduced off target effects, increased efficiency, improved specificity and even permitted mutation of single bases (208–225).

CRISPR-Cas genome editing has been adapted to modelling a variety of tumor types either through loss of function mutations, chromosomal engineering or gain of expression [reviewed in (226, 227)]. CRISPR-Cas models of B cell malignancy are rare although there is now an extensive literature on conditions that increase the efficiency of editing primary B cells or HSCs. Some researchers use cells from mice expressing Cas9 and transduce these with viruses expressing sgRNAs (228–233). In one of these studies, activated B cells from mice expressing a Cre inducible Cas9 IRES GFP from the *Rosa26* locus were transduced with sgRNA viruses, achieving up to 80% knockout efficiency in cultured primary B cells (231). Another study transduced lipopolysaccharide (LPS) stimulated B cells expressing Cas9 from the *Rosa26* locus with virus expressing sgRNA and a puromycin resistance marker, followed by selection with puromycin to enrich for edited cells (230). Others have used Cas9 expressing Lineage- Sca-1+ Kit+ (LSK) HSCs from bone marrow, transduced these with lentivirus sgRNA constructs, yielding edited cells of multiple hematopoietic lineages in reconstituted recipients including B cells (232). B cell specificity has also been achieved *via* the transduction of LSK HSCs bearing a *Cre* switchable Cas9 under control of a CD19-*Cre* transgene (233). The knockout efficiency of target genes in CD34+ HSPCs from human cord blood can also be improved by changing the order of delivery and the sgRNA structure, and these cells remain transplantable into immunocompromised mice after transduction (234).

Editing can also be made more efficient by delivering Cas9 as a protein, as an mRNA or as a ribonuclear protein of Cas9 precomplexed with sgRNA [reviewed in (217)]. Activating culture conditions also play a role in efficient transduction of B cells. Human peripheral blood B cells can be expanded by IL4 and CD40L cross linking and then electroporated. Electroporation with *CD19* targeting sgRNAs in combination with either Cas9 RNA or Cas9 protein, can achieve knockout of *CD19* in up to 70% of cells (235). Mouse splenic B cells activated using LPS (as a TLR4/CD180 agonist), or human peripheral blood B cells activated by anti-CD180 antibody can be edited by electroporated Cas9/sgRNA ribonuclear protein combined with adeno associated virus templates (236) or transfection of Cas9/sgRNA ribonuclear protein with ssDNA template (237). Human peripheral B cells cultured in IL-2, IL-10, IL-15, multimerized CD40 ligand and CpG oligodeoxynucleotide are efficiently edited by electroporation with CRISPR/Cas9 ribonuclear protein and adeno associated virus template constructs (238).

Although CRISPR-Cas has not been used to study lymphoma and leukemia as often as shRNAs, the technology has proven utility in validation of tumor suppressor candidates. One of the earliest proof of concept experiments used a vector expressing both Cas9 and an sgRNA against *Trp53*. When established Eμ-*Myc p19*$^{ARF-/-}$ lymphomas were transduced and transplanted into recipients, lymphoma growth *in vivo* was accelerated (138). Another model used a vector constitutively expressing Cas9 with a doxycycline inducible vector expressing *Trp53* sgRNA in Eμ-*Myc* HSCs. This yielded rapid 100% penetrant disease where both *Trp53* alleles could be found modified by a range of insertions, indels, deletions and large deletions (173). A similar model was subsequently developed using a doxycycline inducible Cas9 transgene in donor cells (183).

Three of the forward genetic studies mentioned previously in this review used similar Eμ-*Myc* fetal liver HSC transplant models to verify the tumor suppressors *Bcor* (using a vector expressing both Cas9 and sgRNA) (54, 108) and *Rfx7* and *Phip* (combining a sgRNA vector with a Cas9 transgene) (48). Eμ-*Myc* HSCs have also been used to perform CRISPR-Cas9 functional genomic screens. In one study a library of 75 sgRNAs was designed against rarely mutated genes in Burkitt's lymphoma

and cloned into a Cas9 expressing vector. Pools of up to 5 sgRNAs were then transduced into Eμ-*Myc* fetal liver cells. Transduced cells were transplanted into irradiated recipients and when lymphomas developed, sgRNAs were quantitated by PCR and sequencing; genomic editing was then measured by T7 endonuclease I mismatch assays. Of the candidate sgRNAs identified by the screen *Phip* and *Sp3* were functionally validated as tumor suppressors using the same assay (177).

Cas/sgRNA targeting has also been expanded to the regulation of transcription by fusing nuclease deficient SpCas9 to transcriptional domains that either activate transcription (referred to as CRISPRa) or inhibit transcription (referred to as CRISPRi) (239). CRISPRi constructs have modified *in vivo* growth of primary Eμ-*Myc*;$p19^{ARF-/-}$ lymphoma and have been used to conduct an *in vivo* screen in *Bcr-Abl* driven B ALL (134). From a 25 gene library of sgRNAs, *Chk2* was identified as a modifier of temozolomide resistance.

CRISPR-Cas has also been used to engineer translocation events in somatic cells for mouse models of cancer. One of the earliest examples was induction of the *EML4/ALK* translocations in a lung cancer model (240) and since then CRISPR-Cas induced translocations have also been adapted to hematological malignancies, with a handful of models generating a subset of B lineage malignancies alongside other subtypes. One small study using mouse donor cells introduced SpCas9 and guide RNAs that translocate *Npm1* to *Alk* in mouse fetal liver HSCs. Transplanting these into recipients lead to two cases of T lineage ALK+ anaplastic large-cell lymphoma and one case of anaplastic ALK+ large B-cell lymphoma (186). Two studies discussed in the next section have also used CRISPR-Cas editing to cause malignancies by introducing these same translocations in human HSCs (182, 185).

Xenotransplantation Models of Human Leukemia

Human cord-blood derived HSCs have been used in a manner similar to mouse derived HSCs to generate adoptive transfer models of various hematologic malignancies. The t(11;19)(q23; p13.3) translocation produces the *MLL/ENL* (*KMT2A/MLLT1*) fusion and is found in acute leukemias of B, T and myeloid lineages. The t(9;11)(p21;q23) translocation produces the *MLL/AF9* (*KMT2A/MLLT3*) fusion and is primarily observed in childhood AML but also in a subset of ALL in children below 1 year of age. Lineage-depleted human umbilical cord blood infected with *MLL/ENL* virus gave rise to B precursor ALL when injected into sublethally irradiated NOD/LtSz-scid/scid mice (164). An *MLL/AF9* virus in the same model gives rise to a phenotypically similar B ALL and less frequently an AML like disease.

The lineage restriction of tumor initiating and tumor propagating cells was also investigated. The use of myeloid promoting suspension culture protocols skewed both transgenes toward a myeloid leukemia when injected. Transplantation of limiting cell numbers of primary tumors into secondary recipients indicated self-renewing leukemia cells were rare. Southern blots of retroviral vector integration and immunoglobulin heavy chain rearrangement suggested that leukemia initiating stem cells with germline immunoglobulin can differentiate into tumor propagating B lineage cell type having undergone immunoglobulin rearrangement. Lineage switching between B and myeloid lineages was also observed in culture.

More recently both translocations have been recreated in human HSCs using CRISPR-Cas. One model used CRISPR-Cas to induce the *MLL/AF9* (*KMT2A/MLLT3*) translocation in cultured human cord blood HSCs. Transplanting these cells into sublethally irradiated NSG mice gave rise to B ALL, acute myeloid leukemia or mixed phenotype acute leukemia, as well as mice with a mixture of AML/ALL (185). Another study induced CRISPR-Cas mediated translocations between *MLL*(*KMT2A*) and *ENL*(*MLLT1*) in human HSCs. When these cells were introduced to NSG mice, myeloid disease was most commonly observed however secondary outgrowths of B ALL were also identified (182).

Other B cell malignancies have also been modelled. Transducing human CD133+ HSCs with MYC^{T58A} mutant and *BCL2* from a lentiviral vector gives rise to a "double hit" lymphoma like disease when transplanted into NOD.*Cg-Prkdc*^{scid}*IL2rg*^{tm1Wjl}/SzJ (NSG) mice (171). NSG mice with a humanized lymphoid compartment can be generated by injecting human fetal liver CD34+ hematopoietic progenitor cells into 1 Gy irradiated NSG recipients and these mice can serve as a model for virus induced primary effusion lymphoma caused by coinfection with Kaposi sarcoma-associated herpesvirus and Epstein-Barr virus (181).

Rapid Generation of Germline Mutations

Historically, developing models using new germline alleles is time consuming. Traditional transgenesis by pronuclear injection of fertilized zygotes leads to unpredictable integration sites of unkown copy number. Gene targetting by homologous recombination in ES cells requires constructs with long homology arms and extensive screening and characterization of clones prior to blastocyst injection. Founder animals must then be crossed to verify germline transmission and to combine multiple alleles in sufficient animals to form experimental cohorts.

Higher throughput strategies to generating these models and cohorts have now been developed using various combinations of CRISPR-Cas, recombinase mediated cassette exchange and routine derivation of new ES cell lines from mice bearing multiple germline alleles [reviewed in (241)]. Superficially, generating null alleles by zygote injection of CRISPR-Cas components is less laborious and time consuming than generating constructs for allele replacement, targeting of ES cells and blastocyst injection. In practice however, the methods used to generate mouse strains have diversified and now vary considerably in the time taken to generate targeting constructs and/or the reliability and efficiency of allele generation.

One of the main advantages of CRISPR-Cas is that the targeting of multiple alleles simultaneously can disrupt both copies of a gene and/or disrupt multiple genes a single founder animal. Simultaneous CRISPR-Cas mutation of both germline alleles of B lymphoma tumor suppressors *Tet1* and *Tet2* have been achieved as inactivating mutations (242) and even

conditional loss of function alleles (243), potentially saving generations of breeding time in order to establish mutant cohorts. The efficiency of generating floxed alleles by injection of zygotes has been improved by the use of Cas9-avidin fusion with biotin tagged replacement template DNA (223). As mentioned previously some versions of CRISPR-Cas editing can generate imprecise lesions and off target effects (203–207). As such the speed gained from generating multiple CRISPR-Cas edited alleles simultaneously may be somewhat offset by the need for backcrossing and the need to repeat experiments using mice derived from independent founders. Where greater precision of allele generation is required (e.g. null alleles are lethal) the use of newly rederived ES cell lines from mouse strains carrying four or more alleles of interest offers an alternative for rapid generation of multiallelic models (244, 245).

CRISPR-Cas also potentially allows novel approaches to increase the throughput of gene editing of many alleles simultaneously (246). Multi sgRNA alleles can be generated by placing a lox71 site downstream of a U6 promoter and then downstream of this a concatemers of alternating sgRNA sequences with loxKR3 lox sites. LoxKR3 sites cannot combine with each other but can recombine with lox71. As such expression of Cre recombinase will lead to a single recombination event where only one of the sgRNA sequences chosen at random will be expressed in each cell. This allows Cre inducible sgRNA mosaicism that can be employed to study a range of genes in a single animal, or using germline switching the generation of many sgRNA strains from a single progenitor allele.

Temporal Control of Germline Alleles and Retroviral Constructs

Studies cited in previous sections drive specific disease subtypes through combinations of germline alleles, viral vectors and the cell types being cultured and transplanted. Additional control can also be achieved though vectors or alleles that are regulated by Cre recombinase or ligands such as doxycycline (for tetracycline regulatable promoters) and 4-hydroxytamoxifen (to regulate nuclear localization of estrogen receptor fusions) (247). Early regulatable models of lymphoma include mouse strains expressing human *MYC* from tetracycline/doxycycline regulatable promoters (248, 249) which develop T, B and myeloid lineage malignancies that regress upon doxycycline induced repression of *MYC* expression. A similar doxycycline repressible *BCL2* transgene when combined with the Eμ-*Myc* transgene gave rise to B lymphoblastic leukemia. These leukemias undergo remission upon repression of *BCL2* expression (250). Studies such as these demonstrate the continued requirement of cancer initiating oncogenes in tumor maintenance and thereby the potential of these proteins as therapeutic targets.

Similar regulation of shRNAs has also been achieved using tetracycline/doxycycline repressible germline alleles. Constitutive knockdown of the *Pax5* tumor suppressor by shRNA in combination with constitutively activated *STAT5b* causes a B ALL like disease (251). Repression of *Pax5* shRNA expression by doxycycline treatment removes a block in differentiation and when these established leukemias are transplanted into *Rag1*$^{-/-}$ recipients, doxycycline treatment causes remission of disease (251). An analogous model of tumor suppressor restoration is a mouse strain that fuses the carboxy terminus of the endogenous *Trp53* open reading frame to the estrogen receptor ligand binding domain. This fusion renders mice functionally *Trp53* null until treated with 4-hydroxytamoxifen (252). Restoring *Trp53* function in established Eμ-*Myc* lymphomas demonstrates the therapeutic potential for *Trp53* restoration (253), which is analogous to the stabilization of Trp53 by treatment with Mdm2/Mdmx inhibitors.

Constructs that express open reading frames or shRNAs from tetracycline/doxycycline regulatable promoters have been transduced into B cell lines or hematopoietic stem cells used for transplant studies (128, 254–258). Placing the expressed sequences of a retrovirus between tandem loxP sequences allows controlled expression of an invertible open reading frame cassette that is limited by lineage specific Cre expression (259). Viral vectors expressing doxycycline regulatable Cas9 (260) or sgRNAs (173) have also been developed. Aside from the previously mentioned strains expressing Cas9 under control of Cre recombinase (228, 233), several mouse strains have also been generated that place Cas9 under the control of tetracycline regulatable promoters (183, 261, 262). In one of these studies, the *Col1a1* locus was targetted in ES cells with a construct expressing multiple sgRNAs constitutively and a tetracycline/doxycyline regulatable Cas9 expression cassette. The resulting mice were crossed to mice with a reverse tetracycline transactivator allowing doxycycline controlled biallelic mutation of multiple genes in somatic cells using only two alleles (262).

CRISPRi gene regulation has similarly been placed under doxycycline control; Sp-dCas9 (nuclease deficient Cas9) is fused with the VP64 transactivation domain (i.e. four copies of the herpesvirus VP16 domain), the RELA p65 transactivation domain and the reverse tetracycline activation domain (263). This fusion has relatively low activity until cells are treated with doxycycline at which point the coexpression of sgRNA sequences causes activated expression of genes determined by the sgRNA target sequence.

CONCLUSIONS AND FUTURE DIRECTIONS

Human populations are highly polymorphic and this, in combination with the mutator phenotype generated by many tumours, can make it difficult to subtract the background noise of unselected passenger mutations from the evidence for driver mutations. The growing volume of human cancer genome sequencing data has created an exponentially expanding number of potential validation experiments. This in turn creates a prioritization bottleneck deciding which combinations of mutations should be tested and the developmental stages in which they should be modeled.

Forward genetics in mice can aid this prioritization by cross species comparative genomics i.e. identifying the overlap of mutation spectra identified between human and mouse cohorts. There is a tradeoff between the extent to which

forward genetic screens recapitulate human disease and the throughput of mutation detection. Exome sequencing arguably better mimics human tumor exomes, however insertional mutagenesis screens better represent the effects of translocation/copy number/non-coding mutations and are relatively lower cost and higher yield in terms of the number of driver mutations identified per mouse. This cost benefit analysis becomes relevant when considering the statistical limits of proving selection of non-coding point mutations from WGS of human cohorts. Insertional mutagenesis models also have greater statistical power to identify cooperating mutations, especially when sequencing coverage is sufficient to identify subclonal mutations.

Forward genetic screens in mice also have limitations. In some cases, the expected homologs of human drivers are not identified because functionally equivalent mutations that are specific to mice are identified instead. Another limitation of both forward and reverse genetic models is that the time frame for development of malignancies in mice is far shorter than observed in human lifespans. Consequently, predisposing mutations must be introduced and this in turn increases the chance of multiple clones arising independently in a single animal. Furthermore, Cre expressing strains used in some studies (such as Cd19 and Aicda) may replace the endogenous gene thereby altering the dosage of crucial B cell development genes.

Since the emphasis of this review is experimental approaches with higher throughput to identify and validate large numbers of candidate genes, for the most part we have not covered reverse genetic models that exclusively employ cohorts generated by germline alleles, which is a vast literature in and of itself. Rapid model prototyping using transplantation of virus transduced cells reduces the commitment of resources for initial testing of candidate genes. This allows more genes to be tested before robust germline models are designed and, in a handful of instances, allows for high throughput screens of dozens or even hundreds of candidate genes within a single cohort. This approach does, however, lack the precision of inducible targeted germline alleles and the dosage of transduced constructs can be highly variable and potentially reach expression levels not observed in human cells. Many cancer genes have physiological roles that are highly sensitive to dosage, and non-physiological expression levels from vectors may block or drive differentiation, sensitize cells to apoptosis or alter proliferation in a manner not typically observed as a result of somatic mutations.

Despite the number of labs working with B cell transplantation models, very few have published functional genomic screens where selection takes place *in vivo*. *In vivo* functional genomic screens are arguably a uniquely powerful application of adoptive transfer protocols, however in writing this review we only identified a limited number of studies using libraries of ORFs, shRNAs or gRNAs in B cell malignancy models. This would suggest that there is unrealized potential for more screens and/or that there are technical barriers to the reproducible identification of constructs selected in parallel. Functional genomic screens are a tradeoff between increasing the number of constructs screened whilst controlling for the stochasticity of selection of each construct relative to others in the library. B cell survival, migration, selection, differentiation and expansion are highly stochastic processes that may obscure selection in complex libraries. One approach to controlling for this stochasticity employed by several researchers is screening smaller pools of limited numbers of constructs to make selection of individual constructs easier to observe. Another approach to increasing confidence in the set of candidates identified in a screen is performing parallel screens using both shRNAs and sgRNAs to find genes that are selected by methodologies (264).

In aggregate, the studies discussed in this review suggest several lines of research that are ripe for further innovation. The literature of transplantation-based models is dominated by the use of Eμ-*Myc* fetal liver HSCs as donor cells (often in combination with mutation of *Trp53* or the *Cdkn2a* locus). Transplantation models could easily be diversified through the use of different germline lesions or culturing and transplanting later stages of B cell development. Many of the studies we discuss have successfully cultured and transduced primary B cells with high efficiency, though currently only a handful have used transplantation of transduced B cells as the basis of lymphoma models.

Another promising direction for future development is the use of humanized models of human HSCs transplanted into immunodeficient mice. Immunodeficient host strains vary considerably in their engraftment potential, and although most are missing later stages of B cell development, they can recapitulate earlier stages of lymphoid development and have formed the basis of useful models for lymphoblastic leukemias. Immunodeficient mouse strains have various defects in the hematopoietic microenvironment and/or stromal cell proteins that are incompatible with their human targets and this can inhibit engraftment. For instance, IL2 receptor common gamma chain null mice (including NSG mice) lack lymphoid tissue inducer cells and innate lymphoid cells and do not express HLA molecules on thymic epithelia thereby preventing MHC restriction of T cells. Some models also develop graft-versus-host disease. There now is a growing literature of newer humanized models that can better recapitulate all aspects of human hematopoiesis (265–268). Newer strains compensate for these deficiencies or enhance engraftment by transgenic expression of human proteins (including SCF, GM-CSF, IL3, SIRPA, HLA, B2M, TPO and TSLP). Other deficiencies can be partly compensated by co-engraftment of human HSCs with human mesenchymal stem/stromal cells. Although this review has mostly emphasized the use of models dissecting the biology and genetics of B cell malignancies, there is likely unrealized potential for transplant models in preclinical studies of treatment efficacy and/or identification of novel therapeutic targets.

Modelling the antigenic context of B cell malignancies is also rarely addressed in the literature. The role of antigenic stimulation or tolerization by commensal flora is frequently overlooked and SPF or germ free conditions may not accurately represent the microbiome of human cancer patients, particularly where disease is influenced by a combination of

normal gut flora and infectious agents, as is the case with *H.pylori* infection in MALT lymphoma (269).

Identification of human cancer drivers and the cell types that are most responsible for tumor initiation and propagation are critical foundations for the discovery of novel targeted therapies. The "post-genomic era" with seemingly limitless genomic data to interrogate has brought its own challenges of how to prioritize the use of this data. Modeling large numbers of mutations over the many stages of B cell development is a vast undertaking, particularly when differentiating between genes responsible for tumor initiation and maintenance and when testing potential targets across diverse genetic contexts of a single disease subtype. As such even the highest throughput experimental approaches discussed here can benefit from the parallel use of complementary methods.

AUTHOR CONTRIBUTIONS

All authors listed have made substantial, direct, and intellectual contribution to the work and approved it for publication.

FUNDING

JD and AU were supported by MRC programme grant MC_A652_5PZ20.

ACKNOWLEDGMENTS

We thank Andrej Alendar, Heather Verkade and Kira Behrens for critical reading of the manuscript.

REFERENCES

1. Willis TG, Dyer MJS. The Role of Immunoglobulin Translocations in the Pathogenesis of B-Cell Malignancies. *Blood* (2000) 96:808–22. doi: 10.1182/blood.V96.3.808
2. Husby S, Grønbæk K. Mature Lymphoid Malignancies: Origin, Stem Cells, and Chronicity. *Blood Adv* (2017) 1:2444–55. doi: 10.1182/bloodadvances.2017008854
3. Busslinger M, Klix N, Pfeffer P, Graninger PG, Kozmik Z. Deregulation of PAX-5 by Translocation of the Emu Enhancer of the IgH Locus Adjacent to Two Alternative PAX-5 Promoters in a Diffuse Large-Cell Lymphoma. *Proc Natl Acad Sci* (1996) 93:6129–34. doi: 10.1073/pnas.93.12.6129
4. Pasqualucci L, Neumeister P, Goossens T, Nanjangud G, Chaganti RS, Küppers R, et al. Hypermutation of Multiple Proto-Oncogenes in B-Cell Diffuse Large-Cell Lymphomas. *Nature* (2001) 412:341–6. doi: 10.1038/35085588
5. Küppers R. Mechanisms of B-Cell Lymphoma Pathogenesis. *Nat Rev Cancer* (2005) 5:251–62. doi: 10.1038/nrc1589
6. Basso K, Dalla-Favera R. Germinal Centres and B Cell Lymphomagenesis. *Nat Rev Immunol* (2015) 15:172–84. doi: 10.1038/nri3814
7. Pasqualucci L, Bhagat G, Jankovic M, Compagno M, Smith P, Muramatsu M, et al. AID Is Required for Germinal Center-Derived Lymphomagenesis. *Nat Genet* (2008) 40:108–12. doi: 10.1038/ng.2007.35
8. Khodabakhshi AH, Morin RD, Fejes AP, Mungall AJ, Mungall KL, Bolger-Munro M, et al. Recurrent Targets of Aberrant Somatic Hypermutation in Lymphoma. *Oncotarget* (2012) 3:1308–19. doi: 10.18632/oncotarget.653
9. Pasqualucci L, Guglielmino R, Malek SN, Novak U, Compagno M, Nanjangud G, et al. Aberrant Somatic Hypermutation Targets an Extensive Set of Genes in Diffuse Large B-Cell Lymphoma. *Blood* (2004) 104:1528–8. doi: 10.1182/blood.V104.11.1528.1528
10. Jäger U, Böcskor S, Le T, Mitterbauer G, Bolz I, Chott A, et al. Follicular Lymphomas' BCL-2/IgH Junctions Contain Templated Nucleotide Insertions: Novel Insights Into the Mechanism of T(14;18) Translocation. *Blood* (2000) 95:3520–9. doi: 10.1182/blood.V95.11.3520
11. Limpens J, Stad R, Vos C, De Vlaam C, De Jong D, Van Ommen GJB, et al. Lymphoma-Associated Translocation T(14;18) in Blood B Cells of Normal Individuals. *Blood* (1995) 85:2528–36. doi: 10.1182/blood.v85.9.2528.bloodjournal8592528
12. Damm F, Mylonas E, Cosson A, Yoshida K, Della Valle V, Mouly E, et al. Acquired Initiating Mutations in Early Hematopoietic Cells of CLL Patients. *Cancer Discovery* (2014) 4:1088–101. doi: 10.1158/2159-8290.CD-14-0104
13. Gahn B, Schäfer C, Neef J, Troff C, Feuring-Buske M, Hiddemann W, et al. Detection of Trisomy 12 and Rb-Deletion in CD34+ Cells of Patients With B-Cell Chronic Lymphocytic Leukemia. *Blood* (1997) 89:4275–81. doi: 10.1182/blood.V89.12.4275
14. Kikushige Y, Ishikawa F, Miyamoto T, Shima T, Urata S, Yoshimoto G, et al. Self-Renewing Hematopoietic Stem Cell Is the Primary Target in Pathogenesis of Human Chronic Lymphocytic Leukemia. *Cancer Cell* (2011) 20:246–59. doi: 10.1016/j.ccr.2011.06.029
15. Montgomery ND, Mathews SP. Transformation in Low-Grade B-Cell Neoplasms. *Surg Pathol Clin* (2016) 9:79–92. doi: 10.1016/j.path.2015.09.004
16. Chan JKC, Ng CS, Isaacson PG. Relationship Between High-Grade Lymphoma and Low-Grade B-Cell Mucosa-Associated Lymphoid Tissue Lymphoma (MALToma) of the Stomach. *Am J Pathol* (1990) 136:1153–64.
17. Peng H, Du M, Diss TC, Isaacson PG, Pan L. Genetic Evidence for a Clonal Link Between Low and High-Grade Components in Gastric MALT B-Cell Lymphoma. *Histopathology* (1997) 30:425–9. doi: 10.1046/j.1365-2559.1997.5450786.x
18. Al-Mansour M, Connors JM, Gascoyne RD, Skinnider B, Savage KJ. Transformation to Aggressive Lymphoma in Nodular Lymphocyte-Predominant Hodgkin's Lymphoma. *J Clin Oncol* (2010) 28:793–9. doi: 10.1200/JCO.2009.24.9516
19. Landgren O, Albitar M, Ma W, Abbasi F, Hayes RB, Ghia P, et al. Caporaso NE. B-Cell Clones as Early Markers for Chronic Lymphocytic Leukemia. *N Engl J Med* (2009) 360:659–67. doi: 10.1056/NEJMoa0806122
20. Weiss BM, Abadie J, Verma P, Howard RS, Kuehl WM. A Monoclonal Gammopathy Precedes Multiple Myeloma in Most Patients. *Blood* (2009) 113:5418–22. doi: 10.1182/blood-2008-12-195008
21. Landgren O, Kyle RA, Pfeiffer RM, Katzmann JA, Caporaso NE, Hayes RB, et al. Monoclonal Gammopathy of Undetermined Significance (MGUS) Consistently Precedes Multiple Myeloma: A Prospective Study. *Blood* (2009) 113:5412–7. doi: 10.1182/blood-2008-12-194241
22. van Lohuizen M, Verbeek S, Scheijen B, Wientjens E, van der Gulden H, Berns A. Identification of Cooperating Oncogenes in E Mu-Myc Transgenic Mice by Provirus Tagging. *Cell* (1991) 65:737–52. doi: 10.1016/0092-8674(91)90382-9
23. Haupt Y, Alexander WS, Barri G, Peter Klinken S, Adams JM. Novel Zinc Finger Gene Implicated as Myc Collaborator by Retrovirally Accelerated Lymphomagenesis in Eμ-Myc Transgenic Mice. *Cell* (1991) 65:753–63. doi: 10.1016/0092-8674(91)90383-A
24. Shinto Y, Morimoto M, Katsumata M, Uchida A, Aozasa K, Okamoto M, et al. Moloney Murine Leukemia Virus Infection Accelerates Lymphomagenesis in E Mu-Bcl-2 Transgenic Mice. *Oncogene* (1995) 11:1729–36.
25. van der Lugt NM, Domen J, Verhoeven E, Linders K, van der Gulden H, Allen J, et al. Proviral Tagging in E Mu-Myc Transgenic Mice Lacking the Pim-1 Proto-Oncogene Leads to Compensatory Activation of Pim-2. *EMBO J* (1995) 14:2536–44. doi: 10.1002/j.1460-2075.1995.tb07251.x
26. Sheppard RD, Samant SA, Rosenberg M, Silver LM, Cole MD. Transgenic N-Myc Mouse Model for Indolent B Cell Lymphoma: Tumor Characterization and Analysis of Genetic Alterations in Spontaneous and Retrovirally Accelerated Tumors. *Oncogene* (1998) 17:2073–85. doi: 10.1038/sj.onc.1202125
27. Mikkers H, Allen J, Knipscheer P, Romeijn L, Hart A, Vink E, et al. High-Throughput Retroviral Tagging to Identify Components of Specific Signaling Pathways in Cancer. *Nat Genet* (2002) 32:153–9. doi: 10.1038/ng950

28. Dang J, Wei L, de Ridder J, Su X, Rust AG, Roberts KG, et al. PAX5 Is a Tumor Suppressor in Mouse Mutagenesis Models of Acute Lymphoblastic Leukemia. *Blood* (2015) 125:3609–17. doi: 10.1182/blood-2015-02-626127
29. Webster P, Dawes JC, Dewchand H, Takacs K, Iadarola B, Bolt BJ, et al. Subclonal Mutation Selection in Mouse Lymphomagenesis Identifies Known Cancer Loci and Suggests Novel Candidates. *Nat Commun* (2018) 9:2649. doi: 10.1038/s41467-018-05069-9
30. Martín-Hernández J, Sørensen AB, Pedersen FS. Murine Leukemia Virus Proviral Insertions Between the N-Ras and Unr Genes in B-Cell Lymphoma DNA Affect the Expression of N-Ras Only. *J Virol* (2001) 75:11907–12. doi: 10.1128/JVI.75.23.11907-11912.2001
31. Ma SL, Sørensen AB, Kunder S, Sørensen KD, Quintanilla-Martinez L, Morris DW, et al. The Icsbp Locus Is a Common Proviral Insertion Site in Mature B-Cell Lymphomas/Plasmacytomas Induced by Exogenous Murine Leukemia Virus. *Virology* (2006) 352:306–18. doi: 10.1016/j.virol.2006.05.006
32. Sørensen AB, Lund AH, Kunder S, Quintanilla-Martinez L, Schmidt J, Wang B, et al. Impairment of Alternative Splice Sites Defining a Novel Gammaretroviral Exon Within Gag Modifies the Oncogenic Properties of Akv Murine Leukemia Virus. *Retrovirology* (2007) 4:46. doi: 10.1186/1742-4690-4-46
33. Liu J, Sørensen A, Wang B, Wabl M, Nielsen A, Pedersen F. Identification of Novel Bach2 Transcripts and Protein Isoforms Through Tagging Analysis of Retroviral Integrations in B-Cell Lymphomas. *BMC Mol Biol* (2009) 10:2. doi: 10.1186/1471-2199-10-2
34. Pyrz M, Wang B, Wabl M, Pedersen FS. A Retroviral Mutagenesis Screen Identifies Cd74 as a Common Insertion Site in Murine B-Lymphomas and Reveals the Existence of a Novel IFNgamma-Inducible Cd74 Isoform. *Mol Cancer* (2010) 9:86. doi: 10.1186/1476-4598-9-86
35. Hartley JW, Chattopadhyay SK, Lander MR, Taddesse-Heath L, Naghashfar Z, Morse HC, et al. Accelerated Appearance of Multiple B Cell Lymphoma Types in NFS/N Mice Congenic for Ecotropic Murine Leukemia Viruses. *Lab Investig* (2000) 80:159–69. doi: 10.1038/labinvest.3780020
36. Suzuki T, Shen H, Akagi K, Morse HC, Malley JD, Naiman DQ, et al. New Genes Involved in Cancer Identified by Retroviral Tagging. *Nat Genet* (2002) 32:166–74. doi: 10.1038/ng949
37. Tsuruyama T, Nakamura T, Jin G, Ozeki M, Yamada Y, Hiai H. Constitutive Activation of Stat5a by Retrovirus Integration in Early Pre-B Lymphomas of SL/Kh Strain Mice. *Proc Natl Acad Sci* (2002) 99:8253–8. doi: 10.1073/pnas.112202899
38. Jin G, Tsuruyama T, Yamada Y, Hiai H. Svi3: A Provirus Common Integration Site in C-Myc in SL/Kh Pre-B Lymphomas. *Cancer Sci* (2003) 94:791–5. doi: 10.1111/j.1349-7006.2003.tb01520.x
39. Shin MS, Fredrickson TN, Hartley JW, Suzuki T, Agaki K, Morse HC. High-Throughput Retroviral Tagging for Identification of Genes Involved in Initiation and Progression of Mouse Splenic Marginal Zone Lymphomas. *Cancer Res* (2004) 64:4419–27. doi: 10.1158/0008-5472.CAN-03-3885
40. Suzuki T, Minehata K, Akagi K, Jenkins NA, Copeland NG. Tumor Suppressor Gene Identification Using Retroviral Insertional Mutagenesis in Blm-Deficient Mice. *EMBO J* (2006) 25:3422–31. doi: 10.1038/sj.emboj.7601215
41. Weiser KC, Liu B, Hansen GM, Skapura D, Hentges KE, Yarlagadda S, et al. Retroviral Insertions in the VISION Database Identify Molecular Pathways in Mouse Lymphoid Leukemia and Lymphoma. *Mamm Genome* (2007) 18:709–22. doi: 10.1007/s00335-007-9060-2
42. Tsuruyama T, Imai Y, Takeuchi H, Hiratsuka T, Maruyama Y, Kanaya K, et al. Dual Retrovirus Integration Tagging: Identification of New Signaling Molecules Fiz1 and Hipk2 That Are Involved in the IL-7 Signaling Pathway in B Lymphoblastic Lymphomas. *J Leukoc Biol* (2010) 88:107–16. doi: 10.1189/jlb.1109748
43. van der Weyden L, Giotopoulos G, Rust AG, Matheson LS, van Delft FW, Kong J, et al. Modeling the Evolution of ETV6-RUNX1–induced B-Cell Precursor Acute Lymphoblastic Leukemia in Mice. *Blood* (2011) 118:1041–51. doi: 10.1182/blood-2011-02-338848
44. Zanesi N, Balatti V, Riordan J, Burch A, Rizzotto L, Palamarchuk A, et al. A Sleeping Beauty Screen Reveals NF-kB Activation in CLL Mouse Model. *Blood* (2013) 121:4355–8. doi: 10.1182/blood-2013-02-486035
45. van der Weyden L, Giotopoulos G, Wong K, Rust AG, Robles-Espinoza CD, Osaki H, et al. Somatic Drivers of B-ALL in a Model of ETV6-RUNX1; Pax5 (+/-) Leukemia. *BMC Cancer* (2015) 15:585. doi: 10.1186/s12885-015-1586-1
46. Heltemes-Harris LM, Larson JD, Starr TK, Hubbard GK, Sarver AL, Largaespada DA, et al. Sleeping Beauty Transposon Screen Identifies Signaling Modules That Cooperate With STAT5 Activation to Induce B-Cell Acute Lymphoblastic Leukemia. *Oncogene* (2016) 35:3454–64. doi: 10.1038/onc.2015.405
47. Rahrmann EP, Wolf NK, Otto GM, Heltemes-Harris L, Ramsey LB, Shu J, et al. Sleeping Beauty Screen Identifies RREB1 and Other Genetic Drivers in Human B-Cell Lymphoma. *Mol Cancer Res* (2019) 17:567–82. doi: 10.1158/1541-7786.MCR-18-0582
48. Weber J, de la Rosa J, Grove CS, Schick M, Rad L, Baranov O, et al. PiggyBac Transposon Tools for Recessive Screening Identify B-Cell Lymphoma Drivers in Mice. *Nat Commun* (2019) 10:1415. doi: 10.1038/s41467-019-09180-3
49. Sander S, Calado DP, Srinivasan L, Köchert K, Zhang B, Rosolowski M, et al. Synergy Between PI3K Signaling and MYC in Burkitt Lymphomagenesis. *Cancer Cell* (2012) 22:167–79. doi: 10.1016/j.ccr.2012.06.012
50. Sungalee S, Mamessier E, Morgado E, Grégoire E, Brohawn PZ, Morehouse CA, et al. Germinal Center Reentries of BCL2-Overexpressing B Cells Drive Follicular Lymphoma Progression. *J Clin Invest* (2014) 124:5337–51. doi: 10.1172/JCI72415
51. Gough SM, Goldberg L, Pineda M, Walker RL, Zhu YJ, Bilke S, et al. Spontaneous Mutations of Bcor and Jak1/2 Genes Lead to an Aggressive Leukemia of B-1 Progenitor B Cells. *Blood* (2014) 124:3573–3. doi: 10.1182/blood.V124.21.3573.3573
52. Martín-Lorenzo A, Hauer J, Vicente-Dueñas C, Auer F, González-Herrero I, García-Ramírez I, et al. Infection Exposure Is a Causal Factor in B-Cell Precursor Acute Lymphoblastic Leukemia as a Result of Pax5 -Inherited Susceptibility. *Cancer Discovery* (2015) 5:1328–43. doi: 10.1158/2159-8290.CD-15-0892
53. Duque-Afonso J, Feng J, Scherer F, Lin C-H, Wong SHK, Wang Z, et al. Comparative Genomics Reveals Multistep Pathogenesis of E2A-PBX1 Acute Lymphoblastic Leukemia. *J Clin Invest* (2015) 125:3667–80. doi: 10.1172/JCI81158
54. Lefebure M, Tothill RW, Kruse E, Hawkins ED, Shortt J, Matthews GM, et al. Genomic Characterisation of Eμ-Myc Mouse Lymphomas Identifies Bcor as a Myc Co-Operative Tumour-Suppressor Gene. *Nat Commun* (2017) 8:14581. doi: 10.1038/ncomms14581
55. Rodríguez-Hernández G, Hauer J, Martín-Lorenzo A, Schäfer D, Bartenhagen C, García-Ramírez I, et al. Infection Exposure Promotes ETV6-RUNX1 Precursor B-Cell Leukemia *via* Impaired H3K4 Demethylases. *Cancer Res* (2017) 77:4365–77. doi: 10.1158/0008-5472.CAN-17-0701
56. Gough SM, Goldberg L, Pineda M, Walker RL, Zhu YJ, Bilke S, et al. Progenitor B-1 B-Cell Acute Lymphoblastic Leukemia Is Associated With Collaborative Mutations in 3 Critical Pathways. *Blood Adv* (2017) 1:1749–59. doi: 10.1182/bloodadvances.2017009837
57. Mouly E, Ghamlouch H, Della-Valle V, Scourzic L, Quivoron C, Roos-Weil D, et al. B-Cell Tumor Development in Tet2-Deficient Mice. *Blood Adv* (2018) 2:703–14. doi: 10.1182/bloodadvances.2017014118
58. Jamrog L, Chemin G, Fregona V, Coster L, Pasquet M, Oudinet C, et al. PAX5-ELN Oncoprotein Promotes Multistep B-Cell Acute Lymphoblastic Leukemia in Mice. *Proc Natl Acad Sci* (2018) 115:10357–62. doi: 10.1073/pnas.1721678115
59. Zaborsky N, Gassner FJ, Höpner JP, Schubert M, Hebenstreit D, Stark R, et al. Exome Sequencing of the TCL1 Mouse Model for CLL Reveals Genetic Heterogeneity and Dynamics During Disease Development. *Leukemia* (2019) 33:957–68. doi: 10.1038/s41375-018-0260-4
60. Flümann R, Rehkämper T, Nieper P, Pfeiffer P, Holzem A, Klein S, et al. An Autochthonous Mouse Model of Myd88 - and BCL2 -Driven Diffuse Large B-Cell Lymphoma Reveals Actionable Molecular Vulnerabilities. *Blood Cancer Discovery* (2021) 2:70–91. doi: 10.1158/2643-3230.BCD-19-0059
61. Vicente-Dueñas C, Janssen S, Oldenburg M, Auer F, González-Herrero I, Casado-García A, et al. An Intact Gut Microbiome Protects Genetically Predisposed Mice Against Leukemia. *Blood* (2020) 136:2003–17. doi: 10.1182/blood.2019004381
62. Kool J, Berns A. High-Throughput Insertional Mutagenesis Screens in Mice to Identify Oncogenic Networks. *Nat Rev Cancer* (2009) 9:389–99. doi: 10.1038/nrc2647

63. Fan H. Leukemogenesis by Moloney Murine Leukemia Virus: A Multistep Process. *Trends Microbiol* (1997) 5:74–82. doi: 10.1016/S0966-842X(96)10076-7
64. Hanecak R, Pattengale PK, Fan H. Addition of Substitution of Simian Virus 40 Enhancer Sequences Into the Moloney Murine Leukemia Virus (M-MuLV) Long Terminal Repeat Yields Infectious M-MuLV With Altered Biological Properties. *J Virol* (1988) 62:2427–36. doi: 10.1128/JVI.62.7.2427-2436.1988
65. Lovmand J, Sorensen AB, Schmidt J, Ostergaard M, Luz A, Pedersen FS. B-Cell Lymphoma Induction by Akv Murine Leukemia Viruses Harboring One or Both Copies of the Tandem Repeat in the U3 Enhancer. *J Virol* (1998) 72:5745–56. doi: 10.1128/JVI.72.7.5745-5756.1998
66. Sørensen KD, Kunder S, Quintanilla-Martinez L, Sørensen J, Schmidt J, Pedersen FS. Enhancer Mutations of Akv Murine Leukemia Virus Inhibit the Induction of Mature B-Cell Lymphomas and Shift Disease Specificity Towards the More Differentiated Plasma Cell Stage. *Virology* (2007) 362:179–91. doi: 10.1016/j.virol.2006.12.016
67. Mucenski ML, Bedigian HG, Shull MM, Copeland NG, Jenkins NA. Comparative Molecular Genetic Analysis of Lymphomas From Six Inbred Mouse Strains. *J Virol* (1988) 62:839–46. doi: 10.1128/jvi.62.3.839-846.1988
68. Yamada Y, Matsushiro H, Ogawa MS, Okamoto K, Nakakuki Y, Toyokuni S, et al. Genetic Predisposition to Pre-B Lymphomas in SL/Kh Strain Mice. *Cancer Res* (1994) 54:403–7.
69. Gilbert DJ, Neumann PE, Taylor BA, Jenkins NA, Copeland NG. Susceptibility of AKXD Recombinant Inbred Mouse Strains to Lymphomas. *J Virol* (1993) 67:2083–90. doi: 10.1128/jvi.67.4.2083-2090.1993
70. Fredrickson TN, Morse HC, Rowe WP. Spontaneous Tumors of NFS Mice Congenic for Ecotropic Murine Leukemia Virus Induction Loci2. *JNCI J Natl Cancer Inst* (1984) 73:521–4. doi: 10.1093/jnci/73.2.521
71. Fredrickson TN, Morse HC, Yetter RA, Rowe WP, Hartley JW, Pattengale PK. Multiparameter Analyses of Spontaneous Nonthymic Lymphomas Occurring in NFS/N Mice Congenic for Ecotropic Murine Leukemia Viruses. *Am J Pathol* (1985) 121:349–60.
72. Beckmann PJ, Largaespada DA. Transposon Insertion Mutagenesis in Mice for Modeling Human Cancers: Critical Insights Gained and New Opportunities. *Int J Mol Sci* (2020) 21:1172. doi: 10.3390/ijms21031172
73. Kawakami K, Largaespada DA, Ivics Z. Transposons As Tools for Functional Genomics in Vertebrate Models. *Trends Genet* (2017) 33:784–801. doi: 10.1016/j.tig.2017.07.006
74. O'Donnell KA. Advances in Functional Genetic Screening With Transposons and CRISPR/Cas9 to Illuminate Cancer Biology. *Curr Opin Genet Dev* (2018) 49:85–94. doi: 10.1016/j.gde.2018.03.006
75. Kuiper RP, Schoenmakers EFPM, van Reijmersdal SV, Hehir-Kwa JY, van Kessel AG, van Leeuwen FN, et al. High-Resolution Genomic Profiling of Childhood ALL Reveals Novel Recurrent Genetic Lesions Affecting Pathways Involved in Lymphocyte Differentiation and Cell Cycle Progression. *Leukemia* (2007) 21:1258–66. doi: 10.1038/sj.leu.2404691
76. Mullighan CG, Goorha S, Radtke I, Miller CB, Coustan-Smith E, Dalton JD, et al. Genome-Wide Analysis of Genetic Alterations in Acute Lymphoblastic Leukaemia. *Nature* (2007) 446:758–64. doi: 10.1038/nature05690
77. Mansouri L, Papakonstantinou N, Ntoufa S, Stamatopoulos K, Rosenquist R. NF-κb Activation in Chronic Lymphocytic Leukemia: A Point of Convergence of External Triggers and Intrinsic Lesions. *Semin Cancer Biol* (2016) 39:40–8. doi: 10.1016/j.semcancer.2016.07.005
78. Zapata JM, Krajewska M, Morse HC, Choi Y, Reed JC. TNF Receptor-Associated Factor (TRAF) Domain and Bcl-2 Cooperate to Induce Small B Cell Lymphoma/Chronic Lymphocytic Leukemia in Transgenic Mice. *Proc Natl Acad Sci* (2004) 101:16600–5. doi: 10.1073/pnas.0407541101
79. Pérez-Chacón G, Llobet D, Pardo C, Pindado J, Choi Y, Reed JC, et al. TNFR-Associated Factor 2 Deficiency in B Lymphocytes Predisposes to Chronic Lymphocytic Leukemia/Small Lymphocytic Lymphoma in Mice. *J Immunol* (2012) 189:1053–61. doi: 10.4049/jimmunol.1200814
80. Pérez-Chacón G, Zapata JM. Mouse Models of Chronic Lymphocytic Leukemia. In: Oppezzo P (Ed.) *Chronic Lymphocytic Leukemia*. London, United Kingdom: IntechOpen Limited (2012)
81. Lenz G, Wright GW, Emre NCT, Kohlhammer H, Dave SS, Davis RE, et al. Molecular Subtypes of Diffuse Large B-Cell Lymphoma Arise by Distinct Genetic Pathways. *Proc Natl Acad Sci* (2008) 105:13520–5. doi: 10.1073/pnas.0804295105
82. Pfeifer M, Lenz G. PI3K/AKT Addiction in Subsets of Diffuse Large B-Cell Lymphoma. *Cell Cycle* (2013) 12:3347–8. doi: 10.4161/cc.26575
83. Bronner IF, Otto TD, Zhang M, Udenze K, Wang C, Quail MA, et al. Quantitative Insertion-Site Sequencing (QIseq) for High Throughput Phenotyping of Transposon Mutants. *Genome Res* (2016) 26:980–9. doi: 10.1101/gr.200279.115
84. Arnold C, Hodgson IJ. Vectorette PCR: A Novel Approach to Genomic Walking. *Genome Res* (1991) 1:39–42. doi: 10.1101/gr.1.1.39
85. Devon RS, Porteous DJ, Brookes AJ. Splinkerettes—improved Vectorettes for Greater Efficiency in PCR Walking. *Nucleic Acids Res* (1995) 23:1644–5. doi: 10.1093/nar/23.9.1644
86. Hui EKWW, Wang PC, Lo SJ. Strategies for Cloning Unknown Cellular Flanking DNA Sequences From Foreign Integrants. *Cell Mol Life Sci* (1998) 54:1403–11. doi: 10.1007/s000180050262
87. Koudijs MJ, Klijn C, van der Weyden L, Kool J, ten Hoeve J, Sie D, et al. High-Throughput Semiquantitative Analysis of Insertional Mutations in Heterogeneous Tumors. *Genome Res* (2011) 21:2181–9. doi: 10.1101/gr.112763.110
88. Sherman E, Nobles C, Berry CC, Six E, Wu Y, Dryga A, et al. INSPIIRED: A Pipeline for Quantitative Analysis of Sites of New DNA Integration in Cellular Genomes. *Mol Ther Methods Clin Dev* (2017) 4:39–49. doi: 10.1016/j.omtm.2016.11.002
89. Berry CC, Gillet NA, Melamed A, Gormley N, Bangham CRM, Bushman FD. Estimating Abundances of Retroviral Insertion Sites From DNA Fragment Length Data. *Bioinformatics* (2012) 28:755–62. doi: 10.1093/bioinformatics/bts004
90. Mann KM, Newberg JY, Black MA, Jones DJ, Amaya-Manzanares F, Guzman-Rojas L, et al. Analyzing Tumor Heterogeneity and Driver Genes in Single Myeloid Leukemia Cells With SBCapSeq. *Nat Biotechnol* (2016) 34:962–72. doi: 10.1038/nbt.3637
91. Mann M, Mann KM, Guzman-Rojas L, Amaya-Manzanares F, Jones DJ, Newberg JY, et al. SBCapSeq Protocol: A Method for Selective Cloning of Sleeping Beauty Transposon Insertions Using Liquid Capture Hybridization and Ion Torrent Semiconductor Sequencing. *Protoc Exch* (2016). doi: 10.1038/protex.2016.053
92. Dawes JC, Webster P, Iadarola B, Garcia-Diaz C, Dore M, Bolt BJ, et al. LUMI-PCR: An Illumina Platform Ligation-Mediated PCR Protocol for Integration Site Cloning, Provides Molecular Quantitation of Integration Sites. *Mob DNA* (2020) 11:7. doi: 10.1186/s13100-020-0201-4
93. Huser CA, Gilroy KL, de Ridder J, Kilbey A, Borland G, Mackay N, et al. Insertional Mutagenesis and Deep Profiling Reveals Gene Hierarchies and a Myc/p53-Dependent Bottleneck in Lymphomagenesis. *PloS Genet* (2014) 10:e1004167. doi: 10.1371/journal.pgen.1004167
94. van Galen P, Hovestadt V, Wadsworth MHII, Hughes TK, Griffin GK, Battaglia S, et al. Single-Cell RNA-Seq Reveals AML Hierarchies Relevant to Disease Progression and Immunity. *Cell* (2019) 176:1265–1281.e24. doi: 10.1016/j.cell.2019.01.031
95. Wu J, Xiao Y, Sun J, Sun H, Chen H, Zhu Y, et al. A Single-Cell Survey of Cellular Hierarchy in Acute Myeloid Leukemia. *J Hematol Oncol* (2020) 13:128. doi: 10.1186/s13045-020-00941-y
96. Petti AA, Williams SR, Miller CA, Fiddes IT, Srivatsan SN, Chen DY, et al. A General Approach for Detecting Expressed Mutations in AML Cells Using Single Cell RNA-Sequencing. *Nat Commun* (2019) 10:3660. doi: 10.1038/s41467-019-11591-1
97. Miles LA, Bowman RL, Merlinsky TR, Csete IS, Ooi AT, Durruthy-Durruthy R, et al. Single-Cell Mutation Analysis of Clonal Evolution in Myeloid Malignancies. *Nature* (2020) 587:477–82. doi: 10.1038/s41586-020-2864-x
98. de Ridder J, Uren A, Kool J, Reinders M, Wessels L. Detecting Statistically Significant Common Insertion Sites in Retroviral Insertional Mutagenesis Screens. *PloS Comput Biol* (2006) 2:e166. doi: 10.1371/journal.pcbi.0020166
99. Sarver AL, Erdman J, Starr T, Largaespada DA, Silverstein KAT. TAPDANCE: An Automated Tool to Identify and Annotate Transposon Insertion CISs and Associations Between CISs From Next Generation Sequence Data. *BMC Bioinf* (2012) 13:134. doi: 10.1186/1471-2105-13-154
100. de Jong J, de Ridder J, van der Weyden L, Sun N, van Uitert M, Berns A, et al. Computational Identification of Insertional Mutagenesis Targets for Cancer Gene Discovery. *Nucleic Acids Res* (2011) 39:e105–5. doi: 10.1093/nar/gkr447

101. de Jong J, Akhtar W, Badhai J, Rust AG, Rad R, Hilkens J, et al. Chromatin Landscapes of Retroviral and Transposon Integration Profiles. *PloS Genet* (2014) 10:e1004250. doi: 10.1371/journal.pgen.1004250
102. Uren AG, Kool J, Matentzoglu K, de Ridder J, Mattison J, van Uitert M, et al. Large-Scale Mutagenesis in P19arf- and P53-Deficient Mice Identifies Cancer Genes and Their Collaborative Networks. *Cell* (2008) 133:727–41. doi: 10.1016/j.cell.2008.03.021
103. Kool J, Uren AG, Martins CP, Sie D, de Ridder J, Turner G, et al. Insertional Mutagenesis in Mice Deficient for p15Ink4b, p16Ink4a, p21Cip1, and p27Kip1 Reveals Cancer Gene Interactions and Correlations With Tumor Phenotypes. *Cancer Res* (2010) 70:520–31. doi: 10.1158/0008-5472.CAN-09-2736
104. Quivoron C, Couronné L, Della Valle V, Lopez CK, Plo I, Wagner-Ballon O, et al. TET2 Inactivation Results in Pleiotropic Hematopoietic Abnormalities in Mouse and Is a Recurrent Event During Human Lymphomagenesis. *Cancer Cell* (2011) 20:25–38. doi: 10.1016/j.ccr.2011.06.003
105. Dominguez PM, Ghamlouch H, Rosikiewicz W, Kumar P, Béguelin W, Fontán L, et al. TET2 Deficiency Causes Germinal Center Hyperplasia, Impairs Plasma Cell Differentiation, and Promotes B-Cell Lymphomagenesis. *Cancer Discovery* (2018) 8:1632–53. doi: 10.1158/2159-8290.CD-18-0657
106. Cimmino L, Dawlaty MM, Ndiaye-Lobry D, Yap YS, Bakogianni S, Yu Y, et al. TET1 Is a Tumor Suppressor of Hematopoietic Malignancy. *Nat Immunol* (2015) 16:653–62. doi: 10.1038/ni.3148
107. Li H, Kaminski MS, Li Y, Yildiz M, Ouillette P, Jones SSS, et al. Mutations in Linker Histone Genes HIST1H1 B, C, D, and E; OCT2 (POU2F2); IRF8; and ARID1A Underlying the Pathogenesis of Follicular Lymphoma. *Blood* (2014) 123:1487–98. doi: 10.1182/blood-2013-05-500264
108. Yin M, Chung YJ, Lindsley RC, Walker RL, Zhu YJ, Ebert BL, et al. Engineered Bcor Mutations Lead to Acute Leukemia of Progenitor B-1 Lymphocyte Origin in a Sensitized Background. *Blood* (2019) 133:2610–4. doi: 10.1182/blood.2018864173
109. Familiades J, Bousquet M, Lafage-Pochitaloff M, Béné M-C, Beldjord K, De Vos J, et al. PAX5 Mutations Occur Frequently in Adult B-Cell Progenitor Acute Lymphoblastic Leukemia and PAX5 Haploinsufficiency Is Associated With BCR-ABL1 and TCF3-PBX1 Fusion Genes: A GRAALL Study. *Leukemia* (2009) 23:1989–98. doi: 10.1038/leu.2009.135
110. Coyaud E, Struski S, Prade N, Familiades J, Eichner R, Quelen C, et al. Wide Diversity of PAX5 Alterations in B-ALL: A Groupe Francophone De Cytogénétique Hématologique Study. *Blood* (2010) 115:3089–97. doi: 10.1182/blood-2009-07-234229
111. Bastian L, Schroeder MP, Eckert C, Schlee C, Tanchez JO, Kämpf S, et al. PAX5 Biallelic Genomic Alterations Define a Novel Subgroup of B-Cell Precursor Acute Lymphoblastic Leukemia. *Leukemia* (2019) 33:1895–909. doi: 10.1038/s41375-019-0430-z
112. Shah S, Schrader KA, Waanders E, Timms AE, Vijai J, Miething C, et al. A Recurrent Germline PAX5 Mutation Confers Susceptibility to Pre-B Cell Acute Lymphoblastic Leukemia. *Nat Genet* (2013) 45:1226–31. doi: 10.1038/ng.2754
113. Auer F, Rüschendorf F, Gombert M, Husemann P, Ginzel S, Izraeli S, et al. Inherited Susceptibility to Pre B-ALL Caused by Germline Transmission of PAX5 C.547G<A. *Leukemia* (2014) 28:1136–8. doi: 10.1038/leu.2013.363
114. Yazdanparast S, Khatami SR, Galehdari H, Jaseb K. One Missense Mutation in Exon 2 of the PAX5 Gene in Iran. *Genet Mol Res* (2015) 14:17768–75. doi: 10.4238/2015.December.22.1
115. Duployez N, Jamrog LA, Fregona V, Hamelle C, Fenwarth L, Lejeune S, et al. Germline PAX5 Mutation Predisposes to Familial B-Cell Precursor Acute Lymphoblastic Leukemia. *Blood* (2021) 137:1424–8. doi: 10.1182/blood.2020005756
116. Smeenk L, Fischer M, Jurado S, Jaritz M, Azaryan A, Werner B, et al. Molecular Role of the PAX 5- ETV 6 Oncoprotein in Promoting B-Cell Acute Lymphoblastic Leukemia. *EMBO J* (2017) 36:718–35. doi: 10.15252/embj.201695495
117. Tarantul V. Transgenic Mice as an In Vivo Model of Lymphomagenesis. *Int Rev Cytol* (2004) 236:123–80. doi: 10.1016/S0074-7696(04)36004-3
118. You MJ. Mouse Models of Lymphoma and Lymphoid Leukemia. In: *Neoplastic Hematopathology*. Totowa, NJ: Humana Press. (2009) p. 583–96. doi: 10.1007/978-1-60761-384-8_36
119. Kohnken R, Porcu P, Mishra A. Overview of the Use of Murine Models in Leukemia and Lymphoma Research. *Front Oncol* (2017) 7:22. doi: 10.3389/fonc.2017.00022
120. Mossadegh-Keller N, Brisou G, Beyou A, Nadel B, Roulland S. Human B Lymphomas Reveal Their Secrets Through Genetic Mouse Models. *Front Immunol* (2021) 12:683597. doi: 10.3389/fimmu.2021.683597
121. Pasqualucci L, Meyer SN, Koul S. Mouse Models in the Study of Germinal Center Derived B-Cell Malignancies. *Front Immunol* (2021) 12:710711. doi: 10.3389/fimmu.2021.710711
122. Donnou S, Galand C, Touitou V, Sautès-Fridman C, Fabry Z, Fisson S. Murine Models of B-Cell Lymphomas: Promising Tools for Designing Cancer Therapies. *Adv Hematol* (2012) 2012:1–13. doi: 10.1155/2012/701704
123. Schmitt CA, Rosenthal CT, Lowe SW. Genetic Analysis of Chemoresistance in Primary Murine Lymphomas. *Nat Med* (2000) 6:1029–35. doi: 10.1038/79542
124. Schmitt CA, Lowe SW. Bcl-2 Mediates Chemoresistance in Matched Pairs of Primary Eμ-Myc Lymphomas *In Vivo*. *Blood Cells Mol Dis* (2001) 27:206–16. doi: 10.1006/bcmd.2000.0372
125. Schmitt CA, Fridman JS, Yang M, Lee S, Baranov E, Hoffman RM, et al. A Senescence Program Controlled by P53 and P16ink4a Contributes to the Outcome of Cancer Therapy. *Cell* (2002) 109:335–46. doi: 10.1016/s0092-8674(02)00734-1
126. Refaeli Y, Young RM, Turner BC, Duda J, Field KA, Bishop JM. The B Cell Antigen Receptor and Overexpression of MYC Can Cooperate in the Genesis of B Cell Lymphomas. *PloS Biol* (2008) 6:e152. doi: 10.1371/journal.pbio.0060152
127. Young RM, Hardy IR, Clarke RL, Lundy N, Pine P, Turner BC, et al. Mouse Models of Non-Hodgkin Lymphoma Reveal Syk as an Important Therapeutic Target. *Blood* (2009) 113:2508–16. doi: 10.1182/blood-2008-05-158618
128. Zuber J, McJunkin K, Fellmann C, Dow LE, Taylor MJ, Hannon GJ, et al. Toolkit for Evaluating Genes Required for Proliferation and Survival Using Tetracycline-Regulated RNAi. *Nat Biotechnol* (2011) 29:79–83. doi: 10.1038/nbt.1720
129. Cao Z, Ding B-S, Guo P, Lee SB, Butler JM, Casey SC, et al. Angiocrine Factors Deployed by Tumor Vascular Niche Induce B Cell Lymphoma Invasiveness and Chemoresistance. *Cancer Cell* (2014) 25:350–65. doi: 10.1016/j.ccr.2014.02.005
130. Hoellein A, Fallahi M, Schoeffmann S, Steidle S, Schaub FX, Rudelius M, et al. Myc-Induced SUMOylation Is a Therapeutic Vulnerability for B-Cell Lymphoma. *Blood* (2014) 124:2081–90. doi: 10.1182/blood-2014-06-584524
131. Matthews GM, Mehdipour P, Cluse LA, Falkenberg KJ, Wang E, Roth M, et al. Functional-Genetic Dissection of HDAC Dependencies in Mouse Lymphoid and Myeloid Malignancies. *Blood* (2015) 126:2392–403. doi: 10.1182/blood-2015-03-632984
132. Duque-Afonso J, Lin C-H, Han K, Wei MC, Feng J, Kurzer JH, et al. E2A-PBX1 Remodels Oncogenic Signaling Networks in B-Cell Precursor Acute Lymphoid Leukemia. *Cancer Res* (2016) 76:6937–49. doi: 10.1158/0008-5472.CAN-16-1899
133. Li X, Zhang Y, Zheng L, Liu M, Chen CD, Jiang H. UTX Is an Escape From X-Inactivation Tumor-Suppressor in B Cell Lymphoma. *Nat Commun* (2018) 9:2720. doi: 10.1038/s41467-018-05084-w
134. Braun CJ, Bruno PM, Horlbeck MA, Gilbert LA, Weissman JS, Hemann MT. Versatile *In Vivo* Regulation of Tumor Phenotypes by Dcas9-Mediated Transcriptional Perturbation. *Proc Natl Acad Sci USA* (2016) 113:E3892–900. doi: 10.1073/pnas.1600582113
135. Schmitt CA, Fridman JS, Yang M, Baranov E, Hoffman RM, Lowe SW. Dissecting P53 Tumor Suppressor Functions *In Vivo*. *Cancer Cell* (2002) 1:289–98. doi: 10.1016/S1535-6108(02)00047-8
136. Meacham CE, Ho EE, Dubrovsky E, Gertler FB, Hemann MT. *In Vivo* RNAi Screening Identifies Regulators of Actin Dynamics as Key Determinants of Lymphoma Progression. *Nat Genet* (2009) 41:1133–7. doi: 10.1038/ng.451
137. Mu P, Han Y-C, Betel D, Yao E, Squatrito M, Ogrodowski P, et al. Genetic Dissection of the miR-17 92 Cluster of microRNAs in Myc-Induced B-Cell Lymphomas. *Genes Dev* (2009) 23:2806–11. doi: 10.1101/gad.1872909
138. Malina A, Mills JR, Cencic R, Yan Y, Fraser J, Schippers LM, et al. Repurposing CRISPR/Cas9 for *In Situ* Functional Assays. *Genes Dev* (2013) 27:2602–14. doi: 10.1101/gad.227132.113
139. Eva A, Pierce JH, Aaronson SA. Interactions of Retroviral and Cellular Transforming Genes With Hematopoietic Cells. *Ann N Y Acad Sci* (1987) 511:148–70. doi: 10.1111/j.1749-6632.1987.tb36245.x
140. Pierce JH, Eva A, Aaronson SA. Interactions of Oncogenes With Haematopoietic Cells. *Clin Haematol* (1986) 15:573–96. doi: 10.1016/S0308-2261(18)30003-1

141. Kitayama H, Tsujimura T, Matsumura I, Oritani K, Ikeda H, Ishikawa J, et al. Neoplastic Transformation of Normal Hematopoietic Cells by Constitutively Activating Mutations of C-Kit Receptor Tyrosine Kinase. *Blood* (1996) 88:995–1004. doi: 10.1182/blood.V88.3.995.995
142. Hawley TS, Fong AZC, Griesser H, Lyman SD, Hawley RG. Leukemic Predisposition of Mice Transplanted With Gene-Modified Hematopoietic Precursors Expressing Flt3 Ligand. *Blood* (1998) 92:2003–11. doi: 10.1182/blood.V92.6.2003.418k11_2003_2011
143. Schwartz RC, Stanton LW, Riley SC, Marcu KB, Witte ON. Synergism of V-Myc and V-Ha-Ras in the *In Vitro* Neoplastic Progression of Murine Lymphoid Cells. *Mol Cell Biol* (1986) 6:3221–31. doi: 10.1128/mcb.6.9.3221-3231.1986
144. Heard JM, Roussel MF, Rettenmier CW, Sherr CJ. Multilineage Hematopoietic Disorders Induced by Transplantation of Bone Marrow Cells Expressing the V-Fms Oncogene. *Cell* (1987) 51:663–73. doi: 10.1016/0092-8674(87)90135-8
145. Kelliher MA, McLaughlin J, Witte ON, Rosenberg N. Induction of a Chronic Myelogenous Leukemia-Like Syndrome in Mice With V-Abl and BCR/ABL. *Proc Natl Acad Sci* (1990) 87:6649–53. doi: 10.1073/pnas.87.22.9072c
146. Hawley RG, Fong AZC, Ngan BY, Hawley TS. Hematopoietic Transforming Potential of Activated Ras in Chimeric Mice. *Oncogene* (1995) 11:1113–23.
147. Thome KC, Radfar A, Rosenberg N. Mutation of Tp53 Contributes to the Malignant Phenotype of Abelson Virus-Transformed Lymphoid Cells. *J Virol* (1997) 71:8149–56. doi: 10.1128/JVI.71.11.8149-8156.1997
148. McLaughlin J, Chianese E, Witte ON. *In Vitro* Transformation of Immature Hematopoietic Cells by the P210 BCR/ABL Oncogene Product of the Philadelphia Chromosome. *Proc Natl Acad Sci* (1987) 84:6558–62. doi: 10.1073/pnas.84.18.6558
149. Daley G, Van Etten R, Baltimore D. Induction of Chronic Myelogenous Leukemia in Mice by the P210bcr/abl Gene of the Philadelphia Chromosome. *Sci (80-)* (1990) 247:824–30. doi: 10.1126/science.2406902
150. Elefanty AG, Hariharan IK, Cory S. Bcr-Abl, the Hallmark of Chronic Myeloid Leukaemia in Man, Induces Multiple Haemopoietic Neoplasms in Mice. *EMBO J* (1990) 9:1069–78. doi: 10.1002/j.1460-2075.1990.tb08212.x
151. Kuefer MU, Look AT, Pulford K, Behm FG, Pattengale PK, Mason DY, et al. Retrovirus-Mediated Gene Transfer of NPM-ALK Causes Lymphoid Malignancy in Mice. *Blood* (1997) 90:2901–10. doi: 10.1182/blood.V90.8.2901
152. Li S, Ilaria RL, Million RP, Daley GQ, Van Etten RA. The P190, P210, and P230 Forms of the BCR/ABL Oncogene Induce a Similar Chronic Myeloid Leukemia–like Syndrome in Mice But Have Different Lymphoid Leukemogenic Activity. *J Exp Med* (1999) 189:1399–412. doi: 10.1084/jem.189.9.1399
153. Alexander WS, Adams JM, Cory S. Oncogene Cooperation in Lymphocyte Transformation: Malignant Conversion of E Mu-Myc Transgenic Pre-B Cells *In Vitro* Is Enhanced by V-H-Ras or V-Raf But Not V-Abl. *Mol Cell Biol* (1989) 9:67–73. doi: 10.1128/mcb.9.1.67-73.1989
154. Sexl V, Piekorz R, Moriggl R, Rohrer J, Brown MP, Bunting KD, et al. Stat5a/b Contribute to Interleukin 7–Induced B-Cell Precursor Expansion, But Abl-Andbcr/Abl-Induced Transformation Are Independent of Stat5. *Blood* (2000) 96:2277–83. doi: 10.1182/blood.V96.6.2277
155. Hemann MT, Fridman JS, Zilfou JT, Hernando E, Paddison PJ, Cordon-Cardo C, et al. An Epi-Allelic Series of P53 Hypomorphs Created by Stable RNAi Produces Distinct Tumor Phenotypes *In Vivo*. *Nat Genet* (2003) 33:396–400. doi: 10.1038/ng1091
156. Hemann MT, Zilfou JT, Zhao Z, Burgess DJ, Hannon GJ, Lowe SW. Suppression of Tumorigenesis by the P53 Target PUMA. *Proc Natl Acad Sci* (2004) 101:9333–8. doi: 10.1073/pnas.0403286101
157. Wendel H-G, de Stanchina E, JS F, Malina A, Ray S, Kogan S, et al. Survival Signalling by Akt and Eif4e in Oncogenesis and Cancer Therapy. *Nature* (2004) 428:332–7. doi: 10.1038/nature02369
158. Hu Y, Liu Y, Pelletier S, Buchdunger E, Warmuth M, Fabbro D, et al. Requirement of Src Kinases Lyn, Hck and Fgr for BCR-ABL1-Induced B-Lymphoblastic Leukemia But Not Chronic Myeloid Leukemia. *Nat Genet* (2004) 36:453–61. doi: 10.1038/ng1343
159. Hemann MT, Bric A, Teruya-Feldstein J, Herbst A, Nilsson JA, Cordon-Cardo C, et al. Evasion of the P53 Tumour Surveillance Network by Tumour-Derived MYC Mutants. *Nature* (2005) 436:807–11. doi: 10.1038/nature03845
160. He L, Thomson JM, Hemann MT, Hernando-Monge E, Mu D, Goodson S, et al. A microRNA Polycistron as a Potential Human Oncogene. *Nature* (2005) 435:828–33. doi: 10.1038/nature03552
161. Herbst A, Hemann MT, Tworkowski KA, Salghetti SE, Lowe SW, Tansey WP. A Conserved Element in Myc That Negatively Regulates its Proapoptotic Activity. *EMBO Rep* (2005) 6:177–83. doi: 10.1038/sj.embor.7400333
162. Williams RT, Roussel MF, Sherr CJ. Arf Gene Loss Enhances Oncogenicity and Limits Imatinib Response in Mouse Models of Bcr-Abl-Induced Acute Lymphoblastic Leukemia. *Proc Natl Acad Sci* (2006) 103:6688–93. doi: 10.1073/pnas.0602030103
163. Hoelbl A, Kovacic B, Kerenyi MA, Simma O, Warsch W, Cui Y, et al. Clarifying the Role of Stat5 in Lymphoid Development and Abelson-Induced Transformation. *Blood* (2006) 107:4898–906. doi: 10.1182/blood-2005-09-3596
164. Barabe F, Kennedy JA, Hope KJ, Dick JE. Modeling the Initiation and Progression of Human Acute Leukemia in Mice. *Sci (80-)* (2007) 316:600–4. doi: 10.1126/science.1139851
165. Wang P-Y, Young F, Chen C-Y, Stevens BM, Neering SJ, Rossi RM, et al. The Biologic Properties of Leukemias Arising From BCR/ABL-Mediated Transformation Vary as a Function of Developmental Origin and Activity of the P19arf Gene. *Blood* (2008) 112:4184–92. doi: 10.1182/blood-2008-02-142190
166. Bric A, Miething C, Bialucha CU, Scuoppo C, Zender L, Krasnitz A, et al. Functional Identification of Tumor-Suppressor Genes Through an In Vivo RNA Interference Screen in a Mouse Lymphoma Model. *Cancer Cell* (2009) 16:324–35. doi: 10.1016/j.ccr.2009.08.015
167. Hoelbl A, Schuster C, Kovacic B, Zhu B, Wickre M, Hoelzl MA, et al. Stat5 Is Indispensable for the Maintenance of Bcr/Abl -Positive Leukaemia. *EMBO Mol Med* (2010) 2:98–110. doi: 10.1002/emmm.201000062
168. Nakagawa M, Tsuzuki S, Honma K, Taguchi O, Seto M. Synergistic Effect of Bcl2, Myc and Ccnd1 Transforms Mouse Primary B Cells Into Malignant Cells. *Haematologica* (2011) 96:1318–26. doi: 10.3324/haematol.2011.041053
169. Bouquet C, Melchers F. Pim1 and Myc Reversibly Transform Murine Precursor B Lymphocytes But Not Mature B Lymphocytes. *Eur J Immunol* (2012) 42:522–32. doi: 10.1002/eji.201141987
170. Kovacic B, Hoelbl A, Litos G, Alacakaptan M, Schuster C, Fischhuber KM, et al. Diverging Fates of Cells of Origin in Acute and Chronic Leukaemia. *EMBO Mol Med* (2012) 4:283–97. doi: 10.1002/emmm.201100208
171. Leskov I, Pallasch CP, Drake A, Iliopoulou BP, Souza A, Shen C-HH, et al. Rapid Generation of Human B-Cell Lymphomas *via* Combined Expression of Myc and Bcl2 and Their Use as a Preclinical Model for Biological Therapies. *Oncogene* (2013) 32:1066–72. doi: 10.1038/onc.2012.117
172. Arita K, Maeda-Kasugai Y, Ohshima K, Tsuzuki S, Suguro-Katayama M, Karube K, et al. Generation of Mouse Models of Lymphoid Neoplasm Using Retroviral Gene Transduction of *In Vitro*-Induced Germinal Center B and T Cells. *Exp Hematol* (2013) 41:731–741.e9. doi: 10.1016/j.exphem.2013.04.001
173. Aubrey BJ, Kelly GL, Kueh AJ, Brennan MS, O'Connor L, Milla L, et al. An Inducible Lentiviral Guide RNA Platform Enables the Identification of Tumor-Essential Genes and Tumor-Promoting Mutations *In Vivo*. *Cell Rep* (2015) 10:1422–32. doi: 10.1016/j.celrep.2015.02.002
174. Ortega-Molina A, Boss IW, Canela A, Pan H, Jiang Y, Zhao C, et al. The Histone Lysine Methyltransferase KMT2D Sustains a Gene Expression Program That Represses B Cell Lymphoma Development. *Nat Med* (2015) 21:1199–208. doi: 10.1038/nm.3943
175. Scheicher R, Hoelbl-Kovacic A, Bellutti F, Tigan A-S, Prchal-Murphy M, Heller G, et al. CDK6 as a Key Regulator of Hematopoietic and Leukemic Stem Cell Activation. *Blood* (2015) 125:90–101. doi: 10.1182/blood-2014-06-584417
176. Jiang Y, Ortega-Molina A, Geng H, Ying H-Y, Hatzi K, Parsa S, et al. CREBBP Inactivation Promotes the Development of HDAC3-Dependent Lymphomas. *Cancer Discovery* (2017) 7:38–53. doi: 10.1158/2159-8290.CD-16-0975
177. Katigbak A, Cencic R, Robert F, Sénécha P, Scuoppo C, Pelletier J. A CRISPR/Cas9 Functional Screen Identifies Rare Tumor Suppressors. *Sci Rep* (2016) 6:38968. doi: 10.1038/srep38968
178. Wolf I, Bouquet C, Melchers F. cDNA-Library Testing Identifies Transforming Genes Cooperating With C-Myc in Mouse Pre-B Cells. *Eur J Immunol* (2016) 46:2555–65. doi: 10.1002/eji.201646419

179. Wolf I, Bouquet C, Naumann F, Melchers F. Generation of Precursor, Immature, and Mature Murine B1-Cell Lines From C-Myc/bcl-xL-Overexpressing Pre-BI Cells. *Eur J Immunol* (2017) 47:911–20. doi: 10.1002/eji.201746937
180. van Oosterwijk JG, Li C, Yang X, Opferman JT, Sherr CJ. Small Mitochondrial Arf (Smarf) Protein Corrects P53-Independent Developmental Defects of Arf Tumor Suppressor-Deficient Mice. *Proc Natl Acad Sci* (2017) 114:7420–5. doi: 10.1073/pnas.1707292114
181. McHugh D, Caduff N, Barros MHM, Rämer PC, Raykova A, Murer A, et al. Persistent KSHV Infection Increases EBV-Associated Tumor Formation In Vivo *via* Enhanced EBV Lytic Gene Expression. *Cell Host Microbe* (2017) 22:61–73.e7. doi: 10.1016/j.chom.2017.06.009
182. Reimer J, Knöß S, Labuhn M, Charpentier EM, Göhring G, Schlegelberger B, et al. CRISPR-Cas9-Induced T(11;19)/MLL-ENL Translocations Initiate Leukemia in Human Hematopoietic Progenitor Cells *In Vivo*. *Haematologica* (2017) 102:1558–66. doi: 10.3324/haematol.2017.164046
183. Katigbak A, Robert F, Paquet M, Pelletier J. Inducible Genome Editing With Conditional CRISPR/Cas9 Mice. *G3 Genes Genomes Genet* (2018) 8:1627–35. doi: 10.1534/g3.117.300327
184. Janic A, Valente LJ, Wakefield MJ, Di Stefano L, Milla L, Wilcox S, et al. DNA Repair Processes Are Critical Mediators of P53-Dependent Tumor Suppression. *Nat Med* (2018) 24:947–53. doi: 10.1038/s41591-018-0043-5
185. Jeong J, Jager A, Domizi P, Pavel-Dinu M, Gojenola L, Iwasaki M, et al. High-Efficiency CRISPR Induction of T(9;11) Chromosomal Translocations and Acute Leukemias in Human Blood Stem Cells. *Blood Adv* (2019) 3:2825–35. doi: 10.1182/bloodadvances.2019000450
186. Rajan SS, Li L, Kweh MF, Kunkalla K, Amin AD, Agarwal NK, et al. CRISPR Genome Editing of Murine Hematopoietic Stem Cells to Create Npm1-Alk Causes ALK+ Lymphoma After Transplantation. *Blood Adv* (2019) 3:1788–94. doi: 10.1182/bloodadvances.2018025247
187. Verma D, Zanetti C, Godavarthy PS, Kumar R, Minciacchi VR, Pfeiffer J, et al. Bone Marrow Niche-Derived Extracellular Matrix-Degrading Enzymes Influence the Progression of B-Cell Acute Lymphoblastic Leukemia. *Leukemia* (2020) 34:1540–52. doi: 10.1038/s41375-019-0674-7
188. Williams DA, Lemischka IR, Nathan DG, Mulligan RC. Introduction of New Genetic Material Into Pluripotent Haematopoietic Stem Cells of the Mouse. *Nature* (1984) 310:476–80. doi: 10.1038/310476a0
189. Whitlock CA, Witte ON. Long-Term Culture of B Lymphocytes and Their Precursors From Murine Bone Marrow. *Proc Natl Acad Sci* (1982) 79:3608–12. doi: 10.1073/pnas.79.11.3608
190. Nojima T, Haniuda K, Moutai T, Matsudaira M, Mizokawa S, Shiratori I, et al. *In-Vitro* Derived Germinal Centre B Cells Differentially Generate Memory B or Plasma Cells *In Vivo*. *Nat Commun* (2011) 2:465. doi: 10.1038/ncomms1475
191. Adams JM, Harris AW, Pinkert CA, Corcoran LM, Alexander WS, Cory S, et al. The C-Myc Oncogene Driven by Immunoglobulin Enhancers Induces Lymphoid Malignancy in Transgenic Mice. *Nature* (1985) 318:533–8. doi: 10.1038/318533a0
192. Marsden VS, O'Connor L, O'Reilly LA, Silke J, Metcalf D, Ekert PG, et al. Apoptosis Initiated by Bcl-2-Regulated Caspase Activation Independently of the Cytochrome C/Apaf-1/Caspase-9 Apoptosome. *Nature* (2002) 419:634–7. doi: 10.1038/nature01101
193. Scott CL, Schuler M, Marsden VS, Egle A, Pellegrini M, Nesic D, et al. Apaf-1 and Caspase-9 do Not Act as Tumor Suppressors in Myc-Induced Lymphomagenesis or Mouse Embryo Fibroblast Transformation. *J Cell Biol* (2004) 164:89–96. doi: 10.1083/jcb.200310041
194. Nishikawa S-I, Ogawa M, Nishikawa S, Kunisada T, Kodama H. B Lymphopoiesis on Stromal Cell Clone: Stromal Cell Clones Acting on Different Stages of B Cell Differentiation*. *Eur J Immunol* (1988) 18:1767–72. doi: 10.1002/eji.1830181117
195. Rolink A, Kudo A, Karasuyama H, Kikuchi Y, Melchers F. Long-Term Proliferating Early Pre B Cell Lines and Clones With the Potential to Develop to Surface Ig-Positive, Mitogen Reactive B Cells *In Vitro* and *In Vivo*. *EMBO J* (1991) 10:327–36. doi: 10.1002/j.1460-2075.1991.tb07953.x
196. von Muenchow L, Tsapogas P, Albertí-Servera L, Capoferri G, Doelz M, Rolink H, et al. Pro-B Cells Propagated in Stromal Cell-Free Cultures Reconstitute Functional B-Cell Compartments in Immunodeficient Mice. *Eur J Immunol* (2017) 47:394–405. doi: 10.1002/eji.201646638
197. Gonzalez-Martin A, Adams BD, Lai M, Shepherd J, Salvador-Bernaldez M, Salvador JM, et al. The microRNA miR-148a Functions as a Critical Regulator of B Cell Tolerance and Autoimmunity. *Nat Immunol* (2016) 17:433–40. doi: 10.1038/ni.3385
198. Zhao R, Zhang H, Zhang Y, Li D, Huang C, Li F. *In Vivo* Screen Identifies Zdhhc2 as a Critical Regulator of Germinal Center B Cell Differentiation. *Front Immunol* (2020) 11:1025. doi: 10.3389/fimmu.2020.01025
199. Gaj T, Gersbach CA, Barbas CF. ZFN, TALEN, and CRISPR/Cas-Based Methods for Genome Engineering. *Trends Biotechnol* (2013) 31:397–405. doi: 10.1016/j.tibtech.2013.04.004
200. Cong L, Ran FA, Cox D, Lin S, Barretto R, Habib N, et al. Multiplex Genome Engineering Using CRISPR/Cas Systems. *Sci (80-)* (2013) 339:819–23. doi: 10.1126/science.1231143
201. Mali P, Yang L, Esvelt KM, Aach J, Guell M, DiCarlo JE, et al. RNA-Guided Human Genome Engineering *via* Cas9. *Sci (80-)* (2013) 339:823–6. doi: 10.1126/science.1232033
202. Jain S, Shukla S, Yang C, Zhang M, Fatma Z, Lingamaneni M, et al. TALEN Outperforms Cas9 in Editing Heterochromatin Target Sites. *Nat Commun* (2021) 12:606. doi: 10.1038/s41467-020-20672-5
203. Canver MC, Bauer DE, Dass A, Yien YY, Chung J, Masuda T, et al. Characterization of Genomic Deletion Efficiency Mediated by Clustered Regularly Interspaced Palindromic Repeats (CRISPR)/Cas9 Nuclease System in Mammalian Cells*. *J Biol Chem* (2014) 289:21312–24. doi: 10.1074/jbc.M114.564625
204. Parikh BA, Beckman DL, Patel SJ, White JM, Yokoyama WM. Detailed Phenotypic and Molecular Analyses of Genetically Modified Mice Generated by CRISPR-Cas9-Mediated Editing. *PloS One* (2015) 10:e0116484. doi: 10.1371/journal.pone.0116484
205. Boroviak K, Fu B, Yang F, Doe B, Bradley A. Revealing Hidden Complexities of Genomic Rearrangements Generated With Cas9. *Sci Rep* (2017) 7:12867. doi: 10.1038/s41598-017-12740-6
206. Adikusuma F, Piltz S, Corbett MA, Turvey M, McColl SR, Helbig KJ, et al. Large Deletions Induced by Cas9 Cleavage. *Nature* (2018) 560:E8–9. doi: 10.1038/s41586-018-0380-z
207. Kosicki M, Tomberg K, Bradley A. Repair of Double-Strand Breaks Induced by CRISPR–Cas9 Leads to Large Deletions and Complex Rearrangements. *Nat Biotechnol* (2018) 36:765–71. doi: 10.1038/nbt.4192
208. Ran FA, Hsu PD, Lin C-Y, Gootenberg JS, Konermann S, Trevino AE, et al. Double Nicking by RNA-Guided CRISPR Cas9 for Enhanced Genome Editing Specificity. *Cell* (2013) 154:1380–9. doi: 10.1016/j.cell.2013.08.021
209. Fu Y, Sander JD, Reyon D, Cascio VM, Joung JK. Improving CRISPR-Cas Nuclease Specificity Using Truncated Guide RNAs. *Nat Biotechnol* (2014) 32:279–84. doi: 10.1038/nbt.2808
210. Kleinstiver BP, Sousa AA, Walton RT, Tak YE, Hsu JY, Clement K, et al. Engineered CRISPR–Cas12a Variants With Increased Activities and Improved Targeting Ranges for Gene, Epigenetic and Base Editing. *Nat Biotechnol* (2019) 37:276–82. doi: 10.1038/s41587-018-0011-0
211. Walton RT, Christie KA, Whittaker MN, Kleinstiver BP. Unconstrained Genome Targeting With Near-PAMless Engineered CRISPR-Cas9 Variants. *Sci (80-)* (2020) 368:290–6. doi: 10.1126/science.aba8853
212. Hirakawa MP, Krishnakumar R, Timlin JA, Carney JP, Butler KS. Gene Editing and CRISPR in the Clinic: Current and Future Perspectives. *Biosci Rep* (2020) 40(4):BSR20200127. doi: 10.1042/BSR20200127
213. Manghwar H, Li B, Ding X, Hussain A, Lindsey K, Zhang X, et al. CRISPR/Cas Systems in Genome Editing: Methodologies and Tools for sgRNA Design, Off-Target Evaluation, and Strategies to Mitigate Off-Target Effects. *Adv Sci* (2020) 7:1902312. doi: 10.1002/advs.201902312
214. Koblan LW, Doman JL, Wilson C, Levy JM, Tay T, Newby GA, et al. Improving Cytidine and Adenine Base Editors by Expression Optimization and Ancestral Reconstruction. *Nat Biotechnol* (2018) 36:843–6. doi: 10.1038/nbt.4172
215. Doman JL, Raguram A, Newby GA, Liu DR. Evaluation and Minimization of Cas9-Independent Off-Target DNA Editing by Cytosine Base Editors. *Nat Biotechnol* (2020) 38:620–8. doi: 10.1038/s41587-020-0414-6
216. Anzalone AV, Randolph PB, Davis JR, Sousa AA, Koblan LW, Levy JM, et al. Search-And-Replace Genome Editing Without Double-Strand Breaks or Donor DNA. *Nature* (2019) 576:149–57. doi: 10.1038/s41586-019-1711-4
217. Filippova J, Matveeva A, Zhuravlev E, Stepanov G. Guide RNA Modification as a Way to Improve CRISPR/Cas9-Based Genome-Editing Systems. *Biochimie* (2019) 167:49–60. doi: 10.1016/j.biochi.2019.09.003
218. Nakade S, Tsubota T, Sakane Y, Kume S, Sakamoto N, Obara M, et al. Microhomology-Mediated End-Joining-Dependent Integration of Donor

DNA in Cells and Animals Using TALENs and CRISPR/Cas9. *Nat Commun* (2014) 5:5560. doi: 10.1038/ncomms6560
219. Slaymaker IM, Gao L, Zetsche B, Scott DA, Yan WX, Zhang F. Rationally Engineered Cas9 Nucleases With Improved Specificity. *Sci (80-)* (2016) 351:84–8. doi: 10.1126/science.aad5227
220. Kleinstiver BP, Pattanayak V, Prew MS, Tsai SQ, Nguyen NT, Zheng Z, et al. High-Fidelity CRISPR-Cas9 Nucleases With No Detectable Genome-Wide Off-Target Effects. *Nature* (2016) 529:490–5. doi: 10.1038/nature16526
221. Lee K, Mackley VA, Rao A, Chong AT, Dewitt MA, Corn JE, et al. Synthetically Modified Guide RNA and Donor DNA Are a Versatile Platform for CRISPR-Cas9 Engineering. *Elife* (2017) 6:e25312. doi: 10.7554/eLife.25312.001
222. Yao X, Wang X, Hu X, Liu Z, Liu J, Zhou H, et al. Homology-Mediated End Joining-Based Targeted Integration Using CRISPR/Cas9. *Cell Res* (2017) 27:801–14. doi: 10.1038/cr.2017.76
223. Ma M, Zhuang F, Hu X, Wang B, Wen XZ, Ji JF, et al. Efficient Generation of Mice Carrying Homozygous Double-Floxp Alleles Using the Cas9-Avidin/Biotin-Donor DNA System. *Cell Res* (2017) 27:578–81. doi: 10.1038/cr.2017.29
224. Miura H, Quadros RM, Gurumurthy CB, Ohtsuka M. Easi-CRISPR for Creating Knock-in and Conditional Knockout Mouse Models Using Long ssDNA Donors. *Nat Protoc* (2018) 13:195–215. doi: 10.1038/nprot.2017.153
225. Gu B, Posfai E, Rossant J. Efficient Generation of Targeted Large Insertions by Microinjection Into Two-Cell-Stage Mouse Embryos. *Nat Biotechnol* (2018) 36:632–7. doi: 10.1038/nbt.4166
226. Weber J, Rad R. Engineering CRISPR Mouse Models of Cancer. *Curr Opin Genet Dev* (2019) 54:88–96. doi: 10.1016/j.gde.2019.04.001
227. Weber J, Braun CJ, Saur D, Rad R. In Vivo Functional Screening for Systems-Level Integrative Cancer Genomics. *Nat Rev Cancer* (2020) 20:573–93. doi: 10.1038/s41568-020-0275-9
228. Platt RJ, Chen S, Zhou Y, Yim MJ, Swiech L, Kempton HR, et al. CRISPR-Cas9 Knockin Mice for Genome Editing and Cancer Modeling. *Cell* (2014) 159:440–55. doi: 10.1016/j.cell.2014.09.014
229. Gundry MC, Brunetti L, Lin A, Mayle AE, Kitano A, Wagner D, et al. Highly Efficient Genome Editing of Murine and Human Hematopoietic Progenitor Cells by CRISPR/Cas9. *Cell Rep* (2016) 17:1453–61. doi: 10.1016/j.celrep.2016.09.092
230. Chu VT, Weber T, Graf R, Sommermann T, Petsch K, Sack U, et al. Efficient Generation of Rosa26 Knock-in Mice Using CRISPR/Cas9 in C57BL/6 Zygotes. *BMC Biotechnol* (2016) 16:4. doi: 10.1186/s12896-016-0234-4
231. Chu VT, Graf R, Wirtz T, Weber T, Favret J, Li X, et al. Efficient CRISPR-Mediated Mutagenesis in Primary Immune Cells Using CrispRGold and a C57BL/6 Cas9 Transgenic Mouse Line. *Proc Natl Acad Sci* (2016) 113:12514–9. doi: 10.1073/pnas.1613884113
232. LaFleur MW, Nguyen TH, Coxe MA, Yates KB, Trombley JD, Weiss SA, et al. A CRISPR-Cas9 Delivery System for *In Vivo* Screening of Genes in the Immune System. *Nat Commun* (2019) 10:1668. doi: 10.1038/s41467-019-09656-2
233. Ten Hacken E, Yin S, Clement K, Redd RA, Hernandez-Sanchez M, Li S, et al. Interrogation of Individual CLL Loss-Of-Function Lesions By CRISPR In Vivo Editing Reveals Common and Unique Pathway Alterations. *Blood* (2019) 134:684–4. doi: 10.1182/blood-2019-127673
234. Yudovich D, Bäckström A, Schmiderer L, Žemaitis K, Subramaniam A, Larsson J. Combined Lentiviral- and RNA-Mediated CRISPR/Cas9 Delivery for Efficient and Traceable Gene Editing in Human Hematopoietic Stem and Progenitor Cells. *Sci Rep* (2020) 10:22393. doi: 10.1038/s41598-020-79724-x
235. Johnson MJ, Laoharawee K, Lahr WS, Webber BR, Moriarity BS. Engineering of Primary Human B Cells With CRISPR/Cas9 Targeted Nuclease. *Sci Rep* (2018) 8:12144. doi: 10.1038/s41598-018-30358-0
236. Nahmad AD, Raviv Y, Horovitz-Fried M, Sofer I, Akriv T, Nataf D, et al. Engineered B Cells Expressing an Anti-HIV Antibody Enable Memory Retention, Isotype Switching and Clonal Expansion. *Nat Commun* (2020) 11:5851. doi: 10.1038/s41467-020-19649-1
237. Hartweger H, McGuire AT, Horning M, Taylor JJ, Dosenovic P, Yost D, et al. HIV-Specific Humoral Immune Responses by CRISPR/Cas9-Edited B Cells. *J Exp Med* (2019) 216:1301–10. doi: 10.1084/jem.20190287
238. Moffett HF, Harms CK, Fitzpatrick KS, Tooley MR, Boonyaratanakornkit J, Taylor JJ. B Cells Engineered to Express Pathogen-Specific Antibodies Protect Against Infection. *Sci Immunol* (2019) 4:eaax0644. doi: 10.1126/sciimmunol.aax0644
239. Gilbert LA, Horlbeck MA, Adamson B, Villalta JE, Chen Y, Whitehead EH, et al. Genome-Scale CRISPR-Mediated Control of Gene Repression and Activation. *Cell* (2014) 159:647–61. doi: 10.1016/j.cell.2014.09.029
240. Maddalo D, Manchado E, Concepcion CP, Bonetti C, Vidigal JA, Han Y-C, et al. In Vivo Engineering of Oncogenic Chromosomal Rearrangements With the CRISPR/Cas9 System. *Nature* (2014) 516:423–7. doi: 10.1038/nature13902
241. Huijbers IJ. Generating Genetically Modified Mice: A Decision Guide. In: . *Methods Mol Biol* (2017) 1642:1–19. doi: 10.1007/978-1-4939-7169-5_1
242. Wang H, Yang H, Shivalila CS, Dawlaty MM, Cheng AW, Zhang F, et al. One-Step Generation of Mice Carrying Mutations in Multiple Genes by CRISPR/Cas-Mediated Genome Engineering. *Cell* (2013) 153:910–8. doi: 10.1016/j.cell.2013.04.025
243. Yang H, Wang H, Shivalila CS, Cheng AW, Shi L, Jaenisch R. One-Step Generation of Mice Carrying Reporter and Conditional Alleles by CRISPR/Cas-Mediated Genome Engineering. *Cell* (2013) 154:1370–9. doi: 10.1016/j.cell.2013.08.022
244. Huijbers IJ, Bin Ali R, Pritchard C, Cozijnsen M, Kwon MC, Proost N, et al. Rapid Target Gene Validation in Complex Cancer Mouse Models Using Re-Derived Embryonic Stem Cells. *EMBO Mol Med* (2014) 6:212–25. doi: 10.1002/emmm.201303297
245. Huijbers IJ, Del Bravo J, Bin Ali R, Pritchard C, Braumuller TM, van Miltenburg MH, et al. Using the GEMM-ESC Strategy to Study Gene Function in Mouse Models. *Nat Protoc* (2015) 10:1755–85. doi: 10.1038/nprot.2015.114
246. Chen Y, Mao S, Liu B, Jing Z, Zang Y, Xia J, et al. Novel Mosaic Mice With Diverse Applications. *bioRxiv* (2020). doi: 10.1101/2020.03.21.001388
247. Zhang J, Chen L, Zhang J, Wang Y. Drug Inducible CRISPR/Cas Systems. *Comput Struct Biotechnol J* (2019) 17:1171–7. doi: 10.1016/j.csbj.2019.07.015
248. Felsher DW, Bishop JM. Reversible Tumorigenesis by MYC in Hematopoietic Lineages. *Mol Cell* (1999) 4:199–207. doi: 10.1016/S1097-2765(00)80367-6
249. Marinkovic D, Marinkovic T, Mahr B, Hess J, Wirth T. Reversible Lymphomagenesis in Conditionally C-MYC Expressing Mice. *Int J Cancer* (2004) 110:336–42. doi: 10.1002/ijc.20099
250. Letai A, Sorcinelli MD, Beard C, Korsmeyer SJ. Antiapoptotic BCL-2 Is Required for Maintenance of a Model Leukemia. *Cancer Cell* (2004) 6:241–9. doi: 10.1016/j.ccr.2004.07.011
251. Liu GJ, Cimmino L, Jude JG, Hu Y, Witkowski MT, McKenzie MD, et al. Pax5 Loss Imposes a Reversible Differentiation Block in B-Progenitor Acute Lymphoblastic Leukemia. *Genes Dev* (2014) 28:1337–50. doi: 10.1101/gad.240416.114
252. Christophorou MA, Martin-Zanca D, Soucek L, Lawlor ER, Brown-Swigart L, Verschuren EW, et al. Temporal Dissection of P53 Function *In Vitro* and *In Vivo*. *Nat Genet* (2005) 37:718–26. doi: 10.1038/ng1572
253. Martins CP, Brown-Swigart L, Evan GI. Modeling the Therapeutic Efficacy of P53 Restoration in Tumors. *Cell* (2006) 127:1323–34. doi: 10.1016/j.cell.2006.12.007
254. Scheijen B, Ngo HT, Kang H, Griffin JD. FLT3 Receptors With Internal Tandem Duplications Promote Cell Viability and Proliferation by Signaling Through Foxo Proteins. *Oncogene* (2004) 23:3338–49. doi: 10.1038/sj.onc.1207456
255. Klucher KM, Lopez DV, Daley GQ. Secondary Mutation Maintains the Transformed State in BaF3 Cells With Inducible BCR/ABL Expression. *Blood* (1998) 91:3927–34. doi: 10.1182/blood.v91.10.3927
256. Dickins RA, Hemann MT, Zilfou JT, Simpson DR, Ibarra I, Hannon GJ, et al. Probing Tumor Phenotypes Using Stable and Regulated Synthetic microRNA Precursors. *Nat Genet* (2005) 37:1289–95. doi: 10.1038/ng1651
257. Fellmann C, Hoffmann T, Sridhar V, Hopfgartner B, Muhar M, Roth M, et al. An Optimized microRNA Backbone for Effective Single-Copy RNAi. *Cell Rep* (2013) 5:1704–13. doi: 10.1016/j.celrep.2013.11.020
258. Dugray A, Geay J, Foudi A, Bonnet M, Vainchenker W, Wendling F, et al. Rapid Generation of a Tetracycline-Inducible BCR-ABL Defective Retrovirus Using a Single Autoregulatory Retroviral Cassette. *Leukemia* (2001) 15:1658–62. doi: 10.1038/sj.leu.2402225
259. Csikós T, Reijmers RM, Uren AG, Spaargaren M, Pals ST. Instant Conditional Transgenesis in the Mouse Hematopoietic Compartment. *J Immunol Methods* (2008) 339:259–63. doi: 10.1016/j.jim.2008.08.009
260. Cao J, Wu L, Zhang S-M, Lu M, Cheung WKC, Cai W, et al. An Easy and Efficient Inducible CRISPR/Cas9 Platform With Improved Specificity for

Multiple Gene Targeting. *Nucleic Acids Res* (2016) 44:e149. doi: 10.1093/nar/gkw660
261. Lundin A, Porritt MJ, Jaiswal H, Seeliger F, Johansson C, Bidar AW, et al. Development of an ObLiGaRe Doxycycline Inducible Cas9 System for Pre-Clinical Cancer Drug Discovery. *Nat Commun* (2020) 11:4903. doi: 10.1038/s41467-020-18548-9
262. Dow LE, Fisher J, O'Rourke KP, Muley A, Kastenhuber ER, Livshits G, et al. Inducible *In Vivo* Genome Editing With CRISPR-Cas9. *Nat Biotechnol* (2015) 33:390–4. doi: 10.1038/nbt.3155
263. Chavez A, Scheiman J, Vora S, Pruitt BW, Tuttle M, Iyer E PR, et al. Highly Efficient Cas9-Mediated Transcriptional Programming. *Nat Methods* (2015) 12:326–8. doi: 10.1038/nmeth.3312
264. Morgens DW, Deans RM, Li A, Bassik MC. Systematic Comparison of CRISPR/Cas9 and RNAi Screens for Essential Genes. *Nat Biotechnol* (2016) 34:634–6. doi: 10.1038/nbt.3567
265. De La Rochere P, Guil-Luna S, Decaudin D, Azar G, Sidhu SS, Piaggio E. Humanized Mice for the Study of Immuno-Oncology. *Trends Immunol* (2018) 39:748–63. doi: 10.1016/j.it.2018.07.001
266. Saito Y, Shultz LD, Ishikawa F. Understanding Normal and Malignant Human Hematopoiesis Using Next-Generation Humanized Mice. *Trends Immunol* (2020) 41:706–20. doi: 10.1016/j.it.2020.06.004
267. Martinov T, McKenna KM, Tan WH, Collins EJ, Kehret AR, Linton JD, et al. Building the Next Generation of Humanized Hemato-Lymphoid System Mice. *Front Immunol* (2021) 12:643852. doi: 10.3389/fimmu.2021.643852
268. Stripecke R, Münz C, Schuringa JJ, Bissig K, Soper B, Meeham T, et al. Innovations, Challenges, and Minimal Information for Standardization of Humanized Mice. *EMBO Mol Med* (2020) 12:e8662. doi: 10.15252/emmm.201708662
269. Espinoza JL, Matsumoto A, Tanaka H, Matsumura I. Gastric Microbiota: An Emerging Player in Helicobacter Pylori -Induced Gastric Malignancies. *Cancer Lett* (2018) 414:147–52. doi: 10.1016/j.canlet.2017.11.009

Conflict of Interest: The authors declare that the research was conducted in the absence of any commercial or financial relationships that could be construed as a potential conflict of interest.

Publisher's Note: All claims expressed in this article are solely those of the authors and do not necessarily represent those of their affiliated organizations, or those of the publisher, the editors and the reviewers. Any product that may be evaluated in this article, or claim that may be made by its manufacturer, is not guaranteed or endorsed by the publisher.

frontiers in Immunology

ORIGINAL RESEARCH
published: 20 October 2021
doi: 10.3389/fimmu.2021.670338

Mitochondrial Fission Factor Is a Novel Interacting Protein of the Critical B Cell Survival Regulator TRAF3 in B Lymphocytes

*Yingying Liu[1], Samantha Gokhale[1,2], Jaeyong Jung[1,2], Sining Zhu[1,2], Chang Luo[1], Debanjan Saha[1], Jessie Yanxiang Guo[3,4,5], Huaye Zhang[6], Saw Kyin[7], Wei-Xing Zong[3,5], Eileen White[3,8] and Ping Xie[1,3]**

[1] Department of Cell Biology and Neuroscience, Rutgers University, Piscataway, NJ, United States, [2] Graduate Program in Cellular and Molecular Pharmacology, Rutgers University, Piscataway, NJ, United States, [3] Rutgers Cancer Institute of New Jersey, New Brunswick, NJ, United States, [4] Department of Medicine, Rutgers Robert Wood Johnson Medical School, New Brunswick, NJ, United States, [5] Department of Chemical Biology, Rutgers Ernest Mario School of Pharmacy, Piscataway, NJ, United States, [6] Department of Neuroscience and Cell Biology, Rutgers Robert Wood Johnson Medical School, Piscataway, NJ, United States, [7] Department of Molecular Biology, Princeton University, Princeton, NJ, United States, [8] Department of Molecular Biology and Biochemistry, Rutgers University, Piscataway, NJ, United States

OPEN ACCESS

Edited by:
Gema Perez-Chacon, Spanish National Cancer Research Center (CNIO), Spain

Reviewed by:
Nik Georgopoulos, University of Huddersfield, United Kingdom
John D. Colgan, The University of Iowa, United States

***Correspondence:**
Ping Xie
xie@dls.rutgers.edu

Specialty section:
This article was submitted to B Cell Biology, a section of the journal Frontiers in Immunology

Received: *21 February 2021*
Accepted: *04 October 2021*
Published: *20 October 2021*

Citation:
Liu Y, Gokhale S, Jung J, Zhu S, Luo C, Saha D, Guo JY, Zhang H, Kyin S, Zong W-X, White E and Xie P (2021) Mitochondrial Fission Factor Is a Novel Interacting Protein of the Critical B Cell Survival Regulator TRAF3 in B Lymphocytes. Front. Immunol. 12:670338. doi: 10.3389/fimmu.2021.670338

Proteins controlling mitochondrial fission have been recognized as essential regulators of mitochondrial functions, mitochondrial quality control and cell apoptosis. In the present study, we identified the critical B cell survival regulator TRAF3 as a novel binding partner of the key mitochondrial fission factor, MFF, in B lymphocytes. Elicited by our unexpected finding that the majority of cytoplasmic TRAF3 proteins were localized at the mitochondria in resting splenic B cells after *ex vivo* culture for 2 days, we found that TRAF3 specifically interacted with MFF as demonstrated by co-immunoprecipitation and GST pull-down assays. We further found that in the absence of stimulation, increased protein levels of mitochondrial TRAF3 were associated with altered mitochondrial morphology, decreased mitochondrial respiration, increased mitochondrial ROS production and membrane permeabilization, which eventually culminated in mitochondria-dependent apoptosis in resting B cells. Loss of TRAF3 had the opposite effects on the morphology and function of mitochondria as well as mitochondria-dependent apoptosis in resting B cells. Interestingly, co-expression of TRAF3 and MFF resulted in decreased phosphorylation and ubiquitination of MFF as well as decreased ubiquitination of TRAF3. Moreover, lentivirus-mediated overexpression of MFF restored mitochondria-dependent apoptosis in TRAF3-deficient malignant B cells. Taken together, our findings provide novel insights into the apoptosis-inducing mechanisms of TRAF3 in B cells: as a result of survival factor deprivation or under other types of stress, TRAF3 is mobilized to the mitochondria through its interaction with MFF, where it triggers mitochondria-dependent apoptosis. This new role of TRAF3 in controlling mitochondrial homeostasis might have key implications in

TRAF3-mediated regulation of B cell transformation in different cellular contexts. Our findings also suggest that mitochondrial fission is an actionable therapeutic target in human B cell malignancies, including those with *TRAF3* deletion or relevant mutations.

Keywords: TRAF3, MFF, mitochondria, apoptosis, B lymphocytes, B cell malignancies

HIGHLIGHTS

- Cytoplasmic TRAF3 is mainly localized at mitochondria and interacts with MFF in B lymphocytes after 2 days in culture.
- TRAF3 regulates the phosphorylation and ubiquitination of MFF, mitochondrial morphology, respiration and ROS production to induce apoptosis.
- Overexpression of MFF restores mitochondria-dependent apoptosis in TRAF3-deficient malignant B cells.

INTRODUCTION

B cell malignancies comprise the majority of human blood cancers and represent the most common types of lymphoid tumors (1–3). One essential pathogenic mechanism underlying B cell malignant transformation is the dysregulation of the survival and apoptosis pathways, including the B cell receptor (BCR)-Btk, NF-κB1/2-Bcl-2, PI-3K-Akt-mTOR, c-Myc-ERK and Jak-STAT signaling axes (4–12). Recurrent genetic alterations that lead to the activation/elevation of the survival signaling pathways or inhibition/reduction of the apoptosis signaling pathways are frequently detected in various B cell malignancies. Typical examples are gene amplifications, chromosomal translocations or activating mutations that result in increased expression levels or constitutive activation of critical pro-survival and anti-apoptotic proteins such as NIK, c-Rel, c-Myc, Bcl-2, Btk, and $p110^{\delta}$ of PI-3K (4–12). Alternative examples include gene deletions, chromosomal loss or inactivating mutations that cause decreased expression levels or impaired activities of inhibitors of the survival pathways and pro-apoptotic proteins such as IκBα, A20, PTEN, DUSP2, Fas and Bim (4–12). Such deregulation of the survival and apoptosis pathways not only contributes to the pathogenesis but also mediates resistance to various therapies in patients with B cell malignancies (4–11). Therefore, therapeutic strategies and drugs aimed at targeting the survival pathways or restoring the apoptosis pathways are being developed and tested in clinical trials as effective treatments for B cell malignancies, and particularly as useful adjuvants to overcome resistance to other therapies (4–11). Better understanding of the regulatory mechanisms of B cell survival and apoptosis will facilitate the development and improvement of these therapeutic strategies.

One of the most frequently deleted or mutated survival regulator in human B cell malignancies is TRAF3 (13, 14), a cytoplasmic adaptor protein that has been identified as a critical regulator of cell survival in mature B lymphocytes (13, 15–19). Deletions and inactivating mutations of the *TRAF3* gene have been documented in almost all malignancies of mature B cells, including multiple myeloma (MM), diffuse large B-cell lymphoma (DLBCL), B-cell chronic lymphocytic leukemia (B-CLL), gastric and splenic marginal zone lymphoma (MZL), Hodgkin lymphoma (HL) and Waldenstrom's macroglobulinemia (WM) (13, 14). Specific deletion of the *Traf3* gene from B lymphocytes in mice results in severe peripheral B cell hyperplasia due to the prolonged survival of mature B cells independent of the principle B cell survival factor BAFF (15, 16), which eventually leads to spontaneous development of splenic MZL and B1 lymphomas (19). Mechanistically, the TRAF3-TRAF2-cIAP1/2 complex constitutively targets the NF-κB-inducing kinase (NIK) for K48-linked polyubiquitination and proteasome-dependent degradation (20–23). Ablation of TRAF3 as well as TRAF2 or cIAP1/2 all results in constitutive NF-κB2 activation and prolonged survival of mature B lymphocytes (15, 16, 24). Furthermore, we recently elucidated that TRAF3 also regulates the choline kinase α (Chkα)-mediated phosphocholine and phosphatidylcholine (PC)/phosphatidylethanolamine (PE) biosynthesis pathways to control the survival of mature B cells (25). Paradoxically, transgenic overexpression of *TRAF3* in B cells promotes B cell differentiation and results in plasmacytosis and autoimmunity in mice (26), while double transgenic overexpression of both *TRAF3* and *BCL-2* in B cells leads to the development of multiple classes of mature non-Hodgkin B cell lymphomas in mice (27). Detailed mechanisms underlying such seemingly opposite roles of TRAF3 in B cell tumorigenesis were unknown, but all the above findings consistently indicate that TRAF3 is a master regulator of B cell survival and function.

It is known that in the absence of stimulation, TRAF3 proteins are distributed in the cytoplasm and nucleus (28, 29). In the present study, we were interested to determine whether TRAF3 proteins are evenly distributed within the cytoplasm in resting B cells. We obtained an unexpected finding that the majority of cytoplasmic TRAF3 proteins were localized at the mitochondria in resting splenic B cells after 2 days in culture. Given the central importance of mitochondria in regulating cell survival and apoptosis (30–32), our unexpected finding of the mitochondrial localization of TRAF3 proteins led us to test a novel hypothesis that in addition to the previously elucidated TRAF3-NIK-NF-κB2 and Chkα-phosphocholine-PC/PE pathways, TRAF3 can directly regulate the physiology of mitochondria to control B cell apoptosis. Our results described in this paper provide interesting evidence to support this hypothesis. We identified mitochondrial fission factor (MFF), a mitochondrial outer membrane (MOM) protein, as a novel TRAF3-interacting protein in B cells. We demonstrated that

TRAF3 inhibited the posttranslational modifications of MFF, regulated mitochondrial morphology and function, and promoted mitochondria-dependent apoptosis in B cells. Our findings thus shed new light into the complex apoptosis-inducing mechanisms of TRAF3 in B cells. Furthermore, our study discovered additional targetable points, MFF and mitochondrial fission, for the treatment of human B cell malignancies, especially those involving *TRAF3* deletion or relevant mutations.

MATERIALS AND METHODS

Mice and Cell Lines

Traf3$^{flox/flox}$CD19$^{+/Cre}$ (B-*Traf3*$^{-/-}$) and *Traf3*$^{flox/flox}$ (littermate control, LMC) mice were generated as previously described (15). All experimental mice for this study were produced by breeding *Traf3*$^{flox/flox}$ mice with *Traf3*$^{flox/flox}$CD19$^{+/Cre}$ mice. All mice were kept in specific pathogen-free conditions in the Animal Facility at Rutgers University, and were used in accordance with NIH guidelines and under an animal protocol (Protocol # 08-048) approved by the Animal Care and Use Committee of Rutgers University. Equal numbers of male and female mice were used in this study.

The human multiple myeloma (MM) cell line 8226, which contains bi-allelic *TRAF3* deletions, was kindly provided by Dr. Leif Bergsagel (Mayo Clinic, Scottsdale, AZ) and was cultured as previously described (33). The human embryonic kidney 293T cell line was purchased from American Type Culture Collection (ATCC, Manassas, VA) and was cultured according to the manufacturer's protocol.

Reagents and Antibodies

Mitoprobe JC-1 Assay Kit, MitoSOX Red, and tissue culture supplements including stock solutions of sodium pyruvate, L-glutamine, non-essential amino acids and HEPES (pH 7.55) were from Invitrogen (Carlsbad, CA). Fluorochrome-labeled antibodies (Abs) against Annexin V and mouse Thy1.1 were purchased from BioLegend (San Diego, CA). Propidium iodide (PI), MG-132 and the sarkosyl detergent (N-laurylsarcosine sodium) were purchased from Sigma-Aldrich Corp. (St. Louis, MO). Mitochondria Isolation Kit was purchased from ThermoFisher (Waltham, MA). Recombinant BAFF was from PeproTech (Rocky Hill, NJ) and agonistic anti-CD40 (HM40-3) was purchased from eBioscience (San Diego, CA). The TnT® Quick T7 Coupled Transcription/Translation System was from Promega (Madison, WI). Seahorse XF Cell Mito Stress Test Kit was obtained from Agilent Technologies (Lexington, MA). EDTA-free Protease Inhibitor Cocktail Tablets were obtained from Roche Diagnostics Corp (Indianapolis, IN). Phosphatase Inhibitor Mini Tablets, the deubiquitinase inhibitor N-ethylmaleimide (NEM), GelCode Blue Stain reagent and Streptavidin-Sepharose beads were purchased from Pierce (Rockford, IL). Glutathione-Sepharose 4B beads were from GE Healthcare (Chicago, IL). Anti-c-Myc Tag (9E10) Affinity Gel was from BioLegend (San Diego, CA). Bradford Assay was purchased from Bio-Rad (Hercules, CA). Polyclonal or monoclonal rabbit Abs against total or phosphorylated MFF, Caspase 9, Caspase 3, Calreticulin, COX IV, YY1, Bcl-xL, Bcl-2, Mcl-1, Bax, ubiquitin (Ub), K48-Ub, K63-Ub and HA tag were from Cell Signaling Technology (Beverly, MA). Polyclonal rabbit Abs to TRAF3 (H122) and Myc tag were from Santa Cruz Biotechnology (Santa Cruz, CA). Mouse monoclonal Abs to SBP tag was purchased from EMD Millipore Corp (Burlington, MA). Anti-β-actin Ab was from Chemicon (Temecula, CA). HRP-labeled secondary Abs were from Jackson ImmunoResearch Laboratories, Inc. (West Grove, PA).

DNA Constructs

The full-length coding cDNA sequence of human TRAF3 was cloned and the lentiviral expression vector pUB-TRAF3-Thy1.1 was generated as previously described (25). To facilitate co-immunoprecipitation and affinity purification, we engineered an N-terminal FLAG tag or a C-terminal streptavidin-binding peptide-6xHistidine (SBP-6xHis) tag (34) in frame with the TRAF3 coding sequence, respectively. We subsequently generated two lentiviral expression vectors of tagged human TRAF3, including pUB-FLAG-TRAF3 and pUB-TRAF3-SBP-6xHis. For GST pull-down studies, we cloned the human TRAF3 coding sequence into the pGEX vector (provided by Dr. Mike Kiledjian, Rutgers University) (35) and generated the pGEX-GST-TRAF3 plasmid that expresses the GST-TRAF3 fusion protein. We also engineered several deletion mutants of human TRAF3 that lack different structural domains (28) using PCR cloning, including ΔTRAF-C (lacks the TRAF-C domain), ΔTRAF-N&C (lacks the TRAF-N and TRAF-C domains), ΔZnR (lacks the Zinc RING domain) and ΔZnR&F (lacks the Zinc RING domain and all 5 Zinc fingers). The coding cDNA sequences of MFF were cloned from the human MM cell line 8226 cells using reverse transcription PCR with the high fidelity polymerase Pfu UltraII (Agilent, Santa Clara, CA). Primers used for the cloning of human MFF include hMFF isoform 1-F (5'-ATT TAA ATG AGT AAA GGA ACA AGC A -3') or hMFF isoform 2 or isoform 3-F (5'- GCT GAG ATG GCA GAA ATT AGT CGA ATT -3') paired with hMFF-R (5'- CTC TAG CGG CGA AAC CAG AGC CA -3'). No PCR products of human MFF isoform 1 were amplified from 8226 cells. PCR products of human MFF isoform 2 or 3 were gel-purified and verified by DNA sequencing. To facilitate immunoprecipitation studies, we engineered an N-terminal Myc tag (34) in frame with the human MFF coding sequences and subsequently cloned them into the expression vector pcDNA3.0. The coding cDNA sequence of each Myc-tagged MFF isoform was also subcloned into the lentiviral expression vector pUB-eGFP-Thy1.1 (36) (generously provided by Dr. Zhibin Chen, the University of Miami, Miami, FL) by replacing the eGFP coding sequence with Myc-MFF. The lentiviral expression vector of HA-tagged ubiquitin LPC-HA-Ub was described previously (37). Each DNA construct was verified by DNA sequencing at GenScript (Piscataway, NJ).

Splenic B Cell Purification and Culture

Mouse splenic B cells were purified using anti-mouse CD43-coated magnetic beads and a MACS separator (Miltenyi Biotec Inc.) following the manufacturer's protocols as previously described

(15). The purity of the isolated B cell population was monitored by FACS analysis and cell preparations of >98% B220+CD3- purity (**Supplementary Figure 1**) were used for protein preparation and mitochondrial analyses. An aliquot of purified splenic B cells was cultured *ex vivo* in mouse B cell medium (15, 25) for 1 or 2 days before protein preparation and mitochondrial analyses.

Transduction of Human MM Cells With Lentiviral Expression Vectors

Lentiviruses of pUB-TRAF3-SBP-6xHis, pUB-FLAG-TRAF3, pUB-Myc-MFF, pUB-Myc-MFF3 and an empty vector pUB-Thy1.1 were packaged and lentiviral titers were determined as previously described (33, 38). Human MM 8226 cells were transduced with the packaged lentiviruses at an MOI of 1:5 (cell:virus) in the presence of 8 μg/mL polybrene (33, 38). Transduction efficiency of cells was analyzed at day 3 post transduction using Thy1.1 immunofluorescence staining followed by flow cytometry. Transduced cells were subsequently used for mitochondrial isolation and affinity purification or apoptosis analyses.

Flow Cytometry

For analysis of apoptosis, cells were stained with annexin V according to the manufacturer's protocol (Invitrogen) and analyzed by flow cytometry as previously described (19). For cell cycle analysis, cells were fixed with ice-cold 70% ethanol. Cell cycle distribution was subsequently determined by propidium iodide (PI) staining followed by flow cytometry as previously described (39). For the measurement of mitochondrial membrane permeabilization, cells were stained with a MitoProbe JC-1 Assay Kit (Molecular Probes) following the manufacturer's instructions. Briefly, 2 x 10^6 cells of each condition were resuspended in 1 ml PBS and incubated for 5 minutes at 37°C. Subsequently, 10 μl of 200 μM JC-1 (final concentration: 2 μM) was added to the cells and incubated at 37°C for 30 minutes. Cells were subsequently washed with 2 ml of PBS, fixed with 1% formaldehyde, and then analyzed by flow cytometry. Listmode data were acquired on a Northern Lights spectral flow cytometer (Cytek, Fremont, CA) or a FACSCalibur (Becton Dickinson, Mountain View, CA). The results were analyzed using the FlowJo software (TreeStar, San Carlos, CA).

Total Protein Extraction and Immunoblot Analysis

For total protein lysates, cell pellets were lysed in 2X SDS sample buffer (62.5 mM Tris, pH6.8, 1% SDS, 15% glycerol, 2% β-mercaptoethanol and 0.005% bromophenol blue), sonicated for 30 pulses, and then boiled for 10 minutes (40). Proteins were separated by SDS-PAGE and immunoblotted with antibodies to specific proteins as indicated in the figures followed by HRP-conjugated secondary antibodies (goat anti-rabbit or goat anti-mouse IgG). A chemiluminescent substrate (Pierce) was used to detect HRP-labeled Abs on immunoblots. Images of chemiluminescence signals on immunoblots were acquired and quantitated using a low-light imaging system (LAS-4000 mini, FUJIFILM Medical Systems USA, Inc., Stamford, CT) (19, 33).

Fractionation of Cytosol, Mitochondria and Microsomes (Rich in ER)

For purified mouse splenic B cells (8 x 10^7 cells/condition), mitochondria were fractionated from cells using a Mitochondria Isolation Kit (ThermoFisher) following the manufacturer's protocol. For human MM cells (3 x 10^7 cells/condition), mitochondria were fractionated from cells using 700 μl of Mitochondria Isolation Buffer (250 mM sucrose, 10 mM HEPES, pH7.5, 10 mM KCl, 1 mM EDTA and 0.1 mM EGTA with protease and phosphatase inhibitors) followed by homogenization in a Dounce homogenizer as previously described (40). Nuclei were pelleted from the Mitochondrial Isolation lysates by centrifugation at 1,000 g for 10 minutes at 4°C. The cleared lysates were then centrifuged at 10,000 g for 25 minutes at 4°C to obtain the pellets of mitochondria. The supernatants were further centrifuged at 100,000 g for 2 hours to separate the pellets of microsomes (rich in ER) from cytosolic proteins (S100 fraction). One-fifth volume of 5X SDS sample buffer was added into each S100 fraction. The pellets of mitochondria and microsomes (rich in ER) were lysed and sonicated in 300 μl of 2X SDS sample buffer, respectively. Cytoplasmic and nuclear extracts were prepared as previously described (15, 33). All protein samples were subsequently boiled for 10 minutes for immunoblot analyses.

Co-Immunoprecipitation Assay of Mitochondrial Lysates

Human MM cell line 8226 cells (1.5 x 10^8 cells/condition) transduced with pUB-TRAF3-SBP-6xHis or pUB-FLAG-TRAF3 were used for mitochondrial fractionation as described above. Mitochondrial pellets were lysed and sonicated in CHAPS lysis buffer (1% CHAPS, 20 mM Tris, pH 7.4, 150 mM NaCl, 50 mM β-glycerophosphate, and 5% glycerol with freshly added 1 mM DTT and EDTA-free Mini-complete protease inhibitor cocktail) (39). Mitochondrial lysates were cleared by centrifugation at 10,000 g for 20 minutes at 4°C. Cleared mitochondrial lysates were subsequently incubated with the Streptavidin-Sepharose beads (Pierce) to immunoprecipitate TRAF3-SBP-6xHis. Immunoprecipitates were washed 5 times with the Wash Buffer (39), resuspended in 2X SDS sample buffer, boiled for 10 minutes, and then separated on 4-16% gradient SDS-PAGE (Invitrogen) for mass spectrometry-based sequencing or immunoblot analyses.

Liquid Chromatography-Tandem Mass Spectrometry (LC-MS/MS)-Based Sequencing

Mitochondrial lysates immunoprecipitated with the Streptavidin-Sepharose beads were used for LC-MS/MS-based sequencing. The entire gel lanes of TRAF3-SBP-6xHis and the negative control (FLAG-TRAF3) immunoprecipitates were each sectioned into 15 continuous slices. The gel slice samples were subjected to thiol reduction by TCEP, alkylation with iodoacetamide, and digestion with sequencing-grade modified trypsin (41, 42). Peptides were eluted from the gel slices, desalted, and then subjected to reversed-phase nano-flow ultra high

performance capillary liquid chromatography (uPLC) followed by high-resolution/high-mass accuracy MS/MS analysis using an LC-MS platform consisting of an Eksigent Nano Ultra 2D Plus uPLC system hyphenated to a Thermo Orbi Velos mass spectrometer (40). The MS/MS was set to operate in data dependent acquisition mode using a duty cycle in which the top 15 most abundant peptide ions in the full scan MS were targeted for MS/MS sequencing. Full scan MS1 spectra were acquired at 100,000 resolving power and maintained mass calibration to within 2-3 ppm mass accuracy. LC-MS/MS data were searched against the human IPI and UniProt databases using the Mascot and Proteome Discoverer search engines (41, 42). Protein assignments were considered highly confident using a stringent false discovery rate threshold of <1%, as estimated by reversed database searching. Rough relative protein amounts were estimated using spectra counting values.

Co-Immunoprecipitation From Transfected 293T Cells

For verification of the TRAF3-MFF interaction, 293T cells were co-transfected with pUB-TRAF3-SBP-6xHis and pcDNA3-Myc-MFF, pcDNA3-Myc-MFF3, pcDNA3-Myc-CSNK2A2 or an empty expression vector pcDNA3-Myc. At day 2 post transfection, cells (2 x 10^7 cells/condition) were harvested and total cellular proteins were lysed in 1% CHAPS Lysis Buffer (39), sonicated and cleared by centrifugation. The cleared lysates were immunoprecipitated with the Streptavidin-Sepharose beads. Immunoprecipitates were washed 5 times with the Wash Buffer (39), resuspended in 2X SDS sample buffer, boiled for 10 minutes, and then separated on SDS-PAGE for immunoblot analyses.

In Vitro Transcription and Translation of Myc-MFF

In vitro translation of Myc-MFF proteins was performed using the pcDNA3-Myc-MFF plasmid as the template with a coupled in vitro transcription/translation system from reticulocyte lysates (TnT® Quick T7 Coupled Transcription/Translation System, Promega), following the manufacturer's protocol. The reactions were incubated at 30°C for 90 min. Translation of Myc-MFF was verified by Western blot analysis.

GST Pull-Down Assay

For preparation of GST-TRAF3 fusion proteins, each pGEX-GST-TRAF3 plasmid, including wild type (WT) and the deletion mutants, was transformed into *E. coli* BL21 bacteria. Expression of GST-TRAF3 fusion proteins were induced with 0.2 mM isopropyl-β-D-thiogalactoside (IPTG) for 2 hours as described (35). Bacterial pellets were lysed and sonicated in the Bacteria Lysis Buffer (20 mM Tris-HCl, pH 8.0 and 150 mM NaCl with freshly added 1 mg/ml lysozyme, 1% sarkosyl, 1 mM DTT and 1x EDTA-free Protease Inhibitor cocktail). Bacterial lysates were centrifuged at 10,000 g for 30 minutes to remove insoluble materials. Cleared bacterial lysates were diluted with 3 volumes of the Dilution Buffer (2% Triton X-100, 20 mM Tris, pH 8.0, 150 mM NaCl, 1 mM DTT and 1x EDTA-free Protease Inhibitor cocktail). GST-TRAF3 fusion proteins were subsequently purified from the diluted bacterial lysates using Glutathione–Sepharose 4B beads (GE Healthcare) according to the manufacturer's protocol. After incubation with the lysates, the beads were washed five times in PBS containing 0.5% Triton X-100, and then eluted with 50 mM Tris-HCl (pH 8.0) containing 10 mM of reduced glutathione. The concentrations of eluted GST-TRAF3 proteins were determined by Bradford analysis, and then verified by SDS-PAGE and GelCode Blue staining by comparing to protein standards of known concentrations loaded on the same gel.

For GST pull-down assay of Myc-MFF proteins expressed in 293T cells, whole cell lysates were prepared from 293T cells (2 x 10^7 cells/condition) transfected with pcDNA3-Myc-MFF or pcDNA3-Myc-MFF3 using the 1% CHAPS Lysis Buffer (39). For GST pull-down assay of *in vitro* translated Myc-MFF proteins, the translated proteins (4 x 50 µl of reactions/condition) were also lysed in the 1% CHAPS Lysis Buffer (39). 293T cell lysates or the *in vitro* translated proteins were cleared by centrifugation, and then incubated with Glutathione-Sepharose 4B beads for 1 hour at 4°C to remove non-specific bead interactors. The pre-cleared lysates were subsequently incubated with 10 µg of GST, GST-TRAF3 fusion protein or GST-TRAF3 deletion mutants in the presence of Glutathione-Sepharose 4B beads for 4 hours at 4°C. After incubation, the beads were washed 5 times with the Wash Buffer (39). Proteins pulled-down by the beads were eluted with 100 µl of 2X SDS sample buffer, boiled at 98°C for 10 minutes, and then analyzed by SDS-PAGE and immunoblot analyses. GST, GST-TRAF3 fusion protein or GST-TRAF3 deletion mutants in each pull-down sample were also analyzed by SDS-PAGE and visualized by GelCode blue staining. Band intensity of GelCode Blue stained gels was quantified using the ImageJ software (NIH, Bethesda, MD) (43).

Electron Microscopy

For the electron microscopic (EM) examination of mitochondrial morphology and number, cells were fixed in 0.1 M cacodylate buffer with 2.5% glutaraldehyde, 4% paraformaldehyde and 8 mM $CaCl_2$. The fixed and processed samples were subsequently analyzed on a JOEL 1200EX electron microscope as previously described (44).

Mitochondrial Function Assay

Mitochondrial oxygen consumption rates (OCR) were measured using a Cell Mito Stress Test Kit and a Seahorse XFe24 Analyzer (Seahorse Bioscience, North Billerica, MA) as described previously (45). Briefly, purified splenic B cells were seeded at 2 x 10^6 cells/well in XFe24 plates in Seahorse XF medium (10% FBS, 1% Pen-Strep). To derive different parameters of mitochondrial respiration, OCRs were measured sequentially before and after injecting oligomycin (a complex V inhibitor), p-trifluoromethoxy carbonyl cyanide phenyl hydrazine (FCCP, a protonophore and mitochondrial uncoupler), and antimycin A (a complex III inhibitor) plus rotenone (a complex I inhibitor), respectively, from XFe24 reagent ports. The following inhibitor concentrations were used for the mitochondrial stress test: oligomycin, 1 µM; FCCP, 1 µM; rotenone/antimycin A, 1 µM.

All OCR measurements were normalized to cell number (per million cells).

Mitochondrial ROS Analysis

For mitochondrial superoxide analysis, mouse splenic B cells were washed with PBS and stained with 1 μM of MitoSOX Red (Molecular Probes) for 30 minutes at 37°C in a 5% CO_2 incubator. Stained cells were washed twice with pre-warmed PBS and subsequently analyzed by flow cytometry on a Northern Lights spectral flow cytometer.

Ubiquitination Analysis

For ubiquitination analysis, 293T cells were co-transfected with LPC-HA-Ub and pUB-TRAF3-SBP-6xHis, pUB-Myc-MFF or an empty lentiviral vector pUB-Thy1.1. At day 2 post transfection, cells were treated with 10 μM of the proteasome inhibitor MG-132 at 37°C for 4 h, and then harvested at 2 x 10^7 cells/condition. Total cellular proteins were lysed in 1% CHAPS Lysis Buffer (39) containing 1x Phosphatase Inhibitors (Pierce) and 1 mM NEM. The insoluble pellets were removed by centrifugation at 10,000 g for 20 minutes at 4°C. The CHAPS lysates were subsequently immunoprecipitated with the Anti-c-Myc Tag (9E10) Affinity Gel (BioLegend) or Streptavidin-Sepharose beads (Pierce). Immunoprecipitates were washed 5 times with the Wash Buffer (39) containing 1x Phosphatase Inhibitors and 1 mM NEM. Ubiquitination of the immunoprecipitated MFF or TRAF3 was analyzed by immunoblot analyses.

Statistics

Statistical analyses were performed using the Prism software (GraphPad, La Jolla, CA). For direct comparison of the levels of cell apoptosis and mitochondrial parameters between LMC and *Traf3*$^{-/-}$ B cells, statistical significance was determined with the unpaired *t* test for two-tailed data. For comparison of three or more groups of data such as the relative binding between GST-TRAF3 (WT or mutants) and MFF, a one-way analysis of variance (ANOVA) was used to determine the statistical significance. *P* values less than 0.05 are considered significant, *P* values less than 0.01 are considered very significant, and *P* values less than 0.001 are considered highly significant.

RESULTS

TRAF3 Promotes Mitochondria-Dependent Apoptosis in Resting B Cells

We previously reported that *Traf3* deficiency results in prolonged survival of mature B lymphocytes (15), which eventually leads to spontaneous development of splenic marginal zone lymphoma and B1 lymphoma in B-*Traf3*$^{-/-}$ mice (19). Interestingly, CD95-induced apoptosis is normal in *Traf3*$^{-/-}$ splenic B cells (15), suggesting that the extrinsic apoptotic pathway is not interrupted by *Traf3* deficiency. Here we measured the intrinsic apoptosis in premalignant *Traf3*$^{-/-}$ and TRAF3-sufficient splenic B cells prepared from tumor-free, young adult B-*Traf3*$^{-/-}$ and littermate control (LMC) mice. Approximately 50% of LMC B cells underwent apoptosis at day 2 after *ex vivo* culture as analyzed by annexin V staining (**Figures 1A, B**). DNA fragmentation was detected in the apoptotic LMC B cells by cell cycle analysis (**Figures 1C, D**). However, such cellular apoptosis and DNA fragmentation were drastically reduced in *Traf3*$^{-/-}$ B cells (**Figures 1A–D**). Mitochondria are the gateway of intrinsic apoptosis, which is often preceded by mitochondrial membrane potential change (30–32). We next analyzed the mitochondrial membrane potential changes using JC-1 staining and flow cytometry. We found that *Traf3* deficiency dramatically suppressed the mitochondrial membrane permeabilization in resting splenic B cells at day 2 after *ex vivo* culture (**Figures 1E, F**). Interestingly, treatment with the survival factor BAFF, which is known to induce TRAF3 degradation in B cells (28), was able to prevent apoptosis, DNA fragmentation and mitochondrial membrane permeabilization in LMC B cells but did not have detectable effects on *Traf3*$^{-/-}$ B cells (**Supplementary Figure 2**). We further investigated the downstream biochemical events induced by mitochondrial membrane permeabilization, including activation of the initiator caspase (caspase 9) and the effector caspase (caspase 3) of the intrinsic apoptotic pathway. We observed that activation of both caspase 9 and caspase 3, as demonstrated by the cleavage of both caspases, was substantially inhibited in *Traf3*$^{-/-}$ splenic B cells (**Figure 1G**). Taken together, these data indicate that after 2 days in culture and probably under other stress conditions, TRAF3 promotes the mitochondria-dependent intrinsic apoptotic pathway in resting splenic B cells.

It has been shown that *Traf3* deficiency leads to constitutive activation of NF-κB2 (15, 16), which controls the expression of the Bcl-2 family proteins (28, 46). Given that the Bcl-2 family proteins are important regulators of mitochondria-dependent apoptosis (47, 48), we examined the expression of several members of the Bcl-2 family in purified LMC and *Traf3*$^{-/-}$ splenic B cells. We detected a slight increase in the expression level of the anti-apoptotic protein Bcl-2 in *Traf3*$^{-/-}$ B cells at day 0 and a modest up-regulation in another anti-apoptotic protein Mcl-1 in *Traf3*$^{-/-}$ B cells at day 0 and day 1 after *ex vivo* culture in the absence of stimulation (**Supplementary Figure 3**). Interestingly, BAFF stimulation or CD40 ligation markedly induced up-regulation of the anti-apoptotic proteins Bcl-xL and Mcl-1 in both LMC and *Traf3*$^{-/-}$ B cells. Up-regulation of Bcl-xL and Mcl-1 induced by anti-CD40 was more robust than that induced by BAFF, while BAFF stimulation appeared to have a stronger effect on Bcl-xL and Mcl-1 up-regulation than *Traf3* deficiency in B cells (**Supplementary Figure 3**). However, *Traf3* deficiency was as potent as BAFF stimulation at inhibiting mitochondria-dependent apoptosis in resting splenic B cells (**Supplementary Figure 2**). These results suggest that in addition to the Bcl-2 family proteins, other mechanisms may also be involved in TRAF3-mediated regulation of mitochondria-dependent apoptosis in B cells.

Cytoplasmic TRAF3 Is Mainly Localized at the Mitochondria in *Ex Vivo* Cultured Resting B Cells

In the absence of stimulation, cellular TRAF3 proteins are distributed in the cytoplasm and nucleus (28, 29)

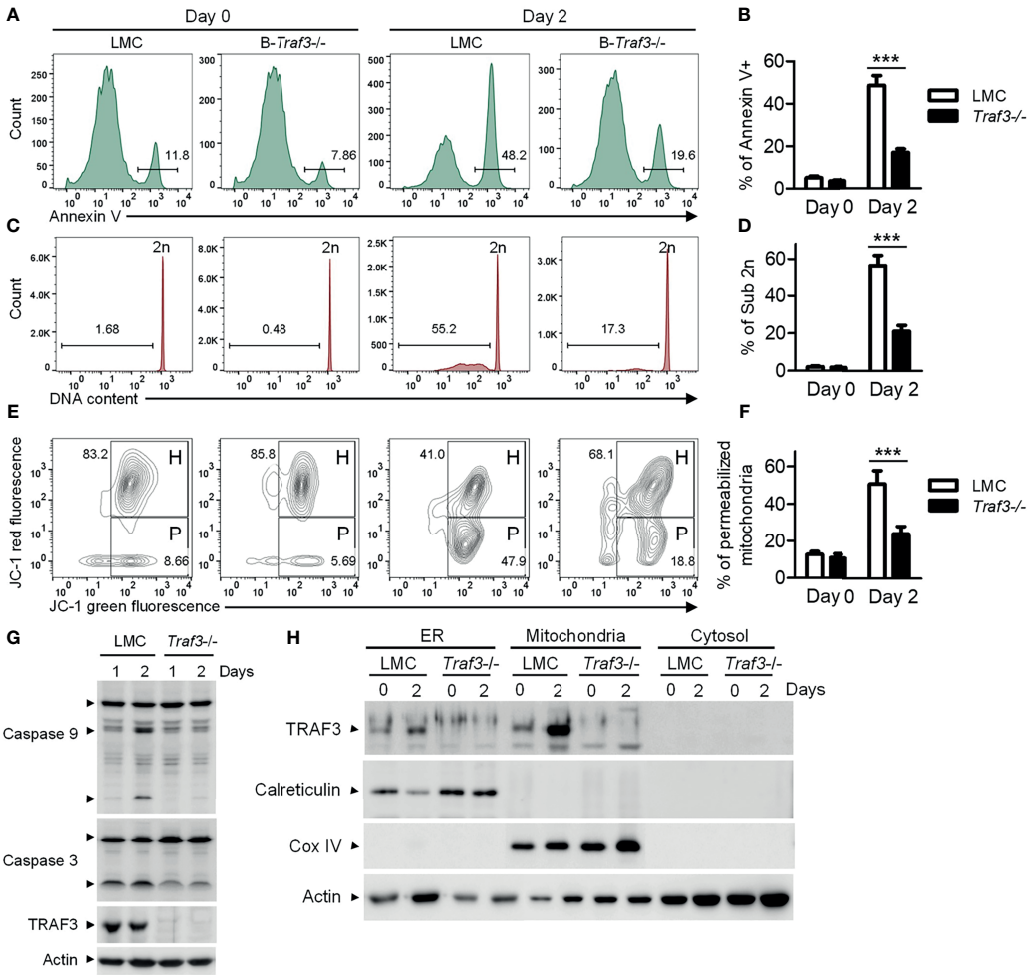

FIGURE 1 | TRAF3 promoted the mitochondria-dependent intrinsic apoptotic pathway and was mainly localized at mitochondria in resting B cells. Splenic B cells were purified from gender-matched, young adult (8-12-week-old) naïve LMC or B-*Traf3*$^{-/-}$ mice. Purified cells were analyzed directly (Day 0) or at day 2 after *ex vivo* culture in mouse B cell medium. **(A)** Representative FACS profiles of annexin V staining. Gated populations indicate the annexin V+ apoptotic cells. **(B)** Graphical results of the percentage of annexin V+ apoptotic cells. **(C)** Representative FACS profiles of cell cycle distribution analyzed by PI staining. Gated populations indicate apoptotic cells with DNA fragmentation (DNA content < 2n). **(D)** Graphical results of the percentage of apoptotic cells with DNA fragmentation. **(E)** Representative FACS profiles of mitochondrial membrane permeabilization measured by MitoProbe JC-1 staining. Gated populations in H show cells with healthy mitochondria and gated populations in P indicate cells with permeabilized mitochondria. **(F)** Graphical results of the percentage of cells with permeabilized mitochondria. **(G)** Cleavage of caspase 9 and caspase 3. Total cellular proteins were prepared at day 1 or day 2 after culture and immunoblotted for caspase 9 and caspase 3, followed by TRAF3 and actin. **(H)** Cytoplasmic TRAF3 proteins were mainly localized at mitochondria in resting B cells. ER, mitochondrial and S100 (cytosolic) proteins were biochemically fractionated and analyzed by immunoblotting. Proteins in each fraction were immunoblotted for TRAF3, calreticulin (an ER protein), COX IV (a mitochondrial protein) and actin. Immunoblots shown are representative of 3 experiments. Graphs shown in **(B, D, F)** are the mean ± SD (n=6/group, including 3 female and 3 male samples). ***$p < 0.001$ by *t* test.

(**Supplementary Figure 4**). BAFF stimulation or CD40 ligation recruits TRAF3 from the cytoplasm to the BAFF receptor or CD40 signaling complex at the sphingolipid-enriched membrane rafts in B cells (49, 50). Viral infection leads to TRAF3 re-localization from the cytoplasm to mitochondria (51, 52). To determine if TRAF3 is evenly distributed within the cytoplasm in the absence of stimulation, we prepared ER, mitochondrial and cytosolic (S100) fractionations from resting splenic B cells of naïve mice. Unexpectedly, we found that the majority of cytoplasmic TRAF3 was in the mitochondrial fraction in resting splenic B cells (**Figure 1H**). We also noticed that in LMC B cells, TRAF3 proteins were remarkably up-regulated in the mitochondria and less robustly in the ER, but not up-regulated in the nucleus, at day 2 after *ex vivo* culture (**Figure 1H** and **Supplementary Figure 4**), probably because endogenous BAFF-induced TRAF3 degradation was eliminated after *ex vivo* culture. These data suggest that BAFF-induced recruitment and subsequent degradation of TRAF3 mainly affect the proteins localized at the mitochondria. Thus, the mitochondrial localization of TRAF3 raises an intriguing possibility that

TRAF3 may also directly regulate mitochondrial physiology to induce mitochondria-dependent apoptosis in B cells.

MFF Is a Novel TRAF3-Interacting Protein

Given that TRAF3 does not contain any mitochondrial targeting motif or transmembrane domain, we reasoned that TRAF3 may be associated with mitochondria in resting B cells by interacting with mitochondrial outer membrane (MOM) proteins. We sought to identify such TRAF3-binding partner(s) in the mitochondrial fraction of B cells using affinity purification followed by LC-MS/MS. To facilitate affinity purification, we generated lentiviral expression vectors of tagged TRAF3, including pUB-TRAF3-SBP-6xHis and pUB-FLAG-TRAF3 (39, 40). To strengthen the clinical relevance of our study and eliminate the interference of endogenous TRAF3 proteins, we used the human MM cell line 8226 that contains biallelic deletions of the *TRAF3* gene for transduction by the lentiviral expression vectors of tagged TRAF3. Transduction efficiency of each lentiviral vector in 8226 cells was > 90% as determined by FACS (**Supplementary Figure 5A**).

We first validated that the C-terminal streptavidin-binding peptide (SBP)-6xHis tag did not affect the function of TRAF3 as demonstrated by its potent induction of cellular apoptosis in transduced 8226 cells (**Figure 2A**), which was comparable to that induced by the untagged, native TRAF3 in transduced 8226 cells as we previously reported (25). We also verified that TRAF3-SBP-6xHis proteins maintained the mitochondrial localization of native TRAF3 (**Supplementary Figure 5B**). We next performed affinity purification using mitochondria isolated from transduced 8226 cells. We solubilized the mitochondrial proteins in 1% CHAPS lysis buffer (39, 40). Using Streptavidin-Sepharose beads, we immunoprecipitated TRAF3-SBP-6xHis and its associated proteins from the solubilized mitochondrial proteins. Cells transduced with FLAG-TRAF3 were subjected to the same biochemical fractionation and immunoprecipitation procedures as a negative control. We confirmed the high recovery rate of TRAF3-SBP-6xHis, but not FLAG-TRAF3, by immunoprecipitation with the Streptavidin-Sepharose beads using immunoblot analyses (**Figure 2B**). We subsequently performed LC-MS/MS of the mitochondrial proteins immunoprecipitated with the Streptavidin-Sepharose beads. Interestingly, we identified the MOM protein MFF (53) as a novel candidate TRAF3-interacting protein. However, our LC-MS/MS analysis did not detect any peptide derived from MAVS, a mitochondrial protein that is known to bind to TRAF3 upon viral infection (54, 55). In addition to MFF, our LC-MS/MS analysis identified a number of other candidate TRAF3-interacting proteins, including GSTP1, CKMT1A, PISD, SLC25A40, HDHD3, PYCARD, GPI, CDS2, DBI, ACAT2, RETSAT, PDE9A, SLC4A7, PRKG2, CDC42, ALDH3A1, ME1, CSNK2A2, CAP1, PGM2, PIK3R2, GSTO1, APEH, PSAT1, UGP2, GUCY1B3 and PRMT1. Bioinformatic analyses revealed that these proteins are predicted to be localized at the mitochondrial inner membrane (MIM), mitochondrial intermembrane space (MIS), mitochondrial matrix, ER membrane, plasma membrane or cytosol (UniProt: https://www.uniprot.org/). Lacking a mitochondrial targeting sequence or transmembrane domain, TRAF3 does not have direct access to the MIM/MIS/matrix under physiological conditions. We speculate that these MIM/MIS/matrix proteins identified in our LC-MS/MS analysis were likely pulled down with TRAF3 *via* post-lysis association. On the other hand, TRAF3-interacting proteins localized at the ER or plasma membrane or cytosol could not directly recruit TRAF3 to the mitochondria. We therefore selected to focus on the MOM protein MFF for further investigation.

There are multiple isoforms of human MFF generated by alternative splicing (53). MFF isoform 2 is a dominant isoform of MFF that is commonly expressed in various cell types, including epithelial cells, fibroblasts, prostate cancer cells and neuroblastoma cells as well as in the brain (56–61). Using PCR cloning, we found that two isoforms of MFF, MFF isoform 2 (291 aa; hereafter referred to as MFF) and MFF isoform 3 (MFF3; 243 aa), were expressed in human MM 8226 cells (**Supplementary Figure 6**). We therefore engineered expression vectors of Myc-tagged MFF and MFF3, and then performed co-immunoprecipitation (co-IP) experiments using 293T cells co-transfected with the expression vectors of TRAF3-SBP-6xHis and Myc-MFF or Myc-MFF3 to verify the interaction between TRAF3 and MFF. We also included Myc-tagged CSNK2A2, another protein identified by our affinity purification and LC-MS/MS, in the co-IP experiments for comparison. Our co-IP experiments verified the association between TRAF3 and MFF or MFF3 (**Figure 2C**). Interestingly, the interaction of TRAF3-MFF or TRAF3-MFF3 appeared to be much stronger than that observed in the TRAF3-CSNK2A2 co-IP (**Figure 2C**). These data demonstrate that MFF and MFF3 are associated with TRAF3 in transfected 293T cells.

The TRAF-C Domain of TRAF3 Is Essential For Binding to MFF

We next investigated the potential direct binding between TRAF3 and MFF/MFF3 using two different GST pull-down assays. In the first assay, whole cell lysates of 293T cells transfected with Myc-tagged MFF or MFF3 were pre-cleared with Glutathione-Sepharose beads, and then incubated with purified GST-TRAF3 fusion proteins or GST native proteins in the presence of Glutathione-Sepharose beads. GST native proteins were used as a negative control to exclude proteins that were pulled down by GST but irrelevant to TRAF3. We did not detect non-specific binding between GST and MFF or MFF3 (**Figure 2D**). However, both MFF and MFF3 were pulled down by GST-TRAF3, indicating that there is a specific binding between TRAF3 and MFF or MFF3 (**Figure 2D**).

Both MFF and MFF3 contain a coiled-coil domain (**Supplementary Figure 6**), which is known to mediate the interactions of other proteins with TRAFs, including the interactions of TRIP-TRAF2/1, p62-TRAF3 and T3JAM-TRAF3 (62–64). We did not find any other known TRAF-interacting motifs such as the (P/S/A/T)-X-(Q/E)-E or (P/S)XQX(T/S/D) motifs in the protein sequences of MFF or MFF3. To map the structural domains of TRAF3 required for its interaction with MFF, we performed GST pull-down experiments using GST fusion proteins of TRAF3 deletion mutants in comparison to wild type GST-TRAF3 with whole cell lysates of 293T cells transfected with Myc-tagged MFF as

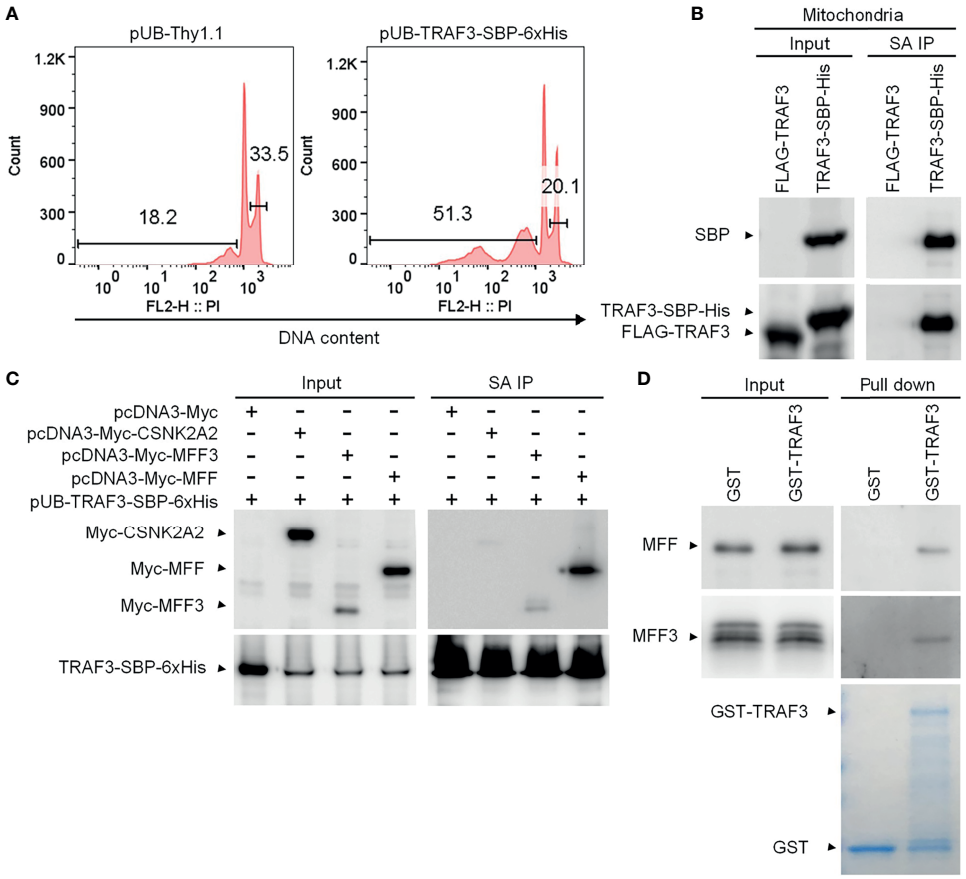

FIGURE 2 | MFF is a novel TRAF3-interacting protein. **(A)** Validation of the functionality of C-terminally SBP-6xHis-tagged TRAF3 in human MM 8226 cells. Reconstitution with the lentiviral expression vector pUB-TRAF3-SBP-6xHis induced apoptosis in 8226 cells as demonstrated by the cell cycle analysis. Cells transduced with an empty lentiviral vector (pUB-Thy1.1) were used as a control. Cell cycle analysis was performed by PI staining and FACS at day 7 post transduction. Gated populations indicate apoptotic cells with DNA fragmentation (DNA content < 2n) and proliferating cells (2n < DNA content ≤ 4n). **(B)** Large scale affinity purification of SBP-6xHis-tagged TRAF3 from isolated mitochondria of transduced 8226 cells. Cells were harvested at day 4 post transduction and were fractionated to isolate mitochondria. Mitochondrial proteins were immunoprecipitated with Streptavidin (SA)-Sepharose beads. Immunoprecipitates of TRAF3-SBP-6xHis (SA IP) from the mitochondrial proteins were analyzed by immunoblotting and used to identify TRAF3-interacting proteins by LC-MS/MS-based sequencing. Immunoblots of mitochondrial proteins before immunoprecipitation were used as the input control. Cells transduced with FLAG-TRAF3 were used as a negative control for SA IP. **(C)** Co-immunoprecipitation of MFF and MFF3 with TRAF3. 293T cells were co-transfected with pUB-TRAF3-SBP-6xHis and pcDNA3-Myc-MFF, pcDNA3-Myc-MFF3, pcDNA3-Myc-CSNK2A2 or an empty expression vector pcDNA3-Myc. Transfected cells were harvested at day 2 post transfection and total cellular proteins were immunoprecipitated with Streptavidin-Sepharose beads. Immunoprecipitates (SA IP) were immunoblotted for the Myc tag followed by the SBP tag. Bands of Myc-tagged proteins are indicated. **(D)** MFF and MFF3 pulled down by GST-TRAF3. Pre-cleared whole cell lysates of 293T cells transfected with pcDNA3-Myc-MFF or pcDNA3-Myc-MFF3 were subjected to the pull-down assay by GST alone or GST-TRAF3 fusion protein in the presence of Glutathione-Sepharose beads. GST and GST-TRAF3 used for pull-down were analyzed by SDS-PAGE and visualized by GelCode blue staining (the bottom panel). Lysates that were purified by the same pull-down procedures with GST were used as a negative control. Myc-tagged MFF and MFF3 in the input lysates and pull-down proteins were detected by immunoblotting (the top panel). Results shown are representative of at least 3 independent experiments.

described above. Different GST-TRAF3 deletion mutants were examined, including GST-TRAF3ΔTRAF-C (with the TRAF-C domain deleted), GST-TRAF3ΔTRAF-N&C (with both the TRAF-N and TRAF-C domains deleted), GST-TRAF3ΔZnR (with the Zinc RING deleted) and GST-TRAF3ΔZnR&F (with the Zinc RING and all 5 Zinc Fingers deleted) (**Figure 3A**). GST, GST-TRAF3 and GST-TRAF3 deletion mutants used for the pull-down experiments were visualized by GelCode blue staining (**Figure 3B**). We found that the interaction between MFF and TRAF3 was severely impaired by the absence of the TRAF-C or TRAF-N&C domains (**Figures 3B, C**). In fact, the TRAF-C deletion almost completely abolished the interaction with MFF, while compound deletion of TRAF-N together with TRAF-C did not further compromise the interaction with MFF (**Figures 3B, C**). Thus, the TRAF-C domain appears to be essential for the binding between TRAF3 and MFF.

To further assess the potential direct binding between TRAF3 and MFF as well as the requirement of the TRAF-C domain in this interaction, we carried out the second GST pull-down assay using *in vitro* translated Myc-MFF proteins. Similar to the results

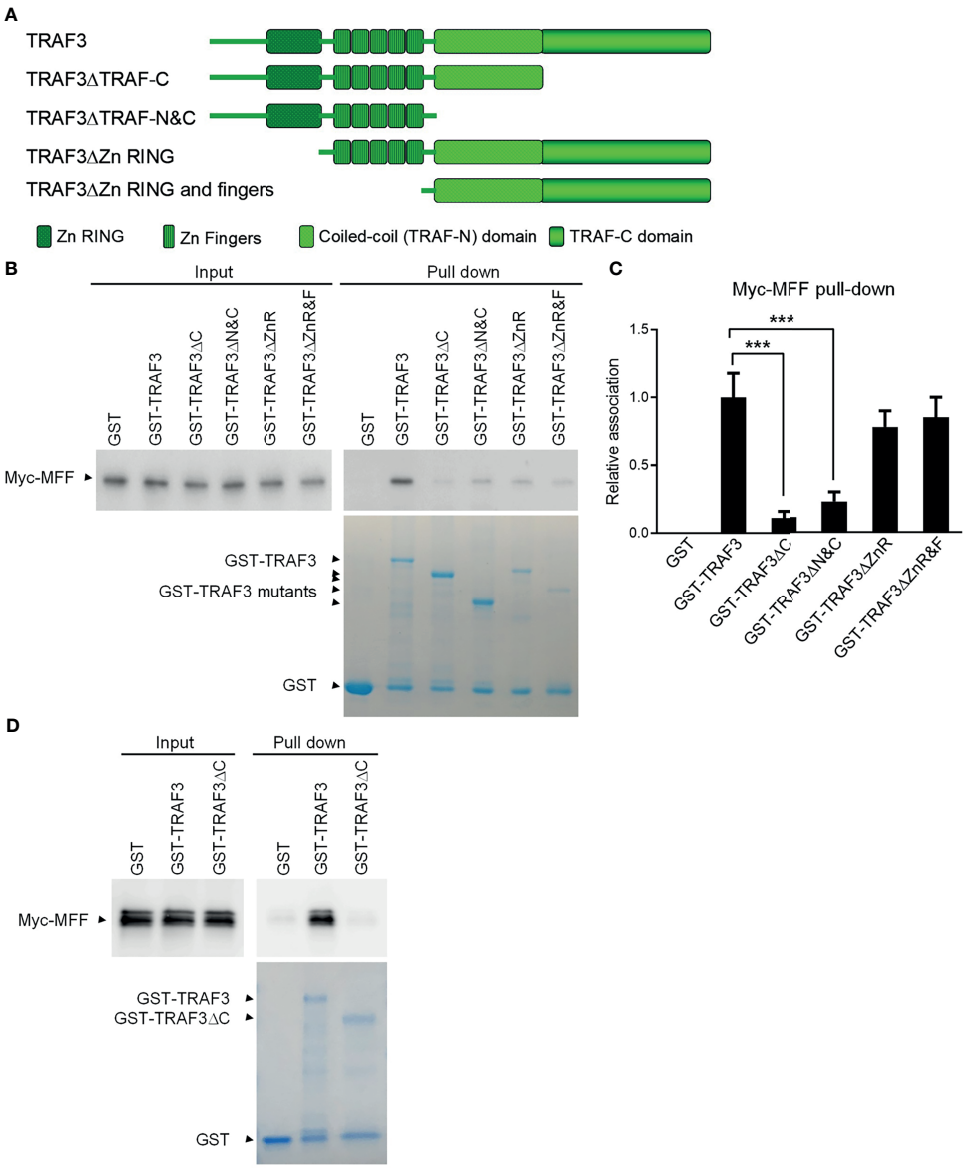

FIGURE 3 | Mapping of the structural domains of TRAF3 required for the interaction with MFF. **(A)** Schematic diagram of the TRAF3 deletion mutants generated in this study and used for the mapping experiments. Structural domains of TRAF3 that were deleted are depicted in the figure. **(B)** Interaction with MFF determined by the GST pull-down assay. Pre-cleared whole cell lysates of 293T cells transfected with pcDNA3-Myc-MFF were used in the pull-down experiments by GST alone or GST fusion proteins of WT or deletion mutants of TRAF3 in the presence of Glutathione-Sepharose beads. GST, GST-TRAF3 and GST-TRAF3 deletion mutants used for pull-down were analyzed by SDS-PAGE and visualized by GelCode blue staining (the bottom panel). GST-TRAF3 deletion mutants examined include GST-TRAF3ΔTRAF-C (ΔC), GST-TRAF3ΔTRAF-N&C(ΔN&C), GST-TRAF3ΔZn RING (ΔZnR), and GST-TRAF3ΔZn RING and fingers (ΔZnR&F). Lysates that were purified by the same pull-down procedures with GST alone were used as a negative control and those with GST-TRAF3 were used as the positive control. Myc-tagged MFF in the input lysates and pull-down proteins were detected by immunoblotting (the top panel). Results shown are representative of 3 experiments. **(C)** Graphical results of the relative association between Myc-MFF and GST fusion proteins of WT or deletion mutants of TRAF3. The Myc-MFF bands on the immunoblots and GST-TRAF3 or mutant bands on the GelCode Blue stained gels in **(B)** were quantitated using a low-light imaging system and the ImageJ Software, respectively. The amount of Myc-MFF in each pull-down lane was first normalized to the intensity of the corresponding input Myc-MFF band and further normalized to the intensity of the corresponding GST-TRAF3 or mutant band. Fold of change of the normalized Myc-MFF pull-down relative to that detected for GST-TRAF3 WT was shown in the graph (mean ± SD, n = 3). ***$p < 0.001$ by one-way ANOVA. **(D)** Direct interaction between TRAF3 and MFF determined by GST pull-down assay of *in vitro* translated proteins. Pre-cleared protein lysates of *in vitro* translated Myc-MFF were used in the pull-down experiments by GST alone, GST-TRAF3 or GST-TRAF3ΔC in the presence of Glutathione-Sepharose beads. Myc-tagged MFF in the input lysates and pull-down proteins were detected by immunoblotting (the top panel). GelCode blue staining of GST, GST-TRAF3 and GST-TRAF3ΔC used for pull-down was shown in the bottom panel. Results shown are representative of 3 experiments.

described for the GST pull-down assay of Myc-MFF proteins expressed in 293T cells, we found that *in vitro* translated MFF proteins were specifically pulled down by GST-TRAF3 but not by GST-TRAF3ΔTRAF-C (**Figure 3D**). These data demonstrate that the TRAF-C domain is required for mediating the direct binding of TRAF3 to MFF. Taken together, we identified MFF as a novel TRAF3-interacting protein, prompting us to test the hypothesis that TRAF3 may directly regulate mitochondrial physiology impacted by MFF.

TRAF3 Regulates the Morphology and Healthy Status of Mitochondria in B Cells

The primary function of MFF is to promote mitochondrial fission, the division process of mitochondria within a cell that contributes to the regulation of mitochondrial number and morphology as well as quality (53, 65). Identification of MFF as a TRAF3-interacting protein led us to test the possibility that TRAF3 may regulate the number, morphology and quality of mitochondria in B cells. We thus compared the number and morphology of mitochondria between LMC and *Traf3*$^{-/-}$ resting splenic B cells using electron microscopy to discern potential changes caused by *Traf3* deficiency. We did not detect a significant difference in the number of mitochondria between the two genotypes of B cells freshly prepared from mouse spleens (**Figures 4A, B**). However, a significant decrease in mitochondrial number was observed in LMC but not in *Traf3*$^{-/-}$ B cells at day 1 after *ex vivo* culture (**Figures 4A, B**). Interestingly, we observed that premalignant *Traf3*$^{-/-}$ splenic B cells generally contained elongated mitochondria as demonstrated by their significantly increased mitochondrial length in comparison to LMC B cells (**Figures 4A, B**). Furthermore, after cultured *ex vivo* in the absence of survival factors for 1 day, the majority of mitochondria in LMC B cells exhibited abnormal and irregular vacuoles as well as loss of mitochondrial cristae, while *Traf3*$^{-/-}$ B cells maintained a healthy morphology of mitochondria (**Figures 4A, B**). These data thus indicate that under certain situations such as growth factor

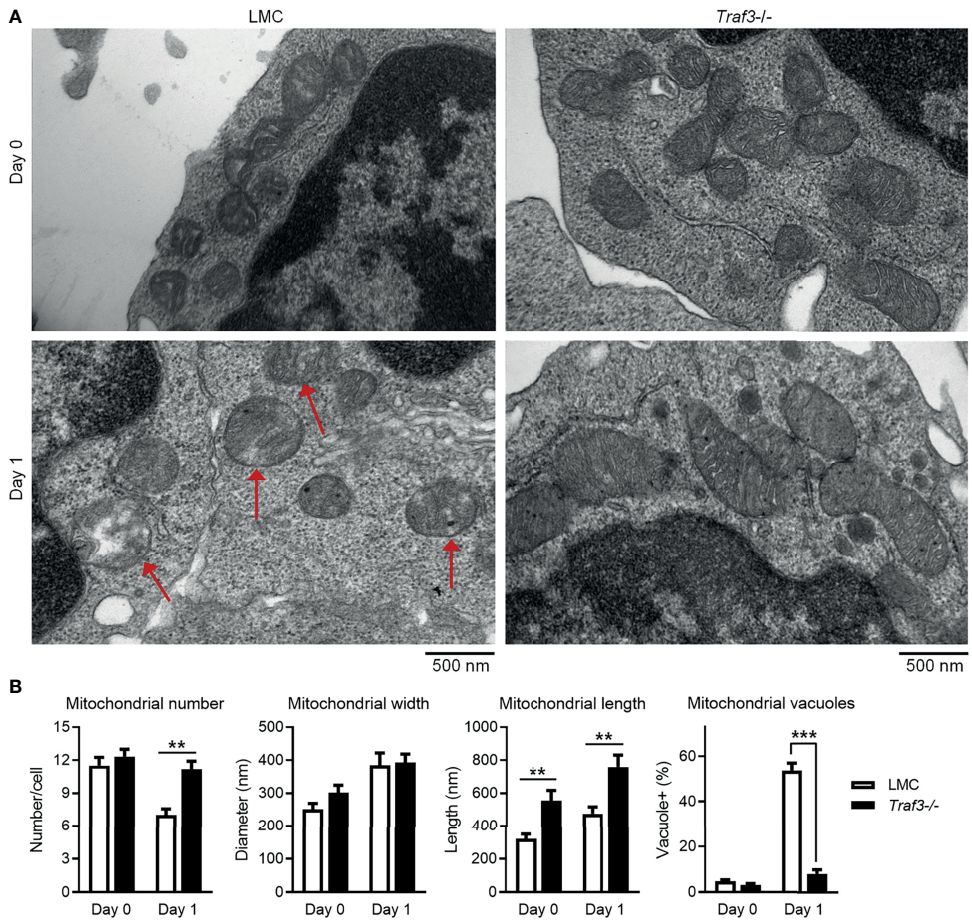

FIGURE 4 | TRAF3 regulated the number and morphology of mitochondria in resting B cells. Splenic B cells were purified from gender-matched, young adult (8-12-week-old) naïve LMC or B-*Traf3*$^{-/-}$ mice. Purified cells were analyzed directly (Day 0) or at day 1 after *ex vivo* culture. The number and morphology of mitochondria in cells were analyzed by electron microscopic (EM) examination. **(A)** Representative EM micrographs of resting B cells. Sick mitochondria are indicated with red arrows in the figure. **(B)** Graphical results of the number, width and length of mitochondria as well as the percentage of cells containing sick mitochondria (vacuole+) determined by EM examination. Graphs shown are the mean ± SD (n = 6/group; $^{**}p < 0.01$; $^{***}p < 0.001$ by *t* test).

deprivation, TRAF3 regulates the number and morphology as well as healthy status of mitochondria in B lymphocytes.

Regulation of Mitochondrial Respiration and ROS Production by TRAF3

It has been shown that MFF-mediated mitochondrial fission not only regulates mitochondrial number and morphology, but also modulates important mitochondrial functions, including mitochondrial respiration and energy production (53, 65). We therefore examined these mitochondrial functions in LMC and *Traf3*$^{-/-}$ resting splenic B cells using the Seahorse Cell Mito Stress Test. Our results showed that mitochondrial basal respiration and ATP production were comparable between the two genotypes of resting B cells freshly prepared from mouse spleens (**Figures 5A, B**). However, at day 1 after *ex vivo* culture in the absence of B cell survival factors, LMC B cells exhibited significantly decreased mitochondrial basal respiration and ATP production as compared to *Traf3*$^{-/-}$ B cells (**Figures 5A, B**). Interestingly, we found that the mitochondrial maximal respiration and spare respiratory capacity were slightly elevated in *Traf3*$^{-/-}$ B cells as compared to LMC B cells freshly prepared from mouse spleens and that these differences were substantially further enlarged at day 1 after

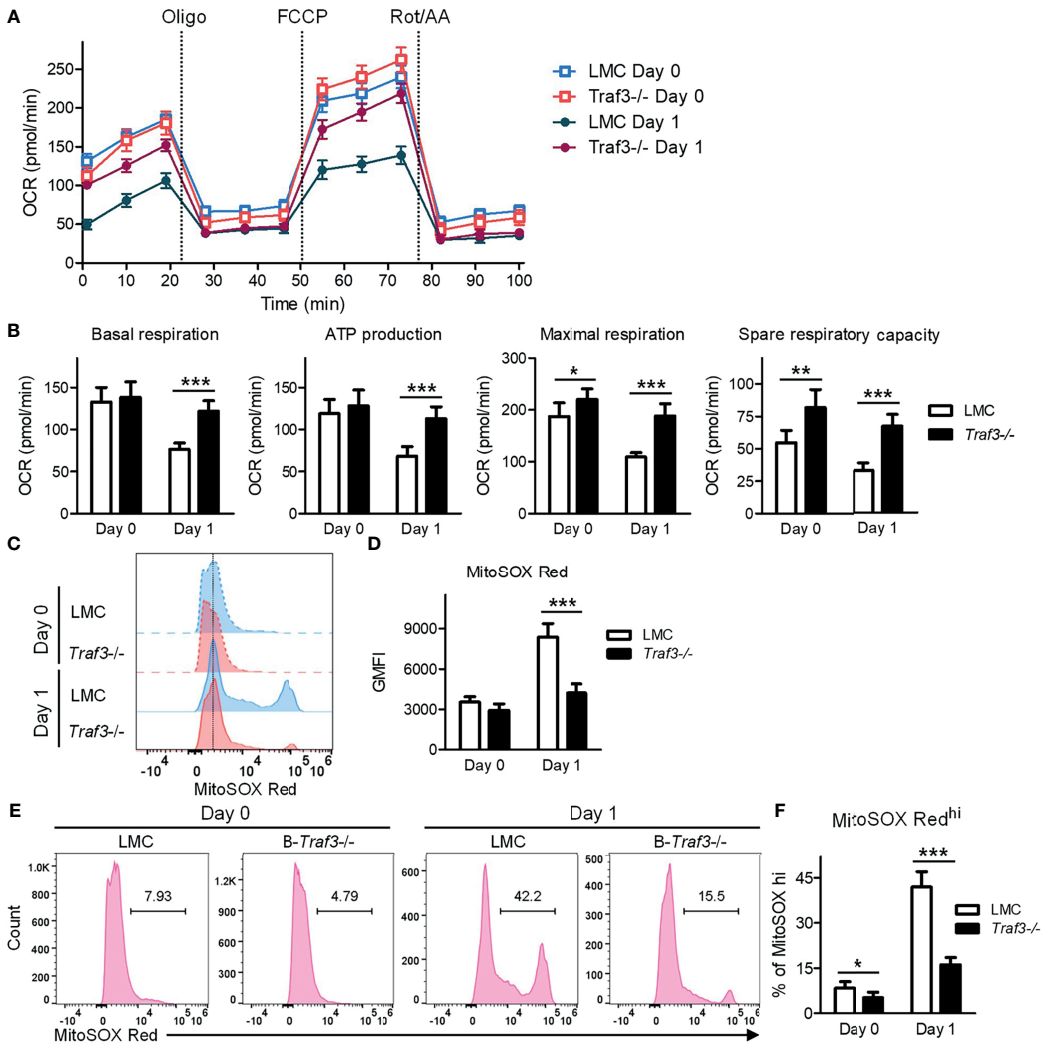

FIGURE 5 | Regulation of mitochondrial function by TRAF3 in resting B cells. Splenic B cells were purified from gender-matched, young adult (8-12-week-old) naïve LMC or B-*Traf3*$^{-/-}$ mice. Purified cells were analyzed directly (Day 0) or at day 1 after *ex vivo* culture. **(A, B)** Mitochondrial respiration and energy production determined by the Seahorse Cell Mito Stress Test. **(A)** Kinetic changes of the oxygen consumption rate (OCR). Injection time points of oligomycin (Oligo), FCCP and rotenone/antimycin A (Rot/AA) are indicated in the figure. **(B)** Graphical results of the OCRs for basal respiration, ATP production, maximal respiration and spare respiratory capacity. **(C–F)** Mitochondrial superoxide levels analyzed MitoSOX Red staining and flow cytometry. **(C)** Representative FACS histogram overlay comparing the levels of MitoSOX Red staining intensity. **(D)** Graphical results of the geometric mean (GM) of MitoSOX Red fluorescence intensity (FI). **(E)** Representative FACS profiles showing the gated MitoSOX Red^{hi} populations. **(F)** Graphical results of the percentage of MitoSOX Red^{hi} subsets. **(B, D, F)** Graphs shown are the mean ± SD (n = 6/group; *$p < 0.05$; **$p < 0.01$; ***$p < 0.001$ by *t* test).

ex vivo culture (**Figures 5A, B**). Thus, TRAF3 inhibited mitochondrial respiration and energy production in *ex vivo* cultured B cells.

MFF-induced mitochondrial functional alterations may lead to increased production of reactive oxygen species (ROS) and consequently oxidative stress, causing deteriorating mitochondrial health (53, 65). To investigate if TRAF3 also regulates mitochondrial ROS production, we measured the levels of mitochondrial superoxide using MitoSOX Red staining followed by flow cytometry. Our FACS data revealed that the mitochondrial superoxide levels were slightly higher in LMC than in *Traf3*$^{-/-}$ B cells freshly prepared from mouse spleens as measured by the geometric mean (GM) of MitoSOX Red fluorescence intensity (FI) and the percentage of MitoSOX Red^{hi} cells (**Figures 5C–F**). The differences in the mitochondrial superoxide levels between the two genotypes of B cells were drastically enlarged at day 1 after *ex vivo* culture (**Figures 5C–F**). We also observed that BAFF treatment effectively inhibited mitochondrial ROS production in LMC B cells but not in *Traf3*$^{-/-}$ B cells (**Supplementary Figure 7**), consistent with the model that BAFF-induced TRAF3 recruitment and degradation would inhibit TRAF3-mediated regulation of mitochondrial ROS production. Taken together, our findings indicate that TRAF3 regulates mitochondrial respiration, energy production and ROS production in resting B cells after 2 days in culture.

The TRAF3-MFF Interaction Affects the Modifications of MFF and TRAF3

The activity of MFF is regulated by its post-translational modifications, including phosphorylation and ubiquitination (53, 65). In light of our evidence that TRAF3 regulates mitochondrial morphology and functions, we sought to analyze if the TRAF3-MFF interaction affects the modifications of MFF to modulate its activity. We first compared the phosphorylation of MFF in cytosolic (S100), mitochondrial and ER fractions between LMC and *Traf3*$^{-/-}$ resting splenic B cells. Consistent with the published literature, we observed that MFF proteins were predominantly localized at mitochondria in resting splenic B cells (**Figure 6A**). MFF phosphorylation was not significantly different between LMC and *Traf3*$^{-/-}$ B cells freshly prepared from mouse spleens (**Figures 6A, B**). However, MFF phosphorylation was significantly reduced in LMC B cells as compared to *Traf3*$^{-/-}$ B cells at day 1 after *ex vivo* culture in the absence of B cell survival factors (**Figures 6A, B**). These data suggest that up-regulation of mitochondrial TRAF3 protein levels may inhibit the phosphorylation of mitochondrial MFF in resting B cells.

We noticed that there were multiple bands of higher molecular weights in the immunoblots of phosphorylated MFF (P-MFF), which exhibited a regulation pattern similar to that described above for MFF phosphorylation and likely represent polyubiquitinated versions of P-MFF (**Figure 6A**). Given that TRAF3 is an E3 ubiquitin ligase (14, 28), we further investigated if the TRAF3-MFF interaction directly impacts the ubiquitination of MFF or TRAF3. We co-transfected lentiviral expression vectors of HA-tagged ubiquitin together with Myc-MFF and/or TRAF3-SBP-6xHis into 293T cells. At day 2 after transfection, ubiquitination of MFF and TRAF3 was analyzed by immunoprecipitation with Myc and SBP, respectively, followed by immunoblotting with anti-HA and ubiquitin (Ub)-specific Abs. We found that overexpression of TRAF3 inhibited both the ubiquitination and phosphorylation of MFF in transfected 293T cells as demonstrated by the HA and P-MFF immunoblots (**Figure 6C**), which is consistent with our results obtained from resting splenic B cells (**Figure 6A**). Subsequently, we attempted to interrogate the type of ubiquitin modification of MFF using Abs specific for K48- or K63-linked polyubiquitination. However, K48-linked polyubiquitination of MFF was not affected by TRAF3 overexpression, while K63-linked polyubiquitin chains were not detected in the Myc-MFF immunoprecipitates (**Figure 6C**), suggesting that TRAF3 inhibits MFF ubiquitination conjugated *via* a type distinct from the canonical K48- or K63-linked polyubiquitination. Interestingly, overexpression of MFF also inhibited the ubiquitination of TRAF3 in transfected 293T cells as demonstrated by the HA immunoblots (**Figure 6D**). Furthermore, we found that the decrease in TRAF3 ubiquitination was mainly attributable to the inhibition on K48-, but not K63-, linked polyubiquitination caused by MFF overexpression as revealed by the K48-Ub and K63-Ub immunoblots (**Figure 6D**). Taken together, our results showed that the TRAF3-MFF interaction inhibits the phosphorylation and ubiquitination of MFF as well as the K48-linked polyubiquitination of TRAF3. It has been shown that K48-linked polyubiquitination of TRAF3 induces the proteasome-dependent degradation of TRAF3 (28) and that phosphorylation and ubiquitination of MFF may increase its activities at promoting mitochondrial fission and facilitating mitophagy (56, 61, 66). In this context, our findings suggest that the TRAF3-MFF interaction may inhibit specific post-translational modifications of MFF and TRAF3 to modulate the activities of MFF and regulate the stability of TRAF3 in B cells.

Overexpression of MFF Induces Mitochondria-Dependent Apoptosis in TRAF3-Deficient Human MM Cells

Our above evidence supports the hypothesis that TRAF3 may induce mitochondria-dependent apoptosis in B cells by regulating the activity of MFF. Altered activities of MFF or MFF overexpression have been shown to induce apoptosis in mammalian cells (53, 65). We reasoned that if MFF acts downstream of TRAF3, MFF overexpression may restore cellular apoptosis in TRAF3-deficient malignant B cells. To address this, we generated lentiviral expression vectors of MFF and MFF3, including pUB-Myc-MFF and pUB-Myc-MFF3. We used these lentiviral expression vectors to transduce human MM 8226 cells and ectopically overexpressed MFF or MFF3 proteins in the transduced cells. Cells transduced with an empty lentiviral expression vector (pUB-Thy1.1) were used as a control in these experiments. We determined the transduction efficiency as > 80% by FACS and verified the overexpression of Myc-tagged MFF and MFF3 proteins by immunoblot analyses (**Figures 7A, B**). We next investigated the functional consequences of ectopic overexpression of MFF and MFF3. We found that overexpression of MFF or MFF3 significantly induced cellular apoptosis in transduced 8226 cells as

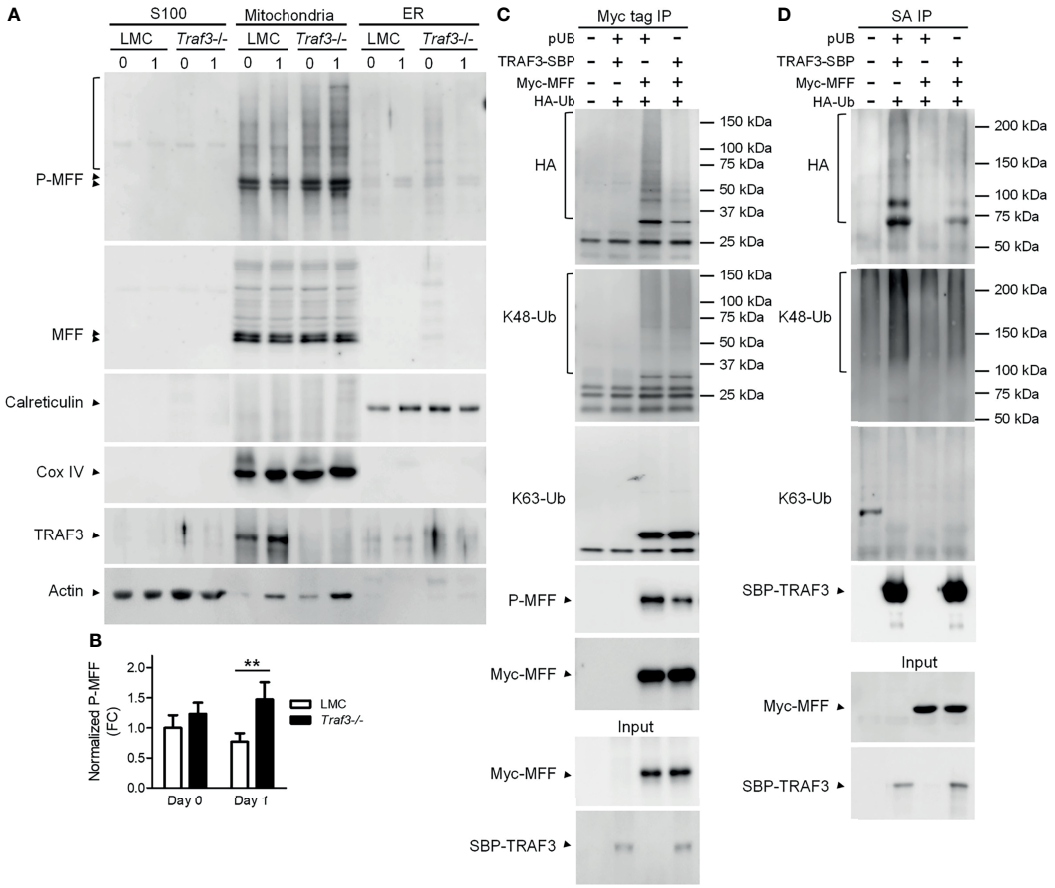

FIGURE 6 | The TRAF3-MFF interaction affected the modifications of MFF and TRAF3. **(A, B)** Phosphorylation of MFF in resting B cells. Splenic B cells were purified from gender-matched, young adult (8-12-week-old) naïve LMC or B-*Traf3*$^{-/-}$ mice. Purified cells were analyzed directly (Day 0) or at day 1 after *ex vivo* culture. S100 (cytosolic), mitochondrial and ER proteins were biochemically fractionated and analyzed by immunoblotting. Proteins in each fraction were immunoblotted for phosphorylated MFF (P-MFF), total MFF, Calreticulin (an ER protein) and COX IV (a mitochondrial protein), followed by TRAF3 and actin. **(B)** Graphical results of the normalized P-MFF in the mitochondrial fraction. The phosphorylated and total MFF bands on the immunoblots in **(A)** were quantitated using a low-light imaging system. The intensity of P-MFF bands in each lane of the mitochondrial fraction was normalized to that of the corresponding total MFF bands. Fold of change of the normalized P-MFF relative to that detected for LMC B cells at Day 0 was shown in the graph (mean ± SD, n = 3). $^{**}p < 0.01$ by *t* test. **(C, D)** Ubiquitination of MFF and TRAF3 was affected by the MFF-TRAF3 interaction in 293T cells. Cells were co-transfected with lentiviral expression vectors of HA-tagged ubiquitin (LPA-HA-Ub) and Myc-tagged MFF (pUB-Myc-MFF), SBP-tagged TRAF3 (pUB-TRAF3-SBP-6xHis) or an empty vector pUB-Thy1.1. Transfected cells were harvested at day 2 post transfection. Total cellular proteins were immunoprecipitated with Anti-c-Myc Tag (9E10) Affinity Gel **(C)** or Streptavidin-Sepharose beads **(D)**. Immunoprecipitates [Myc tag IP in **(C)** or SA IP in **(D)**] were immunoblotted for the HA tag, K48-Ub and K63-Ub to detect the ubiquitination, K48- or K63-linked polyubiquitination of MFF **(C)** and TRAF3 **(D)**, respectively. Phosphorylated MFF (P-MFF) was also analyzed in the Myc tag IP **(C)**. Immunoblotting of Myc-MFF and SBP-TRAF3 was performed with both the immunoprecipitates and input lysates (bottom panels). Immunoblots shown are representative of 3 experiments.

demonstrated by Annexin V staining (**Figures 7C, D**). Our cell cycle analysis revealed that MFF or MFF3 overexpression also induced DNA fragmentation in transduced 8226 cells (**Figures 7E, F**). To elucidate the mechanism of MFF-induced apoptosis, we further investigated whether it was mediated *via* the mitochondria-dependent pathway using JC-1 staining followed by flow cytometry. Our results showed that as compared to cells transduced with the empty lentiviral vector, overexpression of MFF or MFF3 markedly increased the percentage of 8226 cells containing permeabilized mitochondria (**Figures 7G, H**). These data are consistent with the hypothesis that MFF acts downstream of TRAF3 to promote intrinsic apoptosis. However, it is also possible that MFF overexpression may affect apoptosis *via* TRAF3-independent mechanisms such as causing an imbalance of the mitochondrial fission and fusion machineries in cells (53, 65, 67). Although the precise mechanisms remain to be elucidated, our results indicate that overexpression of MFF or MFF3 is able to induce mitochondria-dependent apoptosis in TRAF3-deficient malignant B cells, suggesting that MFF or mitochondrial fission machinery could be targetable points in human B cell malignancies, including those with *TRAF3* deletions or inactivating mutations.

Genetic Alterations of *MFF* and *DNM1L* in Human B Cell Malignancies

MFF acts as a receptor of the fission protein dynamin-related protein 1 (Drp1; encoded by the *DNM1L* gene), a mechano-

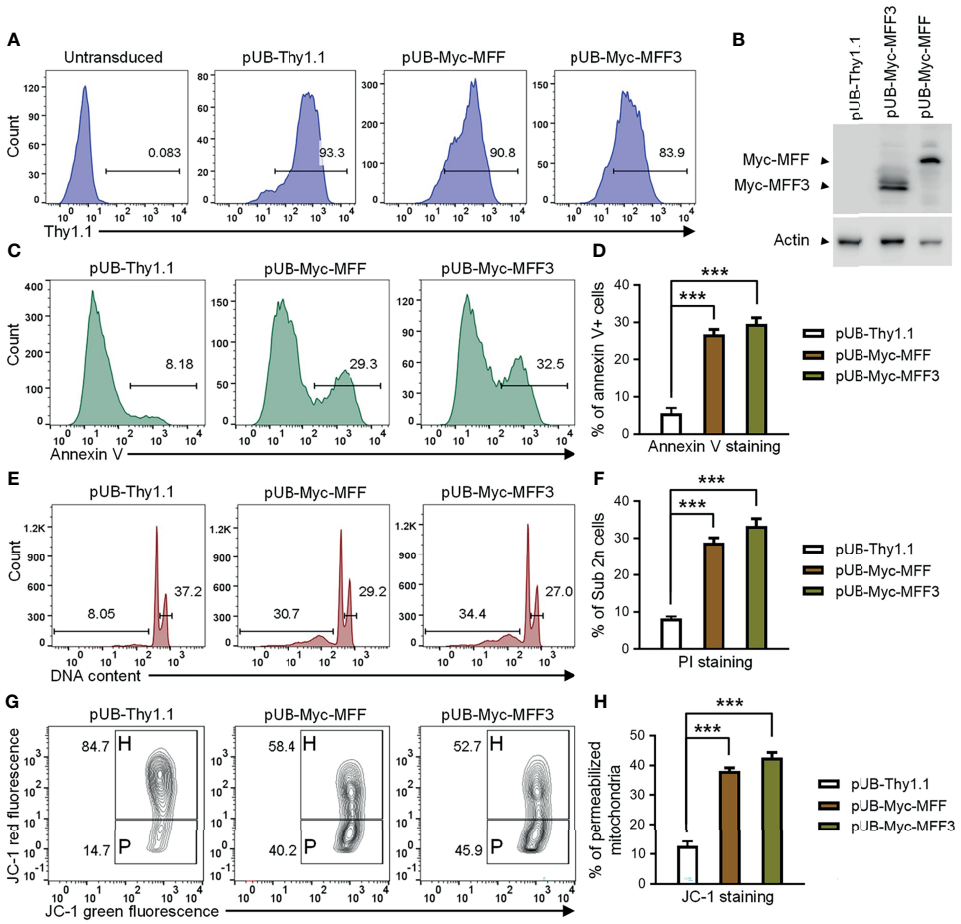

FIGURE 7 | Overexpression of MFF induced mitochondria-dependent apoptosis in human MM 8226 cells. Cells were transduced with individual lentiviral expression vector of MFF (pUB-Myc-MFF), MFF3 (pUB-Myc-MFF3), or an empty vector (pUB-Thy1.1). **(A)** Transduction efficiency of 8226 cells analyzed by Thy1.1 immunofluorescence staining and FACS. Cells were analyzed at day 3 post transduction. Gated population (Thy1.1+) indicates the cells that were successfully transduced with the lentiviral expression vector. **(B)** Ectopic overexpression of MFF and MFF3 in transduced 8226 cells. Total cellular proteins were prepared at day 4 post transduction, and then immunoblotted for the Myc tag, followed by actin. Bands of Myc-MFF and Myc-MFF3 are indicated in the figure. **(C–H)** Cell apoptosis, DNA fragmentation and mitochondrial membrane permeabilization were analyzed at day 6 post transduction. **(C)** Representative FACS profiles of annexin V staining. Gated populations indicate the annexin V+ apoptotic cells. **(D)** Graphical results of the percentage of annexin V+ apoptotic cells. **(E)** Representative FACS profiles of cell cycle analysis by PI staining. Gated populations indicate apoptotic cells with DNA fragmentation (DNA content < 2n) and proliferating cells (2n < DNA content ≤ 4n). **(F)** Graphical results of the percentage of apoptotic cells with DNA fragmentation. **(G)** Representative FACS profiles of mitochondrial membrane permeabilization measured by MitoProbe JC-1 staining. Gated populations in H show cells with healthy mitochondria and gated populations in P indicate cells with permeabilized mitochondria. **(H)** Graphical results of the percentage of cells with permeabilized mitochondria. **(D, F, H)** The graphs depict the results of 3 independent experiments with duplicate samples in each experiment (mean ± SD). ***$p < 0.001$ by one-way ANOVA.

enzymatic GTPase, to recruit the cytosolic Drp1 onto the MOM surface, allowing Drp1 to assemble the mitochondrial constriction machinery at sites of ensuing fission (68–70). Drp1 subsequently hydrolyzes GTP to power membrane constriction and mitochondrial fission (69, 70). The functional importance of both MFF and Drp1 in mitochondrial physiology has been demonstrated by the evidence that genetic mutations of *MFF* and *DNM1L* play causal roles in patients with developmental abnormalities and neurological disorders (65, 71, 72). Given our current finding and the high frequency of deletions and mutations of *TRAF3* detected in human NHL and MM (13, 14), we searched the Cancer Genome Atlas (TCGA) (73) and the Catalog of Somatic Mutations in Cancer (COSMIC) (74) databases for the potential presence of genetic alterations of *MFF* and *DNM1L* in human B cell malignancies. We noticed that genetic alterations of *MFF* are very rare in human B cell cancers with only 0.49% (4 out of 819 cases) in pediatric acute lymphoid leukemia (ALL) identified as deep deletions (TARGET, 2018) (**Supplementary Figure 8A**). Compared to *MFF*, *DNM1L* exhibits relatively higher frequencies of genetic alterations in human B cell malignancies, including 7.1% (1/14) of mutations in NHL (75), 3.8% (2/53) of mutations in DLBCL (76), 0.63% (1/160) of mutations in CLL (77), 0.49% (1/205) of mutations in MM (78) and 0.24% (2/819) of amplifications in pediatric ALL

(TARGET, 2018) (**Supplementary Figure 8B**). We next examined the combined genetic alterations of *MFF*, *DNM1L* and *TRAF3* in human B cell malignancies using the TCGA tool. Interestingly, we noticed that simultaneous genetic alterations of any two among these 3 genes are not documented in patients with B cell malignancies (**Supplementary Figure 9**). However, these genetic data are not conclusive due to the low incidence of mutations in *MFF* and *DNM1L* detected in human B cell malignancies and additional genetic alteration cases need to be analyzed to determine if TRAF3, MFF and Drp1 act in the same or overlapping pathways in B cells.

DISCUSSION

Mitochondria, the executioner organelle for cell death, are exploited by cancer cells and provide a validated therapeutic target in cancers (30–32). Mitochondria are dynamic, constantly undergoing fission and fusion to maintain their diverse functions (53, 65, 67). Mitochondrial dynamics is tightly controlled and crucial for the regulation of cell homeostasis and survival (53, 65, 67). Disruption or an imbalance of mitochondrial dynamics causes functional deterioration of mitochondria, often leading to cell apoptosis and a variety of human diseases ranging from neurodegenerative diseases to cancers (53, 65, 67). Therefore, proteins controlling mitochondrial fission have been recognized as essential regulators of mitochondrial functions, mitochondrial quality control, and cell apoptosis in health and diseases (53, 65, 67). In the present study, we identified the critical B cell survival regulator TRAF3 as a novel binding partner of the key mitochondrial fission protein, MFF, in B lymphocytes.

Elicited by our unexpected finding that the majority of cytoplasmic TRAF3 proteins were localized at the mitochondria in resting B cells after 2 days in culture, we identified MFF as a TRAF3-interacting protein using affinity purification of mitochondrial proteins isolated from human MM cells followed by LC-MS/MS-based sequencing. We verified the TRAF3-MFF interaction using co-immunoprecipitation and GST pull-down assays. In support of the model that the interaction with MFF allows TRAF3 to directly regulate the physiology of mitochondria, we obtained a variety of evidence in the present study. We demonstrated that in the absence of stimulation, increased protein levels of mitochondrial TRAF3 were associated with altered mitochondrial morphology, decreased mitochondrial respiration, increased mitochondrial ROS production and membrane permeabilization, which eventually culminated in caspase 9-dependent apoptotic pathway activation in resting B cells. In concordance with these findings, deletion of TRAF3 had the opposite effects on the morphology, function and healthy status of mitochondria as well as the mitochondria-dependent intrinsic apoptotic pathway in resting B cells. Interestingly, BAFF-induced degradation of TRAF3 appeared to mainly affect mitochondrial TRAF3, which would inhibit TRAF3-MFF-mediated regulation of mitochondrial function and mitochondria-dependent apoptosis in TRAF3-sufficient B cells. Indeed, BAFF stimulation inhibited mitochondrial ROS production and prevented mitochondria-dependent apoptosis in LMC but not in B-*Traf3*$^{-/-}$ splenic B cells. Taken together, our findings support the model that TRAF3 can directly regulate the physiology of mitochondria to promote the intrinsic apoptotic pathway *via* interacting with MFF.

Our findings help to understand some seemingly opposite roles of TRAF3 in B cell function and tumorigenesis. For example, not only *Traf3* deficiency leads to B lymphoma development in mice (19), transgenic overexpression of *TRAF3* in B cells also promotes B cell differentiation and mature non-Hodgkin lymphomas in mice (26, 27). Interestingly, the pro-tumorigenic activities of upregulated TRAF3 in B cells require simultaneous overexpression of the anti-apoptotic protein BCL-2 in B cells (27), suggesting a need for BCL-2-mediated protection of mitochondria in TRAF3-overexpressing B cells. In this context, it is conceivable that BCL-2 overexpression could counteract the TRAF3-MFF-mediated regulation of mitochondrial morphology and function, thereby preventing mitochondria-dependent apoptosis in TRAF3-overexpressing B cells.

Corroborating our evidence that ectopic overexpression of MFF induced mitochondria-dependent apoptosis in TRAF3-deficient malignant B cells, it has been previously reported that overexpression of MFF induced apoptosis and loss of MFF reduced apoptosis in other cell types such as epithelial cells, fibroblasts, cardiomyocytes, mesangial and HeLa cells (67–69, 79–83). Paradoxically, deficiency or silencing of *MFF* also induced apoptosis in cardiomyocytes, HeLa, prostate cancer and KRAS-transformed salivary duct cancer cells (58, 84, 85). These seemingly contradictory observations suggest that the protein and activity levels of MFF are tightly regulated in cells to achieve a delicate balance in mitochondrial dynamics and to appropriately control cell survival and apoptosis.

MFF recruits Drp1, the GTPase that executes mitochondrial fission, to the MOM to induce mitochondrial fission. In the present study, we could not detect co-immunoprecipitation of Drp1 with either MFF or TRAF3 under our experimental condition (data not shown). In addition, the protein levels of Drp1 in the S100, mitochondrial and ER fractions of resting splenic B cells were below the detection limit of immunoblot analyses in our experiments (data not shown). Therefore, we could not determine whether the TRAF3-MFF interaction facilitates or interferes with the recruitment of Drp1 by MFF. Detection of the weak interaction between Drp1 and MFF requires cross-linking prior to co-IP as reported in the literature (68, 86–89). Thus, the interaction between MFF and TRAF3 appears to be much stronger than that observed between MFF and Drp1, highlighting the importance of TRAF3 in modulating the functional properties of MFF. Indeed, we found that TRAF3 inhibits the phosphorylation and ubiquitination of MFF in resting B cells and co-transfected HEK 293T cells.

Phosphorylation of MFF by kinases such as AMPK, JNK, ERK1/2 or CK2α in different cellular contexts has been shown to increase the activity of MFF in recruiting Drp1 to mitochondria and promoting mitochondrial fission (56, 61, 66, 80, 90–94). Ubiquitination of MFF by the E3 ubiquitin ligase Parkin has been

reported to promote the association between MFF and the autophagic adapter protein p62/SQSTM1, thereby facilitating mitophagy and clearance of damaged mitochondria (57). Alternatively, Parkin-mediated ubiquitination of MFF under non-stressed conditions regulates constitutive MFF turnover and induces the degradation of MFF in HEK 293T cells (95). Whether and how the TRAF3-MFF interaction affects the accessibility of MFF to its specific kinase (such as AMPK, JNK, ERK1/2 or CK2α) or E3 ubiquitin ligase (such as Parkin) in B cells await further investigation in future studies. Regardless of the detailed mechanisms, our results suggest that the TRAF3-MFF interaction has functional impacts on MFF modifications, mitochondrial morphology and function as well as mitochondria-dependent apoptosis in B cells.

However, it should be noted that our data do not exclude the possibility that TRAF3 may also indirectly regulate mitochondria-dependent apoptosis in B cells through additional MFF-independent mechanisms. In this regard, it has been shown that the NIK-NF-κB2 pathway is constitutively activated and nuclear CREB is markedly elevated in *Traf3*$^{-/-}$ splenic B cells (15, 16, 96), which lead to increased expression of anti-apoptotic proteins of the Bcl-2 family such as Bcl-2 and Mcl-1 (46, 96). The Bcl-2 family proteins are important regulators of mitochondrial physiology and intrinsic apoptotic pathways (47, 48). Moreover, we recently reported elevated Chkα-driven choline metabolism and increased levels of the phospholipids PC and PE in *Traf3*$^{-/-}$ splenic B cells (25, 97). PC and PE are the two most abundant phospholipids of mitochondrial membranes, critically regulating mitochondrial physiology and mitochondria-dependent apoptosis (98, 99). Therefore, it is likely that the TRAF3-MFF interaction together with the TRAF3-NIK-NF-κB2, TRAF3-CREB-Mcl-1 and TRAF3-Chkα-PC/PE pathways act cooperatively to regulate mitochondrial morphology, function and mitochondria-dependent apoptosis in normal B lymphocytes. Disruption of all these TRAF3-dependent mechanisms in TRAF3-deficient B cells leads to BAFF-independent survival and eventually contributes to B cell malignant transformation.

Interestingly, genetic alterations of the *TRAF3* gene are not limited to B cell malignancies but also detected in human epithelial cancers (14). Most notably, the human papilloma virus-positive (HPV+) head and neck squamous cell carcinomas (HNSCC) exhibit an exceptionally high frequency (~20%) of deep deletions and truncations of the *TRAF3* gene (14, 100, 101). Similar to that described for B cells, elevated activation of the NF-κB2 pathway is detected in TRAF3-deficient HNSCC cells (101). TRAF3 also plays pro-apoptotic roles in human bladder and colorectal carcinoma cells upon CD40 ligation *via* BAX/BAK-caspase 9- and ROS- dependent mechanisms (102, 103). So far, TRAF3-mediated pro-apoptotic effects in epithelial cells have been reported to be mediated *via* transcriptional regulation (101–103). In this study, we detected co-immunoprecipitation of MFF with TRAF3 in transfected 293T epithelial cells. In light of the similarity in the pro-apoptotic role of TRAF3 observed in B cells and epithelial cells, further investigation of the potential direct TRAF3-MFF interaction and its functional impacts in epithelial cancers represent an interesting area in future research. Such investigation would extend our knowledge on the potentially universal functions of the survival/apoptosis regulator TRAF3 in regulating mitochondria-dependent apoptosis.

In summary, our findings provide novel insights into the elaborate pathogenic mechanisms of TRAF3 inactivation-initiated B cell malignant transformation. Our study identified TRAF3 as a novel regulator of mitochondrial physiology in B lymphocytes and elucidated the TRAF3-MFF interaction as one of the underlying mechanisms. Our discovery of the TRAF3-MFF axis in B cells will open up new therapeutic opportunities for the treatment of human B cell malignancies, particularly those with *TRAF3* deletion or relevant mutations. We demonstrated that overexpression of MFF could restore the apoptotic pathway in TRAF3-deficient malignant B cells. Thus, an imbalance in mitochondrial dynamics, caused by either excessive or insufficient levels of MFF proteins or activities, could induce mitochondria-dependent apoptosis in malignant B cells. Interestingly, a cell permeable peptidomimetic MFF has been developed with demonstrated activity on killing melanoma, breast and lung cancer cells but not normal cells in preclinical models, indicating that MFF is an actionable therapeutic target in human cancers (59). Furthermore, pharmaceutical approaches that target mitochondrial dynamics have been developed for the treatment of neurodegenerative diseases and type 2 diabetes, including mitochondrial division inhibitor-1 (mdivi-1, a Drp1-specific inhibitor), dynasore, P110 and 15-oxospiramilactone, etc. (53, 65, 104). All these drugs can be exploited and repurposed to treat human B cell malignancies, overcome resistance to standard therapies and help to improve patient outcome, especially when given in combination with other available chemotherapies, radiotherapies and immunotherapies.

DATA AVAILABILITY STATEMENT

The original contributions presented in the study are included in the article/**Supplementary Material**. Further inquiries can be directed to the corresponding author.

ETHICS STATEMENT

The animal study was reviewed and approved by Rutgers University.

AUTHOR CONTRIBUTIONS

PX, YL, and EW designed the experiments of this study. YL, SG, JJ, SZ, CL, DS, and PX performed the experiments and analyzed the data. SK carried out LC-MS/MS and analyzed the data. W-XZ supervised the ubiquitination studies. JG supervised the mitochondrial functional assays. HZ and EW provided guidance on the mitochondrial morphological examination. PX and YL wrote

the initial manuscript. All authors contributed to the article and approved the submitted version.

FUNDING

This study was supported by the Department of Defense grant W81XWH-13-1-0242 (PX), the National Institutes of Health grant R01 CA158402 (PX), a Pilot Award of Cancer Institute of New Jersey through Grant Number P30CA072720 from the National Cancer Institute (PX) and a Busch Biomedical Grant (PX). The FACS analyses were supported by the Flow Cytometry Core Facility with funding from NCI-CCSG P30CA072720.

ACKNOWLEDGMENTS

We would like to thank Jemmie Tsai, Johann Arceo, Ben Wang Wu and Eton Victor for technical assistance of this study.

SUPPLEMENTARY MATERIAL

The Supplementary Material for this article can be found online at: https://www.frontiersin.org/articles/10.3389/fimmu.2021.670338/full#supplementary-material

REFERENCES

1. Morton LM, Wang SS, Devesa SS, Hartge P, Weisenburger DD, Linet MS. Lymphoma Incidence Patterns by WHO Subtype in the United States, 1992-2001. *Blood* (2006) 107:265–76. doi: 10.1182/blood-2005-06-2508
2. Ruddon R. The Epidemiology of Human Cancer. In: RW Ruddon, editor. *Cancer Biology*, *4th ed.* Oxford, England: Oxford University Press (2007). p. 62–116.
3. Horner MJ, Ries LAG, Krapcho M, Neyman N, Aminou R, Howlader N, et al. *Surveillance, Epidemiology, and End Results (SEER) Program. SEER Cancer Statistics Review, 1975-2006*. Bethesda, MD: National Cancer Institute (2008). Available at: www.seer.cancer.gov. (Nov 2008 Sub).
4. Miao Y, Medeiros LJ, Xu-Monette ZY, Li J, Young KH. Dysregulation of Cell Survival in Diffuse Large B Cell Lymphoma: Mechanisms and Therapeutic Targets. *Front Oncol* (2019) 9:107. doi: 10.3389/fonc.2019.00107
5. Adams CM, Clark-Garvey S, Porcu P, Eischen CM. Targeting the Bcl-2 Family in B Cell Lymphoma. *Front Oncol* (2018) 8:636. doi: 10.3389/fonc.2018.00636
6. Pasqualucci L, Zhang B. Genetic Drivers of NF-kappaB Deregulation in Diffuse Large B-Cell Lymphoma. *Semin Cancer Biol* (2016) 39:26–31. doi: 10.1016/j.semcancer.2016.08.001
7. Waibel M, Gregory G, Shortt J, Johnstone RW. Rational Combination Therapies Targeting Survival Signaling in Aggressive B-Cell Leukemia/Lymphoma. *Curr Opin Hematol* (2014) 21:297–308. doi: 10.1097/MOH.0000000000000045
8. Voutsadakis IA. Apoptosis and the Pathogenesis of Lymphoma. *Acta Oncol* (2000) 39:151–6. doi: 10.1080/028418600430707
9. Cillessen SA, Meijer CJ, Notoya M, Ossenkoppele GJ, Oudejans JJ. Molecular Targeted Therapies for Diffuse Large B-Cell Lymphoma Based on Apoptosis Profiles. *J Pathol* (2010) 220:509–20. doi: 10.1002/path.2670
10. Muris JJ, Meijer CJ, Ossenkoppele GJ, Vos W, Oudejans JJ. Apoptosis Resistance and Response to Chemotherapy in Primary Nodal Diffuse Large B-Cell Lymphoma. *Hematol Oncol* (2006) 24:97–104. doi: 10.1002/hon.774
11. Leslie LA, Younes A. Targeting Oncogenic and Epigenetic Survival Pathways in Lymphoma. *Leuk Lymphoma* (2013) 54:2365–76. doi: 10.3109/10428194.2013.780288
12. Spina V, Rossi D. NF-kappaB Deregulation in Splenic Marginal Zone Lymphoma. *Semin Cancer Biol* (2016) 39:61–7. doi: 10.1016/j.semcancer.2016.08.002
13. Moore CR, Edwards SK, Xie P. Targeting TRAF3 Downstream Signaling Pathways in B Cell Neoplasms. *J Cancer Sci Ther* (2015) 7:67–74. doi: 10.4172/1948-5956.1000327
14. Zhu S, Jin J, Gokhale S, Lu A, Shan H, Feng J, et al. Genetic Alterations of TRAF Proteins in Human Cancers. *Front Immunol* (2018) 9:2111. doi: 10.3389/fimmu.2018.02111
15. Xie P, Stunz LL, Larison KD, Yang B, Bishop GA. Tumor Necrosis Factor Receptor-Associated Factor 3 Is a Critical Regulator of B Cell Homeostasis in Secondary Lymphoid Organs. *Immunity* (2007) 27:253–67. doi: 10.1016/j.immuni.2007.07.012
16. Gardam S, Sierro F, Basten A, Mackay F, Brink R. TRAF2 and TRAF3 Signal Adapters Act Cooperatively to Control the Maturation and Survival Signals Delivered to B Cells by the BAFF Receptor. *Immunity* (2008) 28:391–401. doi: 10.1016/j.immuni.2008.01.009
17. Keats JJ, Fonseca R, Chesi M, Schop R, Baker A, Chng WJ, et al. Promiscuous Mutations Activate the Noncanonical NF-kappaB Pathway in Multiple Myeloma. *Cancer Cell* (2007) 12:131–44. doi: 10.1016/j.ccr.2007.07.003
18. Annunziata CM, Davis RE, Demchenko Y, Bellamy W, Gabrea A, Zhan F, et al. Frequent Engagement of the Classical and Alternative NF-kappaB Pathways by Diverse Genetic Abnormalities in Multiple Myeloma. *Cancer Cell* (2007) 12:115–30. doi: 10.1016/j.ccr.2007.07.004
19. Moore CR, Liu Y, Shao CS, Covey LR, Morse HC3rd, Xie P. Specific Deletion of TRAF3 in B Lymphocytes Leads to B Lymphoma Development in Mice. *Leukemia* (2012) 26:1122–7. doi: 10.1038/leu.2011.309
20. Vince JE, Wong WW, Khan N, Feltham R, Chau D, Ahmed AU, et al. IAP Antagonists Target Ciap1 to Induce TNFalpha-Dependent Apoptosis. *Cell* (2007) 131:682–93. doi: 10.1016/j.cell.2007.10.037
21. Varfolomeev E, Blankenship JW, Wayson SM, Fedorova AV, Kayagaki N, Garg P, et al. IAP Antagonists Induce Autoubiquitination of C-IAPs, NF-kappaB Activation, and TNFalpha-Dependent Apoptosis. *Cell* (2007) 131:669–81. doi: 10.1016/j.cell.2007.10.030
22. Zarnegar BJ, Wang Y, Mahoney DJ, Dempsey PW, Cheung HH, He J, et al. Noncanonical NF-kappaB Activation Requires Coordinated Assembly of a Regulatory Complex of the Adaptors Ciap1, Ciap2, TRAF2 and TRAF3 and the Kinase NIK. *Nat Immunol* (2008) 9:1371–8. doi: 10.1038/ni.1676
23. Vallabhapurapu S, Matsuzawa A, Zhang W, Tseng PH, Keats JJ, Wang H, et al. Nonredundant and Complementary Functions of TRAF2 and TRAF3 in a Ubiquitination Cascade That Activates NIK-Dependent Alternative NF-kappaB Signaling. *Nat Immunol* (2008) 9:1364–70. doi: 10.1038/ni.1678
24. Gardam S, Turner VM, Anderton H, Limaye S, Basten A, Koentgen F, et al. Deletion of Ciap1 and Ciap2 in Murine B Lymphocytes Constitutively Activates Cell Survival Pathways and Inactivates the Germinal Center Response. *Blood* (2011) 117:4041–51. doi: 10.1182/blood-2010-10-312793
25. Gokhale S, Lu W, Zhu S, Liu Y, Hart RP, Rabinowitz JD, et al. Elevated Choline Kinase Alpha-Mediated Choline Metabolism Supports the Prolonged Survival of TRAF3-Deficient B Lymphocytes. *J Immunol* (2020) 204:459–71. doi: 10.4049/jimmunol.1900658
26. Zapata JM, Llobet D, Krajewska M, Lefebvre S, Kress CL, Reed JC. Lymphocyte-Specific TRAF3-Transgenic Mice Have Enhanced Humoral Responses and Develop Plasmacytosis, Autoimmunity, Inflammation, and Cancer. *Blood* (2009) 113:4595–603. doi: 10.1182/blood-2008-07-165456
27. Perez-Chacon G, Adrados M, Vallejo-Cremades MT, Lefebvre S, Reed JC, Zapata JM. Dysregulated TRAF3 and BCL2 Expression Promotes Multiple Classes of Mature Non-Hodgkin B Cell Lymphoma in Mice. *Front Immunol* (2019) 9:3114. doi: 10.3389/fimmu.2018.03114
28. Xie P. TRAF Molecules in Cell Signaling and in Human Diseases. *J Mol Signal* (2013) 8:7. doi: 10.1186/1750-2187-8-7
29. Bishop GA, Stunz LL, Hostager BS. TRAF3 as a Multifaceted Regulator of B Lymphocyte Survival and Activation. *Front Immunol* (2018) 9:2161. doi: 10.3389/fimmu.2018.02161
30. Wang C, Youle RJ. The Role of Mitochondria in Apoptosis*. *Annu Rev Genet* (2009) 43:95–118. doi: 10.1146/annurev-genet-102108-134850

31. Caroppi P, Sinibaldi F, Fiorucci L, Santucci R. Apoptosis and Human Diseases: Mitochondrion Damage and Lethal Role of Released Cytochrome C as Proapoptotic Protein. *Curr Med Chem* (2009) 16:4058–65. doi: 10.2174/092986709789378206
32. Burke PJ. Mitochondria, Bioenergetics and Apoptosis in Cancer. *Trends Cancer* (2017) 3:857–70. doi: 10.1016/j.trecan.2017.10.006
33. Edwards SK, Moore CR, Liu Y, Grewal S, Covey LR, Xie P. N-Benzyladriamycin-14-Valerate (AD 198) Exhibits Potent Anti-Tumor Activity on TRAF3-Deficient Mouse B Lymphoma and Human Multiple Myeloma. *BMC Cancer* (2013) 13:481. doi: 10.1186/1471-2407-13-481
34. Li Y, Franklin S, Zhang MJ, Vondriska TM. Highly Efficient Purification of Protein Complexes From Mammalian Cells Using a Novel Streptavidin-Binding Peptide and Hexahistidine Tandem Tag System: Application to Bruton's Tyrosine Kinase. *Protein Sci* (2010) 20:140–9. doi: 10.1002/pro.546
35. Kiledjian M, Day N, Trifillis P. Purification and RNA Binding Properties of the Polycytidylate-Binding Proteins Alphacp1 and Alphacp2. *Methods* (1999) 17:84–91. doi: 10.1006/meth.1998.0710
36. Zhou S, Kurt-Jones EA, Cerny AM, Chan M, Bronson RT, Finberg RW. MyD88 Intrinsically Regulates CD4 T-Cell Responses. *J Virol* (2009) 83:1625–34. doi: 10.1128/JVI.01770-08
37. Pan JA, Sun Y, Jiang YP, Bott AJ, Jaber N, Dou Z, et al. TRIM21 Ubiquitylates SQSTM1/p62 and Suppresses Protein Sequestration to Regulate Redox Homeostasis. *Mol Cell* (2016) 61:720–33. doi: 10.1016/j.molcel.2016.02.007
38. Edwards SK, Desai A, Liu Y, Moore CR, Xie P. Expression and Function of a Novel Isoform of Sox5 in Malignant B Cells. *Leuk Res* (2014) 38:393–401. doi: 10.1016/j.leukres.2013.12.016
39. Edwards SK, Han Y, Liu Y, Kreider BZ, Grewal S, Desai A, et al. Signaling Mechanisms of Bortezomib in TRAF3-Deficient Mouse B Lymphoma and Human Multiple Myeloma Cells. *Leuk Res* (2016) 41:85–95. doi: 10.1016/j.leukres.2015.12.005
40. Edwards S, Baron J, Moore CR, Liu Y, Perlman DH, Hart RP, et al. Mutated in Colorectal Cancer (MCC) Is a Novel Oncogene in B Lymphocytes. *J Hematol Oncol* (2014) 7:56. doi: 10.1186/s13045-014-0056-6
41. Khan Z, Amini S, Bloom JS, Ruse C, Caudy AA, Kruglyak L, et al. Accurate Proteome-Wide Protein Quantification From High-Resolution 15N Mass Spectra. *Genome Biol* (2011) 12:R122. doi: 10.1186/gb-2011-12-12-r122
42. Ying W, Perlman DH, Li L, Theberge R, Costello CE, McComb ME. Highly Efficient and Selective Enrichment of Peptide Subsets Combining Fluorous Chemistry With Reversed-Phase Chromatography. *Rapid Commun Mass Spectrom* (2009) 23:4019–30. doi: 10.1002/rcm.4343
43. Rueden CT, Schindelin J, Hiner MC, DeZonia BE, Walter AE, Arena ET, et al. ImageJ2: ImageJ for the Next Generation of Scientific Image Data. *BMC Bioinformatics* (2017) 18:529. doi: 10.1186/s12859-017-1934-z
44. Degenhardt K, Mathew R, Beaudoin B, Bray K, Anderson D, Chen G, et al. Autophagy Promotes Tumor Cell Survival and Restricts Necrosis, Inflammation, and Tumorigenesis. *Cancer Cell* (2006) 10:51–64. doi: 10.1016/j.ccr.2006.06.001
45. Guo JY, Chen HY, Mathew R, Fan J, Strohecker AM, Karsli-Uzunbas G, et al. Activated Ras Requires Autophagy to Maintain Oxidative Metabolism and Tumorigenesis. *Genes Dev* (2011) 25:460–70. doi: 10.1101/gad.2016311
46. Sen R. Control of B Lymphocyte Apoptosis by the Transcription Factor NF-kappaB. *Immunity* (2006) 25:871–83. doi: 10.1016/j.immuni.2006.12.003
47. Leibowitz B, Yu J. Mitochondrial Signaling in Cell Death via the Bcl-2 Family. *Cancer Biol Ther* (2010) 9:417–22. doi: 10.4161/cbt.9.6.11392
48. Martinou JC, Youle RJ. Mitochondria in Apoptosis: Bcl-2 Family Members and Mitochondrial Dynamics. *Dev Cell* (2011) 21:92–101. doi: 10.1016/j.devcel.2011.06.017
49. Hostager BS, Catlett IM, Bishop GA. Recruitment of CD40 and Tumor Necrosis Factor Receptor-Associated Factors 2 and 3 to Membrane Microdomains During CD40 Signaling. *J Biol Chem* (2000) 275:15392–8. doi: 10.1074/jbc.M909520199
50. Hildebrand JM, Luo Z, Manske MK, Price-Troska T, Ziesmer SC, Lin W, et al. A BAFF-R Mutation Associated With Non-Hodgkin Lymphoma Alters TRAF Recruitment and Reveals New Insights Into BAFF-R Signaling. *J Exp Med* (2010) 207:2569–79. doi: 10.1084/jem.20100857
51. Mao AP, Li S, Zhong B, Li Y, Yan J, Li Q, et al. Virus-Triggered Ubiquitination of TRAF3/6 by Ciap1/2 Is Essential for Induction of Interferon-Beta (IFN-Beta) and Cellular Antiviral Response. *J Biol Chem* (2010) 285:9470–6. doi: 10.1074/jbc.M109.071043
52. Huang Y, Liu H, Ge R, Zhou Y, Lou X, Wang C. UXT-V1 Facilitates the Formation of MAVS Antiviral Signalosome on Mitochondria. *J Immunol* (2012) 188:358–66. doi: 10.4049/jimmunol.1102079
53. Yu R, Lendahl U, Nister M, Zhao J. Regulation of Mammalian Mitochondrial Dynamics: Opportunities and Challenges. *Front Endocrinol (Lausanne)* (2020) 11:374. doi: 10.3389/fendo.2020.00374
54. Saha SK, Pietras EM, He JQ, Kang JR, Liu SY, Oganesyan G, et al. Regulation of Antiviral Responses by a Direct and Specific Interaction Between TRAF3 and Cardif. *EMBO J* (2006) 25:3257–63. doi: 10.1038/sj.emboj.7601220
55. Paz S, Vilasco M, Werden SJ, Arguello M, Joseph-Pillai D, Zhao T, et al. A Functional C-Terminal TRAF3-Binding Site in MAVS Participates in Positive and Negative Regulation of the IFN Antiviral Response. *Cell Res* (2011) 21:895–910. doi: 10.1038/cr.2011.2
56. Toyama EQ, Herzig S, Courchet J, Lewis TL Jr, Loson OC, Hellberg K, et al. Metabolism. AMP-Activated Protein Kinase Mediates Mitochondrial Fission in Response to Energy Stress. *Science* (2016) 351:275–81. doi: 10.1126/science.aab4138
57. Gao J, Qin S, Jiang C. Parkin-Induced Ubiquitination of Mff Promotes Its Association With P62/SQSTM1 During Mitochondrial Depolarization. *Acta Biochim Biophys Sin (Shanghai)* (2015) 47:522–9. doi: 10.1093/abbs/gmv044
58. Seo JH, Agarwal E, Chae YC, Lee YG, Garlick DS, Storaci AM, et al. Mitochondrial Fission Factor Is a Novel Myc-Dependent Regulator of Mitochondrial Permeability in Cancer. *EBioMedicine* (2019) 48:353–63. doi: 10.1016/j.ebiom.2019.09.017
59. Seo JH, Chae YC, Kossenkov AV, Lee YG, Tang HY, Agarwal E, et al. MFF Regulation of Mitochondrial Cell Death Is a Therapeutic Target in Cancer. *Cancer Res* (2019) 79:6215–26. doi: 10.1158/0008-5472.CAN-19-1982
60. Takamura H, Koyama Y, Matsuzaki S, Yamada K, Hattori T, Miyata S, et al. TRAP1 Controls Mitochondrial Fusion/Fission Balance Through Drp1 and Mff Expression. *PloS One* (2012) 7:e51912. doi: 10.1371/journal.pone.0051912
61. Ducommun S, Deak M, Sumpton D, Ford RJ, Nunez Galindo A, Kussmann M, et al. Motif Affinity and Mass Spectrometry Proteomic Approach for the Discovery of Cellular AMPK Targets: Identification of Mitochondrial Fission Factor as a New AMPK Substrate. *Cell Signal* (2015) 27:978–88. doi: 10.1016/j.cellsig.2015.02.008
62. Lee SY, Choi Y. TRAF-Interacting Protein (TRIP): A Novel Component of the Tumor Necrosis Factor Receptor (TNFR)- and CD30-TRAF Signaling Complexes That Inhibits TRAF2-Mediated NF-kappaB Activation. *J Exp Med* (1997) 185:1275–85. doi: 10.1084/jem.185.7.1275
63. Gamper C, van Eyndhoven WG, Schweiger E, Mossbacher M, Koo B, Lederman S. TRAF-3 Interacts With P62 Nucleoporin, a Component of the Nuclear Pore Central Plug That Binds Classical NLS-Containing Import Complexes. *Mol Immunol* (2000) 37:73–84. doi: 10.1016/S0161-5890(00)00015-8
64. Dadgostar H, Doyle SE, Shahangian A, Garcia DE, Cheng G. T3JAM, a Novel Protein That Specifically Interacts With TRAF3 and Promotes the Activation of JNK(1). *FEBS Lett* (2003) 553:403–7. doi: 10.1016/S0014-5793(03)01072-X
65. El-Hattab AW, Suleiman J, Almannai M, Scaglia F. Mitochondrial Dynamics: Biological Roles, Molecular Machinery, and Related Diseases. *Mol Genet Metab* (2018) 125:315–21. doi: 10.1016/j.ymgme.2018.10.003
66. Seabright AP, Fine NHF, Barlow JP, Lord SO, Musa I, Gray A, et al. AMPK Activation Induces Mitophagy and Promotes Mitochondrial Fission While Activating TBK1 in a PINK1-Parkin Independent Manner. *FASEB J* (2020) 34:6284–301. doi: 10.1096/fj.201903051R
67. Serasinghe MN, Chipuk JE. Mitochondrial Fission in Human Diseases. *Handb Exp Pharmacol* (2017) 240:159–88. doi: 10.1007/164_2016_38
68. Otera H, Wang C, Cleland MM, Setoguchi K, Yokota S, Youle RJ, et al. Mff Is an Essential Factor for Mitochondrial Recruitment of Drp1 During Mitochondrial Fission in Mammalian Cells. *J Cell Biol* (2010) 191:1141–58. doi: 10.1083/jcb.201007152

69. Kornfeld OS, Qvit N, Haileselassie B, Shamloo M, Bernardi P, Mochly-Rosen D. Interaction of Mitochondrial Fission Factor With Dynamin Related Protein 1 Governs Physiological Mitochondrial Function In Vivo. *Sci Rep* (2018) 8:14034. doi: 10.1038/s41598-018-32228-1
70. Singh S, Sharma S. Dynamin-Related Protein-1 as Potential Therapeutic Target in Various Diseases. *Inflammopharmacology* (2017) 25:383–92. doi: 10.1007/s10787-017-0347-y
71. Koch J, Feichtinger RG, Freisinger P, Pies M, Schrodl F, Iuso A, et al. Disturbed Mitochondrial and Peroxisomal Dynamics Due to Loss of MFF Causes Leigh-Like Encephalopathy, Optic Atrophy and Peripheral Neuropathy. *J Med Genet* (2016) 53:270–8. doi: 10.1136/jmedgenet-2015-103500
72. Nasca A, Nardecchia F, Commone A, Semeraro M, Legati A, Garavaglia B, et al. Clinical and Biochemical Features in a Patient With Mitochondrial Fission Factor Gene Alteration. *Front Genet* (2018) 9:625. doi: 10.3389/fgene.2018.00625
73. Weinstein JN, Collisson EA, Mills GB, Shaw KR, Ozenberger BA, Ellrott K, et al. The Cancer Genome Atlas Pan-Cancer Analysis Project. *Nat Genet* (2013) 45:1113–20. doi: 10.1038/ng.2764
74. Forbes SA, Bhamra G, Bamford S, Dawson E, Kok C, Clements J, et al. The Catalogue of Somatic Mutations in Cancer (COSMIC). *Curr Protoc Hum Genet* (2008) Chapter 10:Unit 10 11. doi: 10.1002/0471142905.hg1011s57
75. Morin RD, Mendez-Lago M, Mungall AJ, Goya R, Mungall KL, Corbett RD, et al. Frequent Mutation of Histone-Modifying Genes in Non-Hodgkin Lymphoma. *Nature* (2011) 476:298–303. doi: 10.1038/nature10351
76. Morin RD, Mungall K, Pleasance E, Mungall AJ, Goya R, Huff RD, et al. Mutational and Structural Analysis of Diffuse Large B-Cell Lymphoma Using Whole-Genome Sequencing. *Blood* (2013) 122:1256–65. doi: 10.1182/blood-2013-02-483727
77. Landau DA, Carter SL, Stojanov P, McKenna A, Stevenson K, Lawrence MS, et al. Evolution and Impact of Subclonal Mutations in Chronic Lymphocytic Leukemia. *Cell* (2013) 152:714–26. doi: 10.1016/j.cell.2013.01.019
78. Lohr JG, Stojanov P, Carter SL, Cruz-Gordillo P, Lawrence MS, Auclair D, et al. Widespread Genetic Heterogeneity in Multiple Myeloma: Implications for Targeted Therapy. *Cancer Cell* (2014) 25:91–101. doi: 10.1016/j.ccr.2013.12.015
79. Gandre-Babbe S, van der Bliek AM. The Novel Tail-Anchored Membrane Protein Mff Controls Mitochondrial and Peroxisomal Fission in Mammalian Cells. *Mol Biol Cell* (2008) 19:2402–12. doi: 10.1091/mbc.e07-12-1287
80. Sheng J, Li H, Dai Q, Lu C, Xu M, Zhang J, et al. DUSP1 Recuses Diabetic Nephropathy via Repressing JNK-Mff-Mitochondrial Fission Pathways. *J Cell Physiol* (2019) 234:3043–57. doi: 10.1002/jcp.27124
81. Guido C, Whitaker-Menezes D, Lin Z, Pestell RG, Howell A, Zimmers TA, et al. Mitochondrial Fission Induces Glycolytic Reprogramming in Cancer-Associated Myofibroblasts, Driving Stromal Lactate Production, and Early Tumor Growth. *Oncotarget* (2012) 3:798–810. doi: 10.18632/oncotarget.574
82. Zhou H, Hu S, Jin Q, Shi C, Zhang Y, Zhu P, et al. Mff-Dependent Mitochondrial Fission Contributes to the Pathogenesis of Cardiac Microvasculature Ischemia/Reperfusion Injury via Induction of mROS-Mediated Cardiolipin Oxidation and HK2/VDAC1 Disassociation-Involved mPTP Opening. *J Am Heart Assoc* (2017) 6:1–20. doi: 10.1161/JAHA.116.005328
83. Ma Y, Du M, Yang F, Mai Z, Zhang C, Qu W, et al. Quantifying the Inhibitory Effect of Bcl-Xl on the Action of Mff Using Live-Cell Fluorescence Imaging. *FEBS Open Bio* (2019) 9:2041–51. doi: 10.1002/2211-5463.12739
84. Chen H, Ren S, Clish C, Jain M, Mootha V, McCaffery JM, et al. Titration of Mitochondrial Fusion Rescues Mff-Deficient Cardiomyopathy. *J Cell Biol* (2015) 211:795–805. doi: 10.1083/jcb.201507035
85. Lin HH, Chung Y, Cheng CT, Ouyang C, Fu Y, Kuo CY, et al. Autophagic Reliance Promotes Metabolic Reprogramming in Oncogenic KRAS-Driven Tumorigenesis. *Autophagy* (2018) 14:1481–98. doi: 10.1080/15548627.2018.1450708
86. Strack S, Cribbs JT. Allosteric Modulation of Drp1 Mechanoenzyme Assembly and Mitochondrial Fission by the Variable Domain. *J Biol Chem* (2012) 287:10990–1001. doi: 10.1074/jbc.M112.342105
87. Frohlich C, Grabiger S, Schwefel D, Faelber K, Rosenbaum E, Mears J, et al. Structural Insights Into Oligomerization and Mitochondrial Remodelling of Dynamin 1-Like Protein. *EMBO J* (2013) 32:1280–92. doi: 10.1038/emboj.2013.74
88. Liu R, Chan DC. The Mitochondrial Fission Receptor Mff Selectively Recruits Oligomerized Drp1. *Mol Biol Cell* (2015) 26:4466–77. doi: 10.1091/mbc.E15-08-0591
89. Clinton RW, Francy CA, Ramachandran R, Qi X, Mears JA. Dynamin-Related Protein 1 Oligomerization in Solution Impairs Functional Interactions With Membrane-Anchored Mitochondrial Fission Factor. *J Biol Chem* (2016) 291:478–92. doi: 10.1074/jbc.M115.680025
90. Long A, Klimova N, Kristian T. Mitochondrial NUDIX Hydrolases: A Metabolic Link Between NAD Catabolism, GTP and Mitochondrial Dynamics. *Neurochem Int* (2017) 109:193–201. doi: 10.1016/j.neuint.2017.03.009
91. Zong Y, Zhang CS, Li M, Wang W, Wang Z, Hawley SA, et al. Hierarchical Activation of Compartmentalized Pools of AMPK Depends on Severity of Nutrient or Energy Stress. *Cell Res* (2019) 29:460–73. doi: 10.1038/s41422-019-0163-6
92. Jieensinue S, Zhu H, Li G, Dong K, Liang M, Li Y. Tanshinone IIA Reduces SW837 Colorectal Cancer Cell Viability via the Promotion of Mitochondrial Fission by Activating JNK-Mff Signaling Pathways. *BMC Cell Biol* (2018) 19:21. doi: 10.1186/s12860-018-0174-z
93. Lu YT, Li LZ, Yang YL, Yin X, Liu Q, Zhang L, et al. Succinate Induces Aberrant Mitochondrial Fission in Cardiomyocytes Through GPR91 Signaling. *Cell Death Dis* (2018) 9:672. doi: 10.1038/s41419-018-0708-5
94. Zhou H, Wang J, Zhu P, Zhu H, Toan S, Hu S, et al. NR4A1 Aggravates the Cardiac Microvascular Ischemia Reperfusion Injury Through Suppressing FUNDC1-Mediated Mitophagy and Promoting Mff-Required Mitochondrial Fission by CK2alpha. *Basic Res Cardiol* (2018) 113:23. doi: 10.1007/s00395-018-0682-1
95. Lee L, Seager R, Nakamura Y, Wilkinson KA, Henley JM. Parkin-Mediated Ubiquitination Contributes to the Constitutive Turnover of Mitochondrial Fission Factor (Mff). *PloS One* (2019) 14:e0213116. doi: 10.1371/journal.pone.0213116
96. Mambetsariev N, Lin WW, Stunz LL, Hanson BM, Hildebrand JM, Bishop GA. Nuclear TRAF3 Is a Negative Regulator of CREB in B Cells. *Proc Natl Acad Sci USA* (2016) 113:1032–7. doi: 10.1073/pnas.1514586113
97. Gokhale S, Xie P. ChoK-Full of Potential: Choline Kinase in B Cell and T Cell Malignancies. *Pharmaceutics* (2021) 13:1–15. doi: 10.3390/pharmaceutics13060911
98. Basu Ball W, Neff JK, Gohil VM. The Role of Nonbilayer Phospholipids in Mitochondrial Structure and Function. *FEBS Lett* (2018) 592:1273–90. doi: 10.1002/1873-3468.12887
99. van der Veen JN, Kennelly JP, Wan S, Vance JE, Vance DE, Jacobs RL. The Critical Role of Phosphatidylcholine and Phosphatidylethanolamine Metabolism in Health and Disease. *Biochim Biophys Acta Biomembr* (2017) 1859:1558–72. doi: 10.1016/j.bbamem.2017.04.006
100. Network TCGA. Comprehensive Genomic Characterization of Head and Neck Squamous Cell Carcinomas. *Nature* (2015) 517:576–82. doi: 10.1038/nature14129
101. Zhang J, Chen T, Yang X, Cheng H, Spath SS, Clavijo PE, et al. Attenuated TRAF3 Fosters Activation of Alternative NF-kappaB and Reduced Expression of Antiviral Interferon, TP53, and RB to Promote HPV-Positive Head and Neck Cancers. *Cancer Res* (2018) 78:4613–26. doi: 10.1158/0008-5472.CAN-17-0642
102. Georgopoulos NT, Steele LP, Thomson MJ, Selby PJ, Southgate J, Trejdosiewicz LK. A Novel Mechanism of CD40-Induced Apoptosis of Carcinoma Cells Involving TRAF3 and JNK/AP-1 Activation. *Cell Death Differ* (2006) 13:1789–801. doi: 10.1038/sj.cdd.4401859
103. Dunnill CJ, Ibraheem K, Mohamed A, Southgate J, Georgopoulos NT. A Redox State-Dictated Signalling Pathway Deciphers the Malignant Cell Specificity of CD40-Mediated Apoptosis. *Oncogene* (2017) 36:2515–28. doi: 10.1038/onc.2016.401
104. Rovira-Llopis S, Banuls C, Diaz-Morales N, Hernandez-Mijares A, Rocha M, Victor VM. Mitochondrial Dynamics in Type 2 Diabetes: Pathophysiological Implications. *Redox Biol* (2017) 11:637–45. doi: 10.1016/j.redox.2017.01.013

Conflict of Interest: The authors declare that the research was conducted in the absence of any commercial or financial relationships that could be construed as a potential conflict of interest.

this article, or claim that may be made by its manufacturer, is not guaranteed or endorsed by the publisher.

Advantages of publishing in Frontiers

OPEN ACCESS
Articles are free to read for greatest visibility and readership

FAST PUBLICATION
Around 90 days from submission to decision

HIGH QUALITY PEER-REVIEW
Rigorous, collaborative, and constructive peer-review

TRANSPARENT PEER-REVIEW
Editors and reviewers acknowledged by name on published articles

Frontiers
Avenue du Tribunal-Fédéral 34
1005 Lausanne | Switzerland

Visit us: www.frontiersin.org
Contact us: frontiersin.org/about/contact

REPRODUCIBILITY OF RESEARCH
Support open data and methods to enhance research reproducibility

DIGITAL PUBLISHING
Articles designed for optimal readership across devices

FOLLOW US
@frontiersin

IMPACT METRICS
Advanced article metrics track visibility across digital media

EXTENSIVE PROMOTION
Marketing and promotion of impactful research

LOOP RESEARCH NETWORK
Our network increases your article's readership